

Therya

Volumen 14

Número 1

Enero 2023



www.mastozoologiamexicana.org
AMMAC

La portada

El género de murciélagos *Gardnerycteris* incluye a tres especies neotropicales: *G. keenani* que habita desde el sureste de México hasta el norte de Suramérica, así como *G. koepckeae* y *G. crenulatum*, que se distribuyen en la vertiente oriental andina y las tierras bajas al este de los Andes, respectivamente. Son especies raras y poco conocidas, pero se ha reportado que perchan sobre troncos y árboles huecos, en pequeños grupos cerca de cuerpos de agua. Principalmente se alimentan de insectos como escarabajos, polillas, moscas y hemípteros, pero también de arañas, uropígididos, pequeños vertebrados, néctar, polen y frutos. La etimología *Gardnerycteris* fue propuesta para reconocer las importantes contribuciones al conocimiento de los murciélagos y otros mamíferos neotropicales realizadas por el Dr. Alfred L. Gardner, a quién también dedicamos este número especial de *Therya* (foto tomada por Marco Tschapka).

Nuestro logo "Ozomatli"

El nombre de "Ozomatli" proviene del náhuatl se refiere al símbolo astrológico del mono en el calendario azteca, así como al dios de la danza y del fuego. Se relaciona con la alegría, la danza, el canto, las habilidades. Al signo decimoprimeros en la cosmogonía mexicana. "Ozomatli" es una representación pictórica de los mono arañas (*Ateles geoffroyi*). La especie de primate de más amplia distribución en México. " Es habitante de los bosques, sobre todo de los que están por donde sale el sol en Anáhuac. Tiene el dorso pequeño, es barrigudo y su cola, que a veces se enrosca, es larga. Sus manos y sus pies parecen de hombre; también sus uñas. Los Ozomatin gritan y silban y hacen visajes a la gente. Arrojan piedras y palos. Su cara es casi como la de una persona, pero tienen mucho pelo."

Therya

Volumen 14, número 1

enero 2023

Contenido

EDITORIAL

Special Issue in Honor of Dr. Alfred L. Gardner

Jacob A. Esselstyn, and Giovani Hernández-Canchola _____ 1

ARTICLES

NATURAL HISTORY

Roosting habits of disk-winged bats, especially *Thyroptera discifera*

Ronald H. Pine, Gianfranco Gómez Zamora, Fiona A. Reid, and Robert M. Timm _____ 5

FUNCTIONAL MORPHOLOGY

Skeletal indicators of locomotor adaptations in shrews

Neal Woodman _____ 15

ECOLOGY AND BIOGEOGRAPHY

Ecological niche differentiation among Aztec fruit-eating bat subspecies (*Chiroptera: Phyllostomidae*) in Mesoamerica

Iván Hernández-Chávez, Lázaro Guevara, Joaquín Arroyo-Cabrales, and Livia León-Paniagua _____ 39

Habitat use, richness, and abundance of native mice in the highlands of the Talamanca mountain range, Costa Rica

José D. Ramírez-Fernández, Gilbert Barrantes, Catalina Sánchez-Quirós, and Bernal Rodríguez-Herrera _____ 49

Pleistocene distribution of MacConnell's Bat (*Phyllostomidae*) suggests intermittent connections between Amazonia and Atlantic Forest

Felipe Pessoa Silva, Lucas Gonçalves da Silva, Thiago B. F. Semedo, Tamily C. M. Santos, Gerson Paulino Lopes, Martin Alejandro Montes, and Guilherme S. T. Garbino _____ 55

CONSERVATION

Coming home: modelling the mating roost of the endangered bat *Leptonycteris nivalis* _____ 63
Leonora Torres Knoop, Enrique Martínez-Meyer, and Rodrigo A. Medellín

Human footprint effects on the distribution of the spotted lowland paca (*Cuniculus paca*) _____ 75
Monserrat Sánchez-Reyes, Xavier Chiappa-Carrara, Ella Vázquez-Domínguez, Carlos Yáñez-Arenas, Manuel Falconi, Luis Osorio-Olvera, and Rusby G. Contreras-Díaz

SYSTEMATICS AND TAXONOMY

Current status of the *Peromyscus mexicanus* complex in Oaxaca, México _____ 85
L. Ernesto Pérez-Montes, Sergio Ticul Álvarez-Castañeda, and Consuelo Lorenzo

A propaedeutic to the taxonomy of the Eastern cottontail rabbit (*Lagomorpha: Leporidae: Sylvilagus floridanus*) from Central America _____ 99
Luis A. Ruedas, Lucía I. López, and José M. Mora

Geographic variation in select species of the bat genus *Platyrrhinus* _____ 121
Paúl M. Velazco, Grace Ly, Julia McAllister, and Diego A. Esquivel

Taxonomic reassessment of the Little pocket mouse, *Perognathus longimembris* (Rodentia, Heteromyidae) of southern California and northern Baja California _____ 131
James L. Patton, and Robert N. Fisher

Revisiting species delimitation within *Reithrodontomys sumichrasti* (Rodentia: Cricetidae) using molecular and ecological evidence _____ 161
Elizabeth Arellano, Ana L. Almendra, Daily Martínez-Borrego, Francisco X. González-Cózatl, and Duke S. Rogers

An 1896 specimen helps clarify the phylogenetic placement of the Mexican endemic Hooper's deer mouse _____ 181
Susette Castañeda-Rico, Cody W. Edwards, Melissa T. R. Hawkins, and Jesús E. Maldonado

fascículo 40 <http://www.revistas-conacyt.unam.mx/therya/index.php/THERYA/issue/view/41>

DERECHOS DE AUTOR Y DERECHOS CONEXOS, año 14, No. 1, enero-abril del 2023, es una publicación cuatrimestral editada por la Asociación Mexicana de Mastozoología A. C. Hacienda Vista Hermosa 107, Colonia Villa Quietud, Coyoacan 04960. Distrito Federal, México. Teléfono (612) 123-8486, www.mastozoologiamexicana.org, therya@cibnor.mx. Editor responsable: Dr. Sergio Ticul Álvarez Castañeda. Reservas de Derechos al Uso Exclusivo No. 04-2009-112812171700-102, ISSN: 2007-3364 ambos otorgados por el Instituto Nacional de Derechos de Autor. Responsable de la última actualización de este número, Unidad de informática de la Asociación Mexicana de Mastozoología A. C. Dr. Sergio Ticul Álvarez Castañeda. Instituto Politécnico Nacional 195. La Paz, Baja California Sur, C. P. 23096. Tel. (612) 123-8486, fecha de la última modificación 30 enero 2023.

Las opiniones expresadas por los autores no necesariamente reflejan la postura del editor de la publicación. Queda prohibida la reproducción total o parcial de los contenidos e imágenes de la publicación sin previa autorización de la Asociación Mexicana de Mastozoología, A. C.

Therya

Consejo Editorial

Edward J. Heske. Museum of Southwestern Biology, University of New Mexico, Albuquerque, New Mexico, 87131, Estados Unidos de Norte América.

Douglas A. Kelt. Universidad de California, campus Davis. 1 Shields Ave, Davis, California 95616. Estados Unidos de Norte América.

Víctor Sánchez Cordero. Universidad Nacional Autónoma de México, Instituto de Biología. Coyoacán, Ciudad de México, México.

Therya

Cintya Segura Trujillo. Editora de formato. Instituto Politécnico Nacional 195. La Paz 23096, Baja California Sur., México. E-mail: c.a.bielsegura@gmail.com.

Malinalli Cortés Marcial. Tesorera de la Revista Therya. Universidad Autónoma Metropolitana Unidad Xochimilco. E-mail: therya.tesoreria@gmail.com

Alina Gabriela Monroy Gamboa. Difusión. Instituto de Biología, Universidad Nacional Autónoma de México, Circuito Exterior s/n, Ciudad Universitaria, CP. 04510. Ciudad de México, México. E-mail: beu_ribetzin@hotmail.com

Maria Elena Sánchez Salazar. Traducción.

El objetivo y la intención de *THERYA* es ser una revista científica para la publicación de artículos sobre los mamíferos. Estudios de investigación original, editoriales y artículos de revisión son bienvenidas.

Sergio Ticul Álvarez Castañeda. Editor general. Centro de Investigaciones Biológicas del Noroeste. Av. Instituto Politécnico Nacional 195. La Paz 23096, Baja California Sur. México. E-mail: sticul@cibnor.mx.

Cintya Segura Trujillo. Editor asistente. Universidad de Guadalajara, CUCSUR, Autlán 48900, Jalisco, México. E-mail: c.a.biologsegura@gmail.com.

Jacob A. Esselstyn. Editor asociado. Museum of Natural Science, Louisiana State University, Baton Rouge, LA 70803, USA. E-mail: esselstyn@lsu.edu (JAE).

Lázaro Guevara. Editor asociado. Departamento de Zoología, Instituto de Biología, Universidad Nacional Autónoma de México, 04510, Mexico City, Mexico. E-mail: llg@ib.unam.mx

Guillermo D'Elía. Editor asociado. Instituto de Ciencias Ambientales y Evolutivas, Universidad Austral de Chile, Valdivia, Chile. E-mail: guille.delia@gmail.com.

Monica Díaz. Editor Asociado. CONICET, PIDBA (Programa de Investigaciones de Biodiversidad Argentina), PCMA (Programa de Conservación de los Murciélagos de la Argentina. Facultad de Ciencias Naturales e Instituto Miguel Lillo - Universidad Nacional de Tucumán. Fundación Miguel Lillo, Miguel Lillo 251, (4000) San Miguel de Tucumán, Argentina. E-mail: mmonicadiaz@yahoo.com.ar.

Jesús A. Fernández. Editor asociado. Departamento de Recursos Naturales, Facultad de Zootecnia y Ecología, Universidad Autónoma de Chihuahua, México. E-mail: jaff1789@gmail.com.

Mariana Freitas Nery. Editor asociado. Departamento de Genética, Evolução e Bioagentes, Instituto de Biologia, Universidade Estadual de Campinas. Rua Bertrand Russel, s/n. Caixa Postal 6109 – CEP 13083---970 Campinas/SP. Brasil. E-mail: mariananery@gmail.com.

Giovani Hernández-Canchola. Editor asociado. Departamento de Ecología de la Biodiversidad, Instituto de Ecología, Universidad Nacional Autónoma de México, CP. 04510. Ciudad de México, México. E-mail: giovani@ciencias.unam.mx (GHC).

Mircea Gabriel Hidalgo Mihart. Editor asociado. División Académica de Ciencias Biológicas, Universidad Juárez Autónoma de Tabasco. Carretera Villahermosa-Cárdenas Km. 0.5 S/N, Entronque a Bosques de Saloya. CP. 86150, Villahermosa. Tabasco, México. E-mail: mhidalgo@yahoo.com

Juan Pablo Gallo Reynoso. Editor asociado. Centro de Investigación en Alimentos y Desarrollo. Laboratorio de Ecofisiología. Carretera a Varadero Nacional km 6.6. Col. Las Playitas 85480. Guaymas, Sonora. México. E-mail: jpgallo@ciad.mx.

Consuelo Lorenzo Monterrubio. Editor asociado. El Colegio de la Frontera Sur. Área Conservación de la Biodiversidad. Carretera Panamericana y Periférico Sur s/n. San Cristóbal de Las Casas 29290, Chiapas. México. E-mail: clorenzo@ecosur.mx.

Lia Celina Méndez Rodríguez. Editor asociado. Centro de Investigaciones Biológicas del Noroeste. Av. Instituto Politécnico Nacional 195. La Paz 23096, Baja California Sur. México. E-mail: lmendez04@cibnor.mx.

Eduardo Mendoza. Editor asociado. Instituto de Investigaciones sobre los Recursos Naturales (INIRENA) Universidad Michoacana de San Nicolás de Hidalgo. Av. San Juanito Itzicuaro s/n. Col. Nueva Esperanza C.P. 58337. Morelia, Michoacán, México. E-mail: mendoza.mere@gmail.com.

Robert D. Owen. Editor asociado. Department of Biology. Texas Tech University. Lubbock, Texas 79409. Estados Unidos de Norte América. Dr. Raúl Casal 2230 (ex Martín Barrios) c/Pizarro. C.P. 1371. Barrio Republicano. Asunción, Paraguay. E-mail: rowen@tigo.com.py.

Rafael Reyna Hurtado. Editor asociado. El Colegio de la Frontera Sur, unidad Campeche. Avenida Rancho s/n, Lerma Campeche, 24500. México. E-mail: rafaelcalakmul@gmail.com.

Jorge Servin. Editor asociado. Universidad Autónoma Metropolitana, Unidad Xochimilco. Calz. Del Hueso #1100, Col. Villa Quietud, 14910, Ciudad de México, México. E-mail: Jorge.servin170@gmail.com.

Sergio Solari. Editor asociado. Instituto de Biología. Universidad de Antioquia. Calle 67 No53-108 / AA 1226. Medellín, Colombia. E-mail: solari.udea@gmail.com.

Special Issue in Honor of Dr. Alfred L. Gardner

It is a great pleasure to introduce this special feature honoring Dr. Alfred Lunt Gardner. Al's many contributions to mammalogy span seven decades, two continents, and practically the entire tree of mammals. It is impossible to imagine what mammalogy in the Americas would look like without him. His academic contributions are as significant as his imposing stature.

Al was born in Salem, Massachusetts in 1937 and spent his early childhood there. His first interests in natural history were sparked by his 3rd-grade teacher, an amateur ornithologist who kept a cabinet of specimens in her classroom ([Gardner 2005](#)). In 1947, the Gardner family relocated to a farm in North Andover, Massachusetts, where, according to Al, he "practically lived in the woods fishing, hunting, and trapping" (pg. 277, [Gardner 2005](#)). In his adolescent years, Al would spend considerable time in the outdoors, honing his trapping and skinning skills. By his freshman year of high school, he was selling furs and evading game wardens ([Gardner 2005](#)). In 1953, his family moved to Tucson, Arizona, where Al found a trove of new habitats and wildlife to explore. By 1955, Al graduated high school, signed up for the Army Reserves, and enrolled at the University of Arizona, where his mammalogical interests would be further stimulated by E. Lendell Cockrum and his graduate students.



Figure 1. Al Gardner skinning a bat in 1968 in Perú. Photo credit: John O'Neill.

Al's undergraduate path was a bit circuitous. He dropped out for a while, working as a welder and sheet metal man. His expertise in this area would later prove valuable as they enabled him to fashion traps from scraps, as needed. The capacity to jury rig is invaluable in remote field sites, and one that would serve Al well in many later field excursions. By 1962, Al received his B.S in Wildlife Management and, in 1965, his M.S. in Zoology, both from the University of Arizona. Upon completion of his M.S., Al worked as a professional collector and as a Fellow in Tropical Medicine associated with Louisiana State University (LSU) and based at the International Center for Medical Research and Training in Costa Rica. In 1967, he enrolled at LSU as a PhD student and by 1970 completed his degree in Zoology with a minor in Paleontology. Al's dissertation is an impressive study of the systematics of *Didelphis*, completed under the mentorship of George Lowery. It is remarkable that Al finished his terminal degree so quickly given the amount of time he spent in the field. LSU collecting trips that involved Al always resulted in more specimens, and legend has it that Dr. Lowery always wanted more, so Al was in the field a lot (Figures 1, 2, 3). Today, the LSU collection contains 2498 mammal specimens with ALG field numbers, most of them collected between 1966 and 1971 in the United States (U.S.), México, Costa Rica, Panama, and Perú. Fifty years later, the ALGs from Perú are LSU's most-studied mammal specimens.

During the early 1970s Al worked alternately as an Assistant Professor at LSU and Tulane University. In 1973, he began what would be his long-term position as Curator of North American Mammals at the U.S. National Museum of Natural History. At various times, his position was affiliated

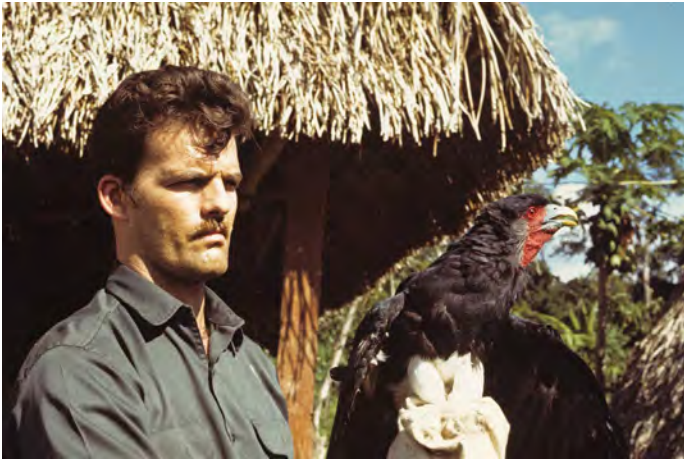


Figure 2. Al Gardner holding a Red-throated Caracara in 1968 in Perú. Photo credit: John O'Neill.

with the U.S. Fish and Wildlife Service (1973–1993), National Biological Survey (1993–1996), and the U.S. Geological Survey (1996–2018). Al retired in 2018, but has remained an active member of the mammal research community.

Al's many significant contributions to mammalogy include at least 162 publications. His first paper appeared in 1960, while he was an undergraduate, providing novel natural history information on a rare mastiff bat in Arizona (Cockrum and Gardner 1960). In 1962, Al would describe his first new species, *Glossophaga commissarisi* Gardner, 1962, named in honor of a fellow student who had died the year before. From this point on, Al's research would use morphology, karyotypes, and a keen sense of natural history to solve taxonomic issues in mammals from North and South America, with much of his attention devoted to bats, but also significant work on marsupials, rodents, and others. In total, he would describe two new genera and 20 new species, while revising countless others (Mammal Diversity Database 2022). Through much of his career, Al also served as a reviewer, editor, and member of the International Commission on Zoological Nomenclature. Al cares deeply about nomenclatural practice, having long recognized its importance to the stability and progress we make in taxonomic research and the many other disciplines that rest upon this foundation. With his nomenclatural expertise, Al has helped countless others by clarifying sometimes complex rules and processes (e. g., Gardner and Hayssen 2004).

Al's work refining taxonomic resolution would culminate in the 2008 publication of Volume 1 of *The Mammals of South America*. Al edited the volume and authored many of its chapters. This beautiful, comprehensive book contains species accounts with synonymys, identification keys, distribution maps, and natural history details of nearly 400 species of bats, xenarthrans, shrews, and marsupials. This massive summation of centuries of investigation has no doubt fostered a wealth of subsequent research and inspired many youngsters to take up mammalogy as a career.

Al's influence on our field of research goes well beyond simple counts of publications, specimens, and the like.

While it is impossible to similarly tally a person's influence on the work of subsequent generations of scientists, it is clear that Al's influence on younger mammalogists has been profound. When Al was just a young graduate student at the University Arizona, he was already inspiring people who would become some of the most significant mammalogists of their generation. Don Wilson counts Al as the single most influential mentor during his early career (Wilson 2005) and Jim Patton credits Al with inspiring a disciplinary shift from Anthropology to Zoology after just one night of trapping kangaroo rats. Al's influence would not end there. Paúl Velazco informs us that, during the late 1990s, as an up and coming young mammalogist in Perú, he considered Al a near mythical mammalogical legend, known as 'gigante con manos grandes'. Al's influence in Latin America continues to the present day, where his publications are required reading for new and experienced mammalogists alike (e. g., Gardner and Hayssen 2004; Ramírez-Pulido *et al.* 2014; Gardner and Ramírez-Pulido 2020) and the specimens he collected, which changed our understanding of Latin American mammal diversity, remain essential material for new generations of researchers. Proof of community-wide respect and admiration is reflected in awards received (e. g., Ticol Álvarez-Solórzano Award; Figure 4) and the patronyms bestowed on Al, including one genus, seven species, and one subspecies named in his honor.

The respect Al garners is due both to the rigor of his scientific contributions and his personality. Jose Ramírez-Pulido describes Al as a serious, formal, persistent, and wise scientist. As a critic, he is direct and objective. As a colleague, he is noble, humble, and magnanimous, all traits that inspire others to be rigorous in their own research while also generously supporting others. We hope that this special feature of *Therya* adequately honors Al's prodigious, careful, and charitable efforts to advance the science of mammalian diversity.

In this special issue, we have assembled a set of papers on the mammals of the Americas. Each builds upon the foundational knowledge established directly and indirectly by Al through his research, fieldwork, and mentorship.



Figure 3. Al Gardner thinking deeply about neotropical mammals in Balta, Perú. Photo credit: Jim Patton.



Figure 4. Al Gardner (center), receiving the Ticul Álvarez-Solórzano Award from the Asociación Mexicana de Mastozoología A. C. in 2018. To Al's left are Javier Sosa Escalante and Rodrigo Medellín; to his right are Cistina Mac Swiney González and Enrique Martínez Meyer. Photo credit: AMMAC archive.

Papers in this volume include work on natural history, functional morphology, ecology, biogeography, conservation, and systematics. These papers stand, both figuratively and literally, on the shoulders of a giant.

Acknowledgements

We thank Sergio Ticul Alvarez Castañeda for the invitation to organize this special feature honoring Dr. Gardner. Melissa Hawkins, Jim Patton, Paúl Velazco, Robb Brumfield, and Jose Ramírez-Pulido were instrumental in tracking down details of Al's personal and professional life. We thank all the authors in this special feature for their valued contributions and the many peer reviewers who examined each manuscript.

JACOB A. ESSELSTYN^{1,2*}, AND GIOVANI HERNÁNDEZ-CANCHOLA³

¹ Museum of Natural Science, Louisiana State University, Baton Rouge, LA 70803, USA. Email: esselstyn@lsu.edu (JAE)

² Department of Biological Sciences, Louisiana State University, Baton Rouge, LA 70803, USA.

³ Departamento de Ecología de la Biodiversidad, Instituto de Ecología, Universidad Nacional Autónoma de México, CP. 04510. Ciudad de México, México. Email: giovani@ciencias.unam.mx (GHC).

*Corresponding author: <https://orcid.org/0000-0002-1823-4062>.

Literature cited

- COCKRUM, E. L., AND A. L. GARDNER. 1960. Underwood's mastiff bat in Arizona. *Journal of Mammalogy* 41:510–511.
- GARDNER, A. L. 1962. A new bat of the genus *Glossophaga* from Mexico. *Contributions in Science, Los Angeles County Museum* 54:1–7.
- GARDNER, A. L. 2005. Been there, done that: After 44 years of preparation, what's next? Pp. 277–284, *in* *Going Afield* (Phillips, C. J., and C. Jones, eds). Museum of Texas Tech University. Lubbock, U.S.A.
- GARDNER, A. L. 2008. *Mammals of South America, Volume 1: Marsupials, Xenarthrans, Shrews, and Bats*. University of Chicago Press. Chicago, U.S.A.
- GARDNER, A. L. and J. RAMÍREZ-PULIDO. 2020. Type localities of Mexican land mammals, with comments on taxonomy and nomenclature. *Special Publications Museum of Texas Tech University* 73: 1–134.
- GARDNER, A. L. AND V. HAYSEN. 2004. A guide to constructing and understanding synonymies for Mammalian Species. *Mammalian Species* 739:1–17.
- MAMMAL DIVERSITY DATABASE. 2022. Mammal diversity database (Version 1.10). Zenodo doi: 10.5281/zenodo.7394529.
- RAMÍREZ-PULIDO, J., N. GONZÁLEZ-RUIZ, A. L. GARDNER, AND J. ARROYO-CABRALES. 2014. List of recent land mammals of Mexico. *Special Publications Museum of Texas Tech University* 63: 1–69.

EDITORIAL

WILSON, D. E. 2005. Bats to biodiversity: Spyder had a pretty good ride. Pg. 217–233, *in* *Going Afield* (Phillips, C. J., and C. Jones, eds). Museum of Texas Tech University. Lubbock, U.S.A.

Roosting habits of disk-winged bats, especially *Thyroptera discifera*

RONALD H. PINE¹, GIANFRANCO GÓMEZ ZAMORA², FIONA A. REID³, AND ROBERT M. TIMM^{4*}

¹ Natural History Museum, University of Kansas, Lawrence, Kansas 66045, United States of America. Email: ronpine@mac.com (RHP).

² 800 meters south of La Paloma Lodge, Drake Bay, Costa Rica. Email: gianfranco.gomez@gmail.com (GG).

³ Center for Biodiversity and Conservation Biology, Royal Ontario Museum, Toronto, Ontario, Canada. M5S 2C6. Email: fiona.reid7243@gmail.com (FAR).

⁴ Natural History Museum and Department of Ecology and Evolutionary Biology, University of Kansas, Lawrence, Kansas 66045, United States of America. Email: btimm@ku.edu (RMT).

*Corresponding author: <https://orcid.org/0000-0001-6203-3316>.

Roosting habits of disk-winged bats of the genus *Thyroptera* (Chiroptera: Thyropteridae) have been unknown to very poorly known except for those of the commonly encountered *T. tricolor*. Many secondary literature publications state that roosting habits of *Thyroptera* in general are those of *tricolor*, known to roost almost exclusively in vertical, unfurling large leaves, especially of native *Heliconia* and introduced banana (genus *Musa*). However, so far as known, no other species of *Thyroptera* chooses such roosts. Until 1993, the only species of *Thyroptera* known were *tricolor* and *discifera*—they had been the only two known for 139 years. During this long period, the unique roosting habits of *tricolor* often were attributed to the genus as a whole, as sometimes still happens today. Now there are three more known species—*lavali*, *devivoi*, and *wynneae*. In this paper, we correct misconceptions concerning roosting habits in *Thyroptera*, summarize what is known for all five species, and provide the first detailed observations on roosting in *discifera*. *Thyroptera discifera* has been found roosting attached to the underside of a palm leaflet or leaflets in Brazil and in conically curled portions of dead banana leaves in Costa Rica.

Los hábitos de selección de refugios de los murciélagos de ventosas del género *Thyroptera* (Chiroptera: Thyropteridae) han sido desconocidos o muy poco conocidos, con excepción a los hábitos de *T. tricolor*, que es la especie que se encuentra comúnmente. Muchas publicaciones de literatura secundaria afirman que los hábitos de selección de refugio de los *Thyroptera* en general son los mismos que los de *tricolor*, que son conocidos por descansar casi exclusivamente en hojas grandes verticales y parcialmente enrolladas, especialmente hojas de *Heliconia* nativa y banano introducido (género *Musa*). Sin embargo, por el momento no se conoce ninguna otra especie de *Thyroptera* que elija este tipo de refugio. Hasta 1993, las únicas especies de *Thyroptera* conocidas eran *tricolor* y *discifera* y habían sido las únicas dos especies conocidas durante 139 años. Durante este largo período, los hábitos particulares de selección de refugios de *tricolor* frecuentemente se atribuyeron a todo género, como a veces todavía sucede hoy en día. Actualmente se conocen tres especies más en este género: *lavali*, *devivoi* y *wynneae*. En este artículo, corregimos los conceptos erróneos sobre selección de refugios en *Thyroptera*, resumimos lo que se conoce de las cinco especies y brindamos las primeras observaciones detalladas sobre la selección de refugios de *discifera*. *Thyroptera discifera* se ha encontrado descansando adherido a la parte inferior de un folíolo o folíolos de palma en Brasil y en porciones de hojas muertas de plátano enrolladas cónicamente en Costa Rica.

Keywords: Banana leaves; Brazil; Costa Rica; *Mauritia*; *Musa*; Neotropics; palm fronds.

© 2023 Asociación Mexicana de Mastozoología, www.mastozoologiamexicana.org

Introduction

The Neotropical disk-winged bat genus *Thyroptera* (Chiroptera: Thyropteridae) contains five known living species occurring from within southern México into southern Brazil and northern Bolivia. The genus is characterized by a number of synapomorphies, the most distinctive being the circular or oval, moist, adhesive disks on the wrists and ankles that are used in attachment to and movement along the roost leaves. Historically, the genus was believed to consist of two species—*Thyroptera tricolor* and *T. discifera*. A third species, *T. lavali* was described based on specimens from a single locality in Perú and is now known from several localities across northern South America ([García et al. 2018](#); [Lee 2019](#); [Morales-Martínez et al. 2021](#)). *Thyroptera devivoi* [Gregorin et al. 2006](#) was described from two localities in eastern Brazil, one in Guyana, and has subsequently been reported from northeastern Colombia by [Rodríguez-Posada et al.](#)

([2017](#)) and additional Brazilian localities by [Semedo et al. \(2020\)](#). *Thyroptera wynneae* [Velazco et al., 2014](#) is known from a locality in eastern Perú and three in southeastern Brazil ([Hoppe et al. 2014](#)).

Thyropterids are seldom captured in the standard mist nets used to sample bats, undoubtedly contributing to our lack of understanding of distributions and ecology. Most observations and specimens of thyropterids are based on individuals found at the roost sites. [Tschapka et al. \(2000\)](#) described the echolocation calls of *T. discifera* as very low intensity and consisting of several frequency-modulated harmonics, which perhaps allow the flying bats to detect mist nets and avoid capture. *Thyroptera tricolor* is the most widely distributed and most frequently encountered species and summaries of the natural history of the genus are primarily based on what is known about that species. Much of what has been written about roosting in the

genus, especially in *discifera*, is in secondary sources and those derived from other secondary sources, and assumes that it is as in *tricolor*. Herein, we review what has been written on roosting in *discifera* and provide new data on roost sites, documenting that this disk-winged bat roosts in the cones formed by dead banana leaves and attached to the underside of palm fronds.

Thyroptera tricolor, the best known and most widely distributed of the species, has frequently been reported as roosting, head up, inside live, still partially rolled *Heliconia* leaves, sometimes of *Musa* (banana) and, occasionally of other genera. As noted above, this roosting predilection of *T. tricolor* has often been assumed to characterize *T. discifera* also, especially in the secondary literature. However, as outlined here, *discifera* has different roosting habits and perhaps never has been found in rolled new leaves.

Findley and Wilson (1974) stated “disk-winged bats are known to roost only inside the rolled new leaves in members of the banana family (Musaceae) or related plants” (p. 562) and that *Heliconia* and *Calathea* are “two genera that provided most bat roosts” (p. 563). Additionally (p. 569), they stated “*Thyroptera* may roost on other types of foliage than musaceous leaves, but none has ever been found in such situations” (but *Calathea* is not musaceous), and “This species is limited to rolled leaves of musaceous plants as roosting sites” (p. 570). In Wilson and Findley (1977:2), we read that *tricolor* is found “occasionally in *Calathea* (Marantaceae)” and that “Morphological specializations of the bats [*tricolor*] probably limit them to rolled leaves as roosting sites” (p. 3). Wilson (1978:2) wrote *tricolor*, unlike *discifera*, “roosts in rolled *Heliconia* leaves and is never found in the open.” Kunz (1982:2) stated, “the ... disks ... of *Thyroptera tricolor* restricts [*sic*] this bat to roosting on the smooth inner surfaces of unfurled [*sic*] leaves ...”

Brosset and Charles-Dominique (1990:543) wrote concerning *tricolor*, “Observed in small groups, harems or bachelor ♂♂, not only in the classical roost of the species: the terminal buds [*sic*] of *Heliconia* and banana-trees, but also in such ... places as between tails of shirts drying on a wire, or between plastic sheets stocked in the station-houses. This species ... adopts artificial [roosts] ... in human settlements ... which suggests that *Thyroptera* may sometimes be short of natural roosts.” In this regard, an adult male *tricolor* (USNM 541439), taken in Chiriquí at Escopeta Camp, ca. 23 km NNE San Félix (= San Félix at 8° 17' N, -81° 52' W), ca. 900 m, was found alive and adhering to the front of an automobile on 1 July 1980 (R. Izor, pers. comm.). The surrounding area is mostly heavily grazed grassland with brush and/or scrubby forest along watercourses. Possibly the bat had been transported there on the vehicle.

Simmons and Voss (1998:133–134) found *tricolor* in the usual semi-furled live *Heliconia* leaves and also in scrolled, dead, hanging leaves of *Phenakospermum guyannense* (Strelitziaceae) along with semi-furled live leaves of the same species. Velazco et al. (2014:18) also mention *Phenakospermum* as providing roosts for *tricolor*. Velazco et al.

(2021:128, 130), writing about *tricolor* in northeastern Peru, found six roosts “at the same locality ... all of them in the rolled new leaves of large *Heliconia* sp. ... about 3.5–4.5 m above the ground in young secondary growth ...” Group size ranged from 4 to “about 12.”

Pine (1993:218), because of the great rarity of *lavalii*, hypothesized that it might roost in the forest canopy. Morales-Martínez et al. (2021:476) stated, incorrectly, that Pine had specifically mentioned palms. Solari et al. (1999:155) wrote concerning *lavalii* “caught from a palm more than 5 m high, where we suppose it was roosting,” and Solari et al. (2004:293) wrote “probably roosts in palms.” Reid et al. (2000:44–45) collected three *lavalii*, each on a different occasion, in or adjacent to a *Mauritia* palm swamp. García et al. (2019:3) reported a specimen of *lavalii* captured in a “morichal, junto a el tapón.” Franger J. García (*in litt.*) informs us that in Venezuelan Spanish this means in a stand of the palm, *Mauritia flexuosa*, next to the dam.

Pérez et al. (2012:1107) reported Guatemalan national park personnel’s having found a *tricolor* “inside a dry unfurled banana leaf” but surmised that it was “probably *Heliconia*.” By “dry leaf” they presumably meant dead leaf. This is the only account that we know of that reports such a roost for *tricolor*.

Rosa et al. (2020:1) state that they “observed a *T. devivoi* colony of 15 living under a dead palm leaf.” But (page 4) an estimated 10–15 individuals “dwelling inside the sheath of a dead palm leaf that was hanging in the forest canopy.” Judging from their two figures (p. 3) and the “2.5 m height roost entrance facing downwards” (p. 5), the roost was not “hanging in the forest canopy.” The roost, as figured, shows a cone-shaped configuration like that of the banana leaf cones described in later accounts here for *discifera*. The species of palm was not indicated. The bats were in the roost for at least four days (p. 1) and the locality was in Chapada das Mesas National Park, Carolina Municipality, Maranhão, Brazil (p. 2). Morales-Martínez et al. (2021:476) state that Rosa et al. incorrectly described “shelters” (plural) of *devivoi* (Rosa et al. also wrote that *Thyroptera* roost in “still furled” leaves). Morales-Martínez et al. (2021:476), however, thought that the bat captured from the colony reported by Rosa et al. might be a *lavalii*, rather than *devivoi*, based on the figure showing no frosting on the venter. They also identified the skull figured by Rosa et al. as of a *Myotis*, rather than of a *Thyroptera*. They themselves (p. 473) reported a *lavalii* mist-netted in an “open *Mauritia flexuosa* palm swamp” that had been cleared at La Chorrera, Amazonas, Colombia. They conclude (p. 476) “*lavalii* is associated with swamp-forest habitats with high *Mauritia flexuosa* palms.”

Gregorin et al. (2006:239) reported two specimens of *devivoi* as having been caught “under an eaté palm leaf” but didn’t state if more had been present. Voss et al. (2016:12) indicate that Gregorin et al. reported *lavalii* as roosting in vegetation, but this is not the case.

Two *Thyroptera wynneae* were recorded by Velazco et al. (2014:15, 18) as roosting in the dark interior of a lobe of a

partially rolled dead *Cecropia* (Urticaceae) leaf hanging by its petiole, about 2 m above the ground. This roosting site resembles those of *discifera*, as described later in this article, in dead leaves of the non-native banana plant.

Uncritical treatments of roosting in Thyroptera

Various authors have treated the genus as a whole, as then known, and including *discifera*, as roosting in partially rolled, live *Heliconia* and/or banana leaves: [Dalquest and Walton \(1970:174\)](#), [Tello \(1979\)](#), [Hill and Smith \(1984:212\)](#), [Patterson \(1992:18\)](#) citing [Taddei \(1988\)](#), and [Rosa et al. \(2020:2\)](#). Other somewhat more complicated uncritical comments follow:

Perhaps the first to write concerning *Thyroptera*'s roosting was [Dobson \(1878:347\)](#) who wrote "... is ... peculiar ... in possessing such highly specialized climbing organs as the adhesive disks." G. M. [Allen \(1939\)](#), wrote (confusingly) that *Thyroptera* are "at times found in the rolled fronds of bananas or in curled large leaves" and "one of their favorite roosting places is inside the long narrow tube formed by an unrolled banana frond." [Cockrum \(1962:250\)](#) cited Allen as stating that *Thyroptera* "usually roost individually" but there is no such statement in Allen's book. [Krumbiegel \(1955\)](#) published redrawn illustrations (of *tricolor*) from [Carvalho \(1940\)](#), and inexplicably, in Krumbiegel's renditions, most of the figured bats were inverted so that they are shown head-down. [Matthews \(1971\)](#), concerning both species of *Thyroptera* then known, stated "These bats roost singly or in groups of up to about half a dozen head upwards in the large curled, faded [?] leaves of heliconias, bananas and other plants," but gave no sources.

[Eisentraut \(1975:143\)](#), writing of the family as then known, stated that suction disks enable "these bats to maintain a firm hold on smooth branches and leaves and to crawl on them," but provided no sources. Eisentraut wrote further, "These bats prefer rolled-up leaves, for example, of bananas, for their sleeping site during the day; several ... can usually be seen sitting one behind the other, with their heads up" (p. 143–144).

[Yalden and Morris \(1975:220\)](#) wrote "Thyropterids ... rest in a head-upwards position, usually beside [*sic*] a curled leaf ..." Concerning *discifera*, [Ascorra et al. \(1993:547\)](#) wrote "This species is usually encountered in rolled leaves of *Heliconia* spp. or *Calathea* spp. but we found no individuals in our searches of these leaves [at a specific site in Perú]." They gave no sources and cited no observations to substantiate their comment.

[Nowak and Paradiso \(1983\)](#) and [Nowak \(1991, 1999\)](#) made no mention of differing habits in the species then known, and seemed to imply that all might be found in rolled leaves, and stated, incorrectly, that all might generally be found only one or two per shelter.

[Bezerra et al. \(2005:169\)](#) wrote "Thyropterids roost inside the rolled leaves of some species of Heliconiaceae ... Roosts inside curled leaves of ... (*Musa* sp.) have also been reported

for *T. discifera*" and cited [Wilson \(1978\)](#), [Torres et al. \(1988\)](#), and [Nowak \(1999\)](#) for the latter comment.

[de Lima and Gregorin \(2007:141\)](#) write that *discifera* uses rolled banana and *Heliconia* leaves for shelters citing [Kennedy \(2002\)](#). [Pérez et al. \(2012:1107\)](#) incorrectly stated that [Medellín et al. \(1986\)](#) had recorded *tricolor* from an unfurled *Heliconia* leaf.

[Lee's \(2019:418\)](#) accounts of *Thyroptera* sometimes attribute habits of *tricolor* to the genus in general, etc. He wrote "... [*tricolor*] roost attached to the undersides [presumably meaning inner sides] of waxy furled leaves ... *Musa* ... *Heliconia*, *Calathea* ... and *Phenokospermum* (Streliziaceae), dead leaves of *Cecropia* ... and palm fronds ... Thyropterids must change roosts almost daily ... diameter of the furl becomes too great after a day or two. Disk-winged bats ... roost in a head-up position ... approximately 4 m aboveground."

Various authors have written that *Thyroptera* are restricted to the lowlands. The latest of these is [Morales-Martinez et al. \(2021:471\)](#) who wrote "*Thyroptera* species inhabit lowland, moist, Neotropical forests." However, authors have recorded *tricolor* from as high as 1,650 m, and Pine has observed disturbed *Thyroptera* exiting from a *Heliconia* leaf at 1,550 to 1,600 m in the Monteverde Reserve, Puntarenas, Costa Rica. [Timm and LaVal \(2018\)](#) reported that *tricolor* was common in the Lower Montane Rain Forest at 1,650 and higher at Monteverde, as well as in the Lower Montane Wet Forest (1,500 to 1,650 m), Premontane Wet Forest (1,300 to 1,500 m), Premontane Moist Forest (700 to 1,300 m), and the Tropical Wet Forest (500 to 700 m) there along the Caribbean slopes of northeastern Costa Rica.

Helpful publications on the roosting habits of *Thyroptera discifera*

Of specimens captured by [Robinson and Lyon \(1901\)](#), fifteen were cataloged as USNM 102923–102928, 105419–105423, 143782–143784. The captures date from 17 and 21 July 1900 at San Julián, Distrito Federal, Venezuela, a settlement at about 10° 37' N, -66° 50' W, at sea level according to [Paynter \(1982\)](#) and located near Caraballeda, ca. 11 km E La Guiara on the Caribbean coast. Most of their labels we've seen state "in plantain" but the field catalog states at least some were caught "under dead leaves of plantain [*sic*]." Eleven of these specimens form the basis of the name *Thyroptera discifera major* Miller, 1931. [Robinson and Lyon \(1901:156\)](#) wrote that one individual, "was placed under an inverted tumbler, to the vertical surface of which it adhered with ease, the vacuum spots under its disks glistening like globules of quicksilver." Concerning the bats caught on 21 July, "The young, although still nursing and clinging to their mothers, were able to fly with ease ... The surface of these disks appears to be constantly moist, so as to insure perfect contact with smooth surfaces ... Young nursing bats cling to their mother's neck or breast with claws and teeth and are carried about as she flies, even when they almost equal her in size and when their weight makes her flight labored

and slow ... the claws are so small and weak as to be almost useless; nevertheless, the young manage to hold on with no risk of falling. The mammae of the female are strap-like, broad and flat, 3 mm wide by 2 mm long. Seizing one in his teeth, the young holds on like a bulldog, dangling by the strength of his jaws alone. One of the young that was brought in hung in this way for twenty minutes, and in all that time made no effort to grasp its mother with its claws."

[Thomas \(1928:257\)](#) reported four males and seven females of *discifera* collected by Hendee at Cumeria [probably = Cumaría and Cumaria according to [Tuttle 1970](#)], Perú (-9° 51' S, -74° 01' W)—for more on this locality see [Pine \(1993\)](#). These bats were "caught roosting in banana leaf." John Edwards Hill of the British Natural History Museum informed Pine "The majority of [these] specimens ... are ... here and are BM(NH) 28-5-2-96-104. Collector's numbers 1290 and 1297 are not in this registration ... all are labelled 'Caught roosting in banana leaf' in accordance with Hendee's collector's notes which are also here, in the archive ... number 1290 has not been registered but is in the collection ... labelled 'Caught with 12 others roosting in banana leaf.'" Hendee's no. 1297 is now cataloged as FMNH 46160 in the Field Museum, its tag bearing the note "Caught with 12 others in banana leaf." This *may* mean that the specimen was one of thirteen bats captured of a group numbering more than thirteen or that there were thirteen bats roosting in the leaf but not all were captured. Only eleven specimens have been accounted for—the same number originally listed by Thomas as having been captured. Unfortunately, the phrase "roosting in banana leaf" is vague. It could refer to something other than a rolled, young banana leaf.

Hill noted "The collection contains a further series 28.7.21.18-25 (4 ♂♂, 4 ♀♀) from Iquitos [-3° 51' S, -71°13' W], Loreto, Peru, 400 ft., also collected by Hendee ... on 9 January 1928. These are marked 'In dry banana leaf' or (28.7.21.22) 'Roosting in dry banana leaf!'" These specimens were reported by [Thomas \(1928\)](#) but no natural history information was provided.

[Wilson \(1978:2\)](#) wrote "The only natural history information recorded for this species is that of [Robinson and Lyon \(1901\)](#) ... One group of 10 was caught by a native with a single sweep of his hand [= "with one grasp of his hand" according to Robinson and Lyon] as they roosted under [and hanging from] a dead banana leaf ... A second group of seven was subsequently captured in the same manner. Both groups contained [adult] males, [adult] females, and flying young. The month of capture for both groups was July." According to Robinson and Lyon, however, the native who caught the seven reported that two or three of the second group had escaped. Earlier, Wilson stated, "Both tightly clustered groups were found by natives who captured them by hand as the bats clung to the under surfaces of dead banana leaves. This roosting habit is quite different from that of *T. tricolor*, which roosts in rolled *Heliconia* leaves" ([Wilson 1976:308, 310](#)). [Robinson and Lyon \(1901:155\)](#), however, specified a "closely grouped" arrangement as having

been observed by the native only for the first group taken—nothing being said about the roosting arrangement of the second group. It seems that the first group at least must not have been roosting single-file as *T. tricolor* does.

[Wilson \(1978:2\)](#) wrote, concerning both *discifera* and *tricolor*, "the colony structure seems similar, with various combinations of sexes and ages represented in a single group." [Kunz \(1982:14, 16\)](#) stated "Virtually nothing is known of the roosting habits of *T. discifera*, but, judging from the similarity of its foot and wrist disks, its roosting habits are probably similar to those of *T. tricolor*."

[Hall \(1981:181\)](#) wrote, "*T. discifera* so far has been found clinging to the under surface of banana leaves. *T. bicolor* roosts in rolled leaves of *Heliconia*." Hall mistakenly used the word *bicolor* here instead of *tricolor*.

[Czaplewski \(1987:25\)](#) wrote that "*Thyroptera discifera* ... unlike *T. tricolor*, roosts in more open situations beneath leaves ..."

[Torres et al. \(1988:434\)](#) were apparently the first to clearly describe *discifera* as roosting in a hanging dead banana leaf. They found a group of 15 *discifera* on 25 January 1985 "in a banana plantation at La Cayoba, ca. 30 km N Magdalena [presumably = Magdalena at -13° 20' S, -64° 08' W at 233 m, as given by [Paynter \(1992\)](#)] on the E bank of the Itonamas River," Prov. Itenez, Depto. Beni, Bolivia. "The bats were inside a dry, furred banana leaf suspended 1.6 m above the ground. The sex ratio of 14 individuals was four males and 10 females. Of 10 specimens studied in detail, three were young with cartilaginous, evenly tapered metacarpo-phalangeal joints and seven were adults with knobby joints." These authors' observations are in keeping with the ones reported in this paper concerning *discifera* in Costa Rica.

[Emmons \(1990:83, 1997:92\)](#) wrote that "*T. discifera* is poorly known, but it has been found roosting beneath open, dead banana leaves."

[Patterson \(1992:18\)](#) reported two specimens of *T. discifera* "secured the same day from the leaves of banana trees" at Aveiros ("= Aveiro; -3° 15' S, -55° 10' W; right bank of lower river [Tapajós] opposite Boim"; p. 6).

[Velazco et al. \(2014:19\)](#) wrote that possibly thyropterids roosting in downward opening roosts may hang head down. They also noted that *tricolor* was the only *Thyroptera* known to roost in partially rolled up *Heliconia* and other green leaves.

[Turcios-Casco et al. \(2020:422\)](#) provided a photo of a dead, shredded, hanging "*Musa × acuminata*" leaf in Costa Rica and which had a colony of *discifera* in it, and a photo of individuals inside. The situation seems to have been in every way similar to some observations given below.

Previously unpublished and new observations on roosting behavior in T. discifera

On 3 November 1983, Toby V. Barrett (*pers. comm.*) captured five *discifera* at Balbina (ca. -1° 50' S, -59° 30' W), Ama-

zonas, Brazil (Field numbers for the bats, an adult female, an immature female, and three immature males, all in fluid, were “morcegos 4–8.” These specimens are currently uncatalogued in the Field Museum). The five were part of a group of no more than 12 attached to the underside of a green leaf of a palm, *Mauritia carana*. The bats were about 12 m above ground and were exposed, visible from the ground, and were collected by cutting down the palm. A frond of *Mauritia carana* consists of radiating strap-like leaflets. The bats were hanging underneath one leaflet along a mid-portion of its length, but some may also have been attached to a corresponding section of an adjacent leaflet (there is some ambiguity in notes and diagrams developed in the course of Pine’s communication with Barrett when the latter’s memory was fresh). Although Barrett wasn’t sure, he thought that each bat was separated from its fellows rather than being in contact with any of them. The collecting locality was characterized by “campina” vegetation and was low-lying but not flooded. The substrate was a wet white sandy soil, possibly a low-humic gley or a quartz sand. The vegetation did not exceed 20 m in height and included many palms (*Mauritia carana*, *Euterpe* sp., and *Desmoncus* sp.) along with numerous *Glycoxylon* (Sapotaceae).

On 30 November 2019, a group of 5 to 7 *discifera* was found in a dry, semi-furled banana leaf at Sylvan Camp and Falls (8.66° N, -83.14° W) in Puntarenas Province, in southwestern Costa Rica by Reid and Jon Hall. Reid had previously observed a bat flying low in this banana plantation and decided to search for bats, focusing on semi-furled, in-a-cone-shape, leaves (as observed by Reid in the painted woolly bat, *Kerivoula picta*, in Thailand). The roost was a cone with the apex at the top closed, and with the lower opening about 1.7 m above ground. The bats were huddled together and roosting in a roughly horizontal manner such that only the backs were visible. One bat, a male, was captured for photos. Unlike most roosting bats, these bats can be removed from the roost without the other bats exiting.

On 20 December 2019, a second observation was made in the same banana patch at Sylvan Camp and Falls, during a bat bioblitz (short duration census of species). Nils Bouillard and Loren Ammerman were present, along with eight students. The banana field was searched by all participants and one roost was found (by Rhianna Connie Dix) at a locality about 100 m from the first roost. All the roost members were caught. There were 7 bats, 6 males and 1 female, and the identification confirmed as *discifera*. This would seem to be an unusual combination sex-wise, and the individuals were not aged. The roost was similar in appearance to the first roost, and at about the same height above ground.

At Cocalito Beach, Drake Bay, near La Paloma Lodge (8° 41' 46" N, -83° 40' 42.8" W), Puntarenas Province, in southwestern Costa Rica, in late November 2020, Gómez and Tracie Stice observed a colony of *discifera* roosting in a dead, brown, vertically hanging portion of a banana leaf,

dangling from the main stalk, and that was partially rolled to form a bugle-like structure with the big open end at the bottom. This roost site was similar to the roosts reported above as at Sylvan Camp and Falls. The cone was lopsided with length 53 cm on one side and 41 cm on the other. The entrance had a diameter of 20 cm and a height of 240 cm from the ground. Stice reports that (*in litt.*) “As we gazed up, into a shadowy fold, we could see more than a half-dozen fluffy rear-ends packed into the leaf.” Thus, their heads were upward, unlike the usual situation in bats but as in *tricolor*. The bats were observed for only one day. On returning a few days later, it was discovered that the leaf had fallen off. Upon searching several other dead leaves in the banana grove on the occasion of the observations made on that single day and on later occasions, no other roost was found.

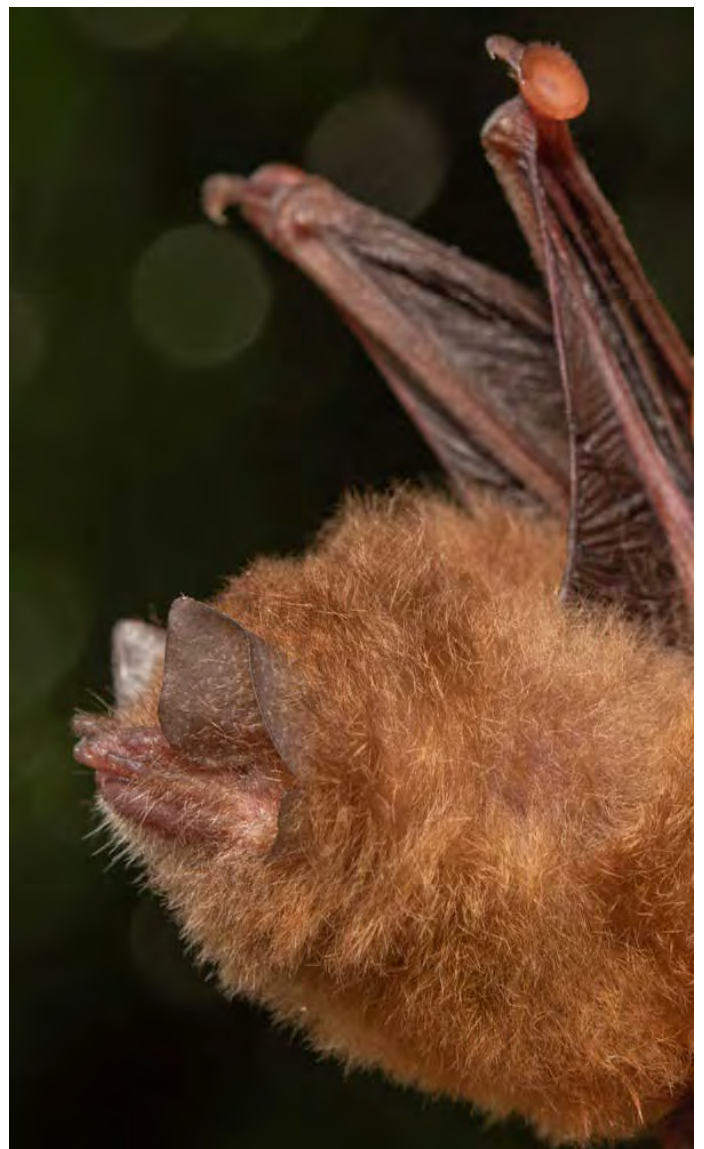


Figure 1. An adult male disk-winged bat, *Thyroptera discifera*, that was observed as part of a roosting colony in a portion of a shredded dead banana leaf and formed a cone-shaped refuge. Note the similar dorsal and ventral coloration and the circular, adhesive disk (seen here at an angle) on the wrist just below the thumb. Photograph taken at Sylvan Camp and Falls, Puntarenas Province, southwestern Costa Rica on 13 January 2020; courtesy of Twan Leenders.

At Sylvan Camp 13 January 2020, a group of students and biologists, led by Reid and Twan Leenders, located *discifera* in the same roost as on 20 December. One bat, a male, was taken out for photos (Figure 1). Since 13 January, the bats have not been located at Sylvan Camp, despite numerous attempts by groups of students and bat enthusiasts. However, on 23 March 2022, Vino de Backer and one other person observed a bat leaving one of the leaf cones in the same banana patch, presumably *discifera*.

Roosting *discifera* were discovered by Gómez at a second site near La Paloma Lodge (8° 41' 40.8" N, -83° 40' 40.5" W) starting on 20 February 2021 and observed for over a month (Figure 2). The bats stayed in the same roost cone except that one individual was observed on 7 March 2021 in a lower cone formed from the same dead leaf and was assumed to have moved there from the colony above.



Figure 2. A “morado” banana (red banana in English, *Musa acuminata*) in a patch that also includes plantains near La Paloma Lodge at Drake Bay, Puntarenas Province, Costa Rica. Portions of shredded dead leaves hanging from the trunk roll back on themselves to create dark, cone-shaped, roosting sites for bats. The top arrow points to where the colony of perhaps nine disk-winged bats, *Thyroptera discifera*, was observed roosting for more than a month during February–March 2021. The lower arrow shows where a single individual was found roosting for a single day. Photograph taken on 7 March 2021 by Gómez.



Figure 3. Two *Thyroptera discifera* roosting in a portion of a dead banana leaf. There had been additional bats in that cone earlier in the evening, but they had already exited. Photograph taken near La Paloma Lodge Drake Bay, Costa Rica on 20 February 2021 by Gómez.

It stayed there for one day. The main conical roost was lopsided with length 50 cm on one side and 40 cm on the other (Figure 3). Height from ground to entrance was 169 cm with roost opening 20 cm wide. The cone that was occupied for one day by a single bat and that was beneath the other cone was of about the same dimensions. Although the bats were not handled, the number occupying the roost varied from only 2 to 5 some days to perhaps 10 or more on others.

Measurements of a roost cone discovered 4 November 2021 at Drake Bay included height 51 cm on longest side, 40 cm on shortest side, and roost opening 20 cm wide; height to entrance from ground 121 cm. The bats did not attempt to fly off when disturbed. A roosting group containing perhaps nine individuals was observed (Figure 4).

The observations of *discifera* using banana leaves as roosts is of interest in that it represents the incorporation of a non-native species for roost sites. The banana plant, also used by *tricolor*, was introduced into the New World tropics within the last 450 years.

Timm has observed *Artibeus jamaicensis* and *Carollia* also roosting in hanging cones of dead banana leaves.

It is clear that, aside from the situation with *tricolor*, there's a good deal that's still unknown concerning the favored roosting sites of the species of *Thyroptera*, and in spite of the new information presented here, that includes *discifera*. There are indications, however, that, in addition to *discifera*, *lavali* and *devivoi* may, at the least, roost occasionally in palms, especially palms of the genus *Mauritia*. The only records of *discifera's* roosting or possibly roosting in association with native Neotropical plants are with their roosting under dead “plantain” leaves, which could mean either *Heliconia* or “cooking banana,” and under a leaf of the palm *Mauritia carana* as recorded here. Otherwise, all certain records are of animals roosting under-



Figure 4. A colony of perhaps 9 *Thyroptera discifera* roosting in a portion of a dead banana leaf. This is the same plant identified in Figure 2 above and the bats were roosting in the top cone shown by the white arrow. Photograph taken near La Paloma Lodge, Drake Bay, Costa Rica on 4 November 2021 by Gómez.

neath dead banana leaves or inside shelters formed from such leaves. In areas where bananas are grown, it may be especially difficult to find *discifera* roosting in association with native plants. The finding of a *wynneae* inside a dead *Cecropia* leaf shelter similar to the dead banana leaf cones described here may indicate one sort of situation that *discifera* may be found in.

[Voss et al. \(2016:16\)](#) noted that no *Thyroptera* had ever been found in any natural roost other than in/on leaves, and that is in keeping with our findings.

Specimens examined of Thyroptera discifera

These include 33 specimens listed by [Pine \(1993:222\)](#) and the 9 listed below. The latter are all in the (U.S.) National Museum of Natural History, Washington, D.C. [USNM]. All skins with skulls unless otherwise indicated: NICARAGUA. Región Autónoma de la Costa Caribe Sur [formerly Zelaya]: Escondido River, 50 mi from Bluefields [See [Genoways and Timm \(2019:484\)](#) concerning this locality], 1 M, 2 F (USNM 51538–51540—in fluid but skull of 51538 removed). PANAMÁ. Chiriquí: 14.5 km NW El Volcán, Finca Santa Clara, 1200–1500 m [El Volcán = “El Hato del Volcán and Lava Flow” at 8° 47' N, -82° 38' W ([Fairchild and Handley 1966](#))], 1 F (USNM 537583—in fluid); Panamá Oeste (formerly Canal Zone): Barro Colorado Is. (PC 21) [= Barro Colorado Island at 9° 09' N, -79° 51' W, [Fairchild and Handley 1966](#)], 1 F (USNM 14799). VENEZUELA. Distrito Federal: San Julian [= San Julián at sea level and at 10° 37' N, -66° 50' W ([Paynter 1982](#))], 1 F [USNM 105419—fluid specimens USNM 102923–102925 from this locality and with sexual composition unrecorded by [Pine \(1993\)](#) are 2 M, 1 F].

Dedication

We dedicate this paper to mammalogist and natural historian par excellence, Dr. Alfred L. Gardner—field biologist first and foremost.

Acknowledgments

L. K. Ammerman, T. V. Barrett, N. Bouillard, S. Graesser, and T. Stice generously shared their observations on roosting in *Thyroptera* with us, contributing significantly to this paper. E. Goldberg, B. A. Morey, V. Musial, L. E. Pine, and D. Shih assisted with the manuscript. J. Esselstyn and two anonymous reviewers made very helpful suggestions, and A. Ferguson and L. Nassef located, examined, and photographed critical specimens for us in the FMNH; their efforts are most appreciated. Staff at La Paloma Lodge helped maintain roosts and potential roosts of *discifera* in place for our studies.

Literature cited

- ALLEN, G. M. 1939. Bats. Harvard University Press. Cambridge, U.S.A.
- ASCORRA, C. F., D. L. GORCHOV, AND F. CORNEJO. 1993. The bats from Jenaro Herrera, Loreto, Peru. *Mammalia* 57:533–552.
- BEZERRA, A. M. R., F. ESCARLATE-TAVARES, AND J. MARINHO-FILHO. 2005. First record of *Thyroptera discifera* (Chiroptera: Thyropteridae) in the Cerrado of central Brazil (Chiroptera: Thyropteridae). *Acta Chiropterologica* 7:165–170.
- BROSSET, A., AND P. CHARLES-DOMINIQUE. 1990. The bats from French Guiana: a taxonomic, faunistic and ecological approach. *Mammalia* 54:509–560.
- CARVALHO, A. L. DE. 1940. Zur Biologie einer Fledermaus (*Thyroptera tricolor* Spix) des Amazonas. *Sitzungsberichte der Gesellschaft Naturforschender Freunde zu Berlin* 1939:249–253.
- COCKRUM, E. L. 1962. Introduction to mammalogy. Ronald Press Company. New York, U.S.A.
- CZAPLEWSKI, N. J. 1987. Deciduous teeth of *Thyroptera tricolor*. *Bat Research News* 28(3-4):23–25.
- DALQUEST, W. W., AND D. W. WALTON. 1970. Diurnal retreats of bats. Pp. 162–187, in *About bats: a chiroptean symposium* (Slaughter B. H., and D. W. Walton, eds.). Southern Methodist University Press. Dallas, U.S.A.
- DE LIMA, I. P., AND R. GREGORIN. 2007. Família Thyropteridae. Pp. 139–143, in *Morcegos do Brasil* (dos Reis, N. R., A. L. Peracchi, W. A. Pedro, and I. P. de Lima, eds.). Biblioteca Central da Universidade Estadual de Londrina. Londrina, Brazil.
- DOBSON, G. E. 1878. Catalogue of the Chiroptera in the collection of the British Museum. Taylor and Francis, London, U.K.
- EISENTRAUT, M. 1975. The bats. Pp. 67–148, in *Mammals III* (Grzimek, B., et al., eds.). Grzimek's animal life encyclopedia 11:1–635.
- EMMONS, L. H. 1990. Neotropical rainforest mammals: A field guide. University of Chicago Press. Chicago, U.S.A.
- EMMONS, L. H. 1997. Neotropical rainforest mammals: A field guide. 2nd ed. University of Chicago Press. Chicago, U.S.A.
- FAIRCHILD, G. B., AND C. O. HANDLEY, JR. 1966. Gazetteer of collecting localities in Panama. Pp. 9–20 in *Ectoparasites of Panama* (Wenzel R. L., and V. J. Tipton, eds.). Field Museum of Natural History. Chicago, U.S.A.

- FINDLEY, J. S., AND D. E. WILSON. 1974. Observations on the Neotropical disk-winged bat, *Thyroptera tricolor* Spix. *Journal of Mammalogy* 55:562–571.
- GARCÍA, F. I., ET AL. 2018. First records of *Thyroptera lavalii* (Chiroptera: Thyropteridae) for the Guiana Shield with an updated distribution of *Thyroptera* species in Venezuela. *Mammalia* 83:219–226.
- GENOWAYS, H. H., AND R. M. TIMM. 2019. The Neotropical variegated squirrel, *Sciurus variegatoides* (Rodentia: Sciuridae) in Nicaragua, with the description of a new subspecies. Pp. 375–409, in *From field to laboratory: A memorial volume in honor of Robert J. Baker* (Bradley, R. D., H. H. Genoways, D. J. Schmidly, and L. C. Bradley, eds.). Special Publications, Museum of Texas Tech University 71:1–957.
- GREGORIN, R., E. GONÇALVES, B. K. LIM, AND M. D. ENGSTROM. 2006. New species of disk-winged bat *Thyroptera* and range extension for *T. discifera*. *Journal of Mammalogy* 87:238–246.
- HALL, E. R. 1981. *The mammals of North America*. 2nd ed. John Wiley and Sons, Inc., New York, U.S.A.
- HILL, J. E., AND J. D. SMITH. 1984. *Bats: a natural history*. British Museum (Natural History), London, U.K.
- HOPPE, J. P. M., V. T. PIMENTA, AND A. D. DITCHFIELD. 2014. First occurrence of the recently described Patricia's disk-winged bat *Thyroptera wynneae* (Chiroptera: Thyropteridae) in Espírito Santo, southeastern Brazil. *Check List* 10:645–647.
- KENNEDY, S. 2002. *Thyroptera discifera*. Animal Diversity Web. https://animaldiversity.org/accounts/Thyroptera_discifera/. Accessed 5 July 2022.
- KRUMBIEGEL, I. 1955. *Biologie der Säugetiere*. Pp. 358–844. 2. Band. Agis-Verlag, Krefeld und Baden-Baden, Germany.
- KUNZ, T. H. 1982. Roosting ecology of bats. Pp. 1–55, in *Ecology of bats* (Kunz, T. H., ed.). Plenum Press. New York, U.S.A.
- LEE, T. E., JR. 2019. Family Thyropteridae (disk-winged bats). Pp. 418–429, in *Handbook of the mammals of the world*. 9. Bats (Wilson, D. E., and R. A. Mittermeier, eds.). Lynx Edicions. Barcelona, Spain.
- MATTHEWS, L. H. 1971. *The life of mammals*. Vol. Two. Universe Books. New York, U.S.A.
- MEDELLÍN, R. A., ET AL. 1986. Notas sobre murciélagos del este de Chiapas. *Southwestern Naturalist* 31:532–535.
- MORALES-MARTÍNEZ, D. M., M. E. RODRÍGUEZ-POSADA, S. G. ACOSTA-MORALES, AND A. M. SILDARRIAGA-GÓMEZ. 2021. First confirmed record of the LaVal's Disk-winged Bat, *Thyroptera lavalii* Pine, 1993 (Chiroptera, Thyropteridae), from Colombia. *Check List* 17:471–478.
- NOWAK, R. M. 1991. *Walker's mammals of the world*. 5th ed. Vol. I. The Johns Hopkins University Press. Baltimore, U.S.A.
- NOWAK, R. M. 1999. *Walker's mammals of the world*. 6th ed. Vol. I. The Johns Hopkins University Press. Baltimore, U.S.A.
- NOWAK, R. M., AND J. L. PARADISO. 1983. *Walker's mammals of the world*. 4th ed. Vol. I. The Johns Hopkins University Press. Baltimore, U.S.A.
- PATTERSON, B. D. 1992. *Mammals in the Royal Natural History Museum, Stockholm, collected in Brazil and Bolivia by A. M. Olalla during 1934–1938*. *Fieldiana: Zoology (New Series)* 66:1–42.
- PAYNTER, R. A., JR. 1982. *Ornithological gazetteer of Venezuela*. Museum of Comparative Zoology, Harvard University. Cambridge, U.S.A.
- PAYNTER, R. A., JR. 1992. *Ornithological gazetteer of Bolivia*, second edition. Museum of Comparative Zoology, Harvard University. Cambridge, U.S.A.
- PAYNTER, R. A., JR., M. A. TRAYLOR, JR., AND B. WINTER. 1975. *Ornithological gazetteer of Bolivia*. Museum of Comparative Zoology, Harvard University. Cambridge, U.S.A.
- PÉREZ, S. G., J. E. LÓPEZ, AND T. J. MCCARTHY. 2012. Five new records of bats for Guatemala, with comments on the checklist of the country. *Chiroptera Neotropical* 18:1106–1110.
- PINE, R. H. 1993. A new species of *Thyroptera* Spix (Mammalia: Chiroptera: Thyropteridae) from the Amazon Basin of north-eastern Perú. *Mammalia* 57:213–225.
- REID, F. A., M. D. ENGSTROM, AND B. K. LIM. 2000. Noteworthy records of bats from Ecuador. *Acta Chiropterologica* 2:37–51.
- ROBINSON, W., AND M. W. LYON, JR. 1901. An annotated list of mammals collected in the vicinity of La Guaira, Venezuela. *Proceedings of the United States National Museum* 24:135–162.
- RODRÍGUEZ-POSADA, M. E., C. FERNÁNDEZ-RODRÍGUEZ, D. M. MORALES-MARTÍNEZ, AND M. C. CALDERÓN-CAPOTE. 2017. First record of De Vivo's disk-winged bat, *Thyroptera devivoi* Gregorin, Gonçalves, Lim, & Engstrom, 2006 (Chiroptera, Thyropteridae), from Colombia, with comments about the record of *Thyroptera lavalii* Pine, 1993 from the country. *Check List* 13:355–361.
- ROSA, R. O. L., ET AL. 2020. Type of shelter and first description of the echolocation call of disk-winged bat (*Thyroptera devivoi*). *Biota Neotropica* 20:e20190821.
- SEMEDO, T. B. F., ET AL. 2020. New records of disk-winged bats *Thyroptera tricolor* Spix, 1823 and *T. devivoi* Gregorin, Gonçalves, Lim & Engstrom, 2006 (Chiroptera: Thyropteridae) for the Brazilian Amazonia and Cerrado. *Boletim do Museu Paraense Emílio Goeldi Ciências Naturais* 15:817–827.
- SIMMONS, N. B., AND R. S. VOSS. 1998. *The mammals of Paracou, French Guiana: a Neotropical lowland rainforest fauna*. Part 1. Bats. *Bulletin of the American Museum of Natural History* 237:1–219.
- SOLARI, S., V. PACHECO, AND E. VIVAR. 1999. New distribution records of Peruvian bats. *Revista Peruana de Biología* 6:152–159.
- SOLARI, S., R. A. VAN DEN BUSSCHE, S. R. HOOFFER, AND B. D. PATTERSON. 2004. Geographic distribution, ecology, and phylogenetic affinities of *Thyroptera lavalii* Pine 1993. *Acta Chiropterologica* 6:293–302.
- TADDEI, V. A. 1988. Morcegos: aspectos ecológicos, econômicos e médico-sanitários, com ênfase para o estado de São Paulo. *Zoo Intertropica*. Instituto de Biociências, Letras e Ciências Exatas, Universidade Estadual Paulista "Júlio de Mesquita Filho" São José do Rio Preto, no 12:1–37.
- TELLO, J. 1979. *Mamíferos de Venezuela*. Fundación La Salle de Ciencias Naturales. Caracas, Venezuela.
- THOMAS, O. 1928. *The Godman-Thomas Expedition to Peru*.—VII. The mammals of the Rio Ucayali. *Annals and Magazine of Natural History, Series 10* 9:249–265.
- TIMM, R. M., AND R. K. LAVAL. 2018. Mammals [of Monteverde]—2000–2018, 17 pp. in *Monteverde: Ecología y conservación de un bosque nuboso tropical* (Wheelwright, N. T., and N. M. Nadkarni, eds.). Bowdoin Scholars' Bookshelf. Book 5.
- TORRES, M. P., T. ROSAS, AND S. I. TIRANTI. 1988. *Thyroptera discifera* (Chiroptera, Thyropteridae) in Bolivia. *Journal of Mammalogy* 69:434–435.
- TSCHAPKA, M., A. P. BROOKE, AND L. T. WASSERTHAL. 2000. *Thyroptera discifera* (Chiroptera: Thyropteridae): a new record for Costa

- Rica and observations on echolocation. *Zeitschrift für Säugetierkunde* 65:193–198.
- TURCIOS-CASCO, M. A., ET AL. 2020. A systematic revision of the bats (Chiroptera) of Honduras: an updated checklist with corroboration of historical specimens and new records. *Zoosystematics and Evolution* 96:411–429.
- TUTTLE, M. D. 1970. Distribution and zoogeography of Peruvian bats, with comments on natural history. *University of Kansas Science Bulletin* 49:45–86.
- VELAZCO, P. M., R. GREGORIN, R. S. VOSS, AND N. SIMMONS. 2014. Extraordinary local diversity of disk-winged bats (Thyropteridae: *Thyroptera*) in northeastern Peru, with description of a new species and comments on roosting behavior. *American Museum Novitates* 3795:1–28.
- VELAZCO, P. M., R. S. VOSS, D. W. FLECK, AND N. B. SIMMONS. 2021. Mammalian diversity and Matses ethnomammalogy in Amazonian Peru. Part 4: Bats. *Bulletin of the American Museum of Natural History* 451:1–199.
- VOSS, R. S., ET AL. 2016. Roosting ecology of Amazonian bats: Evidence for guild structure in hyperdiverse mammalian communities. *American Museum Novitates* 3870:1–43.
- WILSON, D. E. 1976. The subspecies of *Thyroptera discifera* (Lichtenstein and Peters). *Proceedings of the Biological Society of Washington* 89:305–311.
- WILSON, D. E. 1978. *Thyroptera discifera*. *Mammalian Species* 104:1–3.
- WILSON, D. E., AND J. S. FINDLEY. 1977. *Thyroptera tricolor*. *Mammalian Species* 71:1–3.
- YALDEN, D. W., AND P. A. MORRIS. 1975. *The lives of bats*. David & Charles, Newton Abbot, London, U.K.

Associated editor: Jake Esselstyn and Giovani Hernández Canchola

Submitted: July 22, 2022; Reviewed: August 14, 2022

Accepted: October 10, 2022; Published on line: January 27, 2023

Skeletal indicators of locomotor adaptations in shrews

NEAL WOODMAN^{1,2*}¹ U.S. Geological Survey, Eastern Ecological Science Center, Laurel, MD 20708, USA. E-mail: woodmann@si.edu.² Department of Vertebrate Zoology, National Museum of Natural History, Smithsonian Institution, P.O. Box 37012, MRC-108, Washington, DC 20013, USA.*Corresponding author: <https://orcid.org/0000-0003-2689-7373>.

The Soricidae (Mammalia: Eulypotyphla) comprises more than 450 species inhabiting a variety of habitats on five continents. As a family, shrews employ a variety of locomotor modes that incorporate ambulatory, fossorial, aquatic, and scansorial behaviors, illustrating an ability to exploit a variety of natural substrates and their associated resources. In this study, the association of skeletal morphology and three of the dominant locomotor modes in the family—ambulatory, semi-fossorial, and semi-aquatic behaviors—was investigated in up to 52 species of 12 genera representing all three subfamilies of Soricidae. From skeletal measures, 34 morphological indices were calculated, most of which have been used previously to characterize substrate use among shrews, rodents, and other mammals, and analyzed for their individual effectiveness for discriminating the three locomotor modes. To assess their effectiveness in combination, subsets of locomotor indices were analyzed using 1) mean percentile ranks, 2) the first principal component from principal components analysis, and 3) plots and classifications from discriminant function analyses. In general, the three methods effectively identified and grouped the three locomotor modes and identified smaller subsets. Additional analyses were then used to classify the locomotor behaviors of five species whose locomotor modes were unknown or ambiguous. The analyses reinforce and broaden the scope of a previously identified observation of the wide range of grades of morphological variation that may permit an equally diverse range of locomotor abilities among the Soricidae.

La familia Soricidae (Mammalia: Eulypotyphla) comprende más de 450 especies que habitan varios hábitats en los cinco continentes. Como familia, las musarañas emplean una variedad de modos de locomoción que incorporan comportamientos ambulatorios, fosoriales, acuáticos y escansoriales (arborícolas), lo que ilustra su capacidad de explotar diferentes variedades de sustratos y sus recursos asociados. En este estudio, se investigó la asociación de la morfología esquelética y tres de los modos locomotores dominantes en la familia (ambulatorios, semifosoriales y semiacuáticos) en 52 especies de 12 géneros que representan las tres subfamilias de Soricidae. A partir de medidas esqueléticas, se calcularon 34 índices morfológicos, la mayoría de los cuales se han utilizado previamente para caracterizar el uso de sustrato entre musarañas, roedores y otros mamíferos. Se analizaron en cuanto a su eficacia individual para discriminar entre los tres modos de locomoción. Para evaluar su eficacia en combinación, se analizaron subconjuntos de índices locomotores usando 1) intervalos de percentiles medios, 2) el primer componente principal del análisis de componentes principales y 3) gráficas y clasificaciones del análisis de función discriminante. En general, los tres métodos identificaron y agruparon de manera efectiva los tres modos locomotores e identificaron subconjuntos más pequeños. Se usaron análisis adicionales para clasificar los comportamientos locomotores de cinco especies cuyos modos locomotores eran desconocidos o ambiguos. Los análisis refuerzan y amplían el alcance de una observación previamente identificada del intervalo en el grado de variación morfológica que pueden permitir una gama igualmente diversa de habilidades locomotoras entre los Soricidae.

Keywords: Ambulatory; anatomy; aquatic; ecomorphology; fossorial; functional morphology; Soricomorpha; substrate use; terrestrial.

© 2023 Asociación Mexicana de Mastozoología, www.mastozoologiamexicana.org

Introduction

The locomotor behaviors of small, cryptic species of mammals have been studied directly for only a relatively few species. Instead, external and internal morphological characters are typically interpreted to provide insight into how individual species use available substrates, particularly while foraging ([Shimer 1903](#); [Reed 1951](#); [Hildebrand 1985a, 1985b](#); [Hutterer 1985](#); [Price 1993](#); [Samuels and Van Valkenburgh 2008](#); [Hopkins and Davis 2009](#); [Nations et al. 2019](#)).

The typical external morphology of shrews (Mammalia: Eulypotyphla: Soricidae) can be generalized as a long cylindrical body, short legs, and simple feet with five digits used in a plantigrade-to-digitigrade posture, a body plan that is typical of ambulatory small mammals that make use of the ground surface as their primary locomotor substrate ([Hutterer 1985](#); [Churchfield 1990](#); [Woodman and Morgan 2005](#)).

In contrast, the relatively short dense fur, small pinnae, and small eyes of soricids are common mammalian adaptations for fossoriality ([Shimer 1903](#); [Eisenberg 1981](#)). Although ambulation and semi-fossoriality are the two dominant locomotor modes among soricids, members of the family exhibit a range of other locomotor behaviors that assist in exploiting additional substrates. Based on a large sample of 266 species in 20 genera (the recognized diversity of Soricidae at that time), [Hutterer \(1985\)](#) estimated that almost 77 % of soricid species are primarily ambulatory (terrestrial), nearly 11 % are adapted for semi-fossoriality, about 5 % are scansorial, more than 4 % are semi-aquatic, 2 % are anthrophilic, and one species is psammophilic. In a related study based on a similar sample, [Churchfield \(1990:100\)](#) estimated that 82 % of soricid species have a dominantly epigeal foraging mode, 11 % are hypogeal, 5 % are aquatic,

and 3 % are scansorial, illustrating the seemingly close correspondence of primary locomotor mode and resource use.

Previous studies of soricid skeletal adaptations related to locomotor behavior have focused primarily on understanding morphological variation as it relates to ambulation and semi-fossoriality. Ambulatory and semi-fossorial species are distributed among all three subfamilies of the Soricidae (Hutterer 1985; Churchfield 1990), and they exhibit considerable intra-modal variation in morphological characteristics related to substrate use (Woodman and Gaffney 2014; Woodman and Stabile 2015b; Woodman and Wilken 2019). Herein, I explore skeletal variation as it relates to three of the four dominant locomotory modes identified for shrews by testing the discriminatory power of 34 common locomotor indices, mostly calculated from postcranial measurements. Although ambulatory and semi-fossorial locomotor modes occur in all three subfamilies of Soricidae, semi-aquatic modes are confined to a smaller number of species in four genera representing two taxonomic tribes of the subfamily Soricinae: *Chimarrogale*, *Nectogale*, *Neomys*, and *Sorex* (This number increases to five genera if *Crossogale* is recognized as distinct from *Chimarrogale*: Wahab et al. 2020).

Materials and methods

The primary goal of this paper is to better understand skeletal variation among soricids in relation to a traditional, stereotyped classification of locomotor modes. This study of the association between morphology and locomotor behavior is admittedly incomplete, in part because locomotor modes of many soricids are based on inference rather than direct observation. Moreover, phylogeny is a potential primary driver of morphological variation, behavioral variation, or both, but genetic relationships among clades in the Soricidae remain poorly supported at nodes that appear to be crucial to understanding the evolution of locomotor morphology in the family (e. g., He et al. 2015, 2021) and cannot yet be controlled for.

For the purposes of this paper, the word “ambulatory” refers to terrestrial shrews that use the ground surface as their primary locomotor substrate, and lack morphological characters linked to aquatic, fossorial, or scansorial adaptations or behaviors.

In this study, I used measurements and indices from 41 species and subspecies of soricids previously reported by Woodman and Gaffney (2014), Woodman and Stabile (2015a, 2015b), Woodman and Stabile (2015a, 2015b), and Woodman et al. (2019). To these, I added measurements from 180 individuals representing 11 additional species from the mammal collections of the Field Museum of Natural History, Chicago, IL (FMNH), and the National Museum of Natural History, Washington, DC (USNM; Appendix 1). All 52 species were classified *a priori* into one of five locomotor groupings based on reported behaviors and suites of external characteristics: ambulatory ($n = 16$); semi-aquatic ($n = 7$); semi-fossorial ($n = 19$); fossorial ($n = 2$); unknown ($n = 5$). Semi-fossorial and fossorial taxa tend

to have large body size, short tails, small pinnae hidden by the fur, enlarged forefeet, and long, broad foreclaws (Hildebrand 1985b; Hutterer 1985). Semi-aquatic shrews tend to have large body size, long tails that may be laterally flattened or have one or more keels of stiff bristles, long hind feet, and digits and feet fringed with bristles; some have webbed hind feet (Howell 1930; Hutterer 1985). Ambulatory species exhibit the entire range of body size and lack fossorial or aquatic characters. A complete list of species and their *a priori* locomotor classifications is provided in Appendix 2.

Skeletal measurements. To assess relative locomotor adaptations, I followed procedures explained in detail by Woodman and Gaffney (2014; see also Woodman and Stabile 2015b; Woodman and Wilken 2019). Total length and tail length are the standard external measurements recorded from skin tags, and head-and-body length was calculated by subtracting tail length from total length. Forty measurements (Table 1) were obtained from the manus, pes, and long bones of the appendicular skeletons. The scapula, humerus, ulna, radius, femur, and tibiofibula were digitally photographed, and the bones of the manus and pes were digitally x-rayed using a Kevex X-Ray Source 4.1.3 (Kevex, Palo Alto, CA) with Varian Image Viewing and Acquisition 2.0 software (VIVA, Waltham, MA) in the Division of Fishes, National Museum of Natural History, Washington, DC. The resulting digital images from both sources were imported into Adobe Photoshop CS3 Extended 10.0.1 (Adobe Systems, San Jose, CA) and variables (Supplementary Table S1) measured using the Custom Measuring Scale in the Analysis menu following Woodman and Gaffney (2014; see also Woodman and Morgan 2005; Woodman and Stephens 2010; Sargis et al. 2013a, 2013b; Woodman and Stabile 2015b; Woodman and Wilken 2019).

Locomotor indices. Skeletal measurements were used to calculate 34 osteological indices previously employed to characterize locomotor mode and identify potential adaptations for substrate use among soricids (Woodman and Gaffney 2014; Woodman and Stabile 2015a, b; Woodman and Wilken 2019; Woodman et al. 2019), rodents (Price 1993; Samuels and Van Valkenburgh 2008; Elisamburu and De Santis 2011; Nations et al. 2019), and other mammals (Sargis 2002; Hopkins and Davis 2009). To overcome the problem of missing elements, and thereby, missing data, indices (Table 2) were calculated from mean values of variables for each species (Supplementary material Table S1). Abbreviations of measurements used to calculate indices are explained in Table 1.

1. Intermembral index ($IM = [HL+RL]/[FL+TL]$) compares the lengths of the forelimbs and hind limbs (Sargis 2002).

2. Humerofemoral index ($HFI = HL/FL$) represents the length of the humerus as a proportion of the length of the femur (Sargis 2002).

3. Metapodial index ($FOOT = ML/hML$) indicates the relative sizes of the forefeet and hind feet by comparing the length of metacarpal III to that of metatarsal III.

Table 1. Measurements used for calculating locomotor indices (see Woodman and Morgan 2005; Woodman and Stephens 2010; Woodman and Gaffney 2014; Woodman and Stabile 2015a, 2015b; Woodman and Wilken 2019; Woodman *et al.* 2019). See Supplementary material Table S1 for mean measurements.

| | |
|---|--|
| 1. HAR: axis of rotation of the humerus. | 21. UPC: width of proximal crest of the ulna. |
| 2. HL: length of the humerus. | 22. 3CL: length of claw of manus ray III. |
| 3. HDPC: length of deltopectoral crest of the humerus. | 23. 3CW: width of claw of manus ray III. |
| 4. HDW: distal width (epicondylar breadth) of the humerus. | 24. 3DPL: length of distal phalanx of manus ray III. |
| 5. HLD: least mediolateral diameter of humerus. | 25. 3DPW: width of distal phalanx of manus ray III. |
| 6. HTT: length from head of humerus to distal edge of teres tubercle. | 26. 3ML: length of metacarpal of manus ray III. |
| 7. HTRR: breadth of teres tubercle, input lever for rotation of the humerus (measured at a right angle to HAR). | 27. 3MPL: length of middle phalanx of manus ray III. |
| 8. RDW: distal width of radius. | 28. 3MPW: width of middle phalanx of manus ray III. |
| 9. RL: length of radius. | 29. 3PPL: length of proximal phalanx of manus ray III. |
| 10. FDW: distal width (epicondylar breadth) of the femur. | 30. 3PPW: width of proximal phalanx of manus ray III. |
| 11. FL: length of the femur. | 31. 3hCL: length of claw of pes ray III. |
| 12. FLD: least mediolateral diameter of the femur. | 32. 3hCW: width of claw of pes ray III. |
| 13. SL: greatest length of scapula. | 33. 3hDPL: length of distal phalanx of pes ray III. |
| 14. TDA: width of the distal articular surface of the tibiofibula. | 34. 3hDPW: width of distal phalanx of pes ray III. |
| 15. TDW: distal width of the tibiofibula. | 35. 3hML: length of metatarsal of pes ray III. |
| 16. TL: length of the tibiofibula. | 36. 3hMW: width of metacarpal of pes ray III. |
| 17. UFL: functional length (output lever arm) of the ulna. | 37. 3hMPL: length of middle phalanx of pes ray III. |
| 18. UL: total length of the ulna. | 38. 3hMPW: width of middle phalanx of pes ray III. |
| 19. ULD: least mediolateral diameter of the ulna. | 39. 3hPPL: length of proximal phalanx of pes ray III. |
| 20. UOP: length of olecranon process (input lever arm) of the ulna. | 40. 3hPPW: width of proximal phalanx of pes ray III. |

4. Distal phalanx length index ($CLAW = DPL/hDPL$) compares the relative size of distal phalanx III of the manus to distal phalanx III of the pes.

5. Claw length index ($CLI = CL/hCL$) gauges the relative size of claw III of the manus to claw III of the pes.

6. Scapulohumeral index ($SHI = SL/HL$) indicates relative lengths of the scapula and humerus.

7. Brachial index ($BI = RL/HL$) shows the relative proportions of the proximal (humerus) and distal (radius) elements of the forelimb.

8. Shoulder moment index ($SMI = HDPC/HL$) is equivalent to the delto-pectoral crest length index (Sargis 2002). It measures the length of the deltopectoral crest of the humerus relative to the length of the humerus, thereby gauging the size and mechanical advantage of the deltoid and pectoral muscle groups, which are important in the movement, rotation, and counter-rotation of the humerus (Reed 1951).

9. Humeral robustness index ($HRI = HLD/HL$) indicates the robustness of the humerus and its ability to resist bending and shearing stresses.

10. Humeral rotation lever index ($HTI = HTRR/HAR$) shows the relative length of the teres tubercle measured at right angles to the longitudinal axis of rotation of the humerus. The teres tubercle is an elongate process unique to the humerus of talpids, soricids, tachyglossids, and a few early mammals (Reed 1951; Hildebrand 1985b). It serves as the insertion for the latissimus dorsi and teres major muscles and as a lever for rotating the humerus (Reed 1951).

11. Teres tubercle position index ($TTP = HTT/HAR$) represents the relative position of the teres tubercle along the axis of rotation of the humerus (HAR). In more

robust, more fossorially adapted humeri with larger muscle attachment surfaces, the teres tubercle is often more distally positioned (Woodman and Gaffney 2014; Woodman and Stabile 2015).

12. Humeral epicondylar index ($HEB = HDW/HL$) measures the width of the distal humerus relative to the length of the humerus and represents the area available for the origins of muscles involved in flexing, pronating, and supinating the forearm.

13. Radial distal width index ($RDW = RDW/RL$) measures the relative width of the proximal end of the radius, providing a gauge of its robustness and its resistance to stress.

14. Olecranon length index ($OLI = UOP/UFL$) is one of several variations on the index of fossorial ability of Hildebrand (1985a). The ulna acts as a lever that pivots at the trochlear notch, and OLI gauges the force exerted by the triceps brachii muscle on the olecranon process that is transmitted to the functional arm of the ulna. Semi-fossorial and fossorial mammals generally have a longer olecranon process to accommodate a larger triceps brachii, resulting in larger OLI (Reed 1951; Vizcaino and Milne 2002; Samuels and Van Valkenburgh 2008; Woodman and Gaffney 2014).

15. Triceps metacarpal outforce index ($TMO = UOP/[UFL+ML]$), a variant of Hildebrand's (1985a) index of fossorial ability (OLI), gives the length of the olecranon process as a proportion of the functional arm provided by the ulna and metacarpal III together. This index measures the amount of force input on the olecranon process that is transmitted to the tip of the metacarpal of ray III (Price 1993).

16. Triceps claw outforce index ($TCO = UOP/[UFL+ML+PPL+MPL+CL]$) expresses the length of the olecranon process relative to the combined functional lengths of the ulna and the four bones comprising ray III of the

manus. An extension of [Hildebrand's \(1985b\)](#) index of fossorial ability (OLI) and [Price's \(1993\)](#) triceps metacarpal out-force index (TMO), TCO represents the proportion of force input on the olecranon process by the triceps muscle that is transmitted to the tip of the claw of ray III, which is the initial point of contact with the soil.

17. Olecranon crest index (OCI = UPC/UFL) is a measure of the relative length of the olecranon crest on the olecranon process. It serves as the insertion for much of the triceps brachii. OCI is an approximate gauge of muscle size, and, therefore, another measure of the relative input force on the ulna ([Woodman and Gaffney 2014](#)).

18. Ulnar robustness index (URI = ULD/UFL) measures the robustness of the ulna and its ability to resist bending and shearing stresses.

19. Manual distal phalanx index [%DPL = DPL/(ML+PPL+MPL)] is the length of distal phalanx III of the manus relative to the combined length of the proximal three bones of ray III.

20. Manual claw index [%CL = CL/(ML+PPL+MPL)] is the length of claw III of the manus relative to the combined length of the proximal three bones of ray III.

21. Manual claw support index (%CLS = DPL/CL) represents the proportion of claw III of the manus that is supported by the underlying distal phalanx III.

22. Metacarpal width index (MW3 = MW/ML) measures the robustness of metacarpal III of the manus in relation to its length.

23. Phalangeal index (PI = (PPL+MPL)/ML) shows the lengths of the proximal and middle phalanges relative to the metacarpal. This index reflects the degree to which the hand is prehensile and used for grasping (higher index value) versus walking on the ground (lower index value), and it has been used mainly for distinguishing arboreal and scansorial species from ambulatory species. PI varies considerably among rays of an individual, so ray III is typically used for comparisons among species ([Lemelin 1999](#); [Kirk et al. 2008](#)). No arboreal or scansorial shrews were included in the present study.

24. Manus proportions index (MANUS = PPL/ML) measures the size of the proximal phalanx relative to the metacarpal of manual ray III ([Samuels and Van Valkenburgh 2008](#)), and it is the same as [Kirk et al.'s \(2008\)](#) proximal phalangeal index. There appears to be a large phylogenetic component to this index across mammalian orders ([Kirk et al. 2008](#)), but not within rodent families ([Nations et al. 2019](#)), and it is useful for distinguishing arboreally adapted species (larger indices) from ambulatory species (smaller indices).

25. Crural index (CI = TL/FL) measures the relative lengths of proximal (femur) and distal (tibiofibula) long bones of the hind limb.

26. Pes length index (PES = hML/FL) represents the length of metatarsal III relative to femur length and is used to indicate the relative size of the hind foot.

27. Femoral robustness index (FRI = FLD/FL) quantifies the robustness of the femur and its ability to resist bending and shearing stresses.

28. Femoral epicondylar index (FEB = FDW/FL) approximates the area available for the origins of the gastrocnemius and soleus muscles involved in extension of the knee and plantar-flexion of the pes in rodents ([Samuels and Van Valkenburgh 2008](#)). In shrews and talpids, this region is the origin for the plantaris, which flexes the toes, the gastrocnemius, which extends the pes, and the extensor digitorum longus, which extends and adducts the digits and dorsoflexes the foot. It is also the insertion for the caudofemoralis, which retracts the femur, and the adductor longus, which adducts the femur ([Reed 1951](#)).

29. Distal tibiofibular articulation index (DTA = TDA/TDW) measures the width of the articular region for the astragalus between the lateral and medial malleolus relative to the distal width of the tibia ([Woodman and Gaffney 2014](#); [Woodman and Stabile 2015](#)).

30. Pedal distal phalanx index [%hDPL = hDPL/(hML+hPPL+hMPL)] is the length of the distal phalanx of ray III of the pes relative to the combined length of the proximal three bones of that ray.

31. Pedal claw index [%hCL = hCL/(hML+hPPL+hMPL)] is the length of the claw of ray III of the pes relative to the combined length of the proximal three bones of that ray.

32. Pedal claw support index (%hCLS = hDPL/hCL) is the proportion of the claw of ray III of the pes supported by the distal phalanx.

33. Tail length index (%TAIL = tail length/head-and-body length) measures the length of the tail relative to head-and-body length. This index was effective for distinguishing between arboreal and terrestrial species of murid rodents ([Nations et al. 2019](#)).

34. Relative robustness index (RR = HLD/FLD) measures the least breadth of the humerus relative to the least breadth of the femur.

Analyses of locomotor indices. The effectiveness of the 34 indices for distinguishing locomotor mode was initially evaluated by calculating standard univariate statistics (mean, SD, range) in Excel (Microsoft Corporation, Redmond, Washington) for each locomotor group and plotting as box-and-whisker plots (Supplementary material Figure 1). To provide overviews of interspecific variation and to determine relative grades of locomotor modes among taxa, analyses of percentile ranks and multivariate analyses were employed to combine multiple indices. Percentile ranks were calculated for each taxon for each of 23 locomotor indices (IM, HFI, FOOT, CLAW, CLI, SMI, HRI, HTI, TTP, HEB, TCO, OCI, URI, %DPL, %CL, MW3, CI, PES, FEB, %hDPL, %hCL, RR, %TAIL) using the percentile rank calculator at [Statisticshelper.com](https://statisticshelper.com/percentile-rank-calculator/) (<https://statisticshelper.com/percentile-rank-calculator/>). A mean percentile rank was then calculated for each taxon from all indices for which it could be scored. Mean percentile ranks provide a

Table 2. Locomotor indices. See Materials and methods for abbreviations.

| ID | Mode | IM | HFI | FOOT | CLAW | CLI | SHI | BI | SMI | HRI | HTI | TTP | HEB | RDW | OLI | TMO | TCO | OCI | URI | %DPL | %CL | %CLS | MW3 | PI | MANUS | CI | PES | FRI | FEB | DTA | %hDPL | %hCL | %hCLS | %TAIL | RR | No. of indices |
|-------------------------------------|------|----|-----|------|------|-----|-----|-----|-----|-----|-----|-----|-----|-----|-----|-----|-----|-----|-----|------|-----|------|-----|-----|-------|-----|-----|-----|-----|-----|-------|------|-------|-------|-----|----------------|
| <i>Chimarrogale himalayaca</i> | SA | | | 56 | 92 | 88 | 94 | | 45 | 8 | 9 | 42 | 34 | | | | | | | 15 | 24 | 65 | 10 | 93 | 61 | | | | | | | 11 | 17 | 62 | 82 | 19 |
| <i>Nectogale elegans</i> | SA | 68 | 92 | 50 | 89 | 85 | 108 | 109 | 42 | 12 | 13 | 37 | 48 | 15 | 24 | 17 | | | | | | | 64 | 8 | 48 | 182 | 88 | 12 | 35 | 51 | 10 | 16 | 61 | 51 | 93 | 30 |
| <i>Neomys fodiens</i> | SA | 64 | 86 | 56 | 86 | 85 | 103 | 103 | 44 | 9 | 17 | 42 | 41 | 12 | 21 | 15 | 10 | 23 | 5 | 14 | 27 | 53 | 9 | 89 | 55 | 171 | 71 | 9 | 26 | 46 | 11 | 21 | 53 | 71 | 89 | 34 |
| <i>Sorex albibarbis</i> | SA | 68 | 94 | 51 | 85 | 84 | 93 | 105 | 39 | 9 | 13 | 37 | 35 | 11 | 19 | 14 | 10 | 26 | 5 | 14 | 27 | 54 | 9 | 89 | 56 | 184 | 75 | 10 | 28 | 42 | 10 | 19 | 53 | 89 | 86 | 34 |
| <i>Sorex bendirii</i> | SA | 68 | 91 | 53 | 87 | 88 | 99 | 106 | 40 | 10 | 17 | 42 | 38 | 12 | 23 | 17 | 12 | 28 | 6 | 17 | 33 | 51 | 9 | 85 | 53 | 178 | 67 | 10 | 28 | 52 | 12 | 23 | 52 | 82 | 89 | 34 |
| <i>Sorex navigator</i> | SA | 67 | 92 | 51 | 90 | 90 | 95 | 108 | 38 | 9 | 16 | 39 | 37 | 12 | 21 | 15 | 11 | 25 | 5 | 17 | 31 | 54 | 9 | 91 | 57 | 185 | 77 | 10 | 29 | 49 | 11 | 21 | 54 | 96 | 80 | 34 |
| <i>Sorex palustris</i> | SA | 68 | 93 | 55 | 88 | 90 | 96 | 102 | 39 | 8 | 13 | 37 | 34 | 12 | 22 | 15 | 11 | 26 | 5 | 15 | 30 | 50 | 9 | 84 | 52 | 177 | 71 | 10 | 29 | 52 | 11 | 21 | 51 | 79 | 55 | 34 |
| <i>Sorex cinereus</i> | Am | 67 | 90 | 54 | 79 | 86 | 94 | 105 | 38 | 8 | 13 | 35 | 32 | 10 | 20 | 14 | 10 | 23 | 5 | 14 | 27 | 52 | 8 | 90 | 55 | 177 | 64 | 9 | 25 | 55 | 11 | 20 | 57 | 72 | 82 | 34 |
| <i>Sorex hoyi</i> | Am | 67 | 90 | 62 | 89 | 102 | 91 | 102 | 40 | 8 | 15 | 38 | 33 | 11 | 20 | 15 | 10 | 25 | 5 | 15 | 30 | 49 | 8 | 94 | 55 | 169 | 57 | 7 | 26 | 53 | 11 | 20 | 56 | 57 | 94 | 34 |
| <i>Sorex sonomae</i> | Am | 68 | 90 | 59 | 99 | 99 | 97 | 108 | 39 | 10 | 14 | 39 | 37 | 11 | 20 | 15 | 10 | 26 | 6 | 17 | 35 | 49 | 10 | 93 | 55 | 175 | 64 | 9 | 27 | 51 | 12 | 24 | 50 | 73 | 96 | 34 |
| <i>Suncus hututsi</i> | Am | | | 69 | 74 | 81 | | | | | | | | | | | | | | 10 | 19 | 53 | 10 | 86 | 55 | | | | | | 11 | 19 | 59 | 53 | 13 | |
| <i>Cryptotis parvus</i> | Am | 71 | 86 | 67 | 94 | 105 | 100 | 103 | 42 | 9 | 17 | 40 | 36 | 13 | 18 | 13 | 9 | 24 | 6 | 16 | 35 | 44 | 9 | 91 | 54 | 145 | 46 | 8 | 23 | 41 | 13 | 26 | 49 | 28 | 91 | 34 |
| <i>Cryptotis tropicalis</i> | Am | 71 | 87 | 66 | 81 | 105 | 101 | 102 | 45 | 10 | 18 | 42 | 34 | 13 | 17 | 13 | 9 | 24 | 6 | 13 | 30 | 43 | 10 | 98 | 60 | 148 | 48 | 8 | 21 | 43 | 13 | 23 | 55 | 33 | 108 | 34 |
| <i>Cryptotis merriami</i> | Am | 73 | 92 | 68 | 99 | 96 | 94 | 93 | 44 | 9 | 17 | 38 | 35 | 12 | 20 | 15 | 11 | 27 | 7 | 15 | 29 | 52 | 10 | 98 | 62 | 143 | 44 | 10 | 22 | 43 | 12 | 23 | 50 | 41 | 89 | 34 |
| <i>Cryptotis merus</i> | Am | | 88 | 71 | 93 | 98 | 94 | | 46 | 9 | 12 | 37 | 36 | | | | | | | 13 | 30 | 45 | 10 | 92 | 57 | 139 | 45 | 9 | 22 | 41 | 12 | 25 | 48 | 39 | 84 | 26 |
| <i>Cryptotis nigrescens</i> | Am | 73 | 92 | 73 | 89 | 96 | 94 | 87 | 43 | 9 | 18 | 39 | 35 | 13 | 20 | 14 | 10 | 29 | 7 | 16 | 31 | 51 | 12 | 94 | 59 | 136 | 43 | 9 | 22 | 46 | 14 | 26 | 55 | 43 | 88 | 34 |
| <i>Blarinella quadricaudata</i> | Am | 74 | 92 | 71 | 106 | 108 | 100 | 108 | 43 | 10 | 21 | 46 | 39 | 13 | 22 | 16 | 11 | 24 | 6 | 20 | 39 | 51 | 11 | 103 | 60 | 159 | 50 | 10 | 25 | 48 | 15 | 29 | 52 | 52 | 94 | 34 |
| <i>Crocidura olivieri</i> | Am | | 85 | | | | 90 | | 50 | 9 | 8 | 37 | 27 | | | | | | | | | | | | | | 10 | 21 | | | | | 58 | 85 | 11 | |
| <i>Crocidura religiosa</i> | Am | | 91 | | | | 89 | | 52 | 7 | 6 | 36 | 28 | | | | | | | | | | | | | | | 9 | 21 | | | | | 64 | 72 | 11 |
| <i>Crocidura suaveolens</i> | Am | 70 | 87 | | | | 93 | 99 | 47 | 8 | 11 | 35 | 31 | 10 | 18 | | | | | | | | | | | 146 | | 8 | 21 | 32 | | | | 65 | 84 | 19 |
| <i>Myosorex cafer</i> | Am | | 88 | 71 | 100 | 114 | 92 | | 46 | 10 | 15 | 36 | 32 | | | | | | | 19 | 36 | 51 | 11 | 91 | 55 | | 48 | 8 | 21 | | 15 | 26 | 58 | 45 | 101 | 24 |
| <i>Myosorex geata</i> | Am | | 91 | 72 | 93 | 116 | 94 | | 47 | 9 | 16 | 39 | 35 | | | | | | | 21 | 42 | 50 | 13 | 90 | 54 | | 46 | 10 | 23 | | 19 | 31 | 62 | 55 | 84 | 24 |
| <i>Myosorex kilauei</i> | Am | | 90 | 70 | 97 | 117 | 94 | | 46 | 9 | 16 | 40 | 35 | | | | | | | 23 | 46 | 49 | 12 | 88 | 53 | | 47 | 10 | 23 | | 19 | 32 | 59 | 47 | 87 | 24 |
| <i>Blarina brevicauda talpoides</i> | SF | 72 | 88 | 74 | 114 | 130 | 106 | 92 | 45 | 12 | 23 | 45 | 43 | 17 | 32 | 23 | 16 | 35 | 8 | 23 | 43 | 53 | 14 | 89 | 54 | 136 | 41 | 10 | 26 | 52 | 17 | 28 | 60 | 28 | 105 | 34 |
| <i>B. brevicauda jerrychoatei</i> | SF | 73 | 88 | 73 | 108 | 125 | 110 | 92 | 45 | 13 | 24 | 46 | 44 | 17 | 29 | 21 | 14 | 36 | 7 | 23 | 41 | 55 | 14 | 88 | 56 | 133 | 45 | 10 | 25 | 56 | 17 | 27 | 63 | 27 | 110 | 34 |
| <i>Blarina carolinensis</i> | SF | 71 | 86 | 65 | 112 | 126 | 109 | 95 | 48 | 12 | 21 | 45 | 45 | 14 | 28 | 21 | 15 | 30 | 7 | 24 | 45 | 53 | 13 | 98 | 61 | 137 | 41 | 9 | 25 | 34 | 16 | 27 | 59 | 26 | 109 | 34 |
| <i>Blarina hylophaga</i> | SF | | | | | | | | | | | | | | | | | | | | 24 | 45 | 53 | 14 | 93 | 58 | | | | | 17 | 29 | 58 | 27 | 10 | |
| <i>Blarina peninsulae</i> | SF | | | 70 | 117 | 136 | 107 | 94 | 49 | 12 | 19 | 45 | 44 | 15 | 29 | 21 | 14 | 32 | 8 | 23 | 44 | 51 | 13 | 92 | 57 | | | | 44 | 15 | 26 | 60 | 27 | 27 | | |
| <i>Blarina shermani</i> | SF | | | 67 | 106 | 121 | | | | | | | | | | | | | | 21 | 44 | 48 | 13 | 99 | 59 | | | | | | 16 | 28 | 55 | 27 | 13 | |
| <i>B. brevicauda jknoxjonesi</i> | SF | | | | | | | | | | | | | | | | | | | 23 | 46 | 50 | 13 | 89 | 55 | | | | | | 15 | 25 | 61 | 26 | 10 | |
| <i>Cryptotis mexicanus</i> | SF | | | | | | 110 | | 44 | 11 | 25 | 49 | 46 | | | | | | | 26 | 48 | 55 | 15 | 89 | 57 | | | | | | | | 39 | 13 | | |
| <i>Cryptotis phillipsii</i> | SF | | | | | | | | 42 | 11 | 23 | 42 | 42 | | | | | | | | | | | | | | | | | | | | 46 | 6 | | |
| <i>Cryptotis eckerlini</i> | SF | 85 | 61 | 140 | 144 | 113 | 104 | 50 | 12 | 29 | 49 | 55 | 16 | 42 | 29 | 17 | 48 | 11 | | 34 | 63 | 55 | 19 | 105 | 61 | | 45 | 10 | 28 | | 19 | 33 | 56 | 38 | 107 | 31 |
| <i>Cryptotis matsoni</i> | SF | 80 | 60 | 120 | 139 | 121 | | 49 | 13 | 33 | 53 | 55 | | | | | | | | 34 | 59 | 56 | | 94 | 51 | | 46 | 10 | 27 | | 20 | 31 | 65 | 31 | 105 | 23 |
| <i>Cryptotis cavatorculus</i> | SF | | | 69 | 134 | 153 | | 97 | 50 | 12 | 32 | 48 | 52 | 15 | 28 | 21 | 14 | 34 | 7 | 37 | 60 | 61 | 19 | 93 | 60 | | | | | | 22 | 31 | 69 | | 24 | |
| <i>Cryptotis celaque</i> | SF | | 88 | 68 | 123 | 142 | 112 | 107 | 45 | 13 | 31 | 49 | 51 | 14 | 26 | 20 | 13 | 33 | 8 | 33 | 58 | 57 | 17 | 84 | 55 | | 44 | 9 | 28 | | 20 | 31 | 66 | 36 | 119 | 31 |
| <i>Cryptotis mam</i> | SF | 72 | 88 | 64 | 133 | 134 | 113 | 106 | 46 | 13 | 32 | 51 | 52 | 16 | 25 | 19 | 12 | 33 | 7 | 35 | 62 | 56 | 17 | 97 | 60 | 153 | 45 | 9 | 26 | 44 | 20 | 36 | 56 | 38 | 129 | 34 |
| <i>Cryptotis magnimanus</i> | SF | | | | | | | | 43 | 13 | 30 | 50 | 54 | | | | | | | | | | | | | | | | | | | | 31 | | 6 | |
| <i>Cryptotis mcarthyi</i> | SF | | | 64 | 117 | 124 | | | 43 | 13 | 30 | 46 | 51 | | | | | | | 35 | 62 | 57 | 19 | 91 | 59 | | | | | | 22 | 37 | 60 | 30 | 18 | |
| <i>Congosorex phillipsorum</i> | SF | | 90 | 76 | 113 | 107 | 104 | | 50 | 11 | 20 | 39 | 42 | | | | | | | 23 | 39 | 59 | 13 | 87 | 55 | | 46 | 10 | 24 | | 18 | 32 | 56 | 58 | 103 | 24 |
| <i>Myosorex blarina</i> | SF | 72 | 89 | 77 | 107 | 128 | 100 | 96 | 50 | 9 | 19 | 41 | 39 | 15 | 24 | 18 | 12 | 31 | 8 | 28 | 57 | 49 | 15 | 84 | 50 | 142 | 40 | 10 | 24 | 46 | 23 | 39 | 59 | 41 | 81 | 34 |
| <i>Myosorex varius</i> | SF | 70 | 86 | 69 | 109 | 126 | 99 | 103 | 48 | 10 | 18 | 43 | 35 | 13 | 19 | 14 | 10 | 30 | 5 | 27 | 52 | 52 | 14 | 88 | 52 | 149 | 44 | 9 | 22 | 45 | 20 | 34 | 60 | 40 | 99 | 34 |
| <i>Myosorex zinki</i> | SF | | 82 | 75 | 120 | 152 | 108 | | | | | | | | | | | | | | | | | | | | | | | | | | | | | |

convenient means of comparing all 52 taxa on a possible scale from 0 to 100. This permits broader taxonomic coverage, but the lack of data for some taxa means that morphological comparisons are not even across all taxa.

The largest complete dataset (*i. e.*, no missing data) that I could compile included 17 indices (CLI, CLAW, %CL, %DPL, SHI, HEB, HTI, %hCL, FOOT, TTP, SMI, %hDPL, MW3, HRI, PI, MANUS, %TAIL) from six semi-aquatic, 12 ambulatory, 13 semi-fossorial, and two fossorial species. To test the ability of this dataset to discriminate locomotor modes, I carried out both principal components analyses (PCAs) and discriminant function analyses (DFAs) in Past4.03 (Hammer *et al.* 2001).

To investigate the possible locomotory modes of four species (*Cryptotis gracilis*, *C. endersi*, *C. meridensis*, *C. thomasi*) for which locomotory mode was uncertain, I carried out PCA and DFA on a subset of 10 indices (CLAW, CLI, SHI, SMI, HRI, HTI, TTP, %CLS, FEB, %TAIL) from these species and 33 species of known locomotory mode. All four unknown species lacked sufficient data to be included in the 17-variable model (Table S1).

Results

Effectiveness of individual indices. Most of the indices tested individually show identifiable patterns of variation among locomotor modes in soricids, most typically either ascending or descending in mean values from semi-aquatic to ambulatory to semi-fossorial to fossorial. Only a few indices, however, exhibit ranges of variation that are sufficiently constrained to be useful for clearly distinguishing one or more modes.

Individual locomotor indices that appear to be the most reliable for distinguishing semi-aquatic species are PES (*n* =

37 species), FOOT (*n* = 46), CLI (*n* = 44), CI (*n* = 28), %TAIL (*n* = 52), and %hCL (*n* = 45). All but PES have ranges that overlap in value with one or more ambulatory species (Figure 1). The indices CLAW, OCI, MW3, %DPL, %CL, HTI, and CLI are useful for differentiating semi-aquatic and semi-fossorial species.

The ranges of individual locomotor indices of ambulatory species most commonly group with those of semi-aquatic species and often overlap the ranges of some semi-fossorial species. The most reliable indices for distinguishing ambulatory species from semi-aquatic species are PES, FOOT, CLI, FEB (*n* = 41), and %TAIL. The most efficient indices for distinguishing ambulatory species from semi-fossorial species are CLAW (*n* = 43), OCI (*n* = 30), and RDW (*n* = 30), followed by MW3 (*n* = 45), %DPL (*n* = 44), %CL (*n* = 45), HRI (*n* = 49), HTI (*n* = 49), SHI (*n* = 44), CLI, HEB (*n* = 48), TTP (*n* = 49), OLI (*n* = 30), TMO (*n* = 29), and TCO (*n* = 28).

The combination of semi-fossorial and fossorial species can be distinguished most effectively from the other two locomotory modes by OCI and CLAW, followed by MW3, %DPL, CLI, TMO, TCO, HTI, HRI, TTP, RDW, and %CL. The most useful indices for differentiating semi-fossorial from fossorial shrews are %DPL, %CL, %hDPL (*n* = 45), CLI, SMI (*n* = 49), HRI, and HTI, followed by CLAW, HEB, PI (*n* = 45), MANUS (*n* = 46), and %hCL.

1. Intermembral index (IM), which compares the lengths of the forelimbs and hind limbs, typically increases in rodents from semi-aquatic species to ambulatory, to semi-fossorial, and to fossorial species (Samuels and Van Valkenburgh 2008). The index shows a similar pattern with soricids (Supplementary material Figure 1a), indicating a tendency for semi-aquatic species to have relatively longer hind limbs (and/or shorter fore limbs) and for more fossorial forms to have relatively shorter hind limbs. Overlap

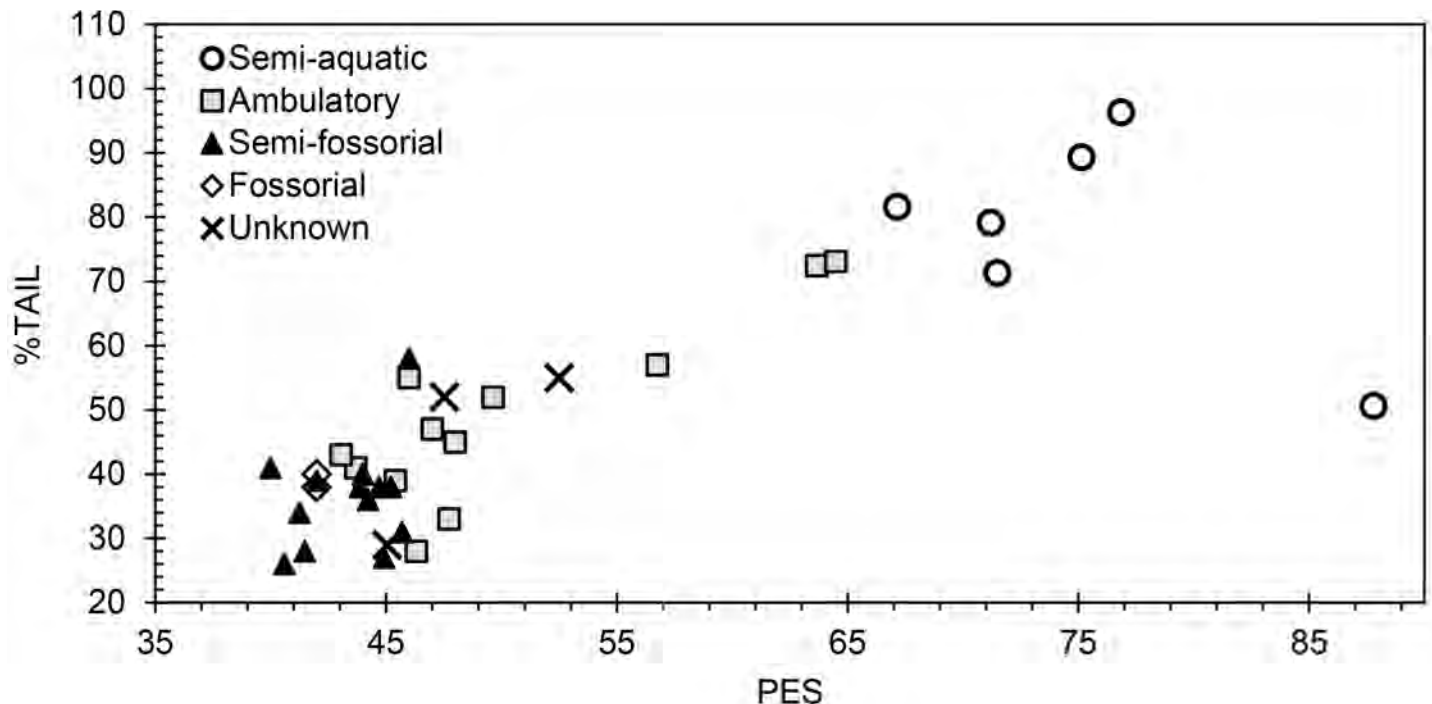


Figure 1. Plot of the indices PES and %TAIL showing separation between semi-aquatic and ambulatory species. The three species of unknown locomotor mode (*C. gracilis*, *C. endersi*, *C. thomasi*) plot with ambulatory and semi-fossorial taxa.

among most locomotor groups, however, limits the usefulness of this index for determining locomotory mode for any one species.

2. Humero-femoral index (HFI) represents the length of the humerus as a proportion of the length of the femur. Among soricids, this index decreases from semi-aquatic species to ambulatory, to semi-fossorial, and to fossorial species (Supplementary material Figure 1b), indicating that semi-aquatic species have a longer humerus relative to the femur, whereas more fossorial species have a shorter humerus. This pattern seems counterintuitive in light of the pattern displayed by the IM, but the longer hind limb in semi-aquatic shrews is a result of their relatively longer tibiofibula (see #25, crural index). Overlap among most locomotor groups makes this index most useful for distinguishing semi-aquatic species from semi-fossorial and fossorial species.

3. Metapodial index (FOOT) indicates the relative sizes of the forefeet and hind feet by comparing the lengths of metacarpal III and metatarsal III. Soricids exhibit an increase in the index from semi-aquatic species to ambulatory to semi-fossorial to fossorial species (Supplementary material Figure 1c), indicating that semi-aquatic species have a relatively longer hind foot (metatarsal III) than other species, particularly the most fossorial species. This index is useful for distinguishing semi-aquatic (low values) and the most fossorial species (high values) from most other species.

4. Distal phalanx length index (CLAW) compares the relative lengths of manual distal phalanx III and pedal distal phalanx III. It increases with increasing fossoriality in rodents (Samuels and Van Valkenburgh 2008), indicating a relatively longer foreclaw than hind claw in more fossorial groups. Among soricids, CLAW clearly distinguishes most semi-fossorial and fossorial species from each other and from other locomotor modes (Supplementary material Figure 1d).

5. Claw length index (CLI) gauges the relative lengths of manual claw III and pedal claw III. CLI increases from semi-aquatic species to ambulatory to semi-fossorial to fossorial species with only minor overlap among locomotor modes (Supplementary material Figure 1e). It clearly distinguishes semi-fossorial and fossorial species from each other and from other locomotor modes, and it also distinguishes semi-aquatic species from most ambulatory species. In this study, only ambulatory *Suncus hututsi* (CLI = 81) and *Sorex cinereus* (86) overlapped with semi-aquatic species, and only semi-fossorial *Congosorex phillipsorum* (107) overlapped with the ambulatory species.

6. Scapulohumeral index (SHI) shows the relative lengths of the scapula and humerus (Supplementary material Figure 1f). This index is typically greater (relatively shorter humerus) for more semi-fossorial and fossorial soricids and lower for ambulatory and aquatic species (Woodman and Gaffney 2014), but its ability to distinguish individual locomotor modes is limited.

7. Brachial index (BI) shows the relative lengths of the humerus and radius. Mean values of this index decrease (relatively shorter radius) among rodents from semi-aquatic to ambulatory to semi-fossorial to fossorial species (Samuels and Van Valkenburgh 2008). The pattern is less apparent among soricids, and ranges of the four modes overlap too extensively for this to be a useful index (Supplementary material Figure 1g).

8. Shoulder moment index (SMI) measures the length of the deltopectoral crest relative to humerus length. In rodents, the index increases from ambulatory to semi-fossorial to semi-aquatic to fossorial species (Samuels and Van Valkenburgh 2008). In contrast, in soricids there is a tendency to increase from semi-aquatic to ambulatory to semi-fossorial to fossorial species (Supplementary material Figure 1h). Extensive overlap among groups makes the index useful only for distinguishing some semi-aquatic and some of the most fossorial species.

9. Humeral robustness index (HRI) indicates the relative thickness of the humerus, which increases (more robust humerus) from ambulatory to semi-fossorial to semi-aquatic to fossorial species among rodents (Samuels and Van Valkenburgh 2008). Among soricids, mean values increase from ambulatory to semi-aquatic to semi-fossorial to fossorial species (Supplementary material Figure 1i). Indices for ambulatory and semi-aquatic species overlap extensively, but most semi-fossorial and fossorial species are distinct. Two exceptions are semi-fossorial *Myosorex blarina* (HRI = 9), which has a lower index than expected, and *Nectogale elegans* (12), which has a higher index than is typical for a semi-aquatic species.

10. Humeral rotation lever index (HTI) shows the relative length of the teres tubercle of the humerus. HTI exhibits little difference between semi-aquatic and ambulatory soricids (Supplementary material Figure 1j), but increases substantially with increased semi-fossoriality and fossoriality (Woodman and Gaffney 2014; Woodman and Stabile 2015). Exceptions are *Myosorex varius* (HTI = 18) and *M. zinki* (18), which have lower index values than is typical for semi-fossorial soricids, and *Blarinella quadricaudata* (21), which has a higher index than expected for an ambulatory species.

11. Teres tubercle position index (TTP) measures the position of the teres tubercle along the humerus. TTP exhibits little difference between semi-aquatic and ambulatory soricids, but increases substantially with increased semi-fossoriality and fossoriality (Supplementary material Figure 1k). Exceptions include *Congosorex phillipsorum* (TTP = 39) and *Myosorex blarina* (41), which have lower index values than expected for semi-fossorial shrews, and ambulatory *Blarinella quadricaudata* (46), with a higher index than expected.

12. Humeral epicondylar index (HEB) is the width of the distal humerus relative to its length. The index typically increases (greater relative width) in mammals with increasing fossoriality (Hildebrand 1985b), and among rodents

HEB increases (broader distal humerus) from ambulatory to semi-fossorial to semi-aquatic to fossorial species (Samuels and Van Valkenburgh 2008). Among soricids, mean values increase from ambulatory to semi-aquatic to semi-fossorial to fossorial species (Supplementary material Figure 1l). There is extensive overlap in index values among ambulatory, semi-aquatic, and semi-fossorial groups, making this index useful for distinguishing only the more fossorial species.

13. Radial distal width index (RDW) measures the relative width of the proximal end of the radius. Ambulatory and semiaquatic soricids tend to have lower RDW (narrower proximal radius), whereas semi-fossorial and fossorial species tend to have larger RDW (Supplementary material Figure 1m). There is extensive overlap, however, between terrestrial and semiaquatic species and between semi-fossorial and fossorial species.

14. Olecranon length index (OLI) represents the relative length of the olecranon process of the ulna. Semi-fossorial and fossorial mammals generally have a longer olecranon process to accommodate a larger triceps brachii, resulting in larger OLI (Reed 1951; Vizcaino and Milne 2002; Samuels and Van Valkenburgh 2008; Woodman and Gaffney 2014). Among rodents, OLI increases from ambulatory to semi-fossorial to semi-aquatic to fossorial species (Samuels and Van Valkenburgh 2008). Among soricids, mean values for this index increase from ambulatory to semi-aquatic to semi-fossorial to fossorial species (Supplementary material Figure 1n). Overlap among groups, however, limits the usefulness of this index for identifying locomotor modes for individual species.

15. Triceps metacarpal outforce index (TMO), like OLI, measures the relative length of the olecranon process. As for OLI, mean values among soricids increase from ambulatory to semi-aquatic to semi-fossorial to fossorial species (Supplementary material Figure 1o), but there is greater separation between semi-aquatic and semi-fossorial species. The one outlier causing overlap between these two groups is semi-fossorial *Myosorex varius* (TMO = 14), which has a lower index than is typical.

16. Triceps claw outforce index (TCO), like OLI and TMO, expresses the relative length of the olecranon process, and it exhibits a pattern similar to those shown by these two indices. Mean values increase from ambulatory to semi-aquatic to semi-fossorial to fossorial species (Supplementary material Figure 1p). Overlap between semi-aquatic and semi-fossorial species is again a result of a lower-than-expected index for semi-fossorial *Myosorex varius* (TMO = 10).

17. Olecranon crest index (OCI) measure of the relative length of the olecranon crest on the olecranon process. Among soricids, there is little difference in TCO between ambulatory and semi-aquatic species, but semi-fossorial and fossorial species exhibit a noticeable increase in the length of the olecranon crest and, therefore, in the index (Supplementary material Figure 1q).

18. Ulnar robustness index (URI) measures the robustness of the ulna. Among rodents, URI increases from ambulatory to semi-fossorial to semi-aquatic to fossorial species (Samuels and Van Valkenburgh 2008). In soricids, this index exhibits a clear pattern of increasing mean values from semi-aquatic to ambulatory to semi-fossorial to fossorial species (Supplementary material Figure 1r). Overlap among groups, however, limits the usefulness of this index for identifying locomotor modes for most individual species. The semi-fossorial *Myosorex varius* (URI = 5), in particular, has a much lower URI than would be predicted.

19. Manual distal phalanx index (%DPL) gauges the length of the manual distal phalanx III. There is little difference in this index between ambulatory and semi-aquatic species, but there are clear distinctions among those two locomotor groups combined, and the semi-fossorial and fossorial species (Supplementary material Figure 1s). The overlap in ranges between ambulatory and semi-fossorial groups results from a lower-than-expected %DPL (and shorter distal phalanx) of semi-fossorial *Blarina shermani* (%DPL = 21) and greater-than-expected index of ambulatory *Myosorex kahaulei* (23).

20. Manual claw index (%CL) is the relative length of manual claw III. Among soricids, %CL shows increases in mean length from semi-aquatic to ambulatory to semi-fossorial to fossorial species (Supplementary material Figure 1t). Overlap between the ranges for semi-aquatic and ambulatory species precludes its use for distinguishing individual species having those locomotor modes. In contrast, the ranges for semi-fossorial and fossorial species are distinct from each other and mostly from the other two modes. Exceptions are greater indices than expected for ambulatory *Myosorex geata* (%CL = 42) and *M. kahaulei* (46) and lower indices than expected for semi-fossorial *Congosorex phillipsorum* (39) and *Blarina brevicauda jerrychoatei* (41).

21. Manual claw support index (%CLS) represents the proportion of manual claw III supported by underlying distal phalanx III. Mean values of this index increase from ambulatory to semifossorial to semi-aquatic to fossorial species (Supplementary material Figure 1u), but the great range of variation among semi-aquatic species and the consequent overlap with other locomotor groups prevents this index from being useful for identifying locomotor modes for individual species.

22. Metacarpal width index (MW3) represents the relative robustness of manual metacarpal III. There is a clear pattern of increase in this index, indicating relatively more robust bones of the manus, from semi-aquatic to ambulatory to semi-fossorial to fossorial species (Supplementary material Figure 1v). Overlaps in values between semi-aquatic and ambulatory species and between semi-fossorial and fossorial species limit the usefulness of this index for distinguishing individual modes, but there is clear separation of most species with adaptations for digging.

23. Phalangeal index (PI) shows the relative lengths of the proximal and middle phalanges of manual ray III. Among the soricid species tested, mean indices increased from fossorial to semi-aquatic species to semi-fossorial species to ambulatory species (Supplementary material Figure 1w). The ranges in values of semi-aquatic, semi-fossorial, and ambulatory species overlap extensively. Fossorial species, however, have extremely low PI.

24. Manus proportions index (MANUS) measures the relative length of the proximal phalanx of manual ray III. Among rodents, mean MANUS increases from fossorial to semi-aquatic to semi-fossorial to ambulatory to arboreal and gliding species (Samuels and Van Valkenburgh 2008; Nations *et al.* 2019). In the Soricidae tested, values for MANUS overlap extensively among semi-aquatic, ambulatory, and semi-fossorial modes (Supplementary material Figure 1x). Fossorial species (*i. e.*, *Surdisorex*) exhibit particularly low MANUS values and are distinct from all other species except semi-aquatic *Nectogale elegans* (MANUS = 48) and semi-fossorial *Myosorex blarina* (50).

25. Crural index (CI) measures the relative lengths of the femur and tibiofibula. Among rodents, this index decreases (longer femur, shorter tibiofibula) with increasing fossoriality, but increases in semi-aquatic species (Samuels and Van Valkenburgh 2008). Although shrews have a relatively longer tibiofibula to begin with, they show a similar pattern, with mean values increasing from fossorial to semi-fossorial to ambulatory to semi-aquatic species (Supplementary material Figure 1y). Overlap in range among fossorial, semi-fossorial, and ambulatory modes is relatively large, making locomotor mode difficult to determine for most individual species. Semi-aquatic species are mostly distinct, overlapping only with *Sorex sonomae* (CI = 175) and *S. cinereus* (177), which have large indices for ambulatory species.

26. Pes length index (PES) represents the relative length of the hind foot. Among rodents, this index increases (relatively longer foot) from fossorial to semi-fossorial to ambulatory to semi-aquatic species (Samuels and Van Valkenburgh 2008). Soricids exhibit a similar pattern, and PES is particularly good for distinguishing semi-aquatic species (Supplementary material Figure 1z).

27. Femoral robustness index (FRI) quantifies the breadth of the femur shaft. Among rodents, this index increases (more robust femur) from ambulatory to semi-fossorial to fossorial to semi-aquatic species (Samuels and Van Valkenburgh 2008). Among rodents, mean values for FRI increase from ambulatory to semi-fossorial to semi-aquatic to fossorial species (Supplementary material Figure 1a). In both groups, there is considerable overlap among locomotor groups, making it difficult to distinguish locomotor mode for a particular species.

28. Femoral epicondylar index (FEB) is the relative distal breadth of the femur. Among rodents, mean FEB is lowest (relatively smaller muscle attachment area) in ambulatory species and is sequentially larger in semi-fossorial, fossorial,

and semi-aquatic species (Samuels and Van Valkenburgh 2008). FEB exhibits a slightly different pattern in soricids, increasing from ambulatory to fossorial to semi-fossorial to semi-aquatic species (Supplementary material Figure 1b). There is extensive overlap among groups, but some ambulatory species and some semi-aquatic species are distinguishable.

29. Distal tibiofibular articulation index (DTA) measures the relative width of the articular region for the astragalus. The ranges of this index overlap extensively among groups, rendering this index essentially useless (Supplementary material Figure 1y).

30. Pedal distal phalanx index (%hDPL) is the relative length of the pedal distal phalanx III. This index shows a clear pattern of increasing (relatively longer distal phalanx) from semi-aquatic to ambulatory to semi-fossorial to fossorial species. Although this index clearly separates semi-fossorial and fossorial locomotor modes, there is considerable overlap between the ranges of semi-aquatic and ambulatory modes (Supplementary material Figure 1d).

31. Pedal claw index (%hCL) is the relative length of the claw of pedal ray III. Like the pedal distal phalanx index (%hDPL), %hCL shows a clear pattern of increasing (longer claw) mean values from semi-aquatic to ambulatory to semi-fossorial to fossorial species (Supplementary material Figure 1e). Although there is greater overlap among the ranges of the four locomotor modes, there is greater separation of some semi-aquatic species from ambulatory species.

32. Pedal claw support index (%hCLS) is the proportion of the claw of pedal ray III supported by the distal phalanx. Values of this index for ambulatory and semi-aquatic species overlap nearly completely but show higher values (relatively greater support) in semi-fossorial and fossorial species (Supplementary material Figure 1z).

33. Tail length index (%TAIL) measures the relative length of the tail. Among shrews, there is a clear pattern of increase in the mean index (greater relative tail length) from fossorial and semi-fossorial species to ambulatory species to semi-aquatic species. There is considerable overlap in ranges among groups, but most semi-aquatic species have longer tails than those in other locomotor modes (Supplementary material Figure 1n). The longer tail of semi-aquatic species may be used to provide added thrust and to prevent yaw rotation while swimming (Fish 1982, 2000). Overlap in the ranges of tail lengths between ambulatory and semi-aquatic shrews is mostly a result of the relatively short tail of semi-aquatic *Nectogale elegans* (%TAIL = 51) and the relatively long tails of ambulatory *Sorex cinereus* (72) and *S. sonomae* (73). As expected (Shimer 1903), semi-fossorial and fossorial species have the shortest tails, with the exception of semi-fossorial *Congosorex phillipsorum*, which has an unexpectedly long tail (58).

34. Relative robustness index (RR) compares the breadths of the humerus and femur. This index exhibits a

progressive increase in mean values (increasing robustness of the humerus) from semi-aquatic to ambulatory to semi-fossorial to fossorial species (Supplementary material Figure 10). There is considerable overlap among ranges of values, making it difficult to distinguish locomotor mode for a particular species.

Mean percentile ranks. A univariate plot of the mean percentile ranks calculated for each of the 52 soricid taxa is shown in Figure 2a. The four locomotor modes mostly form distinct groupings, although there is overlap among some of the modes. As in previous studies of locomotor mode in soricids (Woodman and Gaffney 2014; Woodman and Stabile 2015b; Woodman and Wilken 2019), there is a clear trend of increase in mean percentile rank from ambulatory to semi-fossorial to fossorial taxa. Semi-aquatic species all have relatively low mean ranks, and their range

overlaps that of the lower ranked ambulatory species (*Sorex cinereus*, *Suncus hututsi*, *Sorex hoyi*). There is also overlap of one semi-fossorial species (*Cryptotis phillipsii*) with the highest-ranked ambulatory species. In the latter case, the overlap may result from a lack of data, as *C. phillipsii* is represented by only six indices (Table 3). Among the five species of unknown locomotor mode, four species (*Cryptotis endersi*, *C. gracilis*, *C. meridensis*, *C. monteverdensis*) plot with the higher-ranked ambulatory species. The fifth species (*C. thomasi*) plots between the ambulatory species (and *Cryptotis phillipsii*) and the bulk of the semi-fossorial species, but is more closely allied to the latter.

PCA of locomotor indices. In the PCA of 17 locomotor indices, the first three principal components had high eigenvalues and together accounted for >94% of the variation in the model. Fourteen indices contributed positively

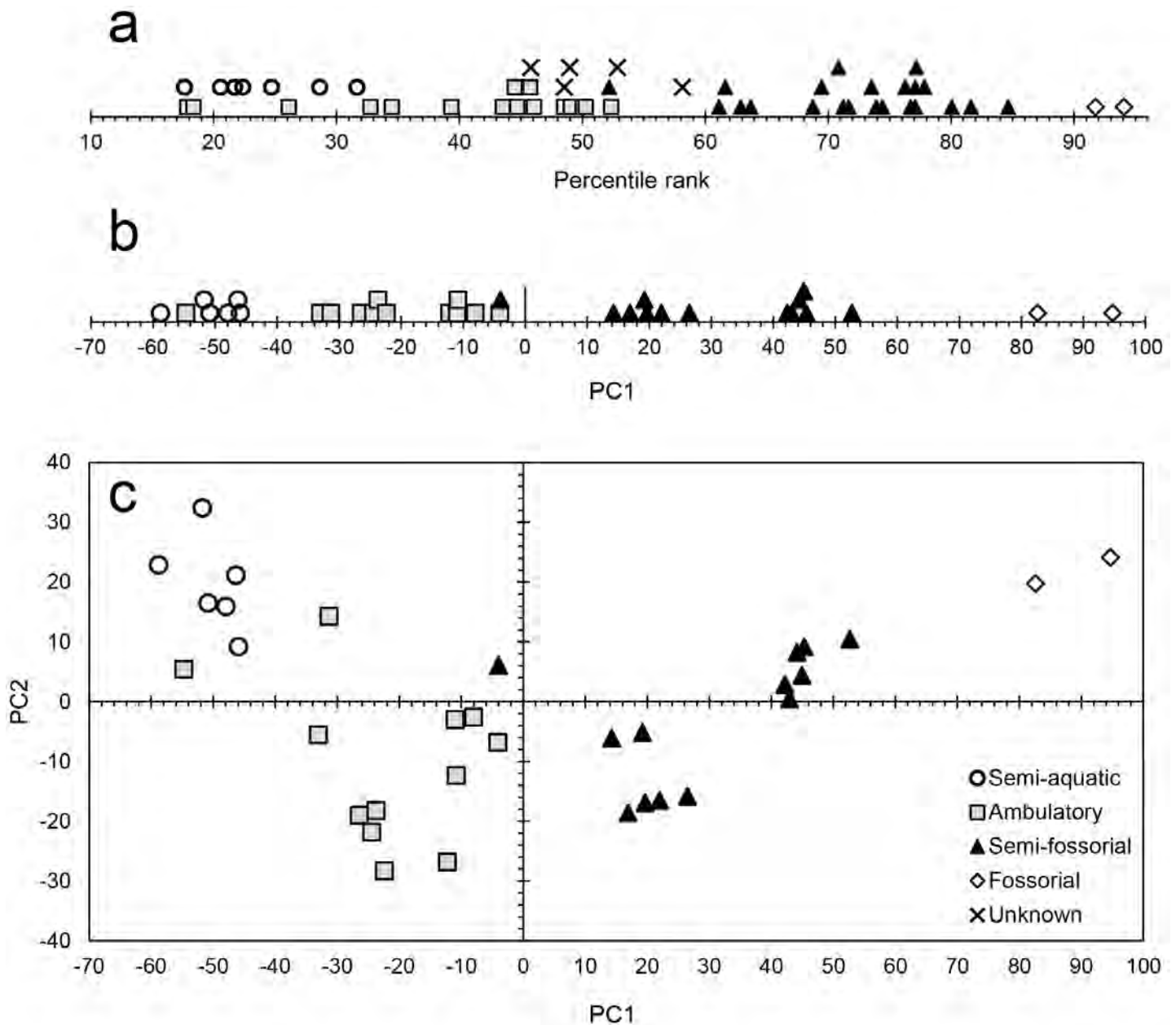


Figure 2. Scaling of locomotory modes: (a) Plot of mean percentile ranks calculated from up to 23 locomotor indices from 52 taxa of soricids, including species of unknown locomotor mode (Table 3). (b) Univariate plot of scores on PC1 (78.8% of variance) from PCA of 17 locomotor indices from 33 taxa (Table 4). (c) Bivariate plot of scores on PC1 and PC2 (12.2% of variance) from a PCA of 17 locomotor indices from 33 taxa (Table 4). Species of unknown locomotor mode were not included in the PCA because of missing data. Key to all symbols is in Figure 2c.

Table 3. Percentile ranks for locomotor indices. See Materials and Methods for abbreviations. Taxa are ordered by increasing mean percentile rank within each *a priori* locomotor mode.

| ID | Mode | IM | HFI | FOOT | CLAW | CLI | SMI | HRI | HTI | TTP | HEB | TCO | OCI | URI | %DPL | %CL | MW3 | CI | PES | FEB | %hDPL | %hCL | RR | %TAIL | Sum of indices | Number of indices | Mean rank | |
|--|------|-----|-----|------|------|-----|-----|-----|-----|-----|-----|-----|-----|-----|------|-----|-----|-----|-----|-----|-------|------|-----|-------|----------------|-------------------|-----------|----|
| <i>Sorex albibarbis</i> | SA | 40 | 3 | 7 | 9 | 5 | 10 | 38 | 19 | 19 | 32 | 33 | 45 | 28 | 14 | 11 | 20 | 7 | 8 | 20 | 5 | 9 | 19 | 4 | 405 | 23 | 18 | |
| <i>Sorex palustris</i> | SA | 40 | 5 | 15 | 19 | 21 | 10 | 13 | 19 | 19 | 19 | 52 | 45 | 28 | 23 | 23 | 20 | 22 | 14 | 8 | 20 | 23 | 3 | 12 | 473 | 23 | 21 | |
| <i>Sorex navigator</i> | SA | 20 | 20 | 7 | 28 | 21 | 4 | 38 | 31 | 33 | 40 | 52 | 28 | 28 | 34 | 27 | 20 | 4 | 6 | 8 | 20 | 23 | 5 | 2 | 499 | 23 | 22 | |
| <i>Chimarrogale himalayaca</i> | SA | - | - | 20 | 30 | 16 | 58 | 13 | 6 | 54 | 19 | - | - | - | 23 | 5 | 34 | - | - | - | 20 | 5 | | 10 | 313 | 14 | 22 | |
| <i>Nectogale elegans</i> | SA | 40 | 20 | 2 | 26 | 9 | 23 | 77 | 19 | 19 | 77 | - | 45 | 28 | - | - | 7 | 11 | 3 | 3 | 5 | 2 | 41 | 37 | 494 | 20 | 25 | |
| <i>Neomys fodiens</i> | SA | 4 | 80 | 20 | 14 | 9 | 48 | 38 | 40 | 54 | 51 | 33 | 10 | 28 | 14 | 11 | 20 | 33 | 14 | 43 | 20 | 23 | 35 | 16 | 658 | 23 | 29 | |
| <i>Sorex bendirii</i> | SA | 40 | 30 | 10 | 16 | 16 | 15 | 54 | 40 | 54 | 43 | 63 | 52 | 52 | 34 | 30 | 20 | 15 | 17 | 20 | 32 | 30 | 35 | 10 | 728 | 23 | 32 | |
| <i>Sorex cinereus</i> | Am | 20 | 48 | 12 | 5 | 12 | 4 | 13 | 19 | 4 | 11 | 33 | 10 | 28 | 14 | 11 | 7 | 22 | 22 | 60 | 20 | 14 | 11 | 10 | 410 | 23 | 18 | |
| <i>Suncus hututsi</i> | Am | - | - | 63 | 2 | 2 | - | - | - | - | - | - | - | - | 2 | 2 | 34 | - | - | - | 20 | 9 | | 31 | 165 | 9 | 18 | |
| <i>Sorex hoyi</i> | Am | 20 | 48 | 32 | 26 | 33 | 15 | 13 | 25 | 23 | 13 | 33 | 28 | 28 | 23 | 23 | 7 | 37 | 25 | 43 | 20 | 14 | 46 | 25 | 600 | 23 | 26 | |
| <i>Crociodura religiosa</i> | Am | - | 30 | - | - | - | 96 | 2 | 2 | 8 | 4 | - | - | - | - | - | - | - | - | 100 | - | - | | 20 | 262 | 8 | 33 | |
| <i>Sorex sonomae</i> | Am | 40 | 48 | 22 | 49 | 30 | 10 | 54 | 21 | 33 | 40 | 33 | 45 | 52 | 34 | 34 | 34 | 30 | 22 | 33 | 32 | 32 | 51 | 14 | 793 | 23 | 34 | |
| <i>Crociodura suaveolens</i> | Am | 56 | 70 | - | - | - | 75 | 13 | 8 | 4 | 6 | - | 3 | 52 | - | - | - | 67 | - | 100 | - | - | | 18 | 472 | 12 | 39 | |
| <i>Cryptotis merus</i> | Am | - | 65 | 80 | 37 | 28 | 69 | 38 | 10 | 19 | 36 | - | - | - | 7 | 23 | 34 | 81 | 67 | 88 | 32 | 36 | 16 | 61 | 827 | 19 | 44 | |
| <i>Cryptotis parvus</i> | Am | 68 | 80 | 51 | 40 | 40 | 23 | 38 | 40 | 38 | 36 | 7 | 21 | 52 | 27 | 34 | 20 | 70 | 53 | 78 | 36 | 45 | 38 | 88 | 1023 | 23 | 44 | |
| <i>Cryptotis tropicalis</i> | Am | 68 | 70 | 44 | 7 | 40 | 58 | 54 | 52 | 54 | 19 | 7 | 21 | 52 | 7 | 23 | 34 | 59 | 39 | 100 | 36 | 30 | 78 | 76 | 1028 | 23 | 45 | |
| <i>Crociodura olivieri</i> | Am | - | 85 | - | - | - | 94 | 38 | 4 | 19 | 2 | - | - | - | - | - | - | - | - | 100 | - | - | | 24 | 366 | 8 | 46 | |
| <i>Cryptotis merriami</i> | Am | 92 | 20 | 56 | 49 | 26 | 48 | 38 | 40 | 23 | 32 | 52 | 48 | 76 | 23 | 14 | 34 | 74 | 78 | 88 | 32 | 30 | 35 | 51 | 1059 | 23 | 46 | |
| <i>Myosorex cafer</i> | Am | - | 65 | 80 | 51 | 51 | 69 | 54 | 25 | 8 | 11 | - | - | - | 41 | 36 | 41 | - | 39 | 100 | 50 | 45 | 62 | 45 | 873 | 18 | 49 | |
| <i>Cryptotis nigrescens</i> | Am | 92 | 20 | 88 | 26 | 26 | 33 | 38 | 52 | 33 | 32 | 33 | 55 | 76 | 27 | 27 | 50 | 93 | 81 | 88 | 39 | 45 | 27 | 47 | 1128 | 23 | 49 | |
| <i>Myosorex geata</i> | Am | - | 30 | 83 | 37 | 53 | 75 | 38 | 31 | 33 | 32 | - | - | - | 50 | 52 | 64 | - | 53 | 78 | 73 | 73 | 16 | 29 | 900 | 18 | 50 | |
| <i>Blarinella quadricaudata</i> | Am | 96 | 20 | 80 | 56 | 44 | 33 | 54 | 67 | 77 | 47 | 52 | 21 | 52 | 43 | 43 | 41 | 44 | 31 | 60 | 50 | 64 | 46 | 35 | 1156 | 23 | 50 | |
| <i>Myosorex kahaulei</i> | Am | - | 48 | 71 | 42 | 56 | 69 | 38 | 31 | 38 | 32 | - | - | - | 64 | 68 | 50 | - | 42 | 78 | 73 | 77 | 24 | 41 | 942 | 18 | 52 | |
| <i>Cryptotis phillipsii</i> | SF | - | - | - | - | - | 23 | 65 | 71 | 54 | 57 | - | - | - | - | - | - | - | - | - | - | - | - | | 43 | 313 | 6 | 52 |
| <i>Blarina shermani</i> | SF | - | - | 51 | 56 | 58 | - | - | - | - | - | - | - | - | 50 | 59 | 64 | - | - | - | 57 | 59 | | 96 | 550 | 9 | 61 | |
| <i>Congosorex phillipsorum</i> | SF | - | 48 | 95 | 67 | 42 | 94 | 65 | 79 | 33 | 57 | - | - | - | 64 | 43 | 64 | - | 53 | 70 | 66 | 77 | 68 | 24 | 1109 | 18 | 62 | |
| <i>Myosorex varius</i> | SF | 56 | 80 | 63 | 63 | 67 | 79 | 54 | 52 | 56 | 32 | 33 | 62 | 28 | 73 | 73 | 73 | 56 | 78 | 88 | 82 | 86 | 57 | 55 | 1446 | 23 | 63 | |
| <i>Blarina brevicauda jknoxjonesi</i> | SF | - | - | - | - | - | - | - | - | - | - | - | - | - | 64 | 68 | 64 | - | - | - | 50 | 36 | | 100 | 382 | 6 | 64 | |
| <i>Myosorex blarina</i> | SF | 80 | 50 | 98 | 58 | 70 | 94 | 38 | 56 | 42 | 47 | 63 | 66 | 90 | 75 | 75 | 77 | 78 | 100 | 70 | 95 | 100 | 8 | 51 | 1581 | 23 | 69 | |
| <i>Cryptotis mexicanus</i> | SF | - | - | - | - | - | 48 | 65 | 77 | 85 | 72 | - | - | - | 70 | 70 | 77 | - | - | - | - | - | | 61 | 625 | 9 | 69 | |
| <i>Blarina peninsulae</i> | SF | - | - | 71 | 77 | 79 | 83 | 77 | 56 | 67 | 68 | 89 | 69 | 90 | 64 | 59 | 64 | - | - | - | 50 | 45 | | 96 | 1204 | 17 | 71 | |
| <i>Blarina carolinensis</i> | SF | 68 | 80 | 41 | 65 | 67 | 79 | 77 | 67 | 67 | 70 | 93 | 62 | 76 | 68 | 64 | 64 | 85 | 97 | 60 | 57 | 50 | 81 | 100 | 1638 | 23 | 71 | |
| <i>Blarina hylophaga</i> | SF | - | - | - | - | - | - | - | - | - | - | - | - | - | 68 | 64 | 73 | - | - | - | 65 | 64 | | 96 | 430 | 6 | 72 | |
| <i>Blarina brevicauda talpoides</i> | SF | 80 | 65 | 90 | 70 | 72 | 58 | 77 | 71 | 67 | 62 | 96 | 83 | 90 | 64 | 55 | 73 | 93 | 97 | 43 | 65 | 59 | 73 | 88 | 1691 | 23 | 74 | |
| <i>Blarina brevicauda jerrychoatei</i> | SF | 92 | 65 | 88 | 60 | 63 | 58 | 94 | 75 | 77 | 68 | 89 | 86 | 76 | 64 | 50 | 73 | 100 | 67 | 60 | 65 | 50 | 84 | 96 | 1700 | 23 | 74 | |
| <i>Cryptotis celaque</i> | SF | - | 65 | 56 | 84 | 86 | 58 | 94 | 85 | 85 | 81 | 67 | 76 | 90 | 80 | 58 | 86 | | 78 | 20 | 82 | 73 | 86 | 72 | 1562 | 21 | 74 | |
| <i>Cryptotis oreoryctes</i> | SF | 20 | 90 | 32 | 88 | 81 | 48 | 94 | 96 | 96 | 89 | 89 | 90 | 76 | 93 | 95 | 86 | 48 | 78 | 33 | 86 | 86 | 89 | 71 | 1754 | 23 | 76 | |
| <i>Cryptotis mam</i> | SF | 80 | 65 | 39 | 91 | 77 | 69 | 94 | 90 | 96 | 85 | 63 | 76 | 76 | 89 | 89 | 86 | 52 | 67 | 43 | 82 | 89 | 95 | 71 | 1764 | 23 | 77 | |
| <i>Cryptotis matsoni</i> | SF | - | 100 | 24 | 81 | 84 | 83 | 94 | 94 | 98 | 94 | - | - | - | 84 | 80 | - | - | 53 | 33 | 82 | 73 | 73 | 80 | 1310 | 17 | 77 | |
| <i>Cryptotis mcarthyi</i> | SF | - | - | 39 | 77 | 60 | 33 | 94 | 83 | 77 | 81 | - | - | - | 89 | 89 | 93 | - | - | - | 91 | 91 | | 82 | 1079 | 14 | 77 | |
| <i>Myosorex zinki</i> | SF | - | 93 | 93 | 81 | 93 | 75 | 94 | 52 | 54 | 74 | - | - | - | 77 | 84 | 80 | - | 89 | 60 | 86 | 86 | 57 | 61 | 1389 | 18 | 77 | |
| <i>Cryptotis magnimanus</i> | SF | - | - | - | - | - | 33 | 94 | 83 | 88 | 89 | - | - | - | - | - | - | - | - | - | - | - | | 80 | 467 | 6 | 78 | |
| <i>Cryptotis eckerlini</i> | SF | - | 85 | 27 | 95 | 88 | 94 | 77 | 79 | 85 | 94 | 100 | 100 | 100 | 84 | 93 | 93 | - | 67 | 20 | 73 | 80 | 76 | 71 | 1681 | 21 | 80 | |
| <i>Cryptotis lacertus</i> | SF | 100 | 20 | 51 | 86 | 74 | 48 | 96 | 94 | 96 | 98 | 89 | 97 | 97 | 93 | 93 | 100 | 63 | 97 | 20 | 95 | 95 | 100 | 75 | 1877 | 23 | 82 | |
| <i>Cryptotis cavatorculus</i> | SF | - | - | 63 | 93 | 95 | 94 | 77 | 90 | 79 | 85 | 89 | 79 | 76 | 95 | 82 | 93 | - | - | - | 91 | 73 | | | 1354 | 16 | 85 | |
| <i>Surdisorex norae</i> | F | 56 | 98 | 80 | 98 | 98 | 100 | 100 | 98 | 96 | 100 | 89 | 97 | 97 | 100 | 100 | 100 | 96 | 89 | 60 | 100 | 95 | 92 | 71 | 2110 | 23 | 92 | |
| <i>Surdisorex polulus</i> | F | - | 90 | 100 | 100 | 100 | 100 | 100 | 100 | 100 | 98 | - | - | - | 98 | 98 | 100 | - | 89 | 70 | 98 | 100 | 97 | 55 | 1693 | 18 | 94 | |
| <i>Cryptotis andersi</i> | UN | - | 48 | - | 77 | 91 | 23 | 38 | 79 | 42 | 57 | - | - | - | - | - | - | - | 39 | 33 | 32 | 23 | 24 | 35 | 641 | 14 | 46 | |
| <i>Cryptotis gracilis</i> | UN | - | 30 | 34 | 37 | 40 | 69 | 65 | 67 | 77 | 68 | - | - | - | 50 | 50 | 50 | 30 | 28 | 33 | 57 | 59 | 49 | 29 | 922 | 19 | 49 | |
| <i>Cryptotis meridensis</i> | UN | 44 | 48 | - | 14 | 47 | 48 | 54 | 52 | 67 | 49 | 52 | 45 | 52 | 41 | 39 | 41 | 41 | | 60 | - | - | 65 | 71 | 930 | 19 | 49 | |
| <i>Cryptotis monteverdensis</i> | UN | - | - | - | - | - | 33 | 54 | 52 | 77 | 62 | - | - | - | - | - | - | - | - | - | - | - | | 39 | 317 | 6 | 53 | |
| <i>Cryptotis thomasi</i> | UN | - | 48 | 71 | 49 | 49 | 48 | 65 | 75 | 58 | - | - | - | - | 41 | 45 | 50 | - | 67 | 70 | 50 | 59 | 59 | 84 | 988 | 17 | 58 | |

to the first principal component (PC1), which alone represented nearly 79 % of the variation. PC1 was most strongly influenced by four variables: CLI, CLAW, %CL, and negatively weighted %TAIL (Table 4). The second principal component (PC2) represented %TAIL and constituted about 12 % of variation. The third principal component (PC3), accounting for <4 % of the variation, was most influenced by PI, SHI, and negatively weighted FOOT.

In a plot of factor scores on PC1 (Figure 2b), *a priori* locomotory groups are mostly separated along PC1, with semi-aquatic species having the lowest scores, and ambulatory, semi-fossorial, and fossorial groups having increasingly greater scores, respectively. Ambulatory species exhibit two distinct clusters along this axis. The ambulatory group with the lower scores includes species of *Sorex* and *Cryptotis*, and the group with the larger scores includes *Cryptotis parvus*, *Blarinella quadricaudata*, and species of *Myosorex*. There are also two clusters of semi-fossorial species. The group with the lower scores includes species of *Myosorex* and *Blarina*, and that with the larger scores is comprised of *Myosorex zinki* and species of *Cryptotis*. The bimodal patterns within the ambulatory and semi-fossorial groups indicate that species in different genera have somewhat different suites of characters associated with a particular locomotor mode (Woodman and Wilken 2019).

One exception to the general pattern is ambulatory *Sorex cinereus*, which plotted with semi-aquatic species. Its low score on PC1 resulted from its low CLI and %CL (relatively short foreclaw) and high %TAIL (relatively long tail). Another exception is semi-fossorial *Congosorex phillipsorum*, which plotted with the ambulatory species. Its low score also resulted from its low CLI, %CL, and %DPL (short foreclaw and distal phalanx relative to other semi-fossorial species) and high %TAIL (long tail). The unique combination of ambulatory and semi-fossorial traits in *C. phillipsorum* previously was discussed in detail in Woodman and Stabile (2015b).

In a plot of factor scores on PC1 and PC2 (Figure 2c), the second factor axis separates fossorial species and most semi-aquatic species from ambulatory and semi-fossorial species. It also separates subgroupings of semi-fossorial shrews with semi-fossorial *Cryptotis* and *Myosorex zinki* plotting along the positive portion of PC2, whereas *Blarina* and other semi-fossorial *Myosorex* plot along the negative part of the axis.

The third factor axis (not shown) provides no discrimination among the *a priori* locomotor groupings. Within the ambulatory group, however, the low scores of the three species of *Myosorex* separate them from ambulatory taxa in other genera. Within the semi-fossorial group, PC3 separates three subgroupings that consist of three species of *Myosorex* (low scores); most taxa of *Blarina*, *Congosorex phillipsorum*, and *Cryptotis celaque* (intermediate scores); and *Blarina carolinensis* and four species of *Cryptotis*.

DFA of locomotor indices. Plots of scores from the DFA of 17 locomotor indices show clear separation of the four

Table 4. Variable loadings and taxon scores from a PCA of 17 locomotor indices from 33 taxa of soricids (Figure 2b, 2c).

| Variable loadings | | | |
|-------------------|----------|---------|--------|
| Variable | PC 1 | PC 2 | PC 3 |
| CLI | 0.575 | 0.030 | -0.359 |
| CLAW | 0.459 | 0.270 | 0.188 |
| %CL | 0.353 | 0.203 | -0.103 |
| %DPL | 0.212 | 0.170 | 0.001 |
| SHI | 0.182 | 0.084 | 0.382 |
| HEB | 0.180 | 0.158 | 0.297 |
| HTI | 0.163 | 0.095 | 0.239 |
| %hCL | 0.135 | 0.014 | -0.121 |
| FOOT | 0.120 | -0.253 | -0.359 |
| TTP | 0.108 | 0.068 | 0.204 |
| SMI | 0.106 | 0.011 | -0.168 |
| %hDPL | 0.104 | 0.027 | -0.112 |
| MW3 | 0.086 | 0.036 | 0.026 |
| HRI | 0.054 | 0.028 | 0.038 |
| PI | -0.009 | -0.098 | 0.422 |
| MANUS | -0.018 | -0.055 | 0.301 |
| %TAIL | -0.347 | 0.855 | -0.192 |
| Eigenvalue | 1682.600 | 260.054 | 80.536 |
| % variance | 78.801 | 12.179 | 3.772 |

| Taxon scores on PC1 | | |
|-----------------------------------|------|---------|
| Taxon | Mode | PC 1 |
| <i>Sorex albibarbis</i> | SA | -58.812 |
| <i>Sorex navigator</i> | SA | -51.795 |
| <i>Chimarrogale himalayaca</i> | SA | -50.854 |
| <i>Sorex palustris</i> | SA | -47.955 |
| <i>Sorex bendirii</i> | SA | -46.349 |
| <i>Neomys fodiens</i> | SA | -45.918 |
| <i>Sorex cinereus</i> | Am | -54.719 |
| <i>Sorex hoyi</i> | Am | -33.033 |
| <i>Sorex sonomae</i> | Am | -31.319 |
| <i>Cryptotis nigrescens</i> | Am | -26.47 |
| <i>Cryptotis merus</i> | Am | -24.479 |
| <i>Cryptotis merriami</i> | Am | -23.749 |
| <i>Cryptotis tropicalis</i> | Am | -22.373 |
| <i>Cryptotis parvus</i> | Am | -12.229 |
| <i>Myosorex geata</i> | Am | -10.973 |
| <i>Myosorex cafer</i> | Am | -10.832 |
| <i>Blarinella quadricaudata</i> | Am | -8.0403 |
| <i>Myosorex kahaulei</i> | Am | -4.0992 |
| <i>Congosorex phillipsorum</i> | SF | -3.981 |
| <i>Myosorex varius</i> | SF | 14.246 |
| <i>B. brevicauda jerrychoatei</i> | SF | 16.908 |
| <i>Myosorex blarina</i> | SF | 19.219 |
| <i>Blarina carolinensis</i> | SF | 19.619 |
| <i>B. brevicauda talpoides</i> | SF | 21.945 |
| <i>Blarina peninsulae</i> | SF | 26.478 |
| <i>Cryptotis celaque</i> | SF | 42.205 |
| <i>Myosorex zinki</i> | SF | 42.961 |
| <i>Cryptotis mam</i> | SF | 44.161 |
| <i>Cryptotis lacertosus</i> | SF | 44.912 |
| <i>Cryptotis oreoryctes</i> | SF | 45.322 |
| <i>Cryptotis eckerlini</i> | SF | 52.677 |
| <i>Surdisorex norae</i> | F | 82.629 |
| <i>Surdisorex polulus</i> | F | 94.698 |

locomotor groups along combinations of the first three canonical variates (Table 5; Figure 3). Fossorial species are strongly separated along CV1, and the other three locomotor groups are separated from each other along CV2 (Figure 3a). Semi-aquatic and semi-fossorial species overlap along CV3, but are separated from both ambulatory and fossorial species (Figure 3b).

The *post hoc* classification matrix indicates that 100 % of taxa were correctly classified into their *a priori* locomotor groups by the DFA (Table 5). In the jack-knifed classification, five species were misclassified as belonging to a locomotor mode other than their *a priori* mode. Ambulatory *Sorex cinereus* and *Cryptotis tropicalis* were both misclassified as being semi-aquatic; ambulatory *Myosorex cafer* was misclas-

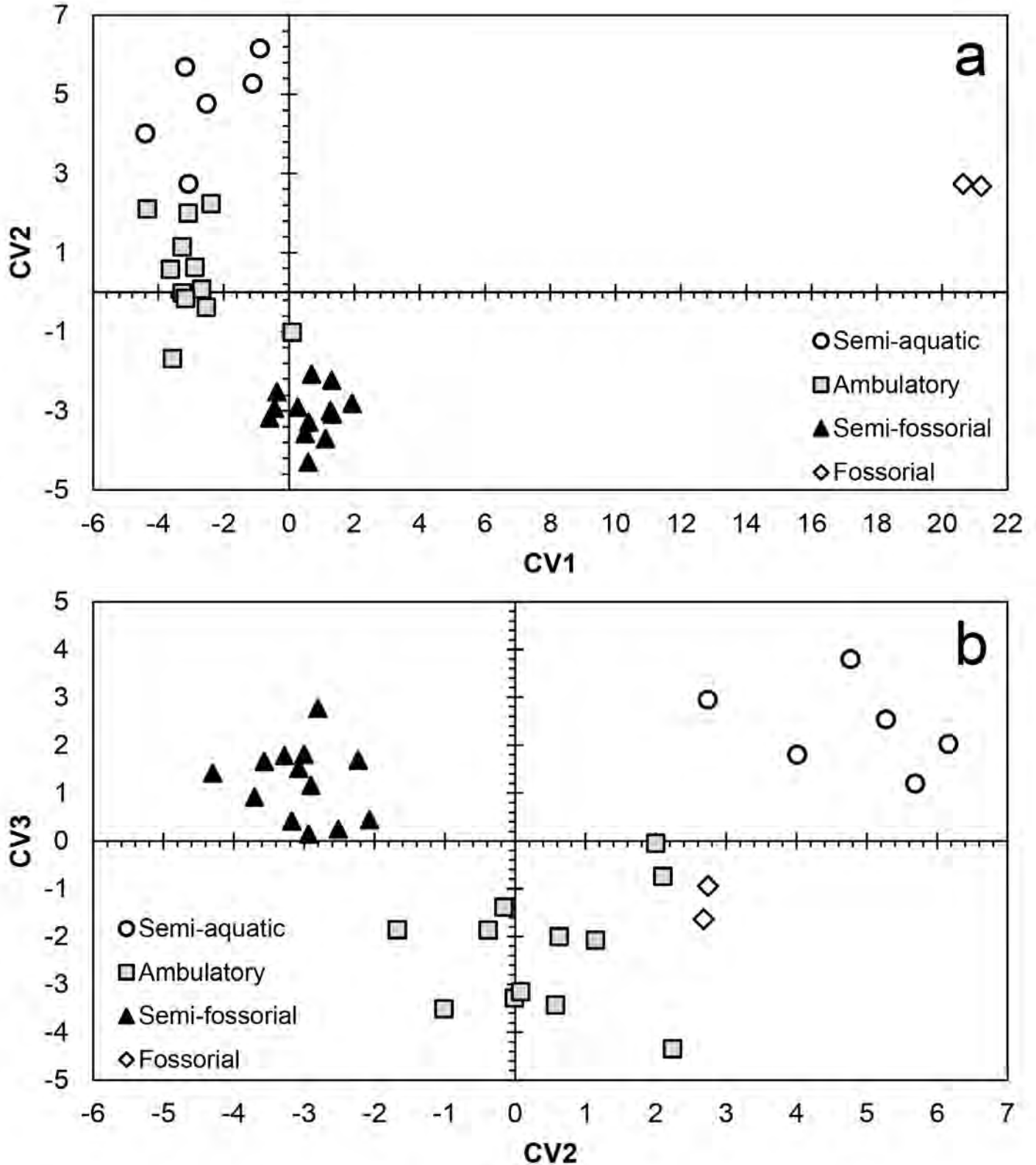


Figure 3. Plots of scores a) on CV1 and CV2 and b) on CV2 and CV3 from a DFA of 17 locomotor indices from 33 species (Table 5).

Table 5. Variable loadings of 17 locomotor indices and classification matrix. A and B classification matrices from a DFA of 17 locomotor indices from 33 taxa of soricids (Figure 3).

| Variable | Variable loadings | | | Axis 3 |
|----------|-------------------|--------|--------|--------|
| | Axis 1 | Axis 2 | Axis 3 | |
| %hCL | -1.139 | -0.730 | 0.569 | |
| MANUS | -0.576 | -0.302 | 0.386 | |
| %hDPL | -0.373 | 0.184 | -0.186 | |
| HEB | -0.345 | 0.158 | -0.129 | |
| CLI | -0.281 | -0.240 | 0.150 | |
| MW3 | -0.162 | 0.000 | 0.522 | |
| TTP | -0.050 | 0.346 | 0.197 | |
| CLAW | -0.010 | -0.057 | 0.098 | |
| %TAIL | 0.031 | 0.050 | 0.060 | |
| SHI | 0.103 | -0.354 | 0.360 | |
| PI | 0.176 | 0.069 | -0.420 | |
| HTI | 0.235 | 0.106 | -0.190 | |
| %DPL | 0.340 | -0.476 | -0.223 | |
| FOOT | 0.351 | 0.068 | -0.266 | |
| %CL | 0.687 | 0.579 | -0.336 | |
| SMI | 0.717 | 0.369 | -0.023 | |
| HRI | 1.096 | 0.754 | -0.737 | |

| | SA | Am | SF | F | Total |
|---|----|----|----|---|-------|
| A | | | | | |
| Classification matrix (100% correct classification) | | | | | |
| Semi-aquatic (SA) | 6 | 0 | 0 | 0 | 6 |
| Ambulatory (Am) | 0 | 12 | 0 | 0 | 12 |
| Semi-fossorial (SF) | 0 | 0 | 13 | 0 | 13 |
| Fossorial (F) | 0 | 0 | 0 | 2 | 2 |
| Total | 6 | 12 | 13 | 2 | 33 |
| B | | | | | |
| Jackknifed classification matrix (81.8% correct classification) | | | | | |
| Semi-aquatic (SA) | 6 | 0 | 0 | 0 | 6 |
| Ambulatory (Am) | 3 | 8 | 1 | 0 | 12 |
| Semi-fossorial (SF) | 0 | 2 | 11 | 0 | 13 |
| Fossorial (F) | 0 | 0 | 0 | 2 | 2 |
| Total | 9 | 10 | 12 | 2 | 33 |

sified as semi-fossorial; and semi-fossorial *Myosorex blarina* and *M. varius* were misclassified as being ambulatory.

PCA of species having unknown locomotor mode. In the PCA carried out in an attempt to classify four species whose locomotor mode was unknown, eight of 10 locomotor indices contributed positively to the first principal component (PC1). PC1 accounted for more than 77 % of the variation in the model (Table 6), and it was most strongly influenced by three variables: CLI, CLAW, and negatively weighted %TAIL. As in the 17-variable model, *a priori* locomotory groups are mostly separated along this axis, from semi-aquatic spe-

cies with the lowest scores to ambulatory to semi-fossorial to fossorial groups having increasingly higher scores (Figure 4). As in the 17-variable model, semi-fossorial species plotted in two primary clusters with the same compositions as in that model. In contrast, ambulatory species were more cohesive. Ambulatory *Sorex cinereus*, which plotted with semi-aquatic species, and semi-fossorial *Congosorex phillipsorum*, which plotted with ambulatory species, again proved to be exceptions to the general pattern.

Among the species of uncertain locomotor mode, *Cryptotis gracilis* and *C. meridensis* plotted within the distribution of ambulatory species; *C. thomasi* occurred between the ambulatory species (and *Congosorex phillipsorum*) and semi-fossorial species; and *C. endersi* plotted with the *Blarina* grouping of semi-fossorial species rather than with the *Cryptotis* grouping of semi-fossorial species (Figure 4, Table 6).

DFA of species of unknown locomotor mode. Plots of scores from the DFA of 10 locomotor indices exhibit similar patterns as those from the 17-variable model, although the separations among locomotor groups are generally not as clear (Table 7; Figure 5). Fossorial species are again strongly separated along CV1, whereas the other three locomotor groups are separated from each other along a combination of CV1 and CV2 (Figure 5a). Semi-aquatic and semi-fossorial species overlap along CV3, but are separated from both ambulatory and fossorial species (Figure 6b).

The *post hoc* classification matrix had a correct classification rate of nearly 97 % (Table 7). The only misclassification was ambulatory *Sorex sonomae*, which was misclassified as semi-aquatic. Among the species of uncertain locomotor mode, *Cryptotis gracilis* was classified as semi-aquatic, *C. meridensis* and *C. thomasi* as ambulatory, and *C. endersi* as semi-fossorial (Figure 5; Table 7). In multivariate space, *C. gracilis* actually plots by itself away from the *a priori* locomotor groups, although it is physically closest to semi-aquatic species. Similarly, *C. endersi* plots in its own multivariate space between the ambulatory and semi-fossorial groups of species, but it is physically closest to the semi-fossorial group.

Discussion

As noted previously, there is considerable variation among soricids in skeletal characteristics that are typically associated with locomotion (Woodman and Gaffney 2014; Woodman and Stabile 2015b; Woodman and Wilken 2019). Such variation suggests that individual species' abilities to use various substrates are more nuanced and diverse (e. g., Mendes-Soares and Rychlik 2009; Tapisso

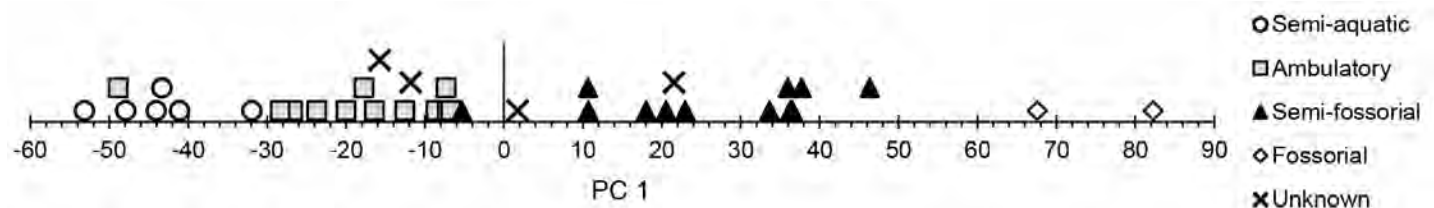
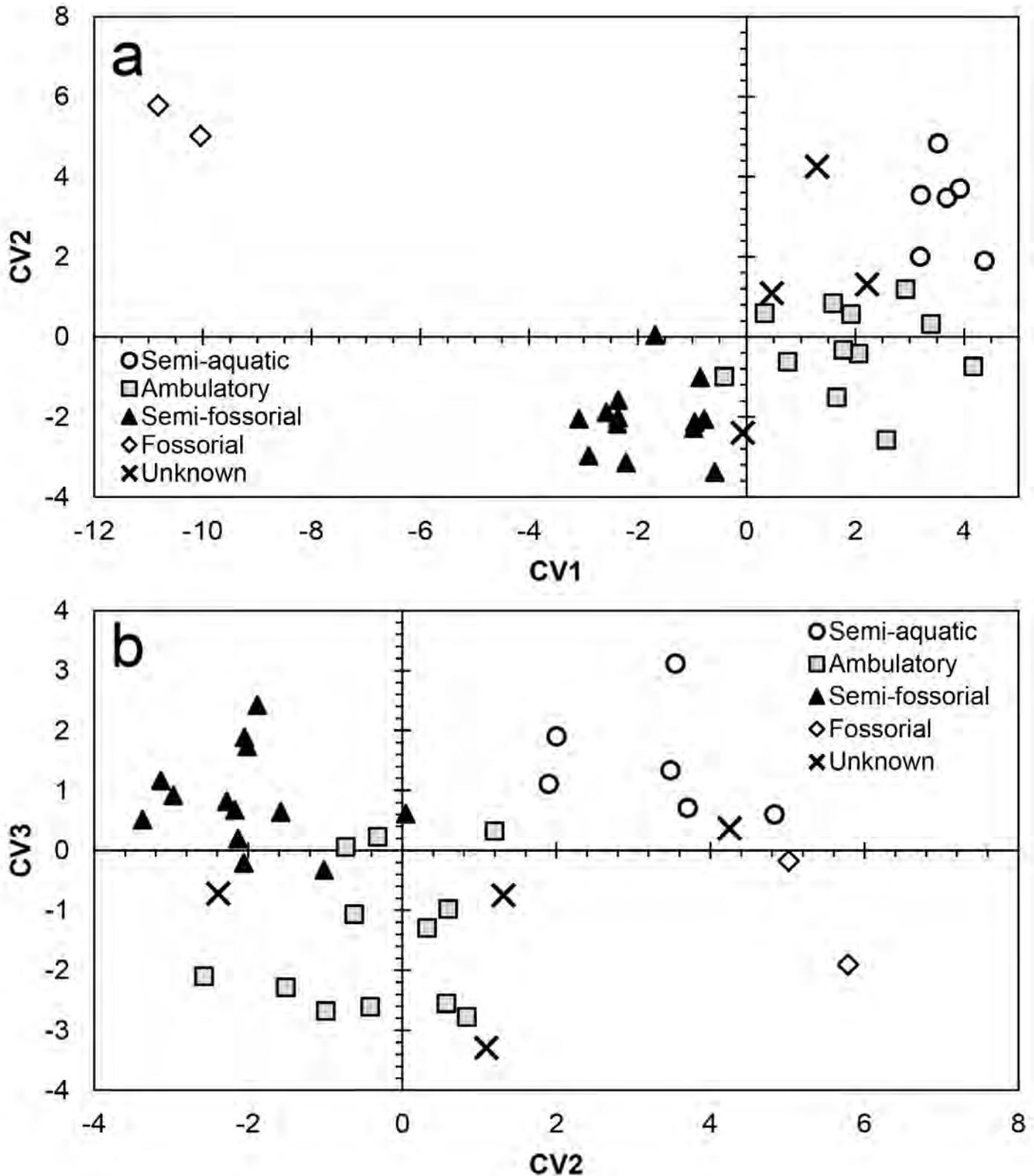


Figure 4. Plot of scores on PC1 from a PCA of 10 locomotor indices from 33 species of known locomotor mode and four species of uncertain locomotor mode (Table 6).



Morphological diversity may also reflect the reality that individuals are not entirely restricted in their use of substrate or in their locomotor behavior by either the possession or lack of specialized traits. Morphological traits that are related to particular modes of locomotion may simply reflect enhanced abilities that permit a species to specialize to a greater extent in certain behaviors that, given a shrew's high metabolism, are most likely related to foraging strategies. This likely accounts for the close correspondence between the numbers of species that appear specialized for ambulatory, semi-fossorial, and semi-aquatic locomotor behaviors (Hutterer 1985) and those that specialize on foraging for epigeal, hypogeal, and aquatic prey (Churchfield 1990). Despite this, ambulatory species can be vigorous scratch-diggers despite the lighter bone structure of their arms and their relatively short foreclaws (Chamberlain 1929). Ambulatory *Cryptotis parvus*, *Sorex cinereus*, and *S. hoyi*, and the semi-aquatic *S. palustris* are reported to excavate subterranean tunnels of varying lengths, depths, and degrees of complexity (Cahn 1937; Davis and Joeris 1945; Sorenson 1962; Tuttle 1964; Beneski and Stinson 1987). Similarly, non-aquatic shrews, such as ambulatory *Sorex araneus*, *S. cinereus*, *S. fumeus*, and *S. minutus*, have been documented to be capable swimmers (Dagg and Windsor 1972; Hanski 1986). Based on the diversity of species and numbers of individuals that have been found in the digestive tracts of various freshwater fishes (e. g., Huish and Hoffmeister 1947; Hodgson 1986; Moore and Kenagy 2004; Jung et al. 2011; Lisi et al. 2013), a number of additional ambulatory and semi-fossorial species readily take to water.

There is also no reason to assume that any particular species cannot possess traits that enhance its abilities for more than one locomotor mode. A ready example in the Talpidae is the *Condylura cristata*, which possesses numerous anatomical traits associated with fossorial locomotion, but which is also an active swimmer and may forage dominantly on hypogeal or aquatic prey, depending on where it lives (Petersen and Yates 1980).

Despite the foregoing caveats, a number of generalizations can be suggested regarding the external and skeletal morphological traits marking common, generalized locomotor modes in soricids.

Ambulatory shrews. Most species of shrews are ambulatory and have short legs and a moderately long tail (Hutterer 1985). The foreclaws and hind claws are short (%DPL, %CL, %hDPL, %hCL), the manual distal phalanges are typically somewhat shorter than the pedal distal phalanges (CLAW), although the claws on the fore feet and hind feet may be of approximately the same length (CLI). This means the foreclaw is less supported by the underlying distal phalanx (%CLS) than the hind claw (%hCLS). This relatively unspecialized body form is assumed to be the basic plan for soricids from which more specialized swimming, climbing, and digging forms evolved, but such singular directionality remains to be substantiated. Regardless, the generalized body morphology of ambulatory shrews represents the

Table 6. Variable loadings and taxon scores from a PCA of 10 locomotor indices from 33 taxa of known locomotor mode and four species for which locomotor mode is uncertain (Figure 4).

| Variable loadings | | |
|---|---------|---------|
| Variable | PC 1 | |
| CLI | 0.674 | |
| CLAW | 0.538 | |
| SHI | 0.201 | |
| HTI | 0.188 | |
| TTP | 0.131 | |
| SMI | 0.121 | |
| HRI | 0.057 | |
| %CLS | 0.049 | |
| FEB | -0.008 | |
| %TAIL | -0.378 | |
| Eigenvalue | 1144.07 | |
| % variance | 77.244 | |
| Taxon scores on PC1 with classification of unknowns | | |
| Taxon | Mode | PC 1 |
| <i>Sorex albibarbis</i> | SA | -53.13 |
| <i>Sorex navigator</i> | SA | -47.943 |
| <i>Sorex bendirii</i> | SA | -44.065 |
| <i>Sorex palustris</i> | SA | -43.347 |
| <i>Neomys fodiens</i> | SA | -41.121 |
| <i>Nectogale elegans</i> | SA | -31.949 |
| <i>Sorex cinereus</i> | Am | -48.893 |
| <i>Sorex sonomae</i> | Am | -28.365 |
| <i>Sorex hoyi</i> | Am | -26.805 |
| <i>Cryptotis nigrescens</i> | Am | -23.709 |
| <i>Cryptotis merus</i> | Am | -20.019 |
| <i>Cryptotis merriami</i> | Am | -17.725 |
| <i>Cryptotis tropicalis</i> | Am | -16.444 |
| <i>Myosorex geata</i> | Am | -12.561 |
| <i>Cryptotis parvus</i> | Am | -8.6015 |
| <i>Myosorex cafer</i> | Am | -7.3472 |
| <i>Blarinella quadricaudata</i> | Am | -7.1599 |
| <i>Myosorex kihaulei</i> | Am | -6.7505 |
| <i>Congosorex phillipsorum</i> | SF | -5.3339 |
| <i>Myosorex varius</i> | SF | 10.644 |
| <i>Myosorex blarina</i> | SF | 10.691 |
| <i>Blarina brevicauda jerrychoatei</i> | SF | 18.017 |
| <i>Blarina carolinensis</i> | SF | 20.531 |
| <i>Blarina brevicauda talpoides</i> | SF | 22.948 |
| <i>Cryptotis lacertosus</i> | SF | 33.638 |
| <i>Myosorex zinki</i> | SF | 35.979 |
| <i>Cryptotis mam</i> | SF | 36.293 |
| <i>Cryptotis celaque</i> | SF | 36.328 |
| <i>Cryptotis oreoryctes</i> | SF | 36.544 |
| <i>Cryptotis matsoni</i> | SF | 37.737 |
| <i>Cryptotis eckerlini</i> | SF | 46.334 |
| <i>Surdisorex norae</i> | F | 67.586 |
| <i>Surdisorex polulus</i> | F | 82.263 |
| <i>Cryptotis gracilis</i> | unknown | -15.742 |
| <i>Cryptotis meridensis</i> | unknown | -11.824 |
| <i>Cryptotis thomasi</i> | unknown | 1.7374 |
| <i>Cryptotis endersi</i> | unknown | 21.566 |

model to which more specialized shrews are compared and contrasted (Woodman and Gaffney 2014; Woodman and Stabile 2015b; Woodman and Wilken 2019).

Semi-aquatic shrews. Externally, semi-aquatic shrews typically possess long tails relative to other shrews, and there may be a dorsal; dorsal and ventral; or dorsal, ventral, and lateral keels of stiff hairs. The tail probably functions like that of a muskrat (*Ondatra zibethicus*) tail, by providing a small amount of forward thrust, but more importantly, by preventing the animal from yawing (Fish 1982). In contrast with the muskrat, which swims with just the hind limbs (Fish 1984), however, semi-aquatic and terrestrial shrews typically paddle by alternately stroking the front and hind limbs (Jackson 1928; Dagg and Windsor 1972; Mendes-Souares and Rychlik 2009). There is also a fringe of stiff hairs on the lateral edges of the digits of the hands and feet. In some species, notably *Nectogale*, the digits are partly webbed (Hutterer 1985). The foreclaws and hind claws are generally short (%DPL, %CL, %hDPL, %hCL), the foreclaws and manual distal phalanges typically are somewhat shorter than the hind claws and pedal distal phalanges (CLI, CLAW). The underlying manual distal phalanx, however, supports a greater proportion of the foreclaw than is typical in, for example, ambulatory shrews (%CLS). Semi-aquatic shrews typically have long hind limbs and hind feet relative to other shrews. Proportionally, the femur averages 28 % (range 27 to 29 %, $n = 6$ species), tibiofibula 50 % (44 to 52), and metacarpal III 22 % (19–26) of their combined length. This is in contrast to ambulatory shrews in which the femur averages 33 % (range 29 to 36 %, $n = 9$ species), tibiofibula 50 % (49 to 52), and metacarpal III 17 % (15 to 19) of their combined length, and to semi-fossorial and fossorial shrews, in which the femur averages 35 % (range 33 to 36 %, $n = 9$ species), tibiofibula 50 % (48 to 52), and metacarpal III 15 % (14 to 16) of their combined length. Moreover, the humerus of semi-aquatic shrews tends to be long in proportion to the femur (HFI), so much of the length of hind limb is a result of the proportionally longer tibiofibula (CI) and hind foot (PES).

Skeletally, the emphasis on the hind limbs in semi-aquatic shrews may be further illustrated by the relatively broad epicondyles of the femur (FEB), from which the plantaris, gastrocnemius, and the extensor digitorum longus muscles originate. The long bones of the limbs and manus bones are not particularly robust (HRI, RDW, URI) and are generally similarly proportioned to those of ambulatory shrews, with the exception of the femur (FRI), which can be considerably more robust than those of ambulatory and even semi-fossorial shrews (RR). The humerus has relatively small muscle attachment areas in the short deltopectoral crest (SMI) and small teres tubercle of the humerus (HTI), but can have a relatively broad epicondylar region (HEB) relative to ambulatory shrews. The olecranon process of the ulna tends to be slightly longer than in ambulatory shrews (OLI, TMO, TCO), suggesting the transmission of greater force from the triceps brachii muscle, although the insertion for that muscle (OCI)

Table 7. Variable loadings from a DFA of 10 locomotor indices from 33 taxa of known locomotor mode and four species for which locomotor mode is uncertain (Figure 5).

| Variable | Variable loadings | | | | | | | | |
|---|-------------------|--------|--------|----|----|----|---|-------|----------|
| | Axis 1 | Axis 2 | Axis 3 | SA | Am | SF | F | Total | Unknowns |
| TTP | 0.177 | -0.034 | 0.285 | | | | | | |
| FEB | 0.123 | 0.734 | -0.021 | | | | | | |
| SHI | 0.006 | -0.339 | 0.262 | | | | | | |
| %TAIL | -0.016 | 0.060 | 0.041 | | | | | | |
| CLAW | -0.016 | -0.091 | 0.015 | | | | | | |
| %CLS | -0.017 | -0.338 | 0.238 | | | | | | |
| CLI | -0.052 | -0.102 | 0.045 | | | | | | |
| HTI | -0.145 | 0.339 | -0.388 | | | | | | |
| SMI | -0.217 | 0.579 | -0.086 | | | | | | |
| HRI | -0.448 | 1.388 | -0.681 | | | | | | |
| Classification matrix (96.97% correct classification) | | | | | | | | | |
| Semi-aquatic (SA) | 6 | 0 | 0 | 0 | 6 | 1 | | | |
| Ambulatory (Am) | 1 | 11 | 0 | 0 | 12 | 2 | | | |
| Semi-fossorial (SF) | 0 | 0 | 13 | 0 | 13 | 1 | | | |
| Fossorial (F) | 0 | 0 | 0 | 2 | 2 | 0 | | | |
| Total | 7 | 11 | 13 | 2 | 33 | 4 | | | |

is no larger than in ambulatory shrews and the ulna averages slightly less breadth, therefore rendering it somewhat less resistant to bending and shearing stresses.

Semi-fossorial and fossorial shrews. In contrast to semi-aquatic shrews, the emphasis in semi-fossorial and fossorial shrews is on the changes in the morphology of the forelimb, particularly the humerus, ulna, and manus (Woodman and Morgan 2005; Woodman and Stephens 2010; Woodman and Gaffney 2014; Woodman and Stabile 2015a, 2015b; Woodman and Timm 2016; Woodman and Wilken 2019; Woodman et al. 2019). Among species in these two locomotor groups, morphological changes can appear to be gradual and progressive (e. g., Figs. 2, 3, 5), but traits do not necessarily co-vary in the same way or to the same degree (e. g., Figs. 1, 4, 6).

Externally, semi-fossorial and fossorial shrews are typically characterized by having small (or absent) pinnae, short tails, broadened forefeet, and elongated and broadened foreclaws (%DPL, %CL). They also have elongated and broadened hind claws (%hDPL, %hCL), although not to the same degree as the foreclaws (CLI, CLAW), and there is increasing support from the underlying distal phalanx as the claws increase in size (%CLS, %hCLS). There may be a tendency to reduce the overall length of the hind limbs relative to the forelimbs (IM) and the hind feet relative to the fore feet (FOOT), but, in contrast, there is a definite trend toward reduction of the length of the humerus relative to that of the femur (HFI).

Skeletally, the long bones of the limbs and manus bones become increasingly robust (HRI, RDW, URI, FRI, RR), particularly relative to those of ambulatory shrews. The humerus shortens, but becomes much broadened with enlarged teres tubercle (HTI), deltopectoral crest (SMI), epicondyles (HEB), and other regions involved in muscle attachment.

The olecranon process of the ulna elongates and broadens relative to the functional arm (OLI, TMO, TCO), allowing for the transmission of much greater force from the triceps brachii muscle, and the insertion for that muscle on the olecranon process (OCI) greatly increases. In contrast, the breadth of the distal epicondyles of the femur (FEB) are only slightly enlarged relative to those of ambulatory shrews, and they are generally smaller than those of semi-aquatic shrews.

Locomotory modes of the “unknowns”. *Cryptotis gracilis* and members of the *C. thomasi* group of species (*C. endersi*, *C. meridensis*, *C. monteverdensis*, *C. thomasi*) have defied easy characterization of their locomotory modes based on external and skeletal characters (Supplementary material Figure 1). These shrews all have relatively long foreclaws and hind claws and associated distal phalanges, like semi-fossorial shrews, but the claws are not particularly broad, and their tails in some cases (*e. g.*, *C. gracilis*, *C. endersi*, *C. monteverdensis*) are rather long, as in ambulatory shrews. Previous analyses of these species showed most of them to plot between the ambulatory and semi-fossorial shrews, with *C. gracilis* somewhat more semi-fossorial (Woodman and Timm 2016; Woodman 2019; Woodman and Wilken 2019).

In the current analyses, most of these species remain ambiguous, in part because of a continued lack of data regarding relevant characters, particularly for the rare *C. endersi* and *C. monteverdensis* (Pine et al. 2002; Woodman and Timm 2016). *Cryptotis gracilis* plots out as ambulatory based on mean percentile ranks (Figure 1; Table 2) and PCA (Figure 5; Table 5), but it was classified by DFA (Figure 6; Table 6) as semi-aquatic. In reality, it is separate from all other species in multivariate space between the ambulatory and semi-aquatic groups of species. It is unlikely to be truly semi-aquatic, as it plots as an ambulatory species for two of the more relevant characteristics of semi-aquatic species, represented by the locomotor indices PES and %TAIL (Figure 1; Table 2), and because it lacks more obvious external characteristics of typical semi-aquatic shrews, such as the fringes of short hairs lining the digits and tail.

The four members of the *C. thomasi* group all plot as ambulatory, semi-fossorial, or intermediate between those two modes. *Cryptotis meridensis* is consistently ambulatory, and *C. monteverdensis* plots as ambulatory based on mean percentile rank, the only analysis in which it could be included. *Cryptotis endersi* plots as ambulatory in the mean percentile rank analysis, and it is classified as semi-fossorial based on both PCA and DFA, but it really plots as somewhat intermediate between both groups (Figure 6; Table 6). In contrast, *C. thomasi* plots as intermediate between the ambulatory and semi-fossorial groupings in both the mean percentile rank analysis and the PCA, but was classified as ambulatory in the DFA.

All five of these species occupy high elevation habitats in southern Central America and Andean South America, and they may represent one or more unique locomotor adaptations or combinations of adaptations for foraging in high-elevation forests and páramo-like habitats.

1. Of 34 locomotor indices tested in this study, 23 (IM, HFI, FOOT, CLAW, CLI, SMI, HRI, HTI, TTP, HEB, TCO, OCI, URI, %DPL, %CL, MW3, CI, PES, FEB, %hDPL, %hCL, RR, %TAIL) proved effective for discriminating one or more of the four *a priori* locomotor groups (ambulatory, semi-aquatic, semi-fossorial, fossorial).

2. Among three analyses of locomotor indices, percentile ranking was the only analysis that permitted the inclusion of all 52 taxa, including species of unknown locomotor mode. The lack of data for some taxa, however, results in uneven morphological comparisons across taxa, and there was considerable overlap of some locomotor groups, particularly the semi-aquatic and ambulatory groups.

In contrast, PCA and DFA require complete datasets, and the largest sample I could compile was 17 indices from 33 taxa, which excluded the unknowns in this study. The first principal component (PC1) from PCA distinguished the major (and some minor) locomotor groupings, but there was overlap between locomotor groups that makes it difficult to identify locomotor mode for some species. Plotting PC1 and PC2 provided greater discrimination among groups, but some overlap remains.

DFA classification of *a priori* locomotor groups provided the best discrimination among locomotor groups, but requires complete datasets.

3. Classification of four species of unknown locomotor mode using PCA and DFA of 10 locomotor indices provided contrasting results. One species was classified as ambulatory by PCA and semi-aquatic by DFA; one species was classified as ambulatory by both analyses; one species was classified as intermediate between ambulatory and semi-fossorial by PCA and semi-fossorial by DFA; and one species was classified as semi-fossorial by both. The lack of complete datasets clearly hampered the analyses, but there is also strong indication that some of these species have unique combinations of morphological traits that are not easily explained by comparison with other shrews, even those in the same genus.

4. Results here confirm that variation in skeletal traits typically exists within defined locomotor modes. Such variation probably results in part from the reality that 1) most species (and individuals) are not restricted to a single mode, but engage in a variety of locomotor behaviors to varying degrees; 2) the traits that we can measure or otherwise gauge are not necessarily adaptive for a particular locomotor mode; and 3) seemingly similar traits may be employed in different ways by different species or populations.

Acknowledgments

Thanks to Jacob Esselstyn and Giovani Hernández-Canchola for organizing this tribute to Al Gardner. This project was made possible by L. Heaney, A. Ferguson, J. Phelps (FMNH), D. Lunde, and I. Rochon (USNM), who permitted access to the invaluable collections under their care, and by Julian C. Kerbis Peterhans, who permitted me to inspect

unique specimens obtained during his field studies. Many thanks to Asante N. Crews, Sarah A. Gaffney, James J. P. Morgan, Frank A. Stabile, Ryan B. Stephens, and Alec T. Wilken, who worked with me on earlier aspects of similar studies. I particularly want to thank Alfred L. Gardner, my valued colleague in the former Biological Survey Unit at the U.S. National Museum of Natural History, for sharing his field expertise, historical knowledge, editorial skills, and comradery during more than two decades. This work benefited from comments by Terry Chesser, Jacob Esselstyn, and two anonymous reviewers. Any use of trade, product, or firm names is for descriptive purposes only and does not imply endorsement by the U.S. government.

Literature cited

- BENESKI, J. T., JR., AND D.W. STINSON. 1987. *Sorex palustris*. *Mammalian Species* 296:1–6.
- CAHN, A. R. 1937. The mammals of Quetico Provincial Park of Ontario. *Journal of Mammalogy* 18:19–30.
- CHAMBERLAIN, E. B. 1929. Behavior of the least shrew. *Journal of Mammalogy* 10:250–251.
- CHURCHFIELD, S. 1990. *The Natural History of Shrews*. Comstock Publishing Associates. Ithaca, U.S.A.
- DAGG, A. I., AND E. E. WINDSOR. 1972. Swimming in northern terrestrial mammals. *Canadian Journal of Zoology* 50:117–139.
- DAVIS, W. B., AND L. JOERIS. 1945. Notes on the life history of the little short-tailed shrew. *Journal of Mammalogy* 26:136–138.
- EISENBERG, J. F. 1981. *The Mammalian Radiations*. The University of Chicago Press. Chicago, U.S.A.
- ELISSAMBURU, A., AND L. DE SANTIS. 2011. Forelimb proportions and fossorial adaptations in the scratch-digging rodent *Ctenomys* (Caviomorpha). *Journal of Mammalogy* 92:683–689.
- FISH, F. E. 1982. Function of the compressed tail of surface swimming muskrats (*Ondatra zibethicus*). *Journal of Mammalogy* 63:591–597.
- FISH, F. E. 1984. Mechanics, power output and efficiency of the swimming muskrat (*Ondatra zibethicus*). *Journal of Experimental Biology* 110:183–201.
- FISH, F. E. 2000. Biomechanics and energetics in aquatic and semiaquatic mammals: platypus to whale. *Physiological and Biochemical Zoology: Ecological and Evolutionary Approaches* 73:683–698.
- HAMMER, Ø., D. A. T. HARPER, AND P. D. RYAN. 2001. PAST: paleontological statistics software package for education and data analysis. *Palaeontologica Electronica* 4:1–9.
- HANSKI, I. 1986. Population dynamics of shrews on small islands accord with the equilibrium model. *Biological Journal of the Linnean Society* 28:23–36.
- HILDEBRAND, M. 1985a. WALKING AND RUNNING. Pp. 38–57, in *Functional Vertebrate Morphology* (Hildebrand, M., D. M. Bramble, K. F. Liem, and D. B. Wake, eds.). Belknap Press, Cambridge, U.S.A.
- HILDEBRAND, M. 1985b. Digging of quadrupeds. Pp. 89–109, in *Functional Vertebrate Morphology* (Hildebrand, M., D. M. Bramble, K. F. Liem, and D. B. Wake, eds.). Belknap Press, Cambridge, U.S.A.
- HODGSON, J. R. 1986. The occurrence of small mammals in the diets of largemouth bass (*Micropterus salmoides*). *Jack-Pine Warbler* 64:39–40.
- HOPKINS, S. S. B., AND E. B. DAVIS. 2009. Quantitative morphological proxies for fossoriality in small mammals. *Journal of Mammalogy* 90:1449–1460.
- HOWELL, H. B. 1930. *Aquatic mammals. Their adaptations to life in the water*. Charles C. Thomas. Springfield, USA.
- HE, K., ET AL. 2015. Molecular phylogeny supports repeated adaptation to burrowing within small-eared shrews, genus of *Cryptotis* (Eulipotyphla, Soricidae). *Plos One* DOI:10.1371/journal.pone.0140280 October 21.
- HE, K., ET AL. 2021. Mitogenome and comprehensive phylogenetic analyses support rapid diversifications among species groups of small eared shrews genus *Cryptotis* (Mammalia: Eulipotyphla: Soricidae). *Zoological Research* 42:739–745.
- HUIISH, M. T., AND D. F. HOFFMEISTER. 1947. The short-tailed shrew (*Blarina*) as a source of food for the green sunfish. *Copeia* 1947:198.
- HUTTERER, R. 1985. Anatomical adaptations of shrews. *Mammal Review* 15:43–55.
- JACKSON, H. H. T. 1928. A taxonomic review of the American long-tailed shrews (genera *Sorex* and *Microsorex*). *North American Fauna* 51:1–238.
- JUNG, T. S., ET AL. 2011. American pygmy shrew, *Sorex hoyi*, consumed by an arctic grayling, *Thymallus arcticus*. *Canadian Field Naturalist* 125:255–256.
- KIRK E. C., P. LEMELIN, M. W. HAMRICK, D. M. BOYER, AND J. I. BLOCH. 2008. Intrinsic hand proportions of euarchontans and other mammals: Implications for the locomotor behavior of plesiadapiforms. *Journal of Human Evolution* 55:278–299.
- LEMELIN P. 1999. Morphological correlates of substrate use in didelphid marsupials: Implications for primate origins. *Journal of Zoology* 247:165–175.
- LISI, P. J., ET AL. 2013. Episodic predation of mammals by stream fishes in a boreal river basin. *Ecology of Freshwater Fish* 23:622–630
- MENDES-SOARES, H., AND L. RYCHLIK. 2009. Differences in swimming and diving abilities between two sympatric species of water shrews: *Neomys anomalus* and *Neomys fodiens* (Soricidae). *Journal of Ethology* 27:317–325
- MOORE, J. W., AND G. J. KENAGY. 2004. Consumption of shrews, *Sorex* spp., by Arctic grayling, *Thymallus arcticus*. *The Canadian Field Naturalist* 118:111–115.
- NATIONS, J. A., ET AL. 2019. A simple skeletal measurement effectively predicts climbing behaviour in a diverse clade of small mammals. *Biological Journal of the Linnean Society* 128:323–336.
- PETERSEN, K. E., AND T. L. YATES. 1980. *Condylura cristata*. *Mammalian Species* 129:1–4.
- PINE, R. H., N. WOODMAN, AND R. M. TIMM. 2002. Rediscovery of Enders's small-eared shrew, *Cryptotis endersi* (Insectivora: Soricidae), with a redescription of the species. *Mammalian Biology* 67:372–377.
- PRICE, M. V. 1993. A functional-morphometric analysis of forelimbs in bipedal and quadrupedal heteromyid rodents. *Biological Journal of the Linnean Society* 50:339–360.
- REED, C. A. 1951. Locomotion and appendicular anatomy in three soricoid insectivores. *American Midland Naturalist* 45:513–670.
- SAMUELS, J. X., AND B. VAN VALKENBURGH. 2008. Skeletal indicators of locomotor adaptations in living and extinct rodents. *Journal of Morphology* 269:1387–1411.

- SARGIS, E. J. 2002. Functional morphology of the forelimb of tupaiids (Mammalia, Scandentia) and its phylogenetic implications. *Journal of Morphology* 253:10–42.
- SARGIS, E. J., ET AL. 2013a. Using hand proportions to test taxonomic boundaries within the *Tupaia glis* species complex (Scandentia, Tupaiidae). *Journal of Mammalogy* 94:183–201.
- SARGIS, E. J., ET AL. 2013b. Morphological distinctiveness of Javan *Tupaia hypochrysa* (Scandentia, Tupaiidae). *Journal of Mammalogy* 94:938–947.
- SHIMER, H. W. 1903. Adaptations to aquatic, arboreal, fossorial and cursorial habits in mammals. III. Fossoriality. *American Naturalist* 37:819–825.
- SORENSEN, M. W. 1962. Some aspects of water shrew behavior. *American Midland Naturalist* 68:445–462.
- TAPISSO, J. T., ET AL. 2013. Ecological release: swimming and diving behavior of an allopatric population of the Mediterranean water shrew. *Journal of Mammalogy* 94:29–39.
- TUTTLE, M. D. 1964. Observation of *Sorex cinereus*. *Journal of Mammalogy* 45:148.
- VIZCAINO, S. F., AND N. MILNE. 2002. Structure and function in armadillo limbs (Mammalia: Xenarthra: Dasypodidae). *Journal of Zoology* 257:117–127.
- WAHAB, M. F. A., ET AL. 2020. Taxonomic assessment of the Malayan water shrew *Chimarrogale hantu* Harrison, 1958 and reclassification to the genus *Crossogale*. *Mammalian Biology* 100:399–409.
- WOODMAN, N. 2019. Three new species of small-eared shrews, genus *Cryptotis*, from El Salvador and Guatemala (Mammalia: Eulipotyphla: Soricidae). *Special Publication of the Museum of Texas Tech University* 72:1–46.
- WOODMAN, N., AND S. A. GAFFNEY. 2014. Can they dig it? Functional morphology and degrees of semi-fossoriality among some American shrews (Mammalia, Soricidae). *Journal of Morphology* 275:745–759.
- WOODMAN, N., AND J. P. J. MORGAN. 2005. Skeletal morphology of the forefoot in shrews (Mammalia: Soricidae) of the genus *Cryptotis*, as revealed by digital x-rays. *Journal of Morphology* 266:60–73.
- WOODMAN, N., AND F. A. STABILE. 2015a. Variation in the mysoricine hand skeleton and its implications for locomotory behavior (Eulipotyphla: Soricidae). *Journal of Mammalogy* 96:159–171.
- WOODMAN, N., AND F. A. STABILE. 2015b. Functional skeletal morphology and its implications for locomotory behavior among three genera of mysoricine shrews (Eulipotyphla: Soricidae). *Journal of Morphology* 276:550–563.
- WOODMAN, N., AND R. B. STEPHENS. 2010. At the foot of the shrew: manus morphology distinguishes closely-related *Cryptotis goodwini* and *Cryptotis griseoventris* (Mammalia, Soricidae) in Central America. *Biological Journal of the Linnean Society* 99:118–134.
- WOODMAN, N., AND R. M. TIMM. 2016. A new species of small-eared shrew in the *Cryptotis thomasi* species group from Costa Rica (Mammalia: Eulipotyphla: Soricidae). *Mammal Research* 62:89–101 (published online 27 August 2016).
- WOODMAN, N., AND A. T. WILKEN. 2019. Comparative functional skeletal morphology among three genera of shrews: implications for the evolution of locomotory behavior in the Soricinae (Eulipotyphla: Soricidae). *Journal of Mammalogy* 100:1750–1764.
- WOODMAN, N., A. T. WILKEN, AND S. IKRAM. 2019. See how they ran: morphological and functional aspects of skeletons from ancient Egyptian shrew mummies (Eulipotyphla: Soricidae: Crocidurinae). *Journal of Mammalogy* 100:1199–1210.

Associated editor: Jake Esselstyn and Giovani Hernández Canchola

Submitted: August 9, 2022; Reviewed: August 15, 2022

Accepted: November 9, 2022; Published on line: January 27, 2023

Appendix 1

New specimens examined and measured.

Specimens used for postcranial measurements (long bones of the appendicular skeleton).

SORICINAE: SORICINI

Sorex cinereus ($n = 20$). NEW HAMPSHIRE: Carroll Co.: Bartlett Experimental Forest (USNM 600625, 600626, 600628, 600629, 600630, 600631, 600633, 600634, 600635, 600637, 600638, 600639, 600642, 600643, 600646, 600648, 600649, 600650, 600651, 600653).

Sorex hoyi ($n = 8$). NEW HAMPSHIRE: Carroll Co.: Bartlett Experimental Forest (USNM 600742, 600743, 601995, 601996, 601999, 602000, 602001, 602001).

Sorex sonomae ($n = 4$). OREGON: Douglas Co.: 24.4 km S, 6 km W of Elkton (USNM 560070). Lane Co.: 0.4 km N, 18.5 km W Lorane (USNM 561167); 3 km N, 19.5 km W Lorane (USNM 561184); 1.6 km S, 5.2 km W McKenzie Bridge (USNM 556750).

Sorex bendirii ($n = 19$). CALIFORNIA: 271162; WASHINGTON: (USNM 250616, 558133, 563996, 563997, 563998, 564000). OREGON: (USNM 556532, 556546, 556554, 556558, 556572, 556583, 557725, 557726, 557734, 561125, 561127, 563080).

Sorex navigator ($n = 10$). COLORADO: (USNM 485409, 485411, 485413, 515058, 515059, 515060). OREGON: (USNM 556780). WASHINGTON: (USNM 241998, 241999, 242003).

Sorex albibarbis ($n = 6$). CANADA: NOVA SCOTIA: 30 mi E of Trenton (USNM 530829). USA: NEW HAMPSHIRE: (USNM 515061, 515062, 600745); MAINE: (USNM 600798). WEST VIRGINIA: Pocahontas Co.: Allegheny Mountains (USNM 569120).

Sorex palustris ($n = 4$). CANADA: ONTARIO: Quetico Provincial Park, side Lake (FMNH 44529). USA: MICHIGAN: Schoolcraft Co.: Seney National Wildlife Refuge (USNM 530501, 551769). MINNESOTA: Cook Co.: Greenwood Lake, 47° 59' 55" N, -90° 8' 30" W (FMNH 163321). WISCONSIN: Douglas Co.: 13 mi W of Salon Springs (USNM 600003).

SORICINAE: NECTOGALINI

Chimarrogale himalayica ($n = 2$). TAIWAN: 6.5 km S of Wu Sheh (USNM 358140); Mupin (USNM 358141).

Nectogale elegans ($n = 2$). CHINA: Sichuan: ca. 17 km SSE of Shimian (USNM 254812, 574296).

Neomys fodiens ($n = 4$). FRANCE: BOURGOGNE: Is-Sur-Tille (USNM 233967). SWEDEN: Lapland (USNM 1058). SPAIN: CANTABRIA: Camargo, Barrio El Juyo, Igollo, 60 m (FMNH 153665, 153666).

Specimens used for measurements of the manus and pes.

SORICINAE: SORICINI

Ambulatory/terrestrial:

Sorex cinereus ($n = 25$). NEW HAMPSHIRE: Carroll Co.: Bartlett Experimental Forest (USNM 601840, 601841, 601842, 601843, 601846, 601847, 601849, 601850, 601855,

601858, 601859, 601862, 601863, 601925); Coos Co.: Lake Umbagog National Wildlife Refuge (USNM 568177, 568178, 568179, 568180, 568184, 568186, 568189, 568190, 568191, 568195); Strafford Co.: 1 mi N, 7 mi W of Rochester (USNM 600627).

Sorex hoyi ($n = 18$). CANADA: NEW BRUNSWICK: Mt. Carleton Provincial Park (USNM 553310, 553311, 553312, 553313, 553314, 553315, 553316, 553317, 553318, 553319, 553320, 553321). USA: NEW HAMPSHIRE: Carroll Co.: Bartlett Experimental Forest (USNM 601998, 602001, 602004); Coos Co.: Bretton Woods (USNM 294773); Lake Umbagog National Wildlife Refuge (USNM 568192, 568198)

Sorex sonomae ($n = 8$). USA: CALIFORNIA: Del Norte Co.: Crescent City (USNM 68166, 68167); Gasquet (USNM 91551, 91552, 91553). Humboldt Co.: Eureka (USNM 47090, 63520, 63521).

Semi-aquatic:

Sorex bendirii ($n = 39$). CALIFORNIA: Del Norte Co.: Crescent City (USNM 97601, 97603, 97604, 97605, 97606, 97607); Gasquet (USNM 91555, 91552, 91553). OREGON: Morrow Co.: Camas Prairie, Mount Hood, eastern base of Cascade Mountains (USNM 79964). Clatsop Co.: Astoria (USNM 89019). Lane Co.: 4.4 km N, 6.8 km E Blue River (USNM 556565); Eugene (USNM 204482); Vida (USNM 204480). Lincoln Co.: Otis (USNM 264398). Linn Co.: 9.2 km N, 1.2 km W McKenzie Bridge (USNM 556534, 556535, 557728). Multnomah Co.: Larch Mountain, T1N, R5E, sec. 36 (USNM 294066); Portland (USNM 140852). WASHINGTON: Grays Harbor Co.: Oakville (USNM 231022, 231024, 231025). Klickitat Co.: Trout Lake (USNM 230235). Lewis Co.: 8 mi W of Chehalis (USNM 230230, 230233, 230234, 230236); Toledo (USNM 231023). Pacific Co.: Ilwaco (USNM 230231, 230237). Pierce Co.: Mount Rainier, Ohanapecosh Springs (USNM 232844, 232845); Mount Rainier, 1 mi W Rainier Park, Meslers Ranch (USNM 233593, 233594, 233595); Pullalup (USNM 227155); 6 mi S of Tacoma (USNM 231019). Snohomish County: Oso (USNM 234503). Wahkiakum Co.: Cathlamet (USNM 230232). Yakima Co.: Yakima Indian Reservation (USNM 226862).

Sorex navigator ($n = 22$). COLORADO: Boulder Co.: Boulder (USNM 112064); Gold Hill (USNM 35671, 73862, 73863). Gilpin Co.: Black Hawk, Dory Hill Pond (USNM 112048, 112049). Larimer Co.: Elkhorn (USNM 148154). Montrose Co.: Maverick Canyon, 2 mi N Coventry (USNM 149968, 149969, 149970, 149972). WASHINGTON: Pierce Co.: Mount Rainier (USNM 232843, 232846, 233093, 233222, 233590, 233591, 233592). Skamania Co.: Mount St. Helens (USNM 90751). Snohomish Co.: Suiattle River, Chiwawa Mountain Fork (USNM 229887). Yakima Co.: Yakima Indian Reservation (USNM 226860, 226861).

Sorex albibarbis ($n = 24$). CANADA: NEW BRUNSWICK: 5.3 km N, 3.5 km N Riverside-Albert (USNM 528207); Mount Carleton Provincial Park (USNM 553303, 553304, 553305, 553306, 553307, 553308). NOVA SCOTIA: Digby (USNM 150056, 150068); Halifax (USNM 288005). 30 km E of Tren-

ton (530829). QUEBEC: St. Rose (USNM 150079). USA: MAINE: Mount Katahdin (USNM 117980, 117981). Somerset Co.: N shore of Russell Pond (USNM 569772). York Co.: Lyman, Massabesic Experimental Forest (USNM 600798). NEW HAMPSHIRE: Coos Co.: Bretton Woods (USNM 294622, 294772); Lake Umbagog National Wildlife Refuge (USNM 568193). Carroll Co.: Bartlett Experimental Forest (USNM 600745). TENNESSEE: Sevier Co.: Great Smoky Mountain National Park (USNM 294409). VERMONT: Rutland Co.: Mondon (USNM 250165). VIRGINIA: Bath Co.: Little Back Creek (USNM 512048).

Sorex palustris ($n = 15$). MICHIGAN: Marquette Co.: Michigamme (USNM 243724, 243725); Schoolcraft Co.: Seney National Wildlife Refuge (USNM 514244, 514382, 524518, 524519, 530499, 530500, 530501, 551765, 551766, 551768, 551770, 551773). MINNESOTA: Cook Co.: Greenwood Lake, 47° 59' 55" N, - 90° 8' 30" W (FMNH 163321).

SORICINAE: NECTOGALINI

Semi-aquatic:

Chimarogale himalayica ($n = 4$). CHINA: Yunnan: West Slope of Likiang (USNM 240167). Taiwan: Nan-T'ou: Meichi (USNM 358139, 358140, 358141).

Nectogale elegans ($n = 4$). CHINA: Qinghai: Bei Zha Forestry Station (USNM 449155). Sichuan: Mupin (USNM 254812); ca. 17 km SSE Shimian (USNM 574296). INDIA: Sikkim: Lachung (USNM 260768).

Neomys fodiens ($n = 20$). FRANCE: BOURGOGNE: Cote-D'Or Department, Is-Sur-Tille (USNM 498756, 498757, 498759, 498760, 498761). SWEDEN: Lapland (USNM 1058); UPPSALA: Uppsala (USNM 84909). Locality unknown (USNM 12330). SWITZERLAND: BERN: Meiringen (USNM 85938, 85939, 85941, 85942, 85943, 85944, 85946, 85947, 85949). NEUCHÂTEL: Neuchâtel (USNM 12329). SANKT GALLEN: Sitterwald (USNM 86497). VAUD: Lausanne (USNM 104486).

CROCIDURINAE:

Ambulatory/terrestrial:

Suncus hututsi ($n = 1$). BURUNDI: Bururi Province: Bururi Commune, 2170 m: Bururi Forest Reserve, Ruhinga Hill. (FMNH 155925).

Appendix 2

A priori locomotor classifications of sorcid species.

CROCIDURINAE:

Ambulatory:

Crocidura olivieri
Crocidura religiosa
Crocidura suaveolens
Suncus hututsi

MYOSORICINAE:

Ambulatory:

Myosorex cafer
Myosorex geata
Myosorex kahaulei

Semi-fossorial:

Congosorex phillipsorum
Myosorex blarina
Myosorex varius
Myosorex zinki

Fossorial:

Surdisorex norae
Surdisorex polulus

SORICINAE: BLARINELLINI

Ambulatory:

Blarinella quadricaudata

SORICINAE: BLARININI

Ambulatory:

Cryptotis parvus
Cryptotis tropicalis
Cryptotis merriami
Cryptotis merus
Cryptotis nigrescens

Semi-fossorial:

Blarina brevicauda jerrychoatei
Blarina brevicauda jknoxjonesi
Blarina brevicauda talpoides
Blarina carolinensis
Blarina hylophaga
Blarina peninsulæ
Blarina shermani
Cryptotis cavatorculus
Cryptotis celaque
Cryptotis eckerlini
Cryptotis lacertosus
Cryptotis magnimanus
Cryptotis mam
Cryptotis matsoni

Cryptotis mccarthyi
Cryptotis mexicanus
Cryptotis oreoryctes
Cryptotis phillipsii

Unknown:

Cryptotis endersi
Cryptotis gracilis
Cryptotis meridensis
Cryptotis monteverdensis
Cryptotis thomasi

SORICINAE: NECTOGALINI

Semi-aquatic:

Chimarroale himalayica
Nectogale elegans
Neomys fodiens

Soricinae: Soricini

Ambulatory:

Sorex cinereus
Sorex hoyi
Sorex sonomae

Semi-aquatic:

Sorex albibarbis
Sorex bendirii
Sorex navigator
Sorex palustris

Ecological niche differentiation among Aztec fruit-eating bat subspecies (Chiroptera: Phyllostomidae) in Mesoamerica

IVÁN HERNÁNDEZ-CHÁVEZ^{1,2}, LÁZARO GUEVARA³, JOAQUÍN ARROYO-CABRALES⁴, AND LIVIA LEÓN-PANIAGUA^{2*}

¹ Posgrado en Ciencias Biológicas, Universidad Nacional Autónoma de México. Av. Ciudad Universitaria 3000, CP. 04360, Coyoacán. Ciudad de México, México. E-mail: ivanhc@ciencias.unam.mx (IH-C).

² Museo de Zoología "Alfonso L. Herrera", Facultad de Ciencias, Universidad Nacional Autónoma de México. Av. Ciudad Universitaria 3000, CP. 04360, Coyoacán. Ciudad de México, México. E-mail: llp@ciencias.unam.mx (LL-P).

³ Departamento de Zoología, Instituto de Biología, Universidad Nacional Autónoma de México. Circuito Zona Deportiva s/n, Ciudad Universitaria, CP. 04510, Coyoacán. Ciudad de México, México. E-mail: llg@ib.unam.mx (LG).

⁴ Laboratorio de Arqueozoología, Subdirección de Laboratorios y Apoyo Académico, Instituto Nacional de Antropología e Historia. Moneda 16, Col. Centro, CP. 06060, Cuauhtémoc. Ciudad de México, México. E-mail: arromatu5@yahoo.com.mx (JA-C).

*Corresponding author: <https://orcid.org/0000-0002-1748-0915>.

Artibeus aztecus is a Mesoamerican montane bat with three currently recognized, allopatric subspecies. No study has evaluated the phylogenetic status of the subspecies. However, through an analysis of its ecological niche and its geographic distribution, here we analyze whether there is differentiation of the climatic requirements for each subspecies, assessing whether niche evolution is a potential factor in subspecies differentiation. We assayed ecological niche models for each subspecies, analyzed the response curves for the most important climatic variables of each model, and generated the potential distribution model for each subspecies. We assayed a background similarity test between the subspecies to determine how similar their niches were. We found differences in climatic requirements for the three allopatric subspecies and the most important variables and their response curves. Potential distribution models concur with Mesoamerican highlands and highlight the lowlands of the isthmus of Tehuantepec and the Nicaraguan depression as possible geographic barriers. Differences found between ecological niches for each subspecies contrast with previous findings for the species and other phyllostomid bats. Niche conservatism may have caused geographic isolation in the past, and differences in environmental requirements may have appeared later. Molecular and morphological analyses are necessary to clarify the taxonomic status of these populations and the evolutionary processes involved in their diversification.

Artibeus aztecus es un murciélago montano mesoamericano, cuyas tres poblaciones alopatricas son reconocidas como subspecies. Sin embargo, no hay estudios filogenéticos que permitan aclarar su situación taxonómica, por lo que, a través del análisis de su nicho ecológico y distribución geográfica, se analizó si existe diferenciación en los requerimientos climáticos para cada subspecie, evaluando si la evolución del nicho es un factor potencial en la diferenciación de las subspecies. Se llevaron a cabo modelos de nicho ecológico para cada subspecie, se analizaron las curvas de respuesta de las variables más importantes y, se generó el modelo de distribución potencial para cada subspecie. Adicionalmente se realizaron pruebas de similitud de *background* entre las tres subspecies para determinar qué tan similares son sus nichos. Se encontraron diferencias en los requerimientos climáticos entre las tres subspecies, así como en las variables más importantes y sus curvas de respuesta. Los modelos de distribución potencial coinciden con las tierras altas de Mesoamérica y destacan las zonas bajas del istmo de Tehuantepec y la depresión de Nicaragua como posibles barreras geográficas. Las diferencias encontradas en los nichos ecológicos de las subspecies contrastan con los hallazgos previos para la especie y otros murciélagos filostómidos. Conservadurismo de nicho ecológico pudo provocar aislamiento geográfico en el pasado y las diferencias en los requerimientos climáticos pudieron aparecer después. Son necesarios análisis moleculares y morfológicos que permitan conocer de manera más amplia los patrones evolutivos involucrados en la diversificación de la especie.

Keywords: Geographic barriers; Mesoamerica; neotropical bats; niche divergence; ecological speciation.

© 2023 Asociación Mexicana de Mastozoología, www.mastozoologiamexicana.org

Introduction

Artibeus aztecus is a medium-sized phyllostomid bat that inhabits the highlands of Mesoamerica. The three allopatric populations of this taxon are recognized as subspecies (Davis 1969): *Artibeus aztecus aztecus*, found from Sinaloa and Nuevo León to Oaxaca in México; *Artibeus aztecus minor*, located from Chiapas, México, to Honduras; and *Artibeus aztecus major*, found from Costa Rica and Panama.

The subspecies *A. a. aztecus* was typical in evergreen forests at relatively high elevations in the mountains bordering the Mexican Plateau, as low as 1000 m in cloud forest and as high as 2,400 m in the pine-fir forest, it has been recorded in pine-oak forest, coniferous forest, *Abies* forest, cloud mon-

tane forest, agricultural areas (López-González and García-Mendoza 2006; Segura-Trujillo and Navarro-Pérez 2010; Briones-Salas et al. 2019; Cerón-Hernández et al. 2022); In Veracruz (México) it is considered vulnerable because it inhabits forest fragments but can use riparian vegetation as corridors to cross grasslands (Cerón-Hernández et al. 2022). In the case of *A. a. minor*, it has been reported in coniferous forest, montane cloud forest, grasslands, areas with secondary vegetation, agricultural landscapes and in human settlements (Davis 1969; Kraker-Castañeda et al. 2017; Lorenzo et al. 2017; Medina-Van Berkum et al. 2020). *Artibeus a. major* is the only subspecies whose distributional pattern was not associated with conifers, but

with “cloud forest” atmospheric conditions ([Davis 1969](#)); there are records of the subspecies in tropical premontane rainforest and tropical lower montane rainforest ([Zamora-Mejías and Rodríguez-Herrera 2017](#); [Pineda-Lizano and Chaverri 2022](#)).

Artibeus aztecus is a frugivorous bat. Fruit-eating bats in *Artibeus* are considered important in seed dispersal ([Saldaña-Vázquez 2019](#)), which is essential for forest regeneration and maintenance of plant genetic diversity and composition ([Wang and Smith 2022](#)), thereby being crucial to forest conservation and management ([Jordano et al. 2011](#)). In central México *A. aztecus* eats wild figs (*Ficus* sp.), capuli cherries (*Prunus serotina*), cypress (*Cupressus* sp), and Mexican hawthorn (*Crataegus Mexicana*; [Solarí et al. 2019](#)).

Previously, [Davis \(1969\)](#) treated the three populations as subspecies, having observed only subtle differences in color and some cranial, mandibular, forearm, and phalanx measurements. He also assumed no interbreeding among the three populations. *Artibeus a. major* is the largest of the three subspecies, and *A. a. minor* is the smallest, while *A. a. aztecus* is the least dark subspecies. Later, a study that tested the degree to which the potential distribution of one taxon predicted the geographic distribution of its putative sister taxon and vice versa, using the chi-squared statistic to evaluate statistical significance. The study found that the subspecies *A. a. aztecus* and *A. a. minor* have similar ecological niches ([Peterson et al. 1999](#)). These conclusions were confirmed with the reanalysis of the data using chi-square test statistic and background similarity test using both *I* and *D* metrics ([Warren et al. 2008](#)).

As in other groups of vertebrates ([Fitzpatrick and Turelli 2006](#); [Zink 2012](#); [Heinicke et al. 2017](#)), including bats ([Roberts 2006](#); [Datzmann et al. 2010](#); [Monteiro and Nogueira 2011](#); [Morales-Martínez et al. 2021](#)), geographic isolation is likely driving the diversification process between the central and northern subspecies of the *A. aztecus* distribution. Long-term geographic isolation of populations could lead to the accumulation of genetic or phenotypic differences through neutral or selective processes ([Baker and Bradley 2006](#)). If distinct ecological conditions are present in each region, they may stimulate the divergence process ([Turelli et al. 2001](#); [Kozak and Wiens 2006](#)).

The study of the environmental requirements of species and the possible differences between them can be a useful tool in evaluating the taxonomic status of populations ([Buermann et al. 2008](#); [Lentz et al. 2008](#); [Tocchio et al. 2015](#); [Guevara and Sánchez-Cordero 2018](#)). Ecological niche-based modeling (ENM) is a tool that permits the exploration of geographic and ecological processes by relating species occurrence records with environmental data ([Kozak and Wiens 2006](#); [Phillips et al. 2006](#); [Kozak et al. 2008](#)). ENM may help make taxonomic decisions by making niche comparisons between populations or species or by identifying regions that could isolate them ([Rissler and Apodaca 2007](#); [Martínez-Gordillo et al. 2010](#); [Arribas et al. 2013](#); [Aguilar 2019](#); [Hending 2021](#)).

Here we evaluate the similarities -or differences- between the climatic requirements of the three subspecies of *A. aztecus*, using background similarity tests (as in [Warren et al. 2008](#); but we used a higher number of specimens for each subspecies) and comparing its potential geographic distributions to better understand the ecological resemblance of the subspecies and clarify the taxonomic status of this bat across Mesoamerica. Based on previous studies, we hypothesize that niche conservatism has caused the isolation of *A. aztecus* populations and possible morphological divergence.

Materials and methods

Occurrence data. We collected georeferenced occurrence records for the three populations from the Mammal Collection of the Zoology Museum, UNAM (Facultad de Ciencias – Universidad Nacional Autónoma de México, México City, México, MZFC-M), the Mammal Collection of CIDIR Durango (Centro Interdisciplinario de Investigación para el Desarrollo Integral Regional, Unidad Durango, Instituto Politécnico Nacional, Durango City, México, CRD), and from the databases of VertNet (downloaded on July 27, 2020) and of the Global Biodiversity Information Facility (GBIF, <http://www.gbif.org>; downloaded on April 30, 2021: <https://doi.org/10.15468/dl.e2b69x>), using the name “*Artibeus aztecus*” recorded from 1960 to the present (2020–2021). To reduce sampling bias, we spatially thinned our original data set using the *spThin* package ([Aiello-Lammens et al. 2015](#)) in R 4.0.3. While retaining the greatest number of localities possible, thinning ensured that the distance between all pairs of localities exceeded 10 km ([Boria et al. 2014](#)). Records for the final database are shown in Supplementary material 1. We follow [Baker et al. \(2016\)](#) and [Cirranello et al. \(2016\)](#) in using *Artibeus* rather than *Dermanura* (*contra* [Burgin et al. 2018](#)).

Environmental data. We used 15 bioclimatic variables (Supplementary material 2; [Hijmans et al. 2005](#), www.worldclim.org) at ~5 km resolution, excluding the four layers that combine precipitation and temperature information into the same layer since they show odd spatial anomalies between neighboring pixels ([Escobar et al. 2014](#)), apparently as a consequence of their linked temperature and precipitation variables ([Campbell et al. 2015](#)). We extracted the climatic data using ArcMap (ArcGIS Desktop: Release 10.4).

We used a Pearson correlation test to detect and exclude highly correlated environmental variables. The analysis was performed in R with the library *ntbox* ([Osorio-Olvera et al. 2020](#)), which filters the variables that summarize the environmental information of the presences (occurrences) data according to a correlation threshold; this algorithm suggests which variables to use for the modeling part. The threshold selected for this analysis was $r < 0.7$.

Calibration area. The dispersal capacity of the species, *M* of the BAM diagram in distribution theory ([Soberón and Nakamura 2009](#)), is useful for choosing the calibration area in niche modeling analysis ([Barve et al. 2011](#)). Since the dispersal ability of *A. aztecus* is unknown, we used ArcMap

(ArcGIS Desktop: Release 10.4) to generate the calibration area for each subspecies, with a buffer distance of 1° (~111 km) around occurrences, as a similar distance has been observed in movements of *A. lituratus*, another species of the genus (Arnore et al. 2016).

Ecological niche modelling. We developed niche models for each of the three subspecies of *A. aztecus* using the maximum entropy method implemented in Maxent version 3.4.4 (Phillips et al. 2006). To select the models with the optimal settings for each subspecies, we built various models with all the possible combinations of linear, quadratic, and product features, with different percentages of training locations (25 % and 50 %) and different regularization multipliers (from 0.0 to 2.0 in 0.5 steps), analyzing 70 models for each subspecies. We used 10,000 randomly selected pixels within each generated calibration area as the background sample. All the models were generated and evaluated with the library *kuenm* (Cobos et al. 2019) in R.

We selected the final models based on two evaluation metrics. First, we used partial receiver-operating characteristic (ROC) approaches, as to avoid at least some of the failings of classical ROC approaches (Peterson et al. 2008). We used an acceptable omission error threshold of $E = 5$ and 100 replicate 50% bootstrap resamplings to establish whether the ROC AUC (area under the curve) ratio was above 1.0. Secondly, we used the 5 % training omission rate (OR05), which shows the proportion of test localities with suitability values lower than those excluding the 5 % of training locations with the lowest predicted suitability. Omission rates above the 10% expectation typically indicate model overfitting (Muscarella et al. 2014). The final models were bootstrapped 10 times and we analyzed the data obtained from the average model.

We analyzed and compared the response curves of the three variables with the highest percentage of contribution and permutation importance for each model. The potential distribution of each subspecies were projected to the Mesoamerican region and to generate binary maps, we chose the 10th percentile training presence threshold (Peterson et al. 2007, 2011). We performed these analyses in ArcMap (ArcGIS Desktop: Release 10.4).

Background similarity test. We used background similarity tests to assess niche differentiation between *A. aztecus* subspecies (Warren et al. 2010). This test determines whether ENMs are more similar than expected by chance, based on the geographical regions where each subspecies reside. This type of analysis is particularly important when allopatric populations are being compared because some differences in niches may inevitably follow from the fact that distinct geographic regions rarely encompass identical distributions of environmental variables (Warren et al. 2010). We developed 100 replicate comparisons of each population's known occurrences against the background (points drawn from the accessible area) of the other (sample size matching those available for the "background" popula-

tion). The background similarity tests were performed with the *ENMTools* package version 1.0.4 (Warren et al. 2021) in R.

We assess similarity in pairwise combinations of subspecies using two similarity measures: Schoener's D (1968) and Hellinger's I . These similarity measures are obtained by comparing the estimates of normalized probability calculated for each grid cell of a study area using a Maxent-generated ENM. Both indexes range from 0, when spaces predicted environmental tolerances do not overlap, to 1, when all grid cells are estimated to be equally suitable for both species. Niche similarity is inferred when the observed value falls above the distribution of expected values. In contrast, the difference is inferred when the observed value falls to the left of the distribution (Warren et al. 2010).

Results

We analyzed 151 confirmed *A. aztecus* occurrences: 104 for *A. a. aztecus*, 38 for *A. a. minor*, and 9 for *A. a. major* (Figure 1). Ten of the original climate variables were highly correlated with other variables and were excluded from analysis. For the final analysis, we used: annual mean temperature (bio01), mean diurnal range (bio02), isothermality (bio03), annual precipitation (bio12), and precipitation of the driest month (bio14). Final models with the optimal settings for each subspecies were as follow: *A. a. aztecus*: linear, quadratic, and product features, and regularization multiplier of 1 (Mean AUC ratio: 1.195, OR05: 0.096); *A. a. minor*: linear and quadratic features, and regularization multiplier of 0.5 (Mean AUC ratio: 1.426, OR05: 0.0); and *A. a. major*: linear, quadratic and product features and regularization multiplier of 1.5 (Mean AUC ratio: 1.687, OR05: 0.5).

The most important variable for the model of all the subspecies was the annual mean temperature, while the annual precipitation was the only variable that was not placed between the the three most important models for any model. The second and third variable for each model were: mean diurnal range and precipitation of the driest

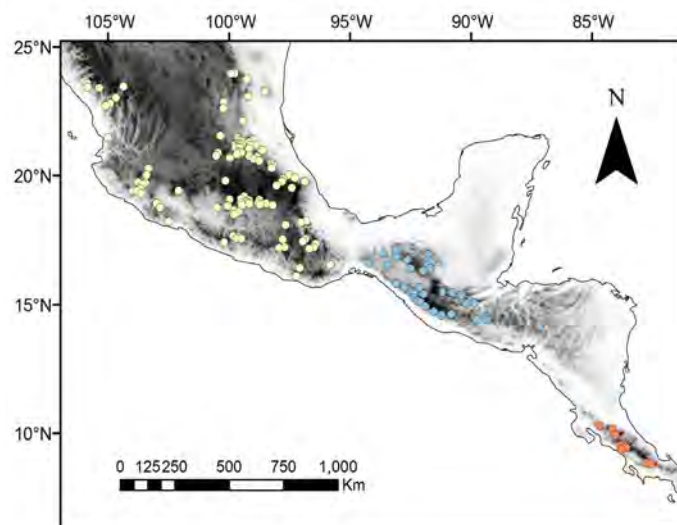


Figure 1. Occurrence records for the three subspecies of *Artibeus aztecus*: *Artibeus aztecus aztecus* (yellow), *Artibeus aztecus minor* (blue) and *Artibeus aztecus major* (light red).

month for *A. a. aztecus*, precipitation of the driest month and isothermality for *A. a. minor*, and isothermality and mean diurnal range for *A. a. major* (Table 1).

Analyzing the response curves for the annual mean temperature, the only important variable in common for the three subspecies, the highest values (> 0.6) of suitability for *A. a. aztecus* are between 14 °C and 20 °C, while for *A. a. minor* they are between 14 and 20 °C, and for *A. a. major* at less than 18 °C (Supplementary material 3). For the mean diurnal range of temperature, in *A. a. aztecus* the highest suitability is between 8 °C and 14.5 °C, while in *A. a. major* it is above 6.5 °C (Supplementary material 3a, c). For the isothermality, the highest suitability for *A. a. minor* was above 70, while for *A. a. major* it was above 76 (Supplementary material 3b, c). For the precipitation of the driest month, the highest suitability for *A. a. aztecus* was found at values over 30 mm and for *A. a. minor* at values between 20 mm and 100 mm (Supplementary material 3a, b).

All potential distribution models showed close correspondence to known distributions of the three populations, showing an association with the highlands of México and Central America (Figure 2). We found relatively wide distributions for the three subspecies, so each model predicted potential distribution areas corresponding with the distribution of the other subspecies. For the three models, the montane regions were separated by less-suitable lowland areas (≤ 500 m), representing potential barriers to the dispersal of each subspecies (e.g., the Isthmus of Tehuantepec and the Nicaraguan Depression).

Pairwise comparisons indicated that *A. a. aztecus* and *A. a. major* have the lowest niche overlap ($D = 0.246$, $I = 0.485$) and *A. a. aztecus* and *A. a. minor* have the highest niche similarity ($D = 0.405$, $I = 0.731$). Observed Schoener's

Table 1. Percentage of contribution and permutation importance of climatic variables used in MaxEnt model for each subspecies of *Artibeus aztecus*.

| Subspecies | Variable | Percentage of contribution | Permutation importance |
|----------------------|-------------------------------|----------------------------|------------------------|
| <i>A. a. aztecus</i> | Annual mean temperature | 55.5 | 52 |
| | Mean diurnal range | 36.8 | 37.7 |
| | Precipitation of driest month | 2.7 | 3.3 |
| | Isothermality | 2.7 | 0.8 |
| | Annual precipitation | 2.3 | 6.2 |
| <i>A. a. minor</i> | Annual mean temperature | 75.8 | 46.3 |
| | Precipitation of driest month | 10.9 | 13.3 |
| | Isothermality | 9.1 | 25 |
| | Annual precipitation | 2.9 | 13.7 |
| | Mean diurnal range | 1.3 | 1.6 |
| <i>A. a. major</i> | Annual mean temperature | 91.4 | 87.5 |
| | Isothermality | 5.7 | 5 |
| | Mean diurnal range | 2.1 | 6.8 |
| | Annual precipitation | 0.8 | 0.7 |
| | Precipitation of driest month | 0 | 0 |

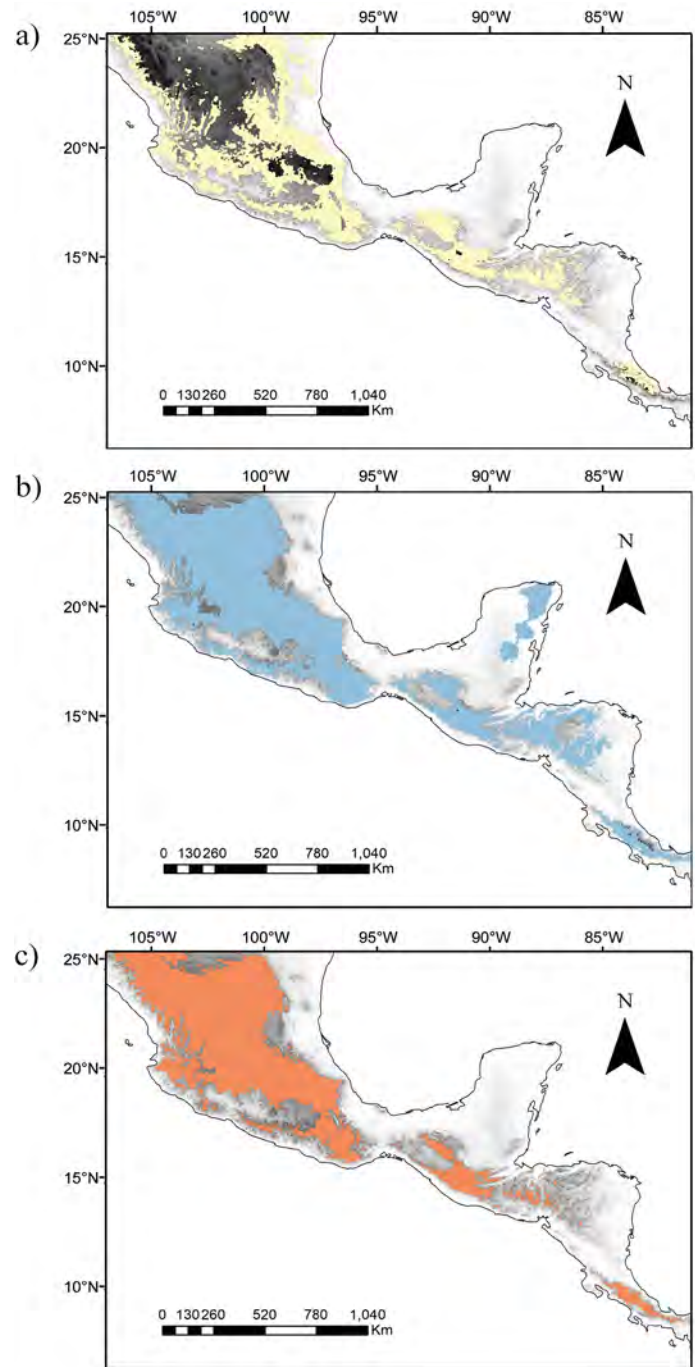


Figure 2. Maxent predicted potential distribution for (a) *Artibeus a. aztecus*, (b) *A. a. minor*, and (c) *A. a. major*.

D and Hellinger's I values were significantly low compared to the null distribution in all cases (Figure 3). Comparisons involving *A. a. minor* showed D and I values closer to those from the left tail of the null distributions, but significantly different than expected (Figure 3a, c). In sum, background similarity tests indicated that the ecological niche models of the three subspecies were more different than expected by chance (Table 2).

Discussion

Potential distributions and geographical barriers. The niche models and potential distribution maps seem to support the findings of the habitat preference of the Aztec fruit-

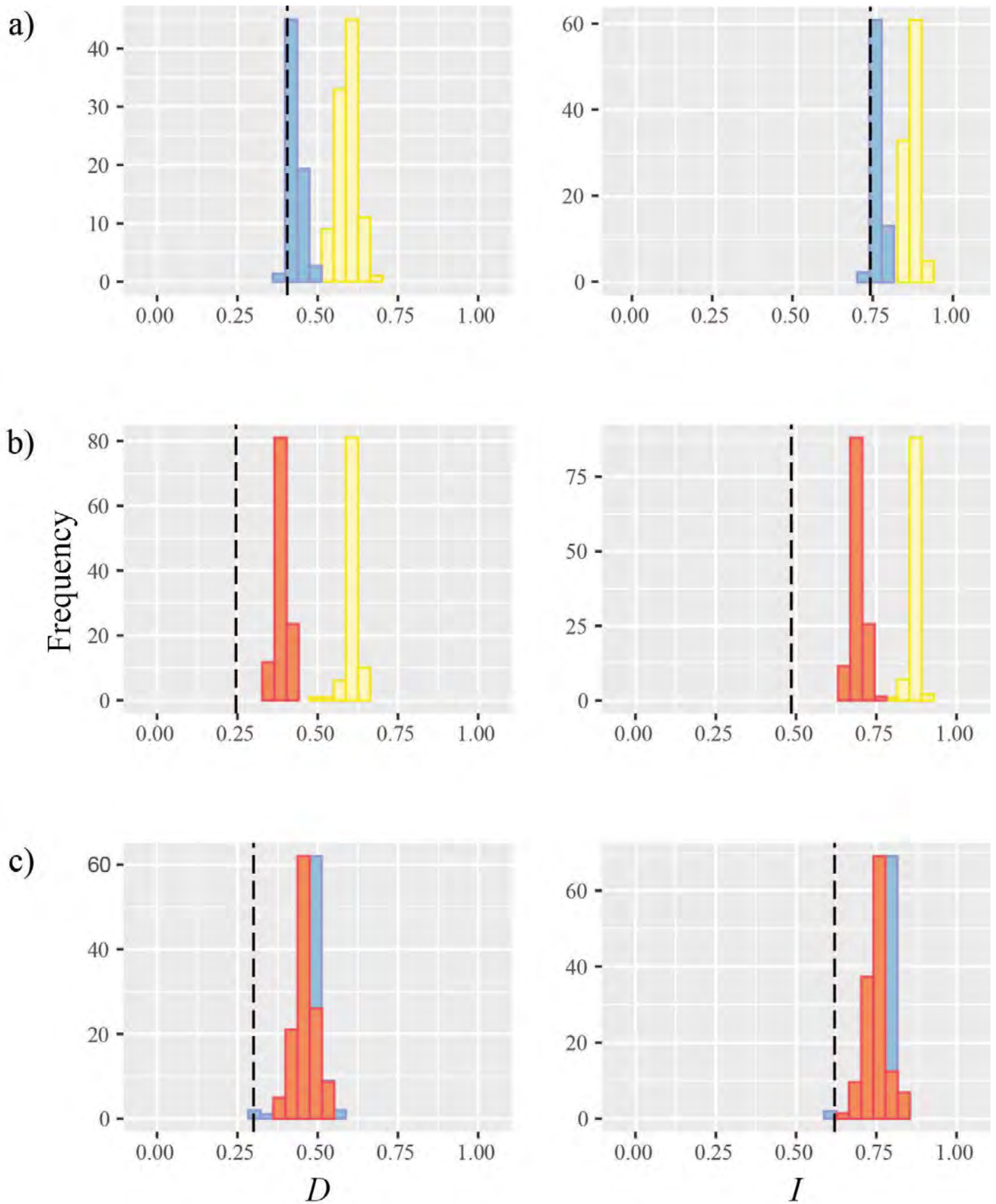


Figure 3. Niche overlap values for Schoener's D and Hellinger's I compared to a null distribution: (a) *Artibeus a. aztecus* (yellow) vs. *A. a. minor* (blue), (b) *A. a. aztecus* vs. *A. A. major* (red), (c) *A. a. minor* vs. *A. A. major*.

eating bat populations reported previously. Mesoamerican highlands, where the models indicate the potential distribution for each subspecies, include a complex assemblage of montane ecosystems containing high biodiversity and endemism (Parra-Olea *et al.* 2012; Bryson *et al.* 2018; Blair *et al.* 2019). Less-suitable areas, such as the Isthmus of Tehuantepec and the Nicaraguan Depression, may act as current geographic barriers to dispersal, limiting contact between the populations, as proposed previously for the subspecies *A. a. aztecus* and *A. a. minor* (Davis 1969; Peterson *et al.* 1999).

Isthmus of Tehuantepec has been proposed as a biogeographic barrier associated with allopatric speciation in a broad range of taxa (Sullivan *et al.* 2000; León-Paniagua *et al.* 2007; Castoe *et al.* 2009; Daza *et al.* 2010; Rodríguez-Gómez *et al.* 2013, 2021) and, climatically, has been considered a barrier for dispersal of oak species, and by separating tropical ecosystems from those with more substantial Nearctic influence (Rodríguez-Correa *et al.* 2015). The climatic effect of this barrier on the subspecies *A. a. aztecus* and *A. a. minor* contrasts with the similar niches found between two haplogroups of the Honduran yellow-shouldered bat *Sturnira hondurensis*, another Mesoamerican highland bat (Hernández-Canchola 2018).

On the other hand, the Nicaraguan Depression has been considered a major feature determining genetic and biogeographic patterns (Gutiérrez-García and Vázquez-Domínguez 2013). The evolutionary impact of this barrier is reflected in genetic differentiation between sister taxa of vertebrates, including birds (Puebla-Olivares *et al.* 2008; Arbeláez-Cortés *et al.* 2010) and snakes (Castoe *et al.* 2009). Our findings about the separation between *A. a. minor* and *A. a. major* are similar to the conclusions of Torres-Morales (2019), who considered Nicaraguan Depression as a significant barrier that limits the distribution of *Sturnira hondurensis*, separating it from its sister species *S. burtonlimi*.

Speciation, and species limits. There is a debate about how conserved the niches between closely related lineages are (Wiens and Graham 2005). Some previous studies have suggested the presence of phylogenetic niche conservatism in phyllostomid bats (Peterson *et al.* 1999; Stevens 2006, 2011; Warren *et al.* 2008), indicating that closely related species share the same climatic preferences. Alternatively, other authors have not found strong support for niche conservatism in phyllostomid bats (Peixoto *et al.* 2017), suggesting their niche may have evolved either under strong selection or randomly (Diniz-Filho *et al.* 2010).

However, former phylogenetic niche conservatism may promote ecological speciation. It can occur in areas with high geographic and ecological variations. In such regions, any geographic distance also results in environmental distance, promoting niche divergence. The combined topographic variation and ecological distance reduce dispersal and gene flow between adjacent populations (Gascon *et al.* 2000; Gehring *et al.* 2012). Lineages may thus adapt to local niches, leading populations to diverge from the ancestral niche (Pyron *et al.* 2015).

Table 2. Results of the background similarity pairwise comparisons among the three subspecies of *Artibeus aztecus*. Observed Schoener's *D* and Hellinger's *I* values and *p*-values (*p*-val) are shown.

| Test | D | p - val | I | p - val |
|---|-------|---------|-------|---------|
| <i>Artibeus a. aztecus</i> vs <i>A. a. minor</i> background | 0.405 | 0.01 | 0.731 | 0.01 |
| <i>Artibeus a. aztecus</i> vs <i>A. a. major</i> background | 0.246 | 0.01 | 0.485 | 0.01 |
| <i>Artibeus a. minor</i> vs <i>A. a. aztecus</i> background | 0.405 | 0.04 | 0.731 | 0.03 |
| <i>Artibeus a. minor</i> vs <i>A. a. major</i> background | 0.300 | 0.03 | 0.620 | 0.03 |
| <i>Artibeus a. major</i> vs <i>A. a. aztecus</i> background | 0.246 | 0.01 | 0.485 | 0.01 |
| <i>Artibeus a. major</i> vs <i>A. a. minor</i> background | 0.300 | 0.01 | 0.620 | 0.01 |

Here, we found signals of ecological niche differentiation among the three subspecies of Aztec fruit-eating bat (Tables 1 and 2, Figures 2 and 3). The three subspecies of *A. aztecus* present different climatic preferences that may indicate they are evolving independently. Therefore, further studies are necessary to learn about the evolutionary history of *A. aztecus* and clarify the taxonomic situation of the three subspecies. Certainly, it is crucial to consider that the outcome and the interpretation of the similarity tests may be sensitive to the definition of the calibration area and environmental background (Warren *et al.* 2010), still, they may offer some guidelines to explore speciation mechanisms (Tocchio *et al.* 2015) and thus determine the taxonomic status of the species. In this study, we defined it using the movement data of a congeneric species of *A. aztecus*, so the results must be carefully interpreted. Further details on the dispersal capacity for each subspecies might improve reference area estimation for niche models.

It is essential to clarify the phylogenetic relationships among the subspecies to better understand their biogeographic history (Martínez-Gordillo *et al.* 2010). Studies that analyzed the diversification of *Artibeus* and the subgenus *Dermanura*, have included a few samples of at least two subspecies, but not *A. a. major* (Owen 1987; Hooper *et al.* 2008; Redondo *et al.* 2008; Solari *et al.* 2009; Baker *et al.* 2016). Solari *et al.* (2009) recovered two clades of *A. aztecus*, represented by samples of *A. a. aztecus* and *A. a. minor*, with a genetic divergence of 3.6 % between them, a value that falls in the range necessary for species recognition suggested by Baker and Bradley (2006), so it is crucial to analyze the genetic divergence between the species using a larger number of samples that includes the three subspecies. In addition, morphological analyses that include all subspecies are necessary to assess phenotypic variation and its potential correlation with environmental conditions. A relationship between environmental conditions and morphology has been documented in other Mesoamerican montane species (Rodríguez-Gómez *et al.* 2013, 2021; Hernández-Canchola 2018).

In sum, our results offer a first look at the ecological variation of *Artibeus aztecus* and an additional view on understanding the processes that have shaped the diversification of montane bats in Mesoamerica. Climatic divergence among the three subspecies probably are due to the inter-

action between former ecological niche conservatism and the emergence of geographic barriers, such as the Isthmus of Tehuantepec and the Nicaraguan Depression that promoted the subsequent ecological differentiation.

Acknowledgements

We thank the Posgrado en Ciencias Biológicas of the Universidad Nacional Autónoma de México (UNAM) and the Consejo Nacional de Ciencia y Tecnología (CONACyT, CVU 1002851) for their support for IHC's masters courses. We thank the following curators and collection managers: Y. Gómez (Mammal Collection of the Zoology Museum of Facultad de Ciencias, UNAM), C. López-González (Mammal Collection of CIDIR Durango, IPN).

Literature cited

- AGUILAR, J. M. 2019. Geographic distribution analysis of the genus *Xenodacnis* (Birds: Thraupidae) using ecological niche modeling. *Revista Peruana de Biología* 26:317–324.
- AIELLO-LAMMENS, M. E., ET AL. 2015. spThin: an R package for spatial thinning of species occurrence records for use in ecological niche models. *Ecography* 38:541–545.
- ANDERSEN, K. 1906. LXI. — Brief diagnoses of a new genus and ten new forms of *Stenodermatous* bats. *Journal of Natural History Series* 7 18:419–423.
- ARBELÁEZ-CORTÉS, E., Á. S. NYÁRI, AND A. G. NAVARRO-SIGÜENZA. 2010. The differential effect of lowlands on the phylogeographic pattern of a Mesoamerican montane species (*Lepidocolaptes affinis*, Aves: Furnariidae). *Molecular Phylogenetics and Evolution* 57:658–668.
- ARNONE, I. S., ET AL. 2016. Long-distance movement by a great fruit-eating bat, *Artibeus lituratus* (Olfers, 1818), in southeastern Brazil (Chiroptera, Phyllostomidae): evidence for migration in Neotropical bats? *Biota Neotropica* 16:1–6.
- ARRIBAS, P., ET AL. 2013. Integrative taxonomy and conservation of cryptic beetles in the Mediterranean region (Hydrophilidae). *Zoologica Scripta* 42:182–200.
- BAKER, R. J., AND R. D. BRADLEY. 2006. Speciation in mammals and the genetic species concept. *Journal of Mammalogy* 87:643–662.
- BAKER, R. J., ET AL. 2016. Higher level classification of Phyllostomid bats with a summary of DNA synapomorphies. *Acta Chiropterologica* 18:1–38.
- BARVE, N., ET AL. 2011. The crucial role of the accessible area in ecological niche modeling and species distribution modeling. *Ecological Modelling* 222:1810–1819.
- BLAIR, C., ET AL. 2019. Cryptic diversity in the Mexican highlands: Thousands of UCE loci help illuminate phylogenetic relationships, species limits and divergence times of montane rattlesnakes (Viperidae: *Crotalus*). *Molecular Ecology Resources* 19:349–365.
- BORIA, R. A., ET AL. 2014. Spatial filtering to reduce sampling bias can improve the performance of ecological niche models. *Ecological Modelling* 275:73–77.
- BRIONES, M., ET AL. 2019. Responses of phyllostomid bats to traditional agriculture in Neotropical montane forests of Southern Mexico. *Zoological Studies* 58:e9.
- BRYSON, R. W., ET AL. 2018. Phylogenomic insights into the diversification of salamanders in the *Isthmura bellii* group across the Mexican highlands. *Molecular Phylogenetics and Evolution* 125:78–84.
- BUERMANN, W., ET AL. 2008. Predicting species distributions across the Amazonian and Andean regions using remote sensing data. *Journal of Biogeography* 35:1160–1176.
- BURGIN, C. J., ET AL. 2018. How many species of mammals are there? *Journal of Mammalogy* 99:1–14.
- CAMPBELL, L., ET AL. 2015. Climate change influences on global distributions of dengue and chikungunya virus vectors. *Philosophical Transactions of the Royal Society B: Biological Sciences* 370:20140135.
- CASTAÑEDA-RICO, S. S. 2005. Variación geográfica de *Dermanura azteca* (Chiroptera: Phyllostomidae) en la República Mexicana (Bachelor thesis). Universidad Nacional Autónoma de México.
- CASTOE, T. A., ET AL. 2009. Comparative phylogeography of pitvipers suggests a consensus of ancient Middle American highland biogeography. *Journal of Biogeography* 36:88–103.
- CERÓN-HERNÁNDEZ, J. A., ET AL. 2022. Diversidad, tipos de dieta de murciélagos y su respuesta a bordes de bosque mesófilo de montaña, Veracruz, México. *Ecosistemas y Recursos Agropecuarios* 9:e3110.
- CIRRANELLO, A., ET AL. 2016. Morphological diagnoses of higher-level Phyllostomid taxa (Chiroptera: Phyllostomidae). *Acta Chiropterologica* 18:39–71.
- COBOS, M. E., ET AL. 2019. kuenm: an R package for detailed development of ecological niche models using Maxent. *PeerJ*:1–15.
- DATZMANN, T., O. VON HELVERSEN, AND F. MAYER. 2010. Evolution of nectarivory in phyllostomid bats (Phyllostomidae Gray, 1825, Chiroptera: Mammalia). *BMC Evolutionary Biology* 10:1–14.
- DAVIS, W. B. 1969. A review of the small fruit bats (genus *Artibeus*) of Middle America. *The Southwestern Naturalist* 14:15–29.
- DAZA, J. M., T. A. CASTOE, AND C. L. PARKINSON. 2010. Using regional comparative phylogeographic data from snake lineages to infer historical processes in Middle America. *Ecography* 33:343–354.
- DINIZ-FILHO, J. A. F., ET AL. 2010. Hidden patterns of phylogenetic non-stationarity overwhelm comparative analyses of niche conservatism and divergence. *Global Ecology and Biogeography* 19:916–926.
- ESCOBAR, L. E., ET AL. 2014. Potential for spread of the white-nose fungus (*Pseudogymnoascus destructans*) in the Americas: Use of Maxent and NicheA to assure strict model transference. *Geospatial Health* 9:221–229.
- FITZPATRICK, B. M., AND M. TURELLI. 2006. The geography of mammalian speciation: mixed signals from phylogenies and range maps. *Evolution* 60:601–615.
- GASCON, C., ET AL. 2000. Riverine barriers and the geographic distribution of Amazonian species. *Proceedings of the National Academy of Sciences of the United States of America* 97:13672–13677.
- GEHRING, P. S., ET AL. 2012. The influence of riverine barriers on phylogeographic patterns of Malagasy reed frogs (*Heterixalus*). *Molecular Phylogenetics and Evolution* 64:618–632.
- GUEVARA, L., AND V. SÁNCHEZ-CORDERO. 2018. Patterns of morphological and ecological similarities of small-eared shrews (Soricidae, *Cryptotis*) in tropical montane cloud forests from Mesoamerica. *Systematics and Biodiversity*:1–14.

- GUTIÉRREZ-GARCÍA, T. A., AND E. VÁZQUEZ-DOMÍNGUEZ. 2013. Consensus between genes and stones in the biogeographic and evolutionary history of Central America. *Quaternary Research (United States)* 79:311–324.
- HEINICKE, M. P., T. R. JACKMAN, AND A. M. BAUER. 2017. The measure of success: geographic isolation promotes diversification in *Pachydactylus geckos*. *BMC Evolutionary Biology* 17:1–17.
- HENDING, D. 2021. Niche-separation and conservation biogeography of Madagascar's fork-marked lemurs (Cheirogaleidae: *Phaner*): Evidence of a new cryptic species? *Global Ecology and Conservation* 29:e01738.
- HERNÁNDEZ-CANCHOLA, G. 2018. Diversificación de dos especies del género *Sturnira* (Chiroptera: Phyllostomidae) en Mesoamérica (PhD thesis). Universidad Nacional Autónoma de México.
- HUIJMAN, R. J., ET AL. 2005. Very high resolution interpolated climate surfaces for global land areas. *International Journal of Climatology* 25:1965–1978.
- HOOPER, S. R., ET AL. 2008. Phylogenetics of the fruit-eating bats (Phyllostomidae: Artibeina) inferred from mitochondrial DNA sequences. *Occasional Papers, Museum of Texas Tech University*:1–15.
- JIMÉNEZ, R. A., AND J. F. ORNELAS. 2016. Historical and current introgression in a Mesoamerican hummingbird species complex: a biogeographic perspective. *PeerJ* 2016.
- JORDANO, P., ET AL. 2011. Frugivores and seed dispersal: mechanisms and consequences for biodiversity of a key ecological interaction. *Biology Letters* 7:321–323.
- KRAKER-CASTAÑEDA, C., ET AL. 2017. Responses of phyllostomid bats to forest cover in upland landscapes in Chiapas southeast Mexico. *Studies on Neotropical Fauna and Environment*: 1–10.
- KOZAK, K. H., C. H. GRAHAM, AND J. J. WIENS. 2008. Integrating GIS-based environmental data into evolutionary biology. *Trends in Ecology and Evolution* 23:141–148.
- KOZAK, K. H., AND J. J. WIENS. 2006. Does niche conservatism promote speciation? a case study in North American salamanders. *Evolution* 60:2604–2621.
- LENTZ, D. L., R. BYE, AND V. SÁNCHEZ-CORDERO. 2008. Ecological niche modeling and distribution of wild sunflower (*Helianthus annuus* L.) in Mexico. *International Journal of Plant Sciences* 169:541–549.
- LEÓN-PANIAGUA, L., ET AL. 2007. Diversification of the arboreal mice of the genus *Habromys* (Rodentia: Cricetidae: Neotominae) in the Mesoamerican highlands. *Molecular Phylogenetics and Evolution* 42:653–664.
- LÓPEZ-GONZÁLEZ, C., AND D. F. GARCÍA-MENDOZA. 2006. Murciélagos de la Sierra Tarahumara, Chihuahua, México. *Acta Zoológica Mexicana* 22:109–135.
- LORENZO, C., ET AL. 2017. Diversidad y conservación de los mamíferos terrestres de Chiapas, México. *Revista Mexicana de Biodiversidad* 88:735–754.
- MARTÍNEZ-GORDILLO, D., O. ROJAS-SOTO, AND A. ESPINOSA DE LOS MONTEROS. 2010. Ecological niche modelling as an exploratory tool for identifying species limits: An example based on Mexican murid rodents. *Journal of Evolutionary Biology* 23:259–270.
- MEDINA-VAN BERKUM, P., ET AL. 2020. Community of bats in Cusco National Park, Honduras, a Mesoamerican Cloud Forest, including new regional and altitudinal records. *Neotropical Naturalist* 3:1–24.
- MONTEIRO, L. R., AND M. R. NOGUEIRA. 2011. Evolutionary patterns and processes in the radiation of phyllostomid bats. *BMC Evolutionary Biology* 11:1–23.
- MORALES-MARTÍNEZ, D. M., H. F. LÓPEZ-ARÉVALO, AND M. VARGAS-RAMÍREZ. 2021. Beginning the quest: Phylogenetic hypothesis and identification of evolutionary lineages in bats of the genus *Micronycteris* (Chiroptera, Phyllostomidae). *ZooKeys* 1028:135–159.
- MUSCARELLA, R., ET AL. 2014. ENMeval: An R package for conducting spatially independent evaluations and estimating optimal model complexity for Maxent ecological niche models. *Methods in Ecology and Evolution* 5:1198–1205.
- OSORIO-OLVERA, L., ET AL. 2020. ntbox: An R package with graphical user interface for modelling and evaluating multidimensional ecological niches. *Methods in Ecology and Evolution* 11:1199–1206.
- OWEN, R. D. 1987. Phylogenetic analyses of the bat subfamily Stenodermatinae (Mammalia: Chiroptera). *Special Publications of the Museum Texas Tech University* 26:1–65.
- PARRA-OLEA, G., ET AL. 2012. Isolation in habitat refugia promotes rapid diversification in a montane tropical salamander. *Journal of Biogeography* 39:353–370.
- PEIXOTO, F. P., F. VILLALOBOS, AND M. V. CIANCARUSO. 2017. Phylogenetic conservatism of climatic niche in bats. *Global Ecology and Biogeography* 26:1055–1065.
- PETERSON, A. T., ET AL. 2008. Rethinking receiver operating characteristic analysis applications in ecological niche modeling. *Ecological Modelling* 213:63–72.
- PETERSON, A. T., ET AL. 2011. *Ecological niches and geographic distributions*. Princeton University Press, New Jersey.
- PETERSON, A. T., M. PAPEŞ, AND M. EATON. 2007. Transferability and model evaluation in ecological niche modeling: a comparison of GARP and Maxent. *Ecography* 30:550–560.
- PETERSON, A. T., J. SOBERÓN, AND V. SÁNCHEZ-CORDERO. 1999. Conservatism of ecological niches in evolutionary time. *Science* 285:1265–1267.
- PHILLIPS, S. J., R. P. ANDERSON, AND R. E. SCHAPIRE. 2006. Maximum entropy modeling of species geographic distributions. *Ecological Modelling* 190:231–259.
- PINEDA-LIZANO, W., AND G. CHAVERRI. 2022. Spatio-temporal distribution and reproductive phenology of Neotropical bat species in an altitudinal gradient in Costa Rica. *Mammalian Biology* 102:1–12.
- PUEBLA-OLIVARES, F., ET AL. 2008. Speciation in the emerald toucanet (*Aulacorhynchus prasinus*) complex. *The Auk* 125:39–50.
- PYRON, R. A., ET AL. 2015. Phylogenetic niche conservatism and the evolutionary basis of ecological speciation. *Biological Reviews* 90:1248–1262.
- REDONDO, R. A. F., ET AL. 2008. Molecular systematics of the genus *Artibeus* (Chiroptera: Phyllostomidae). *Molecular Phylogenetics and Evolution* 49:44–58.
- RISSLER, L. J., AND J. J. APODACA. 2007. Adding more ecology into species delimitation: ecological niche models and phylogeography help define cryptic species in the black salamander (*Aneides flavipunctatus*). *Systematic Biology* 56:924–942.
- ROBERTS, T. E. 2006. Multiple levels of allopatric divergence in the endemic Philippine fruit bat *Haplonycteris fischeri* (Pteropodidae). *Biological Journal of the Linnean Society* 88:329–349.

- RODRÍGUEZ-CORREA, H., ET AL. 2015. How are oaks distributed in the neotropics? A perspective from species turnover, areas of endemism, and climatic niches. *International Journal of Plant Sciences* 176:222–231.
- RODRÍGUEZ-GÓMEZ, F., C. GUTIÉRREZ-RODRÍGUEZ, AND J. F. ORNELAS. 2013. Genetic, phenotypic and ecological divergence with gene flow at the Isthmus of Tehuantepec: the case of the azure-crowned hummingbird (*Amazilia cyanocephala*). *Journal of Biogeography* 40:1360–1373.
- RODRÍGUEZ-GÓMEZ, F., ET AL. 2021. Phylogeography, morphology and ecological niche modelling to explore the evolutionary history of Azure-crowned Hummingbird (*Amazilia cyanocephala*, Trochilidae) in Mesoamerica. *Journal of Ornithology* 162:529–547.
- SALDAÑA-VÁZQUEZ, R. A. 2014. Intrinsic and extrinsic factors affecting dietary specialization in Neotropical frugivorous bats. *Mammal Review* 44:215–224.
- SCHOENER, T. W. 1968. The *Anolis* lizards of Bimini: resource partitioning in a complex fauna. *Ecology* 49:704–726.
- SEGURA-TRUJILLO, C. A., AND S. NAVARRO-PÉREZ. 2010. Escenario y problemática de conservación de los murciélagos (Chiroptera) cavernícolas del Complejo Volcánico de Colima, Jalisco-Colima, México. *Therya* 1:189–206.
- SOBERÓN, J., AND M. NAKAMURA. 2009. Niches and distributional areas: concepts, methods and assumptions. *Proceedings of the National Academy of Sciences* 106:19644–19650.
- SOLARI, S., ET AL. 2009. Operational criteria for genetically defined species: analysis of the diversification of the small fruit-eating bats, *Dermanura* (Phyllostomidae: Stenodermatinae). *Acta Chiropterológica* 11:279–288.
- SOLARI, S., ET AL. 2019. Family Phyllostomidae. Pp. 444–583, in *Handbook of the Mammals of the World - Volume 9. Bats* (Wilson, D. E., and R. A. Mittermeier, eds.). Lynx Edicions. Barcelona, Spain.
- STEVENS, R. D. 2006. Historical processes enhance patterns of diversity along latitudinal gradients. *Proceedings of the Royal Society B: Biological Sciences* 273:2283–2289.
- STEVENS, R. D. 2011. Relative effects of time for speciation and tropical niche conservatism on the latitudinal diversity gradient of phyllostomid bats. *Proceedings of the Royal Society B: Biological Sciences* 278:2528–2536.
- SULLIVAN, ARELLANO, AND ROGERS. 2000. Comparative phylogeography of Mesoamerican highland rodents: concerted versus independent response to past climatic fluctuations. *The American Naturalist* 155:755.
- TOCCHIO, L. J., R., ET AL. 2015. Niche similarities among white-eared opossums (Mammalia, Didelphidae): Is ecological niche modelling relevant to setting species limits? *Zoologica Scripta* 44:1–10.
- TORRES-MORALES, L. 2019. Límites de distribución actual de *Sturnira hondurensis*. *Revista Mexicana de Biodiversidad* 90:1–9.
- TURELLI, M., N. H. BARTON, AND J. A. COYNE. 2001. Theory of Speciation. *Trends in Ecology and Evolution* 16:330–343.
- WANG, B. C., AND T. B. SMITH. 2002. Closing the seed dispersal loop. *Trends in Ecology and Evolution* 17:379–386.
- WARREN, D. L., ET AL. 2021. ENMTools 1.0: an R package for comparative ecological biogeography. *Ecography* 44:1–8.
- WARREN, D. L., R. E. GLOR, AND M. TURELLI. 2008. Environmental niche equivalency versus conservatism: quantitative approaches to niche evolution. *Evolution* 62:2868–2883.
- WARREN, D. L., R. E. GLOR, AND M. TURELLI. 2010. ENMTools: a toolbox for comparative studies of environmental niche models. *Ecography* 33:607–611.
- WIENS, J. J., AND C. H. GRAHAM. 2005. Niche conservatism: integrating evolution, ecology, and conservation biology. *Annual Review of Ecology, Evolution, and Systematics* 36:519–539.
- ZAMORA-MEJÍAS, D., AND B. RODRÍGUEZ-HERRERA. 2017. Murciélagos (Chiroptera) del bosque premontano de San Ramón, Costa Rica. *Revista Pnesamiento Actual* 17:105–113.
- ZINK, R. M. 2012. The geography of speciation: case studies from birds. *Evolution: Education and Outreach* 5:541–546.

Associated editor: Jake Esselstyn and Giovani Hernández Canchola

Submitted: July 26, 2022; Reviewed: November 30, 2022

Accepted: December 1, 2022; Published on line: January 27, 2023

Habitat use, richness, and abundance of native mice in the highlands of the Talamanca mountain range, Costa Rica

JOSÉ D. RAMÍREZ-FERNÁNDEZ^{1*}, GILBERT BARRANTES², CATALINA SÁNCHEZ-QUIRÓS², AND BERNAL RODRÍGUEZ-HERRERA^{2,3}

¹ Fundación Costa Rica Wildlife. Sabanilla, Montes de Oca, CP. 11502. San José, Costa Rica. Email: jramirez@costaricawildlife.org (JDR-F).

² Escuela de Biología, Universidad de Costa Rica. Ciudad Universitaria Rodrigo Facio, CP. 2060. San José, Costa Rica. Email: gilbert.barrantes@gmail.com (GB); catasq@gmail.com (CS).

³ Centro de Investigación en Biodiversidad y Ecología Tropical (CIBET), Universidad de Costa Rica. San Pedro, Montes de Oca, CP. 2060. San José, Costa Rica. Email: bernal.rodriguez@ucr.ac.cr (BR-H).

*Corresponding author: <https://orcid.org/0000-0003-1050-5849>.

The Costa Rican highlands are considered hotspots of diversity and endemism, but studies on rodents are scarce. We compared the richness and abundance of mice between the montane forest and the paramo at the summit of the Talamanca mountain range. We selected two study sites within the Talamanca mountain range: the Cerro de la Muerte Biological Station and the paramo. The former is a montane forest dominated by oaks, and the latter is dominated by an herbaceous layer, and some scattered bushy patches. We captured mice in two different microhabitats within each montane forest and paramo, so we had four different sampling microhabitats: (1) paramo–bush, (2) paramo–*Chusquea*, (3) montane forest–bush, and (4) montane forest–*Chusquea*. Mice were marked to identify recaptures. We captured four mouse species and their abundance varied largely between habitats and among microhabitats (Table 1). The most abundant species, representing 85 % of all mouse captures, was *Peromyscus nudipes*. Mice were more abundant in the montane forest than in the paramo. Within the montane forest, mice were more abundant in the microhabitat containing bushes. The montane forest has a more complex vegetation structure with more diversity of food resources and shelters than the paramo. As well as at the habitat level, we argue that differences in abundance among microhabitats are directly related with the structure of vegetation. A more complex habitat structure may provide rodents with better conditions.

Las tierras altas de Costa Rica son consideradas un punto caliente de diversidad y endemismo, pero los estudios sobre roedores son escasos. Comparamos la riqueza y abundancia de ratones entre el bosque de robledal y el páramo en la cima de la Cordillera de Talamanca. Seleccionamos dos sitios de estudio en la Cordillera de Talamanca: la Estación Biológica Cerro de la Muerte y el páramo. El primero es un bosque montano dominado por robles, y el segundo está dominado por una vegetación herbácea y algunos parches dispersos de arbustos. Capturamos ratones en dos microhábitats diferentes en el robledal y el páramo. Por lo que tuvimos cuatro microhábitats de muestreo: (1) páramo–arbustos, (2) páramo–*Chusquea*, (3) bosque montano–arbustos, y (4) bosque montano–*Chusquea*. Los ratones fueron marcados para identificar recapturas. Capturamos cuatro especies de ratones y sus abundancias variaron considerablemente entre hábitats y microhábitats (Tabla 1). La especie más abundante, con 85 % del total de capturas, fue *Peromyscus nudipes*. Los ratones fueron más abundantes en el robledal que en el páramo. Dentro del robledal, los ratones fueron más abundantes en el microhábitat compuesto por arbustos. El bosque montano posee una estructura vegetal más compleja, con mayor diversidad de recursos alimenticios y refugios que el páramo. Al igual que a nivel de hábitat, discutimos que las diferencias en abundancia entre microhábitats están directamente relacionadas con la estructura de la vegetación. Un hábitat con una estructura más compleja es de esperar que provea a los roedores de mejores condiciones.

Keywords: Cerro de la Muerte; *Chusquea*; Cricetidae; endemic mice; montane forest; paramo; *Peromyscus*; species richness.

© 2023 Asociación Mexicana de Mastozoología, www.mastozoologiamexicana.org

Introduction

Climate change has been identified as one of the main threats to highland ecosystems in the tropics (Epstein 2000; Hughes 2000; Hilbert *et al.* 2004; Rull and Vegas-Vilarrúbia 2006; Laurance *et al.* 2011). In Costa Rica, the negative effects of this global phenomenon have been modeled for highland amphibians, reptiles, and birds (Pounds *et al.* 1999, 2006; Karmalkar *et al.* 2008). As a consequence of climate change, the temperature, dry season length, and number of dry days have increased in tropical highlands (Pounds *et al.* 1999).

These climatic changes have affected the distribution and interaction of species along tropical altitudinal gradients. Many middle elevation species have recently

expanded the upper limit of their altitudinal distribution, moving into the habitat of those species that occur at highest elevations (Morales-Betancourt and Estévez-Varón 2006; Dirnböck *et al.* 2010; Bellard *et al.* 2012; Ripple *et al.* 2014). However, species that inhabit the summit of tropical mountains are trapped in sky islands as their habitat contracts and competition with lowland invading species increases. The synergistic effect of these factors imposes a serious extinction threat on endemic and highland-restricted species (Thomas *et al.* 2004; Malcom *et al.* 2006; Urban 2015; Pyšek *et al.* 2017).

In Costa Rica, the highlands have relatively low diversity but a high percentage of endemic species from different taxonomic groups (Barrantes 2005; Vargas and Sánchez

2005; Barrantes *et al.* 2019). For instance, 22 (73 %) mammal species are endemic at middle and high elevations (Ramírez-Fernández *et al.* in press), and in the highlands many of these species accomplish an important ecological role, such as the dispersal of seed and fungal spores (Lacher *et al.* 2016).

Most Costa Rican mammal research has centered on lowland habitats. Thus, information on the highlands is scarce and fragmented (Carrillo *et al.* 2005). Considering that rodents are an abundant component of the highland fauna (González-Maya *et al.* 2015), and that their role as seed and arthropod predators, fungal spore and seed dispersers, and prey for birds and larger mammals is important, we sought to quantify the richness and abundance of the mice community in the high montane forest and the paramo in the Talamanca mountain range. This is the largest and highest Costa Rican mountain range, and it is recognized as the terrestrial region with the highest endemism in Central America (Holz and Gradstein 2005; Powell *et al.* 2022).

Materials and methods

Study site. To conduct this research, we selected two study sites in the highlands of the Costa Rican Talamanca mountain range: the Cerro de la Muerte Biological Station (CMBS) and the paramo (Figure 1). The CMBS is located in the high montane oak forest at an elevation of 3,100 m (9° 33' N, -83° 44' W) and the paramo at 3,400 m elevation (9° 33' 20" N, -83° 45' 41" W). The two sites are separated by a distance of 2.5 km. The mean annual precipitation is 2,500 mm, with a relatively dry period between December and April, with a mean annual temperature 11° C for the CMBS and 7.6° C for the paramo (Herrera 2005). The temperature oscillates drastically during the day, particularly in the paramo (-5° to 35°). Forests dominated by oaks (*Quercus costaricensis*) with abundant epiphytes, bushes (e. g., ferns, Ericaceae, Asteraceae, Onagraceae), and large patches of bamboo (*Chusquea talamancensis*) cover most of the CMBS study site (Calderón-Sanou *et al.* 2019). On the contrary, the paramo is dominated by an herbaceous layer with a large diversity of Asteraceae and Poaceae (mainly *Chusquea subtessellata*), and some scattered bushy patches in which Ericaceae, Asteraceae, and Hypericaceae are abundant (Vargas and Sánchez 2005).

We selected two microhabitats in each habitat, the montane forest and the paramo, to assess rodent habitat use, species richness, and abundance. In the montane forest, we sampled mice in (1) patches dominated by bamboo (*Chusquea talamancensis*), and in (2) patches dominated by bushes. In the paramo, we sampled in (1) patches dominated by bushes and an herbaceous layer (e. g., Asteraceae, Cyperaceae) and short bushes (e. g., *Pernettya*, *Vaccinium*, and *Hypericum*); and (2) in homogeneous patches dominated by *Chusquea subtessellata*. In each microhabitat we established a circular 10 m-diameter plot, so that we had the following combination of microhabitats in each ecosystem: paramo-bush, paramo-*Chusquea*, montane forest-bush, and montane forest-*Chusquea* (Figure 2).



Figure 1. Sample sites at the Talamanca mountain range, Costa Rica. A) High montane oak forest at Cerro de la Muerte Biological Station; B) paramo habitat.

Capture, recapture, and tattooing mice. We used baited Sherman live traps (5 × 6 × 16 cm; H. B. Sherman Traps, Inc., Florida) to capture mice. The bait was made of barley, oatmeal, banana, peanut butter, and vanilla extract. In each habitat, we placed 50 traps (25 in each microhabitat) for two consecutive nights, each 3 to 4 weeks from May 2015 through April 2016. We placed each trap at 5 to 10 m from a transect we established within each plot and at 5 to 10 m from any other trap. The distance from the transect and from other traps varied depending on the topographic characteristics of the terrain. We registered the geographic position of each trap in each sampling using a GPS Garmin 60Csx (Garmin Corp., Olathe, Kansas) and changed the location of the traps in each sampling to maximize the capture in each microhabitat. In addition, we placed 4 to 8 traps on branches at 1.5 to 3 m above the ground to capture arboreal or climbing mice.

We identified each individual captured to species level using the key published by Villalobos-Chaves *et al.* (2016). For each individual captured, we recorded species, date, habitat, microhabitat, and trap coordinates. Given that taxonomy within the group is in debate, voucher specimens were collected prior and after the sampling period as a reference (Appendix 1).

We tattooed large adult *Peromyscus* using a Spaulding Revolution I (Spaulding and Rogers, Inc., New York) machine for animal tattooing. Individuals were tattooed at the base of the tail. For juvenile *P. nudipes* and small species, we cut a patch (or patches) of hair from the lumbar region to identify each individual; the tattooing machine is not recommended for small animals. In addition, we recorded

any distinctive mark of an individual that facilitated their identification (e. g., tip tail coloration, scars, ear cuts), in case they were recaptured. For the recaptured individuals, we recorded the individual mark or tattoo, trap coordinates, habitat, and microhabitat. After each individual was marked and its information recorded, we released it at the site where it was captured. We then waited until each individual had found a retreat or a protected site before leaving the release site to avoid predation.

Data analyses. We captured four mouse species and compared their abundance among the four microhabitats with a chi-squared contingency analysis and a Fisher paired test. We did not analyze richness since we only captured four species. We used the statistical language R, version 3.4.0 (R Core Team 2017) for the analyses.

Results

Species richness and abundance. We captured 108 mice of four species in the family Cricetidae, from a 2,100 night-trap effort distributed equally between habitats. We captured three species at each habitat, two of which were present in both habitats (Table 1). *Scotinomys xerampelinus* was captured only in montane forest, *Reithrodontomys creper* only in the paramo, *R. sumichrasti* was found in the Montane forest-Chusquea and Paramo-bush microhabitats, and *P. nudipes* was the only species captured in all four microhabitats (Table 1).

Peromyscus nudipes was the most abundant species captured with 85% of all captures (Table 1). The number of mice captured (all species combined) differed between habitats ($X^2 = 43.75$, d. f. = 1, $P < 0.001$) and among microhabitats ($X^2 = 36.83$, d. f. = 9, $P < 0.001$). We captured more mice in the montane forest than in the paramo and more in the montane forest/bush microhabitat ($n = 58$) than in any other microhabitat (Table 1). On the contrary, the microhabitat with the fewest mice captured was paramo-Chusquea with only 6 individuals (Table 1).

Discussion

We found four mouse species in the montane forest and the paramo, the two dominant ecosystems at the Costa Rican highland. At this elevation, richness and abundance of mice vary according to the characteristics of the habitat and microhabitat. For instance, the vegetation structure directly influences density (e. g., Pardini et al. 2005; Blaum et al. 2006), diversity (e. g., Johnson and Vaughan 1993; Muñoz et al. 2009), and richness of small rodents (e. g., Brehme et al. 2011; Thompson and Gese 2013) in Costa Rica and other ecosystems.

Our results showed that some species are present only in a particular habitat and some microhabitats, but not in others. Specifically, we captured *S. xerampelinus* only in the montane forest and *R. creper* only in the paramo; although both species have sporadically previously been recorded in

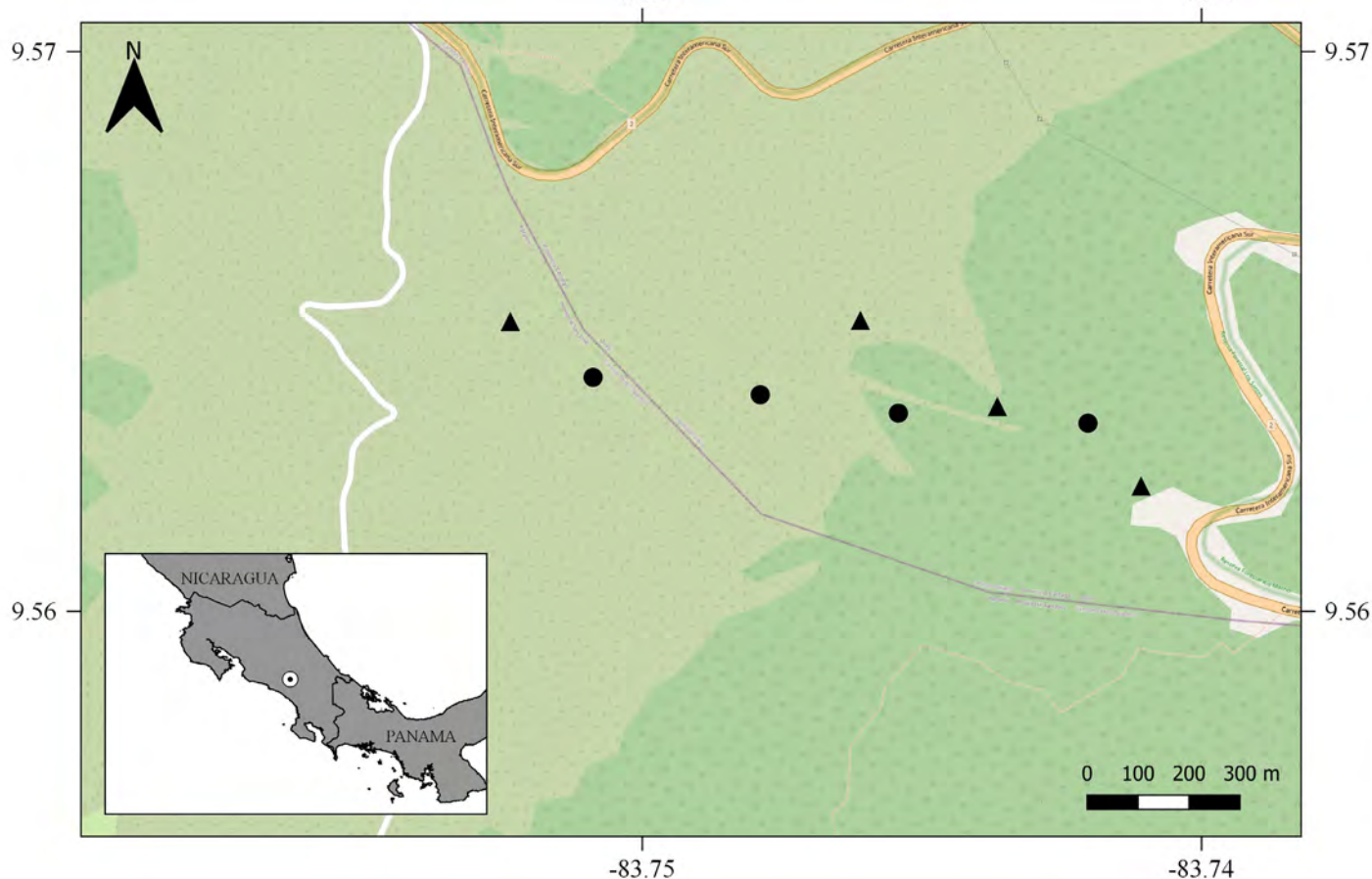


Figure 2. Location of the sample sites in the Talamanca Mountain range. Light green background represents paramo; dark green represents montane forest. Black dots show bush microhabitat; black triangles, *Chusquea* microhabitat.

Table 1. Percentage and number (in parentheses) of mice captured in each microhabitat.

| Species | Montane forest-bush | Montane forest-Chusquea | Paramo-bush | Paramo-Chusquea |
|------------------------------------|---------------------|-------------------------|-------------|-----------------|
| <i>Peromyscus nudipes</i> | 93 (54) | 91 (31) | 66.6 (12) | 67 (4) |
| <i>Scotinomys xerampelinus</i> | 7 (4) | 6 (2) | - | - |
| <i>Reithrodontomys creper</i> | - | - | 16.7 (3) | 33 (2) |
| <i>Reithrodontomys sumichrasti</i> | - | 3 (1) | 16.7 (3) | - |

both habitats (Reid 2009; JDRF unpublished data). Therefore, our findings suggests that even when both species are present in both habitats, each of them preferred one particular habitat over the other, likely related to the structural differences in the vegetation (McCloskey 1976; Johnson and Vaughan 1993).

The abundance of mice varied largely between habitats and among microhabitats, as reported in other studies (Mohammadi 2010). In the montane forest, a more complex vegetation structure and greater diversity of food resources and hiding places likely permit the coexistence of more individuals than in the paramo. The abundance of mice among microhabitats showed a similar pattern. Structurally complex microhabitats, such as the montane forest / bush microhabitat, allow more species to coexist (Torres-Pulliza et al. 2020). On the contrary, the microhabitat dominated by *Chusquea subtessellata* in the paramo, which is structurally simple with large exposed open areas, had the lowest mice abundance.

Differences in abundance among microhabitats of *P. nudipes*, further support that habitat structure influences in the abundance of mice in Costa Rican highlands. This species is present in all microhabitats and its abundance increased with the microhabitat complexity. More complex structure in the vegetation elicits a series of synergetic effects that affect the abundance of different species. For example, a structurally complex vegetation provides a larger number of microhabitats, food resources, and hiding places that can be used for more rodents than those provided by more simple microhabitats (Tews et al. 2004).

The paramo-*Chusquea* is the simplest microhabitat, composed by homogeneous patches of *Chusquea subtessellata* with open spaces in between. The vegetation composition and the simple structure likely provide fewer food resources and retreats than any other microhabitat (Johnson and Vaughan 1993; Mohammadi 2010; García et al. 2011). In addition, rodents tend to avoid foraging in areas deprived of vegetation, since they are more likely detected by predators (Kotler et al. 1988; Morris and Davidson 2000).

Summarizing, the species richness of mice at the highest vegetation ecosystems, the montane forest and paramo, in the Talamanca mountain range is low. However, the abundance of some species is very high, and this abundance varies greatly among microhabitats. The variation in mice abundance is presumably determined by the characteristics of the habitat, primarily related to the structure of veg-

etation. A more complex structure is expected to provide rodents with more diverse and abundant food resources (Johnson and Vaughan 1993; García et al. 2011), more retreats, and better protection from predators (Kotler et al. 1988; Morris and Davidson 2000).

Acknowledgements

We thank Cerro de la Muerte Biological Station for logistic support, and the family of Ramírez-Fernández and Vicerrectoría de Investigación, Universidad de Costa Rica for financial support. Thanks to I. Molina, P. Rodríguez, J. Ramírez, P. Ledezma, and V. Madrigal for helping with field assistance that made possible this study. This work is part of JDRF undergraduate research project (Licenciatura) at UCR.

Literature cited

- BARRANTES, G. 2005. Aves de los páramos de Costa Rica. Pp. 521–532, in *Páramos de Costa Rica* (Kappelle, M., and S. P. Horn, eds.). INBio. Heredia, Costa Rica.
- BARRANTES, G., E. CHACÓN, AND P. HANSON. 2019. Costa Rica y su Riqueza Biológica. Pp. 151–202, in *Biodiversidad e inventario de la naturaleza* (Godoy-Cabrera, C., and N. Ramírez-Albán, eds.). Editorial Universidad Estatal a Distancia. San José, Costa Rica.
- BELLARD, C., ET AL. 2012. Impacts of climate change on the future of biodiversity. *Ecology Letters* 15:365–377.
- BLAUM, N., E. ROSSMANITH, AND F. JELTSCH. 2006. Land use affects rodent communities in Kalahari savannah rangelands. *African Journal of Ecology* 45:189–195.
- BREHME, C. S., ET AL. 2011. Wildfires alter rodent community structure across four vegetation types in Southern California, USA. *Fire Ecology* 7:81–98.
- CALDERÓN-SANOU, I., ET AL. 2019. Lack of negative density-dependence regulation in a dominant oak tree from a neotropical highland forest. *Biotropica* 51:817–825.
- CARRILLO, E., G. WONG, AND J. C. SAENZ. 2005. Mamíferos de los páramos de Costa Rica. Pp. 533–545, in *Páramos de Costa Rica* (Kappelle, M., and S. P. Horn, eds.). INBio. Heredia, Costa Rica.
- CARRILLO, E., G. WONG, AND J. C. SAENZ. 2005. Mamíferos de los páramos de Costa Rica. Pp. 533–545, in *Páramos de Costa Rica* (Kappelle, M., and S. P. Horn, eds.). INBio. Heredia, Costa Rica.
- DIRNBÖCK, T., F. ESSL, AND W. RABITSCH. 2010. Disproportional risk for habitat loss of high-altitude endemic species under climate change. *Global Change Biology* 17:990–996.
- EPSTEIN, P. R. 2000. Is global warming harmful to health? *Scientific American* 283:50–57.
- GARCÍA, D., R. ZAMORA, AND G. C. AMICO. 2011. The spatial scale of plant-animal interactions: effects of resource availability and habitat structure. *Ecological Monographs* 81:103–121.

- GONZÁLEZ-MAYA J. F., ET AL. 2015. Effectiveness of Protected Areas for representing species and populations of terrestrial mammals in Costa Rica. *Plos One* 10:e0124480.
- HERRERA, W. 2005. El clima de los páramos de Costa Rica. Pp. 113–128, in *Páramos de Costa Rica* (Kappelle, M. and S. P. Horn, eds.). INBio. Heredia, Costa Rica.
- HILBERT, D. W., ET AL. 2004. Golden bowerbird (*Prionodura newtonia*) habitat in past, present and future climates: predicted extinction of a vertebrate in tropical highlands due to global warming. *Biological Conservation* 116:367–377.
- HOLZ, I., AND S. R. GRADSTEIN. 2005. Phytogeography of the bryophyte floras of oak forests and páramo of the Cordillera de Talamanca, Costa Rica. *Journal of Biogeography* 32:1591–1609.
- HUGHES, L. 2000. Biological consequences of global warming: is the signal already. *TREE* 15:56–61.
- JOHNSON, W. E., AND C. VAUGHAN. 1993. Habitat use of small terrestrial rodents in the Costa Rican highlands. *Revista Biología Tropical* 41:521–527.
- KARMALKAR, A. V., R. S. BRADLEY, AND H. F. DIAZ. 2008. Climate change scenario for Costa Rican montane forests. *Geophysical Research Letters* 35:1–5.
- KOTLER, B. P., ET AL. 1988. The effects of morphology and body size on rates of owl predation on desert rodents. *Oikos* 53:145–152.
- LACHER, T. E., JR., ET AL. 2016. Evolution, Phylogeny, Ecology, and Conservation of the Clade Glires: Lagomorpha and Rodentia. Pp. 15–26, in *Handbook of the Mammals of the World. Vol. 6. Lagomorphs and Rodents I* (Wilson, D. E., T. E. Lacher, Jr, and R. A. Mittermeier, eds.). Lynx Edicions. Barcelona, Spain.
- LAURANCE, W. F., ET AL. 2011. Global warming, elevational ranges and the vulnerability of tropical biota. *Biological Conservation* 144:548–557.
- MALCOM, J. R., ET AL. 2016. Global warming and extinctions of endemic species from biodiversity hotspots. *Conservation Biology* 20:538–548.
- MCCLOSKEY, R. T. 1976. Community structure in sympatric rodents. *Ecology* 57:728–739.
- MOHAMMADI, S. 2010. Microhabitat selection by small mammals. *Advances in Biological Research* 4:283–287.
- MORALES-BETANCOURT, J. A., AND J. V. ESTÉVEZ-VARÓN. 2006. El páramo: ¿ecosistema en vía de extinción? *Revista Luna Azul* 22:39–51.
- MORRIS, D. W., AND D. L. DAVIDSON. 2000. Optimally foraging mice match path use with habitat differences in fitness. *Ecology* 81:2061–2066.
- MUÑOZ, A., R. BONAL, AND M. DÍAZ. 2009. Ungulates, rodents, shrubs: interactions in a diverse Mediterranean ecosystem. *Basic and Applied Ecology* 10:151–160.
- PARDINI, R., ET AL. 2005. The role of forest structure, fragment size and corridors in maintaining small mammal abundance and diversity in an Atlantic forest landscape. *Biological Conservation* 124:253–266.
- POUNDS, J. A., ET AL. 2006. Widespread amphibian extinctions from epidemic disease driven by global warming. *Nature* 439:161–167.
- POUNDS, J. A., M. P. L. FOGDEN, AND J. H. CAMPBELL. 1999. Biological response to climate change on a tropical mountain. *Nature* 398:611–615.
- POWELL, J. R., ET AL. 2022. Bird species inventory in secondary tropical montane cloud forest at Cloudbridge Nature Reserve, Talamanca Mountains, Costa Rica. *Check List* 18:17–65.
- PYŠEK, P., ET AL. 2017. Displacement and local extinction of native and endemic species. Pp. 157–175, in *Impact of Biological Invasions on Ecosystem Services. Invading Nature – Springer Series in Invasion Ecology, Vol. 12*. Springer. Cham, Switzerland.
- R CORE TEAM. 2017. R: A language and environment for statistical computing. R Foundation for Statistical Computing. Vienna, Austria.
- REID, F. A. 2009. A field guide to the mammals of Central America and Southeast Mexico. Oxford University Press. New York, USA.
- RIPPLE, W. J., ET AL. 2014. Status and ecological effects of the world's largest carnivores. *Science* 343:1241484.
- RULL, V., AND T. VEGAS-VILARRÚBIA. 2006. Unexpected biodiversity loss under global warming in the neotropical Guayana Highlands: a preliminary appraisal. *Global Change Biology* 12:1–9.
- TEWS, J., ET AL. 2004. Animal species diversity driven by habitat heterogeneity/diversity: the importance of keystone structures. *Journal of Biogeography* 31:79–92.
- THOMAS, C. D., ET AL. 2004. Extinction risk from climate change. *Nature* 427:145–148.
- THOMPSON, C. M., AND E. M. GESE. 2013. Influence of vegetation structure on the small mammal community in a shortgrass prairie ecosystem. *Acta Theriologica* 58:55–61.
- TORRES-PULLIZA, D., ET AL. 2020. A geometric basis for surface habitat complexity and biodiversity. *Nature Ecology and Evolution* 4:1495–1501.
- URBAN, M. C. 2015. Accelerating extinction risk from climate change. *Science* 348:571–573.
- VARGAS, G., AND J. J. SÁNCHEZ. 2005. Plantas con flores de los páramos de Costa Rica y Panamá: el páramo ístmico. Pp. 397–435, in *Páramos de Costa Rica* (Kappelle, M., and S. P. Horn, eds.). INBio. Heredia, Costa Rica.
- VILLALOBOS-CHAVES, D., ET AL. 2016. Clave para la identificación de los roedores de Costa Rica. Escuela de Biología, Universidad de Costa Rica. San José, Costa Rica.

Associated editor: Jake Esselstyn and Giovani Hernández Canchola
 Submitted: August 22, 2022; Reviewed: September 29, 2022
 Accepted: November 18, 2022; Published on line: January 27, 2023

Appendix 1

List of voucher specimens of all four species trapped at the study site in the collection of the University of Costa Rica's Zoology Museum.

| Taxa | Museum specimen number |
|------------------------------------|-------------------------------|
| <i>Scotinomys xerampelinus</i> | MZUCR-1929, 4905 |
| <i>Reithrodontomys creper</i> | MZUCR-4372, 4548, 4981, 5097 |
| <i>Peromyscus nudipes</i> | MZUCR-4373 |
| <i>Reithrodontomys sumichrasti</i> | MZUCR-5135 |

Pleistocene distribution of MacConnell's Bat (*Phyllostomidae*) suggests intermittent connections between Amazonia and Atlantic Forest

FELIPE PESSOA SILVA¹, LUCAS GONÇALVES DA SILVA^{2,3}, THIAGO B. F. SEMEDO⁴, FAMILY C. M. SANTOS⁵, GERSON PAULINO LOPES^{5,6}, MARTIN ALEJANDRO MONTES⁷, AND GUILHERME S. T. GARBINO^{8*}

¹ Instituto de Ciências Biológicas, Universidade Federal de Goiás. Avenida Esperança s/n, CEP. 74690-900. Goiânia, Goiás, Brazil. Email: felipe.pessoas@gmail.com (FPS).

² Instituto Nacional da Mata Atlântica (INMA). Avenida José Ruschi, nº 4, Santa Teresa. Espírito Santo, Brazil. Email: lucas_gonca@yahoo.com.br (LGS)

³ Centro de Desenvolvimento Sustentável, Universidade de Brasília. Brasília, Distrito Federal, Brazil.

⁴ Instituto Nacional de Pesquisa do Pantanal (INPP); Museu Paraense Emílio Goeldi (MPEG) - Programa de Capacitação Institucional. Av. Fernando Correia da Costa, CEP. 78060-900. Cuiabá, Mato Grosso, Brazil. Email: thiagosemedo@gmail.com (TBFS)

⁵ Grupo de Pesquisa em Ecologia de Vertebrados Terrestres, Instituto de Desenvolvimento Sustentável Mamirauá. Estrada do Bexiga, 2584, CEP. 69553-225. Tefé, Amazonas, Brazil. Email: family-1fv@hotmail.com (TCMS)

⁶ Programa em Pós-Graduação em Zoologia & Laboratório de Evolução e Genética Animal, Universidade Federal do Amazonas. Avenida General Rodrigo Octavio Jordão Ramos, 1200, CEP. 69067-005. Manaus, Amazonas, Brazil. Email: gersonlps@hotmail.com (GPL)

⁷ Departamento de Biologia, Universidade Federal Rural de Pernambuco, Campus Dois Irmãos, s/n, CEP. 52171-900. Recife, Pernambuco, Brazil. Email: martin.montes@ufrpe.br (MAM)

⁸ Museu de Zoologia João Moojen, Departamento de Biologia Animal, Universidade Federal de Viçosa. Av. P.H. Rolfs s/n, CEP. 36570-900. Viçosa, Minas Gerais, Brazil. Email: guilherme.garbino@ufv.com.br (GSTG).

* Corresponding author: <https://orcid.org/0000-0003-1701-5930>.

The historical biogeography of the major South American forested biomes has long intrigued scientists. Paleoclimatic events during the last 130 thousand years promoted connections between forested biomes in the Neotropical region, leading to disjunct distributions of some of the biota. In this context, MacConnell's Bat, *Mesophylla macconnelli*, appears to represent a forest-restricted species with its current distribution bisected by dry areas. In this study, we infer past connections between the Amazonia and Atlantic Forest using MacConnell's Bat and ecological niche models. We obtained 681 records of the species, and estimated its potential distribution during the Last Interglacial (LIG), Last Glacial Maximum (LGM), and current periods. Our generated models, based on 260 filtered occurrence records, had very good predictive power, with AUC and TSS adherence values above 0.9. Temperature seasonality and annual precipitation had the highest relative contribution. The potential distribution for the LIG suggested a suitable area connection between the southwestern Atlantic Forest and southern Cerrado and Amazonia. The potential distribution in the LGM suggests range expansion toward northern and eastern Amazonia. The current and inferred past distributions of *Mesophylla macconnelli* suggest at least two periods of past connection between Amazon and Atlantic Forest. This pattern is found in other forest-associated vertebrates in South America, suggesting that Pleistocene climatic cycles were central to the generation of disjunct distributions in the region.

La biogeografía histórica de los principales biomas de selvas de América del Sur ha intrigado a los científicos durante mucho tiempo. Los eventos paleoclimáticos durante los últimos 130 mil años promovieron conexiones entre biomas de selvas en la región neotropical, lo que llevó a distribuciones disjuntas de parte de la biota. En este contexto, el murciélago de MacConnell, *Mesophylla macconnelli*, parece ser un ejemplo de especie restringida al bosque con su distribución actual atravesada por las áreas secas de América del Sur. En este estudio, inferimos las conexiones pasadas entre la Amazonía y el Bosque Atlántico utilizando modelos de nicho ecológico y el murciélago de MacConnell. Obtuvimos 681 registros de la especie, y estimamos su distribución potencial durante el Último Interglacial (LIG), Último Máximo Glacial (LGM) y períodos actuales. Nuestros modelos generados, basados en 260 registros de ocurrencia filtrados, tuvieron muy buen poder predictivo, con valores de adherencia AUC y TSS superiores a 0.9. La estacionalidad de la temperatura y la precipitación anual tuvieron la mayor contribución relativa. La distribución potencial en el LIG sugiere una conexión de área adecuada entre el suroeste del Bosque Atlántico y el sur del Cerrado y la Amazonía. La distribución potencial en el LGM sugiere una expansión del rango hacia el norte y el este de la Amazonía. Las distribuciones actuales y pasadas inferidas de *Mesophylla macconnelli* sugieren al menos dos períodos de conexión pasada entre la Amazonía y el Bosque Atlántico. Este patrón se encuentra en otros vertebrados asociados a los bosques en América del Sur, lo que sugiere que los ciclos climáticos del Pleistoceno fueron fundamentales para la generación de distribuciones disjuntas en la región.

Keywords: Fruit-eating bat; *Mesophylla macconnelli*; Last Glacial Maximum; Last Interglacial; Stenodermatinae.

Introduction

The Amazonia and Atlantic Forest are the two major tropical rainforests of South America (Hueck 1972). These two large forests are currently separated by the dry forests of the Caatinga, the Chaco shrublands and the savanic Cerrado (Ab'Saber 1977; Solari *et al.* 2012). Paleoclimatic, biogeographic, and niche modeling studies have suggested intermittent past connections between Amazonia and Atlantic Forest, during the last interglacial period (Wang *et al.* 2004; Sobral-Souza *et al.* 2015; Ledo and Colli 2017).

Traditionally, the disjunct distribution pattern of rainforest-adapted mammals has been considered as evidence that the Amazonia and Atlantic Forest were connected (Coimbra-Filho and Câmara 1996; de Vivo 1997). Notable examples include medium and large arboreal species such as the red-handed howler (*Alouatta belzebul*), the kinkajou (*Potos flavus*), and the silky anteater (*Cyclopes didactylus*). The existence of similar patterns for small mammals, such as bats, has been little investigated (but see Costa 2003 and Rocha *et al.* 2015). To explain these biogeographic patterns, hypotheses often invoke the fragmentation of forests that occurred during the Pleistocene (Vanzolini and Williams 1970; Martins 1971; Haffer 1997). One way to test this hypothesis is to obtain paleoclimatic data from this epoch (Vanzolini and Williams 1970), and to examine the divergence times and amount of genetic divergence among the involved species (Moritz 2000).

MacConnell's Bat, *Mesophylla macconnelli* Thomas, 1901, is one of the smallest species of frugivorous bat in the world, weighing 6 to 8 g (Solari *et al.* 2019). This tent-roosting bat has been recorded from the rainforests of Nicaragua, to the Amazon basin in South America, reaching northern Bolivia and western Brazil (Arroyo-Cabrales 2008). However, recent studies extended its range to the Atlantic Forest and to the Cerrado of, respectively, eastern and central Brazil (Zor-téa and Tomaz 2006; Gregorin *et al.* 2014). With the new records, the disjunct distribution pattern of *M. macconnelli* is strikingly similar to what has been observed for other forest-dependent mammals that occur in both the Amazonia and Atlantic Forest. A recent study identified 127 species of mammals that occur in both ecosystems, suggesting them as good candidates for phylogeographic studies that investigate this putative vicariant pattern, but *M. macconnelli* was not mentioned by the authors (Machado *et al.* 2021).

Using paleoclimatic data and ecological niche models, we estimate the past potential distribution of *M. macconnelli* during the last 130,000 years. Our objective is to assess the potential for past connections between the Amazonia and Atlantic Forest that may explain the apparently disjunct distribution pattern of the species.

Materials and methods

Mesophylla macconnelli occurrence data. Occurrence records for *M. macconnelli* were obtained from museum specimens held in the Instituto de Desenvolvimento Sustentável Mamirauá (IDSM), Natural History Museum, Lon-

don (BMNH), Universidade Federal de Lavras (CMUFLA), Museu de Zoologia da Universidade de São Paulo (MZUSP), Universidade Federal de Mato Grosso (UFMT), Universidade Federal de Minas Gerais (UFMG), and National Museum of Natural History, Smithsonian Institution (USNM).

We also incorporated secondary records in online databases such as Global Biodiversity Information Facility – GBIF (www.gbif.org), SpeciesLink (<http://splink.cria.org.br/>) and Instituto Chico Mendes de Conservação da Biodiversidade – ICMBio (<https://biodiversidade.icmbio.gov.br/>). Additionally, existing records in the scientific literature were included (see Supplementary material 1).

Our database went through a process of cleaning and removing records with missing or repeated geographic coordinates and records outside the known geographic distribution of the species. After this procedure, a single occurrence record was randomly selected within an area equivalent to two cells of resolution of the environmental layers (each cell = 9.24 x 9.24 km; Velazco *et al.* 2019). This was to prevent sampling bias from propagating biased ecological niche models.

Environmental Data. The Neotropical region was determined as our study area to calibrate our model (Olson *et al.* 2001), considering the wide distribution range of *M. macconnelli* in Central and South America, and potential dispersion ability. Ecological niche models (ENM) for current conditions were adjusted based on 19 bioclimatic variables related to temperature and precipitation (Hijmans *et al.* 2005). Detailed information about each variable is available in Supplementary material 2, Table S1. Paleoclimatic conditions for the Last Interglacial (LIG; 120,000 to 140,000 years ago) and Last Glacial Maximum (LGM; ~21,000 years ago) were obtained from the PaleoClim.org database (Brown *et al.* 2018). All variables were obtained at the resolution of 5 arc-minutes and were cropped to the same extent of our study area. To avoid overfitting and to assess correlation among biotic variables a Pearson's correlation test was applied to the bioclimatic variables. This test was performed using the "raster.cor.matrix" function of the ENMTools package in R (Warren *et al.* 2021). From each pair of strongly correlated variables, *i. e.*, $r \geq |0.7|$, we kept the one with the highest biological meaning for the species (Da Silva *et al.* 2020). After this procedure, five variables remained: Mean Diurnal Range (bio2), Temperature Seasonality (bio4), Max Temperature of Warmest Month (bio5), Annual Precipitation (bio12), and Precipitation Seasonality (bio15).

Modelling procedures. We used four algorithms to construct ENM: Bayesian Gaussian – GAU (Golding 2014), Maximum Entropy - MXD (Phillips *et al.* 2017), Random Forest – RDF (Liaw and Wiener 2001), Support Vector Machine – SVM (Karatzoglou *et al.* 2004). The same number of pseudoabsences were generated to fit the models (Barbet-Massin *et al.* 2012). An environmental restriction method was used to allocate the pseudoabsences in climatically different regions of the environmental space in which the species occurs (Engler *et al.* 2004). We used the checkboard

method to calibrate and evaluate models. This method consists of dividing the geographic space into blocks, splitting the occurrences into two groups, one for model adjustment and another for model evaluation (Roberts et al. 2017).

Model performance was evaluated using two metrics: Area Under Curve (AUC) Receiver Operating Characteristic (ROC; Phillips et al. 2006), and True Skill Statistic (TSS = sum of sensibility and specificity - 1; Allouche et al. 2006). AUC ranges from 0 to 1, where values closer to 1 indicate a good distinction between presence and pseudoabsence records. Whereas, values below 0.5 indicate that the model did not perform better than expected by chance (Fielding and Bell 1997). TSS ranges from -1 to +1, values above 0.7 indicate models with statistically reliable performance (Allouche et al. 2006; Zhang et al. 2015). To reduce the uncertainty in the prediction generated by the use of distinct algorithms, we build ensemble models (Araújo and New 2007). The ensemble model was calculated selecting models with TSS value greater than the average TSS value of all algorithms and then calculated the mean suitability model between all algorithms that met this condition. Finally, we projected the current climatic suitability conditions for *M. macconnelli* under past climatic conditions (LIG, ~ 120,000 years ago; LGM, ~21,000 years ago) for each algorithm and then created an ensemble model for each period. For LGM we also

used different climatic conditions estimated by 3 distinct Atmosphere-Ocean General Circulation Models (AOGCMs): CCSM4, MIROC-ESM e MPI-ESM-P (Hijmans et al. 2005). Specifically, for LGM models a final model was created by calculating the average suitability values obtained through the three AOGCM's ensemble models. Finally, we use the threshold that maximizes the sum of sensitivity and specificity (Liu et al. 2005), to turn continuous suitability values into binary presence-absence models.

To test the hypothesis of connection between the distribution of *M. macconnelli* through Amazon and Atlantic Forest, we overlapped the ensemble models of the three time periods. In this way we could identify areas of climate stability, or areas of connection and reconnection that may have been lost in the species current distribution.

Results

Current records. We found 681 records of *Mesophylla macconnelli* in Central and South America and after the filtering process, 260 unique records were used in modelling procedures. Most of the records (565, 83.21 %) are located east of the Andes, but some (114, 16.79 %) occur west of the Cordillera (Figure 1). The majority of the records (627, or 92.7 %) are in Tropical & Subtropical Moist Broadleaf Forests, of which 625 are in the Amazon rainforest and

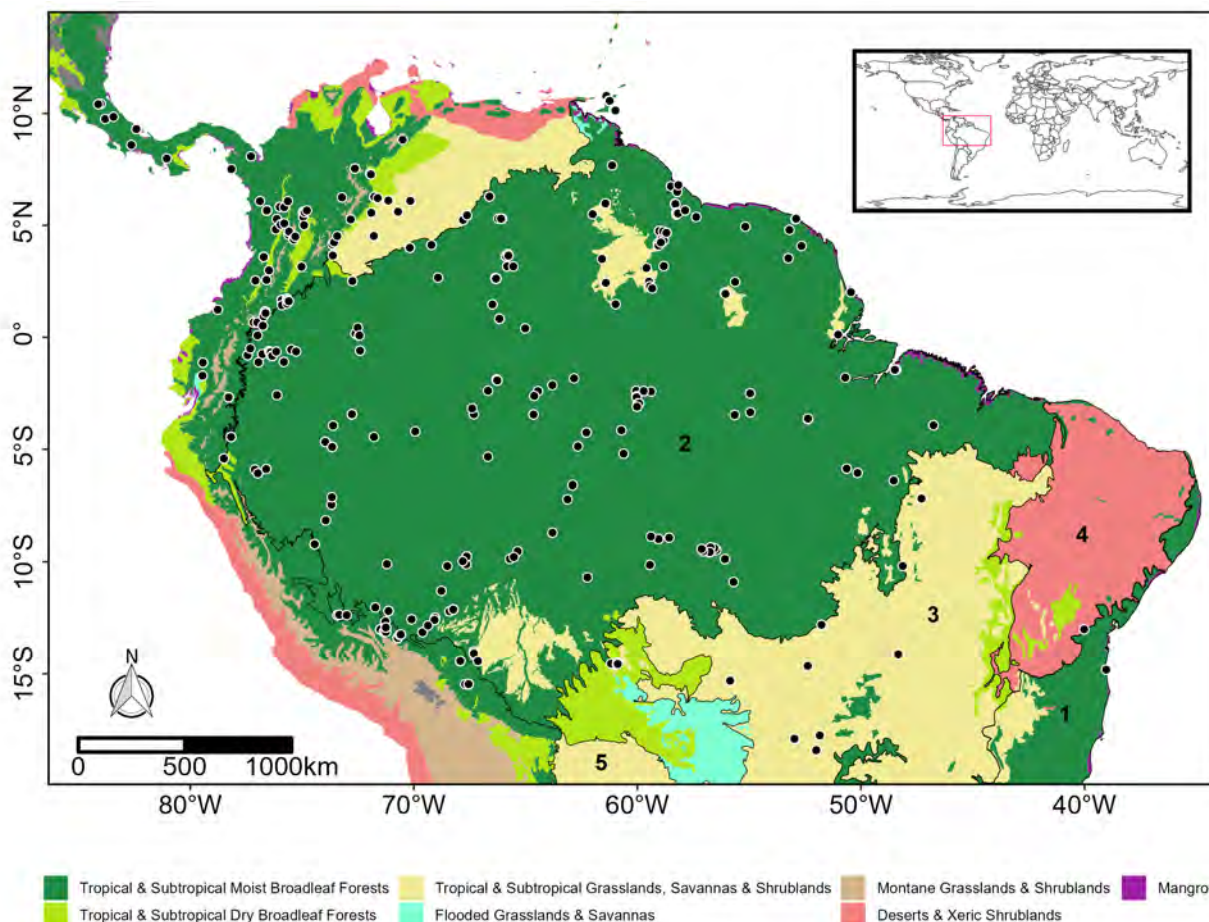


Figure 1. Occurrence records of MacConnell's Bat (*Mesophylla macconnelli*) in the American continent. Colors on map indicate the biomes classified according to Olson (2001). Numbers show the ecoregions of the Neotropical Realm following Olson (2001) (1 - Atlantic Forest, 2 - Amazon Forest, 3 - Cerrado, 4 - Caatinga, 5 - Chaco).

two from the Atlantic Forest. Some records are from the savanna formations of the Cerrado (33, or 4.85 %) and Tropical and Subtropical Dry Broadleaf Forests (21, or 3.08 %). Of all the occurrence points, 85.5 %, or 590, are from altitudes below 900 m above sea level. The remaining 91 localities are from above 900 m, with a maximum altitude of 2,355 m from the cloud forests of Cuzco, Perú.

Geographic distribution models. The evaluation values for the ensemble models, AUC = 0.998 SD=0.028 and TSS = 0.980 SD = 0.027, indicated good performance of the models – for more information about other evaluation metrics and evaluation for each algorithm see Supplementary Material 3. The temperature seasonality (45.3 %) and annual precipitation (36.4 %) provided the highest relative contributions to model *M. macconnelli* distribution. The current distribution model shows a wide area with high suitability values in the Amazon and in the central and northern areas of the Atlantic Forest, with suitable areas also in the Cerrado biome (Figure 2).

During all three projected periods (*i. e.*, LIG, LGM, and Current), the Chocó region, Panama, western Amazonia, and central/northern Atlantic Forest were estimated as highly suitable areas for *M. macconnelli* (Figure 2). The projected distribution for the LIG shows that areas in the southern part of the Amazon, in the Cerrado, and in the Atlantic Forest had suitable climatic conditions, showing a possible connection between the southwestern Atlantic Forest and southern Cerrado (Figure 2). During the LGM we infer a great expansion of appropriate areas towards northern and eastern Amazonia (Figure 3). This occurs concomitantly with a retraction of the southern distribution of the species. This pattern suggests the loss of the connection between the appropriate areas of the Cerrado and Atlantic Forest.

Discussion

The current distribution of *M. macconnelli* seems to be associated with humid forested areas. Even in localities within the Cerrado biome, such as Serra do Roncador (Mato Grosso state, Brazil), and Serranópolis (Goiás state), it has been captured in forest enclaves and riparian areas (Pine *et al.* 1970; Handley 1976; Zortéa and Tomaz 2006). In fact, these transitional areas and forest enclaves in the Cerrado are known to harbor some typical Amazonian mammalian taxa such as *Ateles marginatus*, *Callicebus viefrai*, *Chiroderma trinitatum*, *Didelphis marsupialis*, *Gracilinanus peruanus*, *Marmosops noctivagus*, and *Saguinus niger* (Lacher and Alho 2001; Antunes *et al.* 2021; Garbino *et al.* 2015, 2020; Lima-Silva *et al.* 2022; Semedo *et al.* 2022). Besides forests, temperature seasonality, calculated as the standard deviation of monthly temperature averages, seems to be a limiting factor for the species. This is evident, as *M. macconnelli* occurs in tropical areas between 10° N and -18° S, where there are no abrupt temperature oscillations (Figure 1).

The species is absent in the cooler areas of the Atlantic Forest of southern and southeastern Brazil, which have more seasonal climates than the central Atlantic Forest, where the species occurs. This hypothesis seems more plausible than assuming that the drier formations of the Cerrado acted as a barrier, especially because the Amazon and Atlantic Forest were recently connected by riparian corridors in the region of Goiás, Brazil, where *M. macconnelli* has been recorded (Ab'Saber and Costa-Junior 1950). The dependence on leaves modified into tents to use as daytime roosts (Rodríguez-Herrera *et al.* 2007; Garbino and Tavares 2018) may help explain why the distribution of *M. macconnelli* is intimately associated with forests.

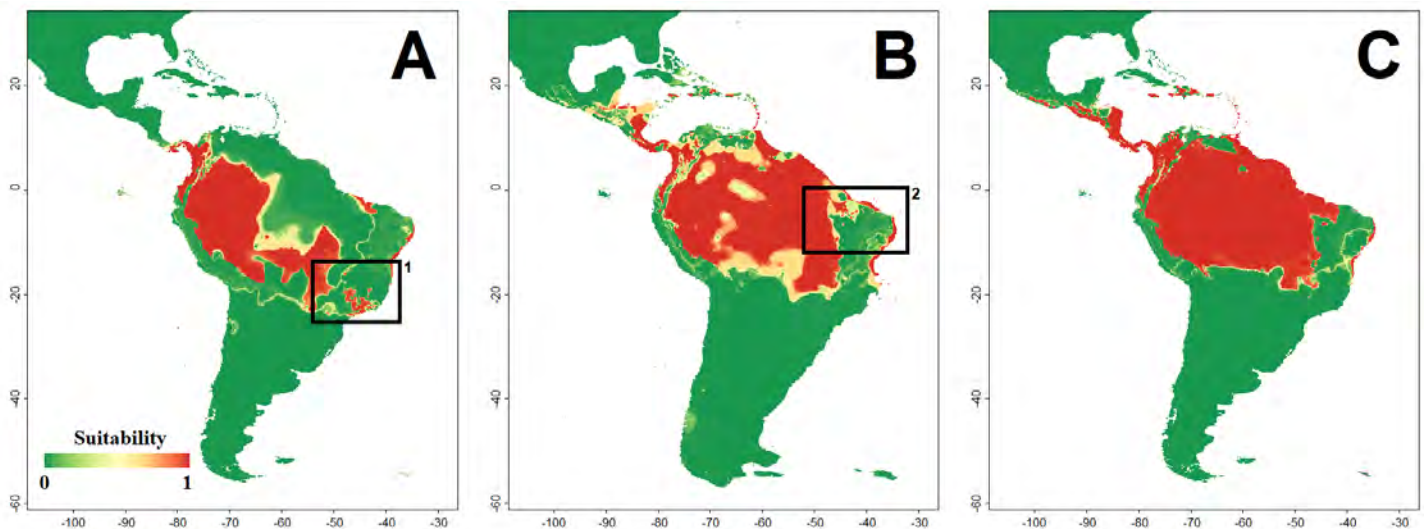


Figure 2. Ecological niche models (ENM) projections of MacConnell's Bat (*Mesophylla macconnelli*) during the (A) Last Interglacial (LIG) – ~120 000 years ago, (B) Last Glacial Maximum (LGM) – ~21 000 years ago, and (C) current distribution. Ensemble models were adjusted based on four algorithms (Bayesian Gaussian – GAU (Golding 2014), Maximum Entropy - MXD (Phillips *et al.* 2017), Random Forest – RDF (Liaw and Wiener 2001), Support Vector Machine – SVM (Karatzoglou *et al.* 2004). Black empty squares indicate possible connections between Atlantic Forest and Amazonia on LIG (1) and LGM (2). The color scale indicates suitability values for *M. macconnelli* occurrence.

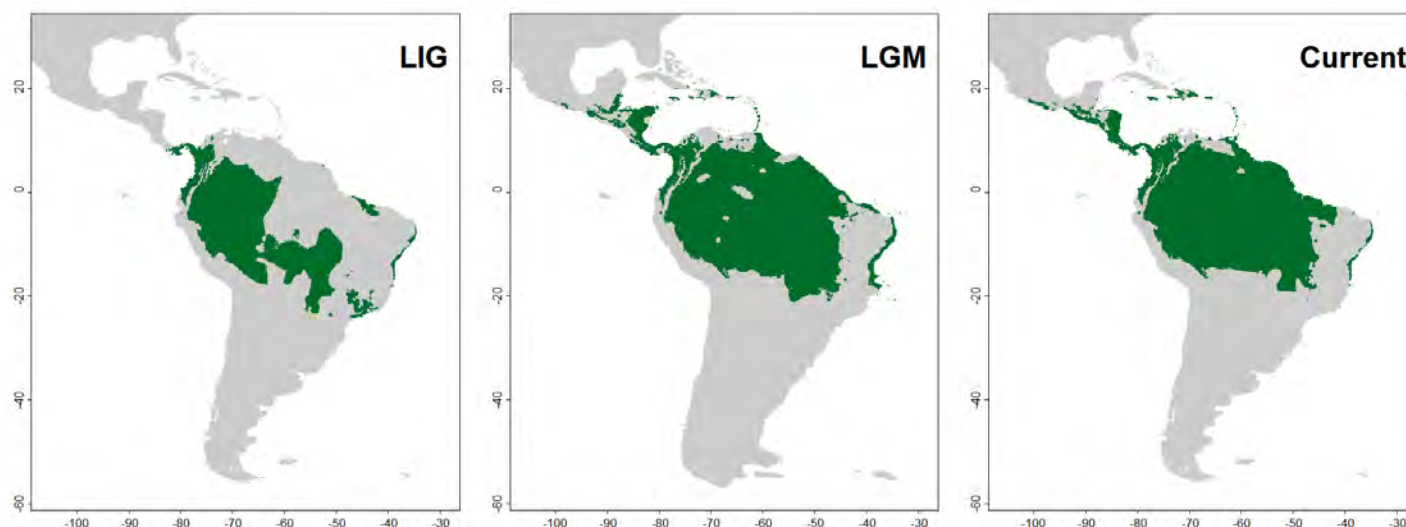


Figure 3. Distributional binary maps of MacConnell's Bat (*Mesophylla macconnelli*) during the transition from the Last Interglacial period to the Last Glacial Maximum (LIG - LGM) and from the Last Glacial Maximum to the current period (LGM - Current). Ensemble models were adjusted based on four algorithms (Bayesian Gaussian – GAU (Golding 2014), Maximum Entropy - MXD (Phillips et al. 2017), Random Forest – RDF (Liaw and Wiener 2001), Support Vector Machine – SVM (Karatzoglou et al. 2004). Green areas indicate predicted species occurrence. Species absence throughout the study area is represented in gray.

According to our model, in the last interglacial period the Andes cordillera acted as a barrier for the species, with suitable areas on the east and west slopes but not in the Andean highlands and plateaus (Figure 2). However, the model suggests that the current period allows for more permeability between the transandean and cisandean populations, which may explain the low genetic structure found in the species (Tavares et al. 2022). The model considering the current distribution also indicates that the populations from the Atlantic Forest (eastern Brazil) are disconnected from the Amazonia/Cerrado populations (Figures 2 and 3). Future surveys in poorly sampled areas where the presence of *M. macconnelli* is not known, may show if the absence of the species in these areas is due to sampling deficiencies.

Some historical biogeographic patterns observed in other vertebrates are suggested in our projected distribution of *M. macconnelli*. The western Amazonia, an area considered an important center of diversity for vertebrates (Hoorn et al. 2010; Oliveira et al. 2017), is recovered as suitable in all three periods (Figure 3). The area where the species occurs in the Atlantic Forest, with climatic stability during all three periods (Figures 2, 3), is known as “Bahia Refuge” and has been identified as a stable climatic area based on other species of vertebrates (Carnaval and Moritz 2008).

The modelled distribution of *M. macconnelli* suggests at least two historical periods of connection between the Atlantic Forest and the Amazonia (Figure 2). In the Last Interglacial, where the climate was more humid, our models recovered suitable areas to the southwest (Figure 2). In the Last Glacial Maximum, when the climate was cooler and drier, our model recovered a northeastern connection of *M. macconnelli*'s range (Figure 2A, B). These two connections may have formed repeatedly over the Pleistocene climatic

oscillations, with the southwest connection between Amazon and Atlantic forests the more ancient and frequent, and the northeast the more recent one (Ledo and Colli 2017). This scenario may have led to the apparent disjunct distribution of *M. macconnelli*. In another forest-dwelling frugivore bat, *Carollia perspicillata*, there is genetic evidence of geographically restricted intraspecific lineages that reflect Pleistocene glacial cycles (Pavan et al. 2011).

Future phylogeographic studies, including genetic samples from the Cerrado of central Brazil, the Atlantic Forest of eastern Brazil, and from eastern and southern Amazonia, will allow verification of the pattern suggested here. We also suggest that niche modelling based on past climates may open new venues of investigation on the biogeographic patterns of the Neotropical fauna.

Acknowledgements

We are thankful to the curators and staff of the visited collections. Thank you also to Jacob Esselstyn and Giovani Hernández-Canchola for the invitation to contribute in this special volume. Two reviewers provided very helpful advice. FPS is supported by the Coordenação de Aperfeiçoamento de Pessoal de Nível Superior – Brasil (CAPES) through a scholarship (Finance Code 001). TCMS and GPL are grateful to the Ministério da Ciência, Tecnologia e Inovação (financial support to the Instituto de Desenvolvimento Sustentável Mamirauá), to the Gordon and Betty Moore Foundation (Grant Agreement to the Instituto de Desenvolvimento Sustentável Mamirauá #5344), and Fundação de Amparo à Pesquisa do Estado do Amazonas (grant to the Instituto de Desenvolvimento Sustentável Mamirauá – FAPEAM PPP 016/2014). TBFS is supported by the Conselho Nacional de Desenvolvimento Científico e Tecnológico (CNPq#301208/2021-2). LGS was supported by FACEPE and INMA/CNPq PCI Program.

Literature cited

- AB'SABER, A. N., AND M. COSTA JUNIOR. 1950. Contribuição ao estudo do sudoeste goiano. *Boletim Paulista de Geografia* 4:3–26.
- AB'SABER, A. N. 1977. Os domínios morfoclimáticos da América do Sul. Primeira aproximação. *Geomorfologia* 53:1–23.
- ALLOUCHE, O., A. TSOAR, AND R. KADMON. 2006. Assessing the accuracy of species distribution models: prevalence, kappa and the true skill statistic (TSS). *Journal of Applied Ecology* 43:1223–1232.
- ANTUNES, P. C., ET AL. 2021. Roedores da Bacia do Alto Paraguai: uma revisão do conhecimento do planalto à planície pantaneira. *Boletim do Museu Paraense Emílio Goeldi. Ciências Naturais* 16:579–649.
- ARAÚJO, M. B., AND M. NEW. 2007. Ensemble forecasting of species distributions. *Trends in Ecology and Evolution* 22:42–47.
- ARROYO-CABRALES, J. 2008. Genus *Mesophylla* O. Thomas, 1901. Pp. 327–329, in *Mammals of South America, Volume 1: marsupials, xenarthrans, shrews, and bats* (Gardner, A. L., ed.). The University of Chicago Press. Chicago, U.S.A.
- BARBET-MASSIN, M., ET AL. 2012. Selecting pseudo-absences for species distribution models: How, where and how many? *Methods in Ecology and Evolution* 3:327–338.
- BROWN, J. L., ET AL. 2018. Paleoclim, high spatial resolution paleoclimate surfaces for global land areas. *Scientific Data* 5:1–9.
- CARNAVAL, A. C., AND C. MORITZ. 2008. Historical climate modeling predicts patterns of current biodiversity in the Brazilian Atlantic forest. *Journal of Biogeography* 35:1187–1201.
- COIMBRA-FILHO, A. F., AND I. G. CÂMARA. 1996. Os limites originais do bioma Mata Atlântica na região Nordeste do Brasil. Fundação Brasileira para Conservação da Natureza, Rio de Janeiro, Brazil.
- COSTA, L. P. 2003. The historical bridge between the Amazon and the Atlantic Forest of Brazil: a study of molecular phylogeography with small mammals. *Journal of Biogeography* 30:71–86.
- ENGLER, R., A. GUISAN, AND L. RECHSTEINER. 2004. An improved approach for predicting the distribution of rare and endangered species from occurrence and pseudo-absence data. *Journal of Applied Ecology* 41:263–274.
- FIELDING, A. H., AND J.F. BELL. 1997. A review of methods for the assessment of prediction errors in conservation presence/absence models. *Environmental Conservation* 24:38–49.
- GARBINO, G. S. T., T. B. SEMEDO, AND A. PANSONATO. 2015. Notes on the western black-handed tamarin, *Saguinus niger* (É. Geoffroy, 1803)(Primates) from an Amazonia-Cerrado ecotone in central-western Brazil: new data on its southern limits. *Mastozoología Neotropical* 22:311–318.
- GARBINO, G. S. T., AND V. C. TAVARES. 2018. Roosting ecology of Stenodermatinae bats (Phyllostomidae): evolution of foliage roosting and correlated phenotypes. *Mammal Review* 48:75–89.
- GARBINO, G. S. T., B. K. LIM, AND V.C. TAVARES. 2020. Systematics of big-eyed bats, genus *Chiroderma* Peters, 1860 (Chiroptera: Phyllostomidae). *Zootaxa* 4846:1–93.
- GOLDING, N. 2014. GRaF: Species Distribution Modelling Using Latent Gaussian Random Fields.
- GREGORIN, R., K. L. VASCONCELOS, AND B. B. GIL. 2014. Two new range records of bats (Chiroptera: Phyllostomidae) for the Atlantic Forest, eastern Brazil. *Mammalia* 79:121–124.
- HAFFER, J. 1997. Alternative models of vertebrate speciation in Amazonia: an overview. *Biodiversity and Conservation* 6:451–476.
- HANDLEY JR., C.O. 1976. Mammals of the Smithsonian Venezuelan Project. *Brigham Young University Science Bulletin, Biological Series* 20:1–89.
- HUIJMANS, R. J., ET AL. 2005. Very high resolution interpolated climate surfaces for global land areas. *International Journal of Climatology* 25:1965–1978.
- HOORN, C., ET AL. 2010. Amazonia through time: Andean uplift, climate change, landscape evolution, and biodiversity. *Science* 330:927–931.
- HUECK, K. 1972. As florestas da América do Sul: ecologia, composição e importância econômica. Polígono. São Paulo, Brazil.
- KARATZOGLU, A., ET AL. 2004. kernlab—An S4 Package for Kernel Methods in R. *Journal of Statistical Software* 11:1–20.
- LACHER, T. E. AND, C. J. R. ALHO. 2001. Terrestrial small mammal richness and habitat associations in an AmazonForest-Cerrado contact zone. *Biotropica* 33:171–181.
- LEDO, R. M. D., AND G. R. COLLI. 2017. The historical connections between the Amazon and the Atlantic Forest revisited. *Journal of Biogeography* 44:2551–2563.
- LIAW, A., AND M. WIENER. 2001. Classification and Regression by RandomForest. *R news* 2:18–22.
- LIMA-SILVA, L. G., ET AL. 2022. New records and geographic distribution extension of two primate species in the Amazonia-Cerrado transition area, Brazil. *Mammalia*. In press.
- LIU, C., P. M. BERRY, T. P. DAWSON, AND R. G. PEARSON. 2005. Selecting thresholds of occurrence in the prediction of species distributions. *Ecography* 28:385–393.
- MACHADO, A. F., ET AL. 2021. Potential mammalian species for investigating the past connections between Amazonia and the Atlantic Forest. *Plos One* 16:e0250016.
- MARTINS, U. R. 1971. Monografia da tribo Ibdionini (Coleoptera, Cerambycinae). Parte VI. *Arquivos de Zoologia* 16:1343–1508.
- MORITZ, C., J. L. PATTON, C. J. SCHNEIDER, AND T. B. SMITH. 2000. Diversification of rainforest faunas: an integrated molecular approach. *Annual Review of Ecology and Systematics* 31:533–563.
- OLIVEIRA, U., M. F. VASCONCELOS, AND A. J. SANTOS. 2017. Biogeography of Amazon birds: rivers limit species composition, but not areas of endemism. *Scientific Reports* 7:1–11.
- OLSON, D. M., ET AL. 2001. Terrestrial Ecoregions of the World: A New Map of Life on Earth A new global map of terrestrial ecoregions provides an innovative tool for conserving biodiversity. *BioScience* 51:933–938.
- PAVAN, A. C., ET AL. 2011. Patterns of diversification in two species of short-tailed bats (*Carollia* Gray, 1838): the effects of historical fragmentation of Brazilian rainforests. *Biological Journal of the Linnean Society* 102:527–539.
- PHILLIPS, S. J., ET AL. 2017. Opening the black box: an open-source release of Maxent. *Ecography* 40:887–893.
- PHILLIPS, S. J., R. P. ANDERSON, AND R. E. SCHAPIRE. 2006. Maximum entropy modeling of species geographic distributions. *Ecological Modelling* 190:231–259.
- PINE, R. H., I. R. BISHOP, AND R. L. JACKSON. 1970. Preliminary list of mammals of the Xavantina/Cachinibo expedition (Central Brazil). *Transactions of the Royal Society of Tropical Medicine and Hygiene* 64:668–670.

- ROBERTS, D. R., *ET AL.* 2017. Cross-validation strategies for data with temporal, spatial, hierarchical, or phylogenetic structure. *Ecography* 40:913–929.
- ROCHA, P. A., *ET AL.* 2015. Zoogeography of South American forest-dwelling bats: Disjunct distributions or sampling deficiencies? *Plos One* 10:e0133276.
- RODRÍGUEZ-HERRERA, B., R. A. MEDELLÍN, R. A., AND R. M. TIMM. 2007. Murciélagos Neotropicales que Acampan en Hojas. Editorial Instituto Nacional de Biodiversidad - INBio. Santo Domingo de Heredia, Costa Rica.
- SEMEDO, T. B. F., *ET AL.* 2022. Distribution limits, natural history and conservation status of the poorly known Peruvian gracile mouse opossum (Didelphimorphia: Didelphidae). *Studies on Neotropical Fauna and Environment. In Press.*
- DA SILVA, F. P., *ET AL.* 2020. Distribution modeling applied to deficient data species assessment: A case study with *Pithecopus nordestinus* (Anura, Phyllomedusidae). *Neotropical Biology and Conservation* 15:165–175.
- SOBRAL-SOUZA, T., M. S. LIMA-RIBEIRO, AND V. N. SOLFERINI. 2015. Biogeography of Neotropical Rainforests: past connections between Amazon and Atlantic Forest detected by ecological niche modeling. *Evolutionary Ecology* 29:643–655.
- SOLARI, S., P. M. VELAZCO, AND B. D. PATTERSON. 2012. Hierarchical organization of Neotropical mammal diversity and its historical basis. Pp. 145–156, *in* Bones, clones, and biomes: the history and geography of Recent Neotropical mammals (Patterson, B. D., and L. P. Costa, eds.). The University of Chicago Press. Chicago, U.S.A.
- SOLARI, S., *ET AL.* 2019. Family Phyllostomidae (New World Leaf-nosed Bats). Pp. 444–583 in *Handbook of the Mammals of the World, Bats*, Vol. 9 (D. E. Wilson, and R. A. Mittermeier, eds.). Lynx Edicions, Barcelona, Spain.
- TAVARES, V. C., *et al.* 2022. Historical DNA of rare Yellow-eared bats *Vampyressa* Thomas, 1900 (Chiroptera, Phyllostomidae) clarifies phylogeny and species boundaries within the genus. *Systematics and Biodiversity* 20:1–13.
- TOMAZ, L. A. G., AND M. ZORTÉA. 2006. Dois novos registros de morcegos (Mammalia, Chiroptera) para o Cerrado do Brasil Central. *Chiroptera Neotropical* 12: 280285.
- VANZOLINI, P. E., AND E. E. WILLIAMS. 1970. South American anoles: the geographic differentiation and evolution of the *Anolis chrysolepis* species group (Sauria, Iguanidae). *Arquivos de Zoologia* 19:1–124.
- VELAZCO, S. J. E., *ET AL.* 2019. A dark scenario for Cerrado plant species: Effects of future climate, land use and protected areas ineffectiveness. *Diversity and Distributions* 25:660–673.
- DE VIVO, M. 1997. Mammalian evidence of historical ecological change in the Caatinga semiarid vegetation of northeastern Brazil. *Journal of Comparative Biology* 2:65–73.
- WANG, X., *ET AL.* 2004. Wet periods in northeastern Brazil over the past 210 kyr linked to distant climate anomalies. *Nature* 432:740–743.
- WARREN, D. L., *ET AL.* 2021. ENMTools 1.0: an R package for comparative ecological biogeography. *Ecography* 44:504–511.
- ZHANG, L., *ET AL.* 2015. Consensus forecasting of species distributions: The effects of niche model performance and niche properties. *Plos One* 10:e0120056.
- ZORTÉA, M., AND L. A. G. TOMAZ. 2006. Dois novos registros de morcegos para o Cerrado do Brasil Central. *Chiroptera Neotropical* 12:280-285.

Associated editor: Jake Esselstyn and Giovani Hernández Canchola
Submitted: August 14, 2022; Reviewed: November 26, 2022
Accepted: December 22, 2022; Published on line: January 27, 2023

Supplementary material

www.revistas-conacyt.unam.mx/theya/index.php/THERYA/article/view/2219/2219_Supplementary%20material

Coming home: modelling the mating roost of the endangered bat *Leptonycteris nivalis*

LEONORA TORRES KNOOP^{1*}, ENRIQUE MARTÍNEZ-MEYER², AND RODRIGO A. MEDELLÍN¹

¹Instituto de Ecología, Universidad Nacional Autónoma de México. Circuito exterior s/n, CP. 04510. Ciudad Universitaria. Ciudad de México, México. Email: ltorresknoop@gmail.com (LTK); medellin@ieciologia.unam.mx (RAM).

²Instituto de Biología, Universidad Nacional Autónoma de México. Circuito exterior s/n, CP. 04510. Ciudad Universitaria. Ciudad de México, México. Email: emm@ib.unam.mx (EM-M).

* Corresponding author: <https://orcid.org/0000-0002-1868-8013>.

The Mexican Long-nosed bat (*Leptonycteris nivalis*) is the largest nectarivorous species in the New World, and one of three migratory nectarivores in Mexico. It is considered an 'Endangered Species' under the U.S. Endangered Species Act and 'Threatened' by the Mexican Federal List of Endangered Species. In 1994, a Recovery Plan was developed by the USFWS with the participation of Mexican and American researchers, and the most urgent actions to ensure the species protection were identified. Locating and protecting roosts are among the most urgent tasks recognized. With this study, we aimed to identify the most suitable areas potentially holding additional mating roosts of *Leptonycteris nivalis*, and we conducted surveys of these areas to confirm its presence, and to assess the reproductive state of individuals. We used Maxent, the Genetic Algorithm for Rule-set Production (GARP), and Bioclim algorithms to generate an agreement map of the potential distribution of additional mating roosts, and we implemented a Euclidian multidimensional distances analysis to identify ecologically similar regions to "La Cueva del Diablo", the only mating roost known for the species. We identified suitable areas in the states of Morelos, Puebla and the State of Mexico. We visited seventeen caves distributed in ten different localities in these areas. For two consecutive years, we found the species in a cave called: "La Cueva de los Coyotes", located in the State of Mexico, where we captured eighteen individuals, including a pregnant female. The location of an unknown roost so far, occupied by individuals of *L. nivalis*, and among them a pregnant female, allows us to reflect about the reproductive dynamics of the species. In that sense, reproductive populations may be splitting into smaller colonies to mate, other than "La Cueva del Diablo", or pregnant females might be moving to additional and nearby roosts to spend the rest of the winter season. Using these tools and further refinements we may be able to locate additional mating roosts, thus, providing more possibilities for the application of conservation measures for the protection of the species.

El murciélago magueyero mayor (*Leptonycteris nivalis*) es el murciélago nectarívoro más grande de América y una de las tres especies nectarívoras migratorias de México. Se encuentra catalogada como especie 'En Peligro de Extinción' en Estados Unidos y como 'Amenazada' bajo la ley federal mexicana. A pesar de que *L. nivalis* tiene una amplia distribución en el país, solamente se ha documentado un refugio de apareamiento de esta especie: "La Cueva del Diablo", localizada en el estado de Morelos, en el centro de México. En 1994, con la participación de investigadores origen mexicano y de Estado Unidos, a través de la USFWS, se elaboró el Plan de Recuperación de *L. nivalis*, donde se identificaron las acciones más urgentes y necesarias para su recuperación. Dentro de dichas acciones se encuentran la localización y protección de refugios. En este estudio identificamos áreas potenciales de distribución de refugios de apareamiento en el centro de México, realizamos visitas a las zonas predichas por los análisis para confirmar la presencia de *L. nivalis* y realizamos una evaluación del estado reproductivo de los individuos. Para los análisis realizamos modelos de nicho ecológico utilizando los algoritmos Maxent, Bioclim y GARP y generamos un mapa consenso de las zonas potenciales de distribución. Adicionalmente, realizamos un análisis de distancias euclidianas multidimensionales para identificar las zonas ecológicamente más similares a la "Cueva del Diablo". Como resultado identificamos áreas potenciales en los estados de Morelos, Puebla y el Estado de México. Visitamos 17 cuevas distribuidas en 10 localidades y encontramos individuos de *L. nivalis* por dos años consecutivos en la "Cueva de los Coyotes", localizada en el suroeste del Estado de México. Capturamos 18 individuos en total, incluyendo una hembra preñada. La ubicación de un refugio ocupado por la especie *L. nivalis*, y particularmente por una hembra preñada, nos permite reflexionar sobre las dinámicas reproductivas de la especie. En ese sentido, las poblaciones reproductivas podrían estarse separando en pequeñas colonias de apareamiento, a parte de "La Cueva del Diablo", o las hembras preñadas podrían estarse moviendo hacia otros refugios para pasar el resto del invierno. Con el mejoramiento de las técnicas utilizadas en este estudio será posible encontrar y proteger refugios de apareamiento adicionales de *L. nivalis*.

Keywords: Cueva del Diablo; ecological multidimensional distances analysis; ecological niche modeling; mating roost; Mexican Long-nosed bat; potential distribution.

© 2023 Asociación Mexicana de Mastozoología, www.mastozoologiamexicana.org

Introduction

The Mexican Long-nosed bat (*Leptonycteris nivalis*) is one of the three nectarivorous migratory species in Mexico and the largest bat within the guild in the American continent. It is considered a relatively rare and scarce species (Arita and Humphrey 1988), and presents a complex biology, therefore,

it is a species difficult to study. Despite the lack of information regarding some basic ecological and biological characteristics of the species, there is relevant information that has been generated in the last decades about foraging behavior, migratory movements, diet, habitat use, and genetics (Hayward and Cockrum 1971; Easterla 1972; Moreno-Valdéz

et al. 2000; Téllez 2001; Sánchez and Medellín 2007; Ammerman et al. 2009; Toledo 2009; Galicia 2013). For instance, a general migration pattern has been proposed by several authors (Baker and Cockrum 1966; Barbour and Davis 1969; Hayward and Cockrum 1971; Easterla 1972; Humphrey and Bonnaccorso 1979; Wilson 1985; Arita 1991; Schmidly 1991; Hoyt et al. 1994; Rojas-Martínez et al. 1999; Moreno-Valdez et al. 2000; Rojas-Martínez 2001; Téllez 2001; Moreno-Valdez et al. 2004; Ammerman et al. 2009; Medellín et al. 2009). While females spend summers in the northern part of the range, in the Chihuahuan Desert, in Mexico, where they give birth and establish maternity roosts (Easterla 1972; Arita and Humphrey 1988; Moreno-Valdez et al. 2004; Ammerman et al. 2009), males supposedly move along an altitudinal gradient throughout the year in the center of Mexico (Rojas-Martínez et al. 1999). Eventually, females and young seem to move towards southwestern United States, to the Big Bend National Park, in Texas (Easterla 1972; Schmidly 1991; Ammerman et al. 2009; Adams and Ammerman 2015) and to the Romney Cave, in the Big Hatchet Mountains, in New Mexico (Hoyt et al. 1994). By the late summer and early autumn, females and sub-adults migrate to the southern part of their distribution, in Central Mexico, where they meet with the males (Arita and Humphrey 1988; Hoyt et al. 1994). It is in this stage of the cycle when mating occurs (Téllez 2001; Toledo 2009). By the end of winter and early spring, only the pregnant females return to the north of México (Moreno-Valdez et al. 2004).

Mating behavior of *L. nivalis* has been reported only in one roost called "La Cueva del Diablo" (Téllez 2001; Toledo 2009; hereafter CDMR for Cueva del Diablo Mating Roost). The CDMR is located in a highly threatened region in the state of Morelos, in Central México. This cave maintains a big population of the species throughout the winter season every year, providing a promising start for the reproduction cycle of the colony.

The region in which CDMR is located is under severe anthropogenic pressure from accelerated urban development. Additionally, the cave is accessible and regular human activity represents a significant detriment on the bat population. Although CDMR consists of one of the most important roosts for the species and have historically maintained a relatively big population, in the last decade, population size has been consistently low with some oscillations. For instance, in 1996 population size was estimated around 5,000 individuals; in 2008 between 8,000 and 10,000 individuals (Medellín 2003; López-Segurajáuregui et al. 2006); in December 2012, approximately 4,000 individuals were present (personal observation, December 2012), and from 2011 to 2016 this colony size has remained this size and stable (USFWS 2018).

Leptonycteris nivalis is considered 'Endangered' by both the IUCN (Medellín 2016) and the United States Endangered Species Act (USFWS 1994) and as 'Threatened' by the México (SEMARNAT 2010). Among the underlying factors for the risk categorization are: the lack of information

regarding the species' population status in its entire distributional range; the general small size of colonies (Arita and Humphrey 1988); the low number of known roosts (USFWS 1994; Téllez 2001); the high dependence on food availability across seasons and range (Easterla and Whitaker 1972; Humphrey and Bonnaccorso 1979; Moreno-Valdez et al. 2000); and the high risk observed in the CDMR (Medellín 2003; López-Segurajáuregui et al. 2006; Galicia 2013).

In order to identify the main threats for the conservation of *L. nivalis*, to detect the most urgent information to obtain, and the main recovery actions to take, in 1994, a Recovery Plan for the species was developed as part of the Endangered Species Act process (USFWS 1994). Later, in 2015, specialists met to review and update the species status assessment (USFWS 2018). In both evaluations, the location and protection of new roosts was recognized as an urgent need.

In this study, we aimed to identify additional potential mating roosts of *L. nivalis* by using Ecological Niche Modeling (ENM) and Euclidian Multidimensional Distances Analysis (EMDA) to assess habitat suitability, by finding ecologically similar areas to the site where the CDMR is located. For doing this, we incorporated environmental variables that could be influencing their presence and, we conducted field surveys to the predicted areas to confirm the presence of the species. The use of these techniques represents the first effort to locate specific bats' roosts, and particularly for *L. nivalis*.

Materials and methods

Study site. With the aim to focus our study to the region where the species has been recorded during winter, our study was held including the entire central region of México and considering the distribution of the main ecosystems used by the species. In terms of biogeographical criteria, this region encompasses the Trans-Mexican Volcanic Belt province and part of the Balsas Basin province. We used the entire area, composed by both physiographic provinces, for the calculation of the environmental Euclidian distances between the CDMR location and the rest of the study area and for the development of Ecological Niche Models. The Trans-Mexican Volcanic Belt is a physiographic province spanning more than 880 km east to west and is characterized by the presence of mountains with peaks above 5,000 meters (Morrone 2001), from which one is the type locality of the species (Saussure 1860). The climate is largely temperate with most of the rainfall occurring in summer C(w) (Köppen classification and modified by García 1998). The vegetation type includes tropical dry forest, pine-oak forest, shrublands, and in a lesser extent, cloud forest and alpine vegetation (Rzedowski 1978; Instituto Nacional de Estadística y Geografía; INEGI 2016). The Balsas Basin province is bound on the north by the Trans-Mexican Volcanic Belt and to the south by the Sierra Madre del Sur province. It is composed mainly of pine-oak forests and tropical dry forests. The predominant climate is tropical with dry winters (Aw; Rzedowski 1978).

The CDMR is located in the Santo Domingo locality, approximately 4 km north of the town of Tepoztlán, in the state of Morelos, at 1960 masl. (Hoffman et al. 1986; López-Segurajáuregui et al. 2006). It is in the buffer zone of the "Corredor Biológico del Chichinautzin", a federally protected area under the category of Protection of Flora and Fauna, decreed by the National Commission of Protected Areas (Comisión Nacional de Áreas Naturales Protegidas; CONANP 2016) and is part of the Trans-Mexican Volcanic Belt province (Figure 1).

Euclidian multidimensional distances analysis (EMDA). Euclidian Multidimensional Distance Analysis are developed by using Geographic Information Systems (GIS) to identify cells or pixels with the least ecological Euclidian distance within a map of an established area according to some ecological variables. For this analysis, we defined ecological Euclidian distance through ecological and environmental variables that we assume are characterizing the site where the CDMR is, and we aim at finding the most ecologically similar areas. For doing that we followed Rice et al. (2003) and Ferreira de Siqueira et al. (2009) methods, which

calculated Euclidian distances in an environmental space between two geographical points. By using ArcGis (ESRI 2011), we set CDMR as a reference point in an environmental space to calculate the multidimensional Euclidean distance between all pixels of the area and the CDMR. For this analysis, we used 19 environmental variables from Worldclim (Hijmans 2005) and three topographical variables: elevation, topographic index, and aspect (U. S. Geological Survey 2001). All variables were z-standardized and combined in ArcGis. Finally, we classified the resulting ecological distances in five unitless categories (0 to 2,500, 2,500 to 5,000, 5,000 to 10,000, and 10,000 to 20,000). Lower values represent greater ecological similarity to CDMR.

Ecological niche modeling (ENM). Ecological Niche Modeling identifies non-random associations between environmental conditions and known species presence (Nix 1986; Guisan and Zimmerman 2000; Soberón and Peterson 2004; Peterson et al. 2011) to identify potential distribution of the species across a delimited area. To generate the models, biological data from species records and data on environmental variables that characterize the ecological niche are required as inputs.

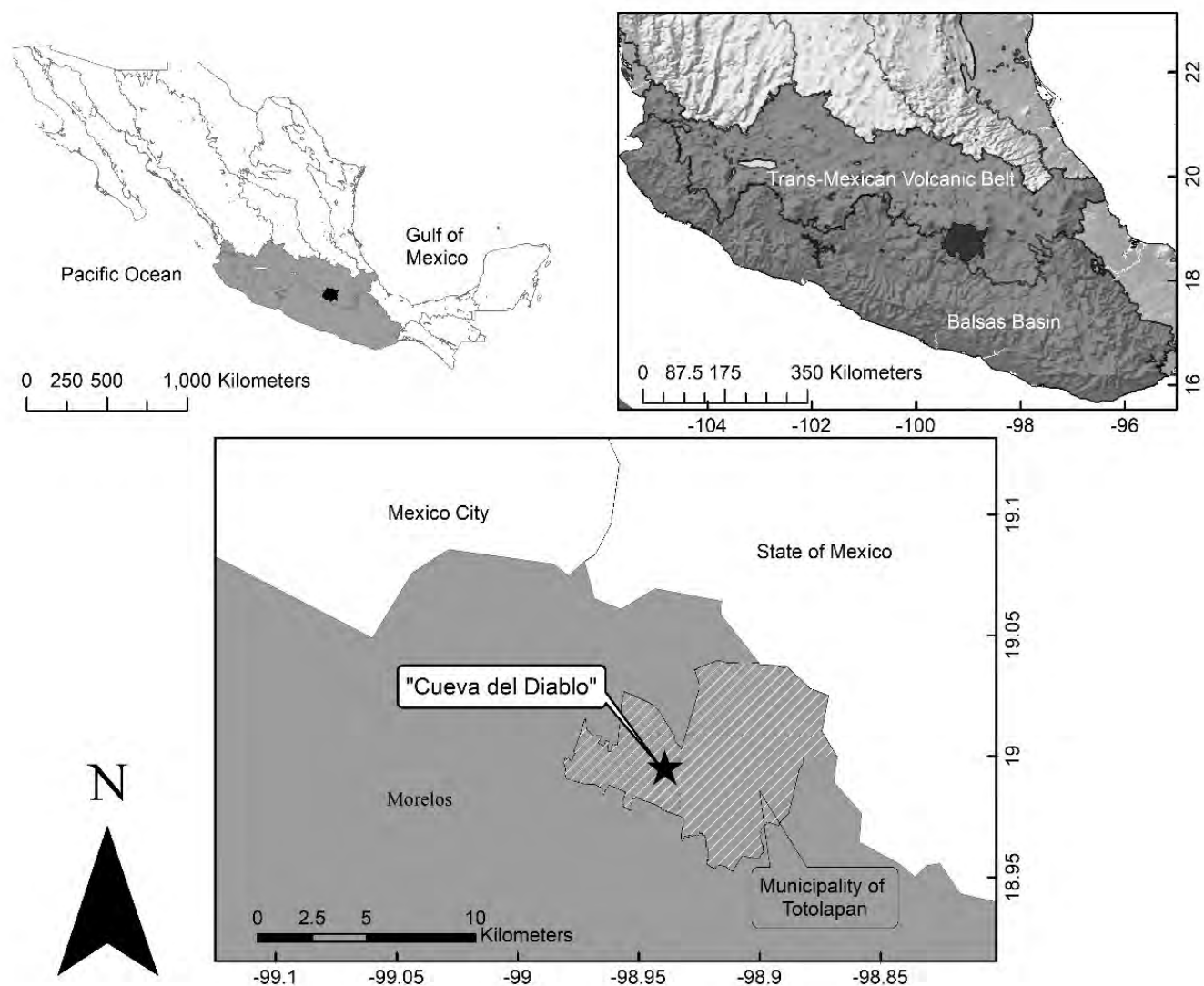


Figure 1. Study site. Top: Location of the Balsas Basin and the Transvolcanic Belt provinces. Bottom: Location of the cave "La Cueva del Diablo".

Biological data. We modeled the potential distribution of the Mexican Long-nosed bat during the autumn and winter seasons in the center of México. We gathered information on the presence records of this species from published literature and scientific collections to obtain different and independent locations for the ENM (Supplementary material 1). When possible, we visited the museum collections to assess the taxonomic identification of every specimen. We examined both skulls and specimens.

We used only museum records of the species corresponding in space and time with the mating season of the species (*i. e.* locations in central México and from late autumn to early spring). To avoid bias in our analyses we only use one record per locality. We generated three stacks of biological data of different length: 1) from August to March, hereafter "8 - M" for the eight months comprised, 2) from September to February, hereafter "6 - M" for the six months comprised, and 3) from November to February, hereafter "4 - M" for the period of four months.

Environmental data. For the ENM we used three monthly environmental surfaces: highest temperature, lowest temperature, and monthly total precipitation (Cuervo-Robayo *et al.* 2013), and the three aforementioned topographical variables. We used the Cuervo-Robayo and collaborators surfaces because they consist in the most up to date high-resolution climate surfaces for México, and they cover a wider and recent period. We consider these variables as appropriate for this analysis not only because of the higher quality of the data, compared to the other three available climate surfaces for the country (Sáenz-Romero *et al.* 2009; Téllez-Valdés *et al.* 2011; Hijmans *et al.* 2005), but also because they represent the base for other derived climate variables that consider annual patterns, and for this study we aimed at model only the winter ecological niche of *L. nivalis*. We generated three environmental data stacks corresponding temporally with the biological data stacks (*i. e.* "8-M", "6 - M" and "4 - M").

Ecological niche models- We generated ecological niche models for the three-time stacks with Maxent 3.3.3k (Phillips *et al.* 2006; Phillips and Dudik 2008), GARP (Stockwell and Noble 1992), and Bioclim (Nix 1986). For GARP and Bioclim we used the OpenModeller platform using the GARP with best subsets mode (Anderson *et al.* 2003; Muñoz *et al.* 2009). We built models corresponding to each period using the three algorithms. As a result, we obtained a total of nine models. We created a binary map for each model by defining a threshold value based on the prediction characteristics of the algorithms (Table 1). For Bioclim a threshold was established considering omission error of 0, for Maxent less than 10 %, and for GARP less than 20 %. For each period, the three binary maps corresponding to each algorithm were overlapped, and those areas that were predicted by the three algorithms were -again- converted to a binary map, generating a period consensus map. For doing this, we established an identifier value for each period model (4, 60, 800 for the 4 - M, 6 - M, 8 - M, respectively). Finally, we

Table 1. Criteria used for each model to establish threshold values.

| Period | Algorithm | Threshold criteria |
|---------------------|-----------|--|
| August - March | Maxent | Logistic threshold value: 0 - 0.199 (absence) and > 0.199 (presence) |
| | GARP | Consensus of eight models |
| | Bioclim | Area containing 100 % of the records |
| September -February | Maxent | Logistic threshold value= 0 - 0.249 (absence) > 0.249 (presence) |
| | GARP | Consensus of seven models |
| | Bioclim | Area containing 100 % of the records |
| November - February | Maxent | Logistic threshold value= 0 - 0.404 (absence) > 0.404 (presence) |
| | GARP | Consensus of nine models |
| | Bioclim | Area containing 100 % of the records |

constructed a final agreement map by overlapping the predicted area of the three resulting period consensus maps using the merge function of the ArcGis (Figure 2).

Most of the museum records that were used for our analyses came from very few unique locations (34); therefore, all models used all data as training data. Additionally, to evaluate the predictive capacity of each model, we generated models using 75 % of records as training data and 25 % as testing data. Furthermore, using the omission error values of the testing data we assessed all model predictions using the area under the ROC curve and a Chi-Square Goodness of Fit test (Supplementary material 2).

Euclidian Multidimensional Distances Analysis and Ecological Niche Modeling. The ENM final map was overlapped with the map obtained from the EMDA. Finally, we used a land cover and vegetation map (Series IV) generated by the National Institute of Geography and Statistics (INEGI 2016) to selected areas with low natural vegetation impact.

Fieldwork. During the winters of 2012 and 2013 we conducted visits to several caves (both in private and protected lands) within the high-suitability areas identified in our analyses. During the day, we entered the caves to look for evidence of the presence of *L. nivalis* (the species' characteristic smell and traces of guano of a nectarivorous bat). During nights, we set mist nets at cave entrances to capture and identify the species present, following the Medellín *et al.* (2008) identification key. For all individuals that we captured, we registered the species and took standardized measurements of body mass and forearm length. For all *L. nivalis* individuals we estimated age, determined the sex, and performed a first assessment of the reproductive state of the individuals. For females, we observed characteristics associated to gestation or lactation, such as the presence of enlarged nipples and milk-filled mammary glands, and the detection of palpable embryos (in small mammals' embryos tend to be palpable after one week; Kunz *et al.* 1996). This allowed us to distinguish between apparently inactive, lactating, and pregnant females. For males, we assessed whether the testes were scrotal or abdominal (Kunz and Parsons 1988).

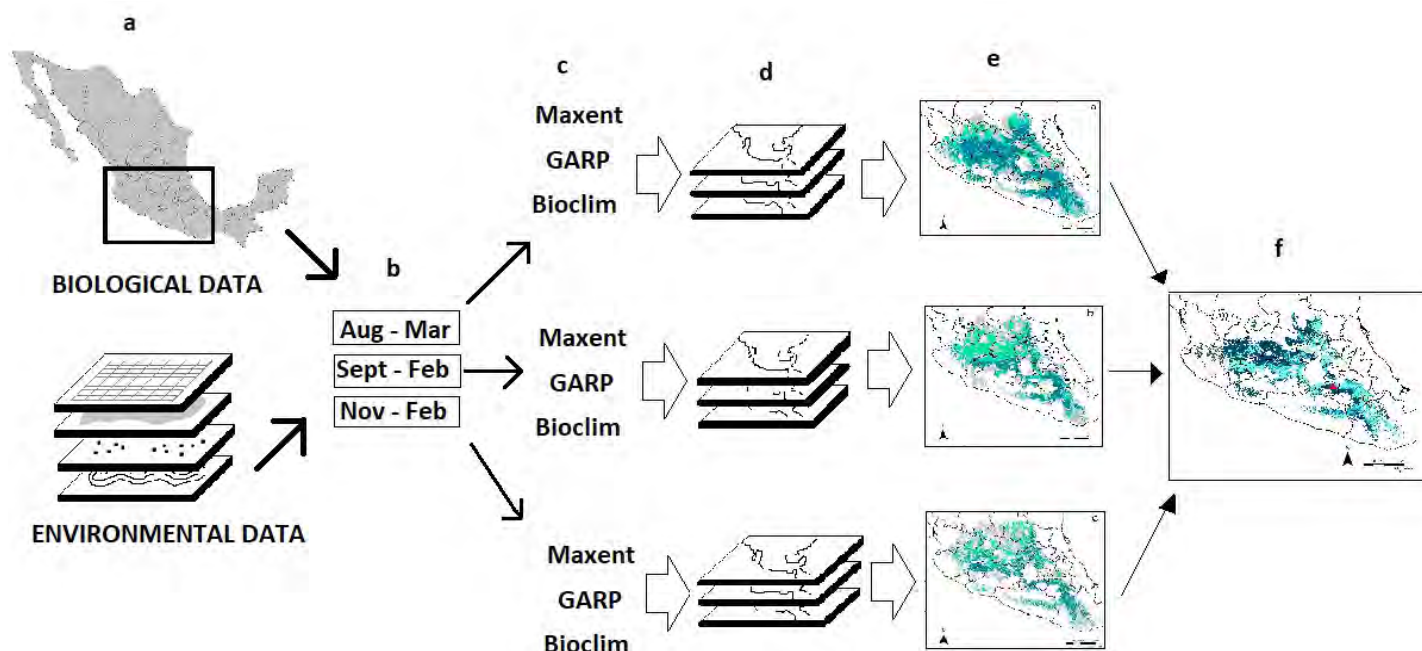


Figure 2. ENM method used in the study. Biological and environmental data (a) were divided into three periods of time (b). Maps were generated with three different algorithms (c), for each period (d). A consensus map of the three algorithms for each period was generated (e). We obtained a final agreement map of all time periods for all algorithms (f).

Additionally, to identify females in their earliest stages of gestation, as well as sexually receptive females, we performed cytological tests following [Goldman et al. \(2007\)](#). We collected vaginal smears to identify the structure of the vaginal epithelial cells. This involved the introduction of 2 μ l of physiological solution into the vaginal orifice using a micropipette (vol. = 0.5–10 μ l) and collecting the wash fluid that carried epithelial cells. We only conducted one trial per female, even if that trial failed. Afterwards, we observed the epithelial cells using an optic microscope (40x and 100x). Furthermore, as an exclusive event, to corroborate the reproductive status of a pregnant female in its earliest stage, in addition to the cytological assessment, we collected one pregnant female of *L. nivalis*. We euthanized this individual by administering an intraperitoneal injection of a lethal dose of Sodium Pentobarbital with a very small-gauge needle two hours after it was collected. We followed the protocol described in the Euthanasia Reference Manual ([The Human Society of United States 2013](#)). Captures and animal management were conducted following the American Society of Mammologists (ASM) guidelines ([Sikes et al. 2016](#)) and using the License of scientific collector (Research permit SGPA/DGVS/06361/16) provided by the Secretary of the Environment and Natural Resources (Secretaría de Medio Ambiente y Recursos Naturales in Spanish; SEMARNAT). All procedures were made ensuring all bats' welfare and the least suffering.

Results

Euclidian Multidimensional Distances Analysis and Ecological Niche Modeling. From 347 individuals that we examined, belonging to five scientific collections: Escuela Nacional de Ciencias Biológicas (ENCB), Colección Nacional de

Mamíferos (CNMA), Universidad Autónoma Metropolitana (UAMI), Colección de Mamíferos del Museo de Zoología de la Facultad de Ciencias (MZFC-M), and the Colección Osteozoológica del Laboratorio de Arqueozoología M. en C Ticul Álvarez Solórzano del Instituto Nacional de Antropología e Historia (INAH), 73 % were correctly identified as *L. nivalis*; the rest corresponded to *L. yerbabuena*. Furthermore, considering four more scientific collections: Colegio de la Frontera Sur (ECOSUR Chiapas), Centro Interdisciplinario de Investigación para el Desarrollo Integral Regional, Unidad Oaxaca and Unidad Durango (CIIDIR), and the Universidad Autónoma de Aguascalientes (UAA), we obtained 51 different localities in central México for the 8 - M period, 26 for the 6 - M period and 16 for the 4 - M period.

The EMDA showed that the region with the most similar environmental characteristics to CDMR is transversally distributed throughout the north of Morelos, across the "Tepozteco" formation, in the south of the State of México, in the northwest region of Puebla, and, scarcely, in the north of Guerrero (Figure 3).

Regarding the ENM, due to a higher number of localities used for the 8 - M period, the predicted area by this approach was considerably larger than the other models (6 - M and 4 - M). This area consisted in a broad band located mainly in the Trans-Mexican Volcanic Belt encompassing of Jalisco, Michoacán, Guanajuato, Querétaro, San Luis Potosí; as well as a more defined area located between México City and a small part of the State of México, in the Balsas Basin province. Finally, this model also predicted a considerable region located between the Balsas Basin and the Southern Sierra Madre provinces, throughout most of Morelos, south of Puebla, and northeastern and northwestern of Guerrero and Oaxaca, respectively (Supplementary material 2).

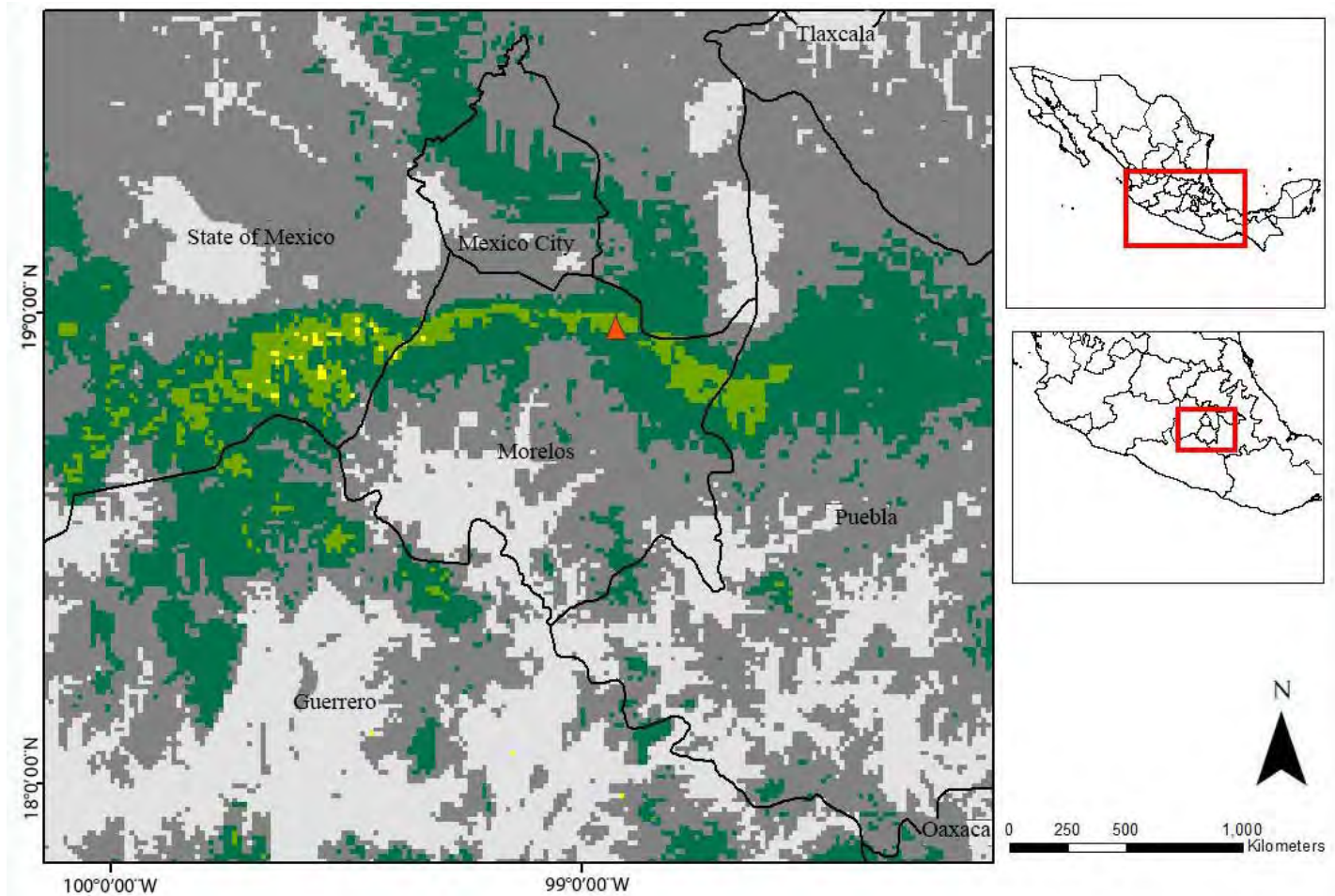


Figure 3. EMDA to “La Cueva del Diablo”, Tepoztlán, Morelos, Mexico. Yellow: region with the lowest ecological distance, hence, the most ecologically similar region to CDMR (distance of 2,500). Light green: the next most environmentally similar region (2,500 - 5,000). Dark green: third distance class (5,000 - 10,000). Dark gray: regions with an ecological distance between (10,000 - 15,000). Light gray: the most ecologically different region to CDMR (> 15,000).

Furthermore, the ecological niche modeling agreement maps from the three periods that were analyzed identified a few common areas of potential distribution, which -although not entirely- corresponded to the regions predicted by the more restricted model (corresponding to the 4-M period). These areas encompass a relatively narrow strip that cross from the southeast of the state of Jalisco, through the north of Michoacan, south of the State of México, north of Morelos, western and south of Puebla, down to the north of Oaxaca, and a small area in the northeast of Guerrero. Additionally, a reduced area located in the north of Guanajuato and Querétaro, and the south of San Luis Potosí was predicted by the three models too (Figure 4).

In addition to differences and similarities found in the areas predicted by the three time periods, variations in performance values, according to the algorithm were also observed. For instance, Bioclim showed 0 omission error, and the highest X^2 values, but it also predicted the wider potential areas. In that sense, a trade-off between omission error and percentage of area predicted by the algorithms was observed. In general terms, GARP predicted a more constrained area (allowing a more precise field search), but it also showed the highest omission error. This

was expected because we established a higher threshold for this algorithm because GARP tends to overpredict. Specifically, for the 4 - M model, Maxent showed the best performance, showing the lowest omission error (12.5 %), and the more constrained area (17.6 %). All the results of the chi-square tests that were performed were significant ($P < 0.005$; Supplementary material 3).

Finally, the map resulting from the overlapping of the EMDA analysis and the final agreement map of the ENM show that a narrow, but well defined, strip crossing transversely the south of the State of México, north of Morelos and southwestern Puebla, holds the most suitable habitat for the location of additional mating roosts for *L. nivalis* (Figure 5A). Nevertheless, this particular region is under severe anthropogenic pressure, therefore, a great proportion of the predicted region is highly disturbed. In that sense, according to the land cover information, the most conserved area of potential suitable habitat consists of a narrower corridor located in the boundary between the south of the state of México, and the northeast of Morelos (Figure 5B).

Field results. In fourteen nights of sampling effort, we visited a total of seventeen caves in eight unique sites in central México (Supplementary material 4). We found *L.*

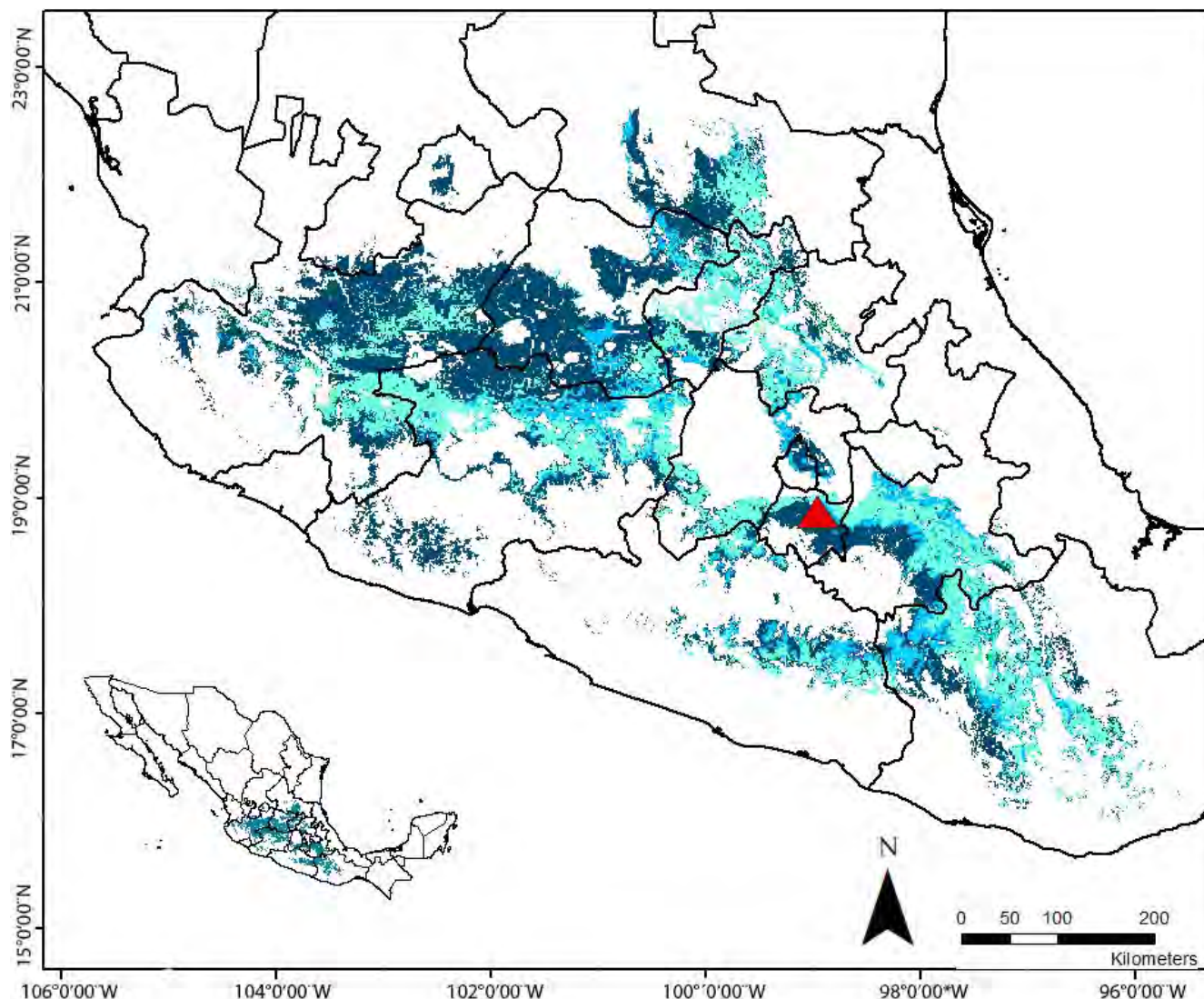


Figure 4. Agreement map of potential distribution of *L. nivalis* generated by three periods of training data (8 - M, 6 - M and 4 - M). Dark blue: Region predicted by the model 8 - M. Light blue: Region predicted by the model 6 - M. Aqua green: Region predicted by the model 4 - M. Red triangle: Location of "La Cueva del Diablo".

nivalis individuals in only one cave: "La Cueva de los Coyotes," located in the Municipality of Tonicaco, south of the State of México, near the boundary with Guerrero.

In four visits conducted to "La Cueva de los Coyotes," we captured a total of 18 individuals of the Mexican Long-nosed bat. Due to our "one trial" procedure for cytological tests we obtained epithelial cells from only one female in January 2014. We found nucleated cells as the predominant cell type and a small number of leukocytes in the smear (Supplementary material 5). This result indicates that the female was probably in a transition process between diestrus and a proestrus stages. In addition, on January 28th of 2013, we collected a female for the corroboration of the reproductive status, and she was carrying a 15 mm embryo.

Discussion

Our results show that the most suitable area for the location of additional mating roosts of *L. nivalis* is located in a narrow strip running from southwestern State of México

to northern Morelos and southwestern Puebla, in Central México. Within this area, we identified a cave called "La Cueva de los Coyotes," in which for two consecutive years we found 18 individuals of *L. nivalis* and at least one pregnant female. Usually, colonies of *L. nivalis* are composed by thousands of individuals (López et al. 2006; Sánchez and Medellín 2007; Toledo 2009), therefore, finding this small number of individuals makes an interpretation of the type and use of this roost difficult. However, the presence of the species for two years may indicate that the area, and specifically, the roost, is being used somehow. It is possible that roosts located among ecologically similar areas to CDMR are being used sparsely for parturition and births, and not specifically for the mating. It is also plausible to think that additional mating roosts are distributed along ecologically similar areas, but they are not used by colonies as large as that of the CDMR. Previous studies have suggested that northern colonies of *L. nivalis* are more numerous than the southern ones (Easterla 1972; Easterla and Whitaker 1972). Additionally, the spreading into smaller colonies following

a decreasing latitudinal gradient pattern has already been documented in the Brazilian Free-Tailed bat (*Tadarida brasiliensis*) maternity colonies (López-González and Best 2006).

Furthermore, the finding of individuals of *L. nivalis* may indicate that their presence is not a fortuitous event, and questions may arise regarding the reproductive dynamics of the species. For instance, is the presence of a pregnant and a sexually receptive female enough evidence to consider “La Cueva de los Coyotes” a mating roost? or, is “La Cueva de los Coyotes” a transitional roost to reach other, -more suitable- caves? Is the occupation of this type of roost a consistent and normal process, or does it constitute a consequence of the perturbation of “La Cueva del Diablo”, and therefore, a reflection of the observed decline in size population in this cave? Despite all possible scenarios, all previous information collected for *L. nivalis* indicates that CDMR represents the most important roost in the southern part of the species distribution range due to the large population it holds yearly during winter, and the consistent mating behavior that has only been documented there (López-Segurajáuregi et al. 2006).

Our ENM showed that, besides the region described above, an additional area was identified as a potentially suitable area for the location of roosts of the species. It is possible that this outcome is the result of a more complex association of *L. nivalis* with the environmental variables used for the models than the one that was assumed for this study. For instance, records of *L. nivalis* that were used for the construction of the ENM could be reflecting a relative ecological plasticity in the species since the models identified potential regions that are not ecologically similar to the CDMR (at least not through the environmental variables used in this study). This region includes the Mixteca region, located in northern Oaxaca and southern Puebla. The capacity of the species to use a variety of habitats, such as tropical dry forest, pine-oak forest, and shrublands (Arita 1991), could be the result of a relative broad tolerance spectrum of *L. nivalis* to different environmental factors. Additionally, a foraging compensatory capacity has been documented for this species (Ayala-Berdon et al. 2013; Galicia 2013). By incorporating this information into further analyses, it could be possible to obtain more accurate estimates of potential areas of distribution of *L. nivalis* as well as the identification of potential mating and maternity roosts.

Limitations of the methods followed in this study include that ecological niche models are very sensitive to the quality and quantity of records. Therefore, the lack of information of the species, along with its complex biology and its ability to take long flights could limit model performance (it has already been documented that the smaller sister species *L. yerbabuena* can make flights of more than 100 km per night; Medellín et al. 2018). Furthermore, since *L. nivalis* is a species that shows a strong cave roosting affinity, it could be also informative to know microclimate requirements of their roosts, in addition to habitat requirements through a landscape perspective. Therefore, future studies

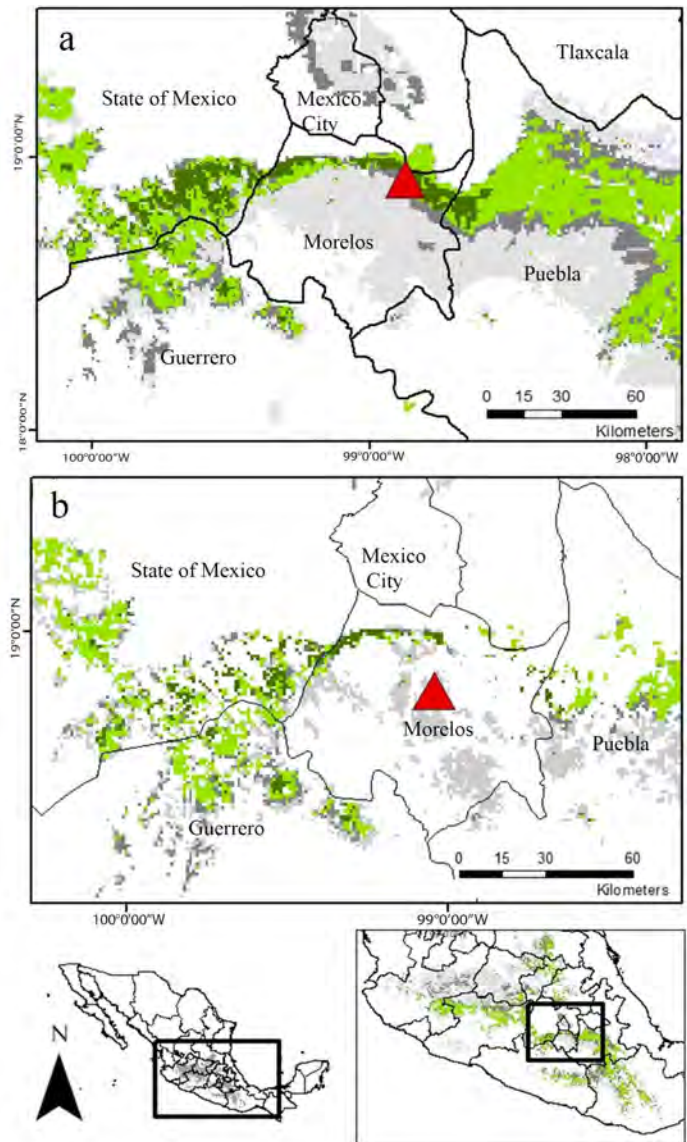


Figure 5. Overlap of EMDA and ENM maps. a. Potential distribution area. b. Conserved patches of the potential distribution area. Dark green: ecologically more similar region to “La Cueva del Diablo” and area predicted in the three periods for ENM analyses. Light green represents regions that were predicted by three of the four analyses we carried out. Dark gray: represents regions that were predicted only by two of the resulting maps. Light gray: areas predicted by only one analysis. Red triangle: Location of “La Cueva del Diablo”. Red triangle: Location of “La Cueva del Diablo”.

could consider not only macroscale habitat characteristics, but also some of the geological and topographical features that may influence roost selection.

Moreover, our study identified regions that met environmental conditions associated with mating roosts during winter season. These predictions could be complemented with a landscape characterization of the area of distribution of *L. nivalis* through the identification of potential foraging patches and assessing their use by the species. In addition, foraging areas can be associated with known roosts, and consequently, information regarding daily movements, energy and environmental requirements can be estimated, providing powerful tools for the conservation of the species.

Although additional refinements of our analyses are required, and the identification of relevant climatic vari-

ables defining ecological niche of *L. nivalis* were not within our goals, we consider that precipitation and temperature acted as appropriate variables to evaluate the habitat suitability for the species because we located a delimited geographical area that corresponded to the distribution of the main ecosystems used by the species (*i. e.* tropical dry forest, pine-oak forest, and the transition zones between them; [Arita 1991](#)). Moreover, nectar-feeding bats depend on the availability of blooming flowers and nectar production; thus, they depend on the phenological patterns of the plant species that conform their diet. In that sense, precipitation and temperature patterns are intimately related to food availability, as they consist in the main environmental triggers for regulating phenological processes ([Lyndon 1992](#); [Marqués et al. 2004](#); [Diaz and Granadillo 2005](#); [Stevenson et al. 2008](#)). Hence, these variables should be influencing the foraging ecology of *L. nivalis* too. Despite there is much to be learned regarding flight ecology, flight daily distances, and foraging ecology for this species, feeding resource distribution and availability appears to influence their distribution and migratory movements ([Fleming et al. 1993](#)). Furthermore, physiological characteristics of the species could also be influencing the distributional patterns observed for the species by giving the species the faculty of inhabiting colder environments relative to other close related species ([Ayala-Berdon et al. 2013](#)). For instance, [Espinosa \(2008\)](#), found that minimum temperature is the variable that remains constant across all localities of *L. nivalis* throughout the entire year. In contrast, precipitation varies considerably between winter and summer localities.

The conservation of the endangered migratory species *L. nivalis* depends on the protection of multiple key elements throughout its entire range of distribution ([USFWS 1994](#)). Within these elements, the temporal mating roosts used by the colonies each year are essential to the long-term conservation of the species. The “Cueva del Diablo” mating roost (CDMR), located in central México, is the only mating roost known for this species and is under threat from disruptive activities in and around the cave; therefore, it is of capital importance to locate additional mating roosts, and to increase our understanding of the population dynamics of this species.

This study represents the first effort to find such a specific target as mating roosts for a bat species. The main potential regions predicted by our analyses covered the “Chichinautzin” corridor (located in the north of Morelos), southwestern Puebla and southeastern State of México. We recommend further exploration of this area to identify more mating roosts of *Leptonycteris nivalis*. Additionally, future monitoring of “La Cueva de los Coyotes” is important to elucidate its role in the reproductive dynamic and the conservation of this species.

Acknowledgments

We dedicate this work to Dr. Alfred Gardner, a pioneer, leader, and steadfast friend whose legacy reaches out to

many mammalogists all over the world. Gracias Alfredo!! Thanks to Bat Conservation International (BCI) and Biocenciencia A.C. for the funding for conducting this project. We thank C. Moreno for technical support. Thanks to the Botanical Garden of the Universidad Nacional Autónoma de México, and to the support and assistance of the authorities of the municipality of Tonatico, State of Mexico. To the Scientific collections and their curators and staff: Colección Zoológica de la Universidad Autónoma de Aguascalientes (UAA), curated by G. de la Riva Hernández; Colección de Vertebrados de la Facultad de Ciencias de la Universidad Autónoma de Baja California (CVUABC), curated by A. A. Guevara; Colección de Mamíferos del Centro de Investigaciones Biológicas del Noroeste (CIBNOR), curated by S. T. Álvarez Castañeda; Colección Mastozoológica de la Universidad Autónoma de Campeche (UAC), curated by O. G. Retana Guascón; Colección Mastozoológica del Colegio de la Frontera Sur (ECOSUR) Unidad San Cristóbal de las Casas, Chiapas, curated by C. Lorenzo Monterrubio; Colección Zoológica Regional (Mammalia) del Instituto de Ecología e Historia Natural de Chiapas (CZRMA), curated by A. Riechers Pérez; Colección de Mastozología de la Escuela Nacional de Ciencias Biológicas (ENCB), curated by J. C. López Vidal; Colección Nacional de Mamíferos del Instituto de Biología de la Universidad Nacional Autónoma de México (CNMA), curated by F. A. Cervantes Reza; Colección de Mamíferos de la Universidad Autónoma Metropolitana (UAMI), curated by N. González; Colección de Mamíferos del Museo de Zoología de la Facultad de Ciencias (MZFC-M), curated by L. S. León Paniagua; Colección Osteozoológica del Laboratorio de Arqueozoología M. en C Ticul Álvarez Solórzano del Instituto Nacional de Antropología e Historia., curated by A. F. Guzmán Camacho; Colección de Mamíferos del Centro Interdisciplinario de Investigación para el Desarrollo Integral Regional (CIIDIR Durango), curated by C. López González; Colección de Mamíferos del Instituto Tecnológico de Huejutla, Hidalgo (HMAM), curated by S. de M. A. Mejenes López; Colección de Vertebrados del Instituto Manantlán de Ecología y Conservación de la Biodiversidad (IMEC BIO), curated by L. I. Íñiguez Dávalos; Centro de Educación Ambiental e Investigación Sierra de Huautla (CEAMISH) de la Universidad Autónoma de Morelos, curated by F. X. González Cózatl; Colección de Mamíferos de la Facultad de Ciencias Biológicas de la Universidad Autónoma de Nuevo León (UANL), curated by J. A. Niño, Colección Mastozoológica del Centro Interdisciplinario de Investigación para el Desarrollo Integral Regional, Unidad Oaxaca (CIIDIR Oaxaca), curated by M.A. Briones Salas; Colección de Mamíferos del Instituto de Ecología y Alimentos (IEA) de la Universidad Autónoma de Tamaulipas (UAT), curated by H. A. Garza Torres; Colección de Mamíferos del Instituto de Investigaciones Biológicas, Universidad Veracruzana, curated by A. González Christen; and Colección Mastozoológica del Museo de Zoología, Universidad Autónoma de Yucatán, curated by S. F. Hernández Betancourt.

Literature cited

- ADAMS, E. R., AND L. K. AMMERMAN. 2015. A serpentine antenna configuration for passive integrated transponder tag readers used at bat roosts. *The Southwestern Naturalist* 60:393–397.
- ANDERSON, R. P., D. LEW, AND A. T. PETERSON. 2003. Evaluating predictive models of species' distributions: Criteria for selecting optimal models. *Ecological Modelling* 162:211–232.
- AMMERMAN, L., *et al.* 2009. Census of the endangered Mexican long-nosed bat *Leptonycteris nivalis* in Texas, USA, using thermal imaging. *Endangered Species Research* 8:87–92.
- ARITA, H. T. 1991. Spatial Segregation in long-nosed Bats, *Leptonycteris nivalis* and *Leptonycteris curasoae*, in Mexico. *Journal Mammalogy* 72:706–714.
- ARITA, H. T., AND S. R. HUMPHREY. 1988. Revisión taxonómica de los murciélagos del género *Leptonycteris*. *Acta Zoológica Mexicana* 29:1–60.
- AYALA-BERDON, J., *ET AL.* 2013. Digestive capacities allow the Mexican long-nosed bat (*Leptonycteris nivalis*) to live in cold environments. *Comparative Biochemistry and Physiology. Part A* 164:622–628.
- BAKER, R. J., AND E. L. COCKRUM. 1966. Geographic and ecological range of the long-nosed bats, *Leptonycteris*. *Journal of Mammalogy* 47:329–331.
- BARBOUR, R. W., AND W. H. DAVIS. 1969. *Bats of America*. University Press of Kentucky, Lexington, U.S.A.
- COMISIÓN NACIONAL DE ÁREAS NATURALES PROTEGIDAS (CONANP). 2016. Corredor Biológico Chichinautzin. <https://www.gob.mx/semarnat/articulos/corredor-biologico-chichinautzin>. Accessed on December, 2016.
- CUERVO-ROBAYO, A. P., *ET AL.* 2013. An update of high-resolution monthly climate surfaces for Mexico. *International Journal of Climatology* 34:2427–2437.
- DÍAZ, M., AND E. GRANADILLO. 2005. The significance of episodic rains for reproductive phenology and productivity of trees in semiarid regions of northwestern Venezuela. *Trees* 19:336–348.
- EASTERLA, D. A., AND J. O. WHITAKER. 1972. Food habits of some bats from Big Bend National Park, Texas. *Journal of Mammalogy* 53:887–890.
- EASTERLA, D. A. 1972. Status of *Leptonycteris nivalis* (Phyllostomidae) in Big Bend National Park, Texas. *The Southwestern Naturalist* 17:287–292.
- ESPINOSA, L. A. 2008. Análisis de los nichos ecológicos estacionales de murciélagos migratorios. M. Sc. thesis. Universidad Nacional Autónoma de México, Ciudad de México, México.
- ESRI. 2011. ArcGis GIS. v9.2. Environmental Systems Research Institute, Inc., Redlands, U.S.A.
- FERRERIRA DE SIQUEIRA, M., *ET AL.* 2009. Something from nothing: Using landscape similarity and ecological niche modeling to find rare plant species. *Journal for Nature Conservation* 17:25–32.
- FLEMING, T. H., R. A. NUÑEZ, AND L. S. L. STERNBERG. 1993. Seasonal changes in the diets of migrant and non-migrant nectarivorous bats as revealed by carbon stable isotope analysis. *Oecologia* 94:72–75.
- GALICIA, R. 2013. *Ipomoea murucoides* (Convolvulaceae) como recurso de invierno para *Leptonycteris nivalis* (Phyllostomidae) en Tepoztlán, Morelos, México. Bachelor's thesis. Universidad Nacional Autónoma de México, Ciudad de México, México.
- GARCÍA, E. 1998. Climas (clasificación de Köppen modificado por García). Comisión Nacional para el Conocimiento y Uso de la Biodiversidad. Scale 1:1,000,000. México.
- GOLDMAN, J. M., A. S. MURR, AND R. L. COOPER. 2007. The rodent estrous cycle: Characterization of vaginal cytology and its utility in toxicological studies. *Birth Defects Research (Part B)* 97:84–97.
- GUISAN, A., AND N. E. ZIMMERMANN. 2000. Predictive habitat distribution models in ecology. *Ecological Modelling* 135:147–186.
- HAYWARD, B. J., AND E. L. COCKRUM. 1971. The natural history of the western long-nosed bat *Leptonycteris sanborni*. *Western New Mexico. University Research in Science* 1:75–123.
- HJUMNAS, R. J., *ET AL.* 2005. Very high resolution interpolated climate surfaces for global land areas. *International Journal of Climatology* 25:1965–1978.
- HOFFMAN, A., J. G. PALACIOS-VARGAS, AND J. B. MORALES-MALACARA. 1986. *Manual de Bioespeleología*, (con nuevas aportaciones para Morelos y Guerrero, México). Universidad Nacional Autónoma de México, Ciudad de México, México.
- HOYT, R. A., J. S. ALTENBACH, AND D. J. HAFNER. 1994. Observations on long-nosed bats (*Leptonycteris*) in New Mexico. *The Southwestern Naturalist* 39:175–179.
- HUMPHREY, S. R., AND F. BONACCORSO. 1979. Population and community ecology. Pp. 409–441, *in* *Biology of Bats of the New World. Family Phyllostomidae. Part 3* (Baker, R. J., J. K. Jones Jr., and D. Carter, eds.). Museum of Texas Tech University, Lubbock, U.S.A.
- INSTITUTO NACIONAL DE ESTADÍSTICA Y GEOGRAFÍA (INEGI). 2016. Conjunto Nacional de Información de Uso de Suelo y Vegetación. Serie IV. Scale 1:250,000, Aguascalientes, México.
- KUNZ, T. H., AND S. PARSONS (EDS.). 1988. *Ecological and Behavioral Methods for the Study of Bats*. Smithsonian Institution Press. Washington, U.S.A.
- KUNZ, T. H., C. WEMMER, AND V. HAYSEN. 1996. Sex, age and reproductive condition. Measuring and monitoring biological diversity. Pp. 279–290, *in* *Standard Methods for Mammals* (Wilson, D. E., F. R. Cole, J. D. Nichols, R. Rudran, and M. S. Foster, eds.). Smithsonian Institution Press. Washington, U.S.A.
- LÓPEZ-SEGURAJÁUREGUI, G., K. GUTIÉRREZ TOLEDO, AND R. A. MEDELLÍN. 2006. Cueva del Diablo: a Bat Cave in Tepoztlán. *AMES Boletín* 7:264–270.
- LÓPEZ-GONZÁLEZ, C., AND T. L. BEST. 2006. Current status of wintering sites of Mexican free-tailed bats *Tadarida brasiliensis mexicana* (Chiroptera: Molossidae) from Carlsbad cavern, New Mexico. *Vertebrata Mexicana* 18:13–22.
- LYNDON, R. F. 1992. *Fruit and Seed Production: Aspects of Development, Environmental Physiology and Ecology*. Cambridge University Press. New York, U.S.A.
- MARQUES, M., J. J. ROPER, AND A. P. B. SALVALAGGIO. 2004. Phenological patterns among plant life-forms in a subtropical forest in southern Brazil. *Plant Ecology* 173: 203–213.
- MEDELLÍN, R. A. 2003. Diversity and conservation of bats in Mexico: research priorities, strategies, and actions. *Wildlife Society Bulletin* 31:87–97.
- MEDELLÍN, R. A., H. T. ARITA, AND O. SÁNCHEZ. 2008. Identificación de los Murciélagos de México: Clave de Campo, 2nd ed. Universidad Nacional Autónoma de México, Ciudad de México, México.
- MEDELLÍN, R. A., *ET AL.* 2009. Conservación de especies migratorias y poblaciones transfronterizas. Pp. 459–515, *in* *Capital*

- Natural de México. Vol. II. Estado de conservación y tendencias de cambio. Comisión Nacional para el Conocimiento y Uso de la Biodiversidad. Ciudad de México, México.
- MEDELLÍN, R. A. 2016. *Leptonycteris nivalis*. In: IUCN 2017. The IUCN Red List of Threatened Species. Version 2018-2. www.iucnredlist.org. Accessed on January, 2022.
- MEDELLÍN, R. A., ET AL. 2018. Follow me: Foraging distances of *Leptonycteris yerbabuena* (Chiroptera: Phyllostomidae) in Sonora determined by fluorescent powder. *Journal of Mammalogy* 2:306-311.
- MORENO-VALDEZ, A., W. E. GRANT, AND R. L. HONEYCUTT. 2000. A simulation model of Mexican long-nosed bat (*Leptonycteris nivalis*) migration. *Ecological Modelling* 134:117-127.
- MORENO-VALDEZ, A., R. L. HONEYCUTT, AND W. E. GRANT. 2004. Colony dynamics of *Leptonycteris nivalis* (Mexican long nosed bat) related to flowering *Agave* in northern Mexico. *Journal of Mammalogy* 85:453-459.
- MORRONE, J. J. 2001. Biogeografía de América Latina y el Caribe. Universidad Nacional Autónoma de México, Ciudad de México, México.
- MUÑOZ, M. E. S., ET AL. 2009. OpenModeller: A generic approach to species' potential distribution modelling. *Geoinformatica* 15:111-135.
- NIX, H. A. 1986. A biogeographic analysis of Australian elapid snakes. *Atlas of elapid snakes of Australia* 7:4-15.
- PETERSON, A. T., ET AL. 2011. *Ecological Niches and Geographic Distributions*. Princeton University Press. Princeton, U.S.A.
- PHILLIPS, S. J., R. P. ANDERSON, AND R. E. SCHAPIRE. 2006. Maximum entropy modeling of species geographic distributions. *Ecological Modelling* 190:231-259.
- PHILLIPS, S. J. AND M. DUDIK. 2008. Modeling of species distributions with Maxent: new extensions and a comprehensive evaluation. *Ecography* 31:161-175.
- RICE, N. H., E. MARTÍNEZ-MEYER, AND A. T. PETERSON. 2003. Ecological niche differentiation in the *Aphelocoma* jays: a phylogenetic perspective. *Biological Journal of the Linnean Society* 80:369-383.
- ROJAS-MARTÍNEZ, A., ET AL. 1999. Seasonal distribution of the long-nosed bat (*Leptonycteris curasoae*) in North America: does a generalized migration pattern really exist? *Journal of Biogeography* 26:1065-1077.
- ROJAS-MARTÍNEZ, A. 2001. Determinación de movimientos altitudinales estacionales de tres especies de murciélagos nectarívoros (Phyllostomidae: Glossophaginae) en el Valle de Tehuacán y la Cuenca del Balsas, México. PhD. Thesis. Universidad Nacional Autónoma de México, Ciudad de México.
- RZEDOWSKI, J. 1978. *Vegetación de México*. 1st ed. Editorial Limusa, S. A., Ciudad de México, México.
- SÁENZ-ROMERO, C., ET AL. 2009. Spline models of contemporary, 2030, 2060 and 2090 climates for Mexico and their use in understanding climate-change impacts on the vegetation. *Climate Change* 102:595-623.
- SÁNCHEZ, R., AND R. MEDELLÍN. 2007. Food habits of the threatened bat *Leptonycteris nivalis* (Chiroptera: Phyllostomidae) in a mating roost in Mexico. *Journal of Natural History* 41:25-28.
- SAUSSURE, M. 1860. Note sur quelques mammifères du Mexique. *Revue Magasin de Zoologie* 12:281-293.
- SOBERÓN, J., AND A. T. PETERSON. 2004. Biodiversity Informatics: Managing and applying primary biodiversity data. *Philosophical Transactions of the Royal Society of London* 359:689-698.
- STEVENSON, P. R., ET AL. 2008. Flowering patterns in a seasonal tropical lowland forest in western Amazonia. *Biotropica* 40:559-567.
- STOCKWELL, D. R. B., AND I. R. NOBLE. 1992. Induction of sets of rules from animal distribution data: A robust and informative method of data analysis. *Mathematics and Computers in Simulation* 33:385-390.
- SECRETARÍA DE MEDIO AMBIENTE Y RECURSOS NATURALES. 2010. Norma Oficial Mexicana NOM-059-SEMARNAT-2010. Protección ambiental-Especies nativas de México de flora y fauna silvestres-Categorías de riesgo y especificaciones para su inclusión, exclusión o cambio-Lista de especies en riesgo. Secretaría del Medio Ambiente y Recursos Naturales. México. February, 2021.
- SCHMIDL, D. J. 1991. *The Bats of Texas*. Texas A&M Press, Lubbock, U.S.A.
- SIKES, R. S. 2016. Guidelines of the American Society of Mammalogists for the use of wild mammals in research and education. *Journal of Mammalogy* 97:663-688.
- THE HUMANE SOCIETY OF THE UNITED STATES. 2013. *Euthanasia Reference Manual*. 2nd ed. Library of Congress. Washington, U.S.A.
- TÉLLEZ, Z. J. 2001. Migración de los murciélagos hocicudos (*Leptonycteris*) en el trópico mexicano. Bachelor thesis. Universidad Nacional Autónoma de México, Ciudad de México, México.
- TÉLLEZ, O., ET AL. 2011. Desarrollo de coberturas digitales climáticas para México. Pp. 15-23, in *Cambio Climático: Aproximaciones para el Estudio de su Efecto sobre la Biodiversidad* (Sánchez Rojas, G., C. Ballesteros Barrera, and N. P. Pavón, eds.). Universidad Autónoma de Hidalgo, Pachuca, México.
- TOLEDO, K. P. 2009. Hábitos reproductivos del murciélago magueyero mayor *Leptonycteris nivalis* (Chiroptera: Phyllostomidae) en la Cueva del Diablo, Tepoztlán, Morelos, México. Bachelor's thesis. Universidad Nacional Autónoma de México, Ciudad de México, México.
- U. S. FISH AND WILDLIFE SERVICE (USFWS). 1994. Mexican Long-nosed Bat (*Leptonycteris nivalis*) Recovery Plan. USFWS, Albuquerque, New Mexico, U.S.A.
- U. S. FISH AND WILDLIFE SERVICE (USFWS). 2018. Species Status Assessment Report for the Mexican Long-nosed Bat (*Leptonycteris nivalis*), Version 1.1. U.S. Fish and Wildlife Service, New Mexico, U.S.A.
- U. S. GEOLOGICAL SURVEY (USGS). 2001. HYDRO 1k. Elevation Derivative Database. http://eros.usgs.gov/#/Find_Data/Products_and_Data_Available/gtopo30_info. Accessed on July 2013.
- WILSON, D. E. 1985. Status Report: *Leptonycteris sanborni* Hoffmeister. Sanborn's Long-nosed Bat. U.S. Fish and Wildlife Service, Washington, U.S.A.

Associated editor: Jake Esselstyn and Giovani Hernández Canchola
Submitted: August 27, 2022; Reviewed: October 5, 2022
Accepted: November 23, 2022; Published on line: January 27, 2023

Supplementary material

www.revistas-conacyt.unam.mx/theya/index.php/THERYA/article/view/2231/2231_Supplementary%20material

Human footprint effects on the distribution of the spotted lowland paca (*Cuniculus paca*)

MONSERRAT SÁNCHEZ-REYES¹, XAVIER CHIAPPA-CARRARA², ELLA VÁZQUEZ-DOMÍNGUEZ¹, CARLOS YAÑEZ-ARENAS³, MANUEL FALCONI⁴, LUIS OSORIO-OLVERA^{1*}, AND RUSBY G. CONTRERAS-DÍAZ^{2*}

¹ Departamento de Ecología de la Biodiversidad, Instituto de Ecología, Universidad Nacional Autónoma de México, Ciudad Universitaria, CP. 04500, Coyoacán. Ciudad de México, México. Email: monse.sanchez.re@gmail.com (MS-R), evazquez@ecologia.unam.mx (EV-D), luis.osorio@ecologia.unam.mx (LO-O).

² Departamento de Sistemas y Procesos Naturales, Escuela Nacional de Estudios Superiores Unidad Mérida, Universidad Nacional Autónoma de México, CP. 97357, Mérida. Yucatán, México. Email: xcc@ciencias.unam.mx (XC-C), rusby.contreras.diaz@gmail.com (RGC-D).

³ Laboratorio de Ecología Geográfica, Unidad de Conservación de la Biodiversidad, Parque Científico y Tecnológico de Yucatán, Unidad Académica Sisal, Facultad de Ciencias, Universidad Nacional Autónoma de México, Carretera Sierra Papacal km 5, CP. 97357, Mérida. Yucatán, México. Email: lichoso@gmail.com (CY-A).

⁴ Departamento de Matemáticas, Facultad de Ciencias, Universidad Nacional Autónoma de México, Ciudad Universitaria, CP. 04510, Coyoacán. Ciudad de México, México. Email: mjfalconi@gmail.com (MF).

*Corresponding authors: <https://orcid.org/0000-0003-0701-5398> (LO-O), <https://orcid.org/0000-0002-0569-8984> (RGC-D).

Human activity has caused the decrease of about 20 % of the planet's vertebrate diversity and 25 % in their abundance. Many large and medium-sized herbivore mammals have gone extinct locally, unleashing a cascade of ecosystem changes. The spotted paca (*Cuniculus paca*) is impacted by hunting and anthropogenic habitat fragmentation and loss. To protect spotted pacas, it is essential to estimate anthropogenic effects on their geographic distribution. Through the use of primary biodiversity data, bioclimatic data, land-cover data, and a human footprint index, we modeled the distribution of *C. paca*. From 105 candidate models, only one model met our selection criteria. The variables with the highest contribution were the human footprint and annual precipitation. According to the model's performance curves, the spotted paca has low to medium tolerance of anthropogenic pressure. *Cuniculus paca* tolerates low to medium anthropogenic disturbance, which we hypothesize is related to reduced predator pressure in habitats modified by humans. Accounting for the costs and benefits of anthropogenic disturbance is essential to paca conservation.

La actividad humana ha disminuido alrededor del 20 % de la diversidad biológica del planeta, así como del 25 % de la abundancia de los vertebrados. Esto ha llevado a mamíferos herbívoros grandes y medianos a extinguirse localmente, desatando una cascada de cambios en los ecosistemas. El tepezcuintle (*Cuniculus paca*) sufre una importante presión antropogénica debido a la cacería y pérdida de hábitat, por lo que es importante estimar sus efectos sobre su distribución para su conservación y manejo. Modelamos la distribución del tepezcuintle mediante el uso de datos primarios de biodiversidad de acceso libre, variables bioclimáticas, cobertura arbórea y un índice de huella humana que refleja la presión antropogénica sobre los ecosistemas. De 105 modelos candidatos, únicamente uno cumplió con los criterios de selección. Las variables con la mayor contribución fueron la huella humana y la precipitación anual. A partir de las curvas de respuesta del modelo, se observó en la especie una tolerancia a la antropización de baja a media. Estos resultados podrían deberse a que en ambientes antropizados los depredadores del tepezcuintle han disminuido sus tamaños poblacionales. Entender los costos y beneficios de la perturbación antropogénica es esencial para la conservación del tepezcuintle.

Keywords: Ecological niche models; species distribution models; spotted paca; human impact.

© 2023 Asociación Mexicana de Mastozoología, www.mastozoologiamexicana.org

Introduction

No other species impacts biodiversity, community composition, and function like human beings (Tillman 1999). In the last century, human impact on Earth has increased so considerably that anthropogenic land cover change is the leading cause of biodiversity loss and the current epoch is now recognized as the Anthropocene (Ehlers and Krafft 2006). Indeed, vegetation biomass has decreased by 53 to 58 % in recent years (Erb et al. 2018) and 20 % of the planet's biodiversity has been lost (Hill et al. 2018; Díaz et al. 2019). These disturbances have greatly affected tropical ecosystems; although quantification of deforestation rates

is difficult, some studies suggest that around 100 million hectares have been lost in recent years (Shimamoto et al. 2018). Approximately 332 terrestrial vertebrates have gone extinct since the 1500s, while around 25 % of vertebrate populations exhibit significant abundance declines, especially tropical birds and mammals (Dirzo et al. 2014). Overall, habitat loss is directly associated with the local extinction of large-and-medium-sized herbivorous mammals, unleashing a cascade of changes in ecosystems (Dirzo et al. 2014). The latter has a tremendous impact on forests because these species help maintain plant diversity via seed dispersal (Martínez-Ramos et al. 2016; Camargo-

[Sanabria et al. 2015](#)). Moreover, herbivorous mammals also have significant anthropogenic pressure due to hunting for their meat, like the spotted paca *Cuniculus paca*. The spotted paca is an endemic species from America and one of the largest rodents in the world ([Emmons 2016](#)). It is distributed from southern Mexico to northern Argentina, from sea level to up to 2800 m elevation ([Padilla-Gómez et al. 2019](#)). This caviomorph frugivore is an important seed disperser, as well as prey for large carnivores (e. g., jaguar and puma; [Figueroa-de León et al. 2016](#)). Although the spotted paca is classified as Least-concern on the Red List of the International Union for Conservation of Nature ([IUCN 2022](#)), the modification and fragmentation of its habitat most likely threatens its populations; hence, it is crucial to assess its habitat status ([Jax et al. 2015](#); [Montes 2005](#)). Correlative species distribution models are a helpful tool that allows estimating the relationship between environmental conditions and the presence of a species in the localities where it has been recorded, under the assumption that those environmental combinations where the species occurs are part of its fundamental niche, that is, where the intrinsic growth rate is positive ([Franklin 2010](#); [Soberón 2010](#); [Falconi et al. 2021](#)). These models have gained relevance for the conservation and monitoring of wildlife, given that they allow the identification of suitable habitats in current and climate change scenarios. Examples using species distribution models include the repopulation and reintroduction of declining or extinct species in the wild ([D'Elia et al. 2015](#)), as well as the identification of areas susceptible to invasion by exotic species, among many other applications ([Jarvie and Svenning 2018](#); [Espindola et al. 2019](#); [Núñez-Penichet et al. 2021](#)).

Although there have been previous attempts to estimate paca's distribution, they did not evaluate the effect of anthropization throughout the species range (e. g., [Cartaya et al. 2016](#); [Contreras-Díaz et al. 2022](#)). Our main objective in this study was to estimate the effect of the human footprint on the distribution of the spotted paca. We used the spatial human footprint index proposed by [Venter et al. \(2016\)](#), which combines different sources of human pressure including human population density, the presence of buildings, crops, induced grasslands, night lights, highways, roads, and navigable waters. By using this as a predictor in distribution models, we determined its effect on distribution and evaluated the paca's tolerance of anthropized environments. We expected *Cuniculus paca* to occur in low anthropized areas across its distribution.

Materials and methods

To estimate the effect of the human footprint on the distribution of *Cuniculus paca*, we evaluated its importance and percentage of contribution to species distribution models. The modeling framework consisted of three stages where we first collected occurrence data and modeling layers from open data repositories. Then we built candidate distribution models using different parameterizations of the Max-

Ent algorithm ([Phillips et al. 2006](#)), selecting those models that passed statistical significance, good performance tests and low complexity. Finally, using the best model, we estimated tolerance ranges to human footprint via MaxEnt's response curves and evaluated variable contribution and importance according to MaxEnt's Jackknife test.

Data collection and preparation. We obtained species occurrence data across the known distribution of the spotted paca from the Global Biodiversity Information Facility (GBIF, <https://www.gbif.org/>) and SpeciesLink (<https://slink.cria.org.br/>). We curated these data following a standard protocol summarized in [Cobos et al. \(2018\)](#). We eliminated fossil observations, wrongly georeferenced localities, duplicated records, and doubtful occurrences. We checked the altitude of all the records, and when they were doubtful, we contacted the data providers to verify their validity. We also removed localities with more than 100 m of uncertainty in their coordinates and to ensure better correspondence with the environmental layers used data from before 1990 were eliminated from our dataset. To avoid spatial autocorrelation, we thinned occurrences at 1 km using the 'ntbox' R package ([Osorio et al. 2020](#)). Finally, we randomly split curated occurrences using 70 % for training and 30% for testing the distribution models.

As modeling layers, we used the bioclimatic variables from WorldClim 2 ([Fick and Hijmans 2017](#)), the percentage of forest cover ([Tuanmu and Jetz 2014](#)), and the 2009 Global terrestrial Human Footprint map (hereafter Human Footprint; [Venter et al. 2016](#)), at a spatial resolution of ~ 1 km². The election of bioclimatic and forest layers is based on the spotted paca's biology since this species lives in humid and forested environments ([Pérez 1992](#); [Beck-King et al. 1999](#); [Gutierrez et al. 2017](#)). The Human Footprint measures direct and indirect human pressures on the environment in 2009; this index ranges from 0 to 50, where 0 means natural environment and 50 high-density built environments. To select the layers to be used in the modeling process, we first removed WorldClim 2 variables 8, 9, 18, and 19 because they present abrupt discontinuities in some areas without geographic breaks ([Anderson and Raza 2010](#); [Escobar et al. 2014](#); [Alkische et al. 2022](#)). Using information from the remaining layers, we estimated Spearman correlations between the environmental values associated with occurrence records and kept only those with correlations ≤ 0.6 to reduce multicollinearity. We clipped the selected layers according to the hypothesis of the accessible area for the species — also known as **M** — ([Soberón and Peterson 2005](#)) to avoid negative impacts of inappropriate background choices ([Alkische et al. 2022](#)). To do this, we added a buffer of 500 km around the native range polygon of the spotted paca ([Emmons 2016](#)), which provided a hypothesis of **M** based on expert knowledge, with an added area likely explored via dispersal.

Calibration and selection of species distribution models. We used MaxEnt 3.4.1 ([Phillips et al. 2006](#)) as a modeling algorithm using the 'kuenm' R package ([Cobos et al.](#)

2019). This package allows fitting and evaluating MaxEnt models using different feature classes and regulation multipliers in an automated fashion. Assessment is done using the partial ROC test for statistical significance, omission rates for model performance, and the Akaike Information criteria for model complexity (Burnham and Anderson 2002; Warren and Seifert 2011). We fitted and evaluated 105 candidate models to select the best parameter settings from our modeling layers. The regularization multipliers assessed were: 0.1, 0.25, 0.5, 0.75, 1, 1.5, 2, 2.5, 3, 3.5, 4, 4.5, 5, 5.5, 6. We used all possible combinations of linear (l), quadratic (q), and product (p) feature classes.

For assessing the overall effect of human footprint on the distribution of the spotted paca, we evaluated its importance and contribution to the model, we performed the Jackknife test in MaxEnt for those models that were statistically significant and presented omission rates < 5% of testing data. Tolerances to human footprint were assessed by examining suitability changes in response curves of MaxEnt models.

Results

We obtained 6,420 occurrences from GBIF and 273 from Species Link. From these data, 5,450 and 32 were collected from 1990 onwards, respectively. After the data curation process, due to the elimination of wrong information and both spatial and temporal duplicates, our final data set included 417 records: 406 and 11 occurrences of GBIF and SpeciesLink, respectively.

Occurrences used in modeling are distributed along an elevation range from 2 to 2,711 m (Figure 1, panel B). However, more than 75 % of the records occur below 1,000 m. Data came from 17 countries along the species distribution (Figure 1, panel C), where Colombia and México had the most georeferenced records (> 80 % of the occurrences in our database; 274 and 64 records, respectively).

Out of 17 predictor variables, seven were the least correlated variables: human footprint, tree cover, annual mean temperature (Bio 1), mean diurnal range (Bio 2), isothermality (Bio 3), annual precipitation (Bio 12), and precipitation seasonality (Bio 15).

With the MaxEnt analyses, we obtained 105 candidate models, but only one model reached the selection criteria: statistically significant, low omission rate, and complexity. The model showed an AUC value of 0.882 ± 0.007 , a regularization multiplier of 0.25, and linear, quadratic, and product features. The most contributing variables were human footprint (26.4 %), annual precipitation (21.4 %), and isothermality (19.1 %), while the least contributing variable was annual mean temperature (3.3 %; Table 1).

Regarding the geography, the model showed the most suitable areas in different zones throughout México, Guatemala, Belize, Costa Rica, Colombia, Venezuela, Ecuador, Perú, and some regions in Brazil and Bolivia (Figure 2).

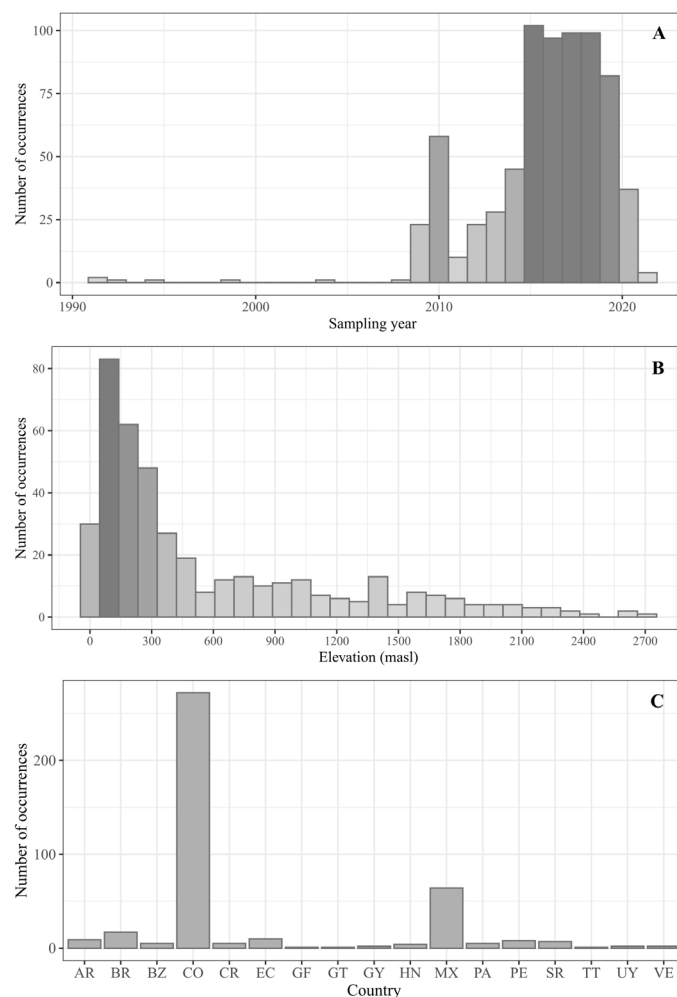


Figure 1. Description of the occurrences used in the modeling selection process: A. Occurrences per sampling year before the temporal and spatial thinning. B. Elevation (masl, meters above sea level) of the occurrences used in the model selection process. C. Occurrences per country used in the model selection process. Country: AR, Argentina; BR, Brazil; BZ, Belize; CO, Colombia; CR, Costa Rica; EC, Ecuador; GF, French Guiana; GT, Guatemala; GY, Guyana; HN, Honduras; MX, México; PA, Panama; PE, Perú; SR, Suriname; TT, Trinidad and Tobago; UY, Uruguay; VE, Venezuela.

The response curves of the model variables showed varying relationships in regard to the environmental suitability for the spotted paca (Figure 3). That is, the relationship between human footprint and environmental suitability showed a normal type form, where suitability decreased at human footprint index values greater

Table 1. Percent contributions for individual environmental variables to the best distribution model.

| Variable | Percent contribution | Permutation importance |
|--|----------------------|------------------------|
| Human footprint map for 2009 (HFP2009) | 26.4 | 30.9 |
| Annual precipitation (Bio 12) | 21.4 | 29.1 |
| Isothermality (Bio 3) | 19.1 | 6.5 |
| Tree cover | 12.3 | 10.1 |
| Mean diurnal range (Bio 2) | 11.6 | 12.0 |
| Precipitation seasonality (Bio 15) | 5.9 | 5.5 |
| Annual mean temperature (Bio 1) | 3.3 | 6.0 |

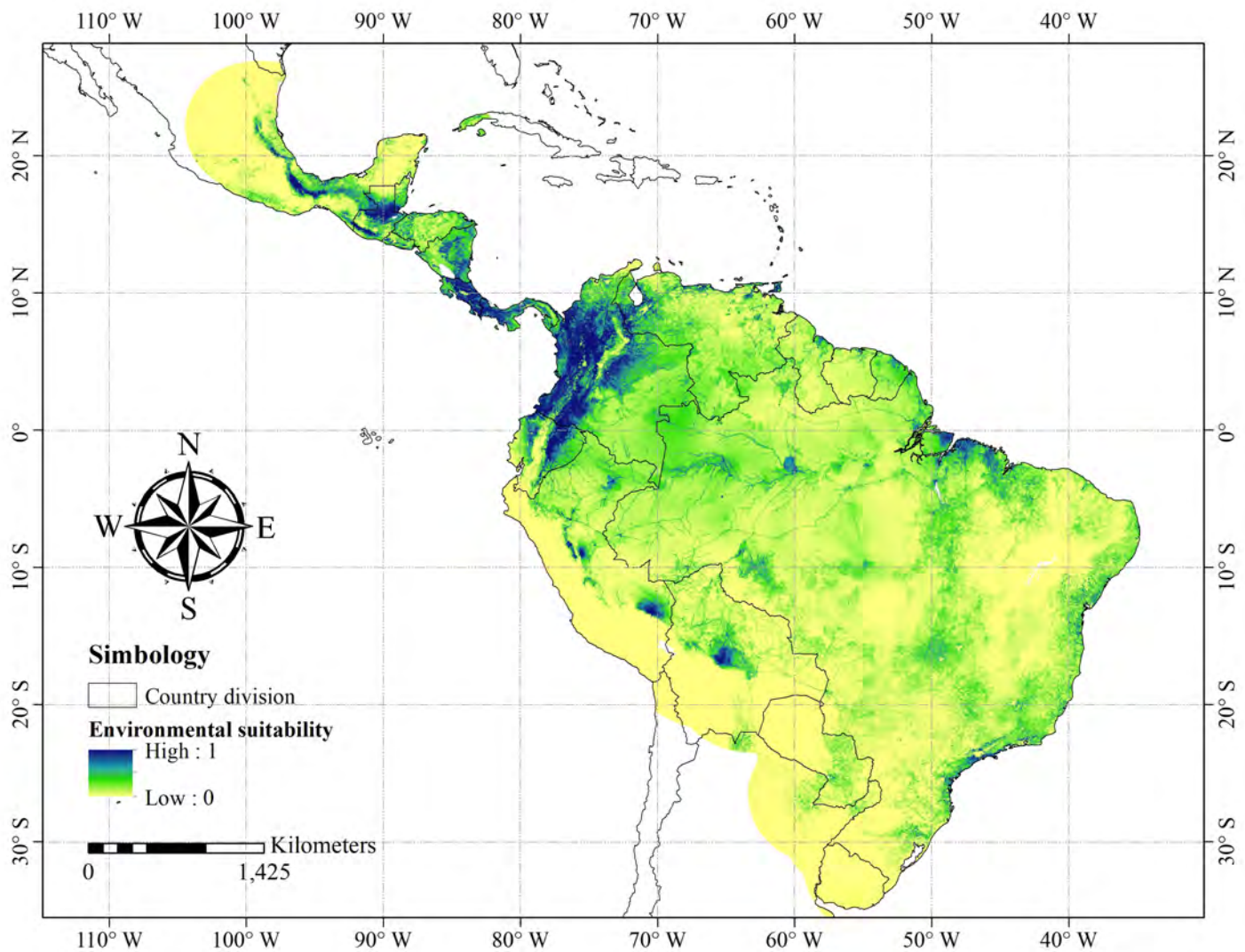


Figure 2. Species distribution model with the best performance. The MaxEnt regularization multiplier and feature type used were 0.25-linear-product-quadratic.

than 20. The same bell curve was found for tree cover and annual mean diurnal range (Bio 2). Regarding tree cover, suitability increased with the percentage of trees and slowly decreased at values of $\sim 70\%$. According to Bio 2, the spotted paca can be found along temperature variations of ± 7 ; higher variations negatively affected suitability. The curve for annual precipitation accumulation (Bio 12) showed a positive relationship with suitability, while as precipitation seasonality (Bio 15, which measures variations in precipitation) increased, suitability decreased. Finally, we found a negative relationship between isothermality (Bio 3) and suitability for values < 60 and a positive relation for higher values (Figure 3). Isothermality quantifies the day-to-night temperature oscillations relative to the summer-to-winter oscillations (measured in percent). An isothermal value of 100 indicates that the daily temperature range is equivalent to the annual temperature range (O'Donnell and Ignizio 2012). Maximum suitability values for Bio 3 were found at 100, which indicates that this species prefers non-fluctuating temperatures.

Discussion

To estimate the effect of the human footprint on the distribution of the spotted paca, we used species distribution modeling and a rigorous process of model selection based on statistical significance, predictive power, and model complexity (Cobos *et al.* 2019). Using these criteria, we found a single model that best characterized the distribution of the species. Most occurrence records are below 1,000 m elevation (see Figure 1, panel B), as reported in previous studies (Beck-King *et al.* 1999; Cartaya *et al.* 2016); however, about 3.3 % of presences occur above 2,000 m, which agrees with recent studies in México where the species has been up to 2,800 m (Padilla-Gómez *et al.* 2019). Based on the theory of species distributions, we hypothesized that some of the higher altitude occurrence patterns are related to exploration activities and might not be part of its fundamental niche (Pulliam 2000; Osorio-Olvera *et al.* 2016). It is known that when primary productivity decreases, *C. paca* explores areas outside of its range in search of food and for predator avoidance (Martínez-Ceceñas *et al.* 2018). Also, this strat-

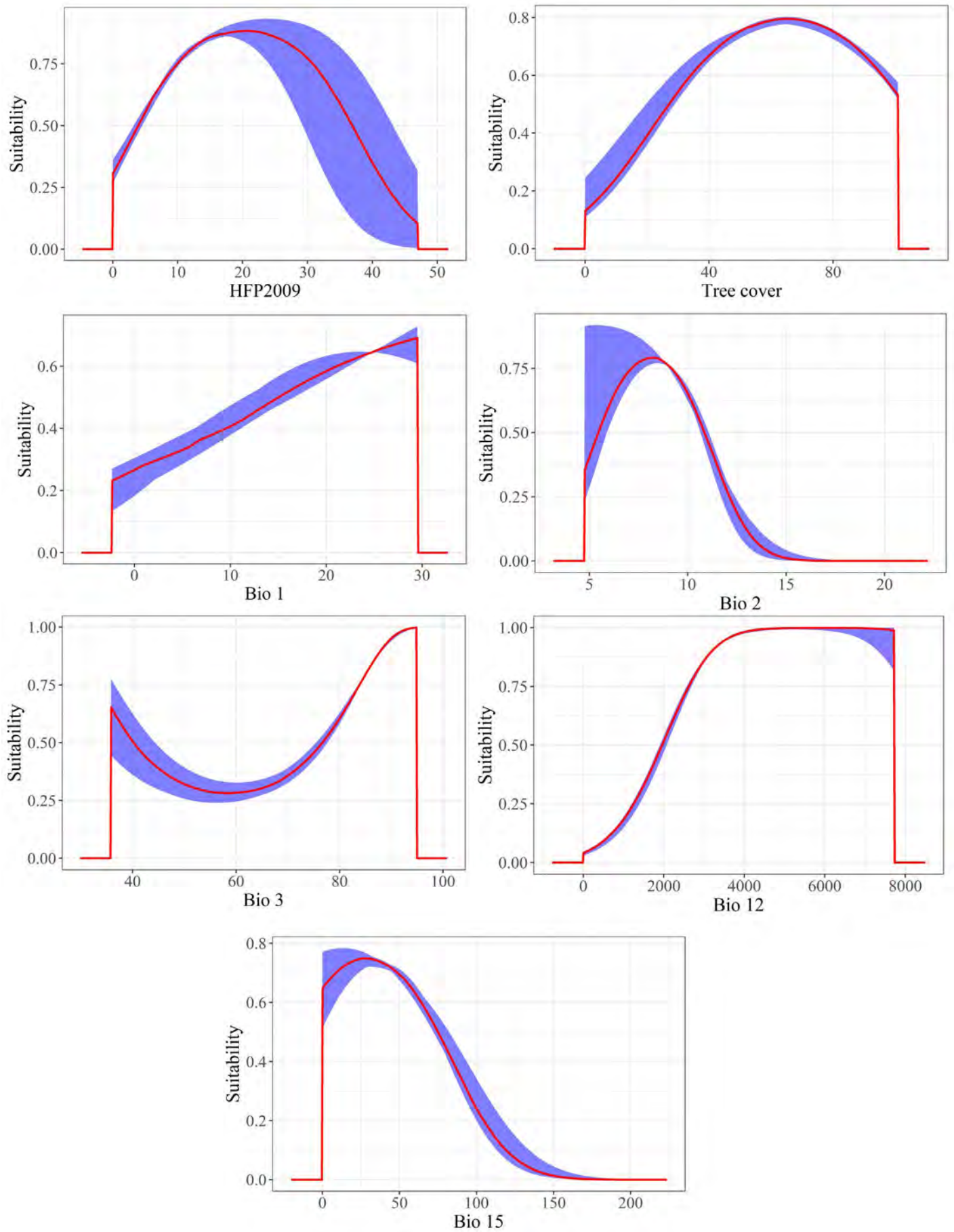


Figure 3. Variable response curves for the best distribution model. HFP2009, human footprint; tree cover; Bio 1, annual mean temperature; Bio 2, mean diurnal range; Bio 3, isothermality; Bio 12, annual precipitation; Bio 15, precipitation seasonality.

egy could be a response to climate change, as it has been documented with changes in latitudinal and altitudinal distribution patterns of many species in the world (Rowe *et al.* 2015; Feldmeier *et al.* 2020; Abbas *et al.* 2021).

The variable that contributed the most to the models was human footprint, followed by precipitation, temperature isothermality, and tree cover. These findings are in agreement with the natural history of the spotted paca given that the last three variables are crucial for its survival (Contreras-Díaz *et al.* 2022). El Bizri *et al.* (2018) found that precipitation fluctuations match reproductive cycles where mating and conception occur in the dry season, while pregnancies and births happen in the rainy season. Our results also show that *C. paca* is found in environments with less seasonal variation. High annual fluctuations in temperature and precipitation can affect food availability because fruit production depends on the rainy season, which also affects tree cover (Dubost and Henry 2017). For the spotted paca, tree cover and precipitation importance cannot be underrated, as it is an herbivore that depends on water bodies for survival and reproduction (Figueroa de León *et al.* 2016; Contreras-Díaz *et al.* 2022).

The contribution of the footprint variable highlighted the crucial role of anthropogenic pressures on spotted paca distribution and movement (Tucker *et al.* 2018). Environmental suitability increases when the human footprint index ranges from 0 to 20. A value of zero corresponds to natural areas with no human impact and values greater than 20 to highly impacted areas (Di Marco *et al.* 2018; Ven-ter *et al.* 2016). Although the paca seems to tolerate low to medium human impacts, an exploration of the components of the human footprint index shows that this species is found in places where the human population density is on average $\leq 15/\text{km}^2$, as well as places with low pressures due to roads and pasture lands (see Supplementary Material). Our results agree with Di Marco *et al.* (2018), who observed that the human footprint is a fundamental predictor of the risk status for different mammal species and found that richness decreases drastically from a value of 20, which supports our conclusion that pacas tolerate a certain level of human disturbances if adequate conditions exist for its reproduction and feeding activities. Although anthropogenic disturbance has negative effects such as habitat fragmentation and roadkill risk, some benefits need to be analyzed (Parsons *et al.* 2018). For example, certain studies report that the spotted paca can be favored by induced vegetation and crops, because it consumes fruits of cultivated species such as mango, avocado, and citrus, among others (Gallina 1981; Zucaratto *et al.* 2010). Using such modified habitat may be related to seasonality and the productivity decrease in the species' environment, forcing it to disperse to areas with higher human impact (Martínez-Ceñañas *et al.* 2018). In addition, movement to these areas could be related to predator evasion behavior (Parsons *et al.* 2018). It has been hypothesized that the spotted paca is flexible in terms of its habitat pref-

erences, where areas with a certain degree of disturbance would present lower predator densities (*e. g.*, felines) and predation risk (Michalski and Norris 2011). It is important to highlight that the apparent tolerance of the spotted paca to medium levels of disturbance could also be linked to biases in presence data due to more intensive sampling along roads, highways, areas near towns, and protected areas. However, this does not seem to be a limiting factor in the predictive power of the distribution models (McCarthy *et al.* 2011). Even if the spotted paca tolerates medium ranges of anthropogenic pressure, the highest values of environmental suitability we found indicated a tree cover of $\geq 60\%$ (see Figure 3), an adequate coverage to carry out their exploration and feeding activities (Pérez 1992; Beck-King *et al.* 1999; Gutierrez *et al.* 2017).

To conclude, we must recognize that humans are the main driver of habitat loss. However, as some species are more or less adapted to these changes, it is crucial to study the mechanisms that enable wildlife species to coexist with us, describe their environmental requirements and how they respond to changes in their habitat. For example, by studying North American mammals, Hantak *et al.* (2021) documented that large species tend to be smaller in anthropized environments. Indeed, more studies assessing species' tolerances to human activities are needed to understand the factors determining species distributions in the Anthropocene. Furthermore, the relationship between species and their environment is not static, it is scale-dependent, and thus we need studies at local and coarse spatial resolutions at different temporal scales to better design and implement conservation strategies.

Acknowledgments

We deeply thank J. A. Esselstyn and G. Hernández-Canchola for the invitation to participate in this tribute to Dr. Alfred L. Gardner. RGC-D thanks the Dirección General de Asuntos del Personal Académico of the Universidad Nacional Autónoma de México (DGAPA-UNAM) for her postdoctoral scholarship. MS-R, XC-C, CY-A, MF, LO-O, and RGC-D are grateful for support from the Programa de Apoyo a Proyectos de Investigación e Innovación Tecnológica of the UNAM (projects IA203922 and IN217123). LO-O and RGC-D thank N. Galvez-Reyes (Instituto de Ecología, UNAM) for her support in the project IA203922. Also, we thank A. Díaz-Pulido and E. Padilla-Gómez for their valuable support in data corroboration. Finally, LO-O and RGC-D thank M. Osorio for her moral encouragement.

Literature cited

- ABBAS, S., J. E. NICHOL, AND M. S. WONG. 2021. Trends in vegetation productivity related to climate change in China's Pearl River Delta. *Plos One* 16:e0245467.
- ALKISHE, A., ET AL. 2022. Ecological niche and potential geographic distributions of *Dermacentor marginatus* and *Dermacentor reticulatus* (Acari: Ixodidae) under current and future climate conditions. *Web Ecology* 22:33–45.

- ANDERSON, R. P., AND A. RAZA. 2010. The effect of the extent of the study region on GIS models of species geographic distributions and estimates of niche evolution: preliminary tests with montane rodents (genus *Nephelomys*) in Venezuela. *Journal of Biogeography* 37:1378–1393.
- BECK-KING, H., O. V. HELVERSEN, AND R. BECK-KING. 1999. Home Range, Population Density, and Food Resources of *Agouti paca* (Rodentia: Agoutidae) in Costa Rica: A Study Using Alternative Methods 1. *Biotropica* 31:675–685.
- BURNHAM, K. P., AND D. R. ANDERSON. 2002. Model selection and multimodel inference: A practical information-theoretic approach. Springer. New York, U.S.A.
- CAMARGO-SANABRIA, A. A., ET AL. 2015. Experimental defaunation of terrestrial mammalian herbivores alters tropical rainforest understory diversity. *Proceedings of the Royal Society B: Biological Sciences* 282:20142580.
- CARTAYA, S., C. ANCHUNDIA, AND R. MANTUANO. 2016. Distribución geográfica potencial de la especie *Cuniculus paca* en el occidente de Ecuador. *La Granja: Revista de Ciencias de la Vida* 24:134–149.
- COBOS, M. E., ET AL. 2018. Sample data and training modules for cleaning biodiversity information. *Biodiversity Informatics* 13:49–50.
- COBOS, M. E., ET AL. 2019. kuenm: an R package for detailed development of ecological niche models using Maxent. *PeerJ* 7:e6281.
- CONTRERAS-DÍAZ, R. G., ET AL. 2022. On the relationship between environmental suitability and habitat use for three neotropical mammals. *Journal of Mammalogy* 103:425–439.
- D'ELIA, J., ET AL. 2015. Activity-specific ecological niche models for planning reintroductions of California condors (*Gymnogyps californianus*). *Biological Conservation* 184:90–99.
- DÍAZ, S., ET AL. 2019. Pervasive human-driven decline of life on Earth points to the need for transformative change. *Science* 366:eaax3100.
- DI MARCO, M., ET AL. 2018. Changes in human footprint drive changes in species extinction risk. *Nature Communications* 9:4621.
- DIRZO, R., ET AL. 2014. Defaunation in the anthropocene. *Science* 345:401–406.
- DUBOST G., AND O. HENRY. 2017. Seasonal reproduction in neotropical rainforest mammals. *Zoological Studies* 56:2.
- EHLERS, E., AND T. KRAFFT. 2006. Managing global change Pp. 5–12, in *Earth System Science in the Anthropocene* (Ehlers, E., and T. Krafft, eds.). Springer. Berlin, Heidelberg.
- EL BIZRI, H. R., ET AL. 2018. Breeding seasonality in the lowland paca (*Cuniculus paca*) in Amazonia: interactions with rainfall, fruiting, and sustainable hunting. *Journal of Mammalogy* 99:1101–1111.
- EMMONS, L. 2016. *Cuniculus paca*. The IUCN Red List of Threatened Species 2016:e.T699A22197347.
- ERB, K. H., ET AL. 2018. Unexpectedly large impact of forest management and grazing on global vegetation biomass. *Nature* 553:73–76.
- ESCOBAR, L. E., ET AL. 2014. Potential for spread of the white-nose fungus (*Pseudogymnoascus destructans*) in the Americas: Use of Maxent and NicheA to assure strict model transference. *Geospatial Health* 9:221–229.
- ESPIÑOLA, S., J. L. PARRA, AND E. VÁZQUEZ-DOMÍNGUEZ. 2019. Fundamental niche unfilling and potential invasion risk of the slider turtle *Trachemys scripta*. *PeerJ* 7:e7923.
- FALCONI, M., L. OSORIO-OLVERA, AND R. G. CONTRERAS-DÍAZ. 2021. Distribución de especies. Un punto de vista teórico. *Revista de Modelamiento Matemático de Sistemas Biológicos* 1:16–24.
- FELDMER, S., ET AL. 2020. Shifting aspect or elevation? The climate change response of ectotherms in a complex mountain topography. *Diversity and Distributions* 26:1483–1495.
- FICK, S. E., AND R. J. HIJMANS. 2017. WorldClim 2: new 1-km spatial resolution climate surfaces for global land areas. *International Journal of Climatology* 37:4302–4315.
- FIGUEROA-DE LEÓN, A. 2016. Dinámica de ocupación de cavidades y uso de hábitat del tepezcuintle (*Cuniculus paca*) en la Selva Lacandona, Chiapas, México. Ph.D. Dissertation. El Colegio de la Frontera Sur. San Cristóbal de Las Casas, Chiapas, México.
- FRANKLIN, J. 2010. Mapping species distributions: spatial inference and prediction (Ecology, biodiversity and conservation). Cambridge University Press. New York, U.S.A.
- GALLINA, S. 1981. Contribución al conocimiento de los hábitos alimenticios del tepezcuintle (*Agouti paca* Lin.) en Lacanjá-Chansayab, Chiapas. Publicación del Instituto de Ecología de México 6:55–67.
- GBIF.ORG. 2021. GBIF Occurrence Download. <https://doi.org/10.15468/dl.5u4dvg>. Accessed on 4 February 2021.
- GUTIÉRREZ, S. M., ET AL. 2017. Ranging behavior and habitat selection of pacas (*Cuniculus paca*) in central Belize. *Journal of Mammalogy* 98:542–550.
- HANTAK, M. M., ET AL. 2021. Mammalian body size is determined by interactions between climate, urbanization, and ecological traits. *Communications Biology* 4:972.
- HILL, S. L. L., ET AL. 2018. Worldwide impacts of past and projected future land-use change on local species richness and the Biodiversity Intactness Index. *BioRxiv* 311787.
- IUCN. 2022. The IUCN Red List of Threatened Species. Version 2022-1. <https://www.iucnredlist.org>. Accessed on 8 July 2022.
- JARVIE, S., AND J. C. SVENNING. 2018. Using species distribution modelling to determine opportunities for trophic rewilding under future scenarios of climate change. *Philosophical Transactions of the Royal Society B* 373:20170446.
- JAX, E., ET AL. 2015. Habitat use and relative abundance of the spotted paca *Cuniculus paca* (Linnaeus, 1766) (Rodentia: Cuniculidae) and the red-rumped agouti *Dasyprocta leporina* (Linnaeus, 1758) (Rodentia: Dasyproctidae) in Guatopo National Park, Venezuela. *Journal of Threatened Taxa* 7:6739–6749.
- MARTÍNEZ-CECEÑAS, Y., ET AL. 2018. Ecología alimentaria del tepezcuintle (*Cuniculus paca*) en áreas conservadas y transformadas de la Selva Lacandona, Chiapas, México. *Revista Mexicana de Biodiversidad* 89:507–515.
- MARTÍNEZ-RAMOS, M., ET AL. 2016. Anthropogenic disturbances jeopardize biodiversity conservation within tropical rainforest reserves. *Proceedings of the National Academy of Sciences* 113:5323–5328.
- MCCARTHY, K. P., ET AL. 2012. Predicting species distributions from samples collected along roadsides. *Conservation Biology* 26:68–77.
- MCCAUGHTON, S. 1975. r- and K-selection in *Typha*. *The American Naturalist*, 109:251–261.
- MICHALSKI, F., AND D. NORRIS. 2011. Activity pattern of *Cuniculus paca* (Rodentia: Cuniculidae) in relation to lunar illumination and other abiotic variables in the southern Brazilian Amazon. *Zoologia* 28:701–708.

- MONTES, R. 2005. El tepezcuintle, un recurso biológico importante. *Biodiversitas* 63:6–10.
- NUÑEZ-PENICHER, C., ET AL. 2021. Geographic potential of the world's largest hornet, *Vespa mandarinia* Smith (Hymenoptera: Vespidae), worldwide and particularly in North America. *PeerJ* 9:e10690.
- O'DONNELL, M. S., AND D. A. IGNIZIO. 2012. Bioclimatic predictors for supporting ecological applications in the conterminous United States. U.S. Geological Survey Data Series 691:1–10.
- OSORIO-OLVERA, L. A., M. FALCONI, AND J. SOBERÓN. 2016. Sobre la relación entre idoneidad del hábitat y la abundancia poblacional bajo diferentes escenarios de dispersión. *Revista Mexicana de Biodiversidad* 87:1080–1088.
- OSORIO-OLVERA, L., ET AL. 2020. ntbox: an R package with graphical user interface for modelling and evaluating multidimensional ecological niches. *Methods in Ecology and Evolution* 11:1199–1206.
- PADILLA-GÓMEZ, E., ET AL. 2019. Noteworthy records of jaguar (*Panthera onca*), tayra (*Eira barbara*), and paca (*Cuniculus paca*) from southern Mexico. *Notas sobre Mamíferos Sudamericanos* 1.
- PARSONS, A. W., ET AL. 2018. Mammal communities are larger and more diverse in moderately developed areas. *eLife* 7:e38012.
- PÉREZ, E. M. 1992. *Agouti paca*. *Mammalian Species* 404:1–7.
- PHILLIPS, S. J., ET AL. 2006. Maximum entropy modeling of species geographic distributions. *Ecological Modelling* 190:231–259.
- PULLIAM, H. R. 2000. On the relationship between niche and distribution. *Ecology Letters* 3:349–361.
- R CORE DEVELOPMENT TEAM. 2019. R: A language and environment for statistical computing. Vienna, Austria. <https://www.R-project.org/>.
- ROWE, K. C., ET AL. 2015. Spatially heterogeneous impact of climate change on small mammals of montane California. *Proceedings of the Royal Society B: Biological Sciences* 282:20141857.
- SOBERÓN, J. 2010. Niche and area of distribution modeling: a population ecology perspective. *Ecography* 33:159–167.
- SOBERÓN J., AND A. T. PETERSON. 2005. Interpretation of models of fundamental ecological niches and species' distributional areas. *Biodiversity Informatics* 2:1–10.
- SPECIESLINK. 2021. Red Species Link. Reference Center for Environmental Information (CRIA), Research Support Foundation of the State of São Paulo (FAPESP). <http://www.splink.org.br>. Accessed on 10 February 2021.
- SHIMAMOTO C. Y., ET AL. 2018. Restoration of ecosystem services in tropical forests: A global meta-analysis. *Plos One* 13:e0208523.
- TILMAN, D. 1999. The ecological consequences of changes in biodiversity: a search for general principles. *Ecology* 80:1455–1474.
- TUANMU, M. N., AND W. JETZ. 2014. A global 1-km consensus land-cover product for biodiversity and ecosystem modelling. *Global Ecology and Biogeography* 23:1031–1045.
- TUCKER, M. A., ET AL. 2018. Moving in the Anthropocene: Global reductions in terrestrial mammalian movements. *Science* 359:466–469.
- VENTER, O., ET AL. 2016. Global terrestrial Human Footprint maps for 1993 and 2009. *Scientific Data* 3:1–10.
- WARREN, D. L., AND S. N. SEIFERT. 2011. Ecological niche modeling in Maxent: The importance of model complexity and the performance of model selection criteria. *Ecological Applications* 21:335–342.
- ZUCARATTO, R., R. CARRARA, AND B. K. SIQUIERA FRANCO. 2010. Dieta da paca (*Cuniculus paca*) usando métodos indiretos numa área de cultura agrícola na Floresta Atlântica brasileira. *Biotemas* 23:235–239.

Associated editor: Jake Esselstyn and Giovani Hernández Canchola
Submitted: September 9, 2022; Reviewed: October 31, 2022
Accepted: January 2, 2023; Published on line: January 27, 2023

Supplementary material

www.revistas-conacyt.unam.mx/theya/index.php/THERYA/article/view/2237/2237_Supplementary%20material

Current status of the *Peromyscus mexicanus* complex in Oaxaca, México

L. ERNESTO PÉREZ-MONTES¹, SERGIO TICUL ÁLVAREZ-CASTAÑEDA^{1*}, AND CONSUELO LORENZO²

¹ Centro de Investigaciones Biológicas del Noroeste, Av. Instituto Politécnico Nacional 195, CP. 23096, La Paz. Baja California Sur, México. Email: ernestomontes364@gmail.com (LEP-M), sticul@cibnor.mx (STA-C).

² Departamento de Conservación de la Biodiversidad, El Colegio de la Frontera Sur, CP. 29290, San Cristóbal de Las Casas. Chiapas, México. Email: clorenzo@ecosur.mx (CL).

*Corresponding author: <https://orcid.org/0000-0002-2689-8758>.

The physiographic, climatic, and ecological characteristics of the mountainous regions of Oaxaca are unique and host geographically isolated populations of *Peromyscus mexicanus*. Populations of *P. mexicanus* from the Sierra Madre del Sur in the Gulf side (SMG) and Pacific side (SMP), Oaxaca, were compared at the craniodental and molecular genetic levels (cytochrome *b* sequences). The geographic isolation of both sides of the Sierra Madre del Sur are expected to have led to genetic isolation between populations of *P. mexicanus* in each area and from populations of eastern México. Our results show that the Oaxacan SMG and SMP populations are genetically different, as are populations of eastern México. Populations in the Oaxaca SMG-SMP are more genetically similar to *P. gymnotis* than to *P. mexicanus* from eastern México. We recommend that the Oaxacan SMG population be classified as *P. totontepecus* and the SMP population as *P. angelensis*, with the Putla population, which is morphologically and morphometrically different, as the subspecies, *P. a. putlaensis*.

Las características fisiográficas, climáticas y ecológicas de las regiones montañosas de Oaxaca son únicas y albergan poblaciones de *Peromyscus mexicanus* aisladas geográficamente. Se compararon a nivel craneodental y genético molecular (secuencias del citocromo *b*) poblaciones de *P. mexicanus* de las Sierras Madre del Sur en la vertiente del Golfo (SMG) y del Pacífico (SMP) de Oaxaca. Por el aislamiento geográfico de ambas vertientes de la Sierra Madre del Sur, se espera aislamiento genético entre las poblaciones de *P. mexicanus* y a su vez con las poblaciones del este de México. Los resultados muestran que las poblaciones de SMG y SMP son genéticamente diferentes, al igual que las poblaciones del este de México. Las poblaciones de SMG-SMP de Oaxaca están más próximas genéticamente a *P. gymnotis* que a *P. mexicanus* del este de México. Se considera que la población de la SMG debe ser conocida como *P. totontepecus*. La población de la SMP como *P. angelensis*, y la población de Putla, morfológica y morfométricamente diferente, como la subespecie, *P. a. putlaensis*.

Keywords: Endemics; nomenclature; taxonomic change; tropical.

© 2023 Asociación Mexicana de Mastozoología, www.mastozoologiamexicana.org

Introduction

In the *mexicanus* complex of the genus *Peromyscus*, 12 species with tropical affinities are recognized, four distributed in México: *P. carolpattonae*, *P. gymnotis*, *P. mexicanus*, and *P. zarhynchus* (Pérez-Consuegra and Vázquez-Domínguez 2017; Álvarez-Castañeda et al. 2019), and eight restricted to Central America: *P. bakeri*, *P. gardneri*, *P. grandis*, *P. guatemalensis*, *P. nicaraguae*, *P. nudipes*, *P. salvadorensis*, and *P. tropicalis* (Ordoñez-Garza et al. 2010; Pérez-Consuegra and Vázquez-Domínguez 2015, 2017; Bradley et al. 2016; Lorenzo et al. 2016; Álvarez-Castañeda et al. 2019). The *Peromyscus mexicanus* complex has been under constant taxonomic review by various authors, with several new species described (Pérez-Consuegra and Vázquez-Domínguez 2015; Lorenzo et al. 2016; Álvarez-Castañeda et al. 2019). The first review of this complex was conducted by Huckaby (1980), where several subspecies described for Central America are now considered valid species (Pérez-Consuegra and Vázquez-Domínguez 2015).

The *Peromyscus mexicanus* complex comprises seven subspecies (Carleton 1989; Trujano-Álvarez and Álvarez-Castañeda 2010): *P. m. angelensis*, distributed in the Sierra Madre del Sur from Guerrero to Oaxaca; *P. m. azulensis*,

restricted to mountains of eastern Oaxaca; *P. m. mexicanus*, in the tropical rainforests of Veracruz and the Gulf of Oaxaca coastal plain; *P. m. putlaensis*, in a region between the western portion of the Sierra Madre del Sur and the southwestern part of the mountains and valleys of western Oaxaca; *P. m. saxatilis*, from the Isthmus of Tehuantepec to Costa Rica; *P. m. teapensis*, in the humid forests of Veracruz, Tabasco, and Chiapas; and *P. m. totontepecus*, restricted to the mountains of the Sierra Madre del Sur in the Gulf side (SMG) of Oaxaca (Huckaby 1980; Hall 1981; Trujano-Álvarez and Álvarez-Castañeda 2010; Figure 1). The populations of *P. m. nicaraguae*, *P. m. salvadorensis*, and *P. m. tropicalis* distributed from Guatemala to Panama are currently recognized as distinct species (Ordoñez-Garza et al. 2010; Pérez-Consuegra and Vázquez-Domínguez 2015, 2017; Bradley et al. 2016; Lorenzo et al. 2016; Álvarez-Castañeda et al. 2019).

The mountainous regions of Oaxaca represent an ideal model for studying evolutionary processes that determine genetic diversity due to their climatic, physiographic, and geological characteristics (Sullivan et al. 1997; García-Mendoza et al. 1994). These characteristics of mountainous regions and their physical separation foster isolation and possible endemism of populations of *P. mexicanus* (Bedford and Hoekstra 2015).

The genetic characterization of other groups of *Peromyscus* species has revealed high genetic divergence among populations inhabiting different mountainous areas (Álvarez-Castañeda *et al.* 2019; Bradley *et al.* 2019; Greenbaum *et al.* 2019; León-Tapia *et al.* 2020). The main mountain ranges of Oaxaca are not currently interconnected, are associated with different climates, and differ in vegetation composition (Ortiz-Pérez *et al.* 2004; McCormack *et al.* 2009). *Peromyscus mexicanus* has been studied in different mountainous regions of Central America and southern México, where a positive correlation has been found between mountain ranges and the presence of different species; hence, the same condition is likely to exist in Oaxaca (Smith *et al.* 1986; Huckaby 1973, 1980; Rogers and Engstrom 1992; Ordoñez-Garza *et al.* 2010; Pérez-Consuegra and Vázquez-Domínguez 2015, 2017; Lorenzo *et al.* 2016; Álvarez-Castañeda *et al.* 2019).

The geographic isolation of mountain regions is likely to restrain gene flow between populations of *P. mexicanus*. Therefore, molecular and morphological-cranial differences are expected to occur between the populations of *P. m. totontepecus* in the Sierra Madre del Sur, Pacific side (SMP), in Oaxaca and *P. m. angelensis* and *P. m. putlaensis* in the Sierra Madre del Sur, Gulf side (SMG), in Oaxaca. To establish the relationship of *P. mexicanus* populations living in both sides of the Sierra Madre del Sur of Oaxaca, these populations were compared with other populations distributed in México and Central America through genetic and morphological analyses.

Materials and methods

The Sierra Madre del Sur are present in the Gulf and Pacific sides of Oaxaca (Morrone 2017). The Gulf side covers an area of 17,519 km² with mountains reaching elevations of 2,500 masl. Vegetation is dominated by mountain cloud forests, tropical forests, and xeric shrubland (Ortiz-Pérez *et al.* 2004). The types of climate are humid, with mean annual temperature between 22 °C and 24 °C and mean annual precipitation of 4,000 mm, and semi-warm humid, with mean annual temperature of 18 °C to 22 °C and mean annual precipitation of 3,800 mm (Trejo 2004).

The Pacific side in Oaxaca covers an area of 12,350 km², with elevations above 2,000 masl. Vegetation is dominated by mountain cloud forests, medium sub-evergreen forests, and shrubland, together with low deciduous forests in restricted areas (García-Mendoza and Torres 1999). The climate is humid and semi-warm humid, with temperatures of 22 °C to 26 °C and, in the highest zones, of 18 °C to 22 °C; the mean annual precipitation ranges between 3,000 mm and 3,500 mm (Trejo 2004).

We used material previously deposited in the Mammal Collection of the Centro de Investigaciones Biológicas del Noroeste (CIB). The specimens were identified based on cranial traits following the taxonomic keys of Álvarez-Castañeda *et al.* (2015, 2017).

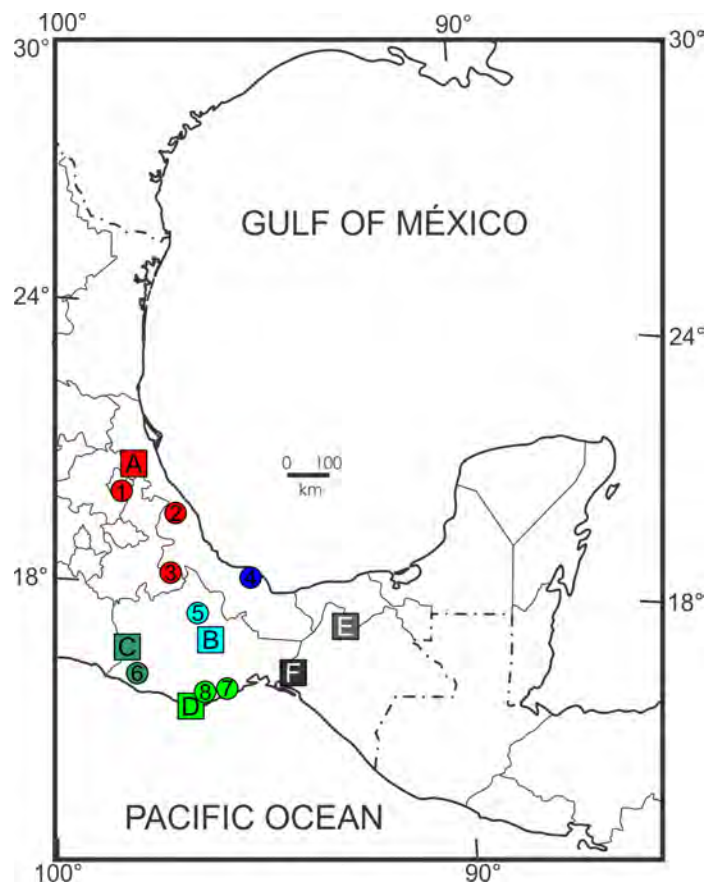


Figure 1. Map of the localities of specimens used for the genetic and morphological analyses. Numbers in the map mark the following localities: 1) Misantla, 2) Tutotepec, 3) Zongolica, 4) Los Tuxtlas, 5) Valle Nacional, 6) San José de las Flores, 7) San Francisco Huamelula, and 8) San Felipe Lachilló. Letters indicate the type localities of A) *P. m. mexicanus* (El Mirador, red), B) *P. m. totontepecus* (Tonotepec, light blue), C) *P. m. putlaensis* (Putla, dark green), D) *P. m. angelensis* (Puerto Ángel, light green), E) *P. m. teapensis* (Teapa, dark gray), and F) *P. m. azulensis* (Cerro Azul, black).

Samples of specimens. For the genetic and morphometric studies, we used specimens from Oaxaca of the following subspecies of *P. mexicanus* (*n* for the molecular analysis / *n* for the morphometric analysis). From the SMP: *P. m. angelensis* (*n* = 7/9) from two localities: 0.5 km W, San Felipe Lachillo (*n* = 2/2) and 0.5 km N, San Francisco Huamelula (*n* = 5/7) and *P. m. putlaensis* (*n* = 1/3) 0.62 km NE, San José de las Flores. From the SMG: *P. m. totontepecus* (*n* = 14/19) 10 km S, 5 km W Valle Nacional. In addition, we used specimens from Los Tuxtlas, Veracruz, which should be assigned to *P. m. mexicanus* (Hall 1981; Carleton 1989; Trujano-Álvarez and Álvarez-Castañeda 2010); however, to include a clear difference from *P. mexicanus* distributed to the north, this population will hereafter be referred to as "*P. m. Tuxtlas*".

DNA sequence data. We sequenced the cytochrome *b* gene (*Cytb*; *n* = 27) for specimens representing *P. m. angelensis*, *P. m. putlaensis*, *P. m. totontepecus*, and *P. m. Tuxtlas*. Genomic DNA was extracted from muscle tissue preserved in 95 % ethanol (stored at -20 °C) using the DNeasy Kit (Qiagen Inc., Valencia, California) protocols. For the proximal 5'-3' ~800 bp of *Cytb*, we used the primer pairs MVZ05/MVZ16 (CGA AGC TTG ATA TGA AAA ACC ATC GTT G/AAA TAG GAA RTA TCA YTC TGG TTT RAT; Smith 1998).

The following conditions were used for the initial double-strand amplification: 12.5 μ l of (10 ng) template; 4.4 μ l ddH₂O; 2.5 μ l of each primer pair (10 nM); 0.474 μ l (0.4 nM) dNTPs; 0.5 μ l (3 mM) MgCl₂; 0.125 μ l *Taq* polymerase (Platinum *Taq* DNA Polymerase High Fidelity, Invitrogen, Carlsbad, California); and 1 \times *Taq* buffer, to make a final volume of 25 μ l. Amplification consisted of a 3-minute initial denaturation at 94 °C followed by 37 denaturation cycles at 94 °C for 45 s each; 45 s annealing at 50 °C; and extension at 72 °C for 60 s. PCR amplicons were cleaned using the QIAquick PCR Purification Kit (Qiagen), and templates were cycle-sequenced in both directions using the Big Dye terminator chemistry (Applied Biosystems Inc., Foster City, California). All products were sequenced by Macrogen Geumcheongu, Seoul, Korea, and deposited in GenBank.

The resulting nucleotide sequences were edited in SEQUENCHER 4.1.4 (GeneCodes Corporation), followed by the alignment of sequences and matrix manipulations. Sequences were manually verified and translated into amino acids to check for spurious stop codons and for alignment confirmation.

Genetic diversity. The DnaSP ver 6.12.03 software was used to estimate the haplotypic and nucleotide diversity of the populations of each side of the Sierra Madre del Sur separately and with the populations combined (Librado and Rozas 2009). Levels of differentiation were assessed with p-distances calculated in Mega X (Kumar et al. 2018) using the Kimura 2-parameter model (Kimura 1980). Nucleotide diversity (P_i), haplotype diversity (H_d), F_s value (F_u) and Tajima's (D) were obtained in Arlequin 3.5 (Excoffier and Lischer 2010).

Phylogenetic analyses. The most appropriate substitution model for the data set was determined using the Akaike information criterion (AIC) as implemented in MrAIC (Nylander et al. 2008). Bayesian analyses were conducted in MrBayes ver. 3.0b4 (Ronquist and Huelsenbeck 2003), using four separate runs with Markov-chain Monte Carlo simulations starting from a random tree. Each run was allowed to go for 20 million generations, sampling at intervals of 1,000 generations. The first 25 % of samples was discarded as burn-in; the remaining sampled trees were analyzed to obtain the posterior probability of the resulting nodes. Partitioned model was assessed using each of the three codon positions separately while applying equal weights and nodal support using non-parametric bootstrapping. ML analyses (Felsenstein 1981) were run in PAUP ver. 4.0b10 (Swofford 2002) using a heuristic search with 1,000 replicates and swapping with the Tree Bisection Reconnection (TBR) algorithm.

In addition to the 27 sequences obtained, we downloaded from GenBank 29 sequences corresponding to specimens of the *mexicanus* group used in previous phylogenetic studies (Supplementary material 1; Bradley et al. 2007; Ordoñez-Garza et al. 2010; Pérez-Consuegra and Vázquez-Domínguez 2015, 2017). Eight species were included as an external group: *P. boylii*, *P. furvus*, *P. maniculatus*, *P. mayensis*,

P. megalops, *P. melanocarpus*, *P. melanophrys*, and *P. sirtoni* (Supplementary material 1; Smith and Patton 1999; Amman et al. 2006; Bradley et al. 2007; Rogers et al. 2007). Phylogenetic trees were observed with the FIGTREE 1.4.4 program (Rambaut 2012).

Morphological analysis. Four somatic measurements of each of the specimens were taken from skin labels: total length (ToL), tail length (TaL), foot length (LHF), and ear length (LE). In addition, we recorded 19 craniodental measurements with a digital vernier to the nearest 0.01 mm: greatest length of skull (GLS), skull height (SKH), condylobasal length (CBL), bullar length (BUL), shield-bullae depth (SBD), diastema length (DIL), rostral height (ROH), rostral breadth (BRR), palatal bridge length (PBL), post-palatal length (POL), basioccipital length (OCL), maxillary toothrow length (MTL), maxillary toothrow breadth (MTB), post-dental breadth (PDB), zygomatic breadth (ZYB), braincase breadth (BAB), nasal length (NAL), interorbital breadth (IOB), and nasal breadth (NAB). Cranial measurements were defined according to Diersing (1981), Williams and Ramírez-Pulido (1984), and Robinson and Dippenaar (1987).

Five age classes were assigned based on tooth growth and wear (Monroy-Gamboa et al. 2005). The specimens assigned to age classes 1 and 2 were considered juvenile and excluded from the analyses. Classes 3 and 4 were classified as adults, while class 5 were considered old. The analysis of sex variation was based on 38 adult specimens (19 females and 19 males) and used an analysis of variance (ANOVA) in STATISTICA ver. 7.0 (Statsoft Inc. 2007). A Kruskal–Wallis test (multiple comparisons with Dunn's method) was used to test for differences among groups.

The four somatic and 19 cranial measures were analyzed through an ANOVA with the Scheffe *post hoc* test to differentiate the populations associated with each subspecies. A Principal Component Analysis (PCA) was performed with the Mahalanobis distance to distinguish populations using STATISTICA ver. 7.0 (Statsoft Inc. 2007) and Paleontological Statistics PAST (ver. 3.26; Hammer et al. 2001). The PCA were performed after the data for the original variables were log-transformed, because in the first analysis all the factorial loads have the same sign in order to reduce the effect of scale differences among them. Somatic measurements were not included in the morphological analyses due to the high coefficient of variation (> 10). Morphological comparisons from each of the geographical areas were made in coloration patterns, shape, and measurements. The LSID for this publication is: urn:lsid:zoobank.org:pub:A8949600-7E9C-4497-92A3-998A32110B25.

Results

The genetic diversity analysis of the 56 sequences of the *mexicanus* group showed a total of 36 non-redundant haplotypes, a nucleotide diversity $P_i = 0.07$, and haplotype diversity $H_d = 0.96$ (Supplementary material 1). The analysis of the 22 sequences of *P. m. angelensis*, *P. m. putlaensis*, and *P. m. totontepecus* yielded nine non-redundant haplotypes

with 45 variable sites, $P_i = 0.03$, $H_d = 0.85$, $F_s Fu = 6.6$, and Tajima's $D = 1.94$. Specifically, within the populations of SMP, *P. m. angelensis*-*P. m. putlaensis* ($n = 7$) showed three non-redundant haplotypes, $P_i = 0.00182$, $H_d = 0.607$, $F_s Fu = 0.671$, and Tajima's $D = -0.73$. In SMG, *P. m. totontepecus* ($n = 16$) showed six non-redundant haplotypes, eight variable sites, $P_i = 0.00286$, $H_d = 0.747$, $F_s Fu = -0.941$, and Tajima's $D = -0.74$.

Phylogenetic analyses. The molecular substitution model that best fitted the sequences was GTR+I+G (General Time reversible using a gamma distribution and assuming that a given fraction of the sites are invariable; Tavaré 1986). The nitrogenous base frequencies were: A = 31.85, C = 26.66, G = 13.25, and T = 28.25; in addition to invariable sites = 0.5427, gamma distribution = 1.0458, AIC = 18,936.53, -LnI = 9,342.92.

The maximum likelihood (tree not shown) and Bayesian inference (Figure 2) tests showed similar topologies and clades within the *P. mexicanus* complex, in addition to those described by Pérez-Consuegra and Vázquez-Domínguez (2017). The results show two clades. The first corresponds to the specimens of *P. m. totontepecus* from Valle Nacional, and *P. m. Tuxtlas*. The second, to the three localities of *P. m. angelensis* and *P. m. putlaensis*: San José de las Flores, Lachilló, and Huamelula. The *P. m. totontepecus*-*P. m. Tuxtlas* and *P. m. angelensis*-*P. m. putlaensis* clades are more closely related to *P. gymnotis* than to the known species of *P. mexicanus* (from central to northern Veracruz).

The *P. m. angelensis*-*P. m. putlaensis* specimens were 5.31 % (p -distance) genetically divergent compared with *P. m. totontepecus*, 7.15 % relative to *P. gymnotis*, and 7.54 %

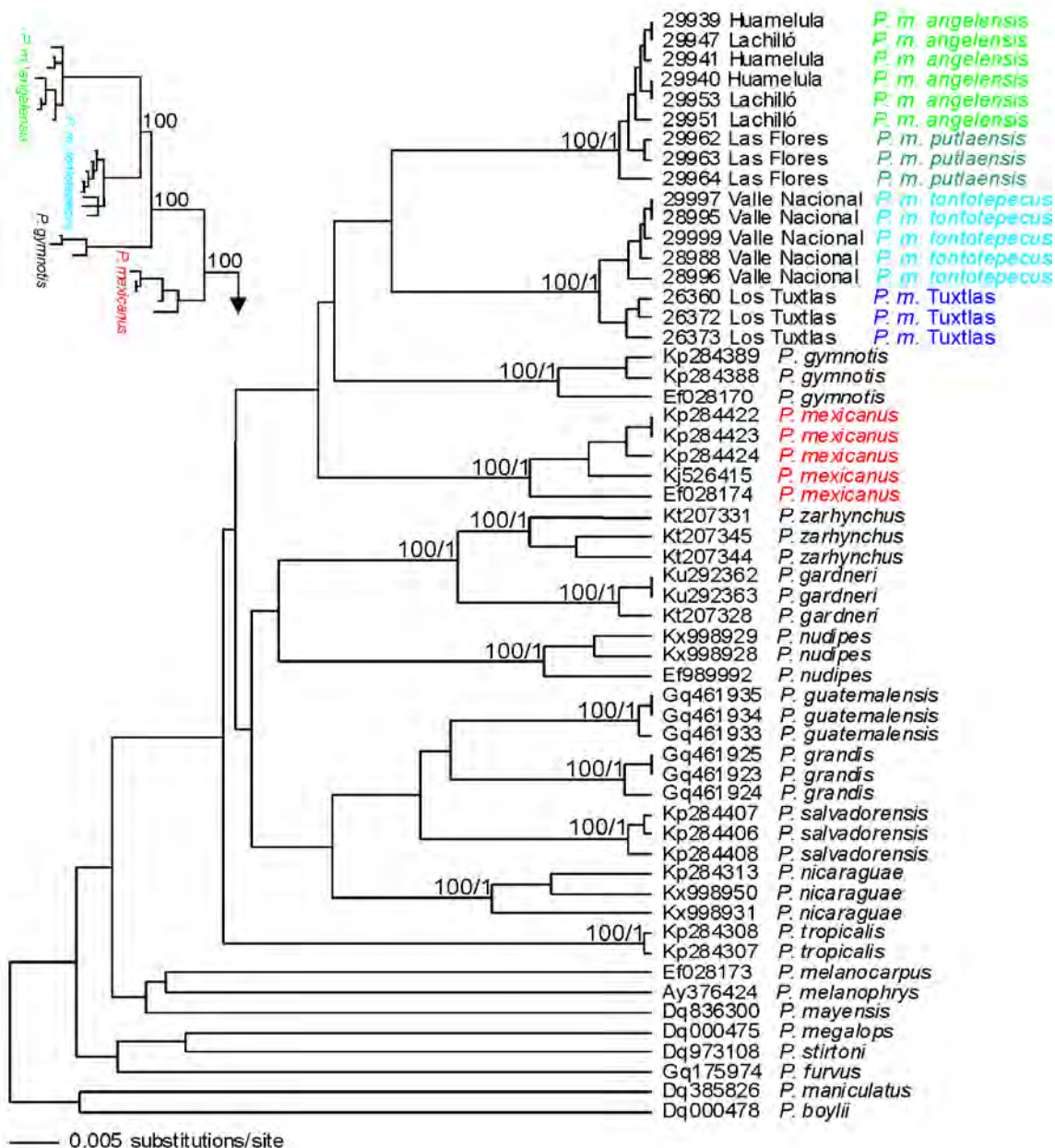


Figure 2. Bayesian inference obtained from the p -distance analysis of *Cytb* sequences of *Peromyscus mexicanus angelensis*, *P. m. putlaensis*, and *P. m. totontepecus*. Species of the *mexicanus* complex are included; other related *Peromyscus* species were used as an external group. Bootstrap / posterior probability support values are shown on the nodes in each branch of the tree.

with respect to *P. mexicanus*. The *P. m. totontepecus* specimens showed a 5.67 % genetic divergence with *P. gymnotis* and 5.98 % with *P. mexicanus* (Table 1). The *P. m. angelensis*-*P. m. putlaensis* and *P. m. totontepecus*-*P. m. Tuxtlas* specimens showed a genetic divergence with the rest of the species of the *mexicanus* group higher (> 5.9 %) than that of *P. gymnotis*. *Peromyscus m. totontepecus* specimens showed an intra-population genetic divergence of 0.70 % and those of *P. m. angelensis*-*P. m. putlaensis*, of 0.37 %.

Morphological comparisons. Specimens from each side of the Sierra Madre del Sur share similar cranial (Figure 3) and external morphologies. The *P. m. angelensis*-*P. m. putlaensis* have a slightly grayish pelage that is lighter-colored and rough, and the abdomen is paler than in *P. m. totontepecus*. The specimens of both sides of the Sierra Madre del Sur have whitish legs, with the proximal part darker and almost black. The tail is long, with very short hair but a hairless appearance, usually dorso-ventrally bicolored or with white spots in the ventral part. *Peromyscus m. totontepecus*

Table 1. Percentage of genetic differentiation (*p*-distance) obtained from *Cytb* sequences within species of the *mexicanus* group among populations of *P. m. totontepecus* - *P. m. Tuxtlas* (SMG) and *P. m. angelensis* - *P. m. putlaensis* (SMP), *P. mexicanus* and more related species.

| | 1 | 2 | 3 | 4 | 5 |
|---|------|------|------|------|------|
| 1 <i>P. m. totontepecus</i> - <i>P. m. Tuxtlas</i> | 0.70 | | | | |
| 2 <i>P. m. angelensis</i> - <i>P. m. putlaensis</i> | 5.31 | 0.37 | | | |
| 3 <i>P. gymnotis</i> | 5.67 | 7.15 | 1.42 | | |
| 4 <i>P. mexicanus</i> | 5.98 | 7.54 | 6.80 | 1.47 | |
| 5 <i>P. zarhynchus</i> | 8.58 | 9.38 | 8.93 | 7.33 | 1.94 |

specimens have a more marked ring spot around the eye than specimens of *P. m. angelensis*-*P. m. putlaensis*. Specimens of *P. m. Tuxtlas* have a darker and softer pelage.

Geographic variation. The means and standard deviation of the somatic and craniodental measurements obtained by ANOVA show that *P. m. totontepecus* is larger (total length; ToL) compared with *P. m. angelensis*, *P. m. putlaensis*, and *P. m. Tuxtlas* ($P < 0,001$; Table 2).

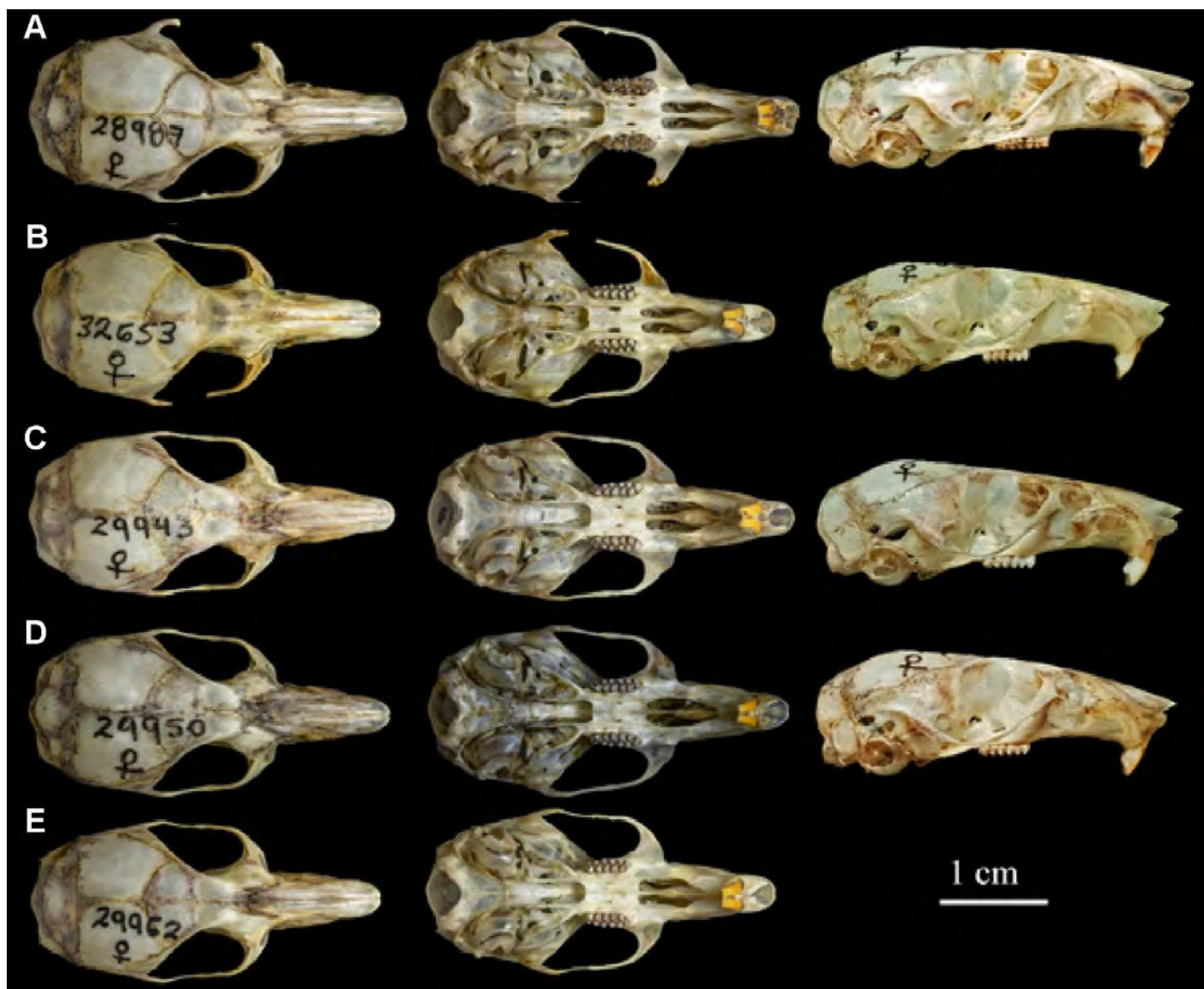


Figure 3. Dorsal, ventral, and lateral views of *Peromyscus m. totontepecus* skulls (A = Valle Nacional, 28987; B = Los Tuxtlas, Veracruz, 32653); *P. m. angelensis* (C = San Francisco Huamelula, 29943; D = San Felipe Lachillo, 29950); *P. m. putlaensis* (E = San José de las Flores, 29962).

The ANOVA *post hoc* Scheffe test between *P. m. angelensis*, *P. m. putlaensis*, *P. m. Tuxtlas* and *P. m. totontepecus* indicate non-significant differences in any variables (somatic and craniodental) between the following pairs of taxa: *P. m. angelensis*-*P. m. putlaensis*; *P. m. angelensis*-*P. m. Tuxtlas*; *P. m. putlaensis*-*P. m. Tuxtlas*. Significant differences were observed between these pairs of taxa: *P. m. putlaensis*-*P. m. totontepecus*, in one somatic variable (LHF); *P. m. totontepecus*-*P. m. Tuxtlas*, in two somatic variables (ToL and LE) and two craniodental variables (CBL, PBL); *P. m. angelensis*-*P. m. totontepecus*, in two somatic variables (ToL and LHF) and five craniodental variables (GLS, CBL, SBD, POL, NAB; Appendix 1).

Principal Component Analysis. The PCA of the 19 craniodental variables showed that the first principal component accounts for 50 % of the data variability; the second, for 9 %; and the third, for 7 %, summing to 66 % of the variation. The scores of the PCA for *P. m. angelensis*, *P. m. putlaensis*, *P. m. Tuxtlas*, and *P. m. totontepecus* indicate that there is no geographic pattern for the differences in “size” in PC1; however, these clades could be distinguished by their respective scores on each of the “shape” axes in PC2, PC3, and PC4, although these axes explain relatively little of the total variation (Appendix 2; Figure 4).

The Mahalanobis distance test determined the absence of outliers in the PCA. The plot of the results of the PCA shows that *P. m. totontepecus* tends to have the largest basi-

occipital region, whereas the smallest was found in *P. m. mexicanus*. We found only a few differences in the interorbital region between *P. m. angelensis*-*P. m. putlaensis* and *P. m. totontepecus*, in which it is larger in size, compared with *P. m. Tuxtlas*, in which it tends to be smaller.

Discussion

The molecular systematics of the *Peromyscus mexicanus* group has been extensively revised for southern México and Central America. However, an in-depth review has not been conducted for populations north of the Isthmus of Tehuantepec. Data obtained from the mountain systems of southern México and Central America (Álvarez-Castañeda *et al.* 2019; Bradley *et al.* 2007, 2016; Lorenzo *et al.* 2016; Ordoñez-Garza *et al.* 2010; Pérez-Consuegra and Vázquez-Domínguez 2015, 2017) suggest that the conditions in the state of Oaxaca have favored the development of *P. mexicanus* into a complex of species.

The results of the phylogenetic analyses of *P. m. angelensis*-*P. m. putlaensis* and *P. m. totontepecus*-*P. m. Tuxtlas* are clearly separate from the nominal taxon, *P. mexicanus* distributed from central Veracruz to the north.

The specimens from Los Tuxtlas, Veracruz, were assigned to *Peromyscus m. mexicanus*, which has its type locality in Veracruz (10 km E Mirador Veracruz; Dalquest 1950), approximately 400 km to the northwest and associ-

Table 2. Arithmetic means ± standard deviation of four external measurements and 19 cranial measurements of each group of *P. mexicanus* from the Sierras of Oaxaca and Veracruz: *P. m. angelensis*: 0.5 km W San Felipe Lachilló, Oaxaca (n = 2) y 0.5 km N San Francisco Huamelula, Oaxaca (n = 7); *P. m. Tuxtla*: Estación de Biología Tropical los Tuxtlas, Veracruz (n = 7); *P. m. putlaensis* 0.62 km NE San José de las Flores, Oaxaca (n = 3); *P. m. totontepecus*: 10 km S, 5 km W Valle Nacional, Oaxaca (n = 19). *F*-values and significance levels (in bold) were obtained through an ANOVA.

| Measuerments | <i>P. m. angelensis</i> | <i>P. m. Tuxtlas</i> | <i>P. m. putlensis</i> | <i>P. m. tontotepecus</i> | <i>F</i> | <i>P-value</i> |
|------------------------------------|-------------------------|----------------------|------------------------|---------------------------|--------------------------------------|----------------|
| Total length (ToL) | 225.13 ± 4.13 | 224.13 ± 5.84 | 225.33 ± 9.53 | 248.36 ± 3.52 | <i>F</i> _(3, 45) = 8.2009 | 0.001 |
| Tail length (TaL) | 124.69 ± 4.28 | 110.25 ± 6.06 | 118.67 ± 9.89 | 129.23 ± 3.65 | <i>F</i> _(3, 46) = 0.4364 | 0.727 |
| Leg length (LHF) | 23.44 ± 0.26 | 25.63 ± 0.37 | 23.67 ± 0.60 | 25.68 ± 0.22 | <i>F</i> _(3, 46) = 2.5723 | 0.065 |
| Ear Length (LE) | 19.44 ± 0.44 | 18.13 ± 0.62 | 21.00 ± 1.01 | 20.73 ± 0.37 | <i>F</i> _(3, 46) = 0.1620 | 0.921 |
| Greatest length of skull (GLS) | 31.03 ± 0.53 | 31.81 ± 0.75 | 31.66 ± 1.23 | 33.45 ± 0.45 | <i>F</i> _(3, 46) = 6.5494 | 0.008 |
| Skull height (SKH) | 8.58 ± 0.16 | 8.53 ± 0.21 | 8.30 ± 0.36 | 8.96 ± 0.13 | <i>F</i> _(3, 47) = 2.1206 | 0.110 |
| Condylobasal length (CBL) | 29.93 ± 0.39 | 30.01 ± 0.55 | 29.72 ± 0.89 | 31.98 ± 0.33 | <i>F</i> _(3, 45) = 7.0671 | 0.005 |
| Bullar length (BUL) | 4.39 ± 0.05 | 4.27 ± 0.07 | 4.40 ± 0.12 | 4.41 ± 0.05 | <i>F</i> _(3, 45) = 0.8697 | 0.463 |
| Shield-bullae depth (SBD) | 1.52 ± 0.03 | 1.41 ± 0.04 | 1.32 ± 0.07 | 1.33 ± 0.02 | <i>F</i> _(3, 45) = 8.3869 | 0.001 |
| Diastema length (DIL) | 8.58 ± 0.13 | 8.49 ± 0.19 | 8.30 ± 0.31 | 9.06 ± 0.11 | <i>F</i> _(3, 45) = 4.3690 | 0.008 |
| Rostral height (ROH) | 5.66 ± 0.11 | 5.75 ± 0.16 | 5.89 ± 0.26 | 6.09 ± 0.10 | <i>F</i> _(3, 45) = 3.0245 | 0.039 |
| Rostral breadth (BRR) | 5.13 ± 0.09 | 5.33 ± 0.12 | 5.06 ± 0.20 | 5.51 ± 0.07 | <i>F</i> _(3, 45) = 4.2968 | 0.009 |
| Palatal bridge length (PBL) | 4.96 ± 0.08 | 4.76 ± 0.11 | 4.87 ± 0.18 | 5.27 ± 0.07 | <i>F</i> _(3, 45) = 6.4797 | 0.009 |
| Postpalatal length (POL) | 4.29 ± 0.05 | 4.46 ± 0.07 | 4.15 ± 0.12 | 4.41 ± 0.04 | <i>F</i> _(3, 46) = 2.8618 | 0.046 |
| Basioccipital length (OCL) | 23.62 ± 0.30 | 23.58 ± 0.43 | 23.29 ± 0.70 | 25.10 ± 0.26 | <i>F</i> _(3, 45) = 6.4665 | 0.009 |
| Maxillary tooththrow length (MTL) | 4.43 ± 1.66 | 4.61 ± 2.34 | 4.20 ± 3.83 | 6.78 ± 1.41 | <i>F</i> _(3, 45) = 0.5025 | 0.682 |
| Maxillary tooththrow breadth (MTB) | 6.24 ± 0.06 | 6.21 ± 0.08 | 6.13 ± 0.13 | 6.49 ± 0.05 | <i>F</i> _(3, 45) = 5.8606 | 0.001 |
| Postdental breadth (PDB) | 4.29 ± 0.05 | 4.43 ± 0.07 | 4.15 ± 0.11 | 4.39 ± 0.04 | <i>F</i> _(3, 45) = 2.4416 | 0.076 |
| Zygomatic breadth (ZYB) | 14.95 ± 0.17 | 15.58 ± 0.24 | 14.78 ± 0.40 | 16.36 ± 0.15 | <i>F</i> _(3, 45) = 14.905 | 0.001 |
| Braincase breadth (BAB) | 13.58 ± 0.08 | 13.48 ± 0.12 | 13.28 ± 0.19 | 13.67 ± 0.07 | <i>F</i> _(3, 45) = 1.6007 | 0.202 |
| Nasal length (NAL) | 11.74 ± 0.19 | 12.79 ± 0.27 | 12.00 ± 0.45 | 12.98 ± 0.16 | <i>F</i> _(3, 45) = 8.6659 | 0.001 |
| Interorbital breadth (IOB) | 4.93 ± 0.06 | 4.71 ± 0.08 | 4.75 ± 0.14 | 4.93 ± 0.05 | <i>F</i> _(3, 45) = 2.2628 | 0.094 |
| Nasal breadth (NAB) | 3.36 ± 0.07 | 3.60 ± 0.09 | 3.39 ± 0.15 | 3.67 ± 0.06 | <i>F</i> _(3, 45) = 4.6992 | 0.006 |

ated with regions covered by tropical forests. The genetic analyses show that the sequences of the Los Tuxtlas specimens are markedly different from those in GenBank for geographic areas close to the type locality of *P. mexicanus*: Misantla, Veracruz (KP284422-23), Tutotepeq [Tutotepec], Hidalgo (KP284424), Puebla (KJ526415), and Zongolica, Veracruz (EF028174). For this reason, the Los Tuxtlas specimens are not considered representatives of *P. m. mexicanus* but of *P. m. totontepecus* instead.

The clades of *P. m. angelensis*-*P. m. putlaensis* and *P. m. totontepecus*-*P. m. Tuxtlas* are also phylogenetically differentiated from the other species in the *mexicanus* group, which clustered more closely with *P. gymnotis*. The *P. m. angelensis*-*P. m. putlaensis* clade had a percentage of dissimilarity of 7.54 % relative to *P. mexicanus*, and the *P. m. totontepecus*-*P. m. Tuxtlas* clade, of 5.98 %. These results show that both sides of the Sierra Madre del Sur of Oaxaca harbor genetically separated lineages of *P. mexicanus*. Genetic distances are consistent with other species in the *mexicanus* group (Table 1).

The biogeographical explanation of the genetic discontinuity among the three clades of *P. mexicanus* analyzed is that *P. m. Tuxtlas* is likely distributed in the SMG from the central part of Veracruz northward. In contrast, *P. m. angelensis*-*P. m. putlaensis* are distributed in various highland areas of the Pacific side in Oaxaca, between 616 and 1,569 masl, and *P. m. totontepecus*, in the SMG and the coastal plains of southeastern Veracruz. In the mid-late Pleistocene, when the forests of Oaxaca originated (Watson 2003), there was a continuous habitat between both sides of the Sierra Madre del Sur, which likely favored the dispersal of *Peromyscus* (Pérez-Consuegra and Vázquez-Domínguez 2015, 2017). The continuity of forests was limited in the late Pleistocene by the appearance of the Central Valleys of Oaxaca, a region with lower altitudes and xeric characteristics covered with a different vegetation type (García-Mendoza et al. 2004), recorded as an environment where no species of the *P. mexicanus* complex are found. Consequently, the Central Valleys functioned as a physiographic barrier between the populations of both sides of the Sierra Madre del Sur, with unique biotic and abiotic conditions that fostered the discontinuity and genetic differentiation of these populations. This is reflected in the genetic discontinuity between the populations of the Sierra Madre del Sur on both slopes of Oaxaca. This is why the *P. m. totontepecus*-*P. m. Tuxtlas* clade is restricted only to the highlands of the SMG in Oaxaca and the coastal plain of southeastern Veracruz. However, this clade is present in part of western Oaxaca and the Tehuantepec area (Hernández-Canchola et al. 2022). In contrast, *P. m. angelensis*-*P. m. putlaensis* is distributed in the Pacific slope in Oaxaca.

The *mexicanus* group may have undergone speciation at about the same time as *P. aztecus* (Sullivan et al. 1997) and *P. melanophrys* (Castañeda-Rico et al. 2014). The local adaptation to different habitats under particular biotic and abiotic conditions (vegetation type, elevation, ecological char-

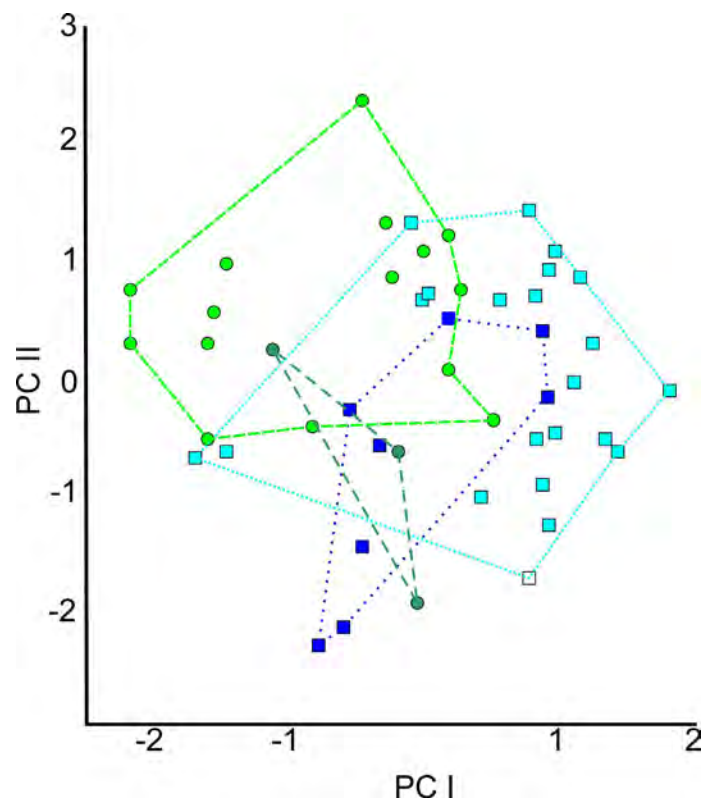


Figure 4. Plot of influences from the Principal Component Analysis (PCA) of the 19 craniodental variables. The analysis included specimens of the *Peromyscus mexicanus* complex from different geographic regions. *P. m. angelensis* (light green), *P. m. putlaensis* (dark green), *P. m. totontepecus* (light blue) and *P. m. Tuxtlas* (dark blue).

acteristics) may have played a key role in the differentiation of the *P. mexicanus* lineages. This is reflected not only in the genetic information, but also in the variations in body size observed. It has been suggested that cranial variations, such as the length of the diastema and the palatal bridge in *P. zarhynchus* (Lorenzo et al. 2006) and the length of the mandible and mandibular tooththrow of *P. mexicanus* (Pérez-Consuegra and Vázquez-Domínguez 2017) are indicators of differences in feeding habits (Lorenzo et al. 2006; Pérez-Consuegra and Vázquez-Domínguez 2017). The same may be happening with the specimens of the *P. mexicanus* complex inhabiting the Oaxaca highlands.

The genetic distance percentages recorded for the populations of *P. m. angelensis*, *P. m. Tuxtlas*, *P. m. putlaensis*, and *P. m. totontepecus* are phylogenetically closer to *P. gymnotis* than to *P. mexicanus*, although these clades have been considered subspecies of *P. mexicanus* based on morphological traits. The morphological variation and genetic diversity observed, compared with other species in the *mexicanus* complex, suggest that the *P. m. angelensis* and *P. m. putlaensis* lineages in the SMP and *P. m. totontepecus* and *P. m. Tuxtlas* of the SMG in Oaxaca and the coastal plain of southeastern Veracruz are valid taxonomic entities at the species level, which differ from *P. mexicanus*. For this reason, *P. totontepecus* (Merriam 1898) should be recognized at the species level in the SMG, including the specimens inhabiting the coastal plain of southeastern Veracruz.

In the Sierra Madre del Sur, following the priority rule of the Nomenclature Code, it is determined that *P. m. putlaensis* (Goodwin 1964) should be considered a subspecies of *P. angelensis* (Osgood 1904).

Peromyscus angelensis Osgood 1904

Distribution. The type locality is Puerto Angel, Oaxaca. Its distribution range includes the Sierra Madre del Sur in the Pacific side highlands, from Guerrero to Oaxaca.

Comments. Morphological variations within the distribution range of *P. angelensis* have been recorded. These variations coincide with the taxa described previously; therefore, we consider that the specimens previously assigned to *putlaensis* should be considered a subspecies of *P. angelensis*.

Peromyscus angelensis can be distinguished from *P. tontotepecus* and *P. mexicanus* by having a dorsal and ventral paler coloration, ring spot around the eye with less contrast to the face flank, smaller somatic and cranial sizes, and a supraorbital bead slightly better developed (Osgood 1904; Musser 1969; Huckaby 1980).

Peromyscus angelensis putlaensis Goodwin 1964

Distribution. The type locality is San Vicente, Putla Municipality, Oaxaca. Its known distribution range is restricted to the high areas adjacent to Putla Villa de Guerrero.

Comments. In *P. a. putlaensis* the braincase proportions are smaller in relation to *P. a. angelensis* with the interorbital breadth, braincase breadth and skull height smaller in relation to the rostral area.

Peromyscus tontotepecus Merriam 1898

Distribution. The type locality is Tontotepec, Oaxaca. Its distribution range includes the highlands of Oaxaca and eastern Puebla. *P. m. mexicanus* is restricted to the Gulf of México coastal plain of Veracruz.

Comments. *Peromyscus tontotepecus* can be distinguished from *P. mexicanus* by having a dorsal and ventral darker coloration, ring spot around the eye with greater contrast to the face flank, and smaller in average in somatic and cranial measurements.

Acknowledgments

The authors gratefully acknowledge Abraham Carranza and Adriana Miranda for their support during the field trips. We thank I. Gutiérrez and M. de la Paz for support in laboratory and curatorial processes of biological material. Thanks to C. Segura and G. Gallegos for DNA amplification and the Node CIBNOR Barcode of Mexican Network of the Barcode of Life for their support in the process of molecular samples. We thank to Dr. Briones Salas for their guidance in Oaxaca's mountains. This research was funded by a scholarship from Consejo Nacional de Ciencia y Tecnología (CONACyT 634990).

This article pays tribute to AL Gardner. He is a key person at the beginning of my professional development (STAC), despite never having been his student or collaborator, he encouraged discipline and love for the profession.

Literature cited

- ÁLVAREZ-CASTAÑEDA, S. T., ET AL. 2019. Two new species of *Peromyscus* from Chiapas and Guatemala. From field to laboratory: a memorial volume in honor of Robert J. Baker (Bradley, R. D., H. H. Genoways, D. J. Schmidly, and L. C. Bradley, eds.). Texas Tech University. Lubbock, U.S.A.
- ÁLVAREZ-CASTAÑEDA, S. T., T. ÁLVAREZ, AND N. GONZÁLEZ-RUIZ. 2015. Guía para la identificación de los mamíferos de México en campo y laboratorio. Centro de Investigaciones Biológicas del Noroeste, S. C. Asociación Mexicana de Mastozoología A. C. Guadalajara, México.
- ÁLVAREZ-CASTAÑEDA, S. T., T. ÁLVAREZ, AND N. GONZÁLEZ-RUIZ. 2017. Keys for identifying mexican mammals. The Johns Hopkins University Press. Baltimore, U.S.A.
- AMMAN, B. R., ET AL. 2006. Intron 2 of the alcohol dehydrogenase gene (Adh1-I2): A Nuclear DNA marker for mammalian systematics. Occasional Papers Texas Tech University 256:1-12.
- BEDFORD, N. L., AND H. E. HOEKSTRA. 2015. *Peromyscus* mice as a model for studying natural variation. eLife 4:e06813.
- BRADLEY, R. D., ET AL. 2007. Toward a molecular phylogeny for *Peromyscus*: evidence from mitochondrial cytochrome-b sequences. Journal of Mammalogy 88:1146-1159.
- BRADLEY, R. D., ET AL. 2016. Molecular systematics and phylogeography of *Peromyscus nudipes* (Cricetidae: Neotominae). Special Publications Museum of Texas Tech University 65:201-213.
- BRADLEY, R. D., ET AL. 2019. Mitochondrial DNA sequence data indicate evidence for multiple species within *Peromyscus maniculatus*. Special Publications of the Museum of Texas Tech University 70:1-59.
- CARLETON, M. D. 1989. Systematics and evolution. Pp. 7-141, in Advances in the study of *Peromyscus* (Rodentia) (Kirkland, G. L., and J. N. Layne, eds.). Texas Tech University Press. Lubbock, U.S.A.
- CASTAÑEDA-RICO, S., ET AL. 2014. Evolutionary diversification and speciation in rodents of Mexican lowlands: The *Peromyscus melanophrys* species group. Molecular Systematics and Evolution 70:454-463.
- DALQUEST, W. W. 1950. Record of mammals from San Luis Potosi. Occasional Papers of the Museum of Zoology, Louisiana State University 23:1-15.
- DIERSING, V. E. 1981. Systematic status of *Sylvilagus brasiliensis* and *S. insonus* from North America. Journal of Mammalogy 62:539-556.
- EXCOFFIER, L., AND H. E. L. LISCHER. 2010. Arlequin suite ver 3.5: a new series of programs to perform population genetics analyses under Linux and Windows. Molecular Ecology Resources 10:564-567.
- FELSENSTEIN, J. 1981. Evolutionary trees from DNA sequences: a maximum likelihood approach. Journal of Molecular Evolution 17:368-376.
- GARCÍA-MENDOZA, A., L. P. TENORIO, AND S. J. REYES. 1994. El endemismo de la flora fanerogámica de la Mixteca Alta, Oaxaca-Puebla, México. Acta Botánica Mexicana 27:53-73.

- GARCÍA-MENDOZA, A. J., M. J. ORDÓÑEZ, AND M. BRIONES-SALAS. 2004. Biodiversidad de Oaxaca. Instituto de Biología, Universidad Nacional Autónoma de México-Fondo Oaxaqueño para la Conservación de la Naturaleza-World Wildlife Found. México City, México.
- GARCÍA-MENDOZA, A., AND C. TORRES. 1999. Estado actual del conocimiento sobre la flora de Oaxaca. *Sociedad y naturaleza en Oaxaca* 3:49-86.
- GOODWIN, G. G. 1964. A new species and a new subspecies of *Peromyscus* from Oaxaca, Mexico. *American Museum Novitates* 2183:1-8.
- GREENBAUM, I. F., R. L. HONEYCUTT, AND S. E. CHIRHART. 2019. Taxonomy and phylogenetics of the *Peromyscus maniculatus* species group. Pp 559-576, in *From field to laboratory: A memorial volume in honor of Robert J. Baker* (Bradley, R. D., H. H. Genoways, D. J. Schmidly, and L. C. Bradley, eds.). Special Publications, Museum of Texas Tech University 71:1- 911.
- HALL, E. R. 1981. *The mammals of North America*. Second edition. John Wiley and Sons. New York, U.S.A.
- HAMMER, Ø., D. A. T. HARPER, AND P. D. RYAN. 2001. PAST: Paleontological statistics software package for education and data analysis. *Paleontologia Electronica* 4:1-9.
- HERNÁNDEZ-CANCHOLA, G., L. LEÓN-PANIAGUA, AND J. A. ESSELSTYN. 2022. Paraphyletic relationships revealed by mitochondrial DNA in the *Peromyscus mexicanus* species group (Rodentia: Cricetidae). *Revista Mexicana de Biodiversidad* 93:e933811.
- HUCKABY, D. G. 1973. Biosystematics of the *Peromyscus mexicanus* group (Rodentia). Ph D. thesis. Michigan University. Michigan, U.S.A.
- HUCKABY, D. G. 1980. Species limits in the *Peromyscus mexicanus* group (Mammalia: Rodentia: Muroidea). *Contributions in Science, Natural History Museum of Los Angeles County* 326:1-24.
- KIMURA, M. 1980. A simple method for estimating evolutionary rates of base substitutions through comparative studies of nucleotide sequences. *Journal of Molecular Evolution* 16:111-120.
- KUMAR, S., ET AL. 2018. MEGA X: molecular evolutionary genetics analysis across computing platforms. *Molecular Biology and Evolution* 35:1547-1549.
- LIBRADO, P., AND J. ROZAS. 2009. DnaSP v5: a software for comprehensive analysis of DNA polymorphism data. *Bioinformatics* 25:1451-1452.
- LEÓN-TAPIA, M. A., ET AL. 2020. A new mouse of the *Peromyscus maniculatus* species complex (Cricetidae) from the highlands of central Mexico. *Journal of Mammalogy* 101:1117-1132.
- LORENZO, C., ET AL. 2006. Intraspecific variation in *Peromyscus zarhynchus* (Rodentia:Muridae) from Chiapas, Mexico. *Journal of Mammalogy* 87:683-689.
- LORENZO, C., ET AL. 2016. Revision of the Chiapan deer mouse, *Peromyscus zarhynchus*, with the description of a new species. *Journal of Mammalogy* 97:910-918.
- MCCORMACK, J. E., H. HUANG, AND L. L. KNOWLES. 2009. Sky islands. *University of Michigan* 839-843.
- MONROY-GAMBOA, A. G., A. UREÑA-RAMÓN, AND L. A. ESPINOSA-ÁVILA. 2005. Variación morfométrica de *Peromyscus maniculatus fulvus* y *Reithrodontomys megalotis saturatus* de la Ciudad de México, D. F. *Revista Mexicana de Mastozoología* 9:72-84.
- MORRONE, J. J. 2017. Biogeographic regionalization of the Sierra Madre del Sur province, Mexico. *Revista Mexicana de Biodiversidad* 88:710-714.
- MUSSER, G. G. 1969. Notes on *Peromyscus* (Muridae) of Mexico and Central America. *American Museum Novitates* 2357:1-23.
- NYLANDER, J. A. A., ET AL. 2008. AWTY (are we there yet?): a system for graphical exploration of MCMC convergence in Bayesian phylogenetics. *Bioinformatics* 24:581-583.
- ORDÓÑEZ-GARZA, N., ET AL. 2010. Patterns of phenotypic and genetic variation in three species of endemic Mesoamerican *Peromyscus* (Rodentia: Cricetidae). *Journal of Mammalogy* 91:848-859.
- ORTIZ-PÉREZ, M. A., J. R. HERNÁNDEZ-SANTANA, AND J. M. FIGUEROA-MAH-ENG. 2004. Reconocimiento fisiográfico y geomorfológico. Pp. 67-85, in *Biodiversidad de Oaxaca*. (García-Mendoza, A. J., M. J. Ordóñez, and M. Briones-Salas, eds.). Instituto de Biología, Universidad Nacional Autónoma de México-Fondo Oaxaqueño para la Conservación de la Naturaleza-World Wildlife Found. Ciudad de México, México.
- OSGOOD, W. H. 1904. Thirty new mice of the genus *Peromyscus* from Mexico and Guatemala. *Proceedings of the Biological Society of Washington* 17:55-77.
- PÉREZ-CONSUEGRA, S. G., AND E. VÁZQUEZ-DOMÍNGUEZ. 2015. Mitochondrial diversification of the *Peromyscus mexicanus* species group in Nuclear Central America: biogeographic and taxonomic implications. *Journal of Zoological Systematics and Evolutionary Research* 53:300-311.
- PÉREZ-CONSUEGRA, S. G., AND E. VÁZQUEZ-DOMÍNGUEZ. 2017. Intricate evolutionary histories in montane species: a phylogenetic window into craniodental discrimination in the *Peromyscus mexicanus* species group (Mammalia: Rodentia: Cricetidae). *Journal of Zoological Systematics and Evolutionary Research* 55:57-72.
- RAMBAUT, A. 2012. FigTree v1.4.2. <http://tree.bio.ed.ac.uk/software/figtree/>.
- ROBINSON, T. J., AND N. J. DIPPENAAR. 1987. Morphometrics of the South African Leporidae. II: *Lepus* Linnaeus, 1758, and *Bunolagus* Thomas, 1929. *Annals Transvaal Museum* 34:379-404.
- ROGERS, D. S., AND M. D. ENGSTROM. 1992. Evolutionary implications of allozymic variation in tropical *Peromyscus* of the *mexicanus* group. *Journal of Mammalogy* 73:55-69.
- ROGERS, D. S., ET AL. 2007. Molecular phylogenetic relationships among crested-tailed mice (Genus *Habromys*). *Journal of Mammalian Evolution* 14:37-55.
- Ronquist, F., and J. P. Huelsenbeck. 2003. MrBayes3: Bayesian phylogenetic inference under mixed models. *Bioinformatics* 19:1572-1574.
- SMITH, S. A., R. D. BRADLEY, AND I. F. GREENBAUM. 1986. Karyotypic conservatism in the *Peromyscus mexicanus* group. *Journal of Mammalogy* 67:584-86.
- SMITH, M. F. 1998. Phylogenetic relationships and geographic structure in pocket gophers in the genus *Thomomys*. *Molecular Phylogenetics and Evolution* 9:1-14.
- SMITH, M. F., AND J. L. PATTON. 1999. Phylogenetic relationships and the radiation of sigmodontine rodents in South America: evidence from cytochrome *b*. *Journal of Mammalian Evolution* 6:89-128.
- STATSOFT, INC. 2007. STATISTICA (data analysis software system), version 8.0. www.statsoft.com.

- SULLIVAN, J., J. A. MARKERT, AND C. WILLIAM- KILPATRICK. 1997. Phylogeography and molecular systematics of the *Peromyscus aztecus* species group (Rodentia: Muridae) inferred using parsimony and likelihood. Society of Systematic Biologists. Oxford University Press 46:426-440.
- SWOFFORD, D. L. 2002. PAUP*: phylogenetic analysis using parsimony (* and other methods). Ver. 4. Sinauer Associates, Inc. Sunderland, U.S.A.
- TAVARÉ, S. 1986. Some probabilistic and statistical problems in the analysis of DNA sequences. Pp. 57-86, *in* Some mathematical questions in biology – DNA sequence analysis (Miura, R. M. ed.). American Mathematics Society. Providence, U.S.A.
- TREJO, I. 2004. Clima. Pp. 67–85, *in* Biodiversidad de Oaxaca (García-Mendoza, A. J., M. J. Ordóñez, and M. Briones-Salas, eds.). Instituto de Biología, Universidad Nacional Autónoma de México-Fondo Oaxaqueño para la Conservación de la Naturaleza-World Wildlife Found. México City, México.
- TRUJANO-ÁLVAREZ, A. L., AND S. T. ÁLVAREZ-CASTAÑEDA. 2010. *Peromyscus mexicanus* (Rodentia: Cricetidae). Mammalian Species. American Society of Mammalogists 42:111-118.
- WATSON, D. M. 2003. Long-term consequences of habitat fragmentation—highland birds in Oaxaca, Mexico. Biological Conservation 111:283-303.
- WILLIAMS, S. L., AND J. RAMÍREZ-PULIDO. 1984. Morphometric variation in the volcano mouse, *Peromyscus (Neotomodon) alstoni* (Mammalia: Cricetidae). Annals of Carnegie Museum 53:163–183.

Associated editor: Jake Esselstyn and Giovani Hernández Canchola

Submitted: May 10, 2022; Reviewed: July 18, 2022

Accepted: November 18, 2022; Published on line: December 14, 2023

Appendix 1

ANOVA *post hoc* Scheffe test between *P. m. angelensis*, *P. m. putlaensis*, *P. m. Tuxtlas* and *P. m. totontepecus*. Numbers in bold mark probability values with significant differences ($P < 0.05$).

Scheffe test; Total length (ToL). MS = 272.63, df = 45,000, $F(3, 45) = 8.2009$, $P = 0.00018$

| | 1 | 2 | 3 | 4 |
|------------------------------|-----------------|-----------------|----------|-----------------|
| 1. <i>P. m. angelensis</i> | | 0.999265 | 0.999998 | 0.001399 |
| 2. <i>P. m. Tuxtlas</i> | 0.999265 | | 0.999660 | 0.010390 |
| 3. <i>P. m. putlaensis</i> | 0.999998 | 0.999660 | | 0.178011 |
| 4. <i>P. m. totontepecus</i> | 0.001399 | 0.010390 | 0.178011 | |

Scheffe test; Tail length (TaL). MS = 293.45, df = 45,000, $F(3, 46) = 0.43645$, $P = 0.72796$

| | 1 | 2 | 3 | 4 |
|------------------------------|----------|----------|----------|----------|
| 1. <i>P. m. angelensis</i> | | 0.298520 | 0.957294 | 0.884198 |
| 2. <i>P. m. Tuxtlas</i> | 0.298520 | | 0.912388 | 0.080262 |
| 3. <i>P. m. putlaensis</i> | 0.957294 | 0.912388 | | 0.800476 |
| 4. <i>P. m. totontepecus</i> | 0.884198 | 0.080262 | 0.800476 | |

Scheffe test; Leg length (LHF). MS = 1.0945, df = 45,000, $F(3, 46) = 2.5723$, $P = 0.06550$

| | 1 | 2 | 3 | 4 |
|------------------------------|-----------------|-----------------|-----------------|-----------------|
| 1. <i>P. m. angelensis</i> | | 0.000275 | 0.989021 | 0.000001 |
| 2. <i>P. m. Tuxtlas</i> | 0.000275 | | 0.067637 | 0.999388 |
| 3. <i>P. m. putlaensis</i> | 0.989021 | 0.067637 | | 0.029852 |
| 4. <i>P. m. totontepecus</i> | 0.000001 | 0.999388 | 0.029852 | |

Scheffe test; Ear length (LE). MS = 3.0484, df = 45,000, $F(3, 46) = 0.16209$, $P = 0.92132$

| | 1 | 2 | 3 | 4 |
|------------------------------|----------|-----------------|----------|-----------------|
| 1. <i>P. m. angelensis</i> | | 0.399521 | 0.572231 | 0.183665 |
| 2. <i>P. m. Tuxtlas</i> | 0.399521 | | 0.131708 | 0.009016 |
| 3. <i>P. m. putlaensis</i> | 0.572231 | 0.131708 | | 0.995670 |
| 4. <i>P. m. totontepecus</i> | 0.183665 | 0.009016 | 0.995670 | |

Scheffe test; Greatest length of skull (GLS). MS = 4.5540, df = 45,000, $F(3, 46) = 6.5494$, $P = 0.00088$

| | 1 | 2 | 3 | 4 |
|------------------------------|-----------------|----------|----------|-----------------|
| 1. <i>P. m. angelensis</i> | | 0.870276 | 0.973705 | 0.013839 |
| 2. <i>P. m. Tuxtlas</i> | 0.870276 | | 0.999718 | 0.339619 |
| 3. <i>P. m. putlaensis</i> | 0.973705 | 0.999718 | | 0.609474 |
| 4. <i>P. m. totontepecus</i> | 0.013839 | 0.339619 | 0.609474 | |

Scheffe test; Skull height (SKH). MS = 0.09275, df = 45,000, $F(3, 47) = 2.1206$, $P = 0.11022$

| | 1 | 2 | 3 | 4 |
|------------------------------|----------|----------|----------|----------|
| 1. <i>P. m. angelensis</i> | | 0.360298 | 0.694643 | 0.935581 |
| 2. <i>P. m. Tuxtlas</i> | 0.360298 | | 0.999983 | 0.592522 |
| 3. <i>P. m. putlaensis</i> | 0.694643 | 0.999983 | | 0.852312 |
| 4. <i>P. m. totontepecus</i> | 0.935581 | 0.592522 | 0.852312 | |

Scheffe test; Condylbasal length (CBL). MS = 2.3922, df = 45,000, $F(3, 45) = 7.0671$, $P = 0.00054$

| | 1 | 2 | 3 | 4 |
|------------------------------|-----------------|-----------------|----------|-----------------|
| 1. <i>P. m. angelensis</i> | | 0.999562 | 0.997178 | 0.002993 |
| 2. <i>P. m. Tuxtlas</i> | 0.999562 | | 0.994252 | 0.034065 |
| 3. <i>P. m. putlaensis</i> | 0.997178 | 0.994252 | | 0.148139 |
| 4. <i>P. m. totontepecus</i> | 0.002993 | 0.034065 | 0.148139 | |

Scheffe test; Bullar length (BUL). MS = 0.04468, df = 45,000, $F(3, 45) = 0.86974$, $P = 0.46380$

| | 1 | 2 | 3 | 4 |
|------------------------------|----------|----------|----------|----------|
| 1. <i>P. m. angelensis</i> | | 0.655027 | 0.999912 | 0.991626 |
| 2. <i>P. m. Tuxtlas</i> | 0.655027 | | 0.854812 | 0.476688 |
| 3. <i>P. m. putlaensis</i> | 0.999912 | 0.854812 | | 0.999739 |
| 4. <i>P. m. totontepecus</i> | 0.991626 | 0.476688 | 0.999739 | |

Scheffe test; Shield-bullae depth (SBD). MS = 0.01364, df = 45, $F(3, 45) = 8.3869$, $P = 0.00015$

| | 1 | 2 | 3 | 4 |
|------------------------------|-----------------|----------|----------|-----------------|
| 1. <i>P. m. angelensis</i> | | 0.269412 | 0.083819 | 0.000259 |
| 2. <i>P. m. Tuxtlas</i> | 0.269412 | | 0.705678 | 0.394302 |
| 3. <i>P. m. putlaensis</i> | 0.083819 | 0.705678 | | 0.999371 |
| 4. <i>P. m. totontepecus</i> | 0.000259 | 0.394302 | 0.999371 | |

Scheffe test; Diastema length (DIL). MS = 0.28388, df = 45,000, $F(3, 45) = 4.3690$, $P = 0.00878$

| | 1 | 2 | 3 | 4 |
|------------------------------|----------|----------|----------|----------|
| 1. <i>P. m. angelensis</i> | | 0.983444 | 0.873214 | 0.071406 |
| 2. <i>P. m. Tuxtlas</i> | 0.983444 | | 0.965141 | 0.094982 |
| 3. <i>P. m. putlaensis</i> | 0.873214 | 0.965141 | | 0.162949 |
| 4. <i>P. m. totontepecus</i> | 0.071406 | 0.094982 | 0.162949 | |

Scheffe test; Rostral height (ROH). MS = 0.20555, df = 45,000, $F(3, 45) = 3.0245$, $P = 0.03921$

| | 1 | 2 | 3 | 4 |
|------------------------------|----------|----------|----------|----------|
| 1. <i>P. m. angelensis</i> | | 0.980188 | 0.890212 | 0.054390 |
| 2. <i>P. m. Tuxtlas</i> | 0.980188 | | 0.975154 | 0.350811 |
| 3. <i>P. m. putlaensis</i> | 0.890212 | 0.975154 | | 0.913528 |
| 4. <i>P. m. totontepecus</i> | 0.054390 | 0.350811 | 0.913528 | |

Scheffe test; Rostral breadth (BRR). MS = 0.11859, df = 45,000, $F(3, 45) = 4.2968$, $P = 0.00949$

| | 1 | 2 | 3 | 4 |
|------------------------------|----------|----------|----------|----------|
| 1. <i>P. m. angelensis</i> | | 0.637648 | 0.988851 | 0.019805 |
| 2. <i>P. m. Tuxtlas</i> | 0.637648 | | 0.718655 | 0.667428 |
| 3. <i>P. m. putlaensis</i> | 0.988851 | 0.718655 | | 0.228049 |
| 4. <i>P. m. totontepecus</i> | 0.019805 | 0.667428 | 0.228049 | |

Scheffe test; Palatal bridge length (PBL). MS = 0.10092, df = 45,000, $F(3, 45) = 6.4797$, $P = 0.00097$

| | 1 | 2 | 3 | 4 |
|------------------------------|----------|-----------------|----------|-----------------|
| 1. <i>P. m. angelensis</i> | | 0.564638 | 0.978362 | 0.041395 |
| 2. <i>P. m. Tuxtlas</i> | 0.564638 | | 0.967061 | 0.004323 |
| 3. <i>P. m. putlaensis</i> | 0.978362 | 0.967061 | | 0.256875 |
| 4. <i>P. m. tototeppecus</i> | 0.041395 | 0.004323 | 0.256875 | |

Scheffe test; Postpalatal length (POL). MS = 0.44998, df = 45,000, $F(3, 46) = 2.8618$, $P = 0.04694$

| | 1 | 2 | 3 | 4 |
|------------------------------|-----------------|----------|----------|-----------------|
| 1. <i>P. m. angelensis</i> | | 0.999248 | 0.937242 | 0.014157 |
| 2. <i>P. m. Tuxtlas</i> | 0.999248 | | 0.924564 | 0.097838 |
| 3. <i>P. m. putlaensis</i> | 0.937242 | 0.924564 | | 0.118085 |
| 4. <i>P. m. tototeppecus</i> | 0.014157 | 0.097838 | 0.118085 | |

Scheffe test; basioccipital length (LCL). MS = 1.4681, df = 45,000, $F(3, 45) = 6.4665$, $P = 0.00098$

| | 1 | 2 | 3 | 4 |
|------------------------------|----------|----------|----------|----------|
| 1. <i>P. m. angelensis</i> | | 0.999905 | 0.979221 | 0.006896 |
| 2. <i>P. m. Tuxtlas</i> | 0.999905 | | 0.988099 | 0.037844 |
| 3. <i>P. m. putlaensis</i> | 0.979221 | 0.988099 | | 0.133576 |
| 4. <i>P. m. tototeppecus</i> | 0.006896 | 0.037844 | 0.133576 | |

Scheffe test; Maxillary tooththrow length (MTL). MS = 43.900, df = 45,000, $F(3, 45) = 0.50259$, $P = 0.68242$

| | 1 | 2 | 3 | 4 |
|------------------------------|----------|----------|----------|----------|
| 1. <i>P. m. angelensis</i> | | 0.999929 | 0.999956 | 0.759835 |
| 2. <i>P. m. Tuxtlas</i> | 0.999929 | | 0.999791 | 0.888461 |
| 3. <i>P. m. putlaensis</i> | 0.999956 | 0.999791 | | 0.939191 |
| 4. <i>P. m. tototeppecus</i> | 0.759835 | 0.888461 | 0.939191 | |

Scheffe test; Maxillary tooththrow breadth (MTB). MS = 0.05356, df = 45,000, $F(3, 45) = 5.8606$, $P = 0.00182$

| | 1 | 2 | 3 | 4 |
|------------------------------|----------|----------|----------|----------|
| 1. <i>P. m. angelensis</i> | | 0.996854 | 0.913134 | 0.016783 |
| 2. <i>P. m. Tuxtlas</i> | 0.996854 | | 0.963846 | 0.048435 |
| 3. <i>P. m. putlaensis</i> | 0.913134 | 0.963846 | | 0.107716 |
| 4. <i>P. m. tototeppecus</i> | 0.016783 | 0.048435 | 0.107716 | |

Scheffe test; Postdental breadth (PDB). MS = 0.03744, df = 45,000, $F(3, 45) = 2.4416$, $P = 0.07650$

| | 1 | 2 | 3 | 4 |
|------------------------------|----------|----------|----------|----------|
| 1. <i>P. m. angelensis</i> | | 0.418908 | 0.721256 | 0.457682 |
| 2. <i>P. m. Tuxtlas</i> | 0.418908 | | 0.212796 | 0.970973 |
| 3. <i>P. m. putlaensis</i> | 0.721256 | 0.212796 | | 0.254528 |
| 4. <i>P. m. tototeppecus</i> | 0.457682 | 0.970973 | 0.254528 | |

Scheffe test; Zygomatic breadth (ZYB). MS = 0.47597, df = 45,000, $F(3, 45) = 14.905$, $P = 0.00000$

| | 1 | 2 | 3 | 4 |
|------------------------------|----------|----------|----------|----------|
| 1. <i>P. m. angelensis</i> | | 0.234420 | 0.983462 | 0.000003 |
| 2. <i>P. m. Tuxtlas</i> | 0.234420 | | 0.409262 | 0.069697 |
| 3. <i>P. m. putlaensis</i> | 0.983462 | 0.409262 | | 0.006489 |
| 4. <i>P. m. tototeppecus</i> | 0.000003 | 0.069697 | 0.006489 | |

Scheffe test; Braincase breadth (BAB). MS = 0.11106, df = 45,000, $F(3, 45) = 1.6007$, $P = 0.20247$

| | 1 | 2 | 3 | 4 |
|------------------------------|----------|----------|----------|----------|
| 1. <i>P. m. angelensis</i> | | 0.929012 | 0.585041 | 0.855249 |
| 2. <i>P. m. Tuxtlas</i> | 0.929012 | | 0.858589 | 0.582648 |
| 3. <i>P. m. putlaensis</i> | 0.585041 | 0.858589 | | 0.319032 |
| 4. <i>P. m. tototeppecus</i> | 0.855249 | 0.582648 | 0.319032 | |

Scheffe test; Nasal length (NAL). MS = 0.59815, df = 45,000, $F(3, 45) = 8.6659$, $P = 0.00012$

| | 1 | 2 | 3 | 4 |
|------------------------------|----------|----------|----------|----------|
| 1. <i>P. m. angelensis</i> | | 0.030782 | 0.962487 | 0.000254 |
| 2. <i>P. m. Tuxtlas</i> | 0.030782 | | 0.529416 | 0.949231 |
| 3. <i>P. m. putlaensis</i> | 0.962487 | 0.529416 | | 0.256447 |
| 4. <i>P. m. tototeppecus</i> | 0.000254 | 0.949231 | 0.256447 | |

Scheffe test; Interorbital breadth (IOB). MS = 0.05626, df = 45,000, $F(3, 45) = 2.2628$, $P = 0.09405$

| | 1 | 2 | 3 | 4 |
|------------------------------|----------|----------|----------|----------|
| 1. <i>P. m. angelensis</i> | | 0.219864 | 0.715751 | 0.999938 |
| 2. <i>P. m. Tuxtlas</i> | 0.219864 | | 0.993875 | 0.169173 |
| 3. <i>P. m. putlaensis</i> | 0.715751 | 0.993875 | | 0.683638 |
| 4. <i>P. m. tototeppecus</i> | 0.999938 | 0.169173 | 0.683638 | |

Scheffe test; Nasal breadth (NAB). MS = 0.06839, df = 45,000, $F(3, 45) = 4.6992$, $P = 0.00614$

| | 1 | 2 | 3 | 4 |
|------------------------------|-----------------|----------|----------|-----------------|
| 1. <i>P. m. angelensis</i> | | 0.226058 | 0.998344 | 0.010247 |
| 2. <i>P. m. Tuxtlas</i> | 0.226058 | | 0.704099 | 0.946611 |
| 3. <i>P. m. putlaensis</i> | 0.998344 | 0.704099 | | 0.411315 |
| 4. <i>P. m. tototeppecus</i> | 0.010247 | 0.946611 | 0.411315 | |

Appendix 2

Factorial loads of the Principal Component Analysis on the log-transformed craniodental variables of *P. m. angelensis* ($n = 16$), *P. m. putlaensis* ($n = 8$), *P. m. Tuxtlas* ($n = 3$), and *P. m. totontepecus* ($n = 22$). The values with the greatest correlation are highlighted in bold.

| | PC 1 | PC 2 | PC 3 | PC 4 |
|----------------------------------|-------------|-------------|-------------|-------------|
| Greatest length of skull (GLS) | 0.76 | -0.01 | 0.04 | 0.04 |
| Skull height (SKH) | 0.28 | 0.67 | -0.23 | -0.08 |
| Bullar length (BUL) | 0.14 | -0.05 | 0.64 | -0.45 |
| Shield-bullae depth (SBD) | -0.54 | 0.20 | -0.37 | 0.19 |
| Diastema length (DIL) | 0.90 | 0.26 | 0.04 | -0.11 |
| Rostral height (ROH) | 0.90 | 0.18 | -0.03 | -0.03 |
| Rostral breadth (BRR) | 0.79 | 0.26 | -0.12 | 0.25 |
| Palatal bridge length (PBL) | 0.65 | 0.31 | 0.25 | -0.13 |
| Postpalatal length (POL) | 0.91 | 0.17 | 0.11 | -0.02 |
| Basioccipital length (OCL) | 0.94 | 0.23 | 0.10 | -0.05 |
| Maxillary toothrow length (MTL) | 0.01 | 0.09 | 0.77 | 0.30 |
| Maxillary toothrow breadth (MTB) | 0.69 | 0.22 | 0.32 | 0.17 |
| Postdental breadth (PDB) | 0.11 | -0.09 | 0.09 | 0.86 |
| Zygomatic breadth (ZYB) | 0.90 | 0.18 | 0.14 | 0.21 |
| Braincase breadth (BAB) | 0.38 | 0.66 | 0.32 | 0.18 |
| Nasal length (NAL) | 0.91 | -0.09 | 0.01 | 0.06 |
| Interorbital breadth (IOB) | 0.20 | 0.83 | 0.03 | -0.11 |
| Nasal breadth (NAB) | 0.79 | 0.10 | 0.07 | 0.04 |
| Explained variation | 8.28 | 2.09 | 1.53 | 1.29 |
| Prp tot | 0.46 | 0.12 | 0.08 | 0.07 |

Supplementary material

www.revistas-conacyt.unam.mx/therya/index.php/THERYA/article/view/2148/2148_Supplementary%20material

A propaedeutic to the taxonomy of the Eastern cottontail rabbit (Lagomorpha: Leporidae: *Sylvilagus floridanus*) from Central America

LUIS A. RUEDAS^{1*}, LUCÍA I. LÓPEZ², AND JOSÉ M. MORA^{1,3}

¹ Department of Biology and Museum of Natural History, Portland State University, SRTC-246, P.O. Box 751, Portland, OR 97207-0751. Email: ruedas@pdx.edu (LAR), jomora@pdx.edu (JMM).

² Área de Ciencias Básicas, Sede Regional de Atenas, Universidad Técnica Nacional, Atenas, Costa Rica. Email: luciaisa2@gmail.com (LIL).

³ Carrera de Gestión Ecoturística, Sede Central, Universidad Técnica Nacional, Alajuela, Costa Rica. Email: josemora07@gmail.com (JMM).

*Corresponding author: <https://orcid.org/0000-0002-4746-4799>.

To ascertain the taxonomic identity of cottontail rabbits from Costa Rica, we examined the holotypes of all the taxa of *Sylvilagus* currently subsumed within the *Sylvilagus floridanus* species complex as defined by Philip Hershkovitz. The almost 40 named taxa contained in *S. floridanus* are widespread from northeastern to north-central North America in the north (including southern Canada), through Central America to northwestern South America. Here, we examine Mesoamerican taxa in the complex, on the basis of holotypes, and test the hypothesis of conspecificity among them. Our examination of the holotypes, along with uni- and multivariate assessments of mensural variation as well as character variation in existing and newly acquired specimens from Costa Rica, indicate that *S. floridanus* (J. A. Allen, 1890) *sensu stricto* is restricted to North America, with its southern limit at the Isthmus of Tehuantepec. *Sylvilagus yucatanicus* (Miller, 1899) is limited to the Yucatan Peninsula. *Sylvilagus hondurensis* Goldman, 1932 is retained as a species, with *S. h. costaricensis* Harris, 1933 as a junior synonym. Costa Rica is revealed to have three described species: *S. gabbi* (J. A. Allen, 1877), *S. hondurensis costaricensis*, and *S. dicei* Harris, 1932. However, there are indications that this taxonomic scheme may in fact underrepresent the existing number of biological species of *Sylvilagus* present in that country.

Para cerciorarnos de la identidad taxonómica de las especies de conejos silvestres en Costa Rica, examinamos los holotipos de todos los taxones de *Sylvilagus* descritos en el grupo *Sylvilagus floridanus* tal como fuera delimitado por Philip Hershkovitz. El grupo comprende cerca de 40 taxones nombrados, ampliamente distribuidos a partir del norte entre el noreste y noroeste de Norteamérica (incluyendo el sur del Canadá), a través de Centroamérica, hasta el noroeste de Sudamérica. En la presente obra, examinamos los taxones Centroamericanos, a partir de holotipos, del complejo *S. floridanus* para así poner a prueba la hipótesis que están todos comprendido en una sola especie. Nuestro examen de estos holotipos, así como análisis de caracteres, y análisis univariado y multivariado de medidas tanto de especímenes en museos como especímenes resultado a partir de nuevos muestreos en Costa Rica, sugieren que *S. floridanus* (J. A. Allen, 1890) *sensu stricto* debe restringirse al norte del Istmo de Tehuantepec. Restringimos *Sylvilagus yucatanicus* (Miller, 1899) a la Península de Yucatán. *Sylvilagus hondurensis* Goldman, 1932 es una especie válida, con *S. h. costaricensis* Harris, 1933 como subespecie incluída. En Costa Rica, distinguimos tres especies descritas: *S. gabbi* (J. A. Allen, 1877), *S. hondurensis costaricensis* y *S. dicei* Harris, 1932. Sin embargo, existen indicios que esta hipótesis taxonómica pueda de hecho infravalorar el actual número de especies biológicas de *Sylvilagus* presentes en ese país.

Keywords: Biogeography; evolution; morphological homogeneity; species limits, taxonomy.

© 2023 Asociación Mexicana de Mastozoología, www.mastozoologiamexicana.org

Introduction

Because of their conservative morphology, lagomorphs are notoriously difficult, to dissemble into biologically realistic evolutionary entities. [Bachman \(1837:282\)](#) notably stated that, “many of the species so greatly resemble each other in many particulars that the student in natural history has sometimes been greatly perplexed in deciding on the exact species referred to by authors.” Forty years later, [Allen \(1877\)](#), in listing examined specimens of *Sylvilagus palustris*— currently understood to be circumscribed to the southeastern United States (western limit to Mobile Bay)— listed specimens from Veracruz and Yucatán, México, as belonging in that species. It was not until the skull had been removed for examination that Allen instead admitted that the specimen from Veracruz should belong

to its own discrete species, *S. truei* [= *S. gabbi truei*] (Allen, 1890b:192), noting that “the single record from so remote a point [*i. e.*, from Florida] as Mirador, México, has of late seemed open to serious [taxonomic] question” thereby first remarking on congruence between geographic features and taxonomy of *Sylvilagus*. Taxonomic decisions at the time were routinely undertaken—with few but notable exceptions— based on external appearance. Since that time, increasingly detailed analyses have been undertaken, and an expanding tool chest of morphological characters have successively been employed to more accurately distinguish among lagomorph taxa ([Baird 1857](#); [Gray 1867](#); [Lyon 1904](#); [Nelson 1909](#); [Thomas 1913](#); [Hummelinck 1940](#); [Hershkovitz 1950](#); [Hall 1951](#); [Palacios et al. 1980](#); [Ruedas 1998, 2017](#); [Ruedas et al. 2017](#)).

Philip Hershkovitz's 1950 treatise in particular, nominally focused on Colombia but in fact covering most, if not all, of South America, stands apart as the first attempt at a comprehensive treatment of the lagomorphs of any continent, albeit closely followed by E. R. Hall's 1951 synopsis of North American lagomorphs. The vast scope, both geographic and taxonomic, of Hershkovitz's work meant that, years later, the taxonomy he proposed for Central and South American cottontails remained in force. For example, for Central American *S. brasiliensis*, [Hall \(1951, 1981\)](#) showed no changes relative to the scheme of [Hershkovitz \(1950\)](#). [Cabrera \(1961\)](#) similarly had few taxonomic changes in either *S. "brasiliensis"* or *S. "floridanus"* (both *sensu lato*) of South America, although *S. nigroneuchalis* Hartert, 1894, the oldest available name for South American taxa considered to be subsumed within *S. floridanus*, was inexplicably omitted from Cabrera's treatment.

However, and notwithstanding its eminent worth, the passage of time has revealed that some errors made their way into Hershkovitz's 1950 treatise. As [Musser et al. \(1998:10\)](#) pointed out with particular respect to oryzomyine rodents, parts of some of Hershkovitz's revisions could represent an "unfortunate example of taxonomic revision undocumented by specimens or other data and one that misleadingly simplified a complex reality". In the case of the treatment of South American cottontails, for example, Hershkovitz did not examine all the pertinent holotypes, and when he did, it is unclear how carefully he scrutinized key morphological characters that could have led to a more accurate reflection of the underlying biological reality ([Ruedas 2017](#)). In fact, Hershkovitz's conclusion (1950:327) that his "review shows [*S. brasiliensis* and *S. floridanus*] to be the only recognizably valid species of leporids indigenous to South America" could not, in retrospect, have been further from the mark, given the recognized presence of a much larger number of species of *Sylvilagus*: at least 12 in the "*brasiliensis*" group alone ([Ruedas et al. 2019](#)).

In the present work, we began by questioning the taxonomy of individuals in the genus *Sylvilagus* from Costa Rica. Costa Rica, at 51,100 km², covers only 0.034 % of the land surface of the Earth, but with over 230 species present of terrestrial mammals, contains approximately 4 % of the World's known mammal species: 121 times more than expected by strict proportionality between area and biodiversity. Insofar as cottontails (*Sylvilagus*) are concerned, that is reflected in the presence of three recognized taxa ([Hall 1951, 1981](#); [Mora 2000](#); [Ruedas and Salazar-Bravo 2007](#); [Rodríguez-Herrera et al. 2014](#)): *S. g. gabbi* (J. A. Allen, 1877), *S. dicei* Harris, 1932, and *S. floridanus costaricensis* Harris, 1933. In describing *S. f. costaricensis*, [Harris \(1933\)](#) undertook comparisons of that taxon with *S. f. aztecus* (J. A. Allen, 1890) and *S. f. hondurensis* Goldman, 1932. Goldman in turn, in his description of *S. f. hondurensis*, undertook comparisons between that taxon and *S. f. chiapensis* (Nelson, 1904).

We accordingly undertook comparisons of taxa in the *Sylvilagus floridanus* group present in Costa Rica and the

region in order to better ascertain their taxonomic identity. The Costa Rican—and indeed, Central American—taxa of *Sylvilagus* remain inadequately described, let alone diagnosed. We therefore undertook a detailed analysis of cranial and dental anatomy of Costa Rican taxa of *S. floridanus* within the broader context of their current nominal identification to species, by undertaking comparisons using all the pertinent holotypes: of *S. floridanus* (J. A. Allen, 1890): those of the species and subspecies listed above, and that of the geographically proximal *S. f. yucatanicus* (Miller, 1899), thereby enabling us to robustly define the species of *S. floridanus* complex in Costa Rica and adjacent areas. Identification of species is, we believe, critical to generating phylogenetic trees that bear any semblance to the reality of life, because accurate trees can only result from the combination of adequate taxon sampling with sufficient data. Otherwise, one is left with what [Coddington and Scharff \(1996:139\)](#) so trenchantly remarked: "A fully resolved tree that makes no sense is still nonsensical."

Materials and methods

Specimens. Specimens examined are listed in Appendix 1, with their original taxonomic designation as well as current taxonomy, localities (georeferenced insofar as possible), repository, and collection number. For geographic and taxonomic reasons, as described above, we chose to focus on the following taxa: *Sylvilagus f. floridanus*, *S. f. costaricensis*, *S. f. hondurensis*, *S. f. aztecus*, *S. f. chiapensis*, *S. f. yucatanicus*, *S. gabbi*, *S. dicei*, and *S. brasiliensis surdaster* (Thomas, 1901). *Sylvilagus b. surdaster* was included because, although the type locality is in Ecuador (Esmeraldas Prov.; Río Bogotá, Carondelet; ca. 1° 07' 27" N, 78° 45' 45" W, ca. 20 m), and there would be scant probability of conspecificity, it is the most proximal lowland taxon affine to *S. brasiliensis* broadly writ and the name *brasiliensis* has previously been used for Costa Rican lowland rainforest rabbits following [Hall \(1981\)](#).

Morphological data: mensural characters. We measured 37 craniodental morphological variables. Terminology of cranial characters and features generally follows [Wible \(2007\)](#), and [Ruedas \(1998\)](#); measurements were defined by [White \(1987\)](#) and [Ruedas \(1998, 2017\)](#), and were extensively detailed and illustrated in [Ruedas et al. \(2017\)](#). Mensural characters included: GLS, greatest length of skull; POSTORB, width of postorbital constriction; BROSTR and DEPROSTR, breadth and depth (height) of rostrum; BBRAIN, breadth of braincase; ZYGO1, greatest width across the masseteric spine; ZYGO2, zygomatic breadth; LZYGO, length of zygomatic arch; NASALL, greatest length of nasal bone; NASALW, greatest width across left and right nasal bones; I2P2, least alveolar length of I2–P2 diastema; P2M3, greatest alveolar length of P2–M3 toothrow; HBRAIN, height of braincase; HBULLA, height of bulla; CONDL, condylopremaxillary length of cranium; LPALFOR, WPALFOR, length and width of incisive foramina; PALONG, palatal length; PALBRDGE, greatest anteroposterior dimension of palatal bridge; BASIOC, anteroposterior length of basioccipital; WIDBULL,

width of auditory bulla; ANTBULL, anteroposterior length of auditory bulla, from the most anterior projection of the ectotympanic to the most posterior point between the occipital and the paracondylar processes of the exoccipital; INTBD, least breadth across the basioccipital between the ectotympanic bones; OCCOND, width across the occipital condyles; INTBOC, length between the posteriormost edge of the palatal bridge and the suture between the basioccipital and basisphenoid bones; CHOANA1, breadth of nasopharynx; CHOANA2, breadth of alisphenoid constriction; MASTOID, greatest breadth across the mastoid exposure of the petrosal; DEPZYGO, least anteroposterior length across the maxillary bone at the base of the masseteric spine on the maxillary portion of the zygomatic arch; IP3, least alveolar length of i–p3; MANDEP, depth of mandibular body; P3M3, greatest alveolar length of p3–m3; HMAND, height of the mandible; HPTT, distance from ventral aspect of angular process (labial to pterygoid shelf) to most dorsal aspect of pterygoid tuberosity; BCON, length of condyloid process; WCON, breadth of articular facet of condyloid process; LMAND, length of mandibular body.

Statistical analyses were carried out using the Statistical Analysis System (SAS) software, version 9.4 (2002–2012; [SAS Institute 1988a, 1988b](#)), generally following [Ruedas \(1995, 1998\)](#); significance in all analyses was set at $\alpha = 0.05$. Due to the paucity of specimens available, little could be made to determine presence or extent of sexual dimorphism in the taxa examined, although sexual dimorphism has been reported in measurements of *Sylvilagus* ([Orr 1940](#)) and could affect results of multivariate analyses ([Reyment et al. 1984](#); [Marcus 1990](#)) given the small intraspecific sample sizes of the present study (Appendix 1). Univariate statistics (mean, standard deviation) were calculated using the UNIVARIATE procedure of SAS. Analysis of variance was carried out using the GLM procedure, enabling the MEANS routine with option REGWQ, which uses the Ryan–Eynot–Gabriel–Welsch multiple range test, and controls for Type I error ([Day and Quinn 1989](#)). A principal component analysis (procedure PRINCOMP) was carried out on the covariance matrix of log-transformed normalized measurement values data. Such a posteriori grouping methods are preferred by us over a priori grouping methods (multiple range tests, discriminant analyses) because there is no prior hypothesis as to the putative identity of specimens examined. These data further are useful to examine ontogenetic growth patterns, which in the sample covariance matrix can be construed as the dispersion of points along the major long axis of each sample, with the first eigenvector representing Huxley's allometric equation ([Voss et al. 1990](#)). We used the broken stick method of [Frontier \(1976\)](#) as implemented by [Jackson \(1993\)](#) to assess the significance of each principal component's eigenvalue; broken-stick distributions for principal component eigenvalues were generated using the "broken.stick" function of R (v. 3.3.1; [R Core Team 2016](#)).

Dental characters. Drawings of p3 were made by tracing from photographs taken using a Canon EOS 30D digital

camera mated to a Canon MP–E 65 mm f/2.8 1–5X Macro Photo lens, or a Canon EOS 6D mated to the same lens or an AmScope CA–CAN–SLR–III camera adapter for microscopes, shooting either through a camera tube on a binocular dissecting microscope or an ocular tube with the ocular removed, also on a binocular dissecting microscope, as made available by the collections housing the specimens under consideration. Among leporids, p3 generally constitutes the most informative dental element for taxonomic and systematic purposes ([Dalquest 1979](#); [Dalquest et al. 1989](#); [Hibbard 1963](#); [Palacios and López Martínez 1980](#); [Ruedas 1998](#); [Ruedas et al. 2017](#); [White 1987, 1991](#); [White and Morgan 1995](#); [Winkler and Tomida 2011](#)). Discrete characters were deemed the most important in this particular research; accordingly, resulting figures were oriented and scaled to the same size in linear dimensions to carry out size-independent comparisons of interspecific characters. Characters considered follow the standard terminology of [Palacios and López Martínez \(1980\)](#), were described in Appendix I of [Ruedas \(1998\)](#) and illustrated here (Figure 1) with some modifications from [Ruedas et al. \(2017\)](#) in that all cusps are identified by incorporating features from [López Martínez \(1974, 1977, 1980, 1989\)](#), [López-Martínez et al. \(2007\)](#), and [Angelone and Sesé \(2009\)](#). Additional characters useful in distinguishing among lagomorph species were extracted from [Palacios \(1996\)](#) and [Palacios et al. \(2008\)](#). The LSID for this publication is: urn:lsid:zoobank.org:pub:601C073B-6DFA-421E-8B4B-F7F44BF62D3F.

Results

Statistical analyses of morphology. Univariate statistics (means \pm standard deviation, minimum–maximum) for the variables measured in each individual taxon (represented in certain taxa only by the holotypes or, in the case of *S. gabbi*, by the lectotype) are shown in Table 1. Also shown in Table 1 are the results of the Ryan–Einot–Gabriel–Welsch multiple range test. Thirty of the 37 characters examined showed some level of significance in discriminating among groups of individuals or taxa. This proportion (81.1 %) is markedly higher than the two characters that would be expected to differ significantly by chance alone with significance set at $\alpha = 0.05$. However, some of the variables that are significantly different among taxa do not discriminate into distinct groups (e. g., depth of rostrum, mastoid breadth, length of mandibular tooththrow, length of mandible). Similarly, most of the significantly different groups displayed a great deal of overlap. The one consistent result obtained from the analysis is that *S. f. yucatanicus* is immoderately larger than remaining taxa in almost all characters. That taxon differs significantly from all taxa but *S. dicei* in breadth of braincase, and from all other taxa in breadth of incisive foramina; it also has the longest skull of any *Sylvilagus* species examined for the present study, and beyond statistical significance ([Moyé 2006](#); [Wasserstein and Lazar 2016](#); [Wasserstein et al. 2019](#)), does not overlap with the GLS of any of the remaining *Sylvilagus* taxa.

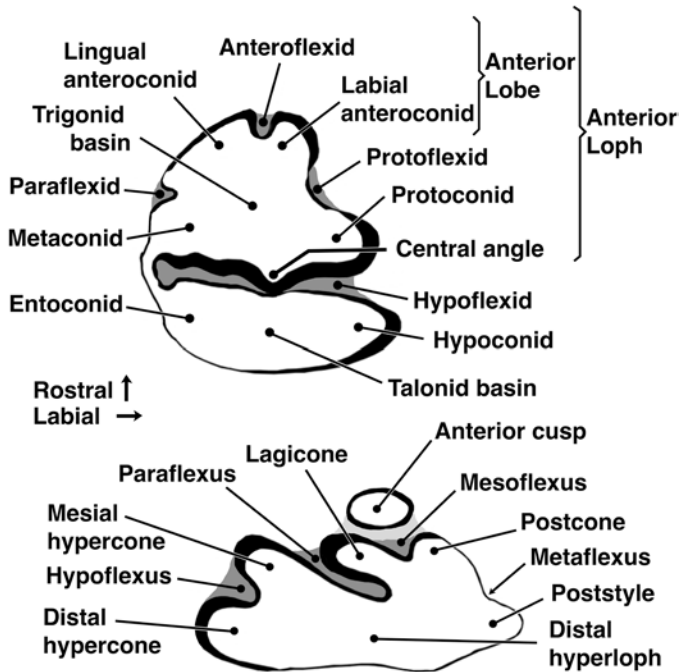


Figure 1. Standard nomenclature for dental features of Recent leporid lagomorphs' third lower premolar (p3, top) and second upper premolar (P2, bottom), adapted from Figure 1 of Palacios and López Martínez (1980:62), and expanded from Ruedas *et al.* (2017) in identifying all cusps by incorporating features from López Martínez (1974, 1977, 1980, 1989) and Angelone and Sesé (2009). The term "anterior loph," preferred herein, was used interchangeably with "trigonid" by Hibbard (1963). López-Martínez *et al.* (2007) considered only the caudal portion of the anterior loph of pm3 to constitute the trigonid, with the rostral portion (anterior lobe) instead collectively constituting the anteroconids.

The results of the principal component analysis, carried out on the covariance matrix of a reduced set of natural log-transformed variables ($n = 22$; reduced as a compromise to embrace as many specimens as possible while maintaining as many measurements as possible), are shown in Figure 2 and Tables 2 and 3. The principal component analysis accounts for 15.4 % of the overall variance. Principal component 1 accounts for 36.2 % of that variation, with PC 2 accounting for 14.9 %; PCs 1–7 jointly account for >80 %, and 1–10 for >90 %. Just over half (50.5 %) of the variation in PC 1 is accounted for by only five of the 22 characters: width of bulla (13.5 %), width of incisive foramina (11.6 %), width of nasal bones (11.3 %), length of nasal bones (8.5 %), and breadth of rostrum (5.6 %). Remaining characters each contribute less than 5 % to the variation in his principal component.

Figure 2 shows the great deal of overlap among most taxa in the *floridanus* species group. Within the limits imposed by a reduced number of samples, the major axis of dispersion for points in these taxa is primarily along principal component 1, which in this instance is a size component. The major axis of dispersion has been shown to be associated with age-correlated growth (Voss *et al.* 1990). In the particular instance of our analysis, this is borne out by the relative homogeneity of the magnitude of the eigenvector scores for PC 1 (Table 3): while some variables have eigenvector scores that are somewhat low (maxillary toothrow, interbullar distance, breadth of braincase) or somewhat high (width of bulla, width of nasal bones, width

of incisive foramina), the remaining characters are fairly homogeneous, and eigenvectors average 0.200 ± 0.08 . The homogeneity of the eigenvectors exhibited in PC1 is not evident in PC 2 through 6 or subsequent principal components (Table 3). For PC2, these average 0.041, but the standard deviation jumps to 0.209, with eigenvectors ranging from -0.456 (width of bulla) to 0.625 (breadth of nasopharynx). Subsequent principal components show similar trends with respect to standard deviation, maxima, and minima, of the characters' eigenvector scores. Such lack of homogeneity in eigenvector scores usually is associated with shape-based, rather than size-based variation.

In Figure 2, principal component 2 (14.9 % of the total variation) distinguishes primarily between the *floridanus* group *Sylvilagus* species and remaining species, including *S. gabbi* and *S. dicei*. Only two characters contribute well over half (59.9 %) of the variation to this principal component: breadth of nasopharynx (39.1 %) and width of bulla (20.8 %).

The results of the principal component analysis reinforce the suggestion derived from the multiple range test that *S. f. yucatanicus* is exceptionally distinct from remaining taxa examined. That taxon is markedly separated in principal component 1 from remaining individuals examined (Figure 2), this despite the fact that we undertook natural log-transformation of the variables in order to minimize the effects of size. Width of incisive foramina is the second most important character in PC1, contributing to 11.6 % of the variation in that PC. Breadth of braincase in contrast only contributes to 1.1 % of the variation in PC 1.

Notwithstanding the informative nature of the exploratory principal components analysis, we acknowledge that said analysis is not without issues. Application of the broken stick method to assess the significance of eigenvalues suggested that only the first two principal components contained meaningful information. These two components cumulatively accounted for 51.1 % of the variation. Because the overall PCA accounted for 15.4 % of the variance, the result is that only 7.9 % of the morphological variation is accounted for in the PCA as implemented in the present study. It is possible that more judicious selection of variables may have influenced the analysis one way or another (*e. g.*, selecting only those variables found to be significant in the multiple range test). We chose however to maintain the variables employed rather than cherry-pick the data. Our PCA results underscore that the morphological conservatism manifested in craniodental mensural variables throughout the genus *Sylvilagus*—and indeed, in other lagomorph genera—is not readily tractable to these morphometric analyses, although the analyses do have certain illuminative properties.

Taxonomic identity of Sylvilagus floridanus costaricensis Harris, 1933.

Analysis of morphological data. To ascertain the taxonomic identity of *S. f. costaricensis*, we undertook comparisons between this taxon and all other pertinent regional

Table 1. Craniodental measurements of holotypes (marked by a superscript star; *S. gabbi* has a lectotype) and taxa (means including holotype ± SD, minimum–maximum) considered in this paper, in mm. Variable abbreviations defined in Ruedas et al. (2017). Our sample sizes made impossible the evaluation of sexual dimorphism within species. *Sylvilagus boylei* was synonymized with *S. floridanus superciliosus* by Hershkovitz (1950); *S. f. chiapensis* was considered a junior synonym of *S. f. aztecus* by Hoffmann and Smith (2005); *S. daulensis* was synonymized with *S. brasiliensis surdaster* by Cabrera (1961); *S. russatus* was synonymized with *S. floridanus* by Nelson (1909); "*Lepus*" [= *Sylvilagus*] *margaritae* was synonymized with *S. floridanus* by Hershkovitz (1950); *S. salentus* was synonymized with *S. brasiliensis* by Hershkovitz (1950); "*Lepus*" [= *Sylvilagus*] *superciliaris* was synonymized with *S. floridanus* by Hershkovitz (1950). Superscripts by variable name indicate significance of variable in the Ryan–Einot–Gabriel–Welsh multiple range test, as follows: †: not significant; 0.05 > * > 0.01; 0.01 > ** > 0.001; 0.001 > *** > 0.0001; 0.0001 > ****. Means or values indicated by the same superscript letters by the variable indicate groups that are not significantly different (not shown for holotypes representing sample sizes greater than 1).

| Taxon | <i>S. f. aztecus</i> * ♂ ANMH 3116/2438 | <i>S. f. aztecus</i> (n = 12) | <i>S. boylei</i> * ♀ ANMH 37794 | <i>S. f. chiapensis</i> * ♀ USNM 75953 | <i>S. f. chiapensis</i> (n = 4) | <i>S. f. connectens</i> * ♂ USNM 63660 | <i>S. f. costaricensis</i> * ♀ UMMZ 65232 | <i>S. daulensis</i> * ♀ AMNH 34671 | <i>S. dicei</i> * ♀ UMMZ 64043 | <i>S. dicei</i> * ♂ TTU 114374 | <i>S. f. floridanus</i> * AMNH 3116/2438 |
|---|---|--|---------------------------------------|---|--|---|--|---------------------------------------|--------------------------------------|--------------------------------------|--|
| Greatest length of skull** | 72.9 | 72.6 ± 3.9, 65.0–77.3 ^{ab} | 76.2 ^b | 78.9 | 77.0 ± 2.1, 74.2–78.9 ^{ab} | 74.4 ^{ab} | 76.3 ^{ab} | 69.2 ^b | 77.3 ^{ab} | 70.5 ^b | 72.9 |
| Postorbital constriction† | 11.2 | 11.7 ± 1.0, 10.0–13.3 | 12.3 | 11.6 | 11.9 ± 0.7, 11.4–12.9 | 12.2 | 12 | 10.9 | 10.1 | 12 | 11.2 |
| Breadth of rostrum† | 20.6 | 18.6 ± 1.5, 15.2–20.6 | 20.7 | 21.2 | 19.9 ± 1.5, 18.4–21.2 | 18.6 | 20.9 | 18 | 22.6 | 17.2 | 17.1 |
| Depth of rostrum*** | 18.2 | 15.8 ± 1.3, 14.0–18.2 ^b | 17.2 ^a | 15.6 | 15.8 ± 0.8, 14.9–16.8 ^b | 17.3 ^a | 15.2 ^a | 15.3 ^b | 16.1 ^a | 14.0 ^a | 15.5 |
| Breadth of braincase**** | 26.1 | 25.4 ± 0.7, 23.9–26.1 ^{bc} | 26.1 ^{bc} | 25.7 | 26.1 ± 0.9, 25.1–27.1 ^{bc} | 26.1 ^{bc} | 25.5 ^{bc} | 23.2 ^a | 27.9 ^{ab} | 27.1 ^{ab} | 26.3 |
| Zygomatic breadth at spine**** | 33.6 | 33.7 ± 1.3, 32.0–36.0 ^{cd} | 35.1 ^{abc} | 35.6 | 35.1 ± 1.2, 33.6–36.4 ^{abc} | 34.4 ^{abcd} | 35.1 ^{abc} | 30.3 ^d | 39.0 ^{ab} | 36.0 ^{ab} | 33.4 |
| Zygomatic breadth** | 35 | 34.4 ± 1.0, 32.3–36.4 ^{bc} | 35.3 ^{abc} | 36.5 | 35.6 ± 1.2, 34.0–36.5 ^{abc} | 35.4 ^{abc} | 34.2 ^{bc} | 31.4 ^e | 38.4 ^{ab} | 36.6 ^{ab} | - |
| Length of zygomatic arch** | 31.1 | 30.7 ± 1.8, 26.4–33.1 ^{ab} | 33.7 ^{ab} | 33.8 | 32.5 ± 0.9, 31.8–33.8 ^{ab} | 33.4 ^{ab} | 32.2 ^{ab} | 29.0 ^f | 33.5 ^{ab} | 31.6 ^{ab} | 31.5 |
| Nasal bone length**** | 33.9 | 31.9 ± 1.9, 27.9–34.2 ^{abcd} | 31.8 ^{abcd} | 36.9 | 34.5 ± 1.6, 33.4–36.9 ^{abcde} | 34.6 ^{abcd} | 35.3 ^{abc} | 27.3 ^f | 33.6 ^{abcd} | 30.5 ^{abcd} | 30.4 |
| Width of nasal bones**** | 17.2 | 15.7 ± 1.2, 13.9–17.4 ^{abcde} | 17.7 ^{ab} | 17.6 | 15.4 ± 1.6, 14.1–17.6 ^{abcde} | 15.4 ^{abcde} | 17.4 ^{abc} | 13.7 ^{abcde} | 14.8 ^{abcde} | 12.7 ^{abcde} | 14.9 |
| Length of upper diastema*** | 19.8 | 19.7 ± 1.1, 17.1–21.4 ^{ab} | 20.4 ^{ab} | 22.3 | 21.2 ± 0.7, 20.8–22.3 ^{ab} | 20.2 ^{ab} | 20.3 ^{ab} | 18.5 ^b | 21.2 ^{ab} | 19.9 ^{ab} | 19.6 |
| Length of maxillary toothrow† | 13.5 | 13.2 ± 0.7, 11.8–14.2 | 14.1 | 14.4 | 13.6 ± 0.9, 12.4–14.4 | 14 | 13.7 | 13.1 | 15 | 13.5 | 14.6 |
| Height of braincase**** | 22.7 | 23.2 ± 1.4, 21.3–25.4 ^{ab} | 23.3 ^{ab} | 24.1 | 24.4 ± 0.3, 24.1–24.7 ^{ab} | 24.2 ^{ab} | 23.1 ^{ab} | 20.7 ^{cd} | 22.8 ^{abcd} | 21.7 ^{abcd} | 23.9 |
| Height of bulla**** | 12.6 | 12.7 ± 0.6, 11.7–13.9 ^{cd} | 12.6 ^{cd} | 14.1 | 13.6 ± 1.3, 13.3–14.1 ^{abc} | 14.1 ^{ab} | 14.0 ^{ab} | 10.3 ^d | 11.6 ^{cd} | 11.1 | 13.1 |
| Condylomaxillary length* | 62.8 | 63.7 ± 3.2, 57.6–67.6 ^{ab} | 67.7 ^{ab} | 70.5 | 67.3 ± 2.8, 64.8–70.5 ^{ab} | 67.3 ^{ab} | 69.0 ^{ab} | 62.2 ^b | 69.4 ^{ab} | 63.0 ^{ab} | 65.7 |
| Length of incisive foramina*** | 16.9 | 16.1 ± 1.0, 13.7–17.4 ^b | 18.9 ^{ab} | 20.4 | 17.9 ± 1.6, 16.7–20.4 ^{ab} | 18.5 ^{ab} | 16.8 ^{ab} | 15.9 ^b | 17.5 ^{ab} | 17.0 ^{ab} | 17.2 |
| Width of incisive foramina*** | 6.5 | 5.9 ± 0.7, 4.7–7.0 ^b | 4.9 ^b | 7.4 | 6.8 ± 0.6, 6.2–7.4 ^b | 6.4 ^b | 6.4 ^b | 5.4 ^b | 7.2 ^b | 5.7 ^b | 6.9 |
| Length of palate** | 27.8 | 27.2 ± 1.4, 23.5–28.6 ^{ab} | 28.2 ^{ab} | 30.4 | 28.9 ± 1.2, 27.6–30.4 ^{ab} | 29.1 ^{ab} | 28.7 ^{ab} | 25.6 ^b | 28.4 ^{ab} | 26.8 ^{ab} | 27.8 |
| Length of palatal bridge** | 7 | 6.8 ± 0.5, 6.0–7.5 ^{ab} | 6.4 ^{ab} | 7.1 | 7.0 ± 0.2, 6.7–7.1 ^{ab} | 7.3 ^{ab} | 7.7 ^{ab} | 6.0 ^b | 6.8 ^{ab} | 6.0 ^{ab} | 7.1 |
| Length of basioccipital*** | 9.4 | 9.2 ± 0.6, 8.1–10.2 ^{ab} | 9.3 ^{ab} | 9.2 | 9.0 ± 0.4, 8.4–9.4 ^{ab} | 9.8 ^a | 9.6 ^a | 8.8 ^{ab} | 9.2 ^{ab} | 8.4 ^{ab} | 9 |
| Width of bulla† | 6.4 | 6.4 ± 1.2, 5.4–9.8 | 7.2 | 6.5 | 6.4 ± 0.3, 6.0–6.5 | 7.1 | 6.5 | 5.2 | 6.5 | 4.6 | 4.4 |
| Anteroposterior length of bulla**** | 9.6 | 9.7 ± 0.5, 8.9–10.6 ^{cd} | 11.2 ^{ab} | 9.6 | 10.0 ± 0.5, 9.6–10.6 ^{abcd} | 10.6 ^{abc} | 9.0 ^{bcde} | 8.2 ^{de} | 8.4 | 9.6 | 10.9 |
| Interbulbar breadth† | 8 | 7.5 ± 0.4, 6.3–8.0 ^{ab} | 7.9 ^{ab} | 7.1 | 6.8 ± 0.6, 5.9–7.4 ^{ab} | 6.9 ^{ab} | 8.5 ^a | 7.4 ^{ab} | 8.5 ^{ab} | 7.5 ^{ab} | 8.3 |
| Breadth of occipital condyles† | 14.1 | 13.8 ± 0.3, 13.4–14.2 | 14.5 | 14.3 | 13.4 ± 0.7, 12.8–14.3 | 13.1 | 14.5 | 13.7 | 14.6 | 12.7 | 12.4 |
| Length of palatal suture† | 20.2 | 19.8 ± 1.3, 17.8–21.8 | 20.5 | 23 | 21.3 ± 1.4, 19.7–23.0 | 21.1 | 21.2 | 18.9 | 22 | 19.1 | 21.1 |
| Breadth of nasopharynx*** | 6.2 | 5.4 ± 0.5, 4.4–6.2 ^{cd} | 5.7 ^{bcd} | 6.2 | 5.9 ± 0.2, 5.7–6.2 ^{bcd} | 5.1 ^{cd} | 6.2 ^{bc} | 4.2 ^{cd} | 7.9 ^b | 7.1 ^a | 6.4 |
| Breadth of alisphenoid constriction**** | - | 8.9 ± 0.3, 8.5–9.6 ^{ab} | - | 10 | 9.2 ± 0.5, 8.8–10.0 ^{ab} | 9.2 ^{ab} | 9.5 ^{ab} | 8.5 ^b | 11.3 ^a | 10.3 ^a | - |
| Mastoid breadth** | 24 | 23.9 ± 1.0, 22.6–25.3 ^a | 24.5 ^a | 24.2 | 24.1 ± 0.6, 23.2–24.8 ^a | 23.7 ^a | 25.6 ^a | 23.1 ^a | 26.7 ^a | 23.5 ^a | 22.4 |
| Depth of zygomatic arch** | 5.3 | 5.06 ± 0.3, 4.4–5.5 ^{ab} | 5.6 ^{ab} | 5 | 5.1 ± 0.4, 4.6–5.7 ^{ab} | 5.8 ^{ab} | 5.3 ^{ab} | 4.4 ^{bc} | 5.2 ^{ab} | 4.8 ^{ab} | 6 |
| Length of mandibular diastema* | 15.8 | 15.6 ± 1.0, 13.2–16.8 ^{ab} | 16.0 ^{ab} | 17 | 16.3 ± 0.5, 15.8–17.0 ^{ab} | 15.6 ^{ab} | 15.2 ^{ab} | 15.2 ^{ab} | 16.4 ^{ab} | 15.0 ^{ab} | 16.1 |
| Depth of mandibular ramus**** | 11.9 | 11.4 ± 0.5, 10.7–12.1 ^{abcd} | 11.2 ^{abcd} | 12.1 | 11.6 ± 0.6, 10.8–12.1 ^{abcd} | 12.2 ^{ab} | 12.6 ^a | 9.8 ^{cd} | 11.0 ^{abcd} | 10.6 ^{abcd} | 11.5 |
| Length of mandibular toothrow** | 14.6 | 13.4 ± 0.6, 12.6–14.6 ^a | 14.4 ^a | 15.1 | 14.2 ± 0.7, 13.5–15.1 ^a | 13.9 ^a | 14.4 ^a | 13.4 ^a | 15.5 ^a | 14.2 ^a | 14.8 |
| Height of mandible**** | 35.8 | 34.9 ± 1.5, 32.1–37.1 ^{bcd} | 38.1 ^{abc} | 38 | 37.1 ± 0.7, 36.4–38.0 ^{abc} | 37.5 ^{abc} | 37.5 ^{abc} | 30.9 ^d | 37.2 ^{abcd} | 34.0 ^{abcd} | 37.2 |
| Length from angular process to pterygoid tuberosity**** | 25 | 24.8 ± 1.3, 22.7–26.7 ^{abc} | 27.8 ^{ab} | 27.8 | 26.6 ± 0.9, 25.6–27.8 ^{ab} | 27.0 ^{ab} | 26.0 ^{abc} | 21.4 ^e | 26.1 ^{abc} | 24.8 ^{abc} | 26.3 |
| Length of condyloid process** | 8.4 | 8.2 ± 0.4, 7.5–8.7 ^a | 8.6 ^a | 8.8 | 8.4 ± 0.5, 7.6–8.8 ^a | 8.8 ^a | 8.9 ^a | 8.7 ^a | 10.2 ^a | 9.5 ^a | 8.9 |
| Width of articular facet** | 3.4 | 3.4 ± 0.1, 3.3–3.7 ^{ab} | 3.1 ^b | 4.1 | 3.6 ± 0.3, 3.4–4.1 ^{ab} | 3.5 ^{ab} | - | 3.3 ^{ab} | - | 4.2 ^a | 4 |
| Length of mandible* | 53 | 52.4 ± 2.6, 48.0–56.2 ^b | 55.2 ^a | 57.5 | 55.7 ± 1.4, 54.2–57.5 ^a | 55.3 ^a | 54.0 ^a | 50.5 ^a | 56.6 ^a | 54.6 ^a | 55 |

Table 1. Continuation...

| Taxon | <i>S. f. floridanus</i> (n = 11) | <i>S. f. russatus</i> ♂ AMNH 17203 | <i>S. g. gabbi</i> ♂ USNM 11371/37794 | <i>S. g. incitatus</i> ♀ MCZ Bangs 8441 | <i>S. g. messorius</i> ♂ USNM 179569 | <i>S. f. hondurensis</i> ♂ USNM 257062 | <i>S. f. hondurensis</i> (n = 13) | <i>S. margaritae</i> ♂ USNM 63217 | <i>S. salentus</i> ♂ AMNH 33050 | <i>S. superciliosus</i> ♀ AMNH 15428 | <i>S. f. yucatanicus</i> ♀ USNM 37772 |
|--|---|---------------------------------------|---|--|---|---|--|--------------------------------------|------------------------------------|---|--|
| Variable (↓); museum number (→) | | | | | | | | | | | |
| Greatest length of skull** | 72.0 ± 1.4, 69.4–73.8 ^b | 78.6 ^b | 70.9 ^b | 73.9 ^b | 72.5 ^{ab} | 74.7 | 76.1 ± 1.4, 73.2–77.6 ^{ab} | 78.8 ^{ab} | - | 78.4 ^{ab} | 81.1 ^a |
| Postorbital constriction† | 11.2 ± 0.8, 10.0–12.7 | 11.2 | 10.5 | 13.2 | 12.4 | 12.4 | 12.2 ± 1.3, 10.4–15.1 | 14.5 | - | 12.9 | 13.2 |
| Breadth of rostrum† | 19.2 ± 1.0, 17.1–20.8 | 20.2 | 17.1 | 20.8 | 18.8 | 19.2 | 19.3 ± 1.0, 17.6–20.7 | 22.3 | - | 20.5 | 21.7 |
| Depth of rostrum*** | 15.3 ± 0.4, 14.7–15.9 ^a | 16.8 ^a | 14.4 ^a | 14.9 ^a | 15.4 ^a | 17.3 | 17.1 ± 0.7, 15.6–18.0 ^a | 17.6 ^a | - | 17.5 ^a | 17.5 ^a |
| Breadth of braincase*** | 25.9 ± 0.6, 25.2–27.4 ^{bc} | 25.6 ^{bc} | 25.0 ^{bc} | 24.0 ^c | 24.0 ^c | 25.5 | 25.8 ± 0.7, 23.9–26.5 ^{bc} | 25.6 ^{bc} | - | 25.3 ^{bc} | 29.0 ^a |
| Zygomatic breadth at spine*** | 33.9 ± 0.6, 33.0–35.0 ^{abcd} | 35.0 ^{abc} | 32.6 ^d | 35.2 ^{bc} | 35.3 ^{abc} | 34.9 | 35.0 ± 1.1, 32.8–36.1 ^{abc} | 36.1 ^{bc} | - | 34.6 ^{abcd} | 38.5 ^a |
| Zygomatic breadth** | 35.2 ± 0.6, 34.5–36.0 ^{bc} | 35.2 ^{abc} | 33.4 ^c | 35.0 ^{bc} | 35.8 ^{ab} | 34.4 | 35.0 ± 1.1, 33.1–36.9 ^{bc} | 36.1 ^{ab} | - | 35.4 ^{abc} | 38.6 ^a |
| Length of zygomatic arch** | 31.0 ± 0.8, 29.4–32.2 ^{ab} | 33.5 ^{ab} | 30.8 ^b | 32.0 ^b | 30.6 ^{ab} | 31 | 32.6 ± 1.1, 31.0–34.3 ^{ab} | 32.5 ^{ab} | - | 33.1 ^{ab} | 34.7 ^a |
| Nasal bone length*** | 30.5 ± 1.0, 14.3 ± 1.1, 28.4–31.9 ^{abcd} | 36.9 ^a | 27.9 ^d | 30.5 ^{abcd} | 28.8 ^{cd} | 34.2 | 34.5 ± 1.3, 32.0–36.3 ^{abcde} | 36.3 ^{ab} | 28.2 ^{def} | 33.5 ^{abcd} | 37.2 ^b |
| Width of nasal bones*** | 12.8–16.5 ^{abcde} | 17.3 ^{abcd} | 12.1 ^e | 13.0 ^{cd} | 12.6 ^{de} | 15.8 | 16.2 ± 0.7, 15.1–17.6 ^{abcde} | 18.2 ^a | 12.7 ^{de} | 16.2 ^{abcde} | 17.1 ^{abcd} |
| Length of upper diastema*** | 19.1 ± 0.6, 18.3–20.4 ^{ab} | 21.1 ^{ab} | 20.4 ^{ab} | 20.4 ^b | 20.0 ^{ab} | 20.7 | 20.5 ± 0.7, 19.8–21.6 ^{ab} | 22.9 ^a | - | 20.4 ^{ab} | 23.2 ^a |
| Length of maxillary toothrow† | 13.9 ± 0.8, 13.0–15.5 | 14.4 | 13.8 | 14.4 | 13.5 | 13.6 | 13.8 ± 0.4, 13.0–14.6 | 14.5 | 12.7 | 14.6 | 14 |
| Height of braincase*** | 22.6 ± 0.7, 21.6–23.9 ^{bc} | 23.2 ^b | 21.1 ^{cd} | 18.6 ^d | 19.0 ^d | 23.1 | 23.7 ± 0.9, 22.1–25.0 ^{ab} | 22.4 ^{abcd} | - | 24.8 ^{ab} | 25.3 ^a |
| Height of bulla*** | 13.4 ± 0.7, 12.4–14.5 ^{bc} | 14.8 ^{ab} | 10.3 ^d | - | 10.3 ^d | 12.9 | 13.3 ± 0.7, 12.5–14.7 ^{bc} | 12.4 ^{cd} | - | 12.0 ^{cd} | 15.5 ^a |
| Condylpremaxillary length* | 64.4 ± 1.7, 61.6–66.5 ^{ab} | 67.4 ^{ab} | 64.4 ^{ab} | 66.3 ^b | 64.2 ^{ab} | 66.2 | 66.8 ± 1.4, 64.5–68.5 ^{ab} | 70.2 ^{ab} | - | 69.3 ^{ab} | 72.2 ^a |
| Length of incisive foramina*** | 15.9 ± 1.0, 14.7–17.2 ^b | 18.8 ^{ab} | 16.2 ^b | 16.2 ^b | 16.2 ^b | 16.6 | 16.8 ± 0.7, 15.5–18.3 ^{ab} | 19.5 ^{ab} | - | 18.7 ^{ab} | 20.5 ^a |
| Width of incisive foramina*** | 6.3 ± 0.5, 5.2–6.9 ^b | 5.3 ^b | 4.6 ^b | 5.7 ^b | 5.9 ^b | 5.9 | 6.1 ± 0.4, 5.1–6.9 ^b | 6.4 ^b | - | 5.0 ^b | 9.1 ^a |
| Length of palate*** | 26.5 ± 1.0, 25.3–28.3 ^b | 29.5 ^{ab} | 27.1 ^{ab} | 28.0 ^b | 27.4 ^{ab} | 28.7 | 28.2 ± 0.7, 27.2–29.4 ^{ab} | 31.3 ^a | - | 28.6 ^{ab} | 31.4 ^a |
| Length of palatal bridge** | 6.6 ± 0.5, 5.8–7.5 ^{ab} | 7.4 ^{ab} | 7.5 ^{ab} | 8.4 ^a | 7.3 ^{ab} | 7.7 | 7.2 ± 0.5, 6.4–8.0 ^{ab} | 7.2 ^{ab} | 7.5 ^{ab} | 6.5 ^b | 7.4 ^{ab} |
| Length of basioccipital*** | 8.5 ± 0.6, 7.7–9.4 ^{ab} | 8.9 ^{ab} | 8.2 ^{ab} | - | 8.2 ^{ab} | 10.5 | 9.5 ± 0.5, 8.7–10.5 ^{ab} | 9.7 ^a | - | 10.6 ^a | 9.6 ^a |
| Width of bulla† | 6.7 ± 0.9, 4.4–7.7 | 7.1 | 5 | 5.3 | 5.7 | 6.7 | 6.4 ± 0.5, 5.4–7.2 | 6.9 | - | 6.7 | 7.9 |
| Anteroposterior length of bulla**** | 10.8 ± 0.6, 9.5–11.5 ^{abc} | 9.8 ^{cd} | 7.2 ^e | 9.1 ^{bcde} | 8.7 ^{de} | 10.5 | 10.2 ± 0.5, 9.4–10.8 ^{abcd} | 10.1 ^{abcd} | - | 11.4 ^{abc} | 12.0 ^a |
| Interbular breadth† | 7.4 ± 0.4, 6.8–8.3 ^{ab} | 6.2 ^b | 7.0 ^{ab} | 8.5 ^b | 7.0 ^{ab} | 7.4 | 7.5 ± 0.6, 6.8–8.7 ^{ab} | 7.8 ^{ab} | - | 7.6 ^{ab} | 8.1 ^{ab} |
| Breadth of occipital condyle† | 13.9 ± 0.8, 12.4–15.1 | 14.1 | 12.8 | 13.4 | 12.3 ^a | 13.1 | 13.3 ± 0.4, 12.6–14.2 ^a | 14.7 ^a | - | 15.6 | - |
| Length palate to basioccipital–basiptenoid suture† | 21.4 ± 0.5, 20.8–22.2 | 20.5 | 20.7 | 21.1 | 21.34 | 20.5 | 21.3 ± 0.9, 19.9–22.8 | 21.9 | - | 21.6 | 22.2 |
| Breadth of nasopharynx**** | 5.9 ± 0.4, 5.2–6.4 ^{abcd} | 6.2 ^{bc} | 6.3 ^{abc} | 7.0 ^{abc} | 7.1 ^{ab} | 5.6 | 5.8 ± 0.4, 4.6–6.4 ^{abcd} | 6.6 ^{abc} | - | 6.2 ^{abc} | 6.6 ^{abc} |
| Breadth of alisphenoid constriction**** | 8.8 ± 0.4, 7.9–9.3 ^b | 9.2 ^{ab} | 9.4 ^{ab} | 10.3 ^b | 10.4 ^{ab} | 9.4 | 9.0 ± 0.4, 8.0–9.4 ^{ab} | 9.8 ^{ab} | - | - | 9.9 ^{ab} |
| Mastoid breadth** | 22.6 ± 1.1, 21.3–25.0 ^a | 23.0 ^a | 24.3 ^a | 23.9 ^a | 23.9 ^a | 24.4 | 24.5 ± 0.5, 23.1–25.4 ^a | 25.6 ^a | - | 24.3 ^b | - |
| Depth of zygomatic arch** | 5.3 ± 0.6, 4.3–6.0 ^{ab} | 5.8 ^{ab} | 3.3 ^c | 5.0 ^{ab} | 5.0 ^{ab} | 4.8 | 5.0 ± 0.2, 4.6–5.3 ^{ab} | 4.8 ^{bc} | - | 5.0 ^{bc} | 6.1 ^a |
| Length of mandibular diastema* | 14.9 ± 0.7, 13.5–16.1 ^{ab} | 15.1 ^{ab} | 16.2 ^{ab} | 15.7 ^{ab} | 16.0 ^{ab} | 16.8 | 16.4 ± 0.7, 15.3–17.8 ^{ab} | 17.2 ^{ab} | - | 16.2 ^{ab} | 18.4 ^a |
| Depth of mandibular ramus**** | 11.5 ± 0.5, 10.6–12.1 ^{abcd} | 11.8 ^{abc} | 9.7 ^{cd} | 12.0 ^b | 9.6 ^d | 12.8 | 12.0 ± 0.5, 11.3–12.9 ^{ab} | 12.0 ^{ab} | 10.9 ^{abcd} | 12.1 ^{abc} | 12.8 ^a |
| Length of mandibular toothrow** | 14.5 ± 0.7, 13.5–15.7 ^a | 14.6 ^a | 14.8 ^a | 15.4 ^a | 14.4 ^a | 14.4 | 13.9 ± 0.4, 13.3–14.5 ^a | 15.0 ^a | 14.4 ^a | 14.6 ^a | 14.2 ^a |
| Height of mandible**** | 35.4 ± 1.0, 33.9–37.2 ^{abcd} | 39.6 ^{ab} | 33.5 ^{cd} | 37.4 ^{abc} | 33.0 ^{cd} | 37.3 | 36.7 ± 1.1, 34.6–38.0 ^{abc} | 35.5 ^{abcd} | - | 36.8 ^{abcd} | 40.8 ^a |
| Length from angular process to pterygoid tuberosity*** | 25.1 ± 1.1, 23.2–27.4 ^{abc} | 28.6 ^a | 24.2 ^{abc} | 25.0 ^{abc} | 23.3 ^{bc} | 26.6 | 26.2 ± 1.0, 24.6–27.8 ^{ab} | 24.9 ^{abc} | - | 24.9 ^{abc} | - |
| Length of condyloid process** | 8.3 ± 0.6, 7.4–9.1 ^a | 9.5 ^a | 9.5 ^a | 8.9 ^a | 10.0 ^a | 7.9 | 8.7 ± 0.5, 7.9–9.4 ^a | 10.1 ^a | - | 9.8 ^a | 8.2 ^a |
| Width of articular facet** | 3.8 ± 0.2, 3.5–4.1 ^{ab} | 4.2 ^a | 3.4 ^{ab} | 4.1 ^a | 3.6 ^{ab} | 3.2 | 3.6 ± 0.3, 3.2–4.1 ^{ab} | 3.2 ^{ab} | - | 3.8 ^{ab} | 4.2 ^a |
| Length of mandible* | 53.8 ± 1.5, 50.9–55.9 ^a | 56.2 | 53.2 ^a | 57.2 ^a | 53.8 ^{ab} | 55 | 55.5 ± 1.4, 53.1–58.2 ^a | 57.0 ^a | - | 56.3 ^b | - |

taxa, as noted in the introduction. Figures 3–5 show the dorsal, ventral, and lateral perspectives, respectively, of the focal taxa: as one might expect from the results of the principal component analysis described above, observed differences among the various taxa are subtle. Nevertheless, they are present and telling. Notwithstanding, one obvious difference between the taxa under consideration is in greatest length of skull. In this character, our sample of *S. f. floridanus* show sexual dimorphism: in males, the mean in mm \pm SD (min–max) is 70.8 ± 1.1 (69.4 to 72.1), whilst in females, it is 72.7 ± 0.9 (71.3 to 73.8); $t_9 = 2.9125$, $P < 0.0172$, $\delta_{\text{means}} = 2.0$ mm, 95 % CI = 0.4–3.5 mm. However, our sample of adults of *S. f. hondurensis* includes only one female (AMNH 126205); remaining individuals are either unknown (AMNH 123378) or males ($n = 7$). Our comparisons in measurements are therefore made grouping the sexes. Between *S. f. floridanus* and *S. f. hondurensis*, the respective data are 72.0 ± 1.4 (69.4 to 73.8), versus 76.4 ± 1.0 (74.6 to 77.6), $t_{18} = 7.6512$, $P < 0.0001$, $\delta_{\text{means}} = 4.4$ mm, 95 % CI = 3.1–5.6 mm. The holotype of *S. f. costaricensis*, at 76.3 mm, is congruent with the mean of *S. f. hondurensis*. The same pattern obtains, albeit without sexual dimorphism in *S. f. floridanus* ($P = 0.1142$), in breadth of skull at the zygomatic spine: 33.9 ± 0.6 (33.0 to 35.0), versus 35.5 ± 0.4 (34.9 to 36.1), $t_{15} = 6.033$, $P < 0.0001$, $\delta_{\text{means}} = 1.7$ mm, 95% CI = 1.1–2.2 mm.

The region of the frontonasal suture, and the shape of the latter, is a character that has been used extensively in previous taxonomic studies of lagomorphs. For a selected subset of the specimens employed herein, that feature is shown in Figure 6. The specimens in the top row all are *S.*

Table 2. Results of the Principal Component analysis showing the eigenvalues for the first 10 principal components of the correlation matrix of the reduced set ($n = 22$) of natural log-transformed variables. The total variance accounted for using the morphometric variables we used was 15.9%.

| Principal component | Eigenvalue | Proportion | Cumulative proportion |
|---------------------|------------|------------|-----------------------|
| 1 | 0.056 | 0.369 | 0.362 |
| 2 | 0.023 | 0.150 | 0.511 |
| 3 | 0.015 | 0.010 | 0.606 |
| 4 | 0.012 | 0.080 | 0.684 |
| 5 | 0.008 | 0.050 | 0.734 |
| 6 | 0.007 | 0.048 | 0.781 |
| 7 | 0.007 | 0.046 | 0.827 |
| 8 | 0.005 | 0.036 | 0.863 |
| 9 | 0.004 | 0.026 | 0.889 |
| 10 | 0.004 | 0.025 | 0.914 |

f. floridanus collected contemporaneously; these all show the posterodorsal process of the premaxilla extending caudad of the frontonasal suture (even with the terminus in USNM 76711), along with a short, marked intrusion of the frontal bone extending between the posterodorsal process of the premaxilla and the nasal bone. The caudally projecting posterodorsal process of the premaxilla is apparent in Central American taxa only in *S. g. gabbi*. The nasal bones themselves are significantly smaller in *S. f. floridanus* than in *S. f. hondurensis*: means in mm \pm SD (min–max) are respectively 30.5 ± 1.0 (28.4 to 31.9), versus $34.8 \text{ mm} \pm 0.9$ (33.2 to 36.3), $t_{17} = 9.2366$, $P < 0.0001$, $\delta_{\text{means}} = 4.3$ mm, 95 % CI = 3.3–5.2 mm. The holotype of *S. f. costaricensis* is congruent with *S. f. hondurensis* in nasal bone length (35.3 mm), and in morphology in that the posterodorsal process of the max-

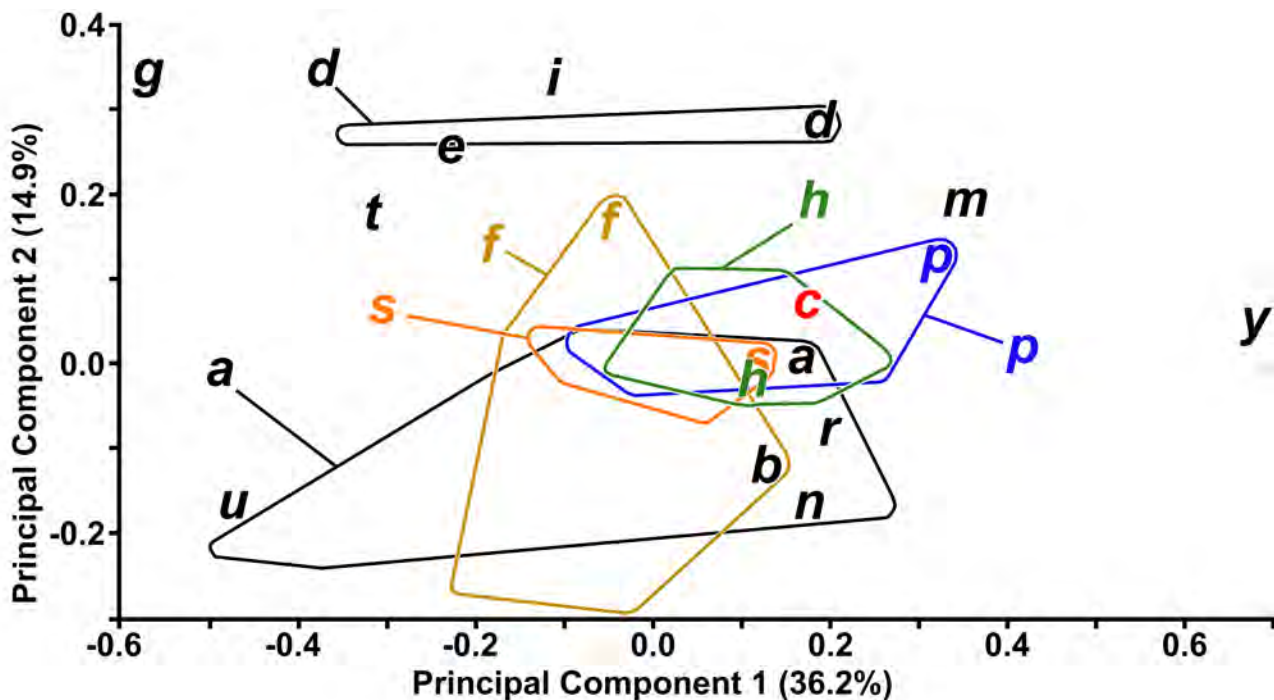


Figure 2. Graphical results of the Principal Component Analysis undertaken on the correlation matrix of the reduced set ($n = 22$) of natural log-transformed variables. Letter codes as follows, **a**: *S. f. aztecus*; **b**: *S. f. boylei*; **c**: *S. f. costaricensis*; **d**: *S. dicei*; **e**: *S. g. messorius*; **f**: *S. f. floridanus*; **g**: *S. g. gabbi*; **h**: *S. f. hondurensis*; **i**: *S. incitatus*; **m**: *S. f. margaritae*; **n**: *S. f. connectens*; **p**: *S. f. chiapensis*; **r**: *S. f. russatus*; **s**: *S. f. superciliaris*; **t**: *S. g. truei*; **u**: *S. f. daulensis*; **y**: *S. f. yucatanicus*. Where the labelled polygon encloses its same designation letter (e.g., **a**, *S. f. aztecus*, or **f**, *S. f. floridanus*), the enclosed letter shows the location of the holotype in the first two dimensions of multivariate space; otherwise, letters refer to holotype (e.g., **m**, *S. f. margaritae*, or **y**, *S. f. yucatanicus*).

Table 3. Results of the Principal Component Analysis showing the eigenvector scores of principal components 1 through 10 for the reduced set of natural log-transformed variables.

| Character | PC 1 | PC 2 | PC 3 | PC 4 | PC 5 | PC 6 | PC 7 | PC 8 | PC 9 | PC 10 |
|-----------|-------|--------|--------|--------|--------|--------|--------|--------|--------|--------|
| POSTORB | 0.173 | 0.032 | 0.135 | 0.020 | 0.387 | 0.291 | -0.791 | -0.122 | 0.017 | 0.106 |
| BROSTR | 0.236 | 0.132 | -0.045 | -0.153 | 0.124 | 0.024 | 0.226 | 0.074 | 0.024 | 0.187 |
| DEPROSTR | 0.225 | -0.023 | 0.198 | -0.022 | -0.012 | 0.121 | 0.002 | 0.013 | -0.353 | 0.152 |
| BBRAIN | 0.104 | -0.015 | -0.052 | 0.053 | -0.014 | -0.040 | 0.070 | -0.037 | 0.192 | -0.067 |
| ZYGO1 | 0.134 | 0.110 | -0.039 | -0.015 | 0.027 | -0.040 | 0.008 | -0.015 | 0.128 | -0.070 |
| NASALL | 0.292 | 0.036 | 0.218 | 0.091 | -0.154 | -0.093 | 0.014 | -0.046 | 0.052 | -0.245 |
| NASALW | 0.336 | -0.099 | 0.344 | 0.146 | -0.027 | 0.300 | 0.231 | -0.044 | -0.266 | -0.268 |
| I2P2 | 0.167 | 0.178 | 0.121 | -0.044 | -0.119 | -0.053 | -0.011 | -0.069 | 0.251 | 0.074 |
| P2M3 | 0.094 | 0.143 | 0.003 | -0.065 | 0.129 | 0.014 | 0.201 | -0.009 | 0.042 | 0.093 |
| HBRAIN | 0.181 | -0.168 | 0.123 | 0.052 | -0.224 | 0.105 | 0.004 | -0.104 | -0.110 | -0.222 |
| HBULL | 0.215 | -0.237 | -0.215 | 0.128 | 0.293 | 0.075 | 0.245 | -0.207 | -0.289 | 0.555 |
| LPALFOR | 0.206 | 0.161 | 0.132 | -0.078 | -0.187 | 0.132 | 0.105 | -0.434 | 0.343 | 0.231 |
| WPALFOR | 0.341 | 0.079 | -0.602 | 0.206 | -0.525 | 0.059 | -0.269 | 0.179 | -0.108 | 0.089 |
| PALLONG | 0.175 | 0.133 | 0.152 | 0.017 | -0.073 | -0.086 | 0.013 | -0.086 | 0.213 | 0.110 |
| PALBRIDG | 0.149 | 0.218 | 0.303 | 0.235 | 0.155 | -0.582 | -0.092 | 0.392 | -0.119 | 0.175 |
| WIDBULL | 0.368 | -0.456 | -0.078 | -0.697 | 0.075 | -0.205 | -0.079 | 0.184 | 0.149 | -0.074 |
| INTBD | 0.103 | 0.141 | -0.098 | 0.103 | 0.277 | 0.518 | 0.197 | 0.579 | 0.331 | -0.082 |
| INTBOC | 0.154 | 0.080 | -0.045 | -0.046 | -0.050 | -0.116 | 0.113 | 0.165 | -0.129 | 0.125 |
| CHOANA1 | 0.136 | 0.625 | -0.292 | -0.291 | 0.265 | -0.072 | 0.039 | -0.245 | -0.289 | -0.344 |
| DEPZYGO | 0.222 | -0.258 | -0.282 | 0.465 | 0.366 | -0.286 | 0.064 | -0.250 | 0.291 | -0.273 |
| IP3 | 0.174 | 0.165 | 0.120 | 0.072 | -0.112 | -0.028 | -0.071 | 0.047 | 0.211 | 0.185 |

illa is retracted rostrally relative to the caudal terminus of the nasal bone. One might expect that because of the longer GLS, the Central American taxon would naturally have a longer nasal bone. However, the Pearson product-moment correlation coefficients between GLS and NASAL suggest that this is not necessarily the case: for *S. f. hondurensis*, $R = 0.611$ ($R^2 = 0.373$, $P = 0.108$), whereas for *S. f. floridanus* $R = 0.753$ ($R^2 = 0.567$, $P = 0.007$); the holotype of *S. f. costaricensis* is almost identical in these two measurements to *S. f. hondurensis* AMNH 126203. We therefore predict that given larger sample sizes, *S. f. costaricensis* will be more closely allied to the pattern displayed by *S. f. hondurensis*.

A corollary of the shorter nasal bone in *S. f. floridanus* is that that bone does not extend as close to the orbit in *S. f. floridanus* as in *S. f. costaricensis* and *S. f. hondurensis* (Figure 3). Measured from the most posterolateral point of the nasal, the distance to the caudalmost point in the notch between the antorbital process and the frontal bone is 6.3 mm in *S. f. floridanus*, 3.5 mm in *S. f. hondurensis*, and 3.8 mm in *S. f. costaricensis*.

In the holotype of *S. f. costaricensis*, there is a small intrusion of frontal bone, the nasopremaxillary process of the frontal, separating the caudal tip of posterodorsal process of the premaxilla from the caudal tip of the nasal bone (measured from the tip of the posterodorsal process of the premaxilla, right: 3.3 mm, left: 4.5 mm). This intrusion is absent from the holotype of *S. f. hondurensis* and largely absent from examined specimens in this taxon, although some (*e. g.*, AMNH 123378, Figure 6) have a minute manifestation of this feature. The frontonasal suture also may vary in shape, being either parallel with a transverse plane

starting laterally then angling rostrally to meet the opposite nasal bone at the medial plane, or on an approximate diagonal plane in a caudo-lateral to rostromedial direction. *Sylvilagus f. floridanus* displays the former, whereas *S. f. costaricensis* represents the latter condition; in this character, *S. f. hondurensis* is more similar to *S. f. floridanus*.

Other characters of the dorsal aspect are somewhat more shrouded. Pitting in the parietal and frontal bones has for example been employed as a character in distinguishing between taxa (Wible 2007; Ruedas *et al.* 2017; Ruedas 2017). However, there is a thin layer of tissue covering this portion of the skull of the holotype of *S. f. costaricensis* that, despite its slenderness, obscures this character. Similarly, the angle of the suture between the parietal and supraoccipital is somewhat descending ventrally from external to medial direction in *S. f. floridanus*, but is horizontal or ascending in *S. f. hondurensis*. However, it is not clearly visible in the holotype of *S. f. costaricensis*.

From a lateral perspective (Figure 5), the length of the zygomatic arches of *S. f. floridanus* differ significantly with little overlap in size from those of *S. f. hondurensis*: 31.0 ± 0.8 (29.3 to 32.2) v. 33.0 ± 1.1 (31.0 to 34.3), $t_{18} = 4.621$, $P = 0.0002$, $\delta_{\text{means}} = 2.0$ mm, 95 % CI = 1.1–2.9 mm. The zygomatic arch of *S. f. costaricensis*, at 32.2 mm, is at the upper limit of those of *S. f. floridanus*, but is firmly ensconced within those of *S. f. hondurensis*. The relative brevity of the zygomatic arch of *S. f. floridanus* gives it a more robust dorsoventral appearance than those of *S. f. costaricensis* and *S. f. hondurensis*; however, vertical depth of the zygomatic arch does not differ significantly among the taxa: 5.3 ± 0.5 (4.3 to 6.0) v. 5.0 ± 0.3 (4.6 to 5.3), $t_{17} = 1.3771$, $P = 0.1863$,

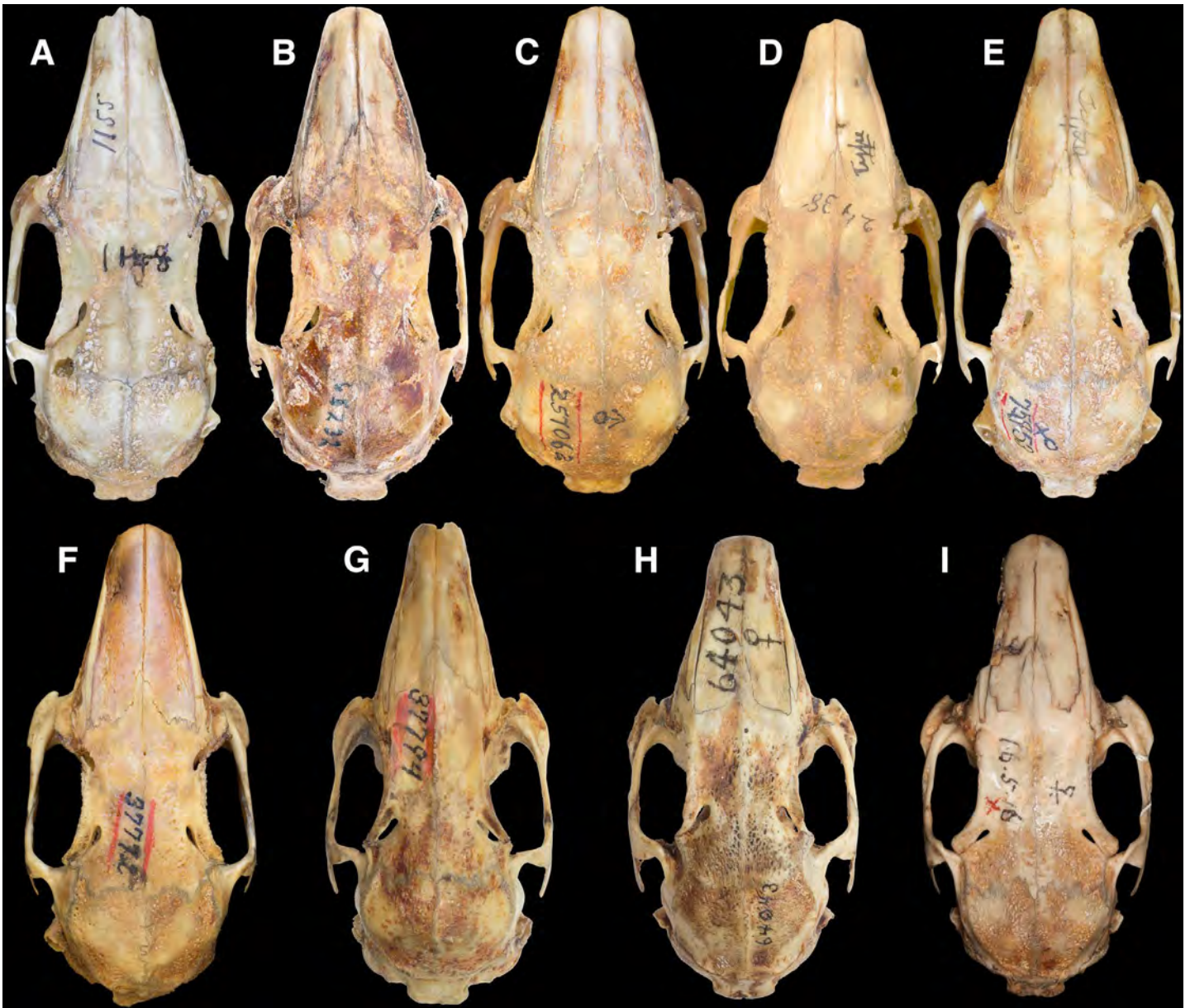


Figure 3. Dorsal views of the crania of the Central and South American taxa under consideration herein (current nomenclature), scaled to the same greatest length of skull. A: *Sylvilagus f. floridanus*, holotype, AMNH 1890/1155 (♀), greatest length of skull (GLS): 71.9 mm; B: *S. f. costaricensis*, holotype, UMMZ 65232 (♀), GLS: 76.3 mm; C: *S. f. hondurensis*, holotype, USNM 257062 (♂), GLS: 74.7 mm; D: *S. f. aztecus*, holotype, AMNH 3116/2438 (♂), GLS: 72.9 mm; E: *S. f. chiapensis*, holotype, USNM 75953 (♀), 78.9 mm; F: *S. f. yucatanicus*, holotype, USNM 37772 (♀), GLS: 81.1 mm; G: *S. g. gabbi*, lectotype, USNM 11371/37794 (♂), GLS: 70.9 mm; H: *S. dicei*, holotype, UMMZ 64043 (♀), 77.3 mm; I: *S. brasiliensis surdaster*, holotype, MNH 1901.6.5.16 (♀), GLS: 72.7 mm.

$\delta_{\text{means}} = 0.3 \text{ mm}$, 95 % CI = $-0.21-0.7 \text{ mm}$; the holotype of *S. f. costaricensis* has a zygomatic depth of 5.3 mm, congruent with either taxon. As in length of nasal bones, this likely is a manifestation of the differences in GLS, given that *S. f. floridanus* and *S. f. hondurensis* have almost identical zygomatic length relative to GLS: 43.0 % and 43.2 %; 42.1 % in *S. f. costaricensis*. Also as in the nasal bones, however, the length of the zygomatic arch is significantly correlated with GLS in *S. f. floridanus* ($R = 0.761$, $R^2 = 0.579$, $P = 0.006$), but not in *S. f. hondurensis* ($R = 0.384$, $R^2 = 0.148$, $P = 0.307$).

Analysis of dental morphology. Substantial and substantive differences are exhibited in the dental morphology the taxa under consideration herein (Figure 7). In the tooth most commonly used to discriminate among species of lagomorphs, lower premolar 3, *S. f. costaricensis* differs

from *S. f. floridanus* in several key features: the anteroflexid is relatively deep and U-shaped, with a narrow constriction on the rostral surface, whereas in *S. f. floridanus*, the anteroflexid is broadly open and V-shaped; *S. f. hondurensis* displays a condition similar to *S. f. costaricensis*. Other Central and South American comparator taxa examined here display a more complex pattern on the rostral surface of pm3, with multiple anteroflexids or, if single, with a complex internal structure (e. g., *S. f. chiapensis*). In *S. dicei*, the rostral architecture of pm3 is of such complexity that a lingual anteroconid is identifiable as a region only, rather than as a distinct feature of the tooth.

The central angle, an almost universal feature of the lagomorph rostral hypoflexid, is present as a singular inflection in *S. floridanus*, but as an unusual double inflection in *S.*

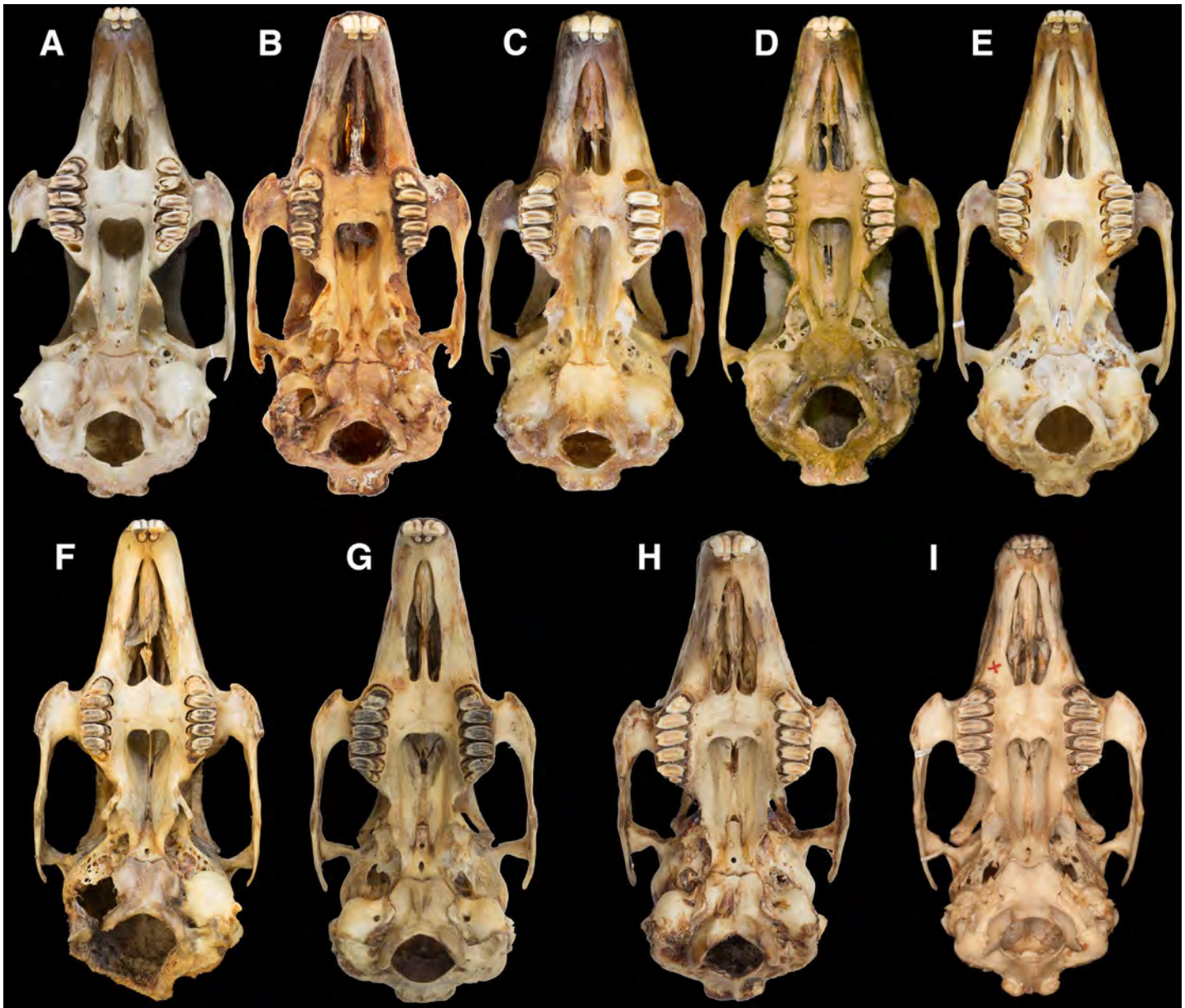


Figure 4. Ventral views of the crania of the Central American taxa under consideration herein, scaled to the same width. Specimens shown are the same as in Figure 3 and disposed in the same order.

f. costaricensis. The central angle is indistinct in *S. f. chiapensis* because of the complexity of the enamel pattern, and possibly double in the lectotype of *S. g. gabbi*. *Sylvilagus brasiliensis surdaster* displays a very weak central angle. The caudal surface of the hypoflexid is relatively smooth (labial portion) to somewhat crenulate (lingual portion) in *S. f. floridanus* versus highly complex and strongly crenulate in *S. f. costaricensis*. Other regional taxa display the range from similarly crenulate morphologies (*S. dicei*, *S. f. yucatanicus*) to somewhat less crenulate (*S. f. aztecus*, *S. f. chiapensis*), to completely smooth (*S. b. surdaster*).

While *S. f. floridanus* definitively does not exhibit a paraflexid (being instead convex), there is a slight inflection in that portion of pm3 of *S. f. costaricensis*. *Sylvilagus f. hondurensis* has a concavity at the base of the anteroconid that we likewise interpret as a paraflexid, as does *S. b. surdaster*. Otherwise, this surface of the tooth is relatively featureless

from slightly convex (*S. f. yucatanicus*) to slightly concave (*S. f. aztecus*, *S. f. chiapensis*).

In PM2 of *S. f. floridanus*, the hypoflexus is marked by a slight depression, barely demarcating mesial from distal hypercones. In *S. f. costaricensis*, there is a distinct, deep, U-shaped hypoflexus in PM2, resulting in distinct mesial and distal hypercones. The area of PM2 between postcone and poststyle PM2 in *S. f. floridanus* is convex, with no trace of a metaflexus. In contrast, *S. f. costaricensis* has a small but distinct inflection marking the metaflexus.

The first upper incisor, although generally neglected as featureless among lagomorphs, also is distinct between the two taxa: in *S. f. costaricensis*, lingual and labial cusps are subequal in height relative to the rostral groove demarcating them; *S. f. hondurensis* is almost identical in the morphology of its I1. In contrast, the lingual cusp of I1 in *S. f. floridanus* is distinctly expanded rostrally relative to the labial cusp.

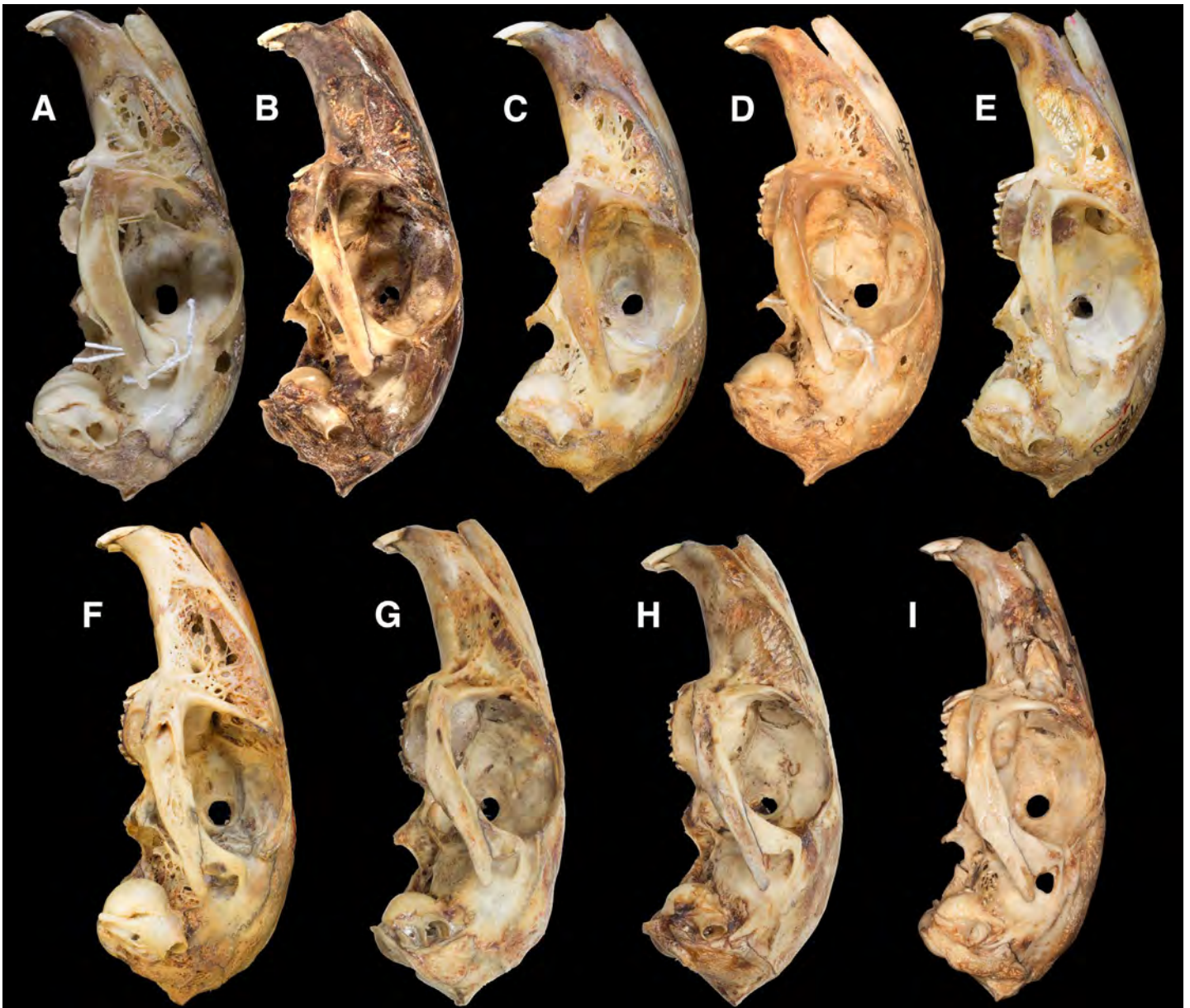


Figure 5. Lateral views of the crania of the Central American taxa under consideration herein, scaled to the same width. Specimens shown are the same as in Figure 3 and disposed in the same order. Inverted for consistency are: *S. f. costaricensis* and *S. f. aztecus*. The latter also was not taken on a completely lateral plane, making the profile appear more dorsoventrally bowed than it is in reality.

An additional, and unusual, feature is present in I2 of *S. f. costaricensis*. This tooth is invariably small, cylindrical, with a circular cross section in every species of *Sylvilagus* we have examined to date. However, in *S. f. costaricensis*, I2 is roughly triangular in cross section, with the base caudal and apex rostral, and has two distinct grooves on the caudal aspect of the tooth (Figure 8). The only other taxon of *Sylvilagus* that we have examined for this study to display these characters is *S. f. hondurensis*.

Taxonomic conclusion: identity of *Sylvilagus floridanus costaricensis*. In light of the foregoing analyses, particularly those based on cranial and dental characters, it is clear that the differences between *S. f. costaricensis* and *S. f. floridanus* are interspecific in nature insofar as taxa of *Sylvilagus* are concerned. As described above, the skulls differ significantly in magnitude in a number of measurements; they also dif-

fer significantly in a number of cranial and dental characters. However, *S. f. costaricensis* are not distinct from *S. f. hondurensis* in the same characters. Most significantly, both taxa share two unique synapomorphies: a triangular cross section to I2, which is marked by two grooves on its caudal facies. We therefore consider that *S. f. costaricensis* are not distinct from *S. f. hondurensis* at the species level. *Sylvilagus floridanus hondurensis* was described by Edward A. Goldman on 30 July 1932; *S. f. costaricensis* by William P. Harris on 28 June 1933. As a consequence, the name *hondurensis* has priority. Until a greater number of specimens are available for examination of population level and broader extent of geographic variation, there are sufficient differences between the two taxa—for example, the comparative extent and degree of crenulation of the caudal aspect of the pm3 hypoflexid—that we recommend the prudent course of action to keep

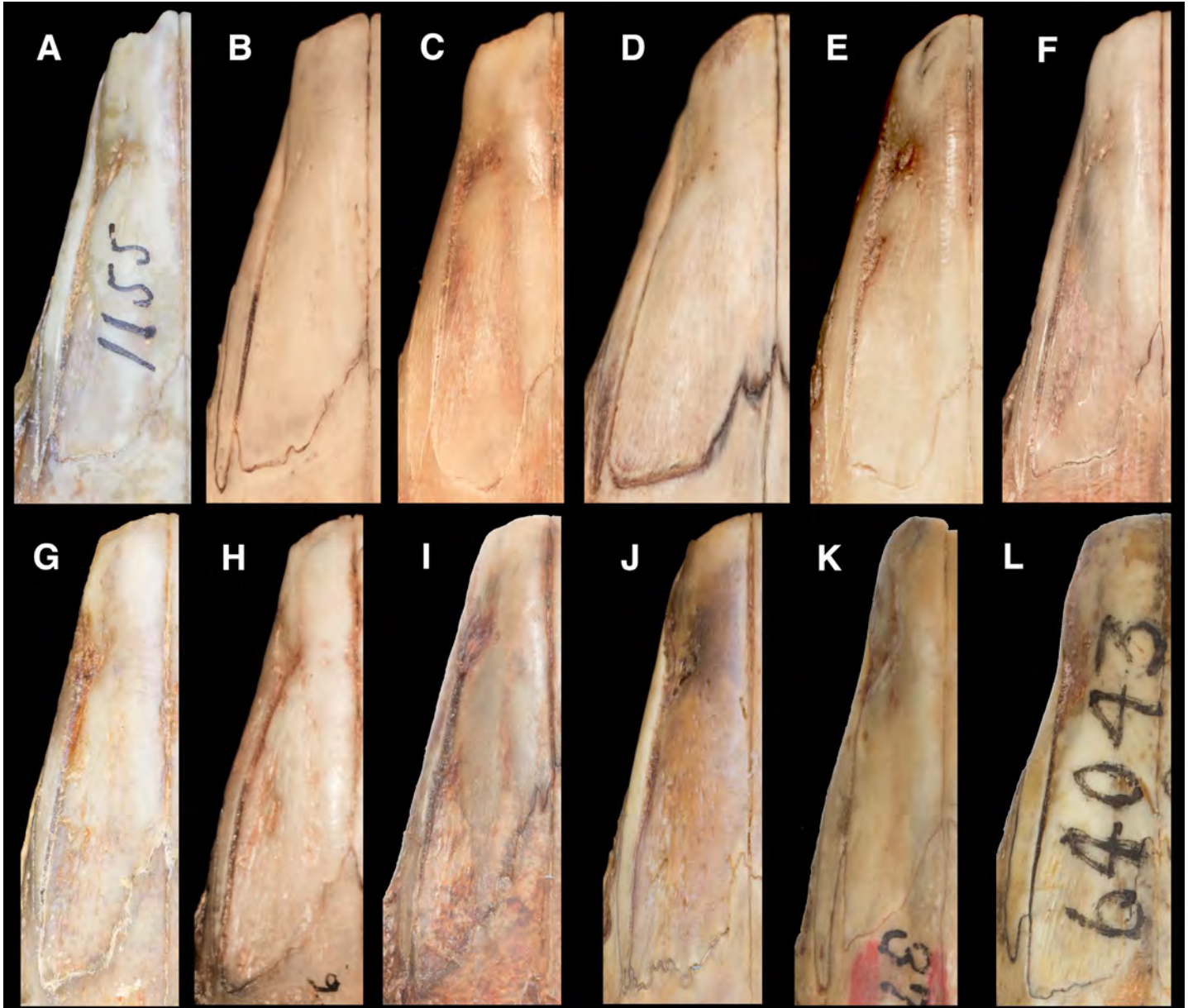


Figure 6. Detail of the left frontonasal suture and posterodorsal process of premaxillary bone in selected individuals, all scaled to the same anteroposterior length for consistency. A: *Sylvilagus f. floridanus*, AMNH 1890/1155 (♀, holotype; greatest length of nasal, in straight line from facialmost to caudalmost point: 30.4 mm); B: USNM 70870 (♀; 30.6 mm); C: USNM 76711 (♂; 29.4 mm); D: USNM 77113 (subadult ♂; 22.4 mm; note the difference in proportions of dimensions); E: USNM 77114 (♀; 31.1 mm); F: USNM 77115 (♂; 31.4 mm); G: *S. f. hondurensis*, USNM 257062 (♂, holotype; 34.2 mm); H: *S. f. hondurensis*, AMNH 126146 (♂; 35.0 mm); I: *S. f. costaricensis*, UMMZ 65232 (♀, holotype; 35.3 mm); J: *S. f. yucatanicus*, USNM 37772 (♀, holotype; 37.2 mm); K: *S. g. gabbi*, USNM 11371/37794 (♂, lectotype; 27.9 mm); L: *S. dicei*, UMMZ 64043 (♀, holotype; 33.6 mm). Key features include: caudal terminus of the posterodorsal process of premaxilla relative to the caudal terminus of the nasal bone, and absence, presence, and rostral extent of process on frontal bone extending between posterodorsal process of premaxilla and posterolateral margin of nasal bone (nasopremaxillary process of frontal bone).

both names, as *Sylvilagus hondurensis hondurensis* E. A. Goldman, 1932, and *S. hondurensis costaricensis* Harris, 1933.

Discussion

We consider our study foundational to any future regional or focused taxonomic study of biogeography, evolution, and phylogeny of cottontails. Revolutions in the practice of taxonomy and phylogenetics have led to a more nuanced understanding of species delimitation and, as a result, of species boundaries. [Ruedas et al. \(2017\)](#) noted that there is a lack of cohesion between philosophical and operational approaches to species; as in that work, we apply what [Sangster \(2014\)](#) called “methodological introgression” of species concepts applied in an operationally coherent manner to

“discover, describe, and order into our classification system” ([Mayden 1997:387](#)) the individuals within, or constituting, the species category, independent of the properties of the species category. We used previously ([Ruedas et al. 2017](#)) an integrative approach to species delimitation (sensu [Padiál et al. 2010](#); [Schlick-Steiner et al. 2010](#)) as implemented by [Naomi \(2011\)](#). This approach, using a morphological character set vastly expanded over that of [Hershkovitz \(1950\)](#), resulted in hypotheses of taxonomic species in *Sylvilagus* that reflected the underlying biological reality imposed by abiotic criteria such as elevation, temperature, and precipitation regimes, soils, etc., as well as the effects of those abiotic factors on vegetation, which ultimately is reflected by the species inhabiting the ecosystems under

consideration. While there have been controversies regarding the application of, for example, the phylogenetic species concept to particular instances (e. g., [Groves and Grubb 2011](#) vs. [Zachos et al. 2013](#); [Zachos 2015](#)), the integrative approach yields coherent and biologically relevant taxonomic hypotheses: a single widespread species of *Sylvilagus* (*S. "brasiliensis" sensu Linnaeus 1758*) distributed from the Atlantic to the Pacific coasts of South America, from 0

to >5,000 m in elevation, and from Veracruz, México, in the north, to Argentina in the south is neither coherent, nor biologically realistic. The taxonomic hypotheses we propose herein for *S. floridanus* follow from Allen's hypothesis that geography, while not the ultimate arbiter of taxonomy, nevertheless strongly affects species limits: "Hence the single record from so remote a point [...] has of late seemed open to serious question" ([Allen 1890:192](#)). The biogeo-

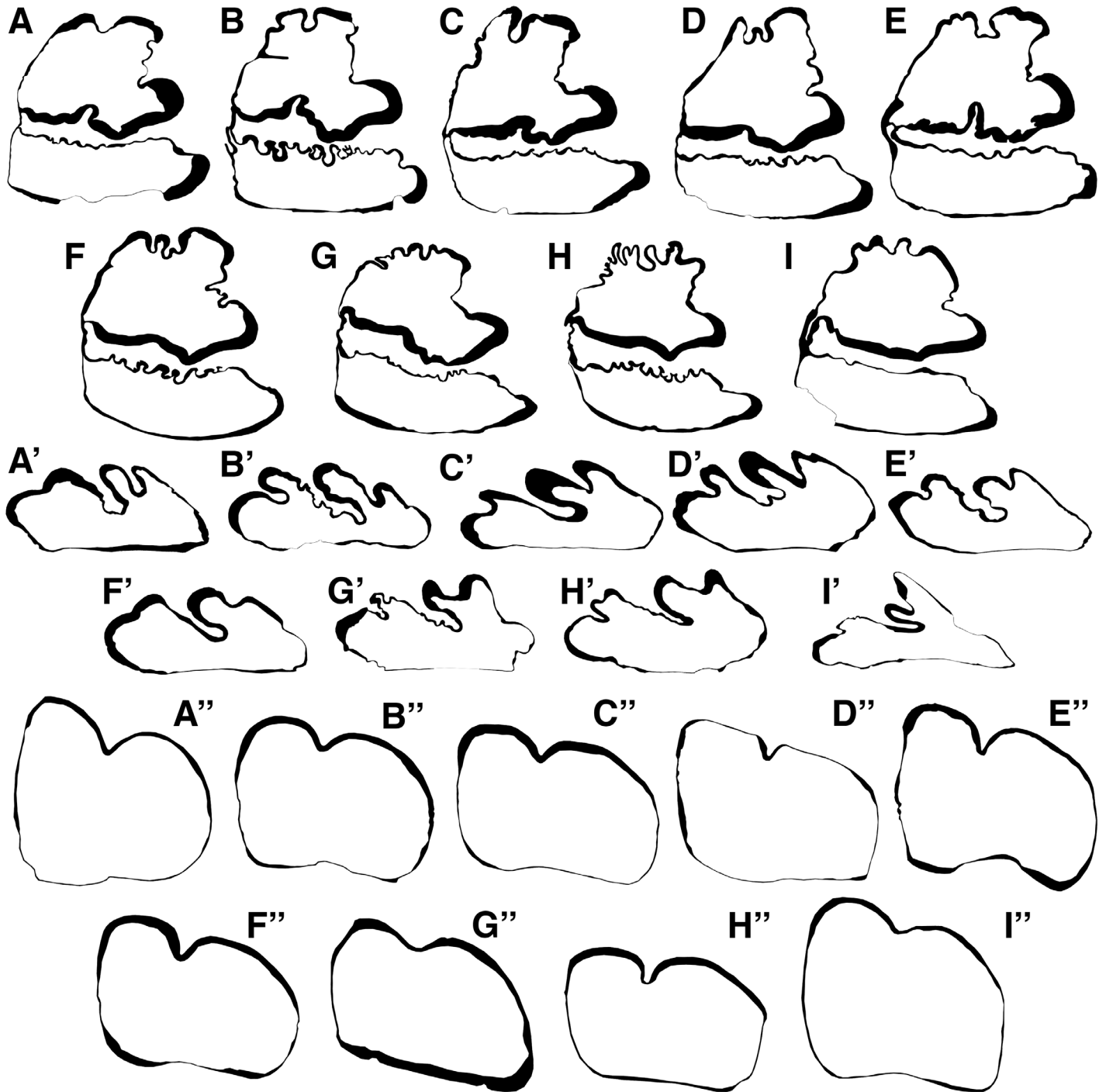


Figure 7. Crown views of the enamel structure of lower premolar 3 (upper two rows), upper premolar 2 (middle two rows), and first upper incisor (lower two rows) for the Central American taxa under consideration herein. Specimens in each triplet are, A: *Sylvilagus f. floridanus*, holotype, AMNH 1890/1155 (♀); B: *S. f. costaricensis*, holotype, UMMZ 65232 (♀); C: *S. f. hondurensis*, holotype, USNM 257062 (♂); D: *S. f. aztecus*, holotype, AMNH 3116/2438 (♂); E: *S. f. chiapensis*, holotype, USNM 75953 (♀); F: *S. f. yucatanicus*, holotype, USNM 37772 (♀); G: *S. g. gabbi*, lectotype, USNM 11371/37794 (♂); H: *S. dicei*, holotype, UMMZ 64043 (♀); I: *S. brasiliensis surdaster*, holotype, MNH 1901.6.5.16 (♀). Some images were rotated horizontally in order for all perspectives to be the same; all images are scaled to the same width so as to show differences in proportion rather than in size. In each image, rostral is to the top of the figure, labial is to the right of the figure.

graphic breaks in Central and South America, reflected in the taxonomy of numerous taxa, are likewise reflected in *Sylvilagus*. In South America, rivers have been implicated in speciation events in small mammals (da Silva and Patton 1998; Matocq et al. 2000; Patton et al. 2000), primates (Wallace 1852; Boubli et al. 2015), and birds (Naka and Brumfield 2018) alike. *Sylvilagus* are similarly affected by vicariant effects. In the instance of *Sylvilagus*, the effects of strong ecological change brought about by the xeric conditions at the Isthmus of Tehuantepec also appear important.

From a biogeographic perspective, the patterns of speciation revealed by our taxonomic framework are congruent with those of other taxa. For example, *Bassariscus astutus* is restricted to the north and west of the Isthmus of Tehuantepec, and its sister species *B. sumichrasti*, while somewhat overlapping the range of *B. astutus* in coastal Guerrero and Oaxaca, México, largely is restricted to the east and south of the isthmus. Similarly, taxa in the *Reithrodontomys sumichrasti* species complex (Rodentia: Cricetidae: Neotominae) show an analogous distribution and hypothesized relationships (Hardy et al. 2013) as we propose here for *Sylvilagus*. In the case of mice of the genus *Habromys* (Rodentia: Cricetidae: Neotominae), six of the seven species in the genus are restricted to the north and west of the isthmus, and only one species, *H. lophurus*, is restricted to the south and east of the isthmus (León-Paniagua et al. 2007). This pattern of sister taxa of mammals exclusively distributed to one or the other side of the Isthmus of Tehuantepec is a repeating evolutionary and biogeographic motif (Sullivan et al. 2000; Rogers et al. 2007).

One result of the integration of distinct data streams to assess taxonomic relationships is the stark difference in taxonomic information content that is brought about by using morphometric (continuously variable measurement data) versus discrete character data. Our principal components analysis (Figure 2) shows that there is substantial overlap in morphology among the distinct taxa of *Sylvilagus* when these are subjected to morphometric analysis. Of note, the principal components analysis is an a posteriori test, thus there is no prior hypothesis imposed on the ensuing result. In contrast, an a priori test such as a discriminant function analysis essentially “forces” the output to conform to the a priori hypothesis (i. e., predict group—species—membership) because it describes a function that will distinguish among the predefined samples groups (i. e., presumptive taxa). As a result, a posteriori tests are preferable in taxonomy because they do not impose a hypothesis on the data, rather the results derived from the data are a reflection of the presumptively true nature of the underlying taxonomic reality. In the present instance, however, the two statistically significant principal components only accounted for 7.9 % of the morphological variation among the groups. That is to say, conversely, that 92.1 % of the mensural variation went unaccounted for. Thus, either a posteriori or a priori tests would be on tenuous grounds in terms of establishing—or even testing—a robust taxonomic hypothesis, no doubt

because of the morphologically conservative, or strongly homomorphic nature of cranial morphology in *Sylvilagus*, and indeed, in Leporidae in general. Because of this, and based on the results of our morphometric analysis, taxa clearly distinguished in the analysis (e. g., *gabbi*, *dicei*, *yucatanicus*) are hypothesized to be definitively distinct; however, taxa in our sample that overlap in multivariate space are not definitively demonstrated to be the same, i. e., subject to Type II error. It is in these circumstances that inspection of character data becomes increasingly valuable: assessment of discretely variable characters in morphologically conservative taxa, particularly when such characters may be discretely distinct in morphometrically indistinguishable groups, can result not only in identification and discrimination of different taxa but also in the possibility of inferring evolutionary relationships among the groups or taxa in question. Character data (qualitative) can be useful for identifying and classifying organisms, while morphometric data (quantitative) may under certain circumstances be useful for identifying organisms, as well as for studying the physical (mensural) characteristics of organisms and their variation. Excessive reliance on either, particularly morphometric data, may result in erroneous taxonomic hypotheses.

Unanswered, however, remains the question of: why are there so many species of *Sylvilagus* present in Costa Rica? We hypothesize that the present biodiversity is a combination of the ecological heterogeneity of Costa Rica, along with its location. We have previously documented, using molecular approaches (Ruedas et al. 2017), that there were multiple invasions of South America by *Sylvilagus*. Some of the remaining biodiversity of Costa Rican *Sylvilagus* may be essentially remnants of these multiple invasions: taxa that resulted from populations that remained in place as other populations continued to expand the dispersal front. As remnant populations, their conservation therefore becomes ever more imperative.

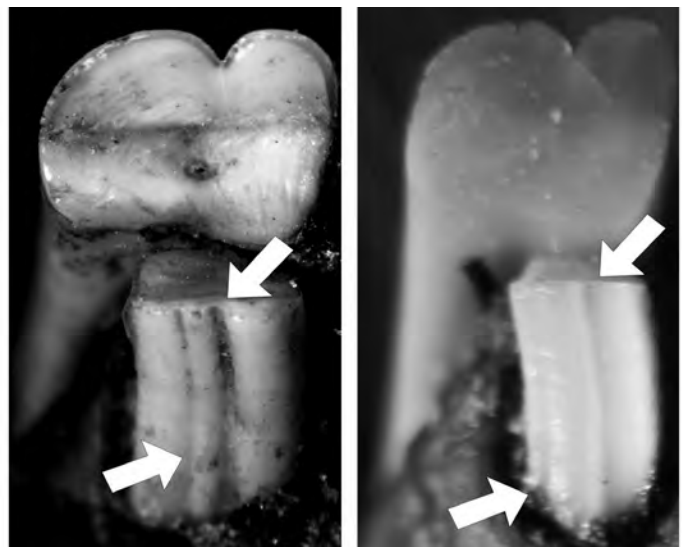


Figure 8. Occlusal perspective of the first and second right upper incisors of *S. f. costaricensis* (left) and *S. f. hondurensis* (right). Arrows mark the two grooves on the caudal aspect of I2. Note the unusual triangular cross section of I2, rather than the almost universal condition for *Sylvilagus* of a circular cross section for this tooth.

Taxonomic Conclusions. On the basis of the foregoing, we recognize the following taxa in Central America south of the Isthmus of Tehuantepec to the Panama–Colombia border: *Sylvilagus dicei*, *S. gabbi*, and *S. hondurensis*.

Sylvilagus hondurensis
Honduras cottontail

Sylvilagus floridanus hondurensis Goldman, 1932:122. Type locality, “From Monte Redondo, about 30 miles northwest of Tegucigalpa, Honduras (altitude about 5,100 feet [1554 m]).” The village of Monte Redondo lies at ca. 860 m rather than, as indicated by Goldman, at 1,554 m. Roads lead NW from Monte Redondo to higher elevations. The 1,554 m contour on a road emanating from Monte Redondo is at ca. 14° 18′ 42″ N, 87° 18′ 24″ W. We speculate that Goldman referred to the higher elevations today contained within the Reserva de Vida Silvestre Corralitos (Francisco Morazán, Honduras), just NW from the village of Monte Redondo. Holotype: USNM 257062.

Sylvilagus floridanus costaricensis Harris, 1933:3. Type locality, “from Hacienda Santa María, Province of Guanacaste, Costa Rica, altitude 3,200 feet” (975 m). The Hacienda Santa María ranger station, inside Guanacaste National Park is located at 10° 45′ 52″ N, 85° 18′ 11″ W, 844 m, thus corresponding fairly closely with Harris’ description. Holotype: UMMZ 65232.

Sylvilagus yucatanicus
Yucatan cottontail

Lepus aquaticus: Allen, 1877:365 (part). Not *Lepus aquaticus* Bachman, 1837. Allen noted that “In the collection are quite a number of specimens from the provinces of Vera Cruz and Yucatan in Southern México. These differ from specimens from Mississippi and Louisiana in no very marked degree.” He later revised his opinion (Allen 1890b) and transferred these specimens to *Lepus sylvaticus* [= *S. floridanus*].

Lepus sylvaticus aztecus: Allen, 1890:191, from “Merida, Yucatan”; not Allen 1890:188, from “Tehuantepec City”.

Lepus floridanus yucatanicus Miller, 1899:384. Type locality, “Merida, Yucatan” (correctly spelled “Mérida, Yucatán” by Hall 1951:159). Holotype, USNM 11441/37772.

Sylvilagus floridanus yucatanicus: Lyon, 1904:336. Name combination.

Acknowledgments

This paper honors the life work of Alfred “Al” Lunt Gardner. Many of the specimens examined here were done so with permission granted by Al, before and after fascinating discussions with him on taxonomy and biogeography of rabbits and American mammals in general. Much of the work was inspired, influenced, and illuminated by Al’s wisdom and phenomenal breadth of knowledge, all of which he generously shared and continues to share with all who visit the

hallowed, specimen-filled hallways of USNM. Costa Rican portions of this work were conducted by JMM under Project SIA 0286-16 of Universidad Nacional (UNA). Other portions of the field work were carried out by JMM during 2018–2021 under academic support of Carrera de Gestión Ecoturística (GEC), Universidad Técnica Nacional (UTN). Additional portions of this work were carried out under the auspices of NSF grant DEB-0616305 to LAR. We acknowledge the support for our field work and permits from CONAGEBIO (project # 332), and the ACC, ACG, ACT, ACAT, ACAHN, ACOPAC, ACLAC, ACLAP, ACTO, and ACOSA conservation areas. JMM acknowledges Emilce Rivera, GEC department head, for her support. LIL acknowledges the support of UTN Sede Atenas to participate in this project. JMM and LAR thank A. L. Gardner, U.S. National Museum of Natural History—Division of Mammals, for permission to examine holotypes under his care, and D. P. Lunde, J. J. Osofsky, and S. Peurach, also at USNM—Mammals, for their invaluable assistance during LAR’s visit to the USNM in 2017, and most particularly for accommodating his unorthodox work schedule. As usual, LAR’s discussions with A. L. Gardner proved insightful and fruitful. JMM and LAR also thank E. Westwig, B. O’Toole, and E. Hoeger, of the American Museum of Natural History for their help during their visit to that institution in 2017, and especially R. S. Voss for granting access to the holotypes, and particularly for taking the time to comment and discuss the work described herein; both his comments and discussions always prove valuable. LAR thanks Carmen Sesé (MNCN, Madrid, Spain) for her valuable help on nomenclature of lagomorph dental features, and Fernando Palacios, of the same institution, for his inestimable conversations and insights into all things lagomorph. Y. Pan (Portland State University, Environmental Science and Management) was extremely generous in providing statistical advice with the principal component analyses.

Literature cited

- ALLEN, J. A. 1877. Monograph No. II—Leporidae. In: E. Coues and J. A. Allen (eds.) Monographs of North American Rodentia. Department of the Interior, Report of the United States Geological Survey of the Territories 11:265–378.
- ALLEN, J. A. 1890a (October). Descriptions of a new species and a new subspecies of the genus *Lepus*. Bulletin of the American Museum of Natural History 3:159–160.
- ALLEN, J. A. 1890b (10 December). Notes on collections of mammals made in Central and Southern Mexico, by Dr. Audley C. Buller, with descriptions of new species of the genera *Vespertilio*, *Sciurus*, and *Lepus*. Bulletin of the American Museum of Natural History 3:175–194.
- ALLEN, J. A. 1899. New rodents from Colombia and Venezuela. Bulletin of the American Museum of Natural History 12:195–218.
- ALLEN, J. A. 1904. Mammals from southern Mexico and Central and South America. Bulletin of the American Museum of Natural History 20:29–80.
- ALLEN, J. A. 1912. Mammals from western Colombia. Bulletin of the American Museum of Natural History 31:71–95.

- ALLEN, J. A. 1913. New mammals from Colombia and Ecuador. *Bulletin of the American Museum of Natural History* 32:469–484.
- ALLEN, J. A. 1914. Two new mammals from Ecuador. *Bulletin of the American Museum of Natural History* 33:199–200.
- ALLEN, J. A. 1916. New South American mammals. *Bulletin of the American Museum of Natural History* 35:83–87.
- ANGELONE, C., AND C. SESÉ. 2009. New characters for species discrimination within the genus *Prolagus* (Ochotonidae, Lagomorpha, Mammalia). *Journal of Paleontology* 83:80–88.
- ANTHONY, H. E. 1923. Preliminary report on Ecuadorean mammals. No. 3. *American Museum Novitates* 55:1–14.
- BACHMAN, J. 1837. Observations, on the different species of hares (genus *Lepus*) inhabiting the United States and Canada. *Journal of the Academy of Natural Sciences of Philadelphia* 7:282–361.
- BAIRD, S. F. 1857. Mammals: General report upon the zoology of several Pacific railroad routes. Vol. 8, pt. 1, in Reports of explorations and surveys to ascertain the most practicable and economical route for a railroad from the Mississippi River to the Pacific Ocean. Senate executive document no. 78, Washington D.C. U.S.A.
- BAIRD, S. F. 1857. Mammals of the boundary. In: United States and Mexican boundary survey, under the order of Lieut. Col. W. H. Emory, Major First Cavalry, and United States Commissioner 2:1–62.
- BANGS, O. 1901. The mammals collected in San Miguel Island, Panama, by W. W. Brown, Jr. *The American Naturalist* 35:631–644.
- BOUBLI, J. P., ET AL. 2015. Spatial and temporal patterns of diversification on the Amazon: a test of the riverine hypothesis for all diurnal primates of Rio Negro and Rio Branco in Brazil. *Molecular Phylogenetics and Evolution* 82:400–412.
- CABRERA, Á. 1961. Catálogo de los mamíferos de América del Sur. *Revista del Museo Argentino de Ciencias Naturales "Bernardino Rivadavia" Ciencias Zoológicas* 4:309–732.
- CODDINGTON, J. A., AND N. SCHARFF. 1996. Problems with "soft" polytomies. *Cladistics* 12:139–145.
- DALQUEST, W. W. 1979. Identification of genera of American rabbits of Blancan Age. *The Southwestern Naturalist* 24:275–278.
- DALQUEST, W. W., F. B. STANGL, JR., AND J. V. GRIMES. 1989. The third lower premolar of the cottontail, genus *Sylvilagus*, and its value in the discrimination of three species. *The American Midland Naturalist* 121:293–301.
- DA SILVA, M. N. F., AND J. L. PATTON. 1998. Molecular phylogeography and the evolution and conservation of Amazonian mammals. *Molecular Ecology* 7:475–486.
- DAY, R. W., AND G. P. QUINN. 1989. Comparison of treatments after an analysis of variance in ecology. *Ecological Monographs* 59:433–463.
- DIERSING, V. 1981. Systematic status of *Sylvilagus brasiliensis* and *S. insonus* from North America. *Journal of Mammalogy* 62:539–556.
- FISCHER, G. 1817. *Adversaria zoologica*. Mémoires de la Société Impériale des Naturalistes de Moscou, 5:357–446 (mispaginated at page 424, skipping to page 443: last page number should have been p. 428).
- FISHER, R. D., AND C. A. LUDWIG. 2015. Catalog of type specimens of Recent mammals: Orders Didelphimorphia through Chiroptera (excluding Rodentia) in the National Museum of Natural History, Smithsonian Institution. *Smithsonian Contributions to Zoology* 644:1–110.
- FRONTIER, S. 1976. Étude de la décroissance des valeurs propres dans une analyse en composantes principales: comparaison avec le modèle du bâton brisé. *Journal of Experimental Marine Biology and Ecology* 25:67–75.
- GOLDMAN, E. A. 1912. New mammals from eastern Panama. *Smithsonian Miscellaneous Collections* 60:1–18.
- GOLDMAN, E. A. 1932. Two new mammals from Honduras. *Proceedings of the Biological Society of Washington*, 45:121–124.
- GOODWIN, G. G. 1942. Mammals of Honduras. *Bulletin of the American Museum of Natural History* 79:107–195.
- GRAY, J. E. 1867. Notes on the skulls of hares (Leporidae) and picas (Lagomyidae) in the British Museum. *Annals and Magazine of Natural History, Series 3* 20:219–225.
- GROVES, C., AND P. GRUBB. 2011. *Ungulate taxonomy*. Johns Hopkins University Press. Baltimore, Maryland, U.S.A.
- GUTIERREZ, E. E., ET AL. 2017. A gene-tree test of the traditional taxonomy of American deer: the importance of voucher specimens, geographic data, and dense sampling. *ZooKeys* 697:87–131.
- HALL, E. R. 1951. A synopsis of the North American Lagomorpha. University of Kansas Publications, Museum of Natural History 5:119–202.
- HALL, E. R. 1981. *The mammals of North America*. 2nd ed. John Wiley & Sons, Inc. New York 1:1–600.
- HARDY, D. K., ET AL. 2013. Molecular phylogenetics and phylogeographic structure of Sumichrast's harvest mouse (*Reithrodontomys sumichrasti*: Cricetidae) based on mitochondrial and nuclear DNA sequences. *Molecular Phylogenetics and Evolution* 68:282–292.
- HARRIS, W. P., JR. 1932. Four new mammals from Costa Rica. *Occasional Papers of the Museum of Zoology, University of Michigan* 248:1–6.
- HARRIS, W. P., JR. 1933. A new tree squirrel and a new cottontail rabbit from Costa Rica. *Occasional Papers of the Museum of Zoology, University of Michigan* 266:1–4.
- HARTERT, E. 1894. *Lepus nigronuchalis* sp. nov. *Novitates Zoologicae* 1:40.
- HERSHKOVITZ, P. 1950. Mammals of northern Colombia. Preliminary report no. 6: Rabbits (Leporidae), with notes on the classification and distribution of the South American forms. *Proceedings of the United States National Museum* 100:327–375.
- HIBBARD, C. W. 1963. The origin of the P₃ pattern of *Sylvilagus*, *Caprolagus*, *Oryctolagus*, and *Lepus*. *Journal of Mammalogy* 44:1–15.
- HOFFMANN, R. S., AND A. T. SMITH. 2005. Order Lagomorpha. Pp. 185–211, in *Mammal species of the world: a taxonomic and geographic reference*. 3rd ed. (Wilson, D. E., and D. M. Reeder, eds.). Johns Hopkins University Press. Baltimore, U.S.A.
- HUMMELINCK, P. W. 1940. Mammals of the genera *Odocoileus* and *Sylvilagus*. *Studies on the Fauna of Curaçao, Aruba, Bonaire and the Venezuelan Islands* 6:83–108.
- JACKSON, D. A. 1993. Stopping rules in principal components analysis: a comparison of heuristic and statistical approaches. *Ecology* 74:2204–2214.
- LAWRENCE, M. A. 1993. Catalog of recent mammal types in the American Museum of Natural History. *Bulletin of the American Museum of Natural History* 217:1–200.

- LEÓN-PANIAGUA, L., ET AL. 2007. Diversification of the arboreal mice of the genus *Habromys* (Rodentia: Cricetidae: Neotomiinae) in the Mesoamerican highlands. *Molecular Phylogenetics and Evolution* 42:653–664.
- LÓPEZ MARTÍNEZ, N. 1974. Évolution de la lignée *Piezodus-Prolagus* (Lagomorpha, Ochotonidae) dans le Cénozoïque d'Europe sud-occidentale. Ph.D. dissertation, Université des Sciences et Techniques du Languedoc. Montpellier, France.
- LÓPEZ MARTÍNEZ, N. 1977. Revisión sistemática y bioestratigráfica de los Lagomorpha (Mammalia) del Terciario y Cuaternario Inferior de España. Ph.D. dissertation, Universidad Complutense de Madrid, Facultad de Ciencias Geológicas. Madrid, Spain.
- LÓPEZ MARTÍNEZ, N. 1980. Los micromamíferos (Rodentia, Insectivora, Lagomorpha y Chiroptera) del Sitio de Ocupación Achelense de Áridos-1 (Arganda, Madrid). Pp. 161–202, in *Ocupaciones Achelenses en el Valle del Jarama; Geología, paleontología, paleoecología y prehistoria*. Vol. 1: Arqueología y Paleontología (M. Santonja, N. López Martínez, and A. Pérez-González, eds.). Servicios de Extensión Cultural y Divulgación de la Diputación Provincial de Madrid. Madrid, Spain 1:1–352.
- LÓPEZ MARTÍNEZ, N. 1989. Revisión sistemática y bioestratigráfica de los Lagomorpha (Mammalia) del Terciario y Cuaternario Inferior de España. *Memorias del Museo de Paleontología de la Universidad de Zaragoza* 3:1–342.
- LÓPEZ-MARTÍNEZ, N, A. ET AL. 2007. A new lagomorph from the Late Miocene of Chad (Central Africa). *Revista Española de Paleontología* 22:1–20.
- LYON, M. W., Jr. 1904. Classification of the hares and their allies. *Smithsonian Miscellaneous Collections* 45:321–447, Pl. 74–100.
- MARCUS, L. 1990. Traditional morphometrics. Pp. 77–122, in *Proceedings of the Michigan Morphometrics Workshop* (Rohlf, F. J., and F. L. Bookstein, eds.). Special Publication number 2, The University of Michigan Museum Zoology. Ann Arbor, U.S.A.
- MATOCQ, M. D., J. L. PATTON, AND M. N. F. DA SILVA. 2000. Population genetic structure of two ecologically distinct Amazonian spiny rats: separating history and current ecology. *Evolution* 54:1423–1432.
- MAYDEN, R. L. 1997. A hierarchy of species concepts: the denouement in the saga of the species problem. Pp. 381–424 in *Species: the units of biodiversity* (Claridge, M. F., H. A. Dawah, and M. R. Wilson, eds.). Chapman & Hall. London, United Kingdom.
- MCCLEARN, D., ET AL. 2001. The Caribbean lowland evergreen moist and wet forests. Pp. 527–587, in *Costa Rican Ecosystems* (Kappelle, M., ed.). University of Chicago Press. Chicago, U.S.A.
- MILLER, G. S. 1898. A new rabbit from Margarita Island, Venezuela. *Proceedings of the Biological Society of Washington* 12:97–98.
- MILLER, G. S. 1899. Descriptions of six new American rabbits. *Proceedings of the Academy of Natural Sciences of Philadelphia* 51:380–390.
- MORA, J. M. 2000. Mamíferos silvestres de Costa Rica. Editorial Universidad Estatal a Distancia. San José, Costa Rica.
- MOYÉ, L. A. 2006. *Statistical reasoning in medicine: the intuitive P-value primer*. 2nd Ed. Springer Science+Business Media. New York, U.S.A.
- MUSSER, G. G., ET AL. 1998. Systematic studies of oryzomyine rodents (Muridae, Sigmodontinae): diagnoses and distributions of species formerly assigned to *Oryzomys "capito"*. *Bulletin of the American Museum of Natural History* 236:1–376.
- NAKA, L. N., AND R. T. BRUMFIELD. 2018. The dual role of Amazonian rivers in the generation and maintenance of avian diversity. *Science Advances* 4:eaar8575.
- NAOMI, S.-I. 2011. On the integrated frameworks of species concepts: Mayden's hierarchy of species concepts and de Queiroz's unified concept of species. *Journal of Zoological Systematics and Evolutionary Research* 49:177–184.
- NELSON, E. W. 1904. Descriptions of seven new rabbits from Mexico. *Proceedings of the Biological Society of Washington* 17:103–110.
- NELSON, E. W. 1909. The rabbits of North America. *North American Fauna* 29:1–287.
- OLSON, D. M., ET AL. 2001. Terrestrial ecoregions of the world: a new map of life on Earth. *BioScience* 51:933–938.
- ORR, R. T. 1940. The rabbits of California. *Occasional Papers of the California Academy of Sciences*, 19:1–207
- PADIAL, J. M., ET AL. 2010. The integrative future of taxonomy. *Frontiers in Zoology* 7:16.
- PALACIOS, F. 1996. Systematics of the indigenous hares of Italy traditionally identified as *Lepus europaeus* Pallas, 1778 (Mammalia: Leporidae). *Bonner Zoologische Beiträge* 46:59–91.
- PALACIOS, F., AND N. LÓPEZ MARTÍNEZ. 1980. Morfología dentaria de las liebres europeas. *Doñana, Acta Vertebrata* 7:61–81.
- PALACIOS, F., ET AL. 2008. Morphological evidence of species differentiation within *Lepus capensis* Linnaeus, 1758 (Leporidae, Lagomorpha) in Cape Province, South Africa. *Mammalian Biology* 73:358–370.
- PATTON, J. L., M. N. DA SILVA, AND J. R. MALCOLM. 2000. Mammals of the Rio Juruá and the evolutionary and ecological diversification of Amazonia. *Bulletin of the American Museum of Natural History* 244:1–306.
- R CORE TEAM. 2016. R: a language and environment for statistical computing. Vienna, Austria. www.R-project.org/.
- REYMENT, R. A., R. E. BLACKITH, AND N. A. CAMPBELL. 1984. *Multivariate morphometrics*. 2nd. ed. Academic Press. London, U.K.
- RODRÍGUEZ-HERRERA, B., ET AL. 2014. Actualización de la lista de especies de mamíferos vivientes de Costa Rica. *Mastozoología Neotropical* 21:275–289.
- ROGERS, D. S., ET AL. 2007. Molecular phylogenetic relationships among crested-tailed mice (genus *Habromys*). *Journal of Mammalian Evolution* 14:37–55.
- RUEDAS, L. A. 1995. Description of a new large-bodied species of *Apomys* Mearns, 1905, (Mammalia: Rodentia: Muridae) from Mindoro Island, Philippines. *Proceedings of the Biological Society of Washington* 108(2):302–318.
- RUEDAS, L. A. 1998. Systematics of *Sylvilagus* Gray, 1867 (Lagomorpha: Leporidae) from southwestern North America. *Journal of Mammalogy* 79:1355–1378.
- RUEDAS, L. A. 2017. A new species of cottontail rabbit (Lagomorpha: Leporidae: *Sylvilagus*) from Suriname, with comments on the taxonomy of allied taxa from northern South America. *Journal of Mammalogy* 98:1042–1059.
- RUEDAS, L. A., AND J. SALAZAR-BRAVO. 2007. Morphological and chromosomal taxonomic assessment of *Sylvilagus brasiliensis gabbi* (Leporidae). *Mammalia* 71:63–69.
- RUEDAS, L. A., S. M. SILVA, J. H. FRENCH, R. N. PLATT, II, J. SALAZAR-BRAVO, J. M. MORA, AND C. W. THOMPSON. 2017. A prolegomenon to the

- systematics of the South American cottontail rabbits (Mammalia, Lagomorpha, Leporidae: *Sylvilagus*): designation of a neotype for *S. brasiliensis* (Linnaeus, 1758), and restoration of *S. andinus* (Thomas, 1897) and *S. tapetillus* Thomas, 1913. *Miscellaneous Publication, Museum of Zoology, University of Michigan* 205:1–67.
- RUEDAS, L. A., *ET AL.* 2019. Taxonomy of the *Sylvilagus brasiliensis* complex in Central and South America (Lagomorpha: Leporidae). *Journal of Mammalogy* 100:1599–1630.
- SAS INSTITUTE, INC. 1988a. SAS/STAT user's guide, release 6.03 edition. SAS Institute Inc. Cary, U.S.A.
- SAS INSTITUTE, INC. 1988b. SAS procedures guide, release 6.03 edition. SAS Institute Inc. Cary, U.S.A.
- SANGSTER, G. 2014. The application of species criteria in avian taxonomy and its implications for the debate over species concepts. *Biological Reviews* 89:199–214.
- SCHLICK-STEINER, B. C., *ET AL.* 2010. Integrative taxonomy: a multi-source approach to exploring biodiversity. *Annual Review of Entomology* 55:421–438.
- STATTERSFIELD, A. J., *ET AL.* 1998. Endemic bird areas of the world: priorities for biodiversity conservation. *BirdLife Conservation Series No. 7*. BirdLife International, Cambridge, U.K.
- SULLIVAN, J. E., E. ARELLANO, AND D. S. ROGERS. 2000. Comparative phylogeography of Mesoamerican Highland rodents: concerted versus independent response to past climatic fluctuations. *American Naturalist* 155:755–768.
- THOMAS, O. 1901. New *Myotis*, *Artibeus*, *Sylvilagus*, and *Metachirus* from Central and South America. *Annals and Magazine of Natural History*, 7th Series 7:541–545.
- THOMAS, O. 1913. Notes on S. American Leporidae. *Annals and Magazine of Natural History*, 8th Series 11:209–214.
- VOSS, R. S., L. F. MARCUS, AND P. ESCALANTE P. 1990. Morphological evolution in muroid rodents I. Conservative patterns of craniometric covariance and their ontogenetic basis in the Neotropical genus *Zygodontomys*. *Evolution* 44:1568–1587.
- WALLACE, A. R. 1852. On the monkeys of the Amazon. *Proceedings of the Zoological Society of London* 10:107–110.
- WASSERSTEIN, R. L., AND N. A. LAZAR. 2016. The ASA Statement on *p*-Values: Context, process, and purpose. *The American Statistician* 70:129–133.
- WASSERSTEIN, R. L., A. L. SCHIRM, AND N. A. LAZAR. 2019. Moving to a world beyond "*p* < 0.05". *The American Statistician* 73:1–19.
- WHITE, J. A. 1987. The Archaeolaginae (Mammalia, Lagomorpha) of North America, excluding *Archaeolagus* and *Panolax*. *Journal of Vertebrate Paleontology* 7:425–450.
- WHITE, J. A. 1991. North American Leporinae (Mammalia: Lagomorpha) from the Late Miocene (Clarendonian) to Latest Pliocene (Blancan). *Journal of Vertebrate Paleontology* 11:67–89.
- WHITE, J. A., AND N. H. MORGAN. 1995. The Leporidae (Mammalia, Lagomorpha) from the Blancan (Pliocene) Taunton local fauna of Washington. *Journal of Vertebrate Paleontology* 15:366–374.
- WIBLE, J. R. 2007. On the cranial osteology of the Lagomorpha. *Bulletin of the Carnegie Museum of Natural History* 39:213–234.
- WINKLER, A. J., AND Y. TOMIDA. 2011. The lower third premolar of *Serengetilagus praecapensis* (Mammalia: Lagomorpha: Leporidae) from Laetoli, Tanzania. Pp. 55–66, in *Paleontology and geology of Laetoli: human evolution in context*. Volume 2: Fossil hominins and the associated fauna (Harrison, T., ed.). Springer, U.S.A.
- ZACHOS, F. E. 2015. Taxonomic inflation, the Phylogenetic Species Concept and lineages in the Tree of Life – a cautionary comment on species splitting. *Journal of Zoological Systematics and Evolutionary Research* 53:180–184.
- ZACHOS, F. E., *ET AL.* 2013. Species inflation and taxonomic artefacts—A critical comment on recent trends in mammalian classification. *Mammalian Biology* 78:1–6.

Associated editor: Jake Esselstyn and Giovani Hernández Canchola

Submitted: July 6, 2022; Reviewed: November 5, 2022

Accepted: December 14, 2022; Published on line: January 27, 2023

Appendix 1

Specimens examined:

The taxa below are listed under their original names, with the currently accepted synonym following in square brackets. Latitude and longitude coordinates are provided in datum WGS84. Museum abbreviations as follows, AMNH: American Museum of Natural History, New York; MCZ: Museum of Comparative Zoology, Harvard University; MVB: Museum of Vertebrate Biology, Portland State University, Portland, Oregon; TTU: Natural Science Research Laboratory, The Museum, Texas Tech University, Lubbock, Texas; UMMZ: University of Michigan Museum of Zoology, Ann Arbor, Michigan; USNM: United States National Museum—Smithsonian Institution, Washington, D.C.

***Sylvilagus daulensis* J. A. Allen, 1914:199** [= *Sylvilagus brasiliensis surdaster*; following circumscription of *S. brasiliensis* to the Pernambuco Endemism Center (Ruedas et al. 2017), we hypothesize that this taxon is unlikely to be conspecific with *S. brasiliensis*]. Ecuador: (Guayas Prov.); Daule [ca. 1° 51' 42" S, 79° 58' 44" W, ~8 m]: holotype, AMNH 34671 (♀).

***Sylvilagus (Tapeti) fulvescens* J. A. Allen, 1912:75** [= *S. fulvescens*; see Ruedas et al. 2019]. Colombia: Departamento de Cauca: "Belén (alt. 6000 ft.) Western Andes" [Lawrence (1993) noted that the label incorrectly gave the altitude as 6,000 feet, and that the actual collecting locality was "Colombia: Cauca; Belén, west of Papayan [sic.], 10,000 ft (3050 m)." There is a town named Belén (Municipio de Inzá) ca. 2° 28' 11" N, 76° 02' 21" W, ~1,705 m, some 65 km airline distance from Popayán (ca. 2° 27' 05" N, 76° 36' 46" W, ~1,725 m) with nearby elevations in the range noted by Lawrence; the eminence closest to Belén of that elevation (~8 km W) is ca. 2° 27' 40.7" N, 76° 06' 22.1" W; the AMNH database lists Belén as Municipio Guapí; however, the Belén in Mpo. Guapí is at ca. 2° 30' 28" N, 77° 35' 49" W, and more pointedly at ~72 m, approximately 173 km (airline distance, bearing 271°) from Belén, Inzá, Cauca]: holotype, AMNH 32360 (♀).

***Sylvilagus kelloggi* Anthony, 1923:9** [*S. b. kelloggi*; following circumscription of *S. brasiliensis* to the Pernambuco Endemism Center (Ruedas et al. 2017), we hypothesize that this taxon is unlikely to be conspecific with *S. brasiliensis*]. Ecuador: Loja Province; Cordillera Occidental, Guachanamá, east of Alamor and northeast of Celica, 9,050 ft (2,760 m), headwaters of the Río Chira [ca. 4° 25' 42" S, 79° 13' 19" W]: holotype, AMNH 60515 (♂).

***Sylvilagus chillae* Anthony, 1923:12** [*S. b. chillae*; following circumscription of *S. brasiliensis* to the Pernambuco Endemism Center (Ruedas et al. 2017), we hypothesize that this taxon is unlikely to be conspecific with *S. brasiliensis*]. Ecuador: El Oro Province; trail between Salvias and Zaraguro, 6,000 ft (1,830 m) SW flank Cordillera de Chilla [ca. 3° 37' 2" S, 79° 30' 12" W; the AMNH catalog lists as locality for this specimen: "Ecuador, Salvias". Salvias is a rural "parroquia" (administrative subdivision) in Sector

Oriental of Cantón Zaruma, El Oro province]: holotype, AMNH 60511 (♀).

***Sylvilagus (Tapeti) salentus* J. A. Allen 1913:476** [= *S. salentus*; see Ruedas et al. 2019]. Colombia: Caldas; Salento, at head of Río Quindio, west of Mount Tolima, western Quindio Andes, 7,000 ft [~2,135 m; ca. 4° 38' 31.6" N, 75° 33' 30.6" W; AMNH catalogue lists as Dept. Chocó, however, Salento currently is in Depto. Quindio; the Depto. Caldas is north of Quindio and separated from the latter by Depto. Risaralda]: holotype AMNH 33050 (♂).

***Sylvilagus dicei* Harris, 1932:1** [*S. dicei*; see Diersing, 1981]. Costa Rica: [San José Prov., Cantón de Dota]: El Copey de Dota [ca. 9° 38' 50" N, 83° 55' 05" W, ~1,850 m]: holotype, UMMZ 64043 (♀). Costa Rica: Provincia de Cartago; 9° 33' 12.3" N, 83° 41' 24.8" W, 2,830 m: TTU 163828 (♂). Puntarenas: Cedral de Miramar, 10° 12' 46.38" N, 84° 40' 34.28" W, MVB 5036 (JMM-001-2018; ♀). Heredia: Los Cartagos, Santa Bárbara, 2,080 m, 10° 08' 55.7" N, 84° 09' 11.6" W: MVB 5065 (JMM-001-2017; ♂). Heredia: Varablanca, 1,700 m, 10° 11' 05.31" N, 84° 09' 18.17" W: MVB 5037 (JMM-002-2017; ♀).

***Lepus sylvaticus aztecus* J. A. Allen, 1890b:188** [= *S. floridanus aztecus*]. México: Oaxaca; Tehuantepec City [ca. 16° 20' N, 95° 14' W, ~50m]: holotype, AMNH 3116/2438, ♂; AMNH 143454, 143455, 143457, 143458 (all ♀), 2439, 2440, 2441, 142550, 143456, 143459, 145166 (all ♂). México: Oaxaca; Dist. Tehuantepec, Las Tejas, AMNH 143460 (♂). México: Oaxaca; Juchitán [ca. 16° 26' N, 95° 01' W, ~25m]: AMNH 186409 (♀). México: Oaxaca; Juchitán, Palomares [possibly ca. 17° 08' 17" N, 95° 03' 45" W, ~120 m], AMNH 254522 (sex unknown).

***Sylvilagus boylei* J. A. Allen, 1916:84** [*S. f. superciliaris*]. Colombia: Departamento del Atlántico; La Playa, near Barranquilla, 150 ft [46 m; La Playa was originally a "corregimiento" (Puerto Colombia) and is currently a district of Barranquilla better known as "Eduardo Santos"; an elevation of ca. 46 m in the vicinity of La Playa could be ca. 11° 01' 04.6" N, 74° 51' 52.6" W]: holotype, AMNH 37794 (♀). [Allen (1916:84) noted that the "skull appears to have been lost in transit." However, Lawrence (1993) subsequently reported that the holotype was constituted by a skin and skull; we examined a *Sylvilagus* with the number corresponding to the holotype of this taxon and characteristics definitively identifying it as a South American species.]

***Lepus floridanus chiapensis* Nelson, 1904:106** [= *S. f. aztecus*]. México: Chiapas; San Cristobal [ca. 16° 43' 57" N, 92° 38' 44" W, ~2,160 m. Fisher and Ludwig (2015) noted that E. W. Nelson and E. A. Goldman, collectors of the holotype (Nelson 1904), listed "8,200 ft" (2,499 m) in their field catalogue]: holotype, USNM 75953 (♀). Guatemala: Dpto. Totonicapán: Momostenango [ca. 15° 02' 42.5" N, 91° 24' 29" W, ~2,210 m]: AMNH 69275 (♂). Guatemala: Jutiapa Dept.; Municipalidad de Moyuta, Colonia Montúfar, Aldea El Paraíso [Moyuta: ca. 14° 2' 19" N, 90° 4' 51" W, ~1,276 m]: AMNH 243827 (♀). México: Chiapas: 3.5 mi S of Comitán; [ca. 16° 12' 28" N, 92° 06' 40" W, ~1,595 m], AMNH 175078 (♂).

***Lepus floridanus connectens* Nelson, 1904:105** [*S. f. connectens*]: México: Veracruz; Chichicaxtle [we located two localities of this name in Veracruz, only ca. 9.5 km distant from each other: at ca. 19° 21' 24.9" N, 96° 22' 43.2" W, ~30 m, and 19° 20' 32.3" N, 96° 28' 02.7" W, ~127 m]: holotype, USNM 63660 (♂).

***Sylvilagus floridanus costaricensis* Harris, 1933:3** [*S. hondurensis costaricensis*; this paper]. Costa Rica: Provincia de Guanacaste: Hacienda Santa María, 3,200 ft [975 m] ("a large ranch just within the cloud forest on the western slope of the Cordillera de Guanacaste, 22 miles northeast of Liberia") [ca. 10° 45' 53" N, 85° 18' 11.8" W, ~845 m]: holotype, UMMZ 65232 (♀). Costa Rica: Provincia de Guanacaste: Parque Nacional Palo Verde, Bagaces, 15 m. 10° 20' 40.46" N, 85° 20' 21.83" W: MVB 5066 (MVB JMM-003-2016; ♀). Costa Rica: Provincia de Puntarenas: Chomes, 11 m. 10° 02' 35.91" N, 84° 54' 32.77" W: MVB 5056 (JMM-015-2017; ♂). Costa Rica: Provincia de Puntarenas: Chomes, 7 m. 10° 02' 26.77" N, 84° 54' 35.55" W: MVB 5067 (JMM-016-2017). Costa Rica: Provincia de Guanacaste: close to Parque Nacional Rincón de la Vieja, 724 m. 10° 46' 15.87" N, 85° 21' 30.78" W: MVB 5057 (JMM-017-2017). Costa Rica: Provincia de Guanacaste: close to Parque Nacional Rincón de la Vieja, 720 m. 10° 46' 05.77" N, 85° 21' 21.87" W: MVB 5058 (JMM-018-2017). Costa Rica: Provincia de Guanacaste: Cañas, 57 m. 10° 24' 52.71" N, 85° 06' 33.91" W: MVB 5059 (JMM-019-2017). Costa Rica: Provincia de Cartago: El Silencio, La Suiza, Turrialba, 897 m. 9° 52' 27.75" N, 83° 36' 50.4" W: MVB 5048 (JMM-020-2017; ♀). Costa Rica: Provincia de Guanacaste: Cañas, 61 m. 10° 25' 17.43" N, 85° 06' 35.91" W: MVB 5068 (JMM-021-2017). Costa Rica: Provincia de Guanacaste: Cañas, 68 m. 10° 24' 02.23" N, 85° 06' 06.67" W: MVB 5060 (JMM-022-2017; ♂). Costa Rica: Provincia de Guanacaste: Cañas, 43 m. 10° 24' 10.84" N, 85° 07' 12.45" W: MVB 5061 (JMM-023-2017; ♀). Costa Rica: Provincia de Guanacaste: main road, 50 m before the entrance to Parque Nacional Rincón de la Vieja, 797 m. 10° 46' 25.22" N, 85° 20' 58.20" W: MVB 5062; JMM-024-2017 (♂).

***Lepus sylvaticus floridanus* J. A. Allen, 1890a:160** [= *Sylvilagus floridanus floridanus*]. United States: Florida: Brevard Co., San Sebastian River, near Micco [ca. 27° 50' 04" N, 80° 30' 24.2" W, ~2 m]: holotype, AMNH 1890/1155 (♀). United States: Florida: Brevard Co.; Micco, Oak Lodge, topotype: USNM 70870 (♀). United States: Florida: Brevard Co.; Micco, topotypes: USNM 77114 (♀), 76711, 77113, 77115 (all ♂). United States: Florida: Seminole and Volusia counties; Lake Harney [ca. 28° 46' 36" N, 81° 03' 19" W, ~1 m]: USNM 78756, 78757, 80334, 80335 (all ♀), 78754, 78755 (all ♂).

***Sylvilagus floridanus hondurensis* Goldman, 1932:122** [*S. hondurensis hondurensis*; this paper]. Honduras: [Departamento de Francisco Morazán]; Monte Redondo, about 30 miles northwest of Tegucigalpa (altitude about 5,100 feet) [the bearing and distance from Tegucigalpa and elevation suggest this locality may more likely be located in the Reserva de Vida Silvestre Corralitos, perhaps ca. 14° 18' 46" N, 87° 18' 18" W]: holotype, USNM 257062 (♂). Honduras: Francisco Morazán: Distrito Central; Comayagua [ca.

14° 06' 38" N, 87° 13' 57" W, ~1205 m]: AMNH 123378 (sex unknown). Honduras: Francisco Morazán; Orica, El Caliche Cedros [Orica is at ca. 14° 42' 56" N, 86° 56' 36.5" W, ~860 m. We were able to locate a nearby locality called Cedros, some 23 km, bearing 235°, at ca. 14° 35' 44" N, 87° 07' 08" W, ~950 m]: AMNH 127564 (♂). Nicaragua: Departamento de Managua; Managua, Laguna de Jiloá [ca. 12° 12' 31.5" N, 86° 18' 14" W, ~52 m]: AMNH 176699 (♀). Honduras: Francisco Morazán; Las Flores, Archaga [Goodwin (1942):110] specified that "Las Flores Archaga" corresponded to La Flor Archaga, "(4500-5000 ft.), a small village on the Talanga road east of Archaga." Archaga is located ca. 14° 17' 7" N, 87° 13' 45" W, ~865 m; Talanga is at ca. 14° 23' 55" N, 87° 04' 57" W, ~810 m]: AMNH 126144, 126145, 126146, 126147 (all ♂). Honduras: Departamento Intibucá; La Florida [specimen label reads "La Flor Intibucá" but Goodwin (1942):110] listed a locality in Intibucá as "La Florida"; La Florida is ca. 14° 11' N, 87° 56' W, ~1,800 m; notwithstanding, Goodwin (1942):150] did not list any *Sylvilagus* with that locality, but did list 8 with a provenance of "La Flor Archaga": AMNH 126203 (♂). Honduras: Departamento Intibucá; El Horno [we could only find "Cerro El Horno", a 1,516 m mountain, in Intibucá at ca. 14° 03' 13" N, 88° 12' 26" W; Goodwin (1942):109] listed a locality with the name of El Horno as being "(4000 ft.), Dept. La Paz, 5 miles north of Marcala." That would situate this locality at ca. 14° 13' 48" N, 88° 02' 36" W, ~1,345m]: AMNH 126205 (♀), 126206 (♂). Nicaragua: Departamento de Chontales: AMNH 28482 (♀). Nicaragua: Departamento de Jinotega; San Rafael del Norte [ca. 13° 12' 46" N, 86° 06' 39" W, ~1085 m]: AMNH 29229 (♀); 29230 (♂). Nicaragua: Departamento de León; León [ca. 12° 26' 06" N, 86° 52' 44" W, ~105 m]: AMNH 28325 (♂). Nicaragua: Departamento de Nueva Segovia; Jalapa [ca. 13° 55' 01" N, 86° 07' 37" W, 685 m]: AMNH 29228 (♂).

***Lepus margaritae* G. S. Miller, 1898:97** [= *S. f. margaritae*]. Venezuela: Nueva Esparta; Isla Margarita [Isla Margarita is a ca. 1,020 km² island off the coast of Venezuela, centered at ca. 10° 56' 11" N, 64° 02' 17" W, rising to 920 m, and containing highly varied terrain; it is unclear where, beyond "Isla Margarita," the type locality might be]: holotype, USNM 63217 (♂).

***Lepus (Sylvilagus) russatus* J. A. Allen, 1904:31** [= *S. f. russatus*]. México: Veracruz; Pasa Nueva [= Paso Nuevo, *vide* Lawrence (1993), ca. 18° 36' 22.8" N, 96° 34' 35.3" W, ~167 m]: holotype, AMNH 17203 (♂).

***Lepus (Sylvilagus) superciliaris* J. A. Allen, 1899:196** [= *S. f. superciliaris*]. Colombia: Departamento de Magdalena: Distrito de Santa Marta; Bonda [ca. 11° 14' 05" N, 74° 07' 32" W, ~65 m]: holotype, AMNH 15428 (♂), 15426, 15429 (all ♂), 23569 (♀), 14634 (sex unknown). "Colombia, S[outh]. A[merica]." [likely near Bonda, "250 ft" (76 m)] AMNH 14848 (♀).

***Lepus floridanus yucatanicus* G. S. Miller 1899:388** [= *S. yucatanicus*; this paper]. México: Yucatán; Mérida [environs of ca. 20° 58' 01.5" N, 89° 37' 25.5" W, ~14 m]: holotype, USNM 37772 (♀).

***Lepus brasiliensis* var. *gabbi* J. A. Allen, 1877:349** [= *S. g. gabbi*; see Ruedas and Salazar–Bravo, 2007]. Costa Rica: Talamanca. Further defined by [Hershkovitz \(1950\)](#) as: “Talamanca (= Sipurio, Río Sixaola, near the Caribbean coast), Costa Rica.” [Sipurio is located ca. 9° 32' 3" N, 82° 56' 58" W, ~71 meters, but Puerto Viejo de Talamanca, ca. 7.5 Km N/NE of the Sixaola River at its closest, is at ca. 9° 39' 20" N, 82° 45' 13" W, ~5 m]: lectotype, USNM 11371/37794 (♂). Heredia; Isla Verde, Chilamate, Sarapiquí, 103 m, 10° 26' 38.83" N, 84° 05' 16.16" W: MVB 5069 (JMM-001-2016; ♀). Heredia; Isla Verde, Chilamate, Sarapiquí, 102 m; 10° 26' 38.83" N, 84° 05' 16.59" W: MVB 5041 (JMM-002-2016; ♂). Heredia; Chilamate, Sarapiquí, 101 m, 10° 26' 39.69" N, 84° 05' 16.53" W: MVB 5042 (JMM-003-2017; ♂). Heredia; Chilamate, Sarapiquí, 95 m, 10° 26' 48.00" N, 84° 05' 21.05" W: MVB 5043 (JMM-004-2017; ♂). Heredia; Chilamate, Sarapiquí, 101 m, 10° 26' 39.75" N, 84° 05' 16.40" W: MVB 5044 (JMM-005-2017; ♀). Alajuela: Guacalito, Las Armenias, Upala, 509 m, 10° 48' 45.4" N, 85° 06' 34.8" N: MVB 5049 (JMM-012-2017; ♂). Alajuela: Esterito, Poco Sol, San Carlos, 10° 38' 57.28" N, 84° 29' 57.32" W, MVB 5050 (JMM-013-2017; ♂). Alajuela: Esterito, Poco Sol, San Carlos, 10° 39' 48.30" N, 84° 32' 20.51" N, MVB 5051 (JMM-014-2017; ♀).

***Lepus (Tapeti) incitatus* Bangs, 1901:633** [= *S. incitatus*; see [Ruedas et al. 2019](#)]. Panamá: Archipiélago de las Perlas; San Miguel Island [= Isla del Rey; this island, centered at ca. 8° 21' 20.4" N, 78° 55' 58" W, covers ca. 234 km², with elevations ranging from sea level to ~212 m; [Bangs \(1901\)](#) provided no additional information as to the provenance of what remains the only specimen of the taxon]: holotype, MCZ, Bangs Collection no. 8441 (♀).

***Sylvilagus gabbi messorius* Goldman, 1912:13** [= *S. g. messorius*]. Panamá: Darién; [Santa Cruz de] Cana, altitude 1,800 ft [549 m], eastern mountains of Panamá. [ca. 7° 45' 25" N, 77° 41' 02" W]: holotype, USNM 179569 (♂).

***Lepus truei* J. A. Allen, 1890b:192** [= *S. g. truei*]. México: Veracruz; Mirador [the exact location of Mirador in Veracruz has never been able to be ascertained: there are numerous locations with that name in Veracruz; it is not our desire in this work to speculate]: holotype, USNM 6357/34878 (sex undetermined) [[Allen \(1890b\):194](#)] listed the number of the skull of the type specimen as 25953; [Fisher and Ludwig \(2015\):30](#) pointed out that Allen's identification was due to a cataloguing error and that the correct number for the skull is 34878, as listed here].

***Sylvilagus surdaster* Thomas, 1901:543** [= *Sylvilagus surdaster*; see [Ruedas et al. 2019](#)]. Ecuador: Esmeraldas; Río Bogotá, Carondelet, 20 m [ca. 1° 07' 26.6" N, 78° 45' 45.4" W]: holotype, MNH 1901.6.5.16 [not listed in original description but so designated, presumably by Thomas, in the MNH collection: data in specimen tags match those in the original description].

Geographic variation in select species of the bat genus *Platyrrhinus*

PAÚL M. VELAZCO^{1,2*}, GRACE LY¹, JULIA McALLISTER¹, AND DIEGO A. ESQUIVEL^{3,4}

¹ Department of Biology, Arcadia University, Glenside, Pennsylvania 19038, United States. Email: velazcop@arcadia.edu (PMV), gly@arcadia.edu (GL), jmcallister_02@arcadia.edu (JM).

² Department of Mammalogy, American Museum of Natural History, New York, New York 10024, United States.

³ Programa de Pós-Graduação em Biologia Animal, Universidade Federal do Rio Grande do Sul, Porto Alegre, Rio Grande do Sul 91501-970, Brasil. Email: diegodaem@gmail.com (DAE).

⁴ Fundación Kurupira, Bogotá, Cundinamarca 110921, Colombia.

*Corresponding author: <https://orcid.org/0000-0001-7195-7422>.

The taxonomy of Neotropical bats is constantly changing, with new species being described and junior synonyms elevated, while other taxa are relegated to junior synonyms or subspecies. The genus *Platyrrhinus* has followed this trend, with some issues persisting about the current status of its subspecies. Here we evaluate variation in cranial shape and size based on geometric morphometric analyses of *Platyrrhinus dorsalis* and *P. umbratus*. *P. dorsalis* occurs at elevations from sea level to above 2,000 m and is found from southern Panama southward into Colombia and along both slopes of the Andes in Ecuador. *P. umbratus* occurs at elevations from 400 m to above 3,150 m in the Andean from Colombia south through Bolivia and Caribbean Mountain systems of Venezuela and Colombia. Our analyses did not support the recognition of subspecies in either species. The difference in skull size and shape between populations of *P. dorsalis* is associated with elevation, suggesting that this species exhibits an altitudinal clinal variation, with individuals being larger in the lower elevation and smaller in higher elevations. In *P. umbratus* the difference in skull size and shape between populations is associated with a latitudinal cline, with individuals tending to be larger in the northern part of their range. Our analyses did not reveal the existence of secondary sexual variation in *P. dorsalis* nor in *P. umbratus*.

La taxonomía de murciélagos Neotropicales está en un estado de constante cambio, con algunas especies siendo descritas, sinónimos menores siendo elevados o especies siendo reconocidas como sinónimos menores o subspecies. El género *Platyrrhinus* no ha sido la excepción a esta tendencia, y presenta una larga historia de cambios taxonómicos persistiendo algunas dudas acerca del estado actual de sus subspecies. Evaluamos la variación en forma y tamaño del cráneo en *Platyrrhinus dorsalis* y *P. umbratus* basándonos en análisis de morfometría geométrica. *P. dorsalis* se encuentra presente en elevaciones desde el nivel del mar hasta por encima de los 2,000 m y se distribuye desde Panamá al sur hasta Colombia, y a lo largo de ambas vertientes de los Andes en Ecuador. *P. umbratus* se encuentra presente en elevaciones desde 400 m hasta los 3,150 m, con distribución en los Andes de Venezuela a Bolivia y el Sistema Montañoso del Caribe de Venezuela y Colombia. Nuestros análisis no apoyan el reconocimiento de subspecies en *P. dorsalis* o *P. umbratus*. La diferencia en el tamaño y forma del cráneo entre poblaciones de *P. dorsalis* está asociada con la elevación, sugiriendo que esta especie presenta una variación clinal altitudinal, con individuos grandes a elevaciones menores y pequeños en las altas. En *P. umbratus* también el tamaño y forma del cráneo está asociada con una clina latitudinal, con los más grandes en la parte septentrional de la distribución. Nuestros análisis no revelan la presencia de variación sexual secundaria en ninguna de las dos especies.

Keywords: Andes, cline, neotropics, *Platyrrhinus dorsalis*, *Platyrrhinus umbratus*, subspecies, taxonomy.

© 2023 Asociación Mexicana de Mastozoología, www.mastozoologiamexicana.org

Introduction

The Neotropical bat genus *Platyrrhinus* is one of the most speciose phyllostomid genera (Simmons and Cirranello 2022). Members of the genus, also known as broad-nosed bats, are widely distributed from Mexico to northern Argentina, with most species found in the Andes region (Velazco and Patterson 2008; Velazco and Gardner 2009; Velazco and Lim 2014; Velazco et al. 2018; Palacios-Mosquera et al. 2020). Over the past two decades, numerous taxonomic changes have been made within the genus, and only since 2005, recognized diversity increased from ten to nineteen species, nearly doubling the number of taxa (Simmons 2005; Simmons and Cirranello 2022; Velazco 2005; Velazco and Gardner 2009; Velazco and Lim 2014; Velazco et al. 2018; Palacios-Mosquera et al. 2020).

Simmons (2005) recognized subspecies in three *Platyrrhinus* species (e. g., *helleri* [*helleri* and *incarum*], *lineatus* [*lineatus* and *nigellus*], and *umbratus* [*aquilus*, *oratus*, and *umbratus*]). However, after several revisionary studies, all of those subspecies were elevated to full species, except for *P. umbratus oratus* which was regarded as a junior synonym of *P. umbratus* (Velazco 2005; Velazco and Gardner 2009; Velazco and Patterson 2008). Velazco et al. (2018) used phylogenetic, linear morphometrics, and ecological niche modeling analyses to review the systematics and taxonomy of *Platyrrhinus nigellus* and *P. umbratus*. The authors suggested that *nigellus* should be recognized as a junior synonym of *umbratus*. Nonetheless, populations of *nigellus* and *umbratus* can be differentiated by subtle external and craniodental morphological differences indi-

cating the possible existence of subspecies or clinal geographic variation (Velazco and Gardner 2009). On the other hand, currently, only subspecies in *Platyrrhinus dorsalis* (*P. d. dorsalis* and *P. d. chocoensis*) are recognized in the genus, but their subspecific status is still controversial. *Platyrrhinus dorsalis* is polytypic, with *chocoensis* and *dorsalis* recognized based on the geographic structure of the morphological variation (Palacios-Mosquera et al. 2020).

Neotropical bat distribution ranges sometimes encompass a variety of biomes, which expose these species to a variety of environments (e. g., climate, vegetation, elevation, etc). Due to this variety of factors some of these species present different degrees of geographic variation throughout their distribution range. These patterns of geographic variation have been suggested to be the result of subspecies (e. g., Molinari et al. 2017; Garbino et al. 2020; Pavan et al. 2021; Tavares et al. 2022), altitudinal (e. g., Moratelli et al. 2013; Castillo-Figueroa 2022), or latitudinal clines (e. g., Nargosen and Tamsitt 1981; Kelly et al. 2018; Méndez-Rodríguez et al. 2021).

Herein we analyzed 2D geometric morphometric data to evaluate whether the populations of *P. dorsalis* and *P. umbratus* deserve subspecific recognition or that the external and craniodental morphological differences between the populations of these two species is the result of an altitudinal or latitudinal cline.

Material and methods

Specimens examined. Our assessment of the taxonomy of *Platyrrhinus dorsalis* and *P. umbratus* was based on the 2D geometric morphometric analyses of the skulls of museum specimens from the following museums: Field Museum of Natural History (FMNH), Chicago, Illinois, United States; Instituto de Investigación de Recursos Biológicos Alexander von Humboldt (IAvH), Villa de Leyva, Boyacá, Colombia; Instituto de Ciencias Naturales (ICN), Universidad Nacional de Colombia, Bogotá, Colombia; Muséum National d'Histoire Naturelle (MNHN-CG), Paris, France; Museo de Historia Natural de la Universidad Nacional Mayor de San Marcos (MUSM), Lima, Peru; Museum of Zoology (UMMZ), University of Michigan, Ann Arbor, Michigan, USA; National Museum of Natural History (formerly U.S. National Museum—USNM), Smithsonian Institution, Washington, D.C., United States; and Sección de Zoología, Departamento de Biología, Universidad del Valle (UV), Cali, Colombia.

Geometric morphometrics analyses. We used 376 skulls of adult individuals from the entire distribution range of *Platyrrhinus dorsalis* and *P. umbratus* (Appendix 1). Dorsal and ventral pictures of the skulls were taken with a Konica Minolta DiMAGE Z6 digital camera. The images were processed with Adobe Photoshop CC. Coordinates of the morphological landmarks (Figure 1) were recorded for each image using tpsDIG version 2.31 (Rohlf 2001). We defined the landmarks based on homology, consistency of relative position, coverage of the form, and repeatability (Zelditch

et al. 2012). Specimens of *P. dorsalis* and *P. umbratus* were grouped into two set of populations (*dorsalis* and *chocoensis* or *nigellus* and *umbratus*) based on external and craniodental morphological differences that distinguished those taxa (Velazco 2005; Velazco and Gardner 2009; Velazco et al. 2018; Palacios-Mosquera et al. 2020). Hereafter, we use *dorsalis* and *chocoensis* or *nigellus* and *umbratus* to refer to the morphological diagnosable groups within each species.

We analyzed a total of 281 images (dorsal view) of *Platyrrhinus dorsalis* (61 from populations assigned to *dorsalis* and 114 from populations assigned to *chocoensis*) and *P. umbratus* (58 from populations assigned to *nigellus* and 48 from populations assigned to *umbratus*; Appendix 1). Dorsal-view landmark definitions were as follows: (1) anteriormost point of the premaxilla; (2) medial point of the anterior edge of the nasal bones; (3) most distal point of the postorbital process; (4) meeting point between the braincase and the anterior edge of the posterior root of the zygomatic arch; (5) posteriormost point of the zygomatic arch opening; (6) meeting point between the braincase and the posterior edge of the posterior root of the zygomatic arch; and (7) posteriormost point of the occipital region (Figure 1A). Landmarks were digitized on the right side of each dorsal image of the skulls, and all the analyses were performed using this configuration.

We analyzed a total of 382 images (ventral view) of *Platyrrhinus dorsalis* (52 from populations assigned to *dorsalis* and 145 from populations assigned to *chocoensis*) and *P. umbratus* (56 from populations assigned to *nigellus* and 129 from populations assigned to *umbratus*; Appendix 1). Ventral view landmark definitions were as follows: (1) anteriormost point of the premaxilla; (2) most posteromedial point on the margin of the incisive foramen; (3) most antero-internal point on M1; (4) most anterolabial point on M2; (5) most antero-internal point on M2; (6) most anterior point on the posterior edge of the palatine; (7) meeting point between

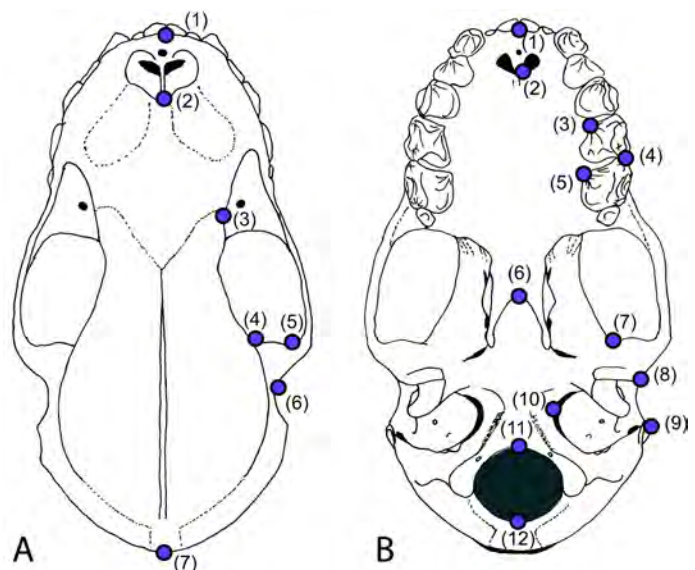


Figure 1. Dorsal (A) and ventral (B) views of a *Platyrrhinus* cranium illustrating the landmarks used in geometric morphometric analyses.

the anterior section of the glenoid fossa and squamosal; (8) most external point on the posterior section of the postglenoid fossa; (9) squamosal lateral extremity, behind the auditory region; (10) most medial point on the margin of the basicochlear fissure; (11) anteriormost point on the margin of the foramen magnum; (12) posteriormost point on the margin of the foramen magnum (Figure 1B). Landmarks were digitized on the left side of each ventral image of the skulls, and all the analyses were performed using this configuration.

The landmark coordinates datasets were converted into Procrustes distances using a Generalized Procrustes Analysis (GPA) that removes undesirable effects of scale, position, and orientation using the *gpagen* function in the R package 'geomorph' (Adams et al. 2021; Baken et al. 2021). We acquired Procrustes shape coordinates, and a size proxy called centroid size (CS) as the square root of the sum of squares of the distance of each landmark to the centroid (mean of all coordinates) of the configuration (Bookstein 1997). Additionally, consensus shapes summarizing the dorsal and ventral views of the skull shape variation among groups were generated. Here, each individual was compared against the consensus shape, which allowed us to visualize differences between groups. Afterwards, we checked the GPA for outliers using the *plotOutliers* function in the 'geomorph' package. Outliers were removed from the analysis and the GPA's were rerun.

Differences in centroid size between females and males (sexual dimorphism) and also among groups were graphically summarized using a series of boxplots in each view. The effects of size, sex, and groups on the dorsal and ventral views of the skull shape and its interactions was tested by evaluating the fit of models using the randomized residual permutation procedure (RRPP) with the *lm.rpp* function in the R package 'RRPP' (Collyer and Adams 2018, 2022). Using the same function, we quantified the differences in size among groups, employing the (log) centroid size of the specimens as the response variable, and sex and groups as independent predictors. All models were fit using the type-II (hierarchical) sum of squares, and its significance was based on 10,000 permutations of residual randomization. We used the *anova.lm.rpp* function to compute analysis of variance (ANOVA) tables for each model, which are based on random statistical distributions and use the F distribution to calculate effect sizes. Pairwise comparisons were conducted on significant factors using the *pairwise* function in the R package 'RRPP' (Collyer and Adams 2018, 2022).

Differences in the dorsal and ventral views of the skull shape among groups were also explored using ordination methods. First, we performed principal component analyses (PCA) on the Procrustes-aligned data using the *gm.prcomp* function in the R package 'geomorph' (Adams et al. 2021; Baken et al. 2021). Of the PCs produced, we chose those that contained significant cumulative variance of shape in each view. Then we generated deformation grids with the extremes (maximum and minimum) of shape

variation along the principal components 1 and 2 (PC1 and PC2). Second, we used a linear discriminant analysis (LDA) using the *lda* function in the R package 'MASS' to determine whether the groups could be reliably distinguished (Venables and Ripley 2002). Jackknife cross-validation was used to estimate the probability of a specimen belonging to any of the predefined groups. Matrices and scripts associated with analyses in this study have been deposited on GitHub (https://github.com/pvelazco/Platyrrhinus_GM.git). The LSID for this publication is: urn:lsid:zoobank.org:pub:4D40F6B2-A27E-461B-8087-401702F7757A.

Results

Platyrrhinus dorsalis variation in skull size. We did not find evidence of sexual dimorphism in size in any of the views examined (Table 1; Figure 2A, B). The two-sample t-test between male and female specimens assigned to *chocoensis* found no statistically significant differences ($t = -0.701$, $d. f. = 112$, $P = 0.484$ [dorsal view]; $t = -0.035$, $d. f. = 143$, $P = 0.971$ [ventral view]). Similarly, the two-sample t-test between male and female specimens assigned to *dorsalis* found no statistically significant differences ($t = 0.046$, $d. f. = 56$, $P = 0.963$ [dorsal view]; $t = 0.233$, $d. f. = 50$, $P = 0.816$ [ventral view]). Finally, the two-sample t-test using all the specimens from both groups found no statistically significant differences between male and females of *P. dorsalis* ($t =$

Table 1. ANOVA results regarding effects of sex, groups, and their interaction on centroid size (log CS).

| | Df | SS | MS | R ² | F | Z | P |
|---|-----|---------|--------|----------------|--------|--------|--------|
| Centroid Size (CS) | | | | | | | |
| (A) Dorsal view – <i>Platyrrhinus dorsalis</i> | | | | | | | |
| Sex | 1 | 0.273 | 0.273 | 0.002 | 0.329 | -0.149 | 0.563 |
| Groups | 1 | 20.718 | 20.718 | 0.129 | 24.923 | 3.580 | < 0.01 |
| Sex x Groups | 1 | 0.162 | 0.162 | 0.001 | 0.195 | -0.447 | 0.672 |
| Residuals | 168 | 139.660 | 0.831 | 0.867 | | | |
| Total | 171 | 161.040 | | | | | |
| (B) Ventral view – <i>Platyrrhinus dorsalis</i> | | | | | | | |
| Sex | 1 | 0.009 | 0.009 | 0.000 | 0.009 | -1.506 | 0.924 |
| Groups | 1 | 0.872 | 0.872 | 0.005 | 0.889 | 0.453 | 0.350 |
| Sex x Groups | 1 | 0.049 | 0.049 | 0.000 | 0.050 | -1.002 | 0.821 |
| Residuals | 193 | 189.315 | 0.981 | 0.995 | | | |
| Total | 196 | 190.236 | | | | | |
| (C) Dorsal view – <i>Platyrrhinus umbratus</i> | | | | | | | |
| Sex | 1 | 1.083 | 1.083 | 0.014 | 1.674 | 0.878 | 0.206 |
| Groups | 1 | 9.236 | 9.236 | 0.121 | 14.273 | 2.919 | < 0.01 |
| Sex x Groups | 1 | 1.280 | 1.280 | 0.017 | 1.978 | 1.027 | 0.160 |
| Residuals | 100 | 64.713 | 0.647 | 0.846 | | | |
| Total | 103 | 76.531 | | | | | |
| (D) Ventral view – <i>Platyrrhinus umbratus</i> | | | | | | | |
| Sex | 1 | 0.128 | 0.128 | 0.001 | 0.137 | -0.592 | 0.714 |
| Groups | 1 | 27.719 | 27.719 | 0.142 | 29.636 | 3.887 | < 0.01 |
| Sex x Groups | 1 | 1.515 | 1.515 | 0.008 | 1.619 | 0.876 | 0.204 |
| Residuals | 177 | 165.555 | 0.935 | 0.848 | | | |
| Total | 180 | 195.321 | | | | | |

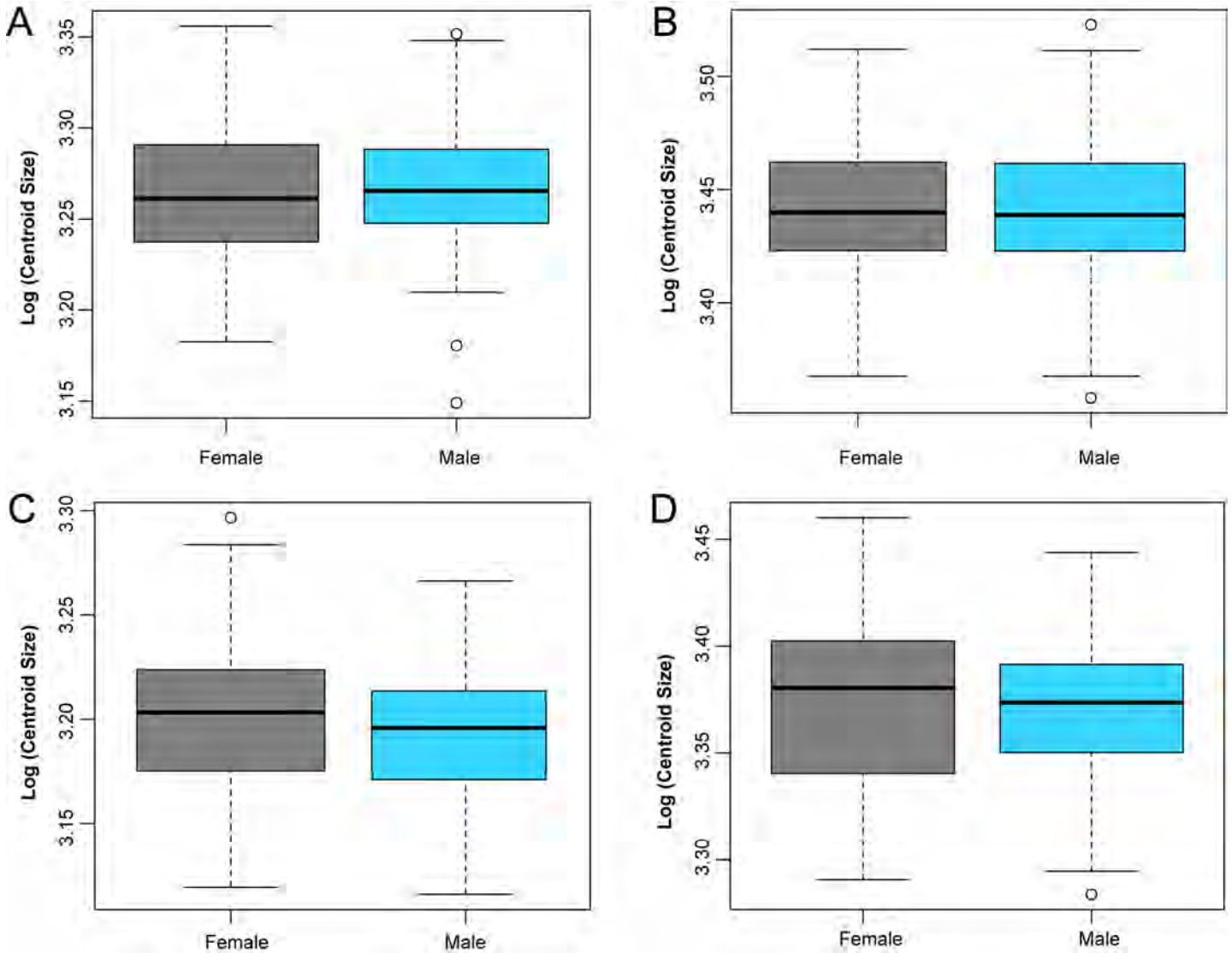


Figure 2. Box plots of the centroid size by species/sex. (A) dorsal view of *Platyrrhinus dorsalis*, (B) ventral view of *P. dorsalis*, (C) dorsal view of *P. umbratus*, and (D) ventral view of *P. umbratus*. Sex: females = gray and males = light blue. Color box limits indicate the first (25%) and third (75%) quartile, the thick black line indicates the median centroid size, and open circles represent outliers.

-0.732, $d. f. = 170$, $P = 0.465$ [dorsal view]; $t = 0.009$, $d. f. = 195$, $P = 0.992$ [ventral view]). The centroid size (CS) in the dorsal view of the cranium was significantly different between the two groups, showing that individuals of *dorsalis* are smaller than *chocoensis* ($P < 0.01$; Table 1; Figure 3A). The variance of the factors tested, represented by mean squares value and the R^2 , showed that most of the variance in cranium size is found between groups (Table 1). However, the centroid size (CS) in the ventral view of the cranium was not significantly different between the two groups ($P = 0.350$; Table 1; Figure 3B).

Platyrrhinus dorsalis variation in skull shape. The ANOVA did not find evidence of sexual dimorphism in cranium shape in either view (Table 2). There were significant differences on both views of the cranial shape variation in the entire Procrustes shape space between the two groups ($P < 0.05$; Table 2). Fitted linear models exhibited significant effect of size on the shape variation in both views; however, the morphological variation explained by size was low

(< 3% in all cases; Table 2) so the allometric effect was not considered, and analyses and graphical representations were carried out on the original shape coordinates.

The PCA showed a clear ordination in both views of the cranium (Figure 4). The first three PC scores accounted for 73% (dorsal view) and 47% (ventral view) of total shape variation. Results are shown from the first two PCs, which accounted for 64% (dorsal view) and 37% (ventral view) of the variation respectively (Figure 4).

The DFA showed a small overlap between the groups indicating that they are different in the shape of the cranium. Specimens were correctly assigned in high percentages to *chocoensis* (93% – dorsal view and 97% – ventral view) and *dorsalis* (71% – dorsal view and 90% – ventral view).

Platyrrhinus umbratus variation in skull size. We did not find evidence of sexual dimorphism in size in any of the views examined (Table 1; Figure 2C, D). The two-sample t-test between male and female specimens assigned to *nigellus* found no statistically significant differences ($t = -0.897$, $d. f. =$

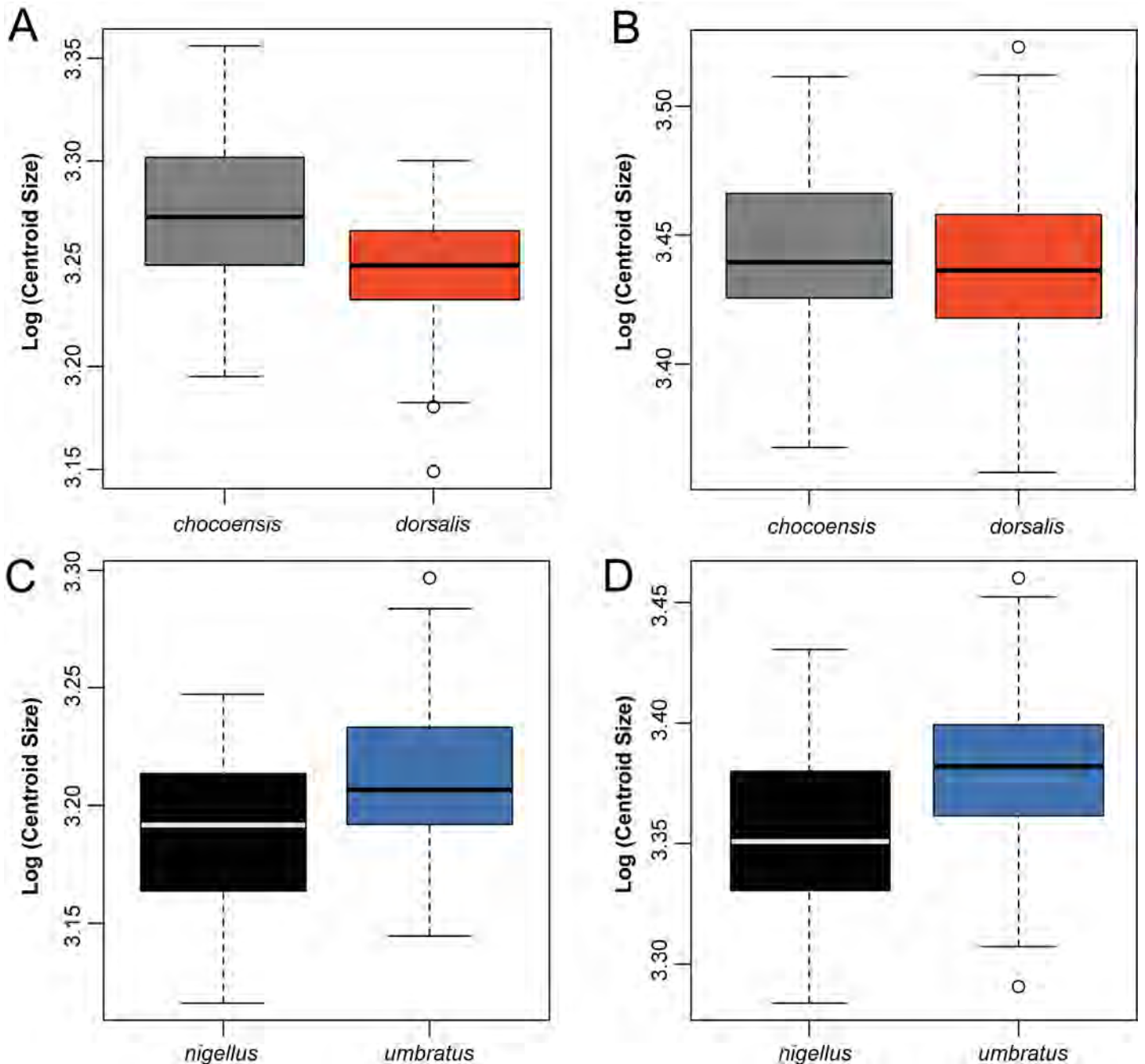


Figure 3. Box plots of the centroid size by groups, showing dorsal (A) and ventral (B) views of *Platyrhinus dorsalis*, and dorsal (C) and (D) ventral views of *P. umbratus*. Groups: *chocoensis* = gray, *dorsalis* = red, *nigellus* = black, and *umbratus* = blue. Color box limits indicate the first (25%) and third (75%) quartile, the thick black line indicates the median centroid size, and open circles represent outliers.

54, $P = 0.374$ [dorsal view]; $t = -0.832$, $d. f. = 54$, $P = 0.409$ [ventral view]). Similarly, the two-sample t-test between male and female specimens assigned to *umbratus* found no statistically significant differences in the ventral view of the cranium ($t = 0.983$, $d. f. = 123$, $P = 0.328$). We were not able to run a similar test for the dorsal view since we did not have enough male specimens ($n = 1$) of *umbratus*. The two-sample t-test using specimens from both groups found no statistically significant differences between males and females of *P. umbratus* ($t = 1.161$, $d. f. = 101$, $P = 0.248$ [dorsal view]; $t = 0.650$, $d. f. = 179$, $P = 0.516$ [ventral view]). The centroid size (CS) in the dorsal and ventral views of the cranium were significantly different

between the two groups showing that individuals of *umbratus* are larger than *nigellus* ($P < 0.01$ in both views; Table 1; Figure 3C, D). The variance of the factors tested, represented by mean squares value and the R^2 , showed that most of the variance in cranium size is found between groups (Table 1).

Platyrhinus umbratus variation in skull shape. The ANOVA did not find evidence of sexual dimorphism in cranium shape in either view (Table 2). There were significant differences on both views of the cranial shape variation in the entire Procrustes shape space between the two groups ($P < 0.05$; Table 2). Fitted linear models exhibited significant effect of size on the shape variation in the dorsal view of the

Table 2. ANOVA results regarding effects of size (allometry), sex (sexual dimorphism), groups and their interactions on shape.

| | Df | SS | MS | R ² | F | Z | P |
|---|-----|-------|-------|----------------|--------|--------|------------------|
| Shape | | | | | | | |
| (A) Dorsal view – <i>Platyrrhinus dorsalis</i> | | | | | | | |
| Size | 1 | 0.003 | 0.003 | 0.017 | 3.215 | 1.999 | 0.025 |
| Sex | 1 | 0.000 | 0.000 | 0.003 | 0.564 | -0.498 | 0.694 |
| Groups | 1 | 0.013 | 0.013 | 0.084 | 15.964 | 4.382 | < 0.01 |
| Size x Sex | 1 | 0.000 | 0.000 | 0.003 | 0.583 | -0.435 | 0.665 |
| Size x Groups | 1 | 0.002 | 0.002 | 0.010 | 1.983 | 1.345 | 0.097 |
| Sex x Groups | 1 | 0.001 | 0.001 | 0.004 | 0.719 | -0.136 | 0.550 |
| Size x Sex x Groups | 1 | 0.001 | 0.001 | 0.005 | 0.991 | 0.337 | 0.361 |
| Residuals | 164 | 0.134 | 0.001 | 0.863 | | | |
| Total | 171 | 0.155 | | | | | |
| (B) Ventral view – <i>Platyrrhinus dorsalis</i> | | | | | | | |
| Size | 1 | 0.004 | 0.004 | 0.029 | 6.716 | 5.234 | < 0.01 |
| Sex | 1 | 0.001 | 0.001 | 0.004 | 0.974 | 0.092 | 0.466 |
| Groups | 1 | 0.020 | 0.020 | 0.147 | 34.584 | 9.196 | < 0.01 |
| Size x Sex | 1 | 0.000 | 0.000 | 0.003 | 0.808 | -0.361 | 0.641 |
| Size x Groups | 1 | 0.001 | 0.001 | 0.007 | 1.660 | 1.482 | 0.066 |
| Sex x Groups | 1 | 0.000 | 0.000 | 0.003 | 0.641 | -0.946 | 0.828 |
| Size x Sex x Groups | 1 | 0.001 | 0.001 | 0.005 | 1.190 | 0.598 | 0.275 |
| Residuals | 189 | 0.108 | 0.001 | 0.805 | | | |
| Total | 196 | 0.135 | | | | | |
| (C) Dorsal view – <i>Platyrrhinus umbratus</i> | | | | | | | |
| Size | 1 | 0.002 | 0.002 | 0.025 | 2.760 | 2.028 | 0.022 |
| Sex | 1 | 0.000 | 0.000 | 0.002 | 0.260 | -1.864 | 0.969 |
| Groups | 1 | 0.002 | 0.002 | 0.033 | 3.677 | 2.575 | 0.005 |
| Size x Sex | 1 | 0.000 | 0.000 | 0.006 | 0.669 | -0.388 | 0.652 |
| Size x Groups | 1 | 0.000 | 0.000 | 0.006 | 0.700 | -0.306 | 0.621 |
| Sex x Groups | 1 | 0.001 | 0.001 | 0.010 | 1.145 | 0.518 | 0.299 |
| Residuals | 97 | 0.054 | 0.001 | 0.873 | | | |
| Total | 103 | 0.062 | | | | | |
| (D) Ventral view – <i>Platyrrhinus umbratus</i> | | | | | | | |
| Size | 1 | 0.001 | 0.001 | 0.007 | 1.430 | 1.074 | 0.141 |
| Sex | 1 | 0.001 | 0.001 | 0.008 | 1.600 | 1.419 | 0.079 |
| Groups | 1 | 0.004 | 0.004 | 0.040 | 7.655 | 5.887 | < 0.01 |
| Size x Sex | 1 | 0.001 | 0.001 | 0.007 | 1.402 | 1.038 | 0.149 |
| Size x Groups | 1 | 0.001 | 0.001 | 0.011 | 2.063 | 2.077 | 0.019 |
| Sex x Groups | 1 | 0.001 | 0.001 | 0.007 | 1.380 | 1.012 | 0.155 |
| Size x Sex x Groups | 1 | 0.001 | 0.001 | 0.005 | 1.012 | 0.196 | 0.424 |
| Residuals | 173 | 0.102 | 0.001 | 0.898 | | | |
| Total | 180 | 0.113 | | | | | |

cranium; however, the morphological variation explained by size was low (< 3 %; Table 2) so the allometric effect was not considered, and analyses and graphical representations were carried out on the original shape coordinates.

The PCA did not show a clear ordination in both views of the cranium (Figure 5). The first three PC scores accounted for 68 % (dorsal view) and 42 % (ventral view) of the cranium total shape variation. Results are shown from the first

two PCs, which accounted for 55 % (dorsal view) and 32 % (ventral view) of the variation respectively (Figure 5).

The DFA showed a small overlap between the groups indicating that they differ in cranial shape. Specimens were correctly assigned to *nigellus* (73 % – dorsal view and 46 % – ventral view) and *umbratus* (75 % – dorsal view and 90 % – ventral view) in high percentages.

Discussion

In the past decade, recognized bat diversity has increased due to new species descriptions and taxa raised from synonymy (Burgin *et al.* 2018). Within Phyllostomidae, examples include *Lophostoma nicaraguae* (Esquivel *et al.* 2022), *Glossophaga bakeri* (Velazco *et al.* 2021), *Tonatia bakeri*, and *T. maresi* (Basantes *et al.* 2020). In a few other cases, species have been downgraded to junior synonyms or subspecies (*e. g.*, *Chiroderma vizottoi* [Garbino *et al.* 2020]; *Vampyressa sinchi* [Tavares *et al.* 2022]; *Lophostoma yasuni* [Camacho *et al.* 2016]). This was the case of *Platyrrhinus chocoensis* that was regarded as a subspecies of *P. dorsalis* based on linear morphometrics and genetic analyses (Palacios-Mosquera *et al.* 2020), and *P. nigellus* that was regarded as a junior synonym of *P. umbratus* based on linear morphometrics, genetic data, and ecological niche modeling analyses (Velazco *et al.* 2018). Our geometric morphometric analyses support the recognition of two morphological groups in *P. dor-*

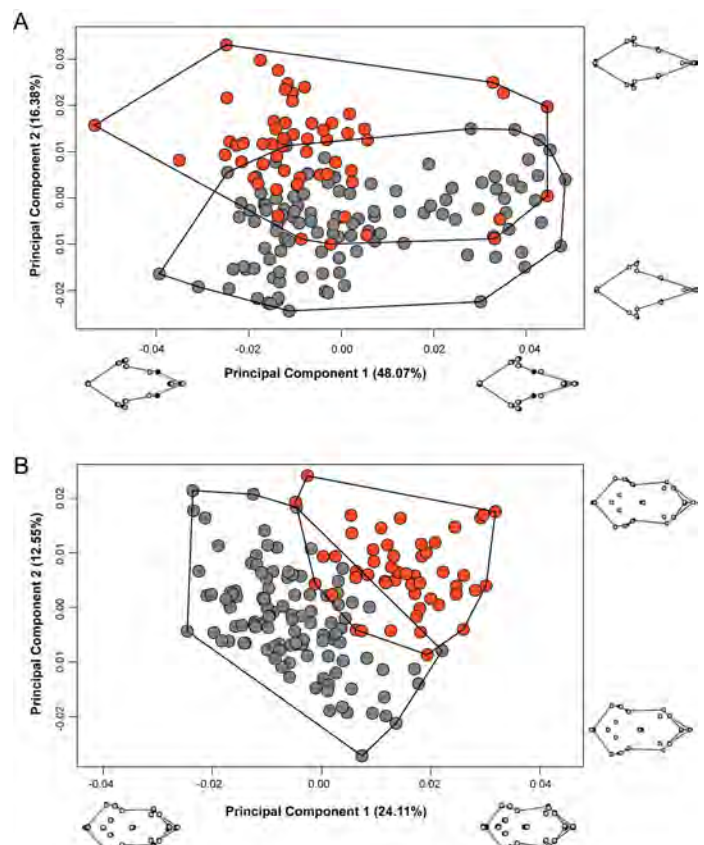


Figure 4. Principal Component Analysis (PCA) of *Platyrrhinus dorsalis* obtained from the (A) dorsal and (B) ventral views of the cranium. Specimens of each group is represented by a dot (*chocoensis*: gray; *dorsalis*: red).

salis (*chocoensis* and *dorsalis*) and in *P. umbratus* (*nigellus* and *umbratus*), but does not support the recognition of these groups as subspecies.

The recognition of subspecies in phyllostomid species has been on the rise in recent years. To mention some examples, [Garbino et al. \(2020\)](#) performed a comprehensive revision of *Chiroderma* and recognized subspecies in *Chiroderma doriae* (*doriae* and *vizottoi*) and *C. villosum* (*jesupi* and *villosum*); [Molinari et al. \(2017\)](#) described *Sturnira adrianae* with two subspecies (*adrianae* and *caripana*) from montane populations in Colombia and Venezuela; and more recently, [Tavares et al. \(2022\)](#) suggested that *Vampyressa sinchi* be recognized as a subspecies of *V. melissa* and not as a separate species based on genetic analyses. One characteristic that all of the aforementioned cases have in common is that the subspecies in each species are not reciprocally monophyletic ([Molinari et al. 2017](#); [Garbino et al. 2020](#); [Tavares et al. 2022](#)). However, [Patten \(2015\)](#) proposed that a morphologically diagnosably distinct, geographically circumscribed group that does not form a distinct genetic clade or is not reciprocally monophyletic in relation to other such clades in the same species could be considered a subspecies. The two morphological groups in *P. dorsalis* (*chocoensis* and *dorsalis*) and *P. umbratus* (*nigellus* and *umbratus*) fulfill all the requirement for subspecies proposed by [Patten \(2015\)](#), with the exception that the groups are geographically circumscribed from each other. In both species there is some overlap in the geographic ranges of both group pairs.

The recognition of *chocoensis* as a subspecies of *Platyrrhinus dorsalis* as suggested by [Palacios-Mosquera et al. \(2020\)](#) was not supported by our analyses. Genetic analyses did not recover the two groups of *dorsalis* to be reciprocally monophyletic ([Palacios-Mosquera et al. 2020](#)). The linear and geometric morphometric analyses showed that populations of *chocoensis* and *dorsalis* are statistically significantly different, with individuals of *dorsalis* being smaller than *chocoensis*. However, *chocoensis* and *dorsalis* occur in sympatry in several localities in Colombia in the departments of Boyacá, Cundinamarca, Meta, Santander, and Valle del Cauca ([Velazco and Gardner 2009](#); [Palacios-Mosquera et al. 2020](#)), precluding their recognition as subspecies of *P. dorsalis*. We found that the difference in skull size and shape between the two groups is associated with elevation, suggesting that this species exhibits an altitudinal clinal variation, with populations of *chocoensis* (larger individuals) being distributed in lowland habitats and *dorsalis* (smaller individuals) in mid to high elevations habitats. Both groups, *chocoensis* and *dorsalis*, exhibit some external and craniodental differences (see below). Furthermore, the linear and geometric morphometric analyses did not reveal the existence of secondary sexual variation among populations of *P. dorsalis* or its groups (this study; [Palacios-Mosquera et al. 2020](#)).

Our results also do not support the recognition of subspecies in *P. umbratus*. As in *P. dorsalis*, the genetic analyses did not recover the two groups of *umbratus* to be reciprocally

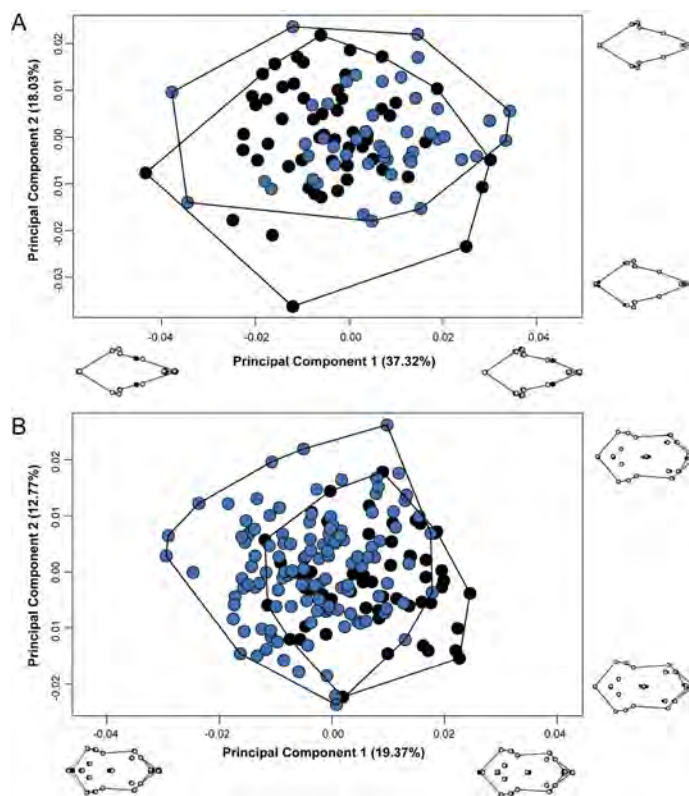


Figure 5. Principal Component Analysis (PCA) of *Platyrrhinus umbratus* obtained from the (A) dorsal and (B) ventral views of the cranium. Specimens of each group is represented by a dot (*nigellus*: black; *umbratus*: blue).

ally monophyletic ([Velazco et al. 2018](#)). The geometric morphometric analyses showed that populations of *nigellus* and *umbratus* are statistically significantly different, with individuals of *umbratus* being larger than *nigellus*. This indicates that *P. umbratus* tend to be larger in the northern part of their range, suggesting that this species exhibits a latitudinal clinal variation. Both groups exhibit some external and craniodental differences (see below). Furthermore, the linear and geometric morphometric analyses did not reveal the existence of secondary sexual variation among populations of *P. umbratus* or its groups (this study; [Velazco et al. 2018](#)).

Our findings indicate that the features used to delineate subspecies within *P. dorsalis* and *P. umbratus* were not phylogenetically relevant but rather represented geographical variation along a cline. Clinal variation in bats has been subject of debate and it has been reported in several neotropical species such as *Myotis nigricans* ([Moratelli et al. 2013](#)), *M. albescens* ([Moratelli and Oliveira 2011](#)), *Anoura cultrata* ([Nagorsen and Tamsitt 1981](#)), *Carollia perspicillata* and *Artibeus lituratus* ([Castillo-Figueroa 2022](#)) among others. Nevertheless, its presence in morphology along environmental gradients must be interpreted with caution, due to the taxonomy of many groups may be heavily impacted by this phenomenon.

Taxonomy. Based on the results of this contribution and other articles (e. g., [Velazco and Gardner 2009](#); [Velazco et al. 2018](#); [Palacios-Mosquera et al. 2020](#)) we present a revised taxonomy of *Platyrrhinus dorsalis* and *P. umbratus*.

Platyrrhinus dorsalis (Thomas, 1900)*Synonyms*

Vampyrops dorsalis Thomas, 1900:269. Type locality: "Paramba, [Imbabura,] N. Ecuador. Alt. 1,100 m."

Platyrrhinus chocoensis Alberico and Velasco, 1991:238. Type locality: Quebrada El Platinerio, 12 km W Istmina (by road), Department of Chocó, Colombia.

Distribution. *Platyrrhinus dorsalis* occurs at elevations from sea level to above 2,000 m from southern Panama southward into Colombia and along both slopes of the Andes in Ecuador.

Diagnosis. Lowland populations assigned to *chocoensis* are medium-size bats (FA [forearm length] 46.9–50.7 mm; CIL [condyloincisive length] 24.3–26.6 mm; Velazco and Gardner [2009]: table 3) characterized by a pale brown dorsal coloration, brownish and bicolored ventral fur; well-marked folds in the pinnae; fossa on the squamosal end of the zygomatic arch lateral to the glenoid fossa absent or almost imperceptible; styler cusp on the lingual face of the M2 metacone absent; only the labial cingulid present on the second lower premolar; and stylid cusp between the metaconid and protoconid of the m2 usually absent. In contrast, mid to high elevation populations assigned to *dorsalis* are medium-size bats (FA 46.6–49.5 mm, CIL 24.1–26.3 mm; Velazco and Gardner [2009]: table 3) characterized by a dark brown dorsal coloration, brownish and tricolored ventral fur; poorly marked but distinguishable folds in the pinnae; deep fossa on the squamosal end of the zygomatic arch lateral to the glenoid fossa; styler cusp on the lingual face of the M2 metacone present; both labial and lingual cingulids present on the second lower premolar; and stylid cusp between the metaconid and protoconid of the m2 present.

Remarks. Linear morphometric analyses did not reveal secondary sexual variation among populations of *chocoensis* or *dorsalis* (Palacios-Mosquera *et al.* 2020). The PCA showed that populations of *chocoensis* and *dorsalis* form two clusters in morphospace (Palacios-Mosquera *et al.* 2020: fig. 2), with individuals of *chocoensis* being larger than *dorsalis*. Molecular analyses recovered specimens of *chocoensis* nested within a larger clade that included specimens only of *dorsalis* (Palacios-Mosquera *et al.* 2020).

Platyrrhinus umbratus (Lyon, 1902)*Synonyms*

Vampyrops umbratus Lyon, 1902:151. type locality: "San Miguel," La Guajira, Colombia.

Vampyrops oratus Thomas, 1914:411. type locality: "Galifari, Sierra del Avila, [Distrito Federal] N. Venezuela. Alt. 6500' " [emend to "Galipán (10° 33' N, -66° 54' W, 1,980 m), Cerro Ávila, 5.7 km NE Caracas, Vargas, Venezuela"].

Vampyrops nigellus Gardner and Carter, 1972:1. type locality: "Huanhuachayo (12° 44' S, -73° 47' W), about 1,660 m, Departamento de Ayacucho, Peru."

Distribution. *Platyrrhinus umbratus* occurs at elevations from 400 m to above 3,150 m in the Andean and Caribbean Mountain systems of Venezuela and Colombia, and along the Andes in Ecuador, Peru, and Bolivia.

Diagnosis. Southern and some northern populations (*nigellus*) of the species are medium-size bats (FA 40.6–48.0 mm, CIL 21.9–25.2 mm; Velazco and Gardner [2009]: table 4) characterized by a tricolored ventral fur; densely haired fringe on the edge of the uropatagium; postorbital process absent or poorly developed; M1 protocone moderately developed; styler cusp on the lingual face of the M2 metacone absent; m2 hypoconid absent; and stylid cusp between the metaconid and protoconid of the m2 present. In contrast, northern populations (*umbratus*) of the species are medium-size bats (FA 42.0–47.8 mm, CIL 23.4–25.1 mm; Velazco and Gardner [2009]: table 4) characterized by a bicolored ventral fur; margin of the uropatagium usually hairy, sometimes sparsely haired; postorbital process moderately developed; M1 protocone well developed; styler cusp on the lingual face of the M2 metacone present; m2 hypoconid present; and stylid cusp between the metaconid and protoconid of the m2 absent.

Remarks. Analyses of linear measurements of *nigellus* populations did not reveal secondary sexual variation among populations (Velazco and Solari 2003). Linear morphometric analyses recovered a high overlap between specimens of *nigellus* and *umbratus*, indicating similarities in size and shape (Velazco *et al.* 2018). Molecular analyses recovered specimens of *nigellus* and *umbratus* clustering together, forming non monophyletic groups (Velazco *et al.* 2018). Ecological niche modeling analyses found that the potential distributions of *umbratus* and *nigellus* in the geographic space were highly similar, suggesting that both groups exhibit broadly overlapping climatic niches with no ecological differentiation (Velazco *et al.* 2018).

Acknowledgments

The following curators and collection staff graciously provided access to specimens under their care: B. D. Patterson and J. Phelps (FMNH), J. E. Castillo (IavH), Y. Muñoz-Saba (ICN), C. Callou (MNHN), V. Pacheco (MUSM), P. Myers (UMMZ), A. L. Gardner and S. C. Peurach (USGS Biological Survey Unit – USNM), and O. Murillo García (UV). Lastly, we thank J. Esselstyn, editor of this volume, and two anonymous reviewers whose comments improved the final draft of our manuscript.

Literature cited

- ADAMS, D. C., *ET AL.* 2021. Geomorph: Software for geometric morphometric analyses. R package version 4.0.2. <https://cran.r-project.org/web/packages/geomorph/index.html>
- ALBERICO, M. S., AND E. VELASCO. 1991. Description of a new broad-nosed bat from Colombia. *Bonner Zoologische Beiträge* 42:237-239.
- BAKEN, E. K., *ET AL.* 2021. Geomorph v4.0 and gmShiny: enhanced analytics and a new graphical interface for a compre-

- hensive morphometric experience. *Methods in Ecology and Evolution* 12:2355-2363.
- BASANTES, M., ET AL. 2020. Systematics and taxonomy of *Tonatia saurophila* Koopman & Williams, 1951 (Chiroptera, Phyllostomidae). *ZooKeys* 915:59-86.
- BOOKSTEIN, F. L. 1997. *Morphometric tools for landmark data: geometry and biology*. Cambridge University Press, Cambridge, U.S.A.
- BURGIN, J. B., ET AL. 2018. How many species of mammals are there? *Journal of Mammalogy* 99:1-14.
- CAMACHO, M. A., D. CHAVEZ, AND S. F. BURNEO. 2016. A taxonomic revision of the Yasuni Round-eared bat, *Lophostoma yasuni* (Chiroptera: Phyllostomidae). *Zootaxa* 4114:246-260.
- CASTILLO-FIGUEROA, D. 2022. Does Bergmann's rule apply in bats? Evidence from two neotropical species. *Neotropical Biodiversity* 8:200-221.
- COLLYER, M. L., AND D. C. ADAMS. 2018. RRPP: An R package for fitting linear models to high-dimensional data using residual randomization. *Methods in Ecology and Evolution* 9:1772-1779.
- COLLYER, M. L., AND D. C. ADAMS. 2022. RRPP: Linear model evaluation with randomized residuals in a permutation procedure version 1.2.3. <https://cran.r-project.org/web/packages/RRPP>
- ESQUIVEL, D. A., ET AL. 2022. Multiple lines of evidence unveil cryptic diversity in the complex *Lophostoma brasiliense* (Chiroptera: Phyllostomidae). *Systematics and Biodiversity* 20: 2110172.
- GARBINO, G. S. T., B. K. LIM, AND V. C. TAVARES. 2020. Systematics of big-eyed bats, genus *Chiroderma* Peters, 1860 (Chiroptera: Phyllostomidae). *Zootaxa* 4846:1-93.
- GARDNER, A. L., AND D. C. CARTER. 1972. A new stenodermine bat (Phyllostomatidae) from Peru. *Occasional Papers of the Museum of Texas Tech University* 2:1-4.
- KELLY, R. M., R. FRIEDMAN, AND S. E. SANTANA. 2018. Primary productivity explains size variation across the Pallid bat's western geographic range. *Functional Ecology* 32:1520-1530.
- LYON, M. W., JR. 1902. Description of a new bat from Colombia. *Proceedings of the Biological Society of Washington* 15:151-152.
- MÉNDEZ-RODRÍGUEZ, A., ET AL. 2021. Genetic introgression and morphological variation in Naked-back bats (Chiroptera: Mormoopidae: *Pteronotus* species) along their contact zone in Central America. *Diversity* 13:194.
- MOLINARI, J., ET AL. 2017. A new polytypic species of yellow-shouldered bats, genus *Sturnira* (Mammalia: Chiroptera: Phyllostomidae), from the Andean and coastal mountain systems of Venezuela and Colombia. *Zootaxa* 4243:75-96.
- MORATELLI, R., AND J. A. D. OLIVEIRA. 2011. Morphometric and morphological variation in South American populations of *Myotis albescens* (Chiroptera: Vespertilionidae). *Zoologia (Curitiba)* 28:789-802.
- MORATELLI, R., ET AL. 2013. Review of *Myotis* (Chiroptera, Vespertilionidae) from northern South America, including description of a new species. *American Museum Novitates* 3780:1-36.
- NAGORSEN, D., AND J. R. TAMSITT. 1981. Systematics of *Anoura cultrata*, *A. brevirostrum* and *A. werckleae*. *Journal of Mammalogy* 62:82-100.
- PALACIOS-MOSQUERA, L., ET AL. 2020. Systematics and taxonomy of *Platyrrhinus chocoensis* (Chiroptera: Phyllostomidae) based on morphometric and genetic analyses: implications for biogeography and conservation. *Mammalian Biology* 100:113-124.
- PATTEN, M. A. 2015. Subspecies and the philosophy of science. *The Auk* 132:481-485.
- PAVAN, A. C., ET AL. 2021. On the taxonomic identity of *Pteronotus davyi incae* Smith, 1972 (Chiroptera: Mormoopidae). *American Museum Novitates* 3966:1-23.
- ROHLF, F. J. 2001. TPSdig32, version 3.31. Geometric morphometric software. <http://www.sbmorphometrics.org/index.html>.
- SIMMONS, N. B. 2005. Order Chiroptera. Pp. 312-529, in *Mammal species of the world, a taxonomic and geographic reference*, 3rd ed. (WILSON, D. E., AND D. M. REEDER, eds.). Johns Hopkins University Press, Baltimore, U.S.A.
- SIMMONS, N. B., AND A. L. CIRRANELLO. 2020. Bat species of the world: a taxonomic and geographic database. <https://bat-names.org/>. Accessed May 20, 2022.
- TAVARES, V. C., ET AL. 2022. Historical DNA of rare Yellow-eared bats *Vampyressa* Thomas, 1900 (Chiroptera, Phyllostomidae) clarifies phylogeny and species boundaries within the genus. *Systematics and Biodiversity* 20: 2117247.
- THOMAS, O. 1900. Descriptions of new Neotropical Mammals. *Annals and Magazine of Natural History*, series 7, 5:269-274.
- THOMAS, O. 1914. Four new small mammals from Venezuela. *Annals and Magazine of Natural History*, series 8, 14:410-414.
- VELAZCO, P. M. 2005. Morphological phylogeny of the bat genus *Platyrrhinus* Saussure, 1860 (Chiroptera: Phyllostomidae) with the description of four new species. *Fieldiana Zoology (new series)* 105:1-53.
- VELAZCO, P. M., AND A. L. GARDNER. 2009. A new species of *Platyrrhinus* (Chiroptera: Phyllostomidae) from western Colombia and Ecuador, with emended diagnoses of *P. aquilus*, *P. dorsalis*, and *P. umbratus*. *Proceedings of the Biological Society of Washington* 122:249-281.
- VELAZCO, P. M., L. GUEVARA, AND J. MOLINARI. 2018. Systematics of the broad-nosed bats, *Platyrrhinus umbratus* (Lyon, 1902) and *P. nigellus* (Gardner and Carter, 1972) (Chiroptera: Phyllostomidae), based on genetic, morphometric, and ecological niche analyses. *Neotropical Biodiversity* 4:118-132.
- VELAZCO, P. M., AND B. K. LIM. 2014. A new species of broad-nosed bat *Platyrrhinus* Saussure, 1860 (Chiroptera: Phyllostomidae) from the Guianan Shield. *Zootaxa* 3796:175-193.
- VELAZCO, P. M., AND B. D. PATTERSON. 2008. Phylogenetics and biogeography of the broad-nosed bats, genus *Platyrrhinus* (Chiroptera: Phyllostomidae). *Molecular Phylogenetics and Evolution* 49:749-759.
- VELAZCO, P. M., AND S. SOLARI. 2003. Taxonomy of *Platyrrhinus dorsalis* and *Platyrrhinus lineatus* (Chiroptera: Phyllostomidae) in Peru. *Mastozoología Neotropical* 10:303-319.
- VELAZCO, P. M., ET AL. 2021. Mammalian Diversity and Matses Ethnomammalogy in Amazonian Peru. Part 4: Bats. *Bulletin of the American Museum of Natural History* 451:1-200.
- VENABLES, W. N., AND B. D. RIPLEY. 2002. *Modern Applied Statistics with S*, Fourth edition. Springer, New York, U.S.A.
- ZELDITCH, M. L., D. L. SWIDERSKI, AND H. D. SHEETS. 2012. *Geometric morphometrics for biologists: a primer*. Elsevier Academic Press, Boston, U.S.A.

Associated editor: Jake Esselstyn and Giovani Hernández Canchola
 Submitted: July 11, 2022; Reviewed: August 12, 2022
 Accepted: October 26, 2022; Published on line: January 27, 2023

Appendix 1

List of *Platyrrhinus dorsalis* and *P. umbratus* voucher specimens used in the geometric morphometric analyses and their associated localities. Collection acronyms are provided in the material and methods section.

Platyrrhinus dorsalis [*chocoensis*] ($n = 122$) — COLOMBIA: **Chocó** (IAvH 3316; UV 3645, 3647, 3648, 3817–3823, 7446, 7447, 7449, 10100–10103, 11289, 11302, 11310, 11332). **Nariño** (USNM 309018). **Valle del Cauca** (MNHN_CG 1989-1; USNM 339395, 339396, 483533–483552, 483554–483567, 483569–483572; UV 281, 972, 2153, 2162–2164, 2167, 2287–2291, 2294, 2810–2812, 3183–3185, 3707–3709, 4257, 4259, 5566–5575, 5748–5751, 5754, 5755, 10539, 10540). PANAMA: **Darién** (USNM 309601–309616).

Platyrrhinus dorsalis [*dorsalis*] ($n = 62$) — COLOMBIA: **Cauca** (IAvH 3313; UV 2165). **Chocó** (UV 4559–4561, 4571, 4575, 7448, 10034, 10035, 10837). **Cundinamarca** (ICN 8742). **Meta** (UV 3851). **Nariño** (UV 2942, 2943, 2947, 2948, 2950, 2953–2955, 2957, 3050, 3052–3055). **Quindío** (IAvH 7040). **Risaralda** (UV 2519). **Santander** (ICN 17502, 17503, 17583). **Valle del Cauca** (UV 806, 1243, 3419–3423, 3521, 3523, 3528, 7175, 7177, 7178, 7180, 7529, 7530, 10578–10580, 10833–10835, 11223, 11224, 11701, 11728, 11952, 12110, 12239, 12305).

Platyrrhinus umbratus [*nigellus*] ($n = 63$) — BOLIVIA: **La Paz** (UMMZ 127174). COLOMBIA: **Boyacá** (ICN 15066). **Cauca** (IAvH 3315). **Cesar** (FMNH 69484). **Cundinamarca** (ICN 5293). **Huila** (IAvH 3311). **Meta** (ICN 14800). **Norte de Santander** (IAvH 6631–6637, 6672, 6678, 6685, 6689, 6702, 6704, 6710, 6715, 6719, 6722, 6734, 6739). **Putumayo** (IAvH 6819, 6825). **Quindío** (ICN 12442, 12448). **Risaralda** (ICN 11934). **Santander** (ICN 8972, 17585–17587). **Valle del Cauca** (UV 12243, 12302, 12304, 12306, 12522, 12559). ECUADOR: **El Oro** (USNM 513465). **Pastaza** (USNM 548189, 548190, 548192, 548194). PERU: **Cuzco** (FMNH 93589, 93592, 93593, 93595–93597, 93599, 93600, 93604, 93606; MUSM 8857, 8858, 8860, 9975). **Madre de Dios** (MUSM 9955). **San Martín** (MUSM 7295, 7296).

Platyrrhinus umbratus [*umbratus*] ($n = 129$) — COLOMBIA: **Chocó** (UV 4149, 4150, 4152). **Cundinamarca** (ICN 5292, 5294, 5537, 5538). **Magdalena** (ICN 5388–5391). **Meta** (UV 3850). **Risaralda** (UV 2517, 2520). **Santander** (ICN 6695–6697). **Valle del Cauca** (UV 769, 1234). VENEZUELA: **Aragua** (USNM 370514, 370515, 517465, 517466). **Carabobo** (USNM 440651–440656). **Distrito Capital** (USNM 370407–370416, 370418, 370429, 370431–370433, 370435–370440, 370442–370444, 370446, 370447, 370452–370456, 370462, 370470, 370472, 370473, 370478, 370480–370492, 370494, 370500–370511, 372128, 408559, 408560, 408562–408564, 562985). **Mérida** (USNM 373837–373839, 387110–387114, 387117, 387118, 387129, 387132, 387137, 387138). **Miranda** (USNM 387126–387128, 387134–387136, 387139–387141; UV 11468). **Mona-gas** (USNM 408566–408568). **Trujillo** (USNM 373834–373836). **Yaracuy** (USNM 440647).

Taxonomic reassessment of the Little pocket mouse, *Perognathus longimembris* (Rodentia, Heteromyidae) of southern California and northern Baja California

JAMES L. PATTON^{1*}, AND ROBERT N. FISHER²

¹ Museum of Vertebrate Zoology, 3101 Valley Life Sciences Building, University of California, Berkeley, CA 94720, USA. Email: patton@berkeley.edu.

² U.S. Geological Survey, Western Ecological Research Center, 4165 Spruance Road, Suite 200, San Diego, CA 92101, USA. Email: rfisher@usgs.gov.

* Corresponding author: <https://orcid.org/0000-0002-8709-7196>.

The Little pocket mouse (*Perognathus longimembris*) encompasses 15 to 16 currently recognized subspecies, six of which are restricted to southern California and adjacent northern Baja California. Using cranial geomorphometric shape parameters and dorsal color variables we delineate six regional groups of populations from this area that we recognize as valid, but these differ in name combination and geographic range from the current taxonomy. We resurrect two names from their current placement in synonymies, synonymize two currently recognized subspecies, and we reassign a third. Importantly, we restrict the U. S. Federally endangered Pacific pocket mouse (*P. l. pacificus* Mearns) to the vicinity of its type locality at the mouth of the Tijuana River in the southwestern corner of San Diego County and resurrect *P. l. cantwelli* von Bloeker for the other two population segments along the coast, those that span the northwestern corner of San Diego County and adjacent Orange County and that in coastal Los Angeles County. The name *cantwelli* would now apply to the only extant populations of the Pacific pocket mouse, a reassignment with obvious management implications. Our taxonomic decisions also reconfigure the ranges of other subspecies of conservation concern, notably *P. l. bangsi* Mearns and *P. l. brevinasus* Osgood.

Para el ratón de abazones menor (*Perognathus longimembris*) se tienen reconocidas quince o dieciséis subespecies, de las cuales seis de ellas tienen una distribución restringida al sur de California y la parte colindante del norte de Baja California. Haciendo uso de parámetros geométricos de la forma craneal y variables en la coloración dorsal, delimitamos y reconocimos como válidos seis grupos regionales de poblaciones, los cuales difieren en el nombre y área geográfica de su actual clasificación taxonómica. Reincorporamos dos nombres de las actuales sinonímias, combinamos dos subespecies que se encuentran actualmente reconocidas y reasignamos una tercera. Es importante destacar que para el ratón de abazones menor (*P. l. pacificus* Mearns), que se encuentra en peligro de extinción a nivel federal de E.U.A., restringimos su distribución a la vecindad de su localidad tipo en la boca del Río Tijuana, localizada en la esquina suroeste de San Diego County. Asimismo, reincorporamos a la subespecie *P. l. cantwelli* von Bloeker a los otros dos segmentos de la población a lo largo de la costa, abarcando la esquina noroeste de San Diego County, colindante con Orange County y la costa de Los Angeles County. El nombre *cantwelli* ahora se aplicaría a las únicas poblaciones del ratón de bolsillo del Pacífico, un reasignamiento con notorias implicaciones en su manejo. Nuestras decisiones taxonómicas también incluyen la reconfiguración en los rangos de otras subespecies que son preocupantes para la conservación, como lo son *P. l. bangsi* Mearns y *P. l. brevinasus* Osgood.

Keywords: Biogeography; colorimetrics; geomorphometrics; management; taxonomy; *aestivus*; *arenicola*; *bangsi*; *brevinasus*; *bombycinus*; *cantwelli*; *internationalis*; *pacificus*.

© 2023 Asociación Mexicana de Mastozoología, www.mastozoologiamexicana.org

Introduction

The Little pocket mouse, *Perognathus longimembris* Coues, occupies desertscrub habitats throughout the Great Basin, Mojave, Colorado, and western parts of the Sonoran deserts in western North America (Hall 1981). It also has a very limited occurrence in the California Floristic Province (CFP) along the Pacific coast in California (Cooper 1869). Intra-specific taxonomy has not been reviewed across the entire range since Osgood (1900); the only treatments subsequent to the last subspecies description (Hall 1941) are those for taxa occurring within Nevada (Hall 1946), Utah (Durrant 1952), and Arizona (Hoffmeister 1986). Of the 22 nominal taxa assigned to the species, recent taxonomic synopses have recognized either 15 (Patton 2005) or 16 (Williams et al. 1993; Hafner 2016) as valid, treating the remainder as

synonyms. A thorough review of the species using modern morphological and molecular approaches is long overdue and also the subject of a larger review of the complex by one of us (JLP and collaborators).

Herein we examine the morphological disparity of Little pocket mice in one relatively small area of the species' range, that across southern California and adjacent northern Baja California. In part, our treatment serves as a companion to available mitochondrial DNA views of population diversity across this same region (Swei et al. 2003). It also, hopefully, will serve as a taxonomic guidepost for population-level genomic studies now initiated by researchers at the San Diego Zoo Wildlife Alliance (Wilder et al. 2022) and the University of California Museum of Vertebrate Zoology, through the California Conservation Genomics Project

(<https://www.ccgproject.org/>) and a refocus on taxa and areas of conservation concern for coordinated management decisions at the local, state, and federal levels.

Our area of interest includes six currently recognized subspecies: *aestivus* Huey, *bangsi* Mearns, *bombycinus* Osgood, *brevinasus* Osgood, *internationalis* Huey, and *pacificus* Mearns. This number represents 37.5 to 40 % of the valid infraspecific taxonomic diversity within *P. longimembris* but represents only about 10 % of the total species' range (approximately 22,000 mi² compared to 213,000 mi²). Despite the small encompassing area, high taxonomic diversity across this region is perhaps not surprising, as was found in a larger analysis of mammal "evolutionary hotspots" in California (Davis *et al.* 2008). Both ecological and topographic diversity are extreme, with five (of the 17) California ecoregions and four (of 11) geomorphic provinces included all or in part. The area also includes the only U.S. federally endangered pocket mouse (the Pacific pocket mouse, *P. l. pacificus* Mearns), now limited to only two small areas along the central coast in Orange and San Diego counties, and three of five other subspecies listed by the California Department of Fish and Wildlife as State Species of Special Concern, with a rank of S1 (Critically Imperiled) or S2 (Imperiled; [CNDDDB 2022](#)).

Two of our six target taxa (*pacificus* Mearns and *bombycinus* Osgood) were originally described as distinct species and two were arranged under different specific epithets (*arenicola* Stephens and *brevinasus* Osgood allocated, as subspecies, to *P. panamintinus* Merriam); [Williams *et al.* \(1993\)](#) included all within their concept of *P. longimembris*. These authors also placed *arenicola* Stephens (following [Grinnell 1913, 1933](#) and [Huey 1928](#)) and *cantwelli* von Bloeker (following [Huey 1939](#) and [Hall 1981](#)) as junior synonyms of *bangsi* Mearns and *pacificus* Mearns, respectively. Of the six taxa [Williams *et al.* \(1993\)](#) treated as valid (*pacificus* Mearns, *bangsi* Mearns, *brevinasus* Osgood, *bombycinus* Osgood, *aestivus* Huey, and *internationalis* Huey), these authors regarded only *internationalis* as of equivocal validity. While California samples along the lower Colorado River are currently assigned to *bombycinus* Osgood (see [Grinnell 1913, 1914, 1933](#); [Hall 1981](#); and [Williams *et al.* \(1993\)](#)), the type locality of this taxon is Yuma, Yuma County, Arizona, on the opposite bank. This river forms the dividing line between multiple subspecies and sister species of heteromyid and other rodents (e. g., [Grinnell 1914](#); [Hoffmeister and Lee 1967](#); [Riddle *et al.* 2000](#)).

Diversity among population samples of *P. longimembris* across the area has been examined, at least limitedly, by morphological and molecular characters. Over 80 years ago, [Huey \(1939\)](#), for example, compared adult specimens of all forms named above and provided tables of mensural character data, but his analyses were limited by small sample sizes, geographic coverage, and analytical scope. He noted (p. 49), however, while "an ultimate revision of the group" was required that "such a work is, owing to the considerable amount of material yet to be gathered, still in the distant

future." At the molecular level, [Swei *et al.* \(2003\)](#) showed that mitochondrial DNA diversity, while extensive within local populations, failed to recover any phylogeographic lineage structure among geographic samples assigned to *pacificus* Mearns, *bangsi* Mearns, *brevinasus* Osgood, and *internationalis* Huey. Species-wide mitochondrial data now available (JLP, unpublished data) place the California populations allocated to *bombycinus* Osgood within the same mitochondrial group as those reported by [Swei *et al.* \(2003\)](#) yet indicate that this group of subspecies differs from topotypic and other samples of *bombycinus* across the lower Colorado River in Arizona. Unfortunately, no molecular data are yet available for *aestivus* Huey.

Huey's "distant future" is today. The population-level genomic studies mentioned above will undoubtedly inform important issues of demographic history while identifying areas of isolation and/or genetic connectedness among extant populations. Eventually, these studies may also identify the underlying genetic basis for key morphological characters we describe below and provide a window into the role that selection has played in generating that diversity. We include analyses that center on colorimetric as well as standard mensural data of the skin and skull, to allow comparison to the limited published studies, and expand cranial analyses by using two-dimensional geometric morphometric approaches to delineate explicit shape differences. Our goal is to describe disparity among available population samples for each of the six taxa in our study area, to assess if the current taxonomy actually reflects geographically defined patterns of character variation, and to inform conservation understanding and management decisions if not.

Materials and methods

We examined a total of 721 museum specimens, of which we digitized 672 intact, adult skulls from 123 separate localities. These we grouped into 20 geographic samples (map, Figure 1; Appendix 1 provides provenance and catalog numbers) based on preliminary analyses that assigned nearby small samples into larger non-significant subsets as determined by oneway ANOVA and Tukey-Kramer post hoc tests. Seven of these samples comprise only the holotype (*pacificus* Mearns, 1898 [USNM 61022], *bangsi* Mearns, 1898 [MCZ 5304; incorrectly listed as AMNH 5304 in [Williams *et al.* \(1993\)](#), *arenicola* Stephens, 1900 [USNM 99828], *brevinasus* Osgood, 1900 [USNM 186515], *aestivus* Huey, 1928 [SDNHM 6110], *cantwelli* von Bloeker, 1932 [MVZ 74680], and *internationalis* Huey, 1939 [SDNHM 11971]) and topotypes of each of the nominal taxa that have been described from our study area. We initially allocated samples to recognized subspecies following range limits given by [Grinnell and Swarth \(1913\)](#) and [Grinnell \(1933\)](#) rather than by [Williams *et al.* \(1993\)](#), who assigned specimens from San Geronio Pass (Banning east to Cabazon) to *P. l. brevinasus* not *P. l. bangsi*. We treated specimens from localities not included within each sample (black circles in Figure 1) as unknown.

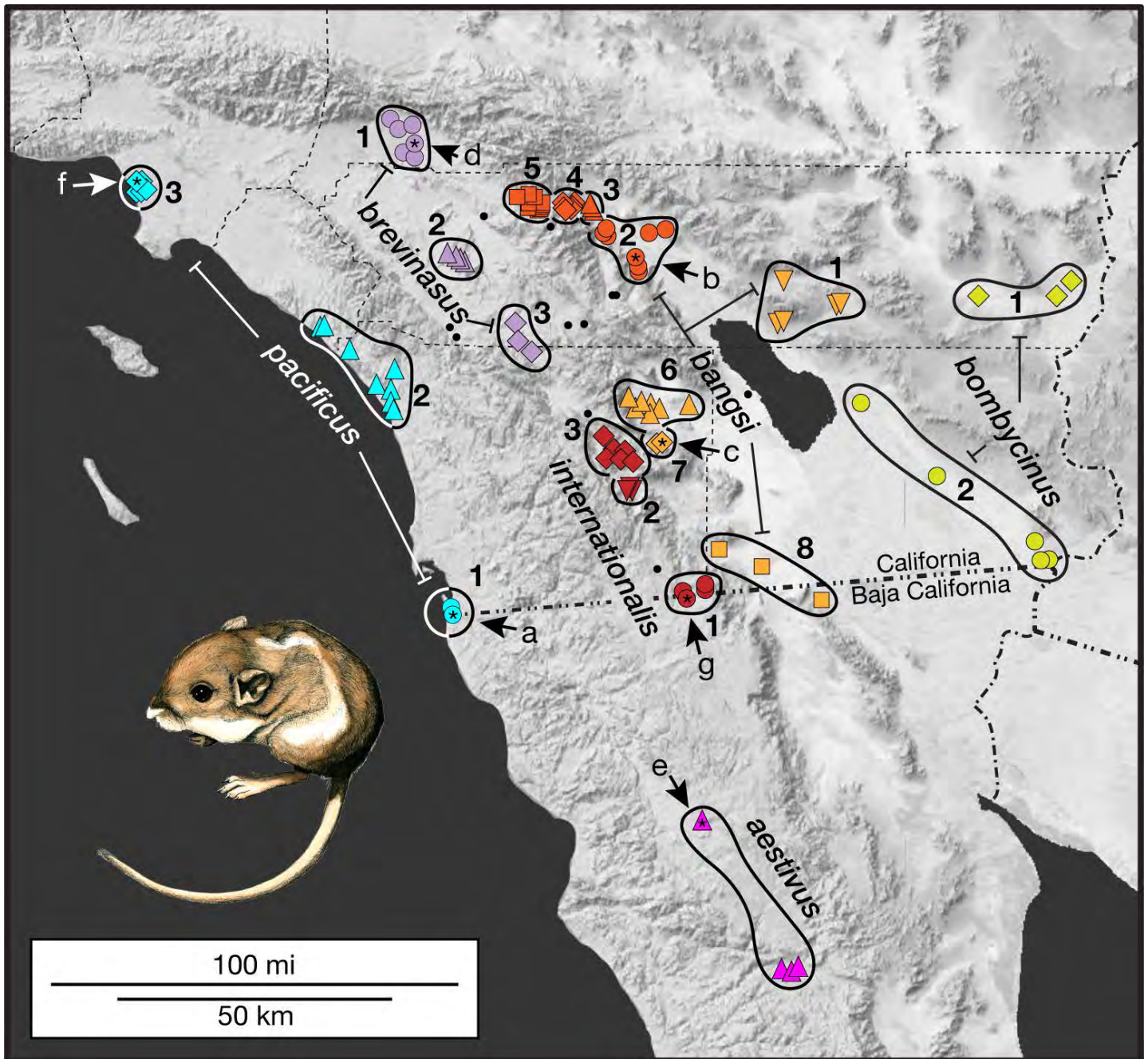


Figure 1. Individual localities allocated to 20 regional samples of *Perognathus longimembris* across southern California and northern Baja California, color coded by subspecies allocation, and population within subspecies by symbol shape. Small black circles are localities with few, mostly singleton, specimens treated as unknown in canonical variate analyses. Arrows and asterisks identify the type locality of each of the seven named taxa allocated to *P. longimembris* in this area (listed by date and page priority: a = *pacificus* Mearns, b = *bangsi* Mearns, c = *arenicola* Stephens, d = *brevinasus* Osgood, e = *aestivus* Huey, f = *cantwelli* von Bloeker, g = *internationalis* Huey). Inset drawing of a Pacific pocket mouse by Tristan Edgarian.

Age criteria. We categorized age classes by maxillary tooth wear similar to the scheme employed by Hoffmeister (1986: Figure 5.131) for Arizona samples of *P. longimembris*, respectively: age class 0 – deciduous premolar 4 still in place or, if gone, permanent PM4 has not reached the molar occlusal plane; age class 1 – PM4 has reached occlusal plane of molar series but all cusps lack evidence of wear; age class 2 – cusps of PM4 and M1-M3 exhibit wear but remain separate or, if partially coalesced, have not unified into complete transverse lophs; age class 3 – cusps of posteroloph of PM4 and anterior and posterior lophs of M1 and M2 have coalesced into separate lophs that remain uncon-

nected on their lingual boundary; age class 4 – anterior cusp of PM4 has coalesced with the posteroloph, lophs of M1-M3 are connected at their lingual border; and age class 5 – the occlusal surface of all teeth are “dished”, with enamel present only around the tooth’s border (occlusal patterns for age classes 2-5 are illustrated in Figure 2c).

Age classes 0 and 1 are considered to be juvenile animals based on porous auditory bullae and unfused basi-cranial sutures; age class 0 individuals are uniformly still in juvenile pelage and, for those specimens for which necropsy data are available, had not attained sexual maturity (i.e., females with thin and translucent uteri and males with

very small, non-vascularized testes). Age class 1 individuals varied from still in juvenile pelage, in molt, or already with adult pelage; available necropsy data indicate that none had reached reproductive maturity. All specimens in age classes 2 through 5 had adult pelage and, especially in spring months, nearly all specimens with necropsy data exhibited signs of present or recent reproductive activity (females with enlarged, swollen uteri, embryos present, or embryo scars visible; males with enlarged, scrotal, and vascularized testes, and enlarged vesicular glands).

Non-geographic variation. To examine sex and age effects, we performed generalized least squares analyses of the 32 linear distance measurements for adult specimens of two samples: pacificus-1 (type and topotypes of *pacificus* Mearns; $n = 66$) and pacificus-3 (type and topotypes of *cantwelli* von Bloeker; $n = 78$). Application of Bonferroni corrections for multiple comparisons yielded no detectable sexual dimorphism nor significant interaction terms in either sample; significant age effects were found for four variables (nasal length, zygomatic breadth, upper incisor breadth, and mesopterygoid width) only in the pacificus-1 sample (Appendix 2). As a result, we combined sexes and ages in all analyses.

Cranial morphological character sets. We photographed the dorsal and ventral aspects of each skull examined using a Nikon D3200 or Nikon D850 digital camera fitted with AF-S AV Micro Nikkor 105 mm lens. Establishing a common plane for all photographed skulls is essential, whether photographs are used to calculate traditional linear measurements or digitized landmarks for geometric morphometrics. To maintain planar uniformity across specimens, we used a bubble level placed on the camera viewfinder and the platform upon which the skull was placed. For the dorsal view, the ventral surfaces of the bullae and the incisor tips established a common 3-point plane. A common plane for the ventral surface was more difficult to establish, as skulls were too small to use a bubble level laid across the molar rows, for example, and the age-related flattening of the dorsal profile made positioning each skull in a consistent position difficult. We thus placed each skull on a bit of putty and positioned the toothrows to a horizontal plane by eye. Damaged skulls that precluded digitizing all landmarks or accurate measurements, such as those with chipped incisors or broken parts, were excluded.

We digitized 28 landmarks (LM) on the dorsal surface of the skull and 25 on the ventral surface (Figure 2a, b) using the on-line XYOM-CLIC module (<http://xyom-clic.eu/>; [Dujardin and Dujardin 2019](#)). Most landmarks were Type 1 in [Bookstein's \(1991\)](#) terminology – those where the intersection of bony sutures is locally defined; others conform to Type 2 as per Bookstein – those defined, for example, by the tip of a structure (dorsal LM 9, L26) or bulge (LM 6). In addition, we placed 21 semilandmarks (SL) along the lateral border of the auditory capsule, nine SL with uniform spacing between LM 13 and 14 along the edge of the epitympanic portion and 12 between LM 14 and 15 on the edge of the mastoid portion.

We then used MorphoJ, version 1.07a ([Klingenberg 2011](#); available at https://morphometrics.uk/MorphoJ_page.html) to generate matrices of Procrustes coordinates, or residuals, that result from superimposition, and principal components of the set of Procrustes residuals (or relative warp scores). MorphoJ uses the latter in canonical variate comparisons of a priori defined samples and to compute matrices of Mahalanobis distances among them. We also used MorphoJ to construct wireframes (sets of lines linking landmarks in a predetermined configuration) and deformation grids to visualize shape changes among taxon samples.

We also took 20 linear measurements from the dorsal surface, including the area (mm^2) of the bullar capsule, and 12 measurements from the ventral surface from each skull photograph using ImageJ, version 1.46r ([Abramoff et al. 2004](#); [Schneider et al. 2012](#); available at <http://imagej.nih.gov/ij/download.html>). ImageJ measurements were given to three decimals; these we rounded to two places, which is consistent with repeated measures of the same variable. Dorsal variables included: occipital-nasal length (1-ONL – midline distance from distal tip of ex-supraoccipital to anterior tip of nasal bones); nasal length (2-NL – midline length of nasal bones); frontal length (3-FL – midline length of frontal bones); parietal length (4-PL – midline length of parietal bones); interparietal length (5-IPL – midline length of interparietal bone); premaxilla tip length (6-premax-ExtL – midline measurement from the distal nasal bones to a line tangential to the two distal premaxillary extensions); rostral width (7-RW – width across the anterior rostrum at the nasal-premaxillary boundary); maxillary width (8-MW – width across the posterior rostrum at the maxillary-premaxillary boundary); premaxillary extension width (9-premax-tipW – width across the most distal portion of the premaxillary distal extensions); interorbital constriction (10-IOC – least width across the interorbital region); zygomatic breadth (11-ZB – maximum width across the zygomatic arches); anterior parietal width (12-antParietalW – maximum width of the parietal bones at their suture junction with the frontal and squamosal elements); anterior interparietal width (13-IPW-ant – maximum width taken at the suture junction with the parietal and ex-supraoccipital); posterior interparietal width (14-IPW-post – maximum width taken across the posterior corners of the interparietal); ex-supraoccipital width (15-exOccW – width across the exposed ex-supraoccipital elements); bullar width (16-bullarW – maximum width across the two bullae); bulla length (17-bullaL – maximum length from the anterior portion of the epitympanic and posterior portion of the mastoid portions); bulla width (18-bullaW – perpendicular width across the left bulla from the epitympanic-mastoid junction to the inner border with the ex-supraoccipital and parietal); bulla perimeter (19-bulla perimeter – the distance of a line circumscribing the left bulla); bulla area (20-bulla area – calculated for the area circumscribed by bulla perimeter, in mm^2). Ventral variables included: anterior nasal extensions (21-anterior border of the upper incisors to the tip of the nasal bones); palatal length (22-posterior border of upper incisors to anterior end of mesopterygoid fossa);

mesopterygoid length (23-anterior end of fossa to a line tangential to the posterior end of the hamular processes); foramen magnum length (24-midline measurement); maxillary tooththrow length (25-alveolar length from upper premolar to third molar), incisor breadth (26-alveolar distance from the lateral margins of the incisors); palatal breadth (27-width across outside of maxilla between first and second molars); squamosal width (28-distance between the squamosal extensions); distal width of mesopterygoid (29-across the end of the hamular processes); stylomastoid foramina width (30-across the two stylomastoid foramina), occipital condyle width (31-across the distal ends of each condyle); ex-supraoccipital width (32-distance between the lateral projections of left and right ex-supraoccipital bones). External measurements of total length (TOL), tail length (TAL), hindfoot length, including claw (HF), and ear length, from notch (E) were taken from specimen labels; we calculated head-and-body length (HBL) by subtracting TAL from TOL.

We obtained dorsal and ventral landmark datasets for all digitized specimens of each taxon, although the final number in each differs slightly after removal of outliers. Sample sizes for ventral measurements were often smaller than those from the dorsum due to damaged structures (e.g., the hamular processes). In general, we employed linear variables primarily for comparisons to previously published studies that reported differences in cranial dimensions or to test character differences identified in diagnoses of taxa when initially described or subsequently compared.

Dorsal color measurement. Of the 721 specimens examined, 565 had preserved skins. These we photographed to obtain measures of the three Commission internationale de l'éclairage (CIE) color variables L^* (lightness, measured on a scale from 0 [= black] to 100 [= diffuse white]), a^* (the position on the color spectrum between red/magenta and green [negative values indicate green while positive values indicate magenta]), and b^* (the position on the color spectrum between yellow and blue [negative values indicate blue and positive values indicate yellow]). To obtain these values, we first took photographs of the dorsal aspect of each skin at a distance of 25 cm using a Nikon DX SWM micro 1:1 lens and under standard lighting conditions at 4600°K; each photograph was then manipulated to yield an approximate uniform white background with $L^* = 90$, $a^* = 0$, and $b^* = 1$. We then recorded, and averaged, color values at three points along the mid-dorsum from each specimen using the Lab Color Mode in Adobe PhotoShop CC™ (Adobe Systems Inc., San Jose, California). Since pelage color at any spot on the dorsum is variable due to a mixture of dark brown or black intertwined with yellow, individual measurements were an average of a 5 x 5 pixel area.

We converted values of a^* and b^* to C^* (chroma, or relative saturation, which is measured on a scale from 0 to 100), as the square root of $a^{*2} + b^{*2}$, and h° (hue, or angle of the hue in the CIELab color wheel), measured as the arctangent of (b^*/a^*). A red hue is at 0°, yellow at 90°, green at 180°, and blue at 270°, with orange, yellow-green, cyan, and magenta at 45°, 135°, 225°, and 315°, respectively).

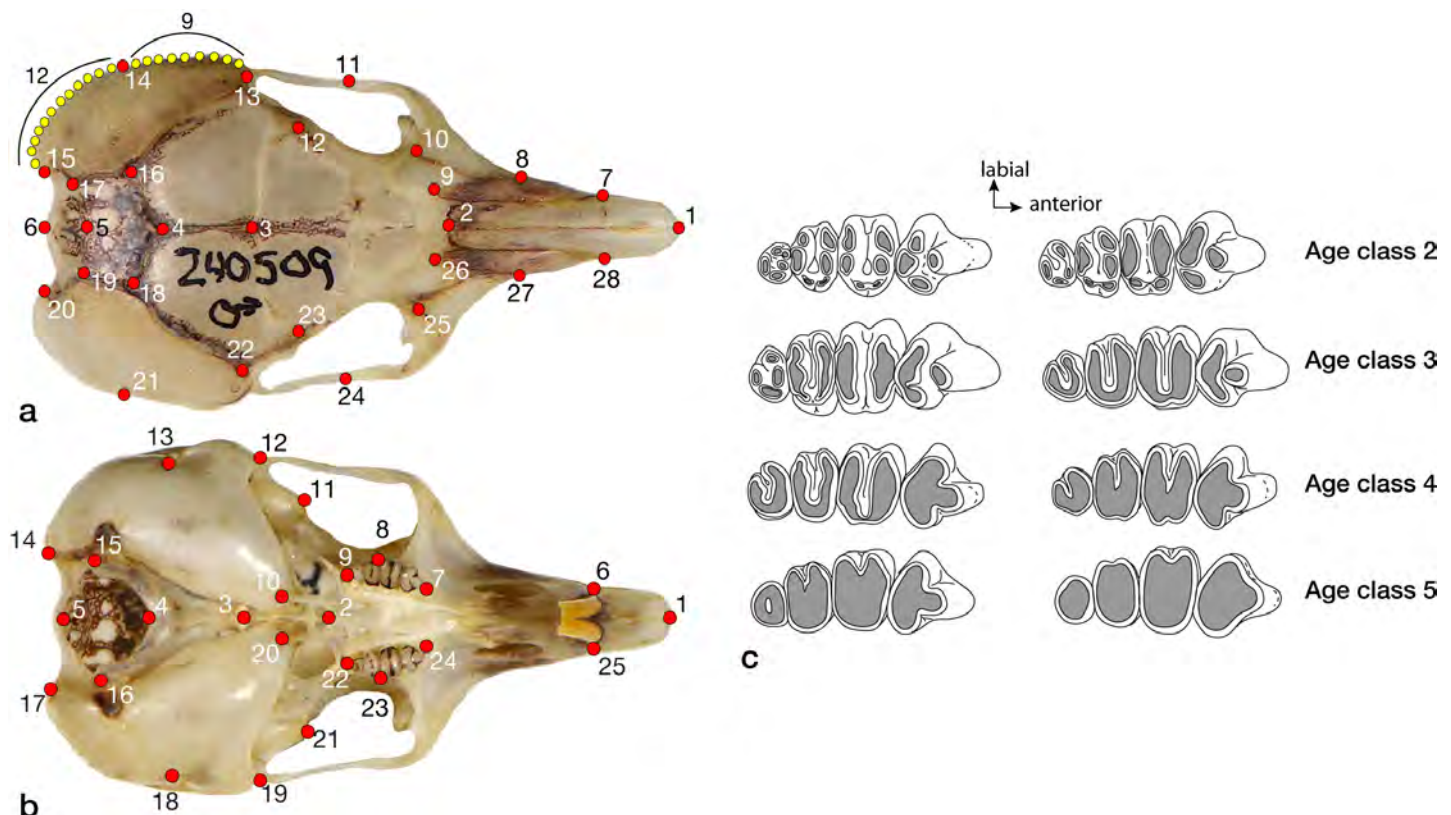


Figure 2. (a) Dorsal view of a skull of *Perognathus longimembris* (MVZ 240590; from East Stone Cabin Valley, Nye Co., Nevada) illustrating the position of 28 dorsal landmarks (LM – red circles) and the 21 semilandmarks (SL – yellow circles) that define the outer margin of the epitympanic (9 SL, black arc) and mastoid (12 SL, black arc) portions of the auditory bulla; (b) ventral view of the same skull with the positions of the 25 ventral landmarks indicated; and (c) maxillary tooththrow occlusal surface wear age classes.

Statistical procedures. We performed all multivariate analyses of landmark-semilandmark coordinates in MorphoJ but used JMP Pro16™ (SAS Institute Inc., Cary, North Carolina) for univariate character or multivariate specimen score comparisons among samples for morphometric and colorimetric data. We used oneway ANOVAs followed by Tukey-Kramer pairwise post hoc tests (with Bonferroni corrected *P*-values for multiple comparisons) in all comparisons of samples to delimit non-significant sample subsets. We also used the hierarchical clustering routine in JMP Pro16, with the Ward algorithm, to generate dendrograms from matrices of sample Mahalanobis distances and the canonical variates routine to obtain posterior probabilities for assignment for unknown specimens, those not allocated a priori to one of the 20 samples. The latter provided an unbiased assessment of each specimen phenetic relationship to a priori samples based on posterior probabilities of assignment. As multivariate ordinations of dorsal and ventral landmark datasets yielded similar patterns of sample dispersion in multivariate space, we present only those derived from the dorsal landmarks and semilandmarks. We performed all MorphoJ canonical analyses with permutation tests for pairwise distances with 10,000 iterations. The LSID for this publication is: urn:lsid:zoobank.org:pub:83CCE2F4-CE8C-4DB7-8116-50C83DA819F2.

Results

We begin by using the 32 linear variable dataset to examine character differences among the seven samples, which include the respective holotype and set of topotypes, or near-topotypes, of each nominal taxon in our study area. Here we wish only to evaluate the univariate characters used in the original descriptions or subsequent reviews upon which the current taxonomy has been based. We then examine disparity among all 20 samples mapped in Figure 1 and follow with analyses focused on more limited geographic areas where multivariate patterns of sharp transition are indicated in the global analysis. For these we employ only the dorsal landmark data since, as noted above, both dorsal and ventral landmark data illustrated the same ordination of samples. As we are interested in the phenetic relationships among samples, we only present results from canonical variates analyses.

Cranial characteristics of type and topotypic series. There are seven nominal taxa whose type localities are within the geographic area of our study (*aestivus* Huey, *arenicola* Stephens, *bangsi* Mearns, *brevinasus* Osgood, *cantwelli* von Bloeker, *internationalis* Huey, and *pacificus* Mearns), each within a separate sample (*aestivus*, *bangsi*-7, *bangsi* 2, *brevinasus*-1, *pacificus*-3, *internationalis*-1, and *pacificus*-1, respectively) that also contain the type series (if identified in the original description) and subsequently collected topotypes.

Earlier comparisons among these taxa centered on body and cranial size as well as the degree of mastoid bulla expansion with concomitant changes in lateral width of

the interparietal and ex-supraoccipital bones. A few other cranial elements are mentioned in some accounts (for example, length and breadth of the nasals, or rostrum, and interorbital region), but these are limited to specific pairs of taxa and have not been reviewed across them all. In these limited comparisons, however, the series representing *pacificus* Mearns are uniformly stated to be exceedingly small in body and skull, darker in dorsal color, and with much smaller mastoid bullae, much wider interparietals, shorter rostra or nasals, and wider interorbital regions. In contrast, the series representing *aestivus* Huey is notable for being larger in body and cranial size, with much larger and inflated mastoid bullae that give a greater width to the posterior skull while compressing the interparietal into an almost equal-sided pentagon (e. g., Huey 1928). The other taxa fall varyingly with intermediate character states between the extremes represented by *pacificus* and *aestivus*.

Huey (1939:49) noted “structurally, there is found to be an entirely different trend of development” among the taxa he examined. Specifically, in contrasting samples from the coast and interior valleys through this region, he wrote “forms living nearest the ocean, such as *pacificus* near the shores of the Pacific and *bombycinus* ... near the shores of the Gulf of California, have the smallest skulls. In fact, the mice themselves are the smallest members of the species. Those occupying the mountain areas are larger and show generally increasing size from north to south. The maximum size of the cranium is found in the specimens of *aestivus*, which occupies the western slopes of the Sierra Juarez and eastern end of El Valle de la Trinidad... Similarly, in the case of altitude, it is found that the greater the elevation, the greater the development of the bullae.”

These general observations are upheld in our comparisons among the type-topotypic series, as evidenced by the minimally non-significant sample subsets for external and selected cranial variables, along with character means, standard errors, and sample sizes provided in Appendix 3. In external characters, Mearns’ *pacificus* is the smallest in total length (mean = 119.64 mm), but Huey’s *aestivus* is largest only in hind foot length (mean 18.83 mm). There is, however, less uniformity among those cranial characters identified by describers and reviewers in the separation of these taxa. Both *pacificus* and *cantwelli* do have the smallest skulls (mean ONL = 19.83 and 19.76 mm, respectively; not significantly different from one another) with especially small bullae, but significantly smaller from one another (mean bulla perimeter = 17.32 and 16.61 mm); the interparietal of *pacificus* is especially wide (mean IPW-ant = 3.85 mm) but that of *cantwelli* is not (mean 3.55 mm). Conversely, *aestivus* does possess the largest skull (mean ONL = 21.57 mm) and largest bullae (mean bulla perimeter = 21.44 mm), significantly so, but shares long nasals with *bangsi* and *internationalis* (mean NL = 7.70 mm versus 7.67 and 7.57) and the narrowest interparietal with *arenicola* (both with mean IPW-ant = 3.10).

Global cranial disparity among all samples. We illustrate differences in dorsal cranial shape in Figure 3a, a biplot of canonical variate scores for the first two CVA axes. Below and to the left of these axes we present deformation grids, with vectors indicating compression or expansion of specific areas of the skull, and wireframe diagrams that compare the resulting shape differences between the most disparate samples aligned on each axis. In Figure 3b, we show the dendrogram of Mahalanobis distances among samples to illustrate hierarchical relationships among them.

The first two CV axes combine to explain 54.8 % of the total pool of variation; each additional axis explains < 8 %. Samples (Figure 3a) are ordered diagonally into three gen-

eral groups that align separately on the two axes: (1) all Colorado Desert floor samples of *bangsi* and *bombycinus* plus *aestivus*; (2), interior basin samples of *brevinasus* and *internationalis* along with *bangsi* samples from San Gorgonio Pass; and (3) coastal samples of *pacificus*. The degree of overlap among samples differs but is notably divergent for the southern (*pacificus*-1) versus central and northern samples (*pacificus*-2 and -3) of *pacificus*. Both deformation grid and wireframe diagram for CV1 emphasize the correlated expansion of the bulla and compression of the posteromedial portion of the braincase, with the *pacificus* samples sharing a small bulla and wide interparietal and ex-supraoccipital relative to desert samples of *bangsi*, *bomby-*

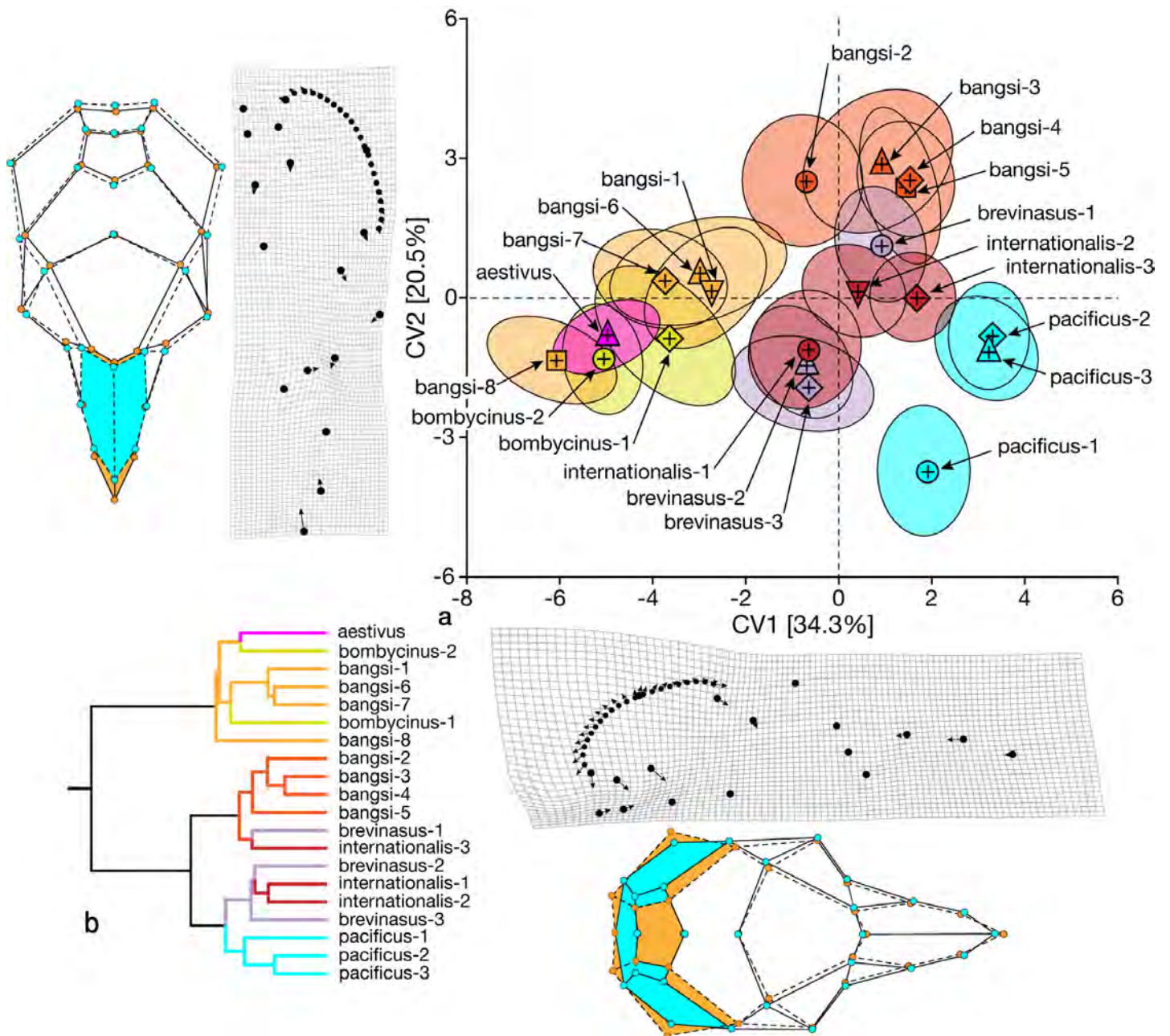


Figure 3. (a) Biplot of canonical variate scores (CV) for the first two axes of dorsal skull landmarks for all 20 samples of *Perognathus longimembris* from southern California and northern Baja California; data are presented as sample means (+) and ellipses that encompass 50 % of specimen scores. Below and to the left are deformation grids for the left side of the skull, which contains the semilandmarks conforming to the bulla perimeter, and wireframe diagrams of the entire skull, excluding the semilandmarks, with colored highlights of cranial areas of major change that compare samples from the extremes on each axis. (b) Dendrogram of Mahalanobis distances depicting hierarchical similarities among all samples. Symbols and colors are those in the map, Figure 1.

cinus, and *aestivus*. In contrast, CV2 emphasizes shape differences in the rostrum, notably contrasting the elongated nasals and narrowed distal premaxillary tips of *bangsi* samples with short nasals and wider premaxillary tips of *pacificus*. The dendrogram separates samples into the desert samples of *bangsi* (*bangsi*-1, -6, -7, and -8) and *bombycinus* plus *aestivus* versus all others. The latter is further subdivided, notably with all three *pacificus* samples grouped together, all northern *bangsi* samples (*bangsi*-2, -3, -4, and -5) grouped, and those allocated to *brevinasus* and *internationalis* split. Centroid size orders samples from largest (*aestivus*) to smallest (all three *pacificus* and the two *bombycinus* samples). Among-sample significant differences are present, but overall samples are ordered from large to small with overlapping non-significant subsets.

The combination of CV1 scores and centroid size ($\log_n CS$; Figure 4) cleanly separates those samples from the desert floor from those of the coast and interior valleys in y-intercept and slope ($z = 5.31, P < 0.001$ and $2.19, P < 0.01$). The single exception is Huey's *aestivus*, which, while occupying the western base of the Sierra Juarez in northern Baja California, shares characteristics of the desert samples. This relationship is contrary to that posited by Huey (1939:49) in his contrast of coastal and interior populations and taxa.

Cranial disparity across transition areas. Three features of the landmark analytical results deserve comment. First, morphological disparity across the entire sample area

reveals two primary groupings of samples: those of the coast, interior valleys, and San Gorgonio Pass and those of the lowland deserts to the east, including the sample from northern Baja California (Figures 3 and 4). Second, there are several geographic areas of sharp transition, both within and between these two geographically structured groups, but also among samples allocated to the same subspecies. And third, samples bordering these sharp transition areas often contain individual specimens that span the mean morphological gap, suggesting phenotypic intermediacy derived from gene flow. Here we examine more closely these transitional areas through CVA. These analyses also permit us to allocate those unknown specimens listed in Appendix 1 by their posterior probabilities to one of the included a priori samples. We organize these analyses by focusing first on transitional areas between the two primary sets of samples identified in figures 3 and 4, specifically (1) *internationalis* versus adjacent *bangsi* samples and (2) *bangsi* versus desert samples. We then consider transitional areas within each of the two global subsets, between (3) coastal *pacificus* versus interior basin *brevinasus* + *internationalis*, (4) *brevinasus* versus *bangsi* samples across San Gorgonia Pass, and (5) northern Baja California *aestivus* versus desert samples of *bangsi* + *bombycinus*. The degree of differentiation across each of these transitions will inform a concluding set of systematic decisions regarding units that warrant taxonomic recognition as well as the geographic range of each. In turn, our

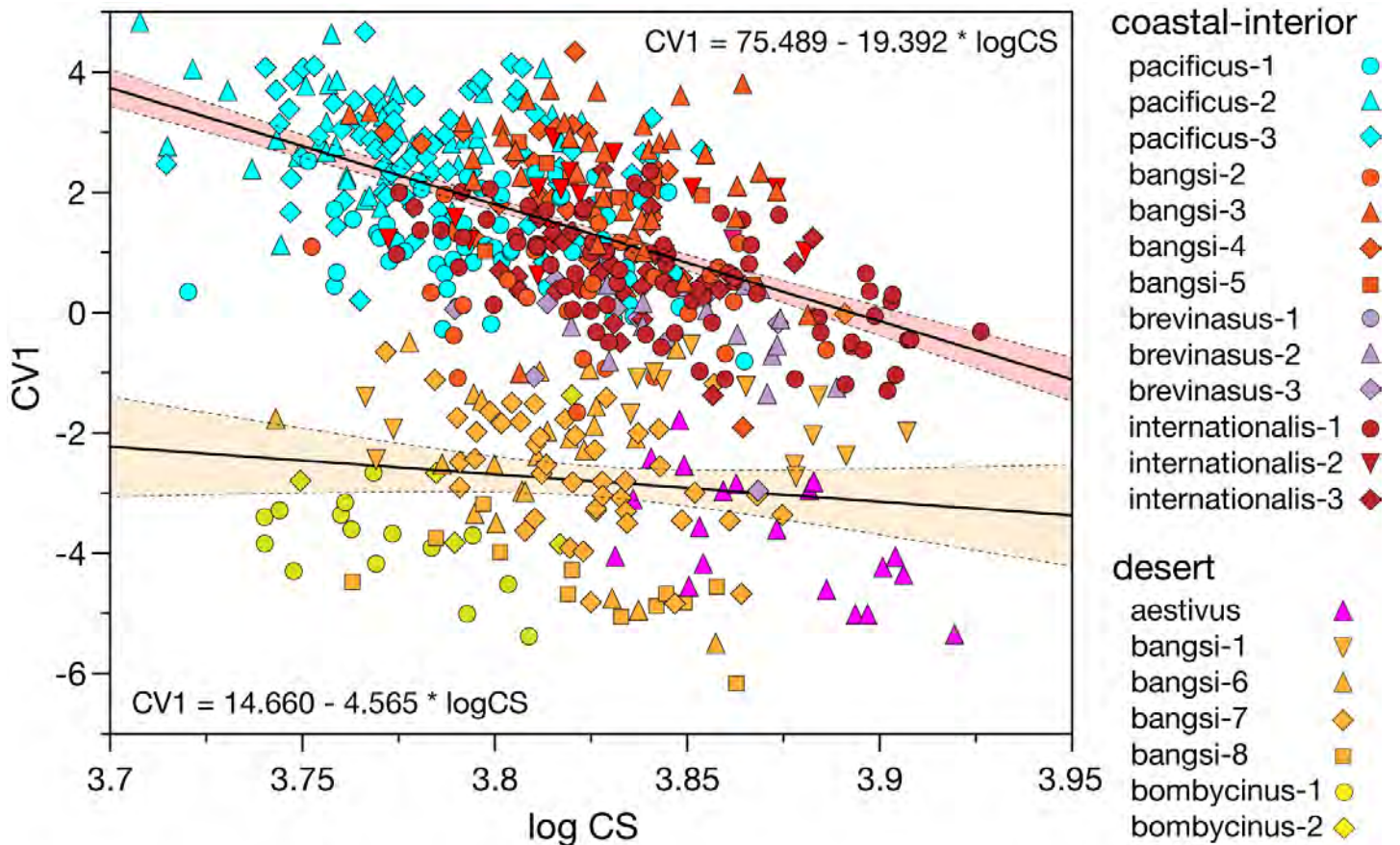


Figure 4. Plot of CV1 scores on log centroid size ($\log_n CS$) for the 20 samples of *Perognathus longimembris* depicted in Figure 3. Regression lines, with 95% confidence limits, and equations are provided. Symbols and colors are those in the map, Figure 1.

suggested taxonomic units will inform conservation status of some, notably *pacificus* and *bangsi*.

1-Southern interior valleys and adjacent desert floor. This area encompasses the phenotypic disparity among the three, southern-most *bangsi* (-6, -7, and -8) and the three *internationalis* samples that are geographically adjacent on the desert floor and interior valleys, respectively (Figure 1). We used the same approach as above, deriving CV scores from CVA in MorphoJ for those specific samples. The combination of CV1 and CV2 scores separates the two taxa on the first axis and orders within-taxon samples geographically (*bangsi* samples from north to south, *internationalis* samples from south to north) on the second (Figure 5a); these two axes combine to explain 70% of the variation. Samples of *bangsi* have a proportionally longer but posteriorly narrowed rostrum, narrowed frontal and parietal elements, and larger bullae coupled with narrowed interparietal and ex-supraoccipital bones in comparison to those of *internationalis* (see Figure 5a, wireframe diagram). Regression relationships of centroid size ($\log_n CS$) on CV1 scores separates the pooled taxon samples (Figure 5b), with significant differences in mean values, y-intercepts, and slopes. The *internationalis* samples are significantly larger in centroid size (pooled *internationalis* $\log_n CS$ mean = 3.609, pooled *bangsi*

= 3.573; oneway ANOVA $P < 0.001$); the two separate along CV1 (mean eigenvector 1.761 versus -1.952, respectively; $P < 0.001$; y-intercept (34.549 versus -16.504; $P < 0.01$); and slope -9.084 versus 4.073; $P < 0.01$).

The two northern-most *bangsi* samples, however, do broadly overlap with their geographic *internationalis* counterparts, with specimens from each spread across their respective 75% inclusion ellipses (Figure 5a). This suggests either past and/or present gene exchange between Mason Valley (*internationalis*-2) and San Felipe Valley (*internationalis*-3) with San Felipe Narrows (*bangsi*-7) and Borrego Valley (*bangsi*-6), perhaps along San Felipe Creek, which connects these areas today. In contrast, there is no overlap of 75% inclusion ellipses nor are specimens of either misplaced between the southern-most *internationalis* sample (*internationalis*-1), which contains the holotype and type series from the vicinity of Jacumba, and the few available specimens from localities in the Yuha Desert region that span the international border (*bangsi*-8). The samples of *bangsi* and *internationalis* thus become progressively more differentiated from north to south along their respective ranges.

2-San Gorgonio Pass and Colorado Desert samples. Here we examine the relationships among samples of *bangsi* Mearns (*bangsi*-1 through -8) and *bombycinus* Osgood

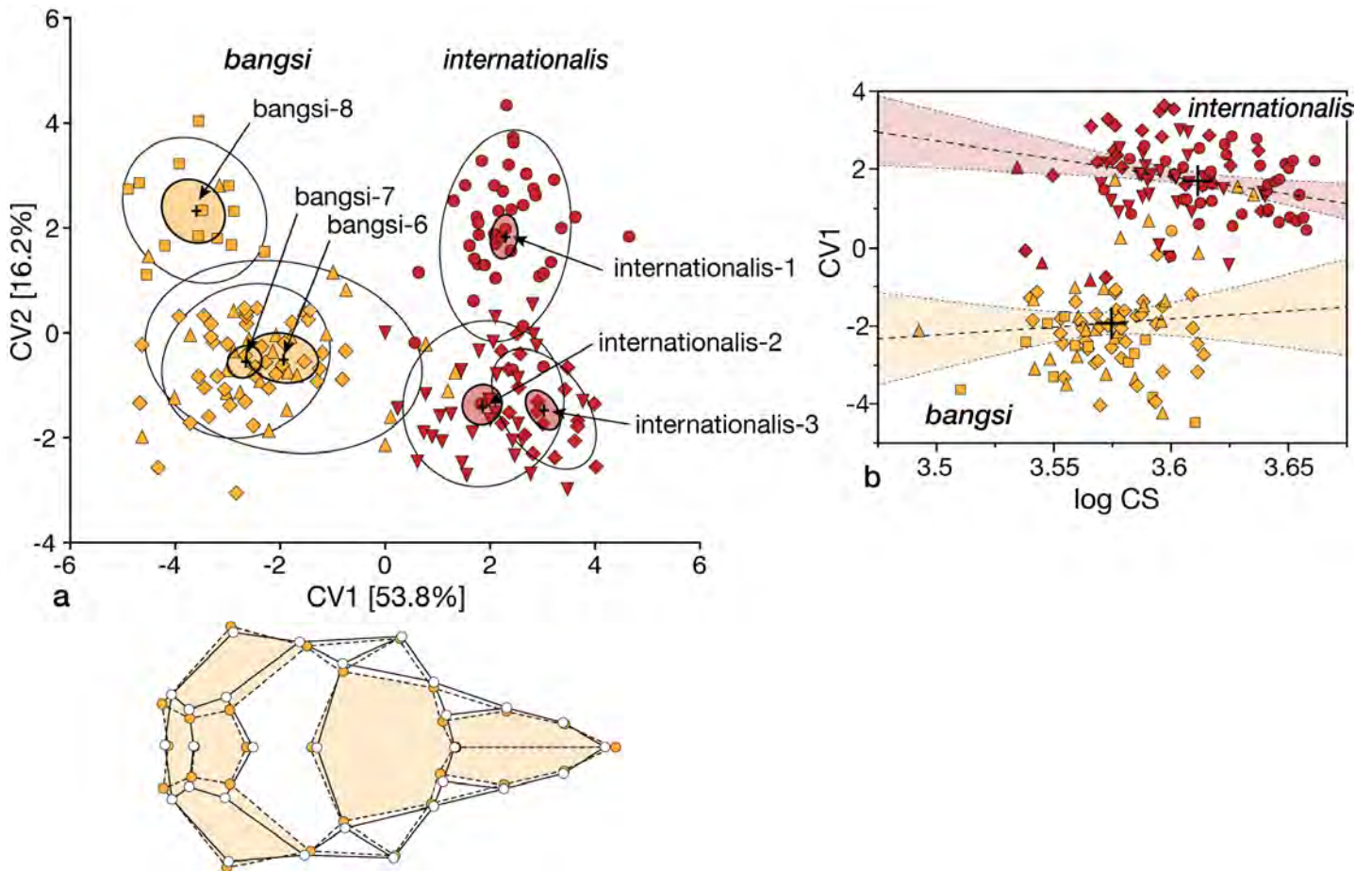


Figure 5. (a) Biplot of canonical variate scores of the first two axes of dorsal cranial landmarks for southern samples of *bangsi* and geographically adjacent samples of *internationalis*; data are presented as sample means (+) and ellipses that encompass 75% of specimen scores (open ellipses) and 95% confidence limits around the mean (colored ellipses). Below is the wireframe diagram depicting areas of dorsal cranial differentiation highlighted in color comparing *bangsi* (dashed lines, cranial elements in pale orange) with the combined *internationalis* samples (solid lines). (b) Linear regression, with 95% confidence limits, of CV1 scores on log centroid size ($\log_n CS$); large crosses indicate mean values. Symbols and colors are those in the map, Figure 1.

(*bombycinus*-1 and -2) from San Gorgonio Pass east through desertscrub vegetation on the floor of the Colorado Desert of southeastern California (Figure 1). As above, we conducted CVA and illustrate the biplot of CV1 and CV2 scores (which combine to explain 71.2 % of the total variation; note that CV1 alone explains 60.3 %) in Figure 6a. Desert floor samples of *bangsi* and *bombycinus* have much larger bullae that project distally from the occiput and, conversely, laterally compressed interparietal and ex-supraoccipital elements (Figure 6a, wireframe diagram). Regression relationships of centroid size ($\log_n CS$) on CV1 scores again separates the pooled taxon samples (Figure 6b), with significant differences in mean values, y-intercepts, and slopes. San Gorgonio Pass samples of *bangsi* are significantly larger in centroid size (pooled samples *bangsi*-2 through -5, $\log_n CS$ mean = 3.597; pooled desert samples = 3.569; oneway ANOVA $P < 0.001$); the two separate along CV1 (mean eigenvector -2.074 versus 2.547, respectively; $P < 0.001$; y-intercept (-8.695 versus 38.390; $P < 0.05$); and slope 1.840 versus -10.040; $P < 0.01$).

The ordination of samples, however, is less discrete than in the previous transition zone analysis, with broader overlap of specimens among samples from the San Gorgonio

Pass (*bangsi*-3 through -5) and the geographically adjacent type and topotype series from Palm Springs (*bangsi*-2). The *bangsi* samples on the desert floor to the immediate east (*bangsi*-1) and south (*bangsi*-6 and -7) along the desert side of the Peninsular Ranges overlap partially with the cluster of *bangsi*-2 through -5, with the two *bombycinus* from the western side of the lower Colorado River, and the *bangsi*-8 sample from the Yuha Desert region. There is broad overlap between desert floor *bangsi* (*bangsi*-1, -6, -7, and -8) and the two eastern *bombycinus* samples along the first CV axis. Despite the overlap of adjacent sample individual specimens, there remains clear separations between the northwestern *bangsi* samples (*bangsi*-2 through -5) and all samples from the floor of the Colorado Desert, with a relatively sharp transition in shape of the distal cranial elements of the bulla, interparietal, and ex-supraoccipital (Figure 6a, wireframe diagram).

3-Coastal versus interior valley samples. This analysis includes the three coastal samples (*pacificus*-1, -2, and -3) and six from interior valleys (*brevinasus*-1, -2, -3 and *internationalis*-1, -2, and 3) that separate from all desert samples further to the east across southern California (see

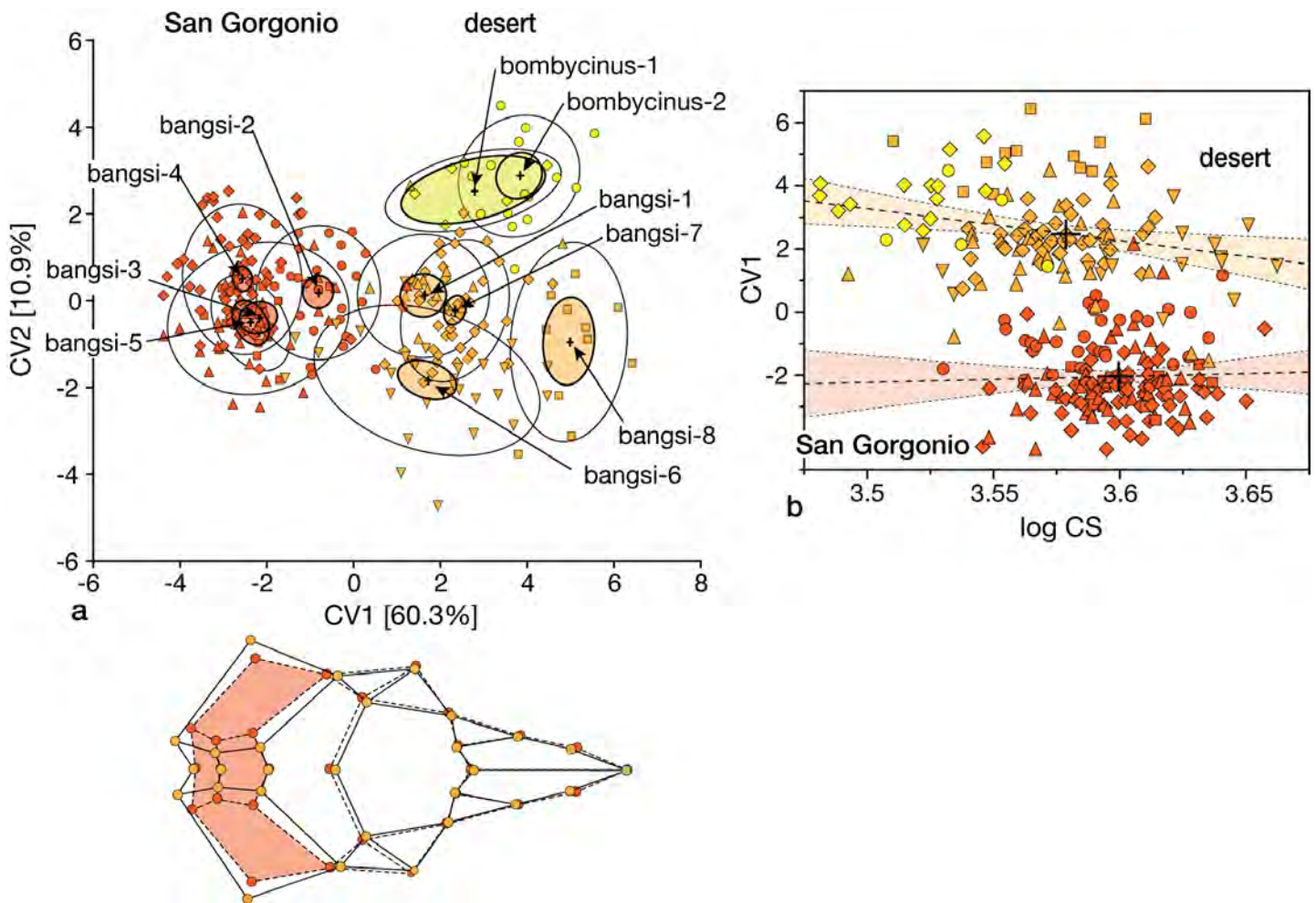


Figure 6. (a) Biplot of canonical variate scores of the first two axes of dorsal cranial landmarks for San Gorgonio Pass and lowland desert samples of *bangsi* and the desert *bombycinus*; data are presented as sample means (+) and ellipses that encompass 75 % of specimen scores (open ellipses) and 95 % confidence limits around the mean (colored ellipses). Below is the wireframe diagram depicting areas of dorsal cranial differentiation highlighted in color comparing northwestern *bangsi* (samples *bangsi*-2, -3, -4, and 5; dark orange circles, dashed lines, and orange cranial elements) with the combined desert samples of *bangsi* and *bombycinus* (pale orange circles, solid lines). (b) Linear regression, with 95 % confidence limits, of CV1 scores on log centroid size ($\log_n CS$); large crosses indicate mean values. Symbols and colors are those in the map, Figure 1.

Figure 3 and Figure 4). We again used canonical analyses to compare the nine samples and then samples pooled by subspecies allocation (Figure 1). We included all unknown specimens (Appendix 1) to determine their respective assignments in the two analyses.

The first two CVA analyses separate the three coastal samples and those from the interior valleys; for simplicity, we present data for only the 9-group analysis (Figure 7a). The first two axes are nearly equivalent in the percentage of the variation explained (32.1 and 29.1 %, respectively, or 62.2 % combined). While the ordination of samples is similar to that depicted in Figure 3, and with the same cranial features emphasized in this separation (compare wireframe in Figure 7a with that in Figure 3a), the degree of disparity in dorsal shape attributes is much less. These differences, nonetheless, do emphasize the smaller auditory bullae with the laterally expanded interparietal and ex-supraoccipital region along with the short and distally broader rostral elements of the coastal samples, *pacificus*-1, -2, and -3. Note the distinction between the *pacificus*-1 (which contains

the type of *pacificus* Mearns) and paired *pacificus*-2 and -3 samples (the latter which contains the type of *cantwelli* von Bloeker). The two samples of *pacificus* versus *brevinasus* + *internationalis* also differ in their relationship of centroid size ($\log_n CS$) and CV1 scores (Fig 7b; mean $\log_n CS$ coastal = 3.786, interior = 3.838; mean CV1 coastal = 1.483, coastal = -1.620; ANOVA $P < 0.001$ in each comparison), similar to that of the global analysis (Figure 4). In contrast, pooled samples of *brevinasus* and *internationalis* share the same means, y-intercepts, and slopes ($P > 0.05$), with each of those measures, except regression slope, differing from those values for the pooled *pacificus* samples ($P < 0.001$ in each comparison).

Assignments of unknown specimens are unambiguous. The three specimens from San Fernando, Los Angeles County (Appendix 1), are assigned to *pacificus*, specifically sample *pacificus*-3, at posterior probabilities above 0.948 in the 9-sample and pooled-taxon analyses. In contrast, all specimens from Riverside (Eden Hot Springs, Hemet, Temecula, and Vallejista) and San Diego (McCain Valley and

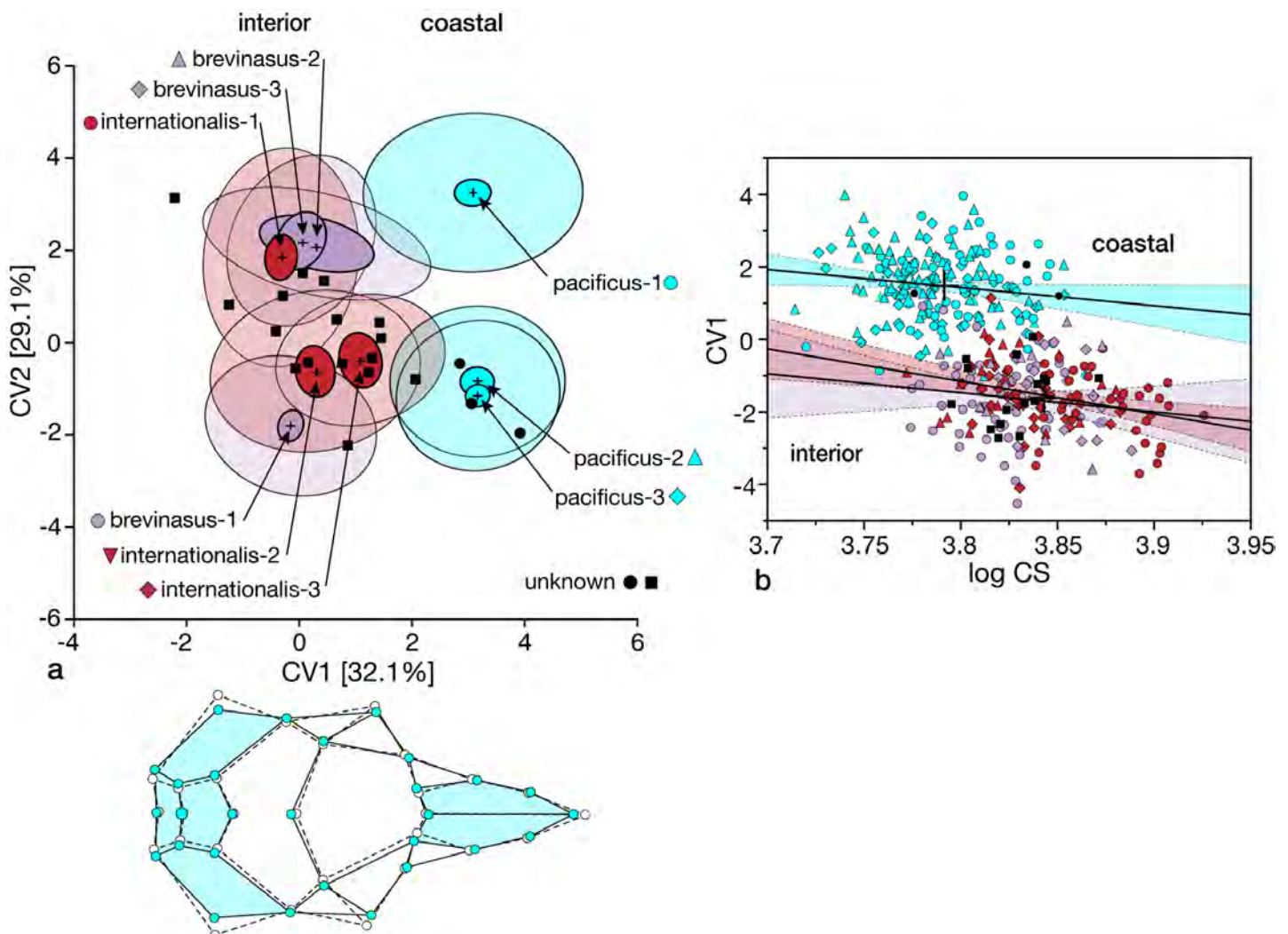


Figure 7. (a) Biplot of canonical variate scores of the first two axes of dorsal cranial landmarks for coastal *pacificus* samples and interior valley samples of *brevinasus*; data are presented as sample means (+) and ellipses that encompass 75 % of specimen scores (open ellipses) and 95 % confidence limits around the mean (colored ellipses). Below is the wireframe diagram depicting areas of dorsal cranial differentiation highlighted in color comparing *pacificus* (solid lines, elements in blue) with the combined *brevinasus* and *internationalis* samples (dashed lines). (b) Linear regression, with 95 % confidence limits, of CV1 scores on log centroid size ($\log_n CS$); large crosses indicate mean values. Symbols and colors are those in the map, Figure 1.

Warner Pass) counties are assigned to the combination of *brevinasus* and *internationalis* samples at posterior probabilities > 0.861. The placement of each is illustrated in Figure 7a, b (black circles are individuals from San Fernando assigned to *pacificus*-3; black squares are those from Riverside and San Diego counties).

The separation of the three coastal samples into two quite distinct geographic groupings was unexpected. All are currently allocated to the endangered Pacific pocket mouse (*P. l. pacificus*) yet, importantly, all three currently known localities of this mouse are located within the *pacificus*-2 sample area (two on Camp Pendleton and Dana Point), which aligns with the northern part of this subspecies range (the *pacificus*-3 sample, which contains the holotype of *cantwelli* von Bloeker) rather than with the southern-most area (*pacificus*-1 sample) where Mearns's holotype of *pacificus* was collected. We thus wished to ascertain to what degree, if any, the *pacificus*-2 sample might be divided into southern (*pacificus*-1 = *pacificus*) and northern (*pacificus*-3 = *cantwelli*) sets of individuals. We thus performed a CVA with these two sample sets as a priori groups and treated all specimens from the *pacificus*-2 sample as unknown. Only singleton specimens from either the *pacificus* ($n = 63$, Appendix 1) or *cantwelli* ($n = 78$) samples were misclassified. Among the 48 *pacificus*-2 specimens, 41 (85.4 %) were assigned to *cantwelli* at posterior probabilities > 0.70 (mean

posterior probability assignment = 0.9796). Seven specimens were assigned to *pacificus* at posterior probabilities of 0.775 or higher (mean assignment = 0.9231). All assignments to *pacificus* came from the southern-most localities in the *pacificus*-2 sample (Oceanside [3 of 26 specimens], 4 mi N Oceanside [1], Santa Margarita River [1], and Santa Margarita Ranch [2]). The four specimens from the northern-most locality of Dana Point were each assigned to *cantwelli* at posterior probabilities > 0.996.

4-San Gorgonio Pass transect. Here we examine phenetic relationships among the type and topotypic specimens of *brevinasus* from the vicinity of San Bernardino (sample *brevinasus*-1) east across San Gorgonio Pass (the three samples of *bangsi* from Banning [*bangsi*-5], Cabazon [*bangsi*-4], and then Whitewater-Snow Creek [*bangsi*-3]) plus the type and topotypic specimens of *bangsi* from the vicinity of Palm Springs (*bangsi*-2). Given differences in subspecies allocation of this set of samples by Grinnell and Swarth (1913; see also Grinnell 1933) and Williams et al. (1993), we are specifically interested where phenotypic gaps might be found.

The first two CV axes combined explain 76.4% of the variation (Figure 8a) with the *brevinasus* sample separating from the four samples from San Gorgonio Pass along the first axis and the latter ordered from east (*bangsi*-2, top) to west (*bangsi*-5, bottom) on the second axis. Skulls of the different sample sets exhibit more subtle shape differences

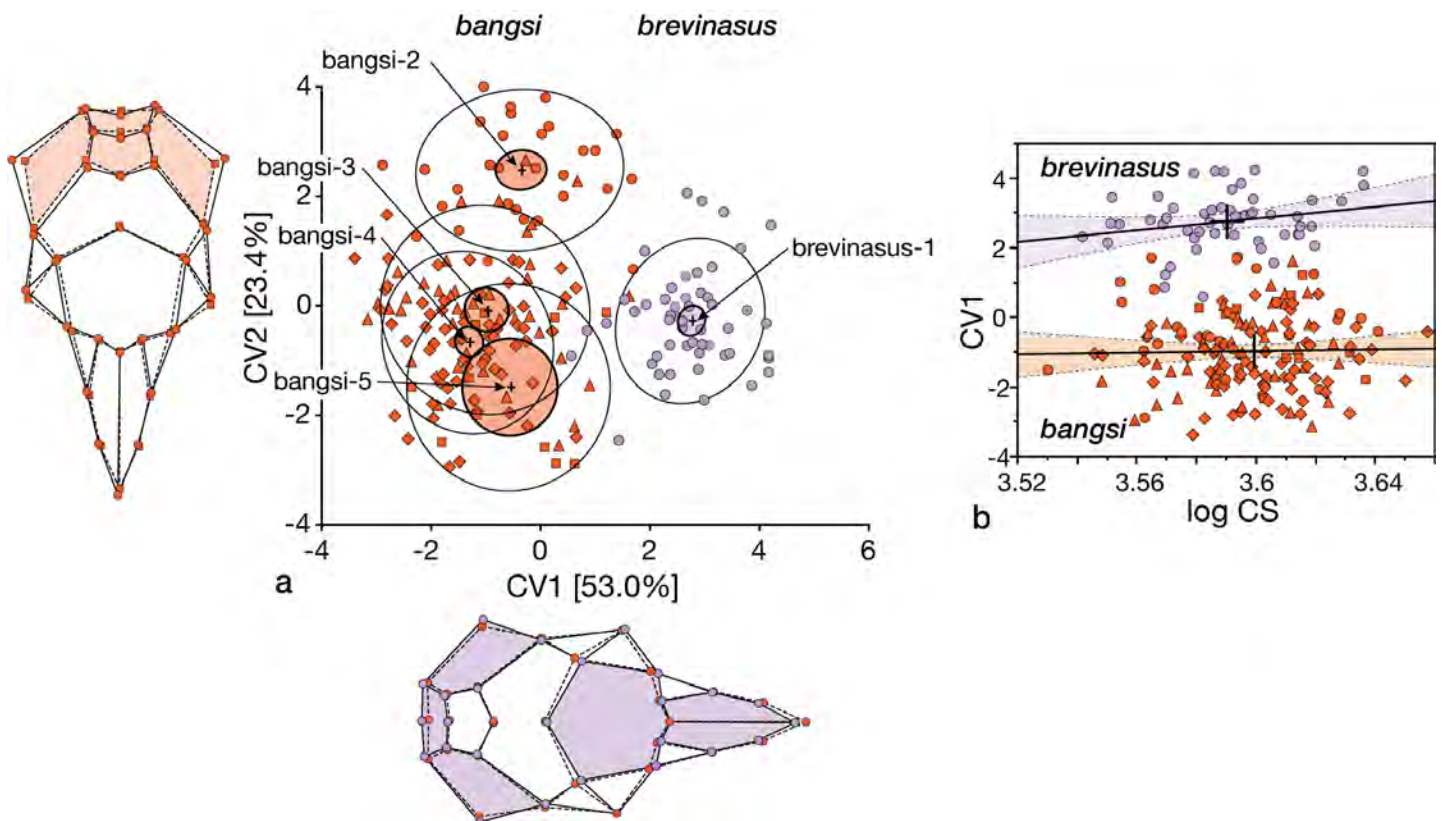


Figure 8. (a) Biplot of canonical variate scores of the first two axes of dorsal cranial landmark for *brevinasus* and *bangsi* samples west to east across San Gorgonio Pass; data are presented as sample means (+) and ellipses that encompass 75 % of specimen scores (open ellipses) and 95 % confidence limits around the mean (colored ellipses). Below is the wireframe diagram depicting areas of dorsal cranial differentiation highlighted in color comparing *brevinasus* (*brevinasus*-1; purple circles, solid lines, and colored cranial elements) with samples of *bangsi* from the Palm Springs area (*bangsi*-2) west across those within San Gorgonio Pass (*bangsi*-3, -4, and -5; orange circles and dashed lines). To the left is the wireframe comparing the *bangsi*-2 (orange circles and solid lines) sample with the other three (orange squares, dashed lines, and colored cranial elements). (b) Regression plot of CV1 scores on log centroid size ($\log_e CS$). Regression lines, with 95% confidence limits, and equations are provided. Symbols and colors are those in the map, Figure 1.

despite the separation of *brevinasus* from all four *bangsi* samples (Figure 8a, bottom wireframe diagram), with limited specimen overlap between *brevinasus* and its immediate *bangsi* neighbor from the vicinity of Banning (bangsi-5). Differences among the *bangsi* samples along CV2 separate bangsi-2 from the three samples located within San Gorgonio Pass, each geographically adjacent pair of samples with more substantial specimen overlap, mostly by changes in the posterior parts of the skull (bullae, interparietals, and ex-supraoccipitals; Figure 8a, wireframe diagram to the left), the same traits that continue the east to west trend illustrated in Figure 6a. The degree of the *bangsi* sample differences along CV2 is nearly as great as that between the two presumptive subspecies (CV1).

The relationship of centroid size ($\log_n CS$) to CV1 scores separates the sample of *brevinasus* from the pooled samples of San Gorgonio *bangsi* (Figure 8b). The *bangsi* samples are marginally larger in centroid size (pooled *bangsi* $\log_n CS$ mean = 3.598, *brevinasus* = 3.590; one way ANOVA $P = 0.03$) and the two separate along CV1 (-0.991 versus 2.764, respectively; $P < 0.001$; y-intercept (-5.253 versus -27.453; $P < 0.01$) but not in slope 8.409 versus 1.184; $P > 0.05$).

As a final comment, the type-topotypic series of *brevinasus* (sample *brevinasus*-1) do not have the shorter nasal bones implied by their name. ANOVA comparisons of the nasal length of *brevinasus*-1 with each *bangsi* sample in this transect, as well as those of *internationalis*, are universally non-significant (pairwise P -values range from 0.546 to 1.000); in comparison to *pacificus*, *brevinasus* has longer nasals, actually and proportionally ($P < 0.001$ in each comparison).

5-Relationship of *aestivus* to desert *bangsi* and *bombycinus*. This final set of comparisons focuses on the desert samples of *bangsi* and *bombycinus* plus the northern Baja California *aestivus*, those samples that collectively contrast

with coastal and interior ones in a dendrogram of among-sample Mahalanobis distances (Figure 3) and in relationships of their centroid sizes with CV1 scores (Figure 4). Huey (1928:87) diagnosed *aestivus* by its large and inflated mastoid bullae that gave it "a much greater width to the skull posteriorly and compressing the interparietal into an almost equal-sided pentagon." While Huey was certainly correct, these same traits apply to desert *bangsi* samples (the eastern-most bangsi-1 and southern bangsi-6, -7, and 8) as well as the two *bombycinus* samples. The major difference, however, is that the skulls of *aestivus* are largest, *bombycinus* are smallest, and *bangsi* samples are intermediate in size (mean \pm standard error for $\log_n CS$: *aestivus* = 3.623 \pm 0.006, pooled desert *bangsi* = 3.579 \pm 0.003, and pooled *bombycinus* = 3.529 \pm 0.006). Furthermore, *aestivus* is broader across the mastoids (bullarW mean = 12.60 mm) than either *bangsi* (range 11.87 mm [bangsi-1] to 11.58 mm [bangsi-6]) or *bombycinus* samples (11.48 mm and 11.33 mm, respectively).

The CVA comparing these seven samples provides limited resolution among them. It takes the first four axes to explain nearly 75 % of the total variation. The first three axes individually explain only 28.5, 18.8, and 15.0 %, respectively. In the biplots of CV1 and CV2 or CV1 and CV3 (Figure 9a, b), most samples align from left to right, along the first CV axis while CV2 and CV3 separate the *aestivus* and one *bangsi* (bangsi-8) samples, respectively. Other combinations of CV axes simply shuffle the positions of these two samples with respect to the core group illustrated in Figure 9 (data not shown). Overall, there is limited resolution on any pair of axes and no clear, well-supported separation among this set of samples.

Pelage color disparity. We provide means, standard errors, sample size, and non-significant sample subsets based on Tukey-Kramer pairwise comparisons in Appen-

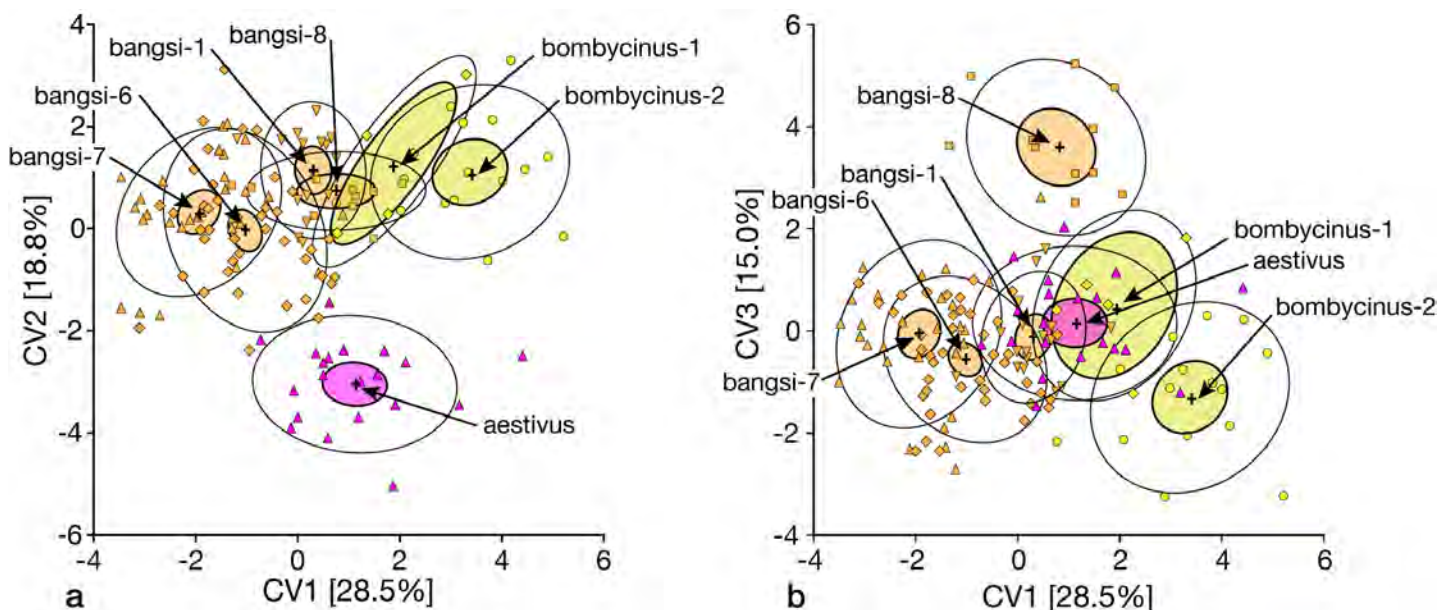


Figure 9. Biplots of canonical variate scores of dorsal cranial landmarks for lowland desert samples of *bangsi* and *bombycinus* plus the northern interior valley sample of *aestivus*; data are presented as sample means (+) and ellipses that encompass 75 % of specimen scores (open ellipses) and 95 % confidence limits around the mean (colored ellipses): A – CV1 and 2 plot; B – CV1 and 3 plot. Symbols and colors are those in the map, Figure 1.

dix 4. All three color variables (lightness, chroma, and hue) vary significantly across the sampled populations (oneway ANOVAs, $P < 0.001$ for each). Lightness varies from quite dark (mean $L^* = 13.99$ [pacificus-1]) to very pale (46.53 [bangsi-1]) and chroma is ordered in the same way, from lower (in the pacificus-1 sample, mean chroma = 9.442) to higher purity (in bangsi-1, 21.855). Hue varies only negligibly among samples (lowest for pacificus-1 [mean 1.083] and highest in bangsi-6 [1.378]), with all specimens within the red spectrum (sample descriptive statistics in Appendix 3). Overall, the *pacificus* samples differ significantly from interior and, especially, desert samples in all three attributes; visually these are easily distinguished by their very dark overall tones; interior samples are intermediate, and desert ones are distinctly lighter.

In PCA and CVA analyses, the first axis explains the vast majority of the total pool of variation (PC1 = 94.75 %; CV1 = 88.31 %), with lightness the only variable that loads significantly on each axis (PC1 eigenvalue = 0.9541 [versus -0.2996 and -0.0041] for chroma and hue, respectively; CV1 standardized scoring coefficient = 0.9867 [versus 0.0246 and 0.001]). These two multivariate methods display the same ordination of samples, whether these are determined

a posteriori (PCA) or a priori (CVA); correlation of specimen PC1 and CV1 scores = 0.998, ANOVA $P < 0.001$. Unsurprisingly, specimen lightness also predicts their individual PC1 and CV1 scores with high efficiency with correlations of 0.997 and 0.999, respectively. One does not need multivariate statistics to see, by eye, differences in pelage lightness among these samples, which we depict as box plots in Figure 10. While some samples are hampered by low numbers of available skins (notably eastern and southern desert bangsi-1 and -8, and bombycinus-1 and -2), the pattern of increasing lightness from coast to desert is obvious. Coastal samples are uniformly darkest but still separate into two significant groups, southern pacificus-1 versus central and northern pacificus-2 and -3 (Figure 10, black bars, which depict non-significant subsets based on Tukey-Kramer HSD). The color separation of these samples mirrors that of their cranial shape (Figs. 3 and 7). Interior basin samples of *brevinasus* and *internationalis*, individually and as a group, are also dark, significantly lighter than coastal *pacificus* but statistically uniform; samples of *bangsi* from west to east across the San Gorgonio Pass form a cline between darker interior and the very light desert samples. Regression of specimen L^* values for the San Gorgonio

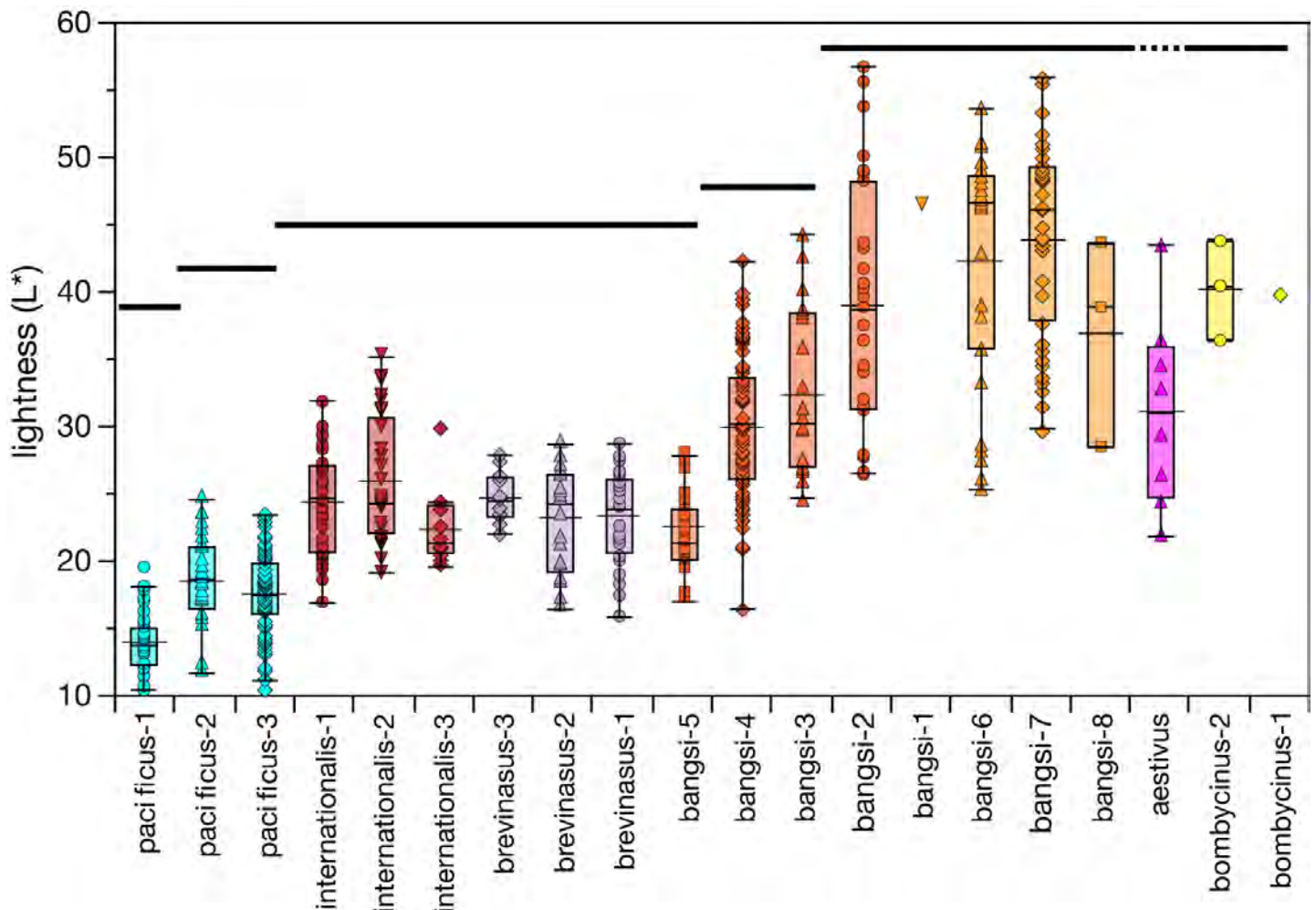


Figure 10. Box plots of pelage lightness, with means and specimen values, for samples of *Perognathus longimembris* from southern California. Samples are arranged from left to right: coastal (*pacificus*), interior valleys (*internationalis* and *brevinasus*), San Gorgonio Pass (*bangsi*, samples 2 through 5), and desert (*bangsi*, samples 1, 6, 7, and -8, *bombycinus*, and including *aestivus* from interior valleys of northern Baja California). Separate heavy lines above samples groups are non-significant subsets (oneway ANOVA, Tukey-Kramer HSD $P > 0.05$). Symbols and colors are those in the map, Figure 1.

Pass localities against longitude is significant ($R^2 = 0.307$, $df_{1,143}$, $F = 62.93$, $P < 0.001$). This observation is consistent with [Grinnell and Swarth's \(1913:360\)](#) statement that some specimens from Banning (sample bangsi-5; Figure 1) "show slightly the darkest coloration, perhaps indicating intergradation towards *brevinasus*" and, along with cranial uniformity (Figure 8), support these authors' allocation of specimens from San Gorgonio Pass to *bangsi* rather than to *brevinasus* (contra [Williams et al. 1993](#)).

Discussion

We organize this section around two important, and inter-related, components of systematic research. The first addresses broad patterns, and degrees, of cranial and color disparity across the sampled region based on the separate transitional area analyses. This is a necessary first-step before tackling the second component, that of the optimal taxonomy that expresses the disparity of the patterns observed. Following these two components, we then posit historical biogeographic factors that might underly the cranial and pelage color disparities we recovered. We then end with potential management considerations as a result of our suggested taxonomic changes, and with a lament that so much of the original ranges of several of the taxa we include have disappeared under concrete and buildings, or been impacted by recent fires, each of which have changed the landscapes and habitats available for pocket mice and many other organisms, some irreversibly. Nonetheless, we believe it important to describe original patterns and processes of organismal diversification even if these exercises are only depictions of the past, not the future.

Synthesis of morphological disparity among samples. Samples of *Perognathus longimembris* from southern California and northern Baja California are diverse in cranial shape and pelage color, but the patterns are somewhat complex yet still geographically ordered. Here we map (Figure 11a) the major axes of cranial shape differentiation that derive from the global analysis (Figs. 3 and 4) and those of the individual transition areas (Figs. 5 – 9). The major axis of differentiation (heavy solid line in Figure 11a) separates eastern (desert plus *aestivus*) samples from those of the coast and interior valleys. Bridges between these two groups are evident in samples bangsi-2 vis-à-vis adjacent samples bangsi-1 to the east, bangsi-3 to the west, and bangsi-6 to the south (Figure 6), and between bangsi-6 and internationalis-2 (Figure 5). Secondary axes of differentiation occur between samples of coastal *pacificus* relative to the interior *brevinasus* and *internationalis* (Figure 7), and *brevinasus* (from the San Bernardino Valley) and *bangsi* samples (from San Gorgonio Pass; Figure 8). Tertiary levels of divergence occur among the three *pacificus* samples, which separate pacificus-1 (the type and topotypic series) from pacificus-2 and -3 from the central and northern coast, respectively (Figure 7). The array of *brevinasus* and *internationalis* samples, while grouped together, do not exhibit an expected clinal phenetic pattern but rather present as coupled pairs (Figure 7). Eastern

desert samples of *bangsi* and *bombycinus*, including *aestivus*, are collectively less cohesive but, at least with available samples, they are not subdivided (Figure 9).

Dorsal pelage color, dominated by lightness (L^*), exhibits the same geographic pattern as cranial shape (compare Figure 10 with Figs. 4 – 9). We have cranial and color data for 358 specimens. For these, we used linear regression to examine the correspondence between individual specimen cranial shape and color CV1 scores (Figure 11b). The relationship between these independent traits is strong ($R^2 = 0.4473$, $df_{1,357}$, $F = 288.13$, $P < 0.001$); specimens from each sample group together and array along the regression line in the consistent coastal to interior to desert pattern.

Taxonomic implications. As the existing subspecific taxonomy implies ([Williams et al. 1993](#), [Patton 2005](#), [Hafner 2016](#)), phenotypic diversity across the entire sample area is substantial. In our opinion, available data support the recognition of four to six infraspecific units, listed below, but also a reshuffling of the current assignments of several populations. Coastal *pacificus* possess the most distinctive skull, with its small overall size, very small bullae and concomitant wide interparietals and supraoccipitals, and short rostrum; its recognition should certainly be retained. A lingering question, however, is whether this taxon should be subdivided, with the name *pacificus* Mearns applied only to the area around its type locality in extreme southwestern San Diego County, and *cantwelli* von Bloeker resurrected to encompass the coastal samples in northwestern San Diego and southwestern Orange counties and those around its type locality of Hyperion (= El Segundo) in Los Angeles County. We believe subdivision is warranted as *pacificus* (sensu stricto) and *cantwelli* differ in multiple morphometric, shape, and color attributes, and at a degree consistent with differences among other subspecies recognized (see Figures. 3 and 7, Appendix 3 and 4).

Lacking any clear distinction between the six interior samples into northern and southern units that would map to the current taxa *brevinasus* Osgood and *internationalis* Huey, respectively, as well as the broad overlap among them, we recommend placing both under the earlier described *brevinasus* Osgood. Such action is consistent with the suggestion of equivocal recognition of the two by [Williams et al. \(1993\)](#). We suggest that samples allocated to *bangsi* Mearns be restricted to those in San Gorgonio Pass and the White-water River outwash, which includes the type locality of Palm Springs. Even though the type and topotypic series share phenetic similarities with samples to the immediate east (Shavers Valley) and south (Borrego Valley), those relationships are more distant than between the Palm Springs and San Gorgonio Pass samples. Eastern and southern *bangsi* samples, which grade into those allocated to *bombycinus* Osgood in the low eastern desert along the western margin of the lower Colorado River, are best considered a single unit. Given that the type locality of Osgood's *bombycinus* is from Yuma, on the Arizona (eastern) side of the lower Colorado River, samples of which are molecularly and phenotypically

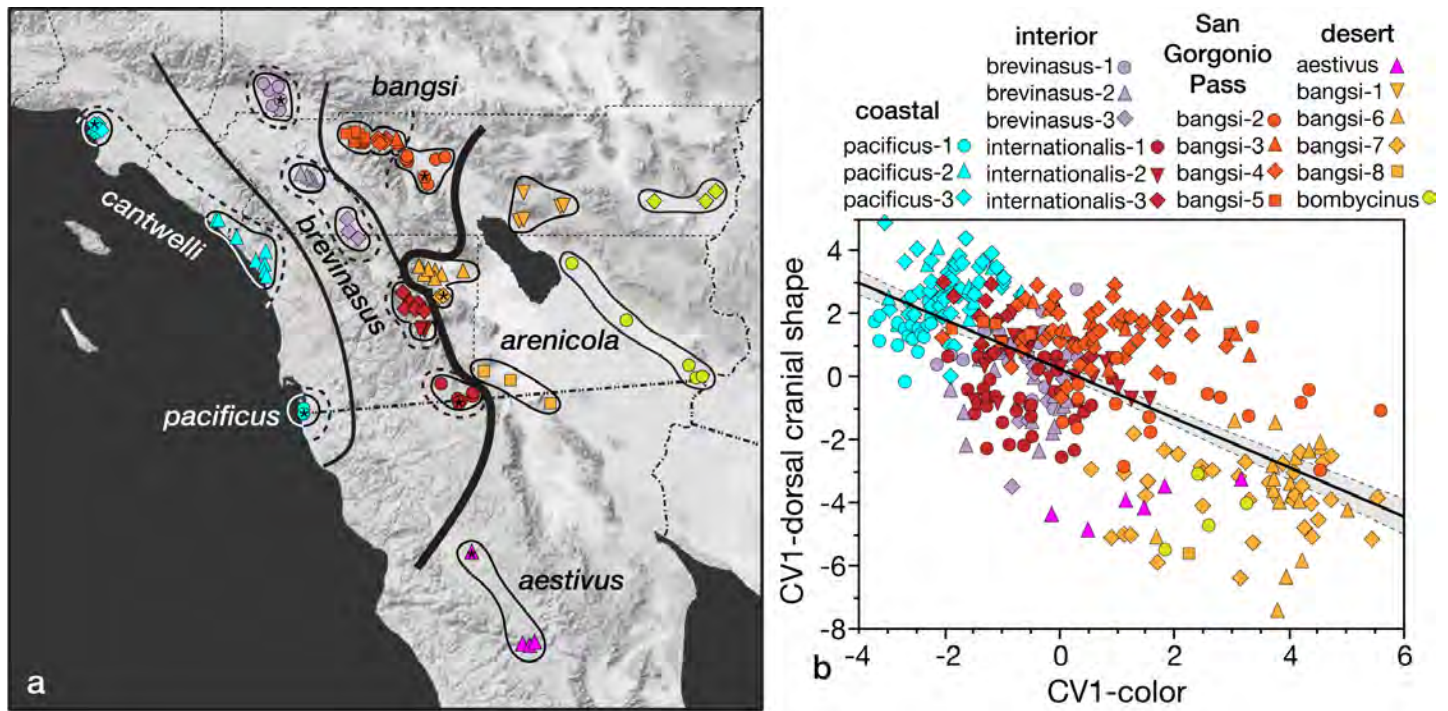


Figure 11. (a) Isophenes of cranial differentiation among samples of *Perognathus longimembris* from southern California and northern Baja California derived from canonical variate analyses presented in Figures 3 through 9. Differentiation is hierarchical, with the heavy line separating regional samples, light solid lines separating units within the western region, and dashed lines separating or grouping samples within current subspecies, but names are provided for infraspecific units we recognize herein. Symbols and colors are those in the map, Figure 1. (b) Regression plot, with 95 % confidence limits around the slope, illustrating the correspondence of individual specimens, as assigned to samples, for dorsal pelage color and cranial shape. Symbols and colors are those in the map, Figure 1.

distinct (JLP, unpublished data), the southeastern California samples cannot be referred to *bombycinus*. Fortunately, the bangsi-7 sample includes the holotype of *arenicola* Stephens; this name is available for these desert populations. As noted by Stephens in his original description, *arenicola* differed from typical *bangsi* by more swollen mastoids that project further posteriorly from the occiput, key features that are demarcated in our analyses (e.g., see wireframe diagram in Figure 6a). Until molecular data are available, we would provisionally retain *aestivus* Huey despite its cranial phenotypic overlap with these desert samples. We note that these suggested rearrangements will impact current conservation strategies for several of these pocket mice. Taxonomy is meant to inform, not to be derivative of those needs. A shortened listing of the valid taxa in southern California and northern Baja California, with range limits, is the following:

Perognathus longimembris pacificus Mearns, 1898

1898. *Perognathus pacificus* Mearns, Bull. Amer. Mus. Nat. Hist., 10:299, 31 August.

1932. *Perognathus longimembris pacificus*: von Bloeker, Proc. Biol. Soc. Washington, 45:127 (first use of current name combination).

Type locality. "Edge of the Pacific Ocean, at the last Mexican boundary monument (No. 258), [San Diego County, California]."

Range. Currently limited to the estuary of the Tijuana River in immediate vicinity of Boundary Monument 258

to 3.2 km north of the monument, San Diego Co., California; likely extends, or used to, even further north along the coast and possibly eastward up the Tijuana River drainage, including into extreme northwestern Baja California, Mexico. Includes localities in sample pacificus-1 (Appendix 1).

Remarks. To our knowledge, this taxon was last collected in the wild in July (von Bloeker 1931b) and October of 1931 (W. H. Burt, Dickey Collection, University of California, Los Angeles).

Perognathus longimembris bangsi Mearns, 1898

1898. *Perognathus longimembris bangsi* Mearns, Bull. Amer. Mus. Nat. Hist., 10:300, 31 August.

1900. *Perognathus panamintinus bangsi*: Osgood, N. Amer. Fauna, 18:29.

Type locality. "Palm Springs, Colorado Desert [Riverside Co.], southern California."

Range. Limited to San Gorgonio Pass (the vicinity of Banning east to Cabezon, Snow Creek, and Whitewater) and outwash of the Whitewater River to the vicinity of Palm Springs, Riverside Co., California. Includes localities of samples bangsi-2, bangsi-3, bangsi-4, and bangsi-5. Localities from San Gorgonio Pass were allocated to *brevinasus* Osgood by Williams et al. (1993) but to *bangsi* by Grinnell and Swarth (1913); some, but not all, specimens from Banning share the darker pelage characteristic of that subspecies but cranially pool with other *bangsi* samples from the Pass.

Perognathus longimembris arenicola Stephens, 1900

1900. *Perognathus panamintinus arenicola* Stephens, Proc. Biol. Soc. Washington, 13:153, 13 June.

1918. *P[erognathus]. I[ongimembris]. arenicola*: Osgood, Proc. Biol. Soc. Washington, 31:96 (first use of current name combination).

Type locality. "San Felipe Narrows, San Diego Co., California."

Range. Colorado Desert of eastern California and north-eastern Baja California, from Shavers Valley east to Blythe (Riverside County) and Borrego Valley south to the Yuha Basin and east to Pilot Knob (Imperial County); range in Baja California unclear but probably extends south along the coast of the Sea of Cortez at least to San Felipe. Includes localities in samples bangsi-1, bangsi-6, bangsi-7, bangsi-8, bombycinus-1, and bombycinus-2.

Remarks. Treated as a synonym of *P. l. bangsi* by [Grinnell \(1913, 1933\)](#), [Hall \(1981\)](#), and [Williams et al. \(1993\)](#). May include *aestivus* Huey, pending molecular data if and when available. [Grinnell \(1914\)](#) assigned specimens from the vicinity of Pilot Knob to *P. l. bombycinus*, the type locality of which is in Arizona (see above).

Perognathus longimembris brevinasus Osgood, 1900

1900. *Perognathus panamintinus brevinasus* Osgood, N. Amer. Fauna, 18:30, September.

1928. *Perognathus longimembris brevinasus*: Huey, Trans. San Diego Soc. Nat. Hist., 8:88 (first use of current name combination).

1939. *Perognathus longimembris internationalis*: Huey, Trans. San Diego Soc. Nat. Hist., 9(11):47. 31 August; type locality "Lower California side of the International Boundary at Jacumba, San Diego County, California," Baja California.

Type locality. "San Bernardino, [San Bernardino Co.], Cal. [California]." Stated by [Grinnell \(1933\)](#) to be "about 2 miles east of present city center."

Range. Interior valleys of southern California from the vicinity of the type locality in San Bernardino County successively south through the interior San Jacinto, Menifee, Aguanga, Oak Grove, Warner, San Felipe, Mason, and McCain valleys to the Jacumba Valley that straddles the international border. Includes localities in samples brevinasus-1, -2, and -3, and internationalis-1, -2, and -3. For assignment of specimens from localities across San Geronimo Pass ([Williams et al. 1993](#)) see comment under *P. l. bangsi*.

Perognathus longimembris aestivus Huey, 1928.

1928. *Perognathus longimembris aestivus* Huey, 1928, Trans. San Diego Soc. Nat. Hist., 5:87, 18 January.

Type locality. "Sangre de Cristo in Valle San Rafael on the western base of the Sierra Juárez, Lower [Baja] California, Mexico (upper Sonoran zone), lat. 31°52' north, long. 116°06' west."

Range. Known only from the type locality and Valle de la Trinidad (localities listed in sample *aestivus*).

Perognathus longimembris cantwelli von Bloeker, 1932.

1869. *Perognathus parvus*, Cooper, Amer. Nat., 3:183

1932. *Perognathus longimembris cantwelli* von Bloeker, Proc. Bio. Soc. Washington, 45:128, 9 September.

1939. *Perognathus longimembris pacificus*: Huey, Trans. San Diego Soc. Nat. Hist., 9(11):49 (first use of synonymy for *cantwelli*).

Type locality. "Hyperion [= El Segundo], Los Angeles County, California."

Range. Currently known from two disjunct areas along the coast of southern California: (1) from Oceanside (San Diego Co.; see [von Bloeker 1931b](#), [Bailey 1939](#)) north to Dana Point (Orange Co.; [Swei et al. 2003](#)) and continuing to Newport in the San Joaquin Hills historically ([M'Closkey 1972](#); [Meserve 1976](#)) and (2) the vicinity of the type locality south along the coast to Wilmington ([Cooper 1869](#)) but herein extended to include specimens from San Fernando, Los Angeles County, that others had previously assigned to *P. l. brevinasus* (e. g., [von Bloeker 1932](#); [Grinnell 1933](#); [Huey 1939](#); [Williams et al. 1993](#)). These two areas correspond to samples pacificus-2 and -3, respectively. When describing this form, [von Bloeker \(1932\)](#) referred the San Fernando samples to *P. l. brevinasus* based on skull characteristics and size although he pointed out it was like his *cantwelli* based on color.

Remarks. Treated as a valid subspecies by [Grinnell \(1933:148\)](#) but as a synonym of *P. l. pacificus* Mearns by most subsequent authors (e. g., [Hall 1981](#); [Williams et al. 1993](#)). So far as known, today this taxon is limited to small areas on Camp Pendleton Marine Corps Base (San Mateo/San Onofre, and Oscar One and Edson training areas, San Diego County) and Dana Point (Orange County). [Bailey \(1939\)](#) kept two living individuals collected at Oceanside in August of 1931 at his home; one died in December 1935 (Bitty) and the other (Bobbity) on 29 June 1937; see photographs (Figure 12) and accompanying poem, below.

Coming together, falling apart, and loss. The populations of *Perognathus longimembris* we studied form a natural monophyletic group that invaded the Pacific Plate and the Salton Sea trough (Rift Zone) from the east on the Continental Plate, where the species is much more widespread, and then diversified into multiple taxa in various habitat types ([Swei et al. 2003](#) and herein). There are multiple other taxa that spread to the Pacific Plate and then diversified; an excellent example is within the plethodontid salamander *Batrachoseps major* complex ([Jochsuch et al. 2020](#); see also [Gottscho 2016](#)). This contrasts with the *Perognathus parvus* complex that is widespread to the northeast in the Great Basin but only gets into southern California on the rim of the Continental Plate where it diversified (i. e., *Perognathus alticola*) but didn't invade the Pacific Plate at all ([Riddle et al. 2014](#)). Reptiles also have multiple lineages in southern California that are specialized for psammophilus habitats; *Perognathus longimembris* is the best example of a small

mammal that shares this niche (Mosauer 1932). These reptile species tend to show regional speciation patterns due to the regionalization of habitats; they serve as useful hypotheses to test our taxonomy (Wood *et al.* 2008; Leaché *et al.* 2009; Parham and Papenfuss 2009; Gottscho *et al.* 2017). Thus, within the Pacific Plate and Rift Zone these mice segregate clearly into five well defined habitat features, and six taxa: San Gorgonio Pass-Coachella Valley (*bangsi*), Colorado Desert (*arenicola*), interior northern Baja valleys (*aestivus*), headwater washes (*brevinasus*), and coastal dunes, washes, and marine terraces (*pacificus* and *cantwelli*). Below we evaluate the biogeography of these major habitat features. Next, we provide a brief history of the focal distributional areas of these mice.

1-San Gorgonio Pass-Coachella Valley: This area at the upper end of the San Andreas Rift Zone is part of the White-water-San Gorgonio River system and is bounded on the south by the head of the Salton Trough, and is a region identified in multi-species genetic hotspots analyses (Davis *et al.* 2008; Wood *et al.* 2013). There were expansive dunes in this landscape and high levels of endemism across taxa including additional mammals like the ground squirrel, *Xerospermophilus tereticaudus chlorus*. For psammophilus

reptiles the best example is *Uma inornata* that is restricted to this area but also the snake *Chionactis annulata/occipitalis* that was shown to have a high endemic divergence here as well (Wood *et al.* 2008, 2014; Gottscho *et al.* 2017). Various invertebrates also show high levels of endemism to the dunes and washes including the beetle *Dinacoma caseyi* and the cricket *Ammopelmatus cahuillaensis* (Tinkham 1968; Rubinoff *et al.* 2020). Thus, our revised definition of *P. l. bangsi* geographically fits well within this landscape with high endemism of dune evolved species.

2-Colorado Desert: This area borders the Salton Sea (Lake Cahuilla) on both sides and extends into desert valleys around Anza Borrego and the dune fields bordering the Chocolate Mountains and across to the Chuckwalla Valley but does not cross the Colorado River; rather, it heads south towards San Felipe in Baja California. Little pocket mice were probably continuous across the basin prior to the 1905 flood that formed the present Salton Sea. This area was also identified in Wood *et al.* (2013); the species most closely overlapping *P. l. arenicola* in distribution is the lizard *Uma notata* (Gottscho *et al.* 2017). Much of the north-eastern part of the mouse's range is bounded by the Bouse Formation (Busing 1990). There are genetic breaks in two

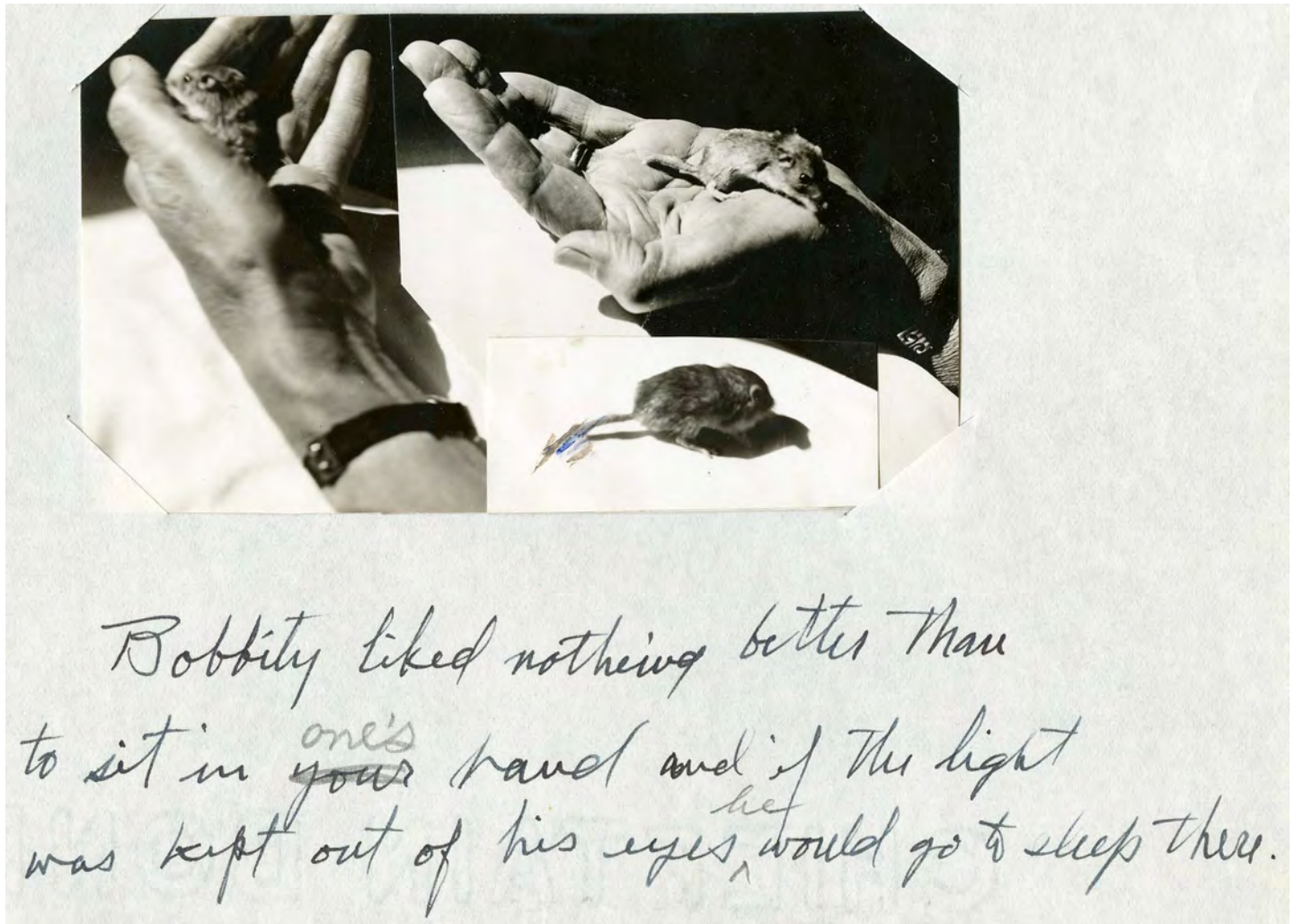


Figure 12. Photographs of Bobbity, Vernon Bailey's pet *P. l. cantwelli* collected at Oceanside, San Diego County on 20 August 1931 and that died on 29 June 1937 at a weight of "26 navy beans" (V. Bailey fieldnotes, Mammal Division archives, National Museum of Natural History, Smithsonian Institution, Washington, D.C.).

different species of horned lizards that match well with this landscape (*Phrynosoma mcallii* and *Phrynosoma platyrhinos*) and occupy the pocket mouse habitats (Mulcahy et al. 2006). The San Andreas fault-line passes through here but both sides of the rift zone are occupied by the same taxa. The eastern margin is the lower Colorado River, which forms a barrier for some taxa, including *P. l. arenicola* and other heteromyids as noted above, but not all. Both *Phrynosoma mcallii* and *Chionactis annulata* cross the river into the Yuma Desert and eastward to the Pinacate region in Sonora, Mexico (e. g., Mulcahy et al. 2006; Wood et al. 2014).

3-Interior northern Baja California valleys: The Trinidad and Ojos Negros/San Rafael valleys are connected to the lower part of the Colorado Desert region via the Paseo de San Matias where there is leakage from the desert to these inland xeric valleys for many taxa (Grismer 1994). The darker pelage of *P. l. aestivus* appears convergent with the darker coloration of the *P. l. brevinasus* further north in similar headwater wash situations on both sides of the Peninsular Ranges. Other desert species leak into these valleys from the desert such as the reptiles *Sceloporus magister*, *Xantusia wigginsi*, and the mammal *Dipodomys merriami trinidadensis* (Lidicker 1960; Grismer 1994; Álvarez-Castañeda et al. 2009). Although these valleys are on the western aspect of the Baja California Peninsula they maintain a more xeric landscape than other coastal areas in northern Baja California. Other valleys to the north and west seem to have appropriate habitat for *Perognathus longimembris* but lack records (Guadalupe Valley and Valle de las Palmas) despite field work conducted by prominent field mammalogists including S. B. Benson, L. M. Huey, and F. Stephens.

4-Headwater washes: These are a set of alluvial fans/basins that extend from north to south along the higher slopes of the Transverse and Peninsular ranges on both coastal and desert slopes. The distribution of *P. l. brevinasus* extends south along the western slope in the upper Santa Ana, Santa Margarita, and San Luis Rey rivers but switches to the eastern slope of the Peninsular Ranges along San Felipe Creek, Vallecito Creek, and Carrizo Creek washes terminating near Jacumba and Mountain Springs on both sides of the international boundary. It is separated spatially from *P. l. arenicola*, occurring at higher elevations within the mountains in appropriate habitat rather than on the Colorado Desert floor. Although this subspecies occurs on coastal and desert slopes, it maintains its phenology along this distribution. A surprising spatial gap in distribution is in the foothills of the San Gabriel Mountains where *P. l. brevinasus* terminates in the west around Etiwanda Wash rather than extending farther to Cucamonga or San Antonio washes where seemingly continuous and appropriate habitats occur. The lack of records from this area across to the San Fernando Valley supports the break we find in our morphologic assessment, where specimens from San Fernando (Lower Big Tujunga Wash) are assigned to *P. l. cantwelli* and not *P. l. brevinasus*. Evidence that this gap is real comes from MacMillen's (1964) Ph.D. thesis studies in

the San Antonio alluvial fan and our recent trapping work at San Antonio and lower San Gabriel River washes where we also failed to detect any *Perognathus longimembris*. In the northern part of its range, *P. l. brevinasus* closely tracks the highly endemic and endangered San Bernardino kangaroo rat (*Dipodomys merriami parvus*) in the Santa Ana Watershed, then overlaps with the endangered Stephens kangaroo rat (*Dipodomys stephensi*) more broadly in the Perris Plain south to Temecula, and lastly switches in the upper Santa Margarita Watershed near Aguanga and overlaps *Dipodomys merriami collinus* and tracks the range of this subspecies into San Felipe Creek (Lidicker 1960) and then south into Mason Valley. Farther south, *P. l. brevinasus* overlaps *Dipodomys merriami trinidadensis* possibly in the Jacumba Valley. This overlap with three different subspecies of *Dipodomys merriami* is worth further investigation, as these overlap combinations coincide with several of the evolutionary hotspots identified in Vandergast et al. (2008).

5-Coastal dunes, washes, and marine terraces: This is a complex of geologically divergent areas that are tied together by being coastal (with the exception of San Fernando Valley, discussed last), extending along the coastline from Playa del Rey in Los Angeles County to the Tijuana River wash just north of the Mexican border. The areas are/were occupied by *P. l. cantwelli* except the Tijuana site that was occupied by *P. l. pacificus*. There is a set of coastal dunes that extended in patches from north to south with the most extensive being the high El Segundo sand dunes feature. This area was known for extreme endemism in invertebrates (Mattoni 1992). Most of this feature is now gone except for a 300+ acre portion on Los Angeles World Airways property that is managed as a reserve. Immediately to the south is the prominent feature of Palos Verdes Peninsula that lacks any appropriate habitat for pocket mice. South of these hills is Wilmington, where three specimens were collected in 1865 (Cooper 1869; now MVZ 5633 to 5635). This area comprises large riverine sandy alluvium and low elevation marine terraces that extend to Newport Back Bay. All three major rivers (Los Angeles, San Gabriel, and Santa Ana) once terminated in this region and often flooded a large landscape as they merged during big storm events. This area has not only the earliest record for mice, but subfossil records are known from Huntington Beach (Tom Wake, pers. comm.); the region is now almost entirely developed.

South of Newport Bay are the San Joaquin Hills where pocket mice have occupied patchy, specific marine terrace features (M'Closkey 1972; Meserve 1976; no museum vouchers exist for these sites). Much of this landscape is now protected but the likely mouse habitats are now housing developments. These hills continue south to Dana Point where pocket mice still persist on top of a small coastal bluff on a paleobeach habitat surrounded by housing (Brehme et al. 2021). South of there the mice occurred in patches in Camp Pendleton on other paleobeach formations (Brehme et al. 2017) and then were common on the sand dune for-

mation on the north side of Oceanside where [Bailey \(1939\)](#) was easily able to capture mice by digging them out of the sand. South of Oceanside there are a few possible records and some paleorecords but no museum vouchers until the Tijuana Estuary where *P. l. pacificus* was apparently endemic. This population was discovered in 1894 by E. A. Mearns and F. X. Holzner but not found again until J. C. von Bloeker rediscovered them in July 1931 on river bottom sand ([von Bloeker 1931a](#)). Previous effort centered on the small mesa-tops by the international border based on Mearns' locality description. At the time of rediscovery in the river valley, mice were abundant and easily collected but abruptly disappeared within a year or so. They have not been documented from this general area for over 90 years. The river valley is very dynamic and experiences large flood events but also became extensively cultivated ([Safran et al. 2017](#)). Small patches of native habitat still occur there with appropriate forbland species that *P. l. pacificus* and *P. l. cantwelli* prefer (see [von Bloeker 1931a, b](#); [Iwanowicz et al. 2016](#)). Historical reconstructions of the pre-development habitats based on the mid-1800's survey maps, in part, show extensive river wash/riparian scrub habitats that *P. l. pacificus* could have occupied in this valley; [Safran et al. \(2017\)](#) estimate this was approximately 1,800 hectares, with 89 % of this habitat lost to date. Additionally, the Pleistocene (glacial maximum) extent of sandy habitats extended well offshore heading towards Coronado Canyon, ~15 km west of the current Tijuana Estuary dune system, greatly extending the potential *P. l. pacificus* habitats historically available in this area ([Graham et al. 2003](#)).

Lastly, we have the isolated population in the upper Los Angeles River tributary of Big Tujunga wash. This very sandy wash bisected the San Fernando Valley and historically *P. l. cantwelli* here were probably continuous along the Los Angeles River as it passed Burbank and headed south into the Los Angeles Basin. As discussed below, much of this basin habitat was broadly underwater for months in the 1860s due to massive flooding, resulting in likely periodic extirpations of populations of low elevation mice. The upper section in San Fernando Valley apparently persisted until the entire area became urbanized. Recent surveys in the Hansen Dam area in sandy soils in lower Big Tujunga wash have failed to detect this species ([Hitchcock et al. 2022](#)).

We end this section posing two questions: First, why is *P. longimembris* lacking from the washes connecting the inland alluvial fans and the coastline dunes and terraces? Surprisingly there is a big gap in many species distributions between the coastal zone and inland occurrences in the upper watersheds of the main Los Angeles Basin drainages, exemplified by the subspecies of the giant fly *Rhaphiomidas terminatus*, where one is endemic in the El Segundo sand dunes and the other is endemic inland in the Colton dune system ([George and Mattoni 2006](#)), a contrast similar to the current distribution of *P. l. cantwelli* and *P. l. brevinaesus*. This appears to be the result of a combination of potential historic and current events. Historic events like the 100

and 1,000 year flood events (in particular the 1862 flood; [Engstrom 1996](#)) drove the shape and structure of the Los Angeles, San Gabriel, and Santa Ana river washes and the flooding of the Los Angeles Basin. Higher areas of marine terraces and hills like San Joaquin Hills and El Segundo dunes must have been important for long term persistence of the psammophilus species, including the mice, by acting as island refugia. The San Fernando Valley records for *P. l. cantwelli* are thus quite important in showing that this taxon remained connected upstream towards the alluvial fan of Big Tujunga Wash as the San Fernando Valley did not flood during the 1862 event (see Figure 1 in [Engstrom 1996](#)) and persisted there at least until the 1930s. Cooper's specimens from Wilmington in 1865 for *P. l. cantwelli* post-date the 1862 flood, so while the landscape was likely inundated by the flood event ([Cooper 1869](#), [Engstrom 1996](#)), clearly not all mouse habitat was lost. Currently the areas between coastal occurrences of the mice and inland alluvial fans are primarily urbanized and lack almost any suitable habitats.

Second, why are there two different coastal mice in southern California? Multiple studies of wide-ranging species show that the coastal occurrences of these species at El Segundo dunes are independent lineages from other dunes in southern California, including dunes to the north ([Dupuis et al. 2020](#)) or those to the south such as the Tijuana River wash ([Vandergast et al. 2008](#); [Leache et al. 2009](#); [Parham and Papenfuss 2009](#)). There are a few species that are coastal dune specific specialists that only occur along the coast; beetles and spiders have, in particular, been studied phylogenetically in this context. These studies show that there is typically isolation by distance in the respective groups with potential north-south speciation between some sets of populations ([Bond et al. 2001](#); [Chatzimanolis and Caterino 2008](#)). [Chatzimanolis and Caterino \(2008\)](#) stated "It is evident that all the dune systems studied harbor great genetic diversity and the protection of one system cannot act as a surrogate for another." Thus, the finding of two similar but different coastal mice, *pacificus* and *cantwelli*, is not surprising but has important evolutionary and conservation implications.

The lament. Close to 28 million people live in southern California and northern Baja California today. As a consequence, this great diversity of pocket mice has been, and continues to be exposed to many stressors. Although these taxa occur in very different habitats, several of them are threatened by the same factors that will likely impact their long-term persistence. Many of these threats have been identified in various planning documents, such as the recovery plan for the Pacific pocket mouse ([U.S. Fish and Wildlife Service 1998](#)), and various actions, such as reserve planning ([Chase et al. 2000](#); [Barrows et al. 2011](#); [Miller et al. 2017](#)) and management ([Brehme et al. 2017](#); [Miller et al. 2017](#); [Brehme et al. 2021](#)), are helping to mitigate and manage for these stressors. Critically, the Central Coastal NCCP, Western Riverside County MSHCP, Coachella Valley MSCP, SBVWCD, and other entities such as the Camp Pendleton

MCB INRMP all work towards these goals (Chase et al. 2000; U.S. Fish and Wildlife Service 2010; Barrows et al. 2011; Chock et al. 2022). We include a potential threats matrix (Table 1) as a useful platform for continued conservation planning for these taxa and the habitats in which they occur (Miller et al. 2017). Sadly, our evidence that *Perognathus l. pacificus* as we define it here (as opposed to recent taxonomy) was endemic to only the Tijuana Watershed and has not been detected since the 1930's supports that this is now the third subspecies of mammal endemic to southern California that is now extinct. Thus, *P. l. pacificus* joins *Perognathus a. alticola* and *Vulpes m. macrotis* as a previously localized endemic in this dynamic and complex habitat to befall the same fate (Davis et al. 2008).

We end on the hopeful note that populations of *P. l. cantwelli* (as defined here as opposed to recent taxonomy in which these populations were considered *P. l. pacificus*) are the focus of conservation efforts by various agencies and landowners (e. g., U.S. Fish and Wildlife Service 2010; Brehme et al. 2017; Miller et al. 2017; Brehme et al. 2021; Chock et al. 2022). First collected in 1901 by Frank Stephens (at San Onofre), viable populations remained in the Oceanside area at least until the late 1930s, and continue, as noted above, at sites on Camp Pendleton and at Dana Point. This animal was special to Vernon Bailey, one of the most eminent mammalogists and naturalists of the early 20th century, who kept a pair at his home in Washington, D.C. Below is a poem, penned by Bailey and edited by his wife, Florence Merriam Bailey, about "Bobbity," their name for the mouse that lived the longest. One of us (RNF) found this document, along with an accompanying set of photographs with Bailey's hand-written notes (Figure 12) in the archives of the National Museum of Natural History, Smithsonian Institution, Washington, D.C.

Bobbity

Dear little mouse with shiny coat
 Bright black eyes and dainty hands
 Watching us with a wistful look
 And a far away gaze that understands
 More than we think of our intent
 And more than we know of distant lands.
 Deserts and wastes of sandy soil
 Where treasures of seeds in a cool deep cell,
 The rich rewards of nights of toil
 With the dainty foods that pleased him well.
 But when he came to share our life
 And freely his valued trust to give
 To accept from our hands protection and care
 And teach us how his people live
 It was only for us to understand
 And write his life with a friendly hand.

Acknowledgments

Work such as this could not be conceived, much less accomplished without acknowledging the efforts of those collectors who assembled, over many decades, the specimens we examined and the staff of those institutions

Table 1. Threat assessments that are currently or are likely to impact each of the six subspecies of *Perognathus longimembris* we recognize within the greater southern California-northern Baja California region.

| Potential Threats | <i>pacificus</i> | <i>cantwelli</i> | <i>brevinasus</i> | <i>bangsi</i> | <i>arenicola</i> | <i>aestivus</i> |
|-------------------------------------|------------------|------------------|-------------------|---------------|------------------|-----------------|
| Agriculture ¹ | X | X | X | X | X | X |
| Argentine ants ² | X | X | X | | | |
| Red imported fire ants ³ | | X | X | X | | |
| Solar development ⁴ | | | X | X | X | |
| Wind development ⁵ | | | X | X | X | |
| Invasive plants ⁶ | X | X | X | X | X | X |
| House cats ⁷ | X | X | X | | | |
| Invasive red fox ⁸ | | X | | | | |
| Mining ¹ | | | | | X | |
| Off-highway vehicles ⁹ | | | X | X | X | X |
| Urbanization ¹⁰ | X | X | X | X | | |
| Flooding ¹¹ | X | X | X | X | | |
| Light pollution ¹² | X | X | X | X | | |
| Connectivity loss ¹³ | X | X | X | X | | |

¹Lovich and Bainbridge 1999; ²Laakkonen et al. 2001; ³Allen et al. 2004; ⁴Lovich and Ennen 2011; ⁵Lovich and Ennen 2013; ⁶Ceradini and Falfoun 2017; ⁷Longcore et al. 2009; ⁸Golightly et al. 1994; ⁹Brooks 1995; ¹⁰Amburgey et al. 2021; ¹¹Engstrom 1996; ¹²Kotler 1984; ¹³Barrows et al. 2011.

who have both maintained and made them available to researchers. In this respect, we are immeasurably grateful to the curators and collection managers who granted our access to their respective collections: Duke S. Rogers at the Monte L. Bean Museum of Natural History, Brigham Young University, Provo, Utah (BYU); Eric A. Rickart, Utah Museum of Natural History, Salt Lake City, Utah (UMNH); Darrin Lunde and Alfred L. Gardner, National Museum of Natural History, Smithsonian Institution, Washington, D.C. (NMNH); Lawrence R. Heaney, Field Museum of Natural History, Chicago, Illinois (FMNH); Joseph A. Cook and Jonathan L. Dunnum, Museum of Southwestern Biology, University of New Mexico, Albuquerque, New Mexico (MSB); James P. Dines, Shannen L. Robson, and Kayce C. Bell, Natural History Museum of Los Angeles County, Los Angeles, California (LACM); Philip Unit and Scott Tremor, San Diego Museum of Natural History, San Diego, California (SDMNH); and Krista Fahy, Santa Barbara Natural History Museum, Santa Barbara, California (SBNHM). Special thanks are due Mark D. Omura, Museum of Comparative Zoology, Harvard University, Cambridge, Massachusetts, for providing digital images of the holotype of *P. l. bangsi* Mearns; Dra. Yocelyn Gutierrez Guerrero for translating the abstract; and especially Cheryl Brehme for her hard work to design, implement, and manage the USGS Pacific pocket mouse research program, where we have learned so much about the natural history of this mouse, information that has had a significant impact on ensuring its future in coastal California. Finally, we are extremely grateful to Jacob Esselstyn, Richard Erickson, and two anonymous reviewers for improving the content of the manuscript. Any use of trade, firm, or product names is for descriptive purposes only and does not imply endorsement by the U.S. Government. RNF was funded by the Ecosystems Mission Area of the U.S. Geological Survey.

We dedicate this paper to Alfred L. Gardner, a close friend and colleague of JLP for nearly 60 years, the person who encouraged him to switch graduate programs from anthropology to zoology in 1963 and who gave him the opportunity to begin long-term mammalogical investigations in the Amazon Basin in 1968. We are immensely grateful for his wisdom, sense of scientific integrity, and philosophy to expend whatever effort necessary “to find out what is on the other side of that hill.”

Literature cited

- ABRAMOFF, M. D., P. J. MAGALHAES, AND S. J. RAM. 2004. Image processing with ImageJ. *Biophotonics International* 11:36-42.
- ALLEN, C. R., D. M. EPPERSON, AND A. S. GARMESTANI. 2004. Red imported fire ant impacts on wildlife: a decade of research. *American Midland Naturalist* 152:88-103.
- ÁLVAREZ-CASTAÑEDA, S. T., W. Z. LIDICKER, JR, AND E. RIOS. 2009. Revision of the *Dipodomys merriami* complex in the Baja California Peninsula, Mexico. *Journal of Mammalogy* 90:992-1008.
- AMBURGEY, S. M., ET AL. 2021. The influence of species life history and distribution characteristics on species responses to habitat fragmentation in an urban landscape. *Journal of Animal Ecology* 90:685-697.
- BAILEY, V. 1939. The solitary lives of two little pocket mice. *Journal of Mammalogy* 20:325-328.
- BARROWS, C. W., K. D. FLEMING, AND M. F. ALLEN. 2011. Identifying habitat linkages to maintain connectivity for corridor dwellers in a fragmented landscape. *Journal of Wildlife Management* 75:682-691.
- BOND, J. E., ET AL. 2001. Deep molecular divergence in the absence of morphological and ecological change in the Californian coastal dune endemic trapdoor spider *Aptostichus simus*. *Molecular Ecology* 10:899-910.
- BOOKSTEIN, F. L. 1991. *Morphometric tools for landmark data: geometry and biology*. Cambridge University Press. New York, U.S.A.
- BREHME, C. S., ET AL. 2017. Marine corps base, Camp Pendleton Pacific pocket mouse monitoring results for 2016: 5-year trend analysis and monitoring program evaluation. MCB, Camp Pendleton. DRAFT Prepared for Environmental Security Department, Marine Corps Base, Camp Pendleton, U.S.A.
- BREHME, C. S., ET AL. 2021. Dana Point headlands (CNLM, City of Dana Point) Pacific pocket mouse monitoring results for 2020. USGS Cooperator Report to U.S. Fish and Wildlife Service, Carlsbad, U.S.A.
- BROOKS, M. L. 1995. Benefits of protective fencing to plant and rodent communities of the western Mojave Desert, California. *Environmental Management* 19:65-74.
- BUSING, A. V. 1990. The Bouse Formation and bracketing units, southeastern California and western Arizona: Implications for the evolution of the proto-Gulf of California and the lower Colorado River. *Journal of Geophysical Research* 95:20111-20132.
- CALIFORNIA NATURAL DIVERSITY DATABASE (CNDDDB). July 2022. Special Animals List. California Department of Fish and Wildlife, Sacramento. California, U.S.A.
- CERADINI, J. P., AND A. D. CHALFOUN. 2017. Species' traits help predict small mammal responses to habitat homogenization by an invasive grass. *Ecological Applications* 27:1451-1465.
- CHASE, M. K., ET AL. 2000. Single species as indicators of species richness and composition in California coastal sage scrub birds and small mammals. *Conservation Biology* 14:474-487.
- CHATZIMANOLIS, S., AND M. S. CATERINO. 2008. Phylogeography of the darkling beetle *Coelus ciliates* in California. *Annals Entomological Society of America* 101:939-949.
- CHOCK, R. Y., ET AL. 2022. Quantitative SWOT analysis: A structured and collaborative approach to reintroduction site selection for the endangered Pacific pocket mouse. *Journal for Nature Conservation* 70:126268.
- COOPER, J. G. 1869. The naturalist in California. *American Naturalist* 3:182-189.
- DAVIS, E. B., ET AL. 2008. The California hotspots project: identifying regions of rapid diversification of mammals. *Molecular Ecology* 17:120-138.
- DUJARDIN, S., AND J.-P. DUJARDIN. 2019. Geometric morphometrics in the cloud. *Infection, Genetics, and Evolution*, 70:189-196.
- DUPIUS, J. R., ET AL. 2020. Genomics confirms surprising ecological divergence and isolation in an endangered butterfly. *Biodiversity and Conservation* 29:1897-1921.

- DURRANT, S. D. 1952. Mammals of Utah, taxonomy and distribution. University of Kansas Publications, Museum of Natural History 6:1-546.
- ENGSTROM, W. N. 1996. The California storm of January 1862. *Quaternary Research* 46:141-148.
- GEORGE, J. N., AND R. MATTONI. 2006. *Rhaphiomidas terminatus terminatus* Cazier, 1985 (Diptera: Mydidae): notes on the re-discovery and conservation biology of a presumed extinct species. *The Pan-Pacific Entomologist* 82:30-35.
- GOLIGHTLY, R. T., ET AL. 1994. Food habits and management of introduced red fox in southern California. *Proceedings Vertebrate Pest Conference* 16:15-20.
- GOTTSCHO, A. D. 2016. Zoogeography of the San Andreas Fault system: Great Pacific Fracture Zones correspond with spatially concordant phylogeographic boundaries in western North America. *Biological Review* 91:235-254.
- GOTTSCHO, A. D., ET AL. 2017. Lineage diversification of fringed-toed lizards (Phrynosomatidae: *Uma notata* complex) in the Colorado Desert: delimiting species in the presence of gene flow. *Molecular Phylogenetics and Evolution* 106:103-117.
- GRAHAM, M. H., P. K. DAYTON, AND J. M. ERLANDSON. 2003. Ice ages and ecological transitions on temperate coasts. *Trends in Ecology and Evolution* 18:33-40.
- GRINNELL, J. 1913. A distributional list of the mammals of California. *Proceedings of the California Academy of Sciences*, 4th series, 3:265-390.
- GRINNELL, J. 1914. An account of the mammals and birds of the lower Colorado Valley, with special reference to the distributional problems presented. University of California Publications in Zoology 12:51-294.
- GRINNELL, J. 1933. Review of the Recent mammal fauna of California. University of California Publications in Zoology 40:71-234.
- GRINNELL, J., AND H. S. SWARTH. 1913. An account of the birds and mammals of the San Jacinto area of southern California. University of California Publications in Zoology 10:197-406.
- GRISMER, L. L. 1994. The origin and evolution of the peninsular herpetofauna of Baja California, Mexico. *Herpetological Natural History* 2:51-106.
- HAFNER, D. J. 2016. Subfamily Perognathinae, Genus *Perognathus*. Pp. 202-209, in *Handbook of mammals of the world*, vol. 6, Lagomorphs and Rodents I (Wilson, D. E., T. E. Lacher, Jr., and R. A. Mittermeier, eds.). Lynx Ediciones, Barcelona, Spain.
- HALL, E. R. 1941. New heteromyid rodents from Nevada. *Proceedings of the Biological Society of Washington* 54:55-61.
- HALL, E. R. 1946. Mammals of Nevada. University of California Press. Berkeley, U.S.A.
- HALL, E. R. 1981. The mammals of North America, vol. 1. John Wiley & Sons. New York, U.S.A.
- HITCHCOCK, C. J., ET AL. 2022. Draft Final: Summary of biodiversity surveys at Hansen Dam Recreational Area, 2020-2021. Report to U.S. Army Corps of Engineers, Los Angeles District, Operations Division.
- HOFFMEISTER, D. F. 1986. Mammals of Arizona. The University of Arizona Press and The Arizona Game and Fish Department, Arizona, U.S.A.
- HUEY, L. M. 1928. A new silky pocket mouse and a new pocket gopher from Lower California, Mexico. *Transactions of the San Diego Society of Natural History* 5:87-90.
- HUEY, L. M. 1939. The silky pocket mice of southern California and northern Lower California, Mexico, with the description of a new race. *Transactions of the San Diego Society of Natural History* 9:47-54.
- IWANOWICZ, D. D., ET AL. 2016. Metabarcoding of fecal samples to determine herbivore diets: a case study of the endangered Pacific pocket mouse. *Plos One* 11:e0165366.
- JOCKUSCH, E. L., ET AL. 2020. Slender salamanders (genus *Batrachoseps*) reveal Southern California to be a center for diversification, persistence, and introduction of salamander lineages. *PeerJ* 8: e9599.
- KLINGENBERG, C. P. 2011. MorphoJ: an integrated software package for geometric morphometrics. *Molecular Ecology Resources* 11:353-357.
- KOTLER, B. P. 1984. Effects of illumination on the rate of resource harvesting in a community of desert rodents. *American Midland Naturalist* 111:383-389.
- LAAKKONEN, J., R. N. FISHER, AND T. J. CASE. 2001. Effect of land cover, habitat fragmentation and ant colonies on the distribution and abundance of shrews in southern California. *Journal of Animal Ecology* 70:776-788.
- LEACHÉ, A. D., ET AL. 2009. Quantifying ecological, morphological, and genetic variation to delimit species in the coast horned lizard species complex (*Phrysonoma*). *Proceedings of the National Academy of Sciences* 106:12418-12423.
- LIDICKER, W. Z., JR. 1960. An analysis of infraspecific variation in the kangaroo rat *Dipodomys merriami*. University of California Publications in Zoology 67:125-218.
- LONGCORE, T., C. RICHE, AND L. M. SULLIVAN. 2009. Critical evaluation of claims regarding management of feral cats by trap-neuter-return. *Conservation Biology* 23:887-894.
- LOVICH, J. E., AND D. BAINBRIDGE. 1999. Anthropogenic degradation of the Southern California desert ecosystem and prospects for natural recovery and restoration. *Environmental Management* 24:309-326.
- LOVICH, J. E., AND J. R. ENNEN. 2011. Wildlife conservation and solar energy development in the desert southwest, United States. *BioScience* 61:982-992.
- LOVICH, J. E., AND J. R. ENNEN. 2013. Assessing the state of the knowledge of utility-scale wind energy development and operation on non-volant terrestrial and marine wildlife. *Applied Energy* 103:52-60.
- M'CLOSKEY, R. T. 1972. Temporal changes in populations and species diversity in a California rodent community. *Journal of Mammalogy* 53:657-676.
- MACMILLEN, R. E. 1964. Population ecology, water relations, and social behavior of a southern California semidesert rodent fauna. University of California Publications Zoology 71:1-66.
- MATTONI, R. H. T. 1992. The endangered El Segundo blue butterfly. *Journal of Research on the Lepidoptera* 29:277-304.
- MEARNS, E. A. 1898. Descriptions of three new forms of Pocket-mice from the Mexican border of the United States. *Bulletin of the American Museum of Natural History* 10:299-302.
- MESERVE, P. L. 1976. Food relationships of a rodent fauna in a California coastal sage scrub community. *Journal of Mammalogy* 57:300-319.
- MILLER, W. B., ET AL. 2017. Little pocket mouse *Perognathus longimembris*. Pp. 85-94, in *San Diego County Mammal Atlas* (Tremor, S., D. Stokes, W. Spencer, J. Diffendorfer, H. Thomas,

- S. Chivers, and P. Unitt, eds.). Proceedings of the San Diego Society of Natural History. San Diego, U.S.A.
- MOSAUER, W. 1932. Adaptive convergence in the sand reptiles of the Sahara and of California: A study of structure and behavior. *Copeia* 1932:72-78.
- MULCAHY, D. G., ET AL. 2006. Phylogeography of the flat-tailed horned lizard (*Phrynosoma mcallii*) and the systematics of the *P. mcallii-platyrrhinus* mtDNA complex. *Molecular Ecology* 15:1807-1826.
- OSGOOD, W. H. 1900. Revision of the pocket mice of the genus *Perognathus*. *North American Fauna* 18:9-65.
- OSGOOD, W. H. 1918. The status of *Perognathus longimembris* Coues. *Proceedings of the Biological Society of Washington* 31:95-96.
- PARHAM, J. F., AND T. J. PAPPENFUSS. 2009. High genetic diversity among fossorial lizard populations (*Anniella pulchra*) in a rapidly developing landscape (Central California). *Conservation Genetics* 10:169-176.
- PATTON, J. L. 2005. Family Heteromyidae. Pp. 844-858, in *Mammal species of the world. A taxonomic and geographic reference* (Wilson, D. E., and D. E. Reeder, eds.). The Johns Hopkins University Press. Baltimore, U.S.A.
- RIDDLE, B. R., ET AL. 2000. Cryptic vicariance in the historical assembly of a Baja California Peninsular Desert biota. *Proceedings of the National Academy of Sciences (USA)* 97:14438-14443.
- RIDDLE, B. R., ET AL. 2014. Cryptic divergence and revised species taxonomy within the Great Basin pocket mouse, *Perognathus parvus* (Peale, 1848), species group. *Journal of Mammalogy* 95:9-25.
- RUBINOFF, D., ET AL. 2020. Phylogenomics reveals conservation challenges and opportunities for cryptic endangered species in a rapidly disappearing desert ecosystem. *Biodiversity and Conservation* 29:2185-2200.
- SAFRAN, S. M., ET AL. 2017. Tijuana River Valley historical ecology investigation. Prepared for the state coastal conservancy. San Francisco Estuary Institute-Aquatic Science Center, Richmond. California, U.S.A.
- SCHNEIDER, C. A., W. S. RASBAND, AND K. W. ELICEIRI. 2012. NIH Image to ImageJ: 25 years of image analysis. *Nature Methods* 9:671-675.
- STEPHENS, F. 1900. Descriptions of two new mammals from southern California. *Proceedings of the Biological Society of Washington* 13:153-158.
- SWEI, A., ET AL. 2003. Hierarchical genetic structure in fragmented populations of the Little Pocket Mouse (*Perognathus longimembris*) in Southern California. *Conservation Genetics* 4:510-514.
- TINKHAM, E. R. 1968. Studies in Nearctic desert sand dune Orthoptera, Part XI. A new arenicolous species of *Stenopelmatus* from Coachella Valley with key and biological notes. *Great Basin Naturalist* 28:124-131.
- USFWS. 1998. Recovery plan for the Pacific pocket mouse (*Perognathus longimembris pacificus*). U.S. Fish and Wildlife Service. Portland, U.S.A.
- USFWS. 2010. Pacific pocket mouse (*Perognathus longimembris pacificus*) 5-Year Review: Summary and Evaluation. Carlsbad Fish and Wildlife Office. Carlsbad, U.S.A.
- VANDERGAST, A. G., ET AL. 2008. Are hotspots of evolutionary potential adequately protected in southern California? *Biological Conservation* 141:1648-1664.
- VON BLOEKER, J. C., JR. 1931a. *Perognathus pacificus* from the type locality. *Journal of Mammalogy* 12:369-372.
- VON BLOEKER, J. C., JR. 1931b. Extension of range of *Perognathus pacificus*. *Journal of Mammalogy* 12:431-432.
- VON BLOEKER, J. C., JR. 1932. A new race of *Perognathus longimembris* from southern California. *Proceedings of the Biological Society of Washington* 45:127-130.
- WILDER, A. P., ET AL. 2022. A chromosome-length reference genome for the endangered Pacific pocket mouse reveals recent inbreeding in a historically large population. *Genome Biology and Evolution* <https://doi.org/10.1093/gbe/evac122>.
- WILLIAMS, D. F., H. H. GENOWAYS, AND J. K. BRAUN. 1993. Taxonomy. Pp. 38-196 in *Biology of the Heteromyidae* (Genoways, H. H., and J. H. Brown, eds.). Special Publication No. 10, American Society of Mammalogists. Lawrence, U.S.A.
- WOOD, D. A., ET AL. 2008. Molecular and phenotypic diversity in *Chionactis occipitalis* (Western shovel-nosed snake), with emphasis on the status of *C. o. klauberi* (Tucson shovel-nosed snake). *Conservation Genetics* 9:1489-1507.
- WOOD, D. A., ET AL. 2013. Comparative phylogeography reveals deep lineages and regional evolutionary hotspots in the Mojave and Sonoran Deserts. *Diversity and Distributions* 19:722-737.
- WOOD, D. A., R. N. FISHER, AND A. G. VANDERGAST. 2014. Fuzzy boundaries: color and gene flow patterns among parapatric lineages of the western shovel-nosed snake and taxonomic implication. *Plos One* 9:e97494.

Associated editor: Jake Esselstyn and Giovani Hernández Canchola

Submitted: August 30, 2022; Reviewed: October 20, 2022

Accepted: November 27, 2022; Published on line: January 27, 2023

Appendix 1

List of measured specimens organized by the sample groups mapped in Figure 1. Sample sizes for each group are given separately for shape and distance data for the dorsal and ventral aspects of the skull ($n_{\text{shape-d}}$, $n_{\text{shape-v}}$, $n_{\text{distance-d}}$, $n_{\text{distance-v}}$) and dorsal color (n_c). The total sample sizes, museum acronyms, and catalog numbers are given for each locality, even if some individuals were not included in every analysis. Specimens not assigned to a sample group are listed at the end as unknown.

aestivus ($n_{\text{shape-d}} = 19$, $n_{\text{shape-v}} = 19$, $n_{\text{distance-d}} = 20$, $n_{\text{distance-v}} = 19$, $n_c = 8$)

MEXICO.—Baja California; Sangre de Cristo ($n = 5$, SDNHM 6050-1, 6098, 6120, 22079); Sangre de Cristo, Valley San Rafael ($n = 1$, SDNHM 6110 [holotype of *aestivus* Huey]); Valle de la Trinidad ($n = 9$, SDNHM 6208, 6323, 6338, 11504, 11642, 11643, 11664-11666); Valle de la Trinidad, Aguajito Spring ($n = 4$, SDNHM 11563, 11591-11593); Valley La Trinidad, La Zapopita ($n = 1$, LACM 13677) – total $n = 20$.

bangsi-1 ($n_{\text{shape-d}} = 17$, $n_{\text{shape-v}} = 15$, $n_{\text{distance-d}} = 22$, $n_{\text{distance-v}} = 23$, $n_c = 1$)

CALIFORNIA.—Riverside Co.; Colorado Desert, Dos Palmas ($n = 1$, LACM 4346); Desert Center, 9.4 mi S, 9.8 mi W; Salt Creek Wash ($n = 21$, LACM 80544-80549, 85070, 86352, 86354-86361, 86363-86364, 86366, 86369); 0.2 mi W Rancho Dos Palmas ($n = 1$, MVZ 195955); Shavers Valley, ca. 9 mi E Cactus City ($n = 1$, MVZ 195954) – total $n = 24$.

bangsi-2 ($n_{\text{shape-d}} = 32$, $n_{\text{shape-v}} = 30$, $n_{\text{distance-d}} = 34$, $n_{\text{distance-v}} = 32$, $n_c = 27$)

CALIFORNIA.—Riverside Co.; Garnet ($n = 2$, MVZ 90652, 90655); Indio Hills, Pushawalla Canyon, 3.5 mi NW junction of Berdoo Canyon road and Dillon road ($n = 1$, MVZ 184650); Palm Springs ($n = 14$, MCZ 5304 [holotype of *bangsi* Mearns]; LACM 3233, 3291, 3294-3295, 3298, 30072; MVZ 31839; SBMNH 6663-6664, 6666; SDNHM 6666-6667, 22081); Palm Springs, 5 mi NW ($n = 1$, LACM 10352); Santa Rosa Mts.; Deep Canyon ($n = 1$, LACM 20676); 3 mi E Thousand Palms ($n = 1$, LACM 90123); 2.5 mi E and 0.5 mi S Whitewater ($n = 6$, MVZ 85064-85069); 2.5 mi E and 1 mi S Whitewater ($n = 12$, MVZ 85050-85057, 85060-85063) – total $n = 38$.

bangsi-3 ($n_{\text{shape-d}} = 41$, $n_{\text{shape-v}} = 37$, $n_{\text{distance-d}} = 41$, $n_{\text{distance-v}} = 37$, $n_c = 20$)

CALIFORNIA.—Riverside Co.; 5 mi E Cabezon ($n = 8$, MVZ 84352-84357, 84373-84374); 7 mi E and 1.2 mi S Cabezon ($n = 2$, MVZ 84358, 84360); 0.5 mi W and 0.1 mi S Palm Springs Station ($n = 1$, MVZ 184651); 2 mi W Palm Springs Station ($n = 1$, MVZ 84363); San Gorgonio River, 0.33 mi S, 0.41 mi W Whitewater ($n = 7$, LACM 80550-80556); Snow Creek, near Whitewater ($n = 11$, MVZ 1471, 1473-1474, 1485-1486, 1492-1493, 1495, 1497, 1499, 1502); 0.95 mi S hwy 111 on Snow Creek Road ($n = 10$, MVZ 184653-184662); Whitewater Station ($n = 1$, MVZ 1506); 0.5 mi S and 0.8 mi W Whitewater ($n = 3$, MVZ 206791-206793) – total $n = 44$.

bangsi-4 ($n_{\text{shape-d}} = 63$, $n_{\text{shape-v}} = 60$, $n_{\text{distance-d}} = 64$, $n_{\text{distance-v}} = 61$, $n_c = 76$)

CALIFORNIA.—Riverside Co.; Cabazon ($n = 68$, LACM 2259, 20505, 20526-20531; SBMNH 6671-6672; SDNHM 5610, 5615-5622, 5624, 5633-5637, 5639-5644, 5653-5661, 5672-5677, 5679-5680, 5686-5689, 7302-7304, 7325-7328, 7341-7343, 7345-7346; USNM 54075-54077); 0.25 mi E Cabazon ($n = 2$, MVZ 90653-90654); 0.5 mi E Cabazon ($n = 1$, MVZ 90654); 1 mi E Cabazon ($n = 6$, MVZ 184645-184649, 195956); 1 mi S Cabazon ($n = 3$, LACM 10360-10362); 2 mi S Cabazon ($n = 7$, LACM 10354-10359); 2 mi W and 1 mi N Cabazon ($n = 2$, MVZ 84347-84348) – total $n = 89$.

bangsi-5 ($n_{\text{shape-d}} = 11$, $n_{\text{shape-v}} = 11$, $n_{\text{distance-d}} = 11$, $n_{\text{distance-v}} = 11$, $n_c = 23$)

CALIFORNIA.—Riverside Co.; Banning ($n = 1$, USNM 160083); Banning, base of San Jacinto Mts ($n = 2$, MVZ 1489-1490); base of San Jacinto Mts, near Cabazon ($n = 2$, MVZ 1367, 1378); 2 mi W and 1 mi N Cabezon ($n = 1$, MVZ 84349); 2 mi W and 1.5 mi N Cabazon ($n = 2$, MVZ 84346-84347); base San Jacinto Mts, near Cabazon ($n = 13$, MVZ 1356-1363, 1366-1367, 1378-1380); San Jacinto Mts., near Cabazon ($n = 7$, MVZ 1370, 1372-1377) – total $n = 28$.

bangsi-6 ($n_{\text{shape-d}} = 28$, $n_{\text{shape-v}} = 24$, $n_{\text{distance-d}} = 27$, $n_{\text{distance-v}} = 27$, $n_c = 31$)

CALIFORNIA.—San Diego Co.; Borrego Springs, 3 mi S, 3.5 mi W ($n = 4$, LACM 38499-38502); below Borrego Springs ($n = 3$, SDNHM 915-916, 918); 3.3 mi S Borrego Springs on hwy 53 ($n = 1$, MVZ 184663); 4 mi S Borrego Springs ($n = 1$, LACM 69588); 10 mi E Borrego Springs ($n = 1$, SDNHM 917); Borrego Valley, Beatty Ranch ($n = 17$, LACM 3039-3055); Borrego Valley, mouth of Coyote Creek ($n = 4$, LACM 29355-29359); Borrego Valley, Palm Canyon ($n = 3$, LACM 3036-3038); Borrego Valley, 3 mi SW Palm Canyon ($n = 1$, SBMNH 6662); Culp Valley, 2 mi E Ranchita ($n = 1$, SDMNHM) – total $n = 36$.

bangsi-7 ($n_{\text{shape-d}} = 43$, $n_{\text{shape-v}} = 39$, $n_{\text{distance-d}} = 42$, $n_{\text{distance-v}} = 38$, $n_c = 43$)

CALIFORNIA.—San Diego Co.; San Felipe Narrows ($n = 43$, LACM 3032-3035, 3171-3186; MVZ 55156; SBMNH 6645-6661; SDNHM 1590, 2625, 2627-2628, 6661, 17621, 19211; USNM 99828 [holotype of *arenicola* Stephens]); San Felipe Narrows, Desert Sand Dunes ($n = 1$, UAZ 17143); E side San Felipe Narrows ($n = 4$; SDNHM 9911-9913, 9923) – total $n = 48$.

bangsi-8 ($n_{\text{shape-d}} = 13$, $n_{\text{shape-v}} = 13$, $n_{\text{distance-d}} = 12$, $n_{\text{distance-v}} = 13$, $n_c = 3$)

MEXICO.—Baja California; Cerro Centinela, 12 mi WSW Mexicali ($n = 1$, MVZ 111306). CALIFORNIA.—Imperial Co.; Crucifixion Thorn Reserve, 0.8 mi S and 7.8 mi E Ocotillo ($n = 1$, MVZ 184644); 3.2 mi W Ocotillo, 0.2 mi S hwy 52; Dos Cabezas Rd ($n = 3$, LACM 46578-46580); Yuha, Smoke Tree Wash ($n = 10$, LACM 65147-65153, 65165, 80014-80015) – total $n = 15$.

Appendix 1

Continuation

bombycinus-1 ($n_{\text{shape-d}} = 6, n_{\text{shape-v}} = 6, n_{\text{distance-d}} = 6, n_{\text{distance-v}} = 5, n_c = 1$)

CALIFORNIA.—Riverside Co.; 9 mi W Blythe ($n = 1$, LACM 4189); 6.5 mi NW Blythe ($n = 1$, MVZ 239809); 26 mi W Blythe; Chuckwalla Rd; I-10, 4 mi W ($n = 3$, LACM 80540-80542); Chuckwalla Valley, 2 mi S, 19 mi W Blythe ($n = 1$, LACM 80543); Hopkins Well ($n = 1$, LACM 7594) – total $n = 7$.

bombycinus-2 ($n_{\text{shape-d}} = 15, n_{\text{shape-v}} = 7, n_{\text{distance-d}} = 15, n_{\text{distance-v}} = 7, n_c = 3$)

CALIFORNIA.—Imperial Co.; Colorado River, Pilot Knob ($n = 1$, MVZ 9976); Colorado River near Pilot Knob ($n = 3$, MVZ 9973-9975); 8.6 mi W, 0.6 mi N Glamis ($n = 5$, UAZ 11185-11188, 15353); 21 mi N Glamis ($n = 1$, UAZ 11299); west side Pilot Knob ($n = 1$, MVZ 239808); 3 mi W Pilot Knob ($n = 2$, SDNHM 4532-4533); 2 mi N I-8 on county hwy S-34 ($n = 2$, MSB 190591-190592) – total $n = 15$.

brevinasus-1 ($n_{\text{shape-d}} = 53, n_{\text{shape-v}} = 48, n_{\text{distance-d}} = 53, n_{\text{distance-v}} = 48, n_c = 29$)

CALIFORNIA.—Riverside Co.; Reche Canyon ($n = 1$, SDNHM 19212). San Bernardino Co.; mouth of Reche Canyon, near Colton ($n = 1$, MVZ 2656); Reche Canyon, 4 mi SE Colton ($n = 1$, MVZ 24496); San Bernardino ($n = 22$, SDNHM 908-909), USNM 22630-22631, 22634, 186515 [holotype of *brevinasus* Osgood], 192214, 192223-192226, 192230, 192233-192234, 192240-192244, 192248-192249); 4.75 mi N San Bernardino ($n = 3$, MVZ 77112-77114); 5 mi NW San Bernardino ($n = 26$, SDNHM 13311-13312, 13314, 13316, 13318-13322, 13328-13339, 13342, 13344-13347); Slover Mt near Colton ($n = 1$, MVZ 16664) – total $n = 55$.

brevinasus-2 ($n_{\text{shape-d}} = 18, n_{\text{shape-v}} = 16, n_{\text{distance-d}} = 17, n_{\text{distance-v}} = 13, n_c = 21$)

CALIFORNIA.—Riverside Co.; Menifee ($n = 16$, LACM 2649-2655, 3997-4006); 1 mi E Menifee ($n = 1$, LACM 48842); Winchester ($n = 3$, LACM 3655-3657); 1.5 mi W Winchester ($n = 1$, LACM 48841) – total $n = 21$.

brevinasus-3 ($n_{\text{shape-d}} = 10, n_{\text{shape-v}} = 7, n_{\text{distance-d}} = 9, n_{\text{distance-v}} = 8, n_c = 11$)

CALIFORNIA.—Riverside Co.; Aguanga ($n = 2$, SDNHM 1780, 13361); 0.25 mi ENE Aguanga ($n = 1$, MVZ 123341); 5 mi N 0.25 mi W Aguanga ($n = 3$, LACM 48843-48845). San Diego Co.; Oak Grove, N side Palomar Mt ($n = 1$, SBMNH 6673); 2.5 mi N Oak Grove ($n = 6$, SDNHM 13369-13374) – total $n = 13$.

internationalis-1 ($n_{\text{shape-d}} = 42, n_{\text{shape-v}} = 42, n_{\text{distance-d}} = 43, n_{\text{distance-v}} = 43, n_c = 39$)

MEXICO.—Baja California; international boundary near Jacumba, CA ($n = 38$, SDNHM 11917-11936, 11944-11957, 11970, 11971 [holotype of *internationalis* Huey], 11972-11973). CALIFORNIA.—San Diego Co.; Jacunta [= Jacumba] ($n = 1$, FMNH 6984); Jacumba, 12 mi N, 4.5 mi E, old hwy 80 ($n = 2$, LACM 81008-81009); Jacumba Range, Smugglers Cave Basin ($n = 1$, LACM 46800); I-8, 4.2 mi N, In-Ko-Pah Valley Rd ($n = 3$, LACM 81005-81007) – total $n = 45$.

internationalis-2 ($n_{\text{shape-d}} = 31, n_{\text{shape-v}} = 23, n_{\text{distance-d}} = 31, n_{\text{distance-v}} = 22, n_c = 29$)

CALIFORNIA.—San Diego Co.; La Puerta Valley ($n = 33$, SBMNH 6674-6680, 6682); SDNHM 1416-1417, 1424, 1431-1432, 1850, 1860, 1866, 1910, 2168, 2198, 2204, 2207, 2214-2217, 2220-2223, 2237, 2256, 2266, 7174, 20398-20399); La Puerta Valley [= Mason Valley] ($n = 5$, MVZ 18847, 18849, 32834, 32836, 32838) – total $n = 38$.

internationalis-3 ($n_{\text{shape-d}} = 19, n_{\text{shape-v}} = 11, n_{\text{distance-d}} = 19, n_{\text{distance-v}} = 11, n_c = 16$)

CALIFORNIA.—San Diego Co.; 5.5 mi N Banner, San Felipe Valley ($n = 2$, MVZ 122457-122458); Coast Range Mountains, Summit ($n = 1$, USNM 60718); Julian, 1 mi N, 7.3 mi E, Scissors Crossing [Earthquake Valley] ($n = 2$, LACM 89253-89254); San Felipe Valley ($n = 2$, MVZ 7541; SDNHM 913); Scissor's Crossing, Earthquake Valley ($n = 9$, MVZ 123345-123354); 3.25 mi S, 3.25 mi E Scissor Crossing, Earthquake Valley ($n = 4$, MVZ 123355-123358) – total $n = 20$.

pacificus-1 ($n_{\text{shape-d}} = 63, n_{\text{shape-v}} = 61, n_{\text{distance-d}} = 66, n_{\text{distance-v}} = 63, n_c = 35$)

CALIFORNIA.—San Diego Co.; Mexican Boundary Monument No. 258, edge of Pacific Ocean at Mexican Boundary Monument No. 258 ($n = 1$, USNM 61022 [holotype of *pacificus* Mearns]); Mexican Boundary Monument No. 258, shore of Pacific Ocean ($n = 1$, USNM 61024); 2 mi N Monument #258, mouth of Tijuana River ($n = 12$, LACM 2702-2705, 2707-2713, 2718); near mouth Tijuana River ($n = 4$, MVZ 47312-47313; SDNHM 19213, 19216); Tijuana River ($n = 1$, SDNHM 9712); Tijuana River; mouth, 2 mi N Monument #258 ($n = 11$, SBMNH 6691, 6693-6694, 6697-6698, 6701, 6703-6704, 6707-6708, 6710); Tijuana River Valley ($n = 8$, SDNHM 22085, 22088, 22408-22413); Tijuana Valley ($n = 35$, SDNHM 9510-9512, 9717-9721, 9724, 9727-9732, 9741-9745, 9747, 9749-9753, 9756-9757, 9762-9765, 9767, 9774, 9775, 10562); US-Mexico border, Monument 258 ($n = 1$, SBMNH 6806) – total $n = 72$.

pacificus-2 ($n_{\text{shape-d}} = 48, n_{\text{shape-v}} = 40, n_{\text{distance-d}} = 48, n_{\text{distance-v}} = 42, n_c = 25$)

CALIFORNIA.—Orange Co.; Dana Point ($n = 1$, MVZ 195949); Dana Pt, 5 mi W Capistrano Beach ($n = 8$, LACM 3282-3289). San Diego Co.; Oceanside ($n = 28$, LACM 3562-3563; MVZ 47101-47103, 47105-47106; SBMNH 6804; SDNHM 16222-

Appendix 1

Continuation

16224, 16226-16229, 16233-16235, 16238-16239, 16241-16243, 17614-17615, 17617, 17620, 18705); 4 mi N Oceanside ($n = 4$, SDNHM 10595-10597, 10599); 4 mi NW Oceanside; Santa Margarita Ranch ($n = 6$, LACM 2720-2727); Oscar One Training Area, Camp Pendleton Marine Corps Base ($n = 7$, MVZ 195952); San Onofre ($n = 1$, SDNHM 923); San Onofre Creek, dry mesa at mouth ($n = 1$, SBMNH 6711); San Onofre, 2 mi E on hwy 101 ($n = 1$, SBMNH 6712); Santa Margarita River, 5 mi N Oceanside ($n = 6$, SBMNH 6713-6718) – total $n = 63$.

pacificus-3 ($n_{\text{shape-d}} = 80$, $n_{\text{shape-v}} = 75$, $n_{\text{distance-d}} = 77$, $n_{\text{distance-v}} = 76$, $n_c = 92$)

CALIFORNIA.—Los Angeles Co.; Clifton ($n = 2$, SBMNH 6737-6738); Del Rey ($n = 9$, LACM 3220-3228, 3233); Del Rey Hills, near Loyola University ($n = 3$, LACM 4486-4488); 0.5 mi NW El Segundo ($n = 1$, MVZ 74750); 1 mi N El Segundo ($n = 5$, SDNHM 13349-13350, 13352, 13354-13355); Hyperion ($n = 79$, LACM 429; SBMNH 6719-6720, 6726-6736, 6740-6802); Hyperion [= El Segundo] ($n = 2$, MVZ 74680 [holotype of *cantwelli* von Bloeker]; UAZ 17145), Palisades Del Rey ($n = 1$, SBMNH 6723); Playa del Rey ($n = 9$, LACM 3529, 3727-3729, 4382, 48822-48825) – total $n = 102$.

unknown ($n_{\text{shape-d}} = 24$, $n_c = 26$)

CALIFORNIA.—Imperial Co.; Salton Sea ($n = 1$, LACM 65146). Los Angeles Co.; San Fernando ($n = 3$, SBMNH 6667-6669). Riverside Co.; Dos Palmas Spring, Santa Rosa Mts ($n = 2$, MVZ 1929-1930); Eden Hot Springs ($n = 1$, MVZ 90713); Hemet ($n = 1$, USNM 149899); Santa Rosa Mts, 0.4 mi E Dos Palmas Spring ($n = 1$, MVZ 184652); Temecula, at I-15 hwy 79 jct, Santa Gertrudis Creek ($n = 1$, LACM 80249); near Temecula, Rancho California Valley ($n = 1$, LACM 89250); Vallevista, San Jacinto Valley ($n = 7$, MVZ 2278-2281, 2283-2285). San Diego Co.; 3.25 mi N Manzanita, McCain Valley ($n = 2$, MVZ 123359-123360); Warner Pass ($n = 14$, MVZ 7620-7629, 7660-7662, 7666) – total $n = 34$.

Appendix 2

Main effects of sex, age, and paired interaction in a least squares analysis of the pooled pacificus-1 (*pacificus* Mearns) and pacific-3 (*cantwelli* von Bloeker) samples ($n = 66$ and 78 , respectively) for cranial variables; only P -values are provided, significant ones in bold (Bonferroni corrected P at $\alpha_{0.05} = 0.0016$).

| Sample | Pacificus-1 [<i>pacificus</i>] | | | Pacificus-3 [<i>cantwelli</i>] | | |
|-------------------------------|----------------------------------|--------------|-----------|----------------------------------|-------|-----------|
| | | $n = 66$ | | $n = 78$ | | |
| Avariable | Sex | Age | Sex * age | Sex | Age | Sex * age |
| Dorsal measurements | | | | | | |
| occipito-nasal length | 0.306 | 0.027 | 0.036 | 0.159 | 0.645 | 0.519 |
| nasal length | 0.179 | 0.001 | 0.020 | 0.248 | 0.489 | 0.604 |
| frontal length | 0.488 | 0.349 | 0.469 | 0.471 | 0.692 | 0.388 |
| parietal length | 0.900 | 0.495 | 0.902 | 0.061 | 0.256 | 0.680 |
| interparietal length | 0.447 | 0.275 | 0.654 | 0.334 | 0.902 | 0.876 |
| premax-extension length | 0.561 | 0.645 | 0.970 | 0.532 | 0.651 | 0.214 |
| rostral width | 0.397 | 0.012 | 0.083 | 0.400 | 0.143 | 0.912 |
| maxillary width | 0.985 | 0.508 | 0.445 | 0.876 | 0.252 | 0.846 |
| premax-extension width | 0.562 | 0.555 | 0.850 | 0.564 | 0.492 | 0.928 |
| interorbital constriction | 0.060 | 0.315 | 0.210 | 0.462 | 0.428 | 0.647 |
| zygomatic breadth | 0.050 | 0.001 | 0.028 | 0.231 | 0.045 | 0.699 |
| parietal width-anterior | 0.016 | 0.359 | 0.513 | 0.788 | 0.301 | 0.467 |
| interparietal width-anterior | 0.690 | 0.958 | 0.635 | 0.714 | 0.026 | 0.128 |
| interparietal width-posterior | 0.739 | 0.588 | 0.504 | 0.393 | 0.108 | 0.441 |
| exoccipital width | 0.429 | 0.124 | 0.859 | 0.940 | 0.749 | 0.149 |
| bullar width | 0.495 | 0.059 | 0.059 | 0.412 | 0.363 | 0.374 |
| bulla length | 0.871 | 0.444 | 0.096 | 0.292 | 0.509 | 0.244 |
| bulla width | 0.786 | 0.336 | 0.011 | 0.458 | 0.039 | 0.723 |
| bulla area | 0.399 | 0.105 | 0.031 | 0.504 | 0.032 | 0.651 |
| bulla perimeter | 0.762 | 0.484 | 0.085 | 0.173 | 0.193 | 0.730 |
| Ventral measurements | | | | | | |
| anterior nasal extension | 0.807 | 0.271 | 0.006 | 0.013 | 0.227 | 0.984 |
| palatal length | 0.568 | 0.005 | 0.019 | 0.312 | 0.158 | 0.855 |
| mesopterygoid fossa length | 0.854 | 0.380 | 0.695 | 0.215 | 0.593 | 0.593 |
| foramen magnum length | 0.649 | 0.009 | 0.257 | 0.955 | 0.084 | 0.436 |
| maxillary toothrow length | 0.800 | 0.643 | 0.145 | 0.603 | 0.849 | 0.321 |
| upper incisor breadth | 0.879 | 0.001 | 0.185 | 0.428 | 0.604 | 0.569 |
| palatal breadth | 0.629 | 0.006 | 0.279 | 0.404 | 0.243 | 0.808 |
| squamosal breadth | 0.036 | 0.267 | 0.083 | 0.868 | 0.440 | 0.135 |
| mesopterygoid width | 0.218 | 0.001 | 0.768 | 0.675 | 0.009 | 0.658 |
| stylomastoid foramina width | 0.619 | 0.166 | 0.065 | 0.395 | 0.072 | 0.884 |
| occipital condyle width | | | | | | |
| | 0.665 | 0.042 | 0.211 | 0.501 | 0.703 | 0.090 |
| exoccipital width | 0.992 | 0.145 | 0.760 | 0.505 | 0.141 | 0.929 |

Appendix 3

External measurements (column A) and selected cranial dimensions (column B) for samples that contain the holotype and topotypic series for each of the seven subspecies described from the study area in southern California and northern Baja California. Data include minimal non-significant subsets based on oneway ANOVAs followed by Tukey-Kramer HSD pairwise tests (with Bonferroni corrected *P*-values for multiple tests), sample mean and standard error (in mm), and sample size. See text for definition of variables.

A: External measurements (from specimen labels)

| variable/taxon | A | B | C | D | mean | std err | n |
|------------------------|---|---|---|---|--------|---------|----|
| TOL | | | | | | | |
| <i>internationalis</i> | A | | | | 141.76 | 0.908 | 38 |
| <i>aestivus</i> | A | | | | 141.35 | 1.357 | 17 |
| <i>arenicola</i> | A | | | | 139.89 | 0.946 | 35 |
| <i>brevinasus</i> | | B | | | 134.07 | 1.077 | 27 |
| <i>bangsi</i> | | | C | | 129.50 | 1.769 | 10 |
| <i>cantwelli</i> | | | C | | 127.62 | 0.735 | 58 |
| <i>pacificus</i> | | | | D | 119.64 | 0.754 | 55 |
| TAL | | | | | | | |
| <i>arenicola</i> | A | | | | 79.03 | 0.793 | 35 |
| <i>internationalis</i> | A | | | | 77.74 | 0.761 | 38 |
| <i>aestivus</i> | A | | | | 77.71 | 1.137 | 17 |
| <i>bangsi</i> | | B | | | 71.00 | 1.483 | 10 |
| <i>brevinasus</i> | | B | | | 70.00 | 0.903 | 27 |
| <i>cantwelli</i> | | | C | | 67.45 | 0.616 | 58 |
| <i>pacificus</i> | | | | D | 61.58 | 0.632 | 55 |
| HBL [TOL-TAL] | | | | | | | |
| <i>brevinasus</i> | A | | | | 64.07 | 0.676 | 27 |
| <i>internationalis</i> | A | | | | 64.03 | 0.569 | 38 |
| <i>aestivus</i> | A | | | | 63.65 | 0.851 | 17 |
| <i>arenicola</i> | | B | | | 60.86 | 0.593 | 35 |
| <i>cantwelli</i> | | B | | | 60.17 | 0.461 | 58 |
| <i>bangsi</i> | | B | C | | 58.50 | 1.110 | 10 |
| <i>pacificus</i> | | | C | | 58.05 | 0.473 | 55 |
| TAL:TOL x 100 | | | | | | | |
| <i>arenicola</i> | A | | | | 56.47 | 0.386 | 35 |
| <i>aestivus</i> | | B | | | 54.94 | 0.554 | 17 |
| <i>bangsi</i> | | B | | | 54.83 | 0.722 | 10 |
| <i>internationalis</i> | | B | | | 54.82 | 0.370 | 38 |
| <i>cantwelli</i> | | | C | | 52.80 | 0.300 | 58 |
| <i>brevinasus</i> | | | C | D | 52.21 | 0.439 | 27 |
| <i>pacificus</i> | | | | D | 51.47 | 0.308 | 55 |
| HF [w/ claw] | | | | | | | |
| <i>aestivus</i> | A | | | | 18.83 | 0.145 | 18 |
| <i>internationalis</i> | A | | | | 18.65 | 0.101 | 37 |
| <i>arenicola</i> | A | | | | 18.63 | 0.104 | 35 |
| <i>brevinasus</i> | A | | | | 18.52 | 0.114 | 29 |
| <i>bangsi</i> | A | B | | | 18.40 | 0.194 | 10 |
| <i>cantwelli</i> | | B | | | 17.78 | 0.080 | 59 |
| <i>pacificus</i> | | | C | | 16.76 | 0.083 | 55 |
| E [notch] | | | | | | | |
| <i>internationalis</i> | A | | | | 7.03 | 0.087 | 37 |
| <i>aestivus</i> | A | | | | 6.94 | 0.124 | 18 |
| <i>brevinasus</i> | A | | | | 6.86 | 0.098 | 29 |
| <i>bangsi</i> | A | B | | | 6.67 | 0.176 | 9 |
| <i>cantwelli</i> | | B | C | | 6.30 | 0.083 | 40 |
| <i>pacificus</i> | | | C | | 6.21 | 0.073 | 53 |
| <i>arenicola</i> | | | C | | 6.10 | 0.12 | 21 |

B: Selected cranial dimensions

| variable/taxon | A | B | C | D | E | mean | std err | n |
|------------------------|---|---|---|---|---|-------|---------|----|
| ONL | | | | | | | | |
| <i>aestivus</i> | A | | | | | 21.57 | 0.116 | 55 |
| <i>internationalis</i> | | B | | | | 21.18 | 0.081 | 39 |
| <i>brevinasus</i> | | B | C | | | 21.06 | 0.073 | 60 |
| <i>bangsi</i> | | | C | | | 20.84 | 0.095 | 48 |
| <i>arenicola</i> | | | | D | | 20.39 | 0.083 | 28 |
| <i>pacificus</i> | | | | | E | 19.83 | 0.068 | 37 |
| <i>cantwelli</i> | | | | | E | 19.76 | 0.065 | 19 |
| NL | | | | | | | | |
| <i>aestivus</i> | A | | | | | 7.70 | 0.066 | 19 |
| <i>bangsi</i> | A | | | | | 7.67 | 0.054 | 28 |
| <i>internationalis</i> | A | B | | | | 7.57 | 0.046 | 39 |
| <i>brevinasus</i> | | B | C | | | 7.49 | 0.042 | 48 |
| <i>arenicola</i> | | | C | | | 7.42 | 0.047 | 37 |
| <i>cantwelli</i> | | | | D | | 6.87 | 0.037 | 60 |
| <i>pacificus</i> | | | | | E | 6.65 | 0.039 | 55 |
| RL | | | | | | | | |
| <i>internationalis</i> | A | | | | | 2.16 | 0.016 | 39 |
| <i>aestivus</i> | A | B | | | | 2.13 | 0.022 | 19 |
| <i>brevinasus</i> | A | B | | | | 2.12 | 0.014 | 48 |
| <i>bangsi</i> | | B | C | | | 2.08 | 0.018 | 28 |
| <i>pacificus</i> | | | C | | | 2.05 | 0.013 | 55 |
| <i>cantwelli</i> | | | | D | | 2.00 | 0.013 | 60 |
| <i>arenicola</i> | | | | D | | 1.98 | 0.016 | 37 |
| IOC | | | | | | | | |
| <i>aestivus</i> | A | | | | | 5.10 | 0.039 | 19 |
| <i>internationalis</i> | A | B | | | | 5.04 | 0.028 | 39 |
| <i>brevinasus</i> | | B | | | | 5.00 | 0.025 | 48 |
| <i>bangsi</i> | | B | | | | 4.98 | 0.033 | 28 |
| <i>pacificus</i> | | | C | | | 4.81 | 0.023 | 55 |
| <i>arenicola</i> | | | | D | | 4.70 | 0.028 | 37 |
| <i>cantwelli</i> | | | | D | | 4.65 | 0.022 | 60 |
| IPW-ant | | | | | | | | |
| <i>brevinasus</i> | A | | | | | 3.88 | 0.036 | 48 |
| <i>pacificus</i> | A | | | | | 3.85 | 0.033 | 55 |
| <i>bangsi</i> | A | | | | | 3.77 | 0.047 | 28 |
| <i>internationalis</i> | | B | | | | 3.63 | 0.040 | 39 |
| <i>cantwelli</i> | | B | | | | 3.55 | 0.032 | 60 |
| <i>arenicola</i> | | | C | | | 3.10 | 0.041 | 37 |
| <i>aestivus</i> | | | C | | | 3.10 | 0.057 | 19 |
| bull perimeter* | | | | | | | | |
| <i>aestivus</i> | A | | | | | 21.44 | 0.162 | 19 |
| <i>arenicola</i> | | B | | | | 19.26 | 0.116 | 37 |
| <i>internationalis</i> | | B | | | | 19.09 | 0.113 | 39 |
| <i>bangsi</i> | | | C | | | 18.17 | 0.133 | 28 |
| <i>brevinasus</i> | | | C | | | 17.86 | 0.102 | 48 |
| <i>pacificus</i> | | | | D | | 17.32 | 0.095 | 55 |
| <i>cantwelli</i> | | | | | E | 16.61 | 0.091 | 60 |

* bulla perimeter is strongly correlated with both bulla length ($R^2 = 0.939$) and bulla width ($R^2 = 0.935$)

Appendix 4

Colorimetric variables for 20 sample groups of *Perognathus longimembris* from the study area in southern California and northern Baja California. Data for each variable (L* [Lightness], Chroma, and Hue) include minimal non-significant subsets based on oneway ANOVAs followed by Tukey-Kramer HSD pairwise tests (with Bonferroni corrected *P*-values for multiple tests), sample mean and standard error, and sample size. See text for definition of variables.

| Variable/taxon | A | B | C | D | E | F | G | H | I | mean | std err | n |
|-----------------------|---|---|---|---|---|---|---|---|---|-------|---------|----|
| L* [Lightness] | | | | | | | | | | | | |
| bangsi-1 | A | B | | | | | | | | 46.53 | 5.106 | 1 |
| bangsi-7 | A | | | | | | | | | 44.03 | 0.779 | 43 |
| bangsi-6 | A | | | | | | | | | 42.34 | 0.917 | 31 |
| bombycinus-2 | A | B | | | | | | | | 40.42 | 2.948 | 3 |
| bangsi-2 | A | | | | | | | | | 39.74 | 0.983 | 27 |
| bombycinus-1 | A | B | | | | | | | | 39.70 | 5.106 | 1 |
| bangsi-8 | A | B | C | | | | | | | 37.02 | 2.948 | 3 |
| bangsi-3 | | B | | | | | | | | 32.44 | 1.142 | 20 |
| aestivus | | B | C | D | E | | | | | 31.16 | 1.805 | 8 |
| bangsi-4 | | B | C | D | | | | | | 29.89 | 0.586 | 76 |
| internationalis-2 | | | C | D | E | F | | | | 25.95 | 0.948 | 29 |
| brevinasus-3 | | | | D | E | F | G | | | 24.77 | 1.539 | 11 |
| internationalis-1 | | | | | E | F | | | | 24.34 | 0.818 | 39 |
| brevinasus-1 | | | | | | F | G | | | 23.40 | 0.948 | 29 |
| brevinasus-2 | | | | | | F | G | | | 22.99 | 1.114 | 21 |
| internationalis-3 | | | | | | F | G | H | | 22.36 | 1.365 | 14 |
| bangsi-5 | | | | | | F | G | H | | 21.62 | 1.065 | 23 |
| pacificus-2 | | | | | | | G | H | I | 18.52 | 1.021 | 25 |
| pacificus-3 | | | | | | | | H | I | 17.53 | 0.532 | 92 |
| pacificus-1 | | | | | | | | | I | 13.99 | 0.863 | 35 |

| Variable/taxon | A | B | C | D | E | F | mean | std err | n |
|-------------------|---|---|---|---|---|---|------|---------|----|
| Hue | | | | | | | | | |
| bangsi-6 | A | B | | | | | 1.27 | 0.013 | 31 |
| bangsi-7 | A | | | | | | 1.27 | 0.011 | 43 |
| bangsi-4 | A | B | | | | | 1.26 | 0.008 | 76 |
| aestivus | A | B | C | | | | 1.26 | 0.026 | 8 |
| bangsi-2 | A | B | | | | | 1.26 | 0.014 | 27 |
| bombycinus-2 | A | B | C | | | | 1.25 | 0.042 | 3 |
| bombycinus-1 | A | B | C | | | | 1.24 | 0.074 | 1 |
| bangsi-3 | A | B | C | | | | 1.24 | 0.016 | 20 |
| internationalis-2 | A | B | C | | | | 1.23 | 0.014 | 29 |
| brevinasus-3 | A | B | C | | | | 1.23 | 0.022 | 11 |
| bangsi-1 | A | B | C | | | | 1.23 | 0.074 | 1 |
| internationalis-1 | A | B | C | | | | 1.23 | 0.012 | 39 |
| internationalis-3 | A | B | C | | | | 1.23 | 0.020 | 14 |
| brevinasus-1 | | B | C | | | | 1.21 | 0.014 | 29 |
| brevinasus-2 | | B | C | D | | | 1.20 | 0.016 | 21 |
| bangsi-8 | A | B | C | D | | | 1.18 | 0.042 | 3 |
| bangsi-5 | | | C | D | E | | 1.17 | 0.015 | 23 |
| pacificus-2 | | | | D | E | F | 1.13 | 0.015 | 25 |
| pacificus-3 | | | | | E | F | 1.13 | 0.008 | 92 |
| pacificus-1 | | | | | | F | 1.08 | 0.012 | 35 |

| Variable/taxon | A | B | C | D | E | F | G | H | mean | std err | n |
|-------------------|---|---|---|---|---|---|---|---|-------|---------|----|
| Chroma | | | | | | | | | | | |
| bangsi-1 | A | B | C | D | | | | | 21.86 | 2.830 | 1 |
| bombycinus-2 | A | B | C | D | | | | | 21.06 | 1.634 | 3 |
| bangsi-2 | A | | | | | | | | 20.16 | 0.545 | 27 |
| bangsi-7 | A | | | | | | | | 19.81 | 0.432 | 43 |
| aestivus | A | B | C | | | | | | 19.56 | 1.001 | 8 |
| bangsi-6 | A | B | | | | | | | 18.84 | 0.508 | 31 |
| bombycinus-1 | A | B | C | D | | | | | 18.69 | 2.830 | 1 |
| bangsi-3 | A | B | C | D | | | G | | 17.87 | 0.633 | 20 |
| bangsi-4 | | B | C | | | | G | | 17.38 | 0.325 | 76 |
| internationalis-2 | | B | C | D | E | | G | | 17.04 | 0.525 | 29 |
| bangsi-8 | A | B | C | D | E | | | | 16.83 | 1.634 | 3 |
| internationalis-3 | | | C | D | E | F | G | | 15.12 | 0.756 | 14 |
| internationalis-1 | | | | D | E | F | | | 15.11 | 0.453 | 39 |
| brevinasus-1 | | | | | E | F | | | 14.38 | 0.525 | 29 |
| brevinasus-3 | | | | | E | F | G | | 14.29 | 0.853 | 11 |
| brevinasus-2 | | | | | E | F | | | 14.17 | 0.618 | 21 |
| bangsi-5 | | | | | | F | | | 14.00 | 0.590 | 23 |
| pacificus-3 | | | | | | F | | | 13.44 | 0.295 | 92 |
| pacificus-2 | | | | | | F | | | 12.73 | 0.566 | 25 |
| pacificus-1 | | | | | | | | H | 9.44 | 0.478 | 35 |

Revisiting species delimitation within *Reithrodontomys sumichrasti* (Rodentia: Cricetidae) using molecular and ecological evidence

ELIZABETH ARELLANO^{1*}, ANA L. ALMENDRA¹, DAILY MARTÍNEZ-BORRERO¹, FRANCISCO X. GONZÁLEZ-CÓZATL¹, AND DUKE S. ROGERS²

¹ Centro de Investigación en Biodiversidad y Conservación, Universidad Autónoma del Estado de Morelos. Avenida Universidad 1001, CP. 62209, Cuernavaca. Morelos, México. Email: elisabet@uaem.mx (EA), al.almendra@gmx.com (ALA), daily.marbo@gmail.com (DM-B), xavier@uaem.mx (FXG-C).

² Life Science Museum and Department of Biology, Brigham Young University. CP. 84602, Provo. Utah, U.S.A. Email: duke_rogers@byu.edu (DSR).

*Corresponding author: <https://orcid.org/0000-0001-8709-9514>.

Reithrodontomys sumichrasti is distributed from central México to Panama. Previous studies using DNA sequences suggest the existence of distinct clades that may deserve species-level recognition. Here, we use multiple methods of species delimitation to evaluate if this taxon is a complex of cryptic species. DNA sequences from the genes Cyt-b, Fgb-I7, and Acp5 were obtained from GenBank to perform molecular analyses. Species boundaries were tested using the bGMYC, STACEY, and BPP species delimitation methods. Divergence times were estimated as well as the Cyt-b genetic distances. We developed Ecological Niche Models and tested hypotheses of niche conservatism. Finally, we estimated the spatiotemporal history of lineage dispersal. The bGMYC proposed two species while STACEY and BPP proposed 4 species (genetic distances ranged from 5.43 % to 7.52 %). The ancestral position of clade I was recovered, with a Pleistocene diversification time within *R. sumichrasti* at ~2.15 Ma. For clade pairwise niche comparisons, the niche identity hypothesis was rejected. The ancestral distribution of *R. sumichrasti* was centered in Central America and spread to the west crossing the Isthmus of Tehuantepec and extending to the mountain regions of Central México. Our taxonomic considerations included the recognition of four clades as distinct species within *R. sumichrasti*.

Reithrodontomys sumichrasti se distribuye desde el centro de México hasta Panamá. Estudios previos con secuencias de ADN sugieren la existencia de clados distintos y su posible reconocimiento como especies. En este estudio, probamos diferentes métodos de delimitación de especies para evaluar si este taxón constituye un complejo de especies crípticas. Las secuencias de ADN de los genes Cyt-b, Fgb-I7 y Acp5 fueron descargadas de GenBank y utilizadas en análisis moleculares. Los límites de especies fueron probados utilizando los métodos de delimitación bGMYC, STACEY y BPP. Se estimaron tiempos de divergencia y distancias genéticas para el gen Cyt-b. Además, construimos Modelos de Nicho Ecológico y probamos hipótesis de conservadurismo de nicho. Finalmente, reconstruimos la historia espaciotemporal de la dispersión de los linajes. El bGMYC propuso dos especies, mientras que STACEY y BPP propusieron 4 especies (las distancias genéticas oscilaron entre 5.43 % y 7.52 %). Se recuperó la posición ancestral del clado I, ubicando en el Pleistoceno la diversificación dentro de *R. sumichrasti*, hace ~2.15 Ma. En las comparaciones de nicho por pares de clados fue rechazada la hipótesis de identidad de nicho. La distribución ancestral de *R. sumichrasti* se centró en América Central desde donde comenzó a extenderse hacia el oeste cruzando el Istmo de Tehuantepec y extendiéndose hacia las regiones montañosas del centro de México. Nuestras consideraciones taxonómicas incluyeron el reconocimiento de cuatro clados como especies distintas dentro de *R. sumichrasti*.

Keywords: Cryptic species; harvest mice; integrative taxonomy; Mesoamerican highlands; phylogeographic patterns.

© 2023 Asociación Mexicana de Mastozoología, www.mastozoologiamexicana.org

Introduction

A special issue of *Therya* dedicated to Dr. Alfred L. Gardner for his long research career on the diversity of neotropical mammals, especially for his work in México, honors this outstanding scientist by contributing important advances to the knowledge of mammalogy. Our contribution adds to the mission of modern systematic biology: the discovery, description, and classification of the biodiversity on the planet from an evolutionary perspective (Daly et al. 2012). This task involves subjects under debate over the past three decades, such as the species concept (what a species is) and species delimitation (how a species is recognized). Both subjects are closely related but conveniently divided for practical applications (see review by de Queiroz 2007), and over time, species delimitation has taken priority over

species concepts (Sites and Marshall 2003, 2004). Given the current rate of species loss, it is urgent to accurately delimit species inasmuch they are the fundamental unit in studies of ecology, systematic, and conservation biology, among other research areas. From the evolutionary standpoint, species delimitation includes the understanding of population-level mechanisms that can be complex (Huang 2020). Populations differentiation through multiple stages at different rates, in part dependent on factors such as generation time, selection pressure, and gene flow. Tracing the process with an acceptable level of certainty depends on the use of appropriate markers (preferably multiple and independent) and the criteria of evaluation (de Queiroz 2007). One of the most reliable strategies is to use multiple sources of evidence (morphology, genet-

ics, ecology, geography, among others) and to base conclusions on their consistency (Knowles and Carstens 2007; Rissler and Apodaca 2007; Carstens et al. 2013).

There are both regions as well as biological groups, which are amenable to test hypotheses about species delimitation. The Mesoamerican region has been repeatedly used as a study model because of its complex physiography and biogeographical history, which is reflected by high biological diversity, including many endemic species (Myers et al. 2000), particularly for highland groups. As for groups of organisms, rodents, reptiles, and insects, among others have served as models to test hypotheses about evolutionary patterns and processes (e. g. Doody et al. 2009; Gilbert and Manica 2015; Maestri et al. 2017). Some species of rodents have been assessed by evaluating their phylogenetic relationships and further used to illuminate the vicariant biogeography of Mesoamerica (e. g. Sullivan et al. 2000; Leon-Paniagua et al. 2007; Almendra et al. 2018; León-Tapia et al. 2021). Such is the case of *Reithrodontomys sumichrasti* (Family Cricetidae; Bradley 2017), with a particular interest in the high levels of intraspecific divergence reported (Sullivan et al. 2000; Urbina et al. 2006; Hardy et al. 2013).

Reithrodontomys sumichrasti is distributed along the highlands of Mesoamerica, from central México at 1,200 masl to Panama above 3,400 masl, inhabiting temperate

pine-oak and cloud forests. Seven subspecies are recognized, which are distributed in three disjunctive spots (Hooper 1952; Hall 1981; Figure 1). The range of *R. s. sumichrasti* includes portions of the Sierra Madre Oriental, the Mexican Transvolcanic Belt, and the Oaxacan Highlands (type locality El Mirador, Veracruz, México). The distribution of *R. s. nerterus* is restricted to the west portion of the Mexican Transvolcanic Belt (type locality Nevado de Colima, Jalisco, México) whereas *R. s. luteolus* is found in the Sierra Madre del Sur (type locality Juquila, Oaxaca, México). *R. s. dorsalis* occurs in the mountains of the Mexican states of Chiapas and Guatemala (type locality Tonicapan, Guatemala) and *R. s. modestus* in the highlands of El Salvador, Honduras, and western Nicaragua (type locality Jinotega, Nicaragua). The southernmost distribution of the species includes the Cordillera Central and Cordillera de Talamanca in Costa Rica for *R. s. australis* (type locality Cartago, Costa Rica) and the extreme east of Costa Rica and high mountains of western Panama for *R. s. vulcanius* (type locality Chiriquí, Panama; Hooper 1952).

Previous phylogenetic studies using DNA sequences of the mitochondrial Cytochrome b (Cyt-b) gene (Sullivan et al. 2000), or also incorporating the seventh intron of nuclear gene beta-fibrinogen (Fgb-17) and the second intron of the acid phosphatase type V (Acp5; Hardy et al. 2013) have

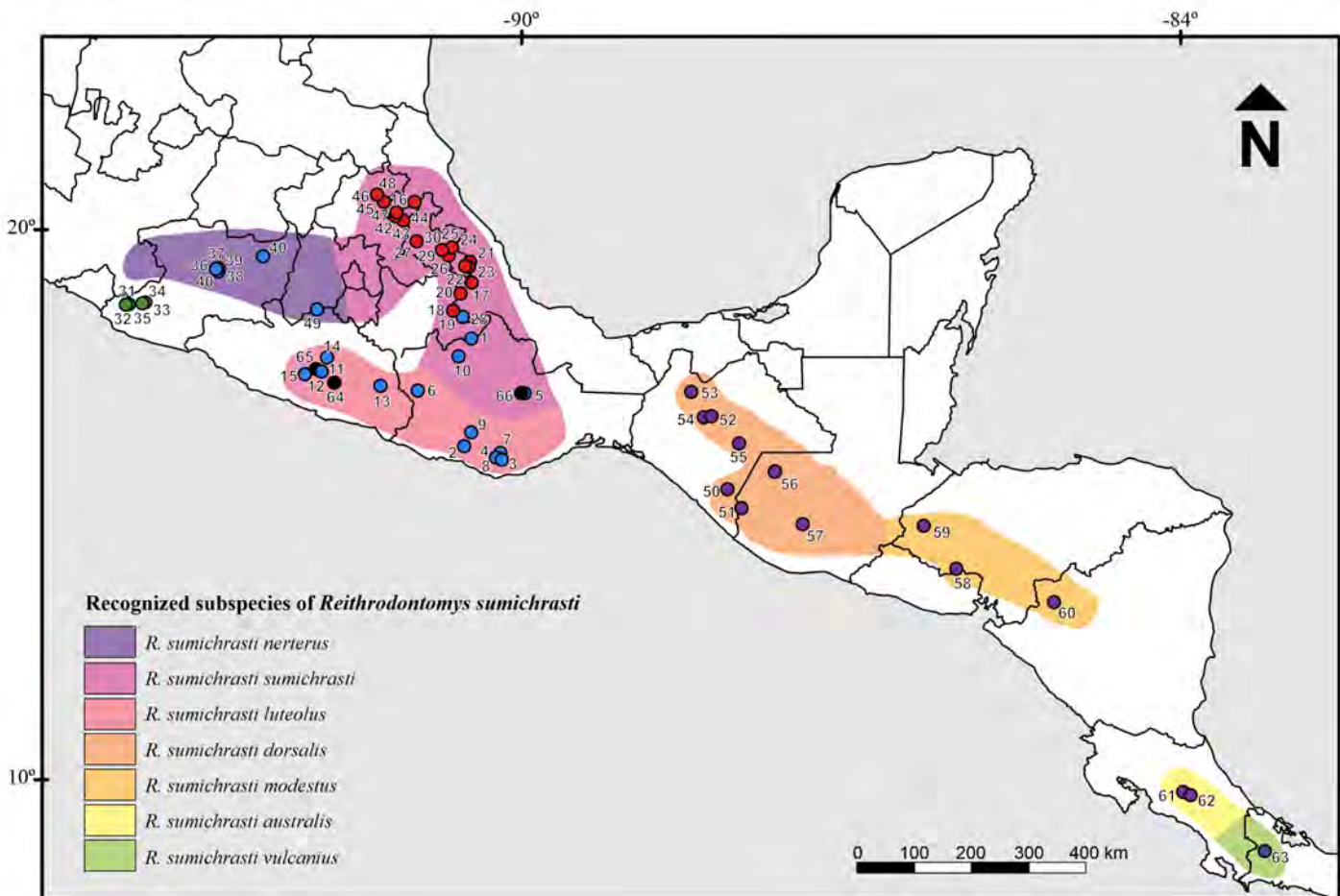


Figure 1. Map of México and Central America (adapted from Hall [1981] and Hardy et al. [2013]) showing geographic distribution of the seven recognized subspecies of *Reithrodontomys sumichrasti*. Dots represent the localities used in this study and follow the clade-color distinction described in Figure 2.

revealed the existence of several distinct clades that may deserve species-level recognition. Lineages on either side of the Isthmus of Tehuantepec in México were proposed as distinct biological species, but this pattern has been supported by only mtDNA sequences (Sullivan et al. 2000; Hardy et al. 2013). Although it was difficult to elucidate the relationships among networks of populations from central México (Hardy et al. 2013; Figure 2), there was a clear pattern of phylogenetic structure.

Here, we evaluate species delimitation within *R. sumichrasti* using different methods of analysis than those previously employed to test the hypothesis that *R. sumichrasti* represents a complex of cryptic species. We also comment on the diversification processes in the region and make taxonomic suggestions.

Materials and methods

Data acquisition. DNA sequences from the mitochondrial gene Cyt-b, and the Fgb-I7 and Acp5 nuclear genes, representing Hardy et al. (2013) populations dataset of *Reithrodontomys sumichrasti* ($n = 226$) were obtained from GenBank. We sequenced an additional 11 specimens of *R. sumichrasti*, five of these from three new geographic localities (64 to 66; Appendix 1). Given the current availability of sequence data for outgroup taxa, we included samples of *R. zacatecae*, *R. megalotis*, *R. chrysopsis*, *R. humulis*, *R. montanus*, and *R. raviventris* from the *R. megalotis* species group (Musser and Carleton 2005). The updated DNA datasets were realigned with MAFFT v7 [L-INS-i refinement, gap penalty = 3, offset = 0.5] (Katoh et al. 2005) for nuclear markers, and manually for Cyt-b using Geneious Pro v6.1.6 (<https://www.geneious.com>). The optimal partition scheme (by gene) and models of nucleotide substitution (Cyt-b: GTR+I+G, Fgb-I7: HKY+I+G, Acp5: K80+I+G); were determined with Partition Finder (Lanfear et al. 2014).

Phylogenetic hypothesis. We considered the phylogenetic relationships proposed by Hardy et al. (2013) as our working hypothesis, where two geographic clades are supported as species-level lineages. One species (spA) split ~2.5 million years ago (Ma) and comprises populations from Chiapas south into Central America (clade I; Figure 2). Species (spB) includes 3 haplogroups restricted to México, west of the Isthmus of Tehuantepec (Figure 2), whose most recent common ancestor was placed ~1.36 Ma (see Hardy et al. 2013). To assess support for this phylogenetic hypothesis (Hardy et al. 2013), and for alternative topological arrangements, we applied three methods for assessing species boundaries and species tree estimation (see below) that do not require a guide topology or species assignments to be specified a priori.

Single locus species delimitation. A time-calibrated Bayesian Inference (BI) analysis of Cyt-b for *R. sumichrasti* samples was run in BEAST2 v.2.6.2 (Bouckaert et al. 2014). We employed a prior rate of evolution of 0.017 substitutions per site per million years (Arbogast et al. 2002) and fossil

calibrations (*R. moorei*, *R. wetmorei*, *R. galushai*, *R. pratincola*, *R. rexroadensis*, and *R. sp.*) with an offset of exponential prior for the age (in Ma) of the root (mean = 2.25, offset = 1.3, HD = 95 % between 1.5 to 5.5 Ma; Dalquest 1978; Czaplewski 1987; Martin et al. 2002; Morgan and White 2005; Lindsay and Czaplewski 2011; Martin and Peláez-Campomanes 2014). BI analysis consisted of four Markov chain Monte Carlo (MCMC) chains of 10 million generations, sampling trees every 1,000 generations and with a burn-in of 20 % of the trees. The last 100 trees sampled from each run were analyzed with 1 million generations of the Bayesian General Mixed Yule-Coalescent (bGMYC) model (Reid and Carstens 2012) in the computing environment R (R Core Team 2018). As advised by Reid and Carstens (2012), outgroup taxa were not included in this analysis. For all Bayesian analyses reported herein, stabilization and appropriate Effective Sample Sizes (ESS ≥ 200) of the posterior distributions for model parameters were examined in Tracer 1.8 (Rambaut et al. 2018).

Time-calibrated multiple loci species delimitation. The multiple loci multiple species dataset was analyzed simultaneously with the multi-tree multi-species coalescent method (Heled and Drummond 2010) and the assignment-free species delimitation technique implemented in STACEY (Jones 2017), using BEAST2. The search strategy implemented in STACEY uses a birth-death-collapse prior to approximate alternative delimitation models and node re-height MCMC move that aims to improve the convergence of the species tree estimation, therefore, its performance is subject to the accuracy of divergence times estimation. As recommended, the analysis was run twice, the second time sampling from the prior only; for 100 million generations, trees were sampled every 5,000 generations. A Fossilized Birth-Death model was set on the speciation rate (Heath et al. 2014), time-calibrated as specified above. Topologies and clock rates from individual loci were left unlinked, and substitution rates among branches were drawn from a log-normal distribution with a prior mean rate of 0.017 substitutions per site per million years for the Cyt-b (Arbogast et al. 2002).

Clock-like multiple loci species delimitation. We assessed the probability of alternative species delimitation models and species trees with the Bayesian Phylogenetics and Phylogeography method (BPPv3.2; Yang and Rannala 2014). This assumes a Jukes-Cantor evolutionary model (strict molecular clock) and applies a species tree search strategy that is grounded on the Nearest Neighbor Interchange (NNI) algorithm, followed by its characteristic rjMCMC move. Although it accounts for the uncertainty on estimated rates of evolution compared to *BEAST-STACEY, this method is applicable to inter- and intra-species datasets that meet the criteria of having clock-like evolutionary rates. For this analysis, uniform rooted species trees were assumed, with gamma priors for the population size (α , β) of $\Theta = (2, 2000)$ and root age ($\text{Tau} = \tau$) $\tau_0 = (4, 2, \text{and } 1)$. The rjMCMC was run with algorithm A11 with fine-tune parameter $\epsilon_{\text{joint}} = 2$ (joint

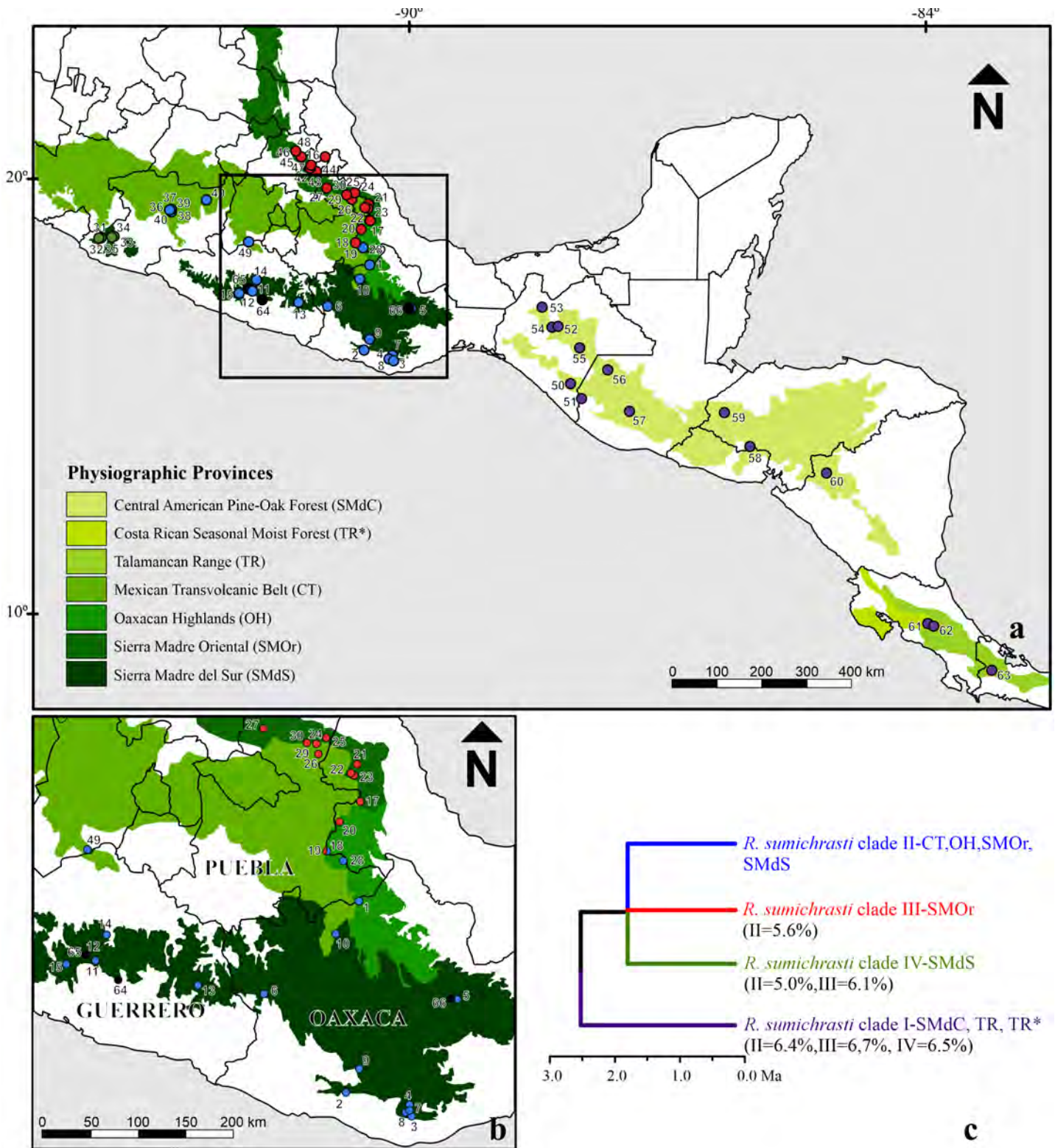


Figure 2. a) Map of México and Central America adapted from Hardy *et al.* (2013) showing collecting localities of *Reithrodontomys sumichrasti* superimposed on a map of the physiographic provinces they occupy. The four clades detected by the authors are demarcated with the colors purple (clade I), blue (clade II), red (clade III), and green (clade IV). Newly incorporated localities are shown as black dots (64-66; Appendix 1). b) Close-up of the area of sympatry of individuals from populations between clade II and clade III. c) Standing time-calibrated phylogenetic hypotheses of the evolutionary relationships among clades within the currently recognized extent of *R. sumichrasti*. Uncorrected Cytochrome-b genetic distances between sister clades are denoted in parentheses as a reference for the level of molecular divergence.

unguided species delimitation and species tree inference) for 500,000 generations with a sampling frequency of 200 after a burn-in period of 10,000.

Genetic distances. Cyt-b genetic distances using the Kimura 2-parameter (K2P; [Kimura 1980](#)) and the uncorrected *P*-distances were estimated between and within clades suggested as distinct species using MEGA X ([Kumar](#)

et al. 2018). This allowed us to make genetic distance comparisons with other values reported for rodents and for *R. sumichrasti* by Bradley and Baker (2001) and Hardy et al. (2013), respectively.

Ecological niche equivalence. For each species-level clade (clades I-IV, see Results section), we developed present-time Ecological Niche Models (ENMs) with MAXENT 4. (Phillips and Dudik 2008). Correlation between the 19 environmental variables from the WORLDCLIM database (1 km² resolution; Hijmans et al. 2005) was calculated with ENMtools v1.4.1 (Warren et al. 2010). Then, 9 environmental variables (correlation = $r \leq 0.80$) and presence points confirmed with molecular data (Appendix 1) were employed to obtain the ENMs. For clades I-III, 10 bootstrap replicates of presence/background points assigning 15 % of the presence points for training were applied. For clade IV, 10-fold cross-validation replicates were applied because of the limited number of presence records.

To test the hypothesis of niche conservatism between the ENMs from sister clades, a null distribution of 99 estimates of the I Statistics (Warren et al. 2008) and the Schoener's D (Schoener 1968) measures of niche overlap was generated for each pair of sister clades with the R package DISMO (Hijmans et al. 2017). In addition, a canonical discriminant function (CF) analysis was executed with the package candisc (Friendly and Fox 2015), to distinguish the potential affecting the extent to which their niches have been conserved. For this analysis, current time ENMs were reclassified so that each pixel predicted by each model would equal 1 and the rest of the grid 0. The resultant ENM masks were used to extract for each clade pixel-level data for the 9 environmental variables.

Lineage dispersal. To reconstruct the spatiotemporal history of lineage dispersal in *R. sumichrasti* we used the Relaxed Random Walk model (RRW; Lemey et al. 2010) as implemented in BEAST2. This model assumes an uncorrelated diffusion rate across the tree and infers the dispersal lineage history in space and time simultaneously, using both the phylogenetic tree and the geographic locations of the samples (Dellicour et al. 2021). To build the RRW we employed the geographic coordinates from each terminal collecting locality as a two-dimensional trait. We assumed a relaxed molecular clock (prior rate = 0.017, SD = 1.0), and the tree priors were calibrated as described above. To visualize the estimated phylogeographic reconstruction, space-time dispersal networks were created using SPREAD 1.0.6 (Bielejec et al. 2011).

Results

Phylogenetic hypothesis and species delimitation. The bGMYC species delimitation analysis of the Cyt-b recovered two species-level clades within *R. sumichrasti* ($P \geq 0.95$), separated by the Isthmus of Tehuantepec (Figure 3; Hypothesis 1). In this phylogeny, samples from new populations 64 to 66 from Guerrero and Oaxaca formed part of clade II. For the BPP and STACEY multiple-loci methods, the

highest probability values (BPP, $pP = 0.56$; STACEY, $pP = 0.91$) supported Hypothesis five which recovered four divergent clades at the species level (Figure 3). One of them (clade I) was confined to the east and south of the Isthmus of Tehuantepec in México and Central America and the other three (clades II, III, and IV) were restricted to México. The K2P genetic distance values ranged from 5.43 % to 7.52 %, with the lowest value between clades II and IV and the highest between clades I and IV (Table 1). Similar genetic distance values among clades were obtained with the uncorrected *P*-distances (Table 1).

Table 1. Matrix of mean genetic distances (%) for Cytochrome b gene sequence data among the 4 clades delimited in *Reithrodontomys sumichrasti*. Values above (uncorrected *P*-distances) and below (Kimura 2-parameter) the diagonal represent genetic distances between clades. Numbers on the diagonal represent Kimura 2-parameter genetic distances within a clade.

| <i>R. sumichrasti</i> | Clade I | Clade II | Clado III | Clado IV |
|-----------------------|---------|----------|-----------|----------|
| Clade I | 1.71 | 6.69 | 6.97 | 7.01 |
| Clade II | 7.16 | 1.66 | 5.74 | 5.17 |
| Clade III | 7.47 | 6.07 | 1.59 | 6.28 |
| Clade IV | 7.52 | 5.43 | 6.67 | 0.25 |

The species delimitation methods and the species tree (Figure 4) recovered the ancestral position of clade I ($pP = 0.84$), with a mean divergence time for the most recent common ancestor (MRCA) of ~2.15 Ma. The bGMYC supported the sister relationship between clades II and IV, whereas the multi-loci methods and the species tree supported the split of clade IV ($pP = 0.79$; mean divergence time 1.42 Ma), and a sister relationship between clades II and III ($pP = 0.70$; mean divergence time 0.90 Ma). In addition, the ancestral position of *R. chrysopsis* with respect to *R. megalotis-R. zacatecae* and *R. sumichrasti* was strongly supported ($pP = 1.00$), with an MRCA mean age estimated at 6.18 Ma. Also, a closer relationship was recovered between *R. humulis* and *R. montanus-R. raviventris* ($pP = 1.00$; mean divergence time 6.43 Ma), although the sister relationship of *R. montanus-R. raviventris* received lower probabilities ($pP = 0.86$; mean divergence time 4.44 Ma).

Ecological niche equivalence. Ecological Niche Models generated for the four species-level clades within *R. sumichrasti* had AUC values above 0.90 for training data. The inter-clade predictability of the ENM of clade I ranged from 95 % when predicting known localities from clade III to 100 % when predicting known localities of clade IV (Figure 5). Clade IV had the most restricted ENM, and its inter-clade predictability ranged from 0 % when predicting clade III (and vice versa), to 18 % when predicting clade II. The ENMs of clades II and III showed the lowest intra-clade predictability values with 90 % and 95 %, respectively. Quantification of niche overlap with the I and Schoener's D statistics (from here forward *I* and *D*) revealed small amounts of overlap between each clade pair. For all clade pairwise comparisons, the niche identity (niche equivalency) hypothesis was rejected regardless of the similarity measure (*I* or *D*; Table 2).

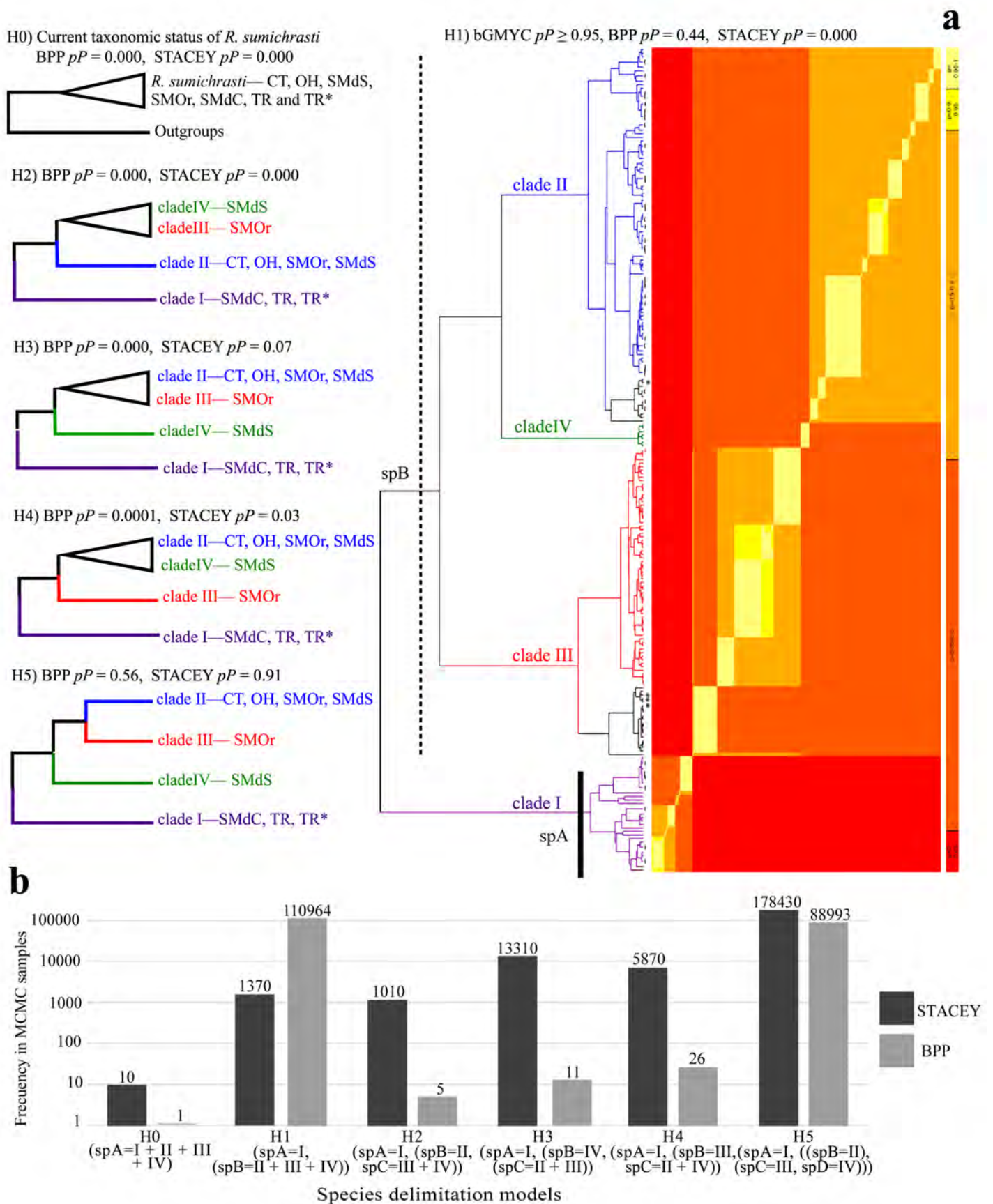


Figure 3. a) Single locus [Hypothesis 1; discontinuous red-yellow heat-map represents the $pP \geq 0.95$ of belonging to different species (red color)] and multiple-loci (Hypothesis 2-Hypothesis 5) species delimitation models for *Reithrodontomys sumichrasti*. Solid and dashed lines denote the species delimitation proposal supported by bGMYC (Hypothesis 1; spA and spB). b) Amount of support for each model in the posterior sample (MCMC) of trees estimated with STACEY and BPP. The abbreviations of the physiographic provinces and clade colors follow Figure 2.

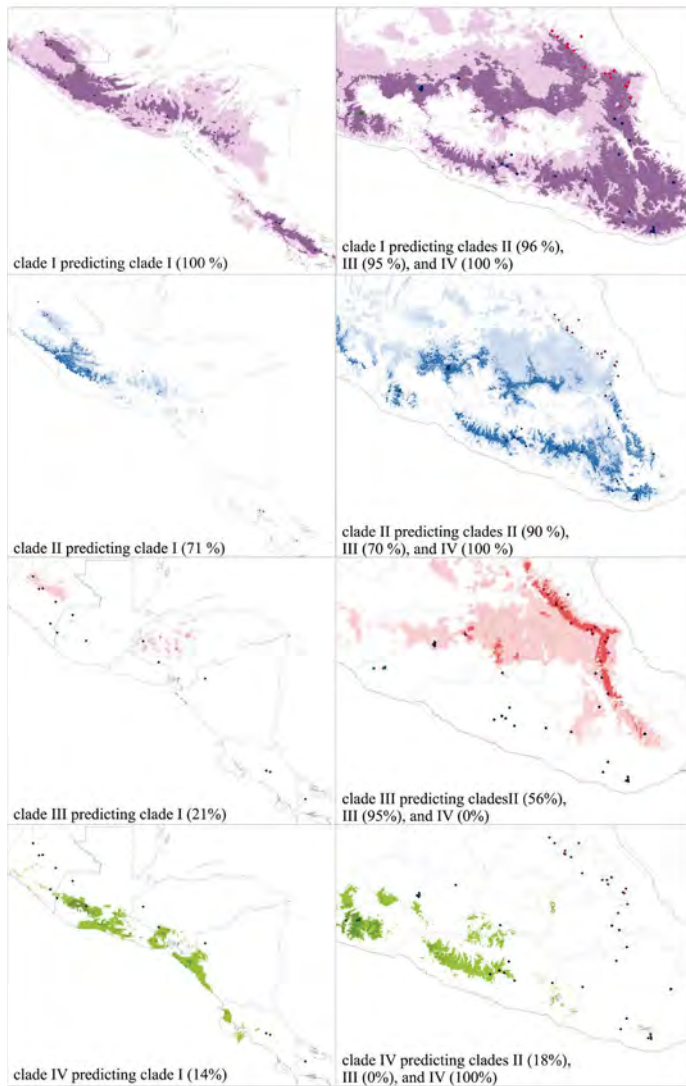


Figure 5. Map projection of the Ecological Niche Models for the 4 clades of *Reithrodontomys sumichrasti* indicating the within-clade and inter-clade localities predictability values. Color dots represent the presence records of each clade and follow the clade-colors in Figure 2. Dark and light colors on the maps represent the suitable and non-suitable areas of each clade, respectively.

(CT as named in [Hardy et al. 2013](#)), and by ~ 0.11 Ma most dispersal events occurred when clade II expanded through the central and east of the CT, but also seemed to expand towards the east by the OH (Figure 7).

Discussion

Species delimitation. The use of innovative tools and methodologies to assess species boundaries has helped to clarify taxonomic problems while facilitating the generation of robust hypotheses to reveal cryptic species and describe the speciation processes ([Dayrat et al. 2005](#); [Padiál et al. 2010](#)). Such is the case of mammals distributed in Mesoamerica, characterized by a peculiar evolutionary history that is linked to the environmental and biogeographical characteristics of this region (see [Almendra and Rogers 2012](#)). We used the cricetid rodent *R. sumichrasti* because it is a good model to evaluate the biogeographical and ecological niche conservatism hypotheses linked to vicariant speciation events in México to Central America. This approach was addressed by other authors ([Sullivan et al. 2000](#); [Martínez-Gordillo et al. 2010](#); [Hardy et al. 2013](#)), but this is the first time that the use of mathematical methods for species delimitation and phylogeographic reconstruction is put into practice for this species.

Our results show that the species delimitation methods support the phylogenetic hypotheses one and five with higher posterior probabilities, suggesting that *R. sumichrasti* is a complex of multiple species. In both hypotheses, clade I was identified as a distinct species, as this result was congruent among the three species delimitation methods. Recognition of clade I at the species level has been suggested previously due to its position in the molecular phylogenies ([Sullivan et al. 2000](#); [Hardy et al. 2013](#)), and to the *P*-distances to the remaining clades (6.15 % to 9.10 %; [Hardy et al. 2013](#)). We agree with this species-level suggestion since this clade was placed as an independent sister lineage to the other clades of *R. sumichrasti* in our phyloge-

Table 3. Coefficients of the three first canonical discriminant functions derived from the bioclimatic variables used in the ecological analyses in *Reithrodontomys sumichrasti*. Mean values of the bioclimatic variables based on the environmental information from occurrence records are given for each clade.

| Climatic Variable | Function 1 Eigen=0.261 | Function 2 Eigen=0.035 | Function 3 Eigen=0.008 | Clade I | Clade II | Clade III | Clade IV |
|-------------------|---------------------------|---------------------------|---------------------------|---------|----------|-----------|----------|
| BIO1 | 0.689 | 0.402 | 0.028 | 17.11 | 16.75 | 14.15 | 18.44 |
| BIO2 | -0.054 | 0.409 | 0.023 | 11.82 | 12.23 | 12.18 | 12.96 |
| BIO4 | 0.632 | 0.086 | 0.021 | 104.09 | 124.54 | 185.44 | 164.25 |
| BIO5 | 0.239 | 0.486 | 0.379 | 24.88 | 25.24 | 23.17 | 27.47 |
| BIO6 | -0.385 | 0.280 | 0.252 | 9.00 | 8.16 | 4.40 | 8.30 |
| BIO7 | -0.614 | 0.671 | 0.015 | 15.88 | 17.09 | 18.77 | 19.17 |
| BIO11 | 0.421 | 0.149 | 0.619 | 15.70 | 15.11 | 11.64 | 16.16 |
| BIO12 | -0.257 | 0.116 | 0.056 | 1723.79 | 1237.19 | 1157.14 | 1086 |
| BIO17 | -0.196 | 0.232 | 0.302 | 79.52 | 34.47 | 98.99 | 14.86 |
| EV (%) | 85.575 | 11.724 | 2.700 | | | | |

BIO1 = Annual Mean Temperature; BIO2 = Mean Diurnal Range (Mean of monthly (max temp - min temp)); BIO4 = Temperature Seasonality (standard deviation *100); BIO5 = Max Temperature of Warmest Month; BIO6 = Min Temperature of Coldest Month, BIO7 = Temperature Annual Range (BIO5-BIO6); BIO11 = Mean Temperature of Coldest Quarter; BIO12 = Annual Precipitation; BIO17 = Precipitation of Driest Quarter; EV (%) = Percent of explained variance.

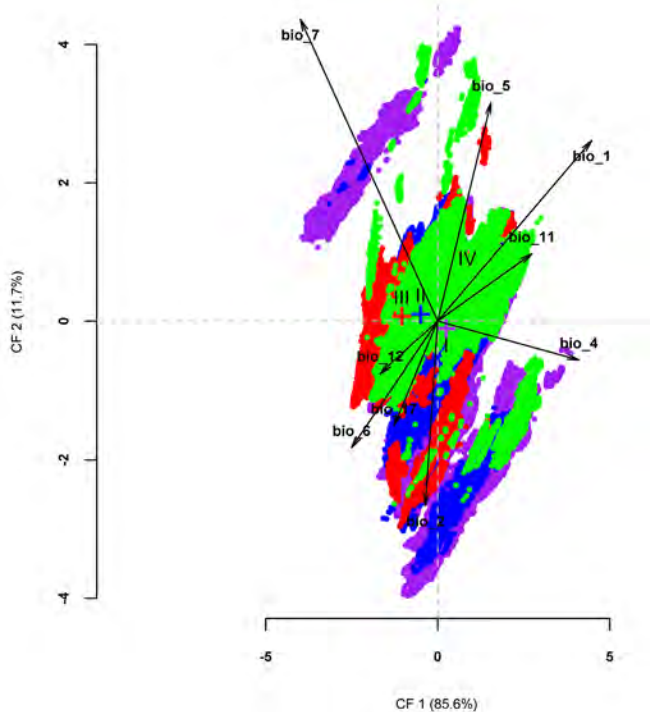


Figure 6. Graphic of the first two discriminant functions among Ecological Niche Models of clades I to IV of *Reithrodontomys sumichrasti*. Colored crosses represent the centroid of each clade environmental niche. Colors follow the clade-color distinction described in Figure 2. Black arrows denote the power and direction of the discrimination for that bioclimatic variable (see text and Table 3 for descriptions of bioclimatic variables).

netic trees and also showed the highest genetic divergence (both K2P and *P*-distances) compared to clades II-IV. The populations belonging to this clade are distributed south-east of the Isthmus of Tehuantepec, from the Sierra Madre de Chiapas, México to western Panama (Hall 1981), and were the first to diverge from a common ancestor ~2.15 Ma. This mean age is close to that reported by Hardy *et al* (2013; ~2.56 Ma), placing the species diversification within *R. sumichrasti* at the Plio-Pleistocene boundary (see discussion below).

The proposal that clade I evolved independently was better supported by molecular data than by ecological data. The environmental niche space that this clade occupies predicted the potential distribution areas of the remaining clades with high percentages, although the inverse was not true. In general, *R. sumichrasti sensu lato* inhabits brush and grass in pine-oak and cloud forests throughout its geographical distribution. However, Hooper (1952) reported a greater diversity of habitats for the subspecies that encompass clade I, particularly for *R. s. dorsalis* and *R. s. australis*. This apparently broad environmental range could explain the high percentages of predictability we found, which was also evidenced in the canonical analysis. Nevertheless, non-equivalency of niche was found in the niche identity test. The remaining ecological analyses showed a relatively high similarity between this clade and clades II-IV, suggesting that their differentiation at the species level within *R. sumichrasti sensu lato* was more favored by geography than by ecology (Peterson *et al.* 1999).

The species delimitation methods were not consistent in the delimitation of clades II, III, and IV. The single-locus bGMYC (Cyt-b) proposed that the three clades form a single species, while the multiple-loci BPP and STACEY (Cyt-b + Fgb-17 + Acp5) considered each clade as a distinct species. Molecular delimitation methods are considered a valuable complement to taxonomy based on morphological traits and are often used as part of an integrative approach to validate putative species (Luo *et al.* 2018). The three delimitation methods used in our study have been recognized for their high performance for this purpose (Jones 2017; Luo *et al.* 2018), but only two of them (BPP and STACEY) were consistent in this work. The performance and accuracy of each method can be affected by factors including both biological (variation in population size, uninterrupted gene flow) and methodological (input tree), among others, so they can over or underestimate the number of species (Rannala 2015; Luo *et al.* 2018). For this reason, the use of different molecular delimitation methods is highly recommended with species hypotheses based on the congruence among them (Carstens *et al.* 2013). In accordance with this suggestion, Hypothesis five (which is based on multiple loci) should be accepted and therefore each clade distributed west of the Isthmus of Tehuantepec constitutes a distinct species-level entity. Hypothesis five (Fig. 2) was also supported by the amount of Cyt-b genetic differentiation among clades. The K2P genetic distance values between pairwise clades II-III, II-IV, and III-IV were 6.07, 5.43, and 6.67, respectively, which are greater than the 5 % value associated with sister species recognition in mammals (Baker and Bradley 2006) including rodents (ranged from 2.70 % to 19.23 %; Bradley and Baker 2001).

Phylogenetic relationships among clades II, III, and IV were different between the Cyt-b tree topology and the species tree, but generally with weak nodal support. In the first case, II and IV were recovered as sister clades, while in the second, clades II and III were more closely related. These results partially coincide with the topologies obtained by Hardy *et al.* (2013), in which their concatenated DNA tree is consistent with our species tree. On the other hand, none of our phylogenies (gene tree or species tree) recovered sister relationships between clades III and IV, such as those obtained in the Cyt-b tree of Hardy *et al.* (2013). This is also supported by the ecological results where there is a greater ecological similarity (based on both directions of area predictability) between clades II and III than between clades II and IV or III and IV.

The ecological niche characteristics (from the bioclimatic variables used) of clade II showed high predictability percentages of the ecological suitability areas of clades III and IV, but these tended to have low or null values when the inverse analysis was performed. For example, clade IV predicted only 18 % of clade II and 0 % of clade III. The geographical distribution of each clade could explain the different percentages of predictability of the environmental niche. The wide geographical distribution of clade II

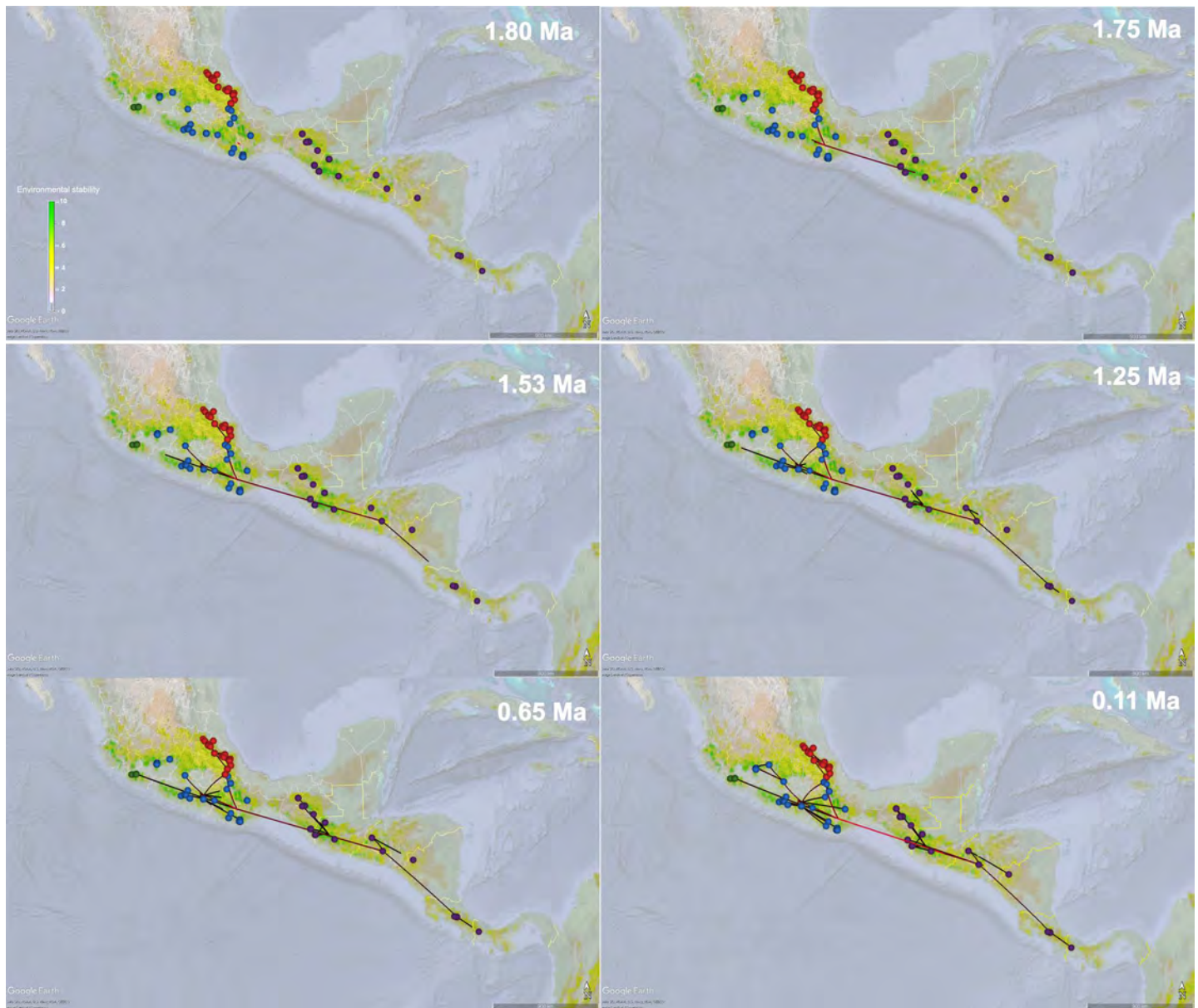


Figure 7. Spatiotemporal dynamics of the *Reithrodontomys sumichrasti* lineages diffusion for 1.80 Ma, 1.75 Ma, 1.53 Ma, 1.25 Ma, 0.65 Ma, and 0.11 Ma. Lines represent the branches of the Maximum Clade Credibility Tree and circles the location of occurrence records of the terminal labels (Appendix 1). An overlay of the sum of current, Last Glacial Maximum, and Last Interglacial ENMs was added to denote areas of relative environmental stability. Line and circle colors follow the clade-color distinction described in Figure 2. Maps were generated using Google Earth (<http://earth.google.com>).

includes localities of the CT, SMdS, extreme south of SMOR, and OH, while clade III is distributed in the SMOR, and clade IV is restricted to Coalcomán and Dos Aguas localities, in Michoacán (Hall 1981; Hardy *et al.* 2013; Figure 1, 2).

Niche pairwise comparisons showed low observed values for *D* and *I* similarity indices, mainly between clades III and IV. This is based on the fact that these indices can take values from 0 (no niche overlap) to 1 (total niche overlap; Warren *et al.* 2008). Closely related species are predicted to share characteristics of their environmental niche due to their common ancestry (Peterson *et al.* 1999), but niche differentiation can occur when allopatric populations exist, and gene flow is assumed to have been disrupted in the past (Avice 2000; Martínez-Gordillo *et al.* 2010). This could explain the non-equivalency of niche between these

clades, as well as the low values of area predictability, which coincides with reports of Martínez-Gordillo *et al.* (2010) for different rodent species, including *R. sumichrasti*.

Bioclimatic data show that clade II shared similar characteristics to the other clades depending on the variable being analyzed. Moreover, clade III was characterized by low temperatures and the second-highest value of annual mean precipitation. These bioclimatic characteristics correspond to the habitat description of *R. s. sumichrasti*, mainly associated with pine and pine-oak forests, in “areas frequently bathed by clouds and rain (Hooper 1952:72)”. In contrast, clade IV was associated with higher temperatures and lower precipitation values, showing extreme values with respect to the other clades in at least five of the nine variables analyzed. Hardy *et al.* (2013) highlighted the pres-

ence of geographical barriers such as low-lying river drainages that have isolated clade IV populations from other *R. sumichrasti sensu lato* populations, which could justify our molecular and ecological results regarding the species recognition of this clade.

Phylogeographic history. Our results suggest that the common ancestor of the *R. sumichrasti sensu lato* originated in the montane regions of northern Central America ~2 Ma ago and expanded to where this species complex currently occurs. Various geographic and environmental factors may have favored and/or limited its dispersal in Central America and México (for more details see [Hardy et al. 2013](#)). The montane and intermontane Central America regions have a deep tectonic and volcanic history, which may have influenced the origin and diversification of montane species such as *Peromyscus guatemalensis*, *P. bakeri*, and *P. carolpattonae* ([Álvarez-Castañeda et al. 2019](#)). Also, the Pleistocene glacial cycles may have played a key role, due to favorable climatic conditions ([Ceballos et al. 2010](#)), which allowed the colonization of new areas and in some cases new habitats, followed by post-glacial isolation that limited the gene flow between populations ([Martin 1961](#)). This has been reported in several groups such as plants (e. g. [Ramírez-Barahona and Eguiarte 2013](#)), reptiles and amphibians (e. g. [Church et al. 2003](#); [Howes et al. 2006](#)), birds (e. g. [Johnson and Cicero 2004](#); [Baker 2008](#)), and mammals (e. g. [Ceballos et al. 2010](#); [Chiou et al. 2011](#)) including other species of *Reithrodontomys* ([Martínez-Borrego et al. 2022](#)). In addition, geographic regions such as the Isthmus of Tehuantepec seem to have acted as an efficient barrier limiting gene flow between populations that are distributed on both sides of the Isthmus, an accepted explanation for *R. sumichrasti* and other rodent species (e. g. [Sullivan et al. 2000](#); [León-Paniagua et al. 2007](#); [Ordoñez-Garza et al. 2010](#); [Hardy et al. 2013](#)).

The lineage dispersal in México was from populations in the west of the OH and SMdS that currently belong to the clade II, which spread into SMO_r (clade III) and the west of CT (clade IV) as well as through the central and east of the CT (clade II). This model would explain the wide geographical distribution of clade II, and also its greater number of haplotypes compared to the other clades ([Hardy et al. 2013](#)). Although these dispersal events seem to have occurred relatively recently, the physiographic characteristics of the Mexican mountainous regions ([Morrone 2005](#); [Escalante et al. 2009](#)) could have favored relatively faster speciation processes within *R. sumichrasti* complex, leading to differentiation, at least genetically and ecologically, among each clade analyzed here. This seems to be a common pattern in several species of small mammals, where the allopatric effect and the habitat characteristics each ancestral species occupied resulted in complete speciation of lineages, often associated with cryptic speciation processes (e. g. [Arellano et al. 2005](#); [Rogers et al. 2007](#); [León-Tapia et al. 2021](#); [Martínez-Borrego et al. 2022](#)).

Taxonomic considerations. Species delimitation methods and values of genetic divergence support the recogni-

tion of populations of *R. sumichrasti* at the east and south of the Isthmus of Tehuantepec, from Chiapas, México to Central America (Clade I), as a valid species which is different from everything occurring to the west of this geographical barrier. According to this hypothesis, then *R. australis* ([Allen 1895](#)) is the taxonomic name that has priority (Article 23; [ICZN 1999](#)). Subspecies distributed across this region of Mesoamerica, beyond the nominotypical would include *R. a. dorsalis* (Merriam 1901), *R. a. modestus* (Thomas 1907), and *R. a. vulcanius* (Bangs 1902).

In addition, the existence of an undescribed species represented by the populations included in clade IV, from Coalcomán and Dos Aguas in Michoacán, México (northwestern SMdS) is supported by species delimitation methods and values of genetic divergence. The disjoint distribution of this genetically distinct clade suggests that it does not belong to *R. s. nerterus* nor *R. s. luteolus*. The mountainous region inhabited by this new species is isolated from other mountain ranges in the area by lowlands of up to approximately 400 masl. This pattern of genetic differentiation coincides with the recent description of a new species of the genus *Peromyscus* (*P. greenbaumi*; [Bradley et al. 2022](#); but see also [León-Tapia et al. 2021](#)). In order to make the formal description based on diagnostic characters that will derive in an appropriate species name, a morphological comparison would be necessary.

Molecular species delimitation and genetic distance values associated to populations from clades II and III indicate that these two lineages should be recognized as valid species. Nomenclatural suggestions are difficult to make due to the sympatry of individuals of some populations from both clades. This was already addressed by [Hardy et al. \(2013\)](#) through nested clade analysis. In our study a phylogeographic pattern of diffusion of the lineages (RRW model) suggests colonization after the separation of clades II and III. Nevertheless, in this work we propose populations comprising clade II should be recognized as *R. nerterus* (Merriam, 1901). Although we did not include specimens from the type locality of *R. nerterus* (El Nevado de Colima, Jalisco, México), we analyzed several individuals from sites reported by [Hooper \(1952\)](#) for this taxon. Because clade II includes populations of the known distribution of *R. s. luteolus*, this taxon should be considered as subspecies of *R. nerterus*. Clade III should be named as *R. sumichrasti*; here we also did not include individuals from the type locality (El Mirador, Veracruz, México), but we used specimens from localities that belong to this species. Populations from south Puebla and Northern Oaxaca (28, 1, and 10 in Figure 2), regarded originally as *R. s. sumichrasti* should be now *R. n. luteolus*. It remains necessary to evaluate sympatric populations from both clades in order to identify plausible evolutionary processes in this region.

Acknowledgements

We acknowledge financial support from the Consejo Nacional de Ciencia y Tecnología (postdoctoral fellowship to ALA)

and the Department of Biology, Brigham Young University (to DSR). We wish to thank D. D. Cruz for his assistance in compiling data for the Ecological Niche Modeling, E. C. Molina for gathering GeneBank data for the molecular analysis, and R. Núñez for his support in editing figures. We also thank two anonymous reviewers who kindly read drafts of this work and supplied valuable comments.

Literature cited

- ALLEN, J. A. 1895. On the species of the genus *Reithrodontomys*. *Bulletin of the American Museum of Natural History* 7:7-143.
- ALMENDRA, A. L., AND D. S. ROGERS. 2012. Biogeography of Central American mammals. Pp. 203-229, in *Bones, clones, and biomes: the history and geography of recent neotropical mammals* (Patterson, B. D., and L. P. Costa, eds.). University of Chicago Press, Illinois, U.S.A.
- ALMENDRA, A. L., ET AL. 2018. Evolutionary relationships and climatic niche evolution in the genus *Handleyomys* (Sigmodontinae: Oryzomyini). *Molecular Phylogenetics and Evolution* 128:12-25.
- ÁLVAREZ-CASTAÑEDA, S. T., ET AL. 2019. Two new species of *Peromyscus* from Chiapas, Mexico, and Guatemala. Pp. 543-558, in *From field to laboratory: a memorial volume in honor of Robert J. Baker* (Bradley, R. D., H. H. Genoways, D. J. Schmidly, and L. C. Bradley, eds.). Special Publications, Museum of Texas Tech University, Lubbock, U.S.A.
- ARBOGAST, B. S., ET AL. 2002. Estimating divergence times from molecular data on phylogenetic and population genetic timescales. *Annual Review of Ecology and Systematics* 33:707-740.
- ARELLANO, E., F. GONZÁLEZ-COZÁTL, AND D. S. ROGERS. 2005. Molecular systematics of Middle American harvest mice *Reithrodontomys* (Muridae), estimated from mitochondrial cytochrome b gene sequences. *Molecular Phylogenetics and Evolution* 37:529-540.
- AVISE, J. C. 2000. *Phylogeography: the history and formation of species*. Harvard University Press, Massachusetts, U.S.A.
- BAKER, A. J. 2008. Islands in the sky: the impact of Pleistocene climate cycles on biodiversity. *Journal of Biology* 7:1-4.
- BAKER, R. J., AND R. D. BRADLEY. 2006. Speciation in mammals and the Genetic Species Concept. *Journal of Mammalogy* 87:643-662.
- BANGS, O. 1902. Chiriqui Mammalia. *Bulletin of the Museum of Comparative Zoology at Harvard College* 39:17-51.
- BIELEJEK, F., ET AL. 2011. SPREAD: spatial phylogenetic reconstruction of evolutionary dynamics. *Bioinformatics* 27:2910-2912.
- BOUCKAERT, R., ET AL. 2014. BEAST 2: a software platform for Bayesian evolutionary analysis. *PLoS Computational Biology* 10:p.e1003537.
- BRADLEY, R. D. 2017. Genus *Reithrodontomys*. Pp. 367-383, in *Handbook of the Mammals of the World: Rodents II* (Wilson, D. E., T. E. Lacher, and R. A. Mittermeier, eds.). Lynx Edicions, Barcelona, Spain.
- BRADLEY, R. D., AND R. J. BAKER. 2001. A test of the Genetic Species Concept: Cytochrome b sequences and mammals. *Journal of Mammalogy* 82:960-973.
- BRADLEY, R. D., ET AL. 2022. Two new species of *Peromyscus* (Cricetidae: Neotominae) from the Transverse volcanic belt of Mexico. *Journal of Mammalogy* 103:255-274.
- CARSTENS, B. C., ET AL. 2013. How to fail at species delimitation. *Molecular Ecology* 22:4369-4383.
- CEBALLOS, G., J. ARROYO-CABRALES, AND E. PONCE. 2010. Effects of Pleistocene environmental changes on the distribution and community structure of the mammalian fauna of Mexico. *Quaternary Research* 73:464-473.
- CHIOU, K. L., ET AL. 2011. Pleistocene diversification of living squirrel monkeys (*Saimiri* spp.) inferred from complete mitochondrial genome sequences. *Molecular Phylogenetics and Evolution* 59:736-745.
- CHURCH, S. A., ET AL. 2003. Evidence for multiple Pleistocene refugia in the postglacial expansion of the eastern tiger salamander, *Ambystoma tigrinum tigrinum*. *Evolution* 57:372-383.
- CZAPLEWSKI, N. J. 1987. Sigmodont rodents (Mammalia; Muridae; Sigmodontinae) from the Pliocene (early Blancan) Verde Formation, Arizona. *Journal of Vertebrate Paleontology* 7:183-99.
- DALQUEST, W. W. 1978. Early Blancan mammals of the Beck Ranch local fauna of Texas. *Journal of Mammalogy* 59:269-98.
- DALY, M., ET AL. 2012. Systematics Agenda 2020: the mission evolves. *Systematic Biology* 61:549-552.
- DAYRAT, B. 2005. Towards integrative taxonomy. *Biological Journal of Linnean Society* 85:407-415.
- DE QUEIROZ, K. 2007. Species concepts and species delimitation. *Systematic Biology* 56:879-886.
- DELLICOUR, S., ET AL. 2021. Relax, keep walking—a practical guide to continuous phylogeographic inference with BEAST. *Molecular Biology and Evolution* 38:3486-3493.
- DOODY, J. S., S. FREEDBERG, AND J. S. KEOGH. 2009. Communal egg-laying in reptiles and amphibians: evolutionary patterns and hypotheses. *The Quarterly Review of Biology* 84:229-252.
- ESCALANTE, T., C. SZUMIK, AND J. J. MORRONE. 2009. Areas of endemism of Mexican mammals: reanalysis applying the optimality criterion. *Biological Journal of the Linnean Society* 98:468-478.
- FRIENDLY, M., AND J. FOX. 2015. candisc: Visualizing generalized canonical discriminant and canonical correlation analysis. R package version 0.6-5. Available from: <https://cran.r-project.org/web/packages/candisc/index.html>
- GILBERT, J. D., AND A. MANICA. 2015. The evolution of parental care in insects: a test of current hypotheses. *Evolution* 69:1255-1270.
- HALL, E. R. 1981. *The Mammals of North America* 2nd ed. John Wiley and Sons, Inc., New York, U.S.A.
- HARDY, D. K., ET AL. 2013. Molecular phylogenetics and phylogeography structure of Sumichrast's harvest mouse (*Reithrodontomys sumichrasti*: Cricetidae) based on mitochondrial and nuclear DNA sequences. *Molecular Phylogenetics and Evolution* 68:282-292.
- HEATH, T. A., J. P. HUELSENBECK, AND T. STADLER. 2014. The fossilized birth-death process for coherent calibration of divergence-time estimates. *Proceedings of the National Academy of Sciences* 111:2957-2966.
- HELED, J., AND A. J. DRUMMOND. 2010. Bayesian inference of species trees from multilocus data. *Molecular Biology and Evolution* 27:570-580.
- HUIJMANS, R. J., ET AL. 2005. Very high-resolution interpolated climate surfaces for global land areas. *International Journal of Climatology* 25:1965-1978.

- HUJMANS, R. J., ET AL. 2017. Package 'dismo'. *Circles* 9:1-68.
- HOOPER, E. T. 1952. A systematic review of harvest mice (genus *Reithrodontomys*) of Latin America. *Miscellaneous Publications Museum of Zoology, University of Michigan* 77:1-255.
- HOWES, B. J., B. LINDSAY, AND S. C. LOUGHEED. 2006. Range-wide phylogeography of a temperate lizard, the five-lined skink (*Eumeces fasciatus*). *Molecular Phylogenetics and Evolution* 40:183-194.
- HUANG, J. P. 2020. Is population subdivision different from speciation? From phylogeography to species delimitation. *Ecology and Evolution* 10:6890-6896.
- INTERNATIONAL COMMISSION ON ZOOLOGICAL NOMENCLATURE. 1999. International code of zoological nomenclature. 4th ed. International Trust for Zoological Nomenclature, London, U.K.
- JOHNSON, N. K., AND C. CICERO. 2004. New mitochondrial DNA data affirm the importance of Pleistocene speciation in North American birds. *Evolution* 58:1122-1130.
- JONES, G. 2017. Algorithmic improvements to species delimitation and phylogeny estimation under the multispecies coalescent. *Journal of Mathematical Biology* 74:447-467.
- KATO, K., ET AL. 2005. MAFFT version 5: improvement in accuracy of multiple sequence alignment. *Nucleic Acids Research* 33:511-518.
- KIMURA, M. 1980. A simple method for estimating evolutionary rates of base substitutions through comparative studies of nucleotide sequences. *Journal of Molecular Evolution* 16:111-120.
- KNOWLES, L. L., AND B. C. CARSTENS. 2007. Delimiting species without monophyletic gene trees. *Systematic Biology* 56:887-895.
- KUMAR, S., ET AL. 2018. MEGA X: molecular evolutionary genetics analysis across computing platforms. *Molecular Biology and Evolution* 35:1547-1549.
- LANFEAR, R., ET AL. 2014. Selecting optimal partitioning schemes for phylogenomic datasets. *BMC Evolutionary Biology* 14:1-14.
- LEMEY, P., ET AL. 2010. Phylogeography takes a relaxed random walk in continuous space and time. *Molecular Biology and Evolution* 27:1877-1885.
- LEÓN-PANIAGUA, L., ET AL. 2007. Diversification of the arboreal mice of the genus *Habromys* (Rodentia: Cricetidae: Neotomiinae) in the Mesoamerican highlands. *Molecular Phylogenetics and Evolution* 42:653-664.
- LEÓN-TAPIA, M. Á., ET AL. 2021. Role of Pleistocene climatic oscillations on genetic differentiation and evolutionary history of the Transvolcanic deer mouse *Peromyscus hylocetes* (Rodentia: Cricetidae) throughout the Mexican central highlands. *Journal of Zoological Systematics and Evolutionary Research* 59:2481-2499.
- LINDSAY, E. H., AND N. J. CZAPLEWSKI. 2011. New rodents (Mammalia, Rodentia, Cricetidae) from the Verde Fauna of Arizona and the Maxum Fauna of California, USA, early Blancan Land Mammal Age. *Palaeontología Electrónica* 14:1-16.
- LUO, A., ET AL. 2018. Comparison of methods for molecular species delimitation across a range of speciation scenarios. *Systematic Biology* 67:830-846.
- MAESTRI, R., ET AL. 2017. The ecology of continental evolutionary radiation: Is the radiation of sigmodontine rodents adaptive? *Evolution* 71:610-632.
- MARTIN, P. S. 1961. Southwestern animal communities in the late Pleistocene. *Biology of the arid and semiarid lands of the Southwest. New Mexico Highlands University Bulletin* 212:56-66.
- MARTIN, R. A., ET AL. 2002. Blancan Lagomorphs and rodents of the Deer Park assemblages, Meade County, Kansas. *Journal of Paleontology* 76:1072-1090.
- MARTIN, R. A., ET AL. 2003. Late Pliocene and early Pleistocene rodents from the northern Borchers Badlands (Meade County, Kansas), with comments on the Blancan-Irvingtonian boundary in the Meade Basin. *Journal of Paleontology* 77:985-1001.
- MARTIN, R. A., AND P. PELÁEZ-CAMPOMANES. 2014. Diversity dynamics of the Late Cenozoic rodent community from south-western Kansas: the influence of historical processes on community structure. *Journal of Quaternary Science* 29:221-231.
- MARTÍNEZ-BORRERO, D., ET AL. 2022. Molecular systematics of the *Reithrodontomys tenuirostris* group (Rodentia: Cricetidae) highlighting the *Reithrodontomys microdon* species complex. *Journal of Mammalogy* 103:29-44.
- MARTÍNEZ-GORDILLO, D., O. ROJAS-SOTO, AND A. ESPINOSA-DE LOS MONTEROS. 2010. Ecological niche modelling as an exploratory tool for identifying species limits: an example based on Mexican muroid rodents. *Journal of Evolutionary Biology* 23:259-270.
- MERRIAM, C. H. 1901. Descriptions of 23 new harvest mice (genus *Reithrodontomys*). *Proceedings of the Washington Academy of Sciences* 3:547-558.
- MORGAN, G. S., AND R. S. WHITE JR. 2005. Miocene and Pliocene vertebrates from Arizona. Pp. 114-135, in *Vertebrate Paleontology in Arizona* (Heckert A. B. and S. G. Lucas, eds.). New Mexico Museum of Natural History and Science Bulletin. Albuquerque, New Mexico, U.S.A.
- MORRONE, J. J. 2005. Toward a synthesis of Mexican biogeography. *Revista Mexicana de Biodiversidad* 76:207-252.
- MUSSER, G. G., AND M. D. CARLETON. 2005. Superfamily Muroidea. Pp. 894-1531, in *Mammal species of the world: a taxonomic and geographic reference*. 3rd ed. (D. E. Wilson and D. M. Reeder, eds.). Johns Hopkins University Press. Baltimore, U.S.A.
- MYERS, N., ET AL. 2000. Biodiversity hotspots for conservation priorities. *Nature* 403:853-858.
- ORDÓÑEZ-GARZA, N., ET AL. 2010. Patterns of phenotypic and genetic variation in three species of endemic Mesoamerican *Peromyscus* (Rodentia: Cricetidae). *Journal of Mammalogy* 91:848-859.
- PADIAL, J., ET AL. 2010. The integrative future of taxonomy. *Frontiers in Zoology* 7:16.
- PETERSON, A. T., J. SOBERÓN, AND V. SÁNCHEZ-CORDERO. 1999. Conservatism of ecological niches in evolutionary time. *Science* 285:1265-1267.
- PHILLIPS, S. J., AND M. DUDÍK. 2008. Modeling of species distributions with Maxent: new extensions and a comprehensive evaluation. *Ecography* 31:161-175.
- R DEVELOPMENT CORE TEAM. 2018. R: A language and environment for statistical computing. R Foundation for Statistical Computing. Vienna, Austria. www.R-project.org/
- RAMBAUT, A., ET AL. 2018. Posterior summarization in Bayesian phylogenetics using Tracer 1.7. *Systematic Biology* 67:901-904.
- RAMÍREZ-BARAHONA, S. AND L. E. EGUIARTE. 2013. The role of glacial cycles in promoting genetic diversity in the Neotropics: the

- case of cloud forests during the Last Glacial Maximum. *Ecology and Evolution* 3:725-738.
- RANNALA, B. 2015. The art and science of species delimitation. *Current Zoology* 61:846-853.
- REID, N. M., AND B. C. CARSTENS. 2012. Phylogenetic estimation error can decrease the accuracy species delimitation: a Bayesian implementation of the General Mixed Yule Coalescent model. *BMC Evolutionary Biology* 12:196.
- RISSLER, L. J., AND J. J. APODACA. 2007. Adding more ecology into species delimitation: ecological niche models and phylogeography help define cryptic species in the black salamander (*Aneides flavipunctatus*). *Systematic Biology* 56:924-942.
- ROGERS, D. S., ET AL. 2007. Molecular phylogenetic relationships among crested-tailed mice (genus *Habromys*). *Journal of Mammalian Evolution* 14:37-55.
- SITES JR., J. W., AND J. C. MARSHALL. 2003. Delimiting species: a renaissance issue in systematic biology. *Trends in Ecology and Evolution* 18:462-470.
- SITES JR., J. W., AND J. C. MARSHALL. 2004. Operational criteria for delimiting species. *Annual Review of Ecology, Evolution, and Systematics* 199-227.
- SCHOENER, T. W. 1968. The *Anolis* lizards of Bimini: resource partitioning in a complex fauna. *Ecology* 49:704-726.
- SULLIVAN, J., E. ARELLANO, AND D. S. ROGERS. 2000. Comparative phylogeography of Mesoamerican highland rodents: concerted versus independent response to past climatic fluctuations. *The American Naturalist* 155:755-768.
- THOMAS, O. 1907. On Neotropical mammals of the genera *Callicebus*, *Reithrodontomys*, *Ctenomys*, *Dasybus*, and *Marmosa*. *The Annals and Magazine of Natural History*, 7:161-168.
- URBINA, S. I., ET AL. 2006. Karyotypes of three species of harvest mice (genus *Reithrodontomys*). *The Southwestern Naturalist* 51:564-568.
- WARREN, D. L., R. E. GLOR, AND M. TURELLI. 2008. Environmental niche equivalency versus conservatism: quantitative approaches to niche evolution. *Evolution: International Journal of Organic Evolution* 62:2868-2883.
- WARREN, D. L., R. E. GLOR, AND M. TURELLI. 2010. ENMTools: a toolbox for comparative studies of environmental niche models. *Ecography* 33:607-611.
- YANG, Z., AND B. RANNALA. 2014. Unguided species delimitation using DNA sequence data from multiple loci. *Molecular Biology and Evolution* 31:3125-3135.

Associated editor: Jake Esselstyn and Giovani Hernández Canchola

Submitted: September 7, 2022; Reviewed: October 26, 2022

Accepted: December 7, 2022; Published on line: January 27, 2023

Appendix 1

Population numbers (corresponding in Figure 2), specimen identification numbers (museum voucher or collector numbers), Collecting locality information; GenBank accession numbers and related clade for each sample of *Reithrodontomys sumichrasti* individuals included in this study. Museum or collector abbreviations are as follows: ASNHC = Angelo State Natural History Collection; BYU = Brigham Young University; CMC = Colección de Mamíferos del CIByC, Universidad Autónoma del Estado de Morelos; MSB = Museum of Southwestern Biology; ROM = Royal Ontario Museum; TTU = Texas Tech University; CWK = C. William Kilpatrick (University of Vermont); JAG = José A. Guerrero (Universidad Autónoma del Estado de Morelos). Country abbreviations are as follows: CR = Costa Rica; GM = Guatemala; HD = Honduras; MX = México; NI = Nicaragua; PN = Panamá. New sequences are denoted by an asterisk.

| Pop. Num. | Voucher number | Country: State | Locality | GenBank accession numbers | | | Clade |
|-----------|----------------|----------------|---|---------------------------|----------|----------|-------|
| | | | | Cyt-b | Fgb-I7 | Acp5 | |
| 1 | BYU15437 | MX: Oaxaca | 1.5 km S Puerto de la Soledad, 2200 m (18.1623667; -96.9975333) | AF211911 | | | II |
| | BYU15438 | | | AF211905 | | | II |
| | BYU16249 | | | HQ269530 | HQ269737 | HQ269468 | II |
| | BYU15433 | | | HQ269531 | | | II |
| | BYU15434 | | | AF211915 | | | II |
| 2 | BYU20806 | MX: Oaxaca | El Polvorín, 5.3 km turn off Lachao Viejo, 1735 m (16.1999333; -97.1339667) | HQ269532 | HQ269738 | HQ269469 | II |
| | BYU20808 | | | HQ269534 | | | II |
| | BYU20807 | | | HQ269533 | HQ269739 | HQ269470 | II |
| 3 | CMC912 | MX: Oaxaca | Finca Copalita, Copalita, 1025 m (15.9655833; 96.4574667) | HQ269535 | HQ269740 | HQ269471 | II |
| | CMC913 | | | HQ269536 | | | II |
| | CMC914 | | | HQ269537 | | | II |
| | CMC915 | | | HQ269538 | HQ269741 | HQ269472 | II |
| | CMC991 | | | HQ269539 | HQ269742 | HQ269473 | II |
| | CMC992 | | | HQ269540 | HQ269743 | HQ269474 | II |
| | CMC993 | | | HQ269541 | | | II |
| | CMC994 | | | HQ269542 | | | II |
| | CMC995 | | | HQ269543 | | | II |
| | CMC996 | | | HQ269544 | | | II |
| | CMC997 | | | HQ269545 | HQ269744 | HQ269475 | II |
| | CMC998 | | | HQ269546 | | | II |
| CMC999 | HQ269547 | | | II | | | |
| 4 | CMC1000 | MX: Oaxaca | Rio Molino, 2353 m (16.0796667; -96.4708833) | HQ269548 | | | II |
| | CMC1001 | | | HQ269549 | HQ269745 | HQ269476 | II |
| | CMC1002 | | | HQ269550 | | | II |
| | CMC1003 | | | HQ269551 | | | II |
| | CMC1004 | | | HQ269552 | HQ269746 | HQ269477 | II |
| | CMC1005 | | | HQ269553 | | | II |
| | CMC1006 | | | HQ269554 | | | II |
| | CMC1007 | | | HQ269555 | | | II |
| | CMC1008 | | | HQ269556 | | | II |
| | CMC1009 | | | HQ269557 | | | II |
| 5 | CMC1010 | MX: Oaxaca | Santa María Yacochi, Cerro Zempoaltepec, 2300 m (17.1583333; -96.0166667) | HQ269558 | | | II |
| | CMC172 | | | HQ269559 | | | II |
| 6 | CMC1650 | MX: Oaxaca | La Cumbre, 1.2 km SE 0.6 km S Agua Fria Juxtlahuaca, 1950 m (17.209; -97.9786667) | HQ269560 | | | II |
| 7 | TTU54952 | MX: Oaxaca | 3.0 mi S. Suchixtepec (16.0166667; -96.4666667) | AF211920 | | | II |
| 8 | CMC989 | MX: Oaxaca | 0.7 km E La Soledad (15.9823; -96.5198167) | HQ269561 | | | II |
| | CMC990 | | | HQ269562 | | | II |
| 9 | CMC734 | MX: Oaxaca | La Cumbre, 18.5 km S Sola de Vega, 2175 m (16.4529; -97.00235) | HQ269563 | | | II |
| 10 | CWK1009 | MX: Oaxaca | Orizaba (17.8333333; -97.2333333) | AF211895 | | | II |
| 11 | FAC1112* | | | AF211907 | | | II |
| | FAC1117* | | | AF211913 | | | II |
| | FAC1118 | | | AF211906 | | | II |
| | FAC1119 | MX: Guerrero | 6.1 km SW Omiltemi, 2490 m (17.5491667; -99.721) | AF211908 | | | II |
| | BYU20801 | | | HQ269564 | HQ269747 | HQ269478 | II |
| | BYU20802 | | | HQ269565 | | | II |
| 12 | CWK1019* | | | AF211921 | | | II |
| | CWK1025* | | | AF211901 | | | II |
| | BYU20799 | MX: Guerrero | 3.4 km W Carrizal, 2480 m (17.6004167; -99.8248333) | HQ269566 | HQ269748 | HQ269479 | II |
| | CMC710 | | | HQ269567 | | | II |

SPECIES LIMITS IN *R. sumichrasti*

| | | | | | | | |
|----|----------|--------------|---|----------|----------|----------|-----|
| | CMC1628 | | | HQ269568 | | | II |
| | CMC1629 | | | HQ269569 | HQ269749 | HQ269480 | II |
| | CMC1630 | | | HQ269570 | HQ269750 | HQ269481 | II |
| | CMC1631 | | | HQ269571 | | | II |
| | CMC1632 | | | HQ269572 | | | II |
| | CMC1633 | | | HQ269573 | | | II |
| | CMC1634 | | | HQ269574 | | | II |
| | CMC1635 | | | HQ269575 | | | II |
| | CMC1636 | | | HQ269576 | | | II |
| | CMC1637 | | | HQ269579 | | | II |
| 13 | CMC1638 | MX: Guerrero | 3 km E El Tejocote, 2620m (17.3048667; -98.6511167) | HQ269580 | | | II |
| | CMC1639 | | | HQ269581 | | | II |
| | CMC1640 | | | HQ269582 | | | II |
| | CMC1641 | | | HQ269583 | | | II |
| | CMC1642 | | | HQ269584 | | | II |
| | CMC1643 | | | HQ269585 | | | II |
| | CMC1644 | | | HQ269586 | | | II |
| | CMC1645 | | | HQ269587 | | | II |
| | CMC1646 | | | HQ269577 | | | II |
| | CMC1647 | | | HQ269578 | | | II |
| | CMC1648 | | | HQ269588 | | | II |
| | CMC1649 | | | HQ269589 | | | II |
| 14 | TK93354 | MX: Guerrero | 4 mi SSW Filo de Caballo (17.8166667; -99.6166667) | AY293810 | | | II |
| | TK93363 | | | AY293811 | | | II |
| 15 | BYU20800 | | | HQ269590 | HQ269751 | HQ269482 | II |
| | CMC712 | MX: Guerrero | 1.1 km E Cruz Nueva, 2650 m (17.513483; -100.0295167) | HQ269591 | | | II |
| | CMC713 | | | HQ269592 | HQ269752 | HQ269483 | II |
| | BYU15967 | | | HQ269594 | | | III |
| | BYU15968 | | | AF211916 | | | III |
| 16 | BYU15969 | MX: Veracruz | La Colonia, 6.5 km W Zacualpan, 6200 ft (20.4666667; -98.3666667) | HQ269595 | HQ269754 | HQ269485 | III |
| | BYU15970 | | | HQ269596 | | | III |
| | BYU15971 | | | AF211902 | | | III |
| | BYU15972 | | | HQ269593 | HQ269753 | HQ269484 | III |
| 17 | CMC873 | MX: Veracruz | Las Cañadas, 1340 m (19.1878333; -96.9834) | HQ269597 | HQ269755 | HQ269486 | III |
| | CMC875 | | | HQ269598 | HQ269756 | HQ269487 | III |
| | CMC876 | | | HQ269599 | | | III |
| 18 | CMC878 | MX: Veracruz | 3.5 km E Puerto del Aire, 2524 m (18.6715667; -97.3318667) | HQ269600 | HQ269757 | HQ269488 | II |
| | CMC879 | | | HQ269601 | HQ269758 | HQ269489 | II |
| | CMC880 | | | HQ269602 | HQ269759 | HQ269490 | II |
| | CMC840 | | | HQ269603 | | | III |
| | CMC843 | | | HQ269604 | | | III |
| 19 | CMC847 | MX: Veracruz | 2.9 km E Puerto del Aire, 2524 m | HQ269605 | | | III |
| | CMC1403 | | | HQ269606 | | | III |
| | CMC1405 | | | HQ269607 | | | II |

| | | | | | | | |
|----|--------------|--|--|----------|----------|----------|-----|
| | | | | AF211914 | | | III |
| | | | | HQ269608 | HQ269760 | HQ269491 | III |
| | | | | HQ269609 | | | III |
| | | | | HQ269610 | | | III |
| | | | | HQ269611 | | | III |
| | | | | HQ269612 | | | III |
| | | | | HQ269613 | | | III |
| | | | | HQ269614 | | | III |
| | | | | HQ269615 | HQ269761 | HQ269492 | III |
| 20 | | | | HQ269616 | | | III |
| | MX: Veracruz | Xometla, 2615 m (18.97775; -97.1910833) | | HQ269617 | | | III |
| | | | | HQ269618 | HQ269762 | HQ269493 | III |
| | | | | HQ269619 | | | III |
| | | | | HQ269620 | | | III |
| | | | | HQ269621 | HQ269763 | HQ269494 | III |
| | | | | HQ269622 | | | III |
| | | | | HQ269623 | HQ269764 | HQ269495 | III |
| | | | | HQ269624 | | | III |
| | | | | HQ269625 | HQ269765 | HQ269496 | III |
| | | | | HQ269626 | | | III |
| | | | | HQ269627 | | | III |
| | | | | HQ269628 | | | III |
| | | | | HQ269629 | | | III |
| | | | | HQ269630 | | | III |
| | | | | HQ269631 | | | III |
| | | | | HQ269632 | | | III |
| 21 | | | | HQ269633 | | | III |
| | MX: Veracruz | Mesa de la Yerba, 3.4 km SW desviación a Mazatepec, 2040 m (19.5593; -97.0185) | | HQ269634 | | | III |
| | | | | HQ269635 | | | III |
| | | | | HQ269636 | | | III |
| | | | | HQ269637 | | | III |
| | | | | HQ269638 | | | III |
| | | | | HQ269639 | | | III |
| | | | | HQ269640 | | | III |
| 22 | | | | HQ269641 | | | III |
| | MX: Veracruz | Cruz Blanca, 2180 m (19.4712; -97.0842) | | HQ269642 | | | III |
| | | | | HQ269643 | | | III |
| | | | | HQ269644 | | | III |
| | | | | HQ269645 | | | III |
| 23 | | | | HQ269646 | | | III |
| | MX: Veracruz | Xico Viejo, 1756 m (19.4517667; -97.0583) | | HQ269648 | | | III |
| | | | | HQ269649 | | | III |
| | | | | HQ269650 | HQ269766 | HQ269497 | III |
| 24 | | | | HQ269651 | | | III |
| | MX: Puebla | 4.7 km NE Teziutlán, 1750 m (19.8353167; -97.34135) | | HQ269652 | HQ269767 | HQ269498 | III |
| 25 | | | | HQ269653 | | | III |
| | MX: Puebla | El Durazno, 0.5 km Libramiento Parada, 1830m (19.8220833; -97.3399833) | | | | | |
| 26 | | | | HQ269654 | HQ269768 | HQ269499 | III |
| | MX: Puebla | 3 km W Cerro Chignaulta, 2176 m | | HQ269656 | HQ269769 | HQ269500 | III |
| | | | | HQ269658 | | | III |
| | | | | HQ269655 | | | III |
| 27 | | | | HQ269657 | | | III |
| | MX: Puebla | Rancho 22 de Marzo, marker 75.8 km Carretera Ahuazotepec-Zacatlán, 2270 m (19.6677; -97.9890333) | | HQ269659 | | | III |
| | | | | HQ269660 | | | III |
| | | | | HQ269661 | | | III |
| 28 | | | | HQ269662 | | | II |
| | MX: Puebla | Alhuaca, 8 km NE Vicente Guerrero, 2680 m (18.5705167; -97.1660833) | | | | | |
| | | | | HQ269663 | | | III |
| 29 | | | | | | | |
| | MX: Puebla | 2 km NW Cuautlamingo, 2171 m (19.7678667; -97.5403333) | | | | | |

SPECIES LIMITS IN *R. sumichrasti*

| | | | | | | | |
|----|-----------|----------------------|---|----------|----------|----------|-----|
| 30 | CMC1710 | MX: Puebla | Los Parajes, 2555 m (19.7664667; -97.4384667) | HQ269664 | | | III |
| | CMC1860 | | | HQ269665 | | | IV |
| 31 | CMC1862 | MX: Michoacán | 11 km NW Coalcomán, 1600 m (18.803; -103.2261667) | HQ269666 | | | IV |
| | CMC1863 | | | HQ269667 | | | IV |
| 32 | CMC1859 | MX: Michoacán | 10.9 km NW Coalcomán, 1680 m (18.7966667; -103.2303333) | HQ269668 | | | IV |
| 33 | CMC1855 | MX: Michoacán | 0.8 km NNE Dos Aguas, 2220 m (18.8075; -102.9263333) | HQ269669 | HQ269770 | HQ269501 | IV |
| 34 | CMC1856 | MX: Michoacán | 4.2 km NNE Dos Aguas, 2370 m (18.8358333; -102.9256667) | HQ269670 | HQ269771 | HQ269502 | IV |
| 35 | CMC1857 | MX: Michoacán | 9.2 km NNE Dos Aguas, 2245 m (18.8046667; -102.9775) | HQ269671 | | | IV |
| | BYU16242 | | | HQ269672 | | | II |
| | BYU16243 | | | HQ269673 | | | II |
| 36 | BYU16244 | MX: Michoacán | 10 km S Pátzcuaro, 2350 m (19.4535; -101.6027333) | HQ269674 | | | II |
| | BYU16245 | | | HQ269675 | | | II |
| | BYU16246 | | | HQ269676 | | | II |
| | BYU16247 | | | HQ269677 | HQ269772 | HQ269503 | II |
| 37 | CMC1870 | MX: Michoacán | 9.6 km S Pátzcuaro, 2350 m (19.45695; -101.6075833) | HQ269678 | | | II |
| 38 | CMC1871 | MX: Michoacán | 4.9 km S Santa Clara, 2415 m (19.3611667; -101.6116667) | HQ269679 | | | II |
| | CMC1872 | | | HQ269680 | | | II |
| 39 | CWK1014 | MX: Michoacán | 2.9 mi E Opopeo (19.4; -101.6) | AF211896 | | | II |
| | CWK1015 | | | AF211923 | | | II |
| | CWK1011 | | | AF211900 | | | II |
| | CMC1864 | | | HQ269681 | HQ269773 | HQ269504 | II |
| 40 | CMC1865 | MX: Michoacán | 9.9 km NW Mil Cumbres, 2820 m (19.6476667; -100.793) | HQ269682 | | | II |
| | CMC1866 | | | HQ269683 | HQ269774 | HQ269505 | II |
| | CMC1867 | | | HQ269684 | | | II |
| | CMC1868 | | | HQ269685 | | | II |
| 41 | CWK1056 | MX: Michoacán | Villa Escalante (19.4; -101.65) | AF211898 | | | II |
| | CMC2001 | | | HQ269688 | | | III |
| 42 | CMC2000 | MX: Hidalgo | Río Chiflón, 9.7 km ENE Crucero los Tules, 1750 m (20.4013333; -98.3840833) | HQ269687 | | | III |
| | CMC2002 | | | HQ269689 | | | III |
| | CMC1982 | | | HQ269686 | HQ269775 | HQ269506 | III |
| 43 | CMC2003 | MX: Hidalgo | 5 km ENE Crucero los Tules, 2070 m (20.3834; -98.3647333) | HQ269690 | | | III |
| | CMC2004 | | | HQ269691 | HQ269776 | HQ269507 | III |
| 44 | CMC1071 | MX: Hidalgo | 22 km NE Metepec, 2210 m (20.3158667; -98.23535) | HQ269693 | | | III |
| | CMC1092 | | | HQ269692 | HQ269777 | HQ269508 | III |
| | BYU15417 | | | HQ269694 | | | III |
| | BYU15418 | | | HQ269695 | | | III |
| 45 | BYU15419 | MX: Hidalgo | La Mojonera, 6 km S Zacualtipán, 2010 m (20.65; -98.6) | HQ269696 | | | III |
| | BYU15420 | | | HQ269697 | | | III |
| | BYU 15421 | | | AF211904 | | | III |
| | BYU 15422 | | | AF211918 | | | III |
| | BYU 15415 | | | AF211899 | | | III |
| 46 | BYU15416 | MX: Hidalgo | El Potrero, 10 km SW Tenango de Doria, 2200 m (20.65; -98.0666667) | HQ269699 | | | III |
| | BYU15414 | | | HQ269698 | | | III |
| 47 | CWK1027 | MX: Hidalgo | 5.0 Km N Zacualtipán (20.65; -98.6) | AF211922 | | | III |
| 48 | CWK1036 | MX: Hidalgo | 0.5 Km N Molango (20.7833333; -98.7166667) | AF211903 | | | III |
| | CMC1786 | | | HQ269703 | | | II |
| 49 | CMC1787 | MX: Estado de México | 9 km SW Zacualpán, 2400 m (18.6882667; -99.80595) | HQ269700 | HQ269778 | HQ269509 | II |
| | CMC1788 | | | HQ269701 | HQ269779 | HQ269510 | II |
| | BYU17083 | | | HQ269704 | HQ269780 | HQ269511 | I |
| 50 | BYU20784 | MX: Chiapas | Cerro Mozotal, 2930 m (15.4311; -92.3379) | HQ269707 | HQ269781 | HQ269512 | I |
| | CMC682 | | | HQ269706 | | | I |
| | BYU17084 | | | HQ269705 | | | I |
| | BYU20795 | | | HQ269710 | HQ269784 | HQ269515 | I |
| 51 | BYU20794 | MX: Chiapas | Rancho la Providencia, 1775 m (15.0913333; -92.0831) | HQ269709 | HQ269783 | HQ269514 | I |
| | CMC694 | | | HQ269708 | HQ269782 | HQ269513 | I |

| | | | | | | | |
|-----|-------------|-------------------|--|----------|----------|----------|----|
| | CNMA 35505 | | | AF211909 | | | I |
| 52 | CNMA 35508 | MX: Chiapas | San Cristobal (16.75; -92.6333333) | AF211910 | | | I |
| | CNMA 35514* | | | AF211917 | | | I |
| | NMA 35506* | | | AF211919 | | | I |
| 53 | ASNHC2150 | MX: Chiapas | 9 km S Rayón (17.2; -93) | AF211894 | | | I |
| | ASNHC2151 | | | AF211897 | HQ269785 | HQ269516 | I |
| 54 | TTU82780 | MX: Chiapas | Yalentay (16.7333333; -92.775) | HQ269711 | | | I |
| | TTU82781 | | | HQ269712 | | | I |
| 55 | ECOSCM1220 | MX: Chiapas | El Vivero, Parque Nacional Lagos de Montebello, 3.55 km NNW El Vivero, 1452 m (16.25; -92.1333333) | HQ269713 | HQ269786 | HQ269517 | I |
| 56 | ROM98287 | GM: Huehuetenango | 10 km NW Santa Eulalia (15.75; -91.4833333) | HQ269714 | | | I |
| | ROM98383 | | | HQ269715 | HQ269787 | HQ269518 | I |
| 57 | ROM98384 | GM: Chimaltenango | 15 km NW Santa Apolonia (14.7913833; -90.9708333) | HQ269716 | HQ269788 | HQ269519 | I |
| 58 | TTU83709 | HD: Copán | Picacho (13.9833333; -88.1833333) | HQ269717 | | | I |
| 59 | TTU84602 | HD: Intibuca | Santa Rosa (14.77; -88.78) | HQ287797 | | | I |
| 60 | JAG417 | NI: Esteli | Reserva de Mirafior, 3 km SE Mirafior (13.3683667; -86.4023) | HQ269718 | | | I |
| 61 | BYU 15246 | CR: San José | El Cascajal de Coronado, 1650 m (9.9166667; -84.0666667) | AF211912 | | | I |
| | ROM113151 | | | HQ269720 | HQ269790 | HQ269521 | I |
| | ROM113178 | | | HQ269724 | | | I |
| | MSB61880 | | | HQ269719 | HQ269789 | HQ269520 | I |
| | ROM113180 | | | HQ269726 | | | I |
| 62 | ROM113153 | CR: Cartago | Volcán Irazú, Route 8 Hwy Sign 28 km, La Pastora (9.8666667; -83.9166667) | HQ269722 | HQ269792 | HQ269523 | I |
| | ROM113181 | | | HQ269727 | | | I |
| | ROM113179 | | | HQ269725 | | | I |
| | ROM113152 | | | HQ269721 | HQ269791 | HQ269522 | I |
| | ROM113154 | | | HQ269723 | | | I |
| 63 | MSB130128 | PN: Chiriqui | Bugaba, Parque Nacional Volcán Baru-Intermedia (8.85; -82.5666667) | HQ269728 | HQ269793 | HQ269524 | I |
| | unavailable | | | AB618727 | | | II |
| 64* | unavailable | MX: Guerrero | Las Truchas, 3 km SE Carrizal de Bravo, 2400 m (17.359739; -99.489833) | AB618732 | | | II |
| | unavailable | | | AB618730 | | | II |
| 65* | unavailable | MX: Guerrero | Carrizal de Bravo, 2.5 km SE, 2400 m (17.609715; -99.820829) | AB618729 | | | II |
| 66* | CNMA42283 | MX: Oaxaca | Municipio Tlahuitoltepec, vicinity Santa María Yacochi, 2,300 m (17.158419; -96.030241) | AY859471 | | | II |

An 1896 specimen helps clarify the phylogenetic placement of the Mexican endemic Hooper's deer mouse

SUSETTE CASTAÑEDA-RICO^{1,2,3*}, CODY W. EDWARDS^{1,3}, MELISSA T. R. HAWKINS⁴, AND JESÚS E. MALDONADO^{1,2,3}

¹ Smithsonian-Mason School of Conservation, Front Royal, VA, U.S.A. Email: susetteazul@gmail.com, castanedaricos@si.edu (SC-R), cedward7@gmu.edu (CWE), maldonadoj@si.edu (JEM).

² Center for Conservation Genomics, Smithsonian National Zoo and Conservation Biology Institute, Washington DC, U.S.A.

³ Department of Biology, George Mason University, Fairfax, VA, U.S.A.

⁴ Department of Vertebrate Zoology, Division of Mammals, National Museum of Natural History, Washington DC, U.S.A. Email: hawkinsmt@si.edu (MTRH).

*Corresponding author: <https://orcid.org/0000-0002-4301-3579>.

Hooper's deer mouse, *Peromyscus hooperi*, is the sole member of the *Peromyscus hooperi* species group. This species is endemic to México where it is restricted to the grassland transition zone in the states of Coahuila, Zacatecas, and San Luis Potosí. Previous studies using mitochondrial and nuclear genes (*Cytb*, *Adh1-12*, *Fgb-17* and *Rbp3*) did not resolve the phylogenetic relationships of this relatively poorly known species. It was hypothesized that *P. hooperi* is sister to *P. crinitus*, and these two taxa are related to *P. melanotis*, *P. polionotus*, *P. maniculatus*, *P. keeni*, *P. leucopus*, *P. gossypinus*, *P. eremicus*, *P. californicus*, and *Osgoodomys banderanus*. Based on morphological characters, karyotypes, and allozymes, *P. hooperi* does not align with either subgenera *Haplomylomys* or *Peromyscus*. However, its unique characteristics (e. g., phallus, karyotype) have been recognized, and therefore it has been retained as its own species group. To better resolve the phylogenetic placement of *P. hooperi*, we performed target-enrichment and high-throughput sequencing and obtained several thousand nuclear ultraconserved elements and a complete mitogenome from a specimen collected in 1896 by Nelson and Goldman in Coahuila, México. We compared these data with 21 other species of neotomines using genome-wide data. Contrary to previous studies, we found high nodal support for the placement of *P. hooperi* as sister to a clade that includes *Podomys floridanus*, *Neotomodon alstoni*, *Habromys simulatus*, *H. ixtlani*, *Peromyscus mexicanus*, *P. megalops*, *P. melanophrys*, *P. perfulvus*, *P. aztecus*, *P. attwateri*, *P. pectoralis*, and *P. boylii*. We dated a Pliocene divergence of *P. hooperi* from its sister group at approximately 3.98 mya, and after the split of *P. crinitus* at ca. 4.31 mya from other peromyscines. We demonstrated that genome-wide data improve the phylogenetic signal, independently of taxon sampling, for a phylogenetically problematic species such as *P. hooperi*. We recommend that future genomic studies expand taxon sampling, including members of the subgenus *Haplomylomys*, to confirm the phylogenetic relationships of *P. hooperi* and the genetic status of its populations.

El ratón de Hooper *Peromyscus hooperi*, es el único miembro del grupo de especies que lleva su mismo nombre. Es una especie endémica de México que se encuentra restringida a las zonas de transición de pastizales en los estados de Coahuila, Zacatecas y San Luis Potosí. Estudios previos en los que se han analizado genes mitocondriales y nucleares (*Cytb*, *Adh1-12*, *Fgb-17* y *Rbp3*) no han podido resolver las relaciones filogenéticas de esta especie poco conocida. Sin embargo, se ha sugerido que *P. hooperi* podría ser la especie hermana de *P. crinitus*, y estar cercanamente relacionada con *P. melanotis*, *P. polionotus*, *P. maniculatus*, *P. keeni*, *P. leucopus*, *P. gossypinus*, *P. eremicus*, *P. californicus* y *Osgoodomys banderanus*. Con base en datos morfológicos, cariotipos y aloenzimas, no se ha podido determinar si esta especie se encuentra más estrechamente relacionada con el subgénero *Haplomylomys* o *Peromyscus*. Sin embargo, las características únicas de *P. hooperi* (e. g., falo, cariotipo) han sido reconocidas, por lo que se ha mantenido en su propio grupo de especies. Con el objetivo de proveer nueva evidencia sobre la posición filogenética de *P. hooperi*, utilizamos el método de captura por hibridación y secuenciación masiva para obtener miles de elementos ultraconservados y el genoma mitocondrial de un ejemplar colectado en 1896 por Nelson y Goldman en Coahuila, México. Además, analizamos datos genómicos de 21 especies de neotominos. Contrario a estudios previos, encontramos altos valores de soporte en el nodo que posiciona a *P. hooperi* como la especie hermana del clado que incluye a *Podomys floridanus*, *Neotomodon alstoni*, *Habromys simulatus*, *H. ixtlani*, *Peromyscus mexicanus*, *P. megalops*, *P. melanophrys*, *P. perfulvus*, *P. aztecus*, *P. attwateri*, *P. pectoralis* y *P. boylii*. Datamos la divergencia de *P. hooperi* de su grupo hermano hace aproximadamente 3.98 millones de años, después de la divergencia de *P. crinitus* y de otros peromiscinos hace aproximadamente 4.31 millones de años, ambos eventos durante el Plioceno. Nuestro estudio es un claro ejemplo de que analizar datos a nivel del genoma mejoran la señal filogenética, independientemente del número de taxones, para especies cuyas relaciones filogenéticas son conflictivas o se encuentran poco resueltas como en el caso de *P. hooperi*. Sin embargo, recomendamos que futuros estudios genómicos incluyan un muestreo taxonómico más amplio, sobre todo de miembros del subgénero *Haplomylomys*, para confirmar las relaciones filogenéticas de *P. hooperi* y el estatus genético de sus poblaciones.

Keywords: Historical DNA; genomics; mitogenomes; museum specimens; *Peromyscus*, Pliocene-Pleistocene; ultraconserved elements.

Introduction

Two of the most important naturalists from the turn of the 20th Century were Edward William Nelson and Edward Alphonso Goldman. They contributed greatly to our knowledge, understanding, and documentation of the biota in the United States and México (López-Medellin and Medellín 2016, <https://sova.si.edu/record/SIA.FARU7364>). The scientific material collected by both naturalists continues to be used as a rich resource in the systematic revision of many groups of birds and mammals (López-Medellin and Medellín 2016). Nelson and Goldman's biological surveys encompassed all of the states in México and lasted 14 years (1892 to 1906). In 1896, Nelson and Goldman conducted field work in Coahuila, México where they collected three individuals, later recognized as *Peromyscus hooperi*. These specimens were deposited and remain housed at the Smithsonian Institution's National Museum of Natural History in Washington DC.

Peromyscus hooperi is a monotypic species, endemic to México and only known from portions of the states of Coahuila, Zacatecas, and San Luis Potosí (Álvarez-Castañeda 2002). This species is sympatric with *P. eremicus*, *P. melanophrys*, and *P. pectoralis* in the states of Coahuila and Zacatecas (Schmidly et al. 1985). Its preferred habitat is the grassland transition zone, a mixture of desert scrub and grassland vegetation (Schmidly et al. 1985; Lee and Schmidly 1977). Its present fragmented and restricted distribution is considered a relict of a much larger historical distribution (Schmidly et al. 1985).

Peromyscus hooperi is poorly represented in mammal collections and little is known about its current status in their restricted distribution; however, it is not protected by the Mexican government (Norma Oficial Mexicana – 059 – 2020, Secretaría de Medio Ambiente y Recursos Naturales 2010) and is classified as Least Concern by the International Union for Conservation of Nature – IUCN – (accessed on August 2022, Álvarez-Castañeda 2016). The species resembles *P. eremicus*, *P. merriami*, and *P. pectoralis* in cranial and external characters but differs in the karyotype (Lee and Schmidly 1977; Schmidly et al. 1985). Fuller et al. (1984) and Schmidly et al. (1985) found that the karyotype of *P. hooperi* is very similar to *P. crinitus*, *P. simulus*, *Osgoodomys banderanus* and northern populations of *P. boylii*. However, *P. hooperi* has been described as a medium size mouse for the genus, with a long and bicolored tail (light grayish brown above and whitish below) with short hair. The upper parts, including face and top of head, are grayish with faint to moderate wash brown; lateral line is faint and near light buff; underparts are cream; and hind feet and lower legs are whitish. The skull contains large auditory bullae, and the first two upper and lower molars lack mesolophes. The glans penis is small but wide with a long protractile tip, and the baculum is long and slender with a cartilaginous tip (Lee and Schmidly 1977). The karyotype (2n = 48, FN = 52) comprises three pairs of biarmed autosomes and 20 pairs of acrocentric acrosomes (Lee and Schmidly 1977; Schmidly et al. 1985).

The taxonomic affinity of Hooper's deer mouse has been problematic (Carleton 1989). Based on a series of morphological characters (*i. e.*, cranial characteristics, accessory lophs, and styles of the anterior molars, structure of the hyoid, and number and placement of the mammae) it was suggested to be closely related to the subgenus *Haplomylomys* (Lee and Schmidly 1977). However, based on the anatomy of the phallus, it was more similar to species representing the subgenus *Peromyscus* (Lee and Schmidly 1977; Schmidly et al. 1985). Therefore, *P. hooperi* was characterized as an intermediate form between these two subgenera (Lee and Schmidly 1977; Fuller et al. 1984; Schmidly et al. 1985). *Peromyscus hooperi* currently is recognized as the sole member of the *Peromyscus hooperi* species group (Schmidly et al. 1985; Carleton 1989), based on morphological characters, karyotypes, allozymes, and mtDNA – cytochrome b (*Cytb*; Carleton 1989; Musser and Carleton 1993, 2005; Hogan et al. 1993; Dawson 2005; Bradley et al. 2007).

Bradley et al. (2007) used *Cytb* sequence data to conduct a phylogenetic analysis of the genus *Peromyscus*. They recovered strong nodal support for a sister group relationship between *P. hooperi* and *P. crinitus* with Maximum Parsimony (MP), however, using Maximum Likelihood (ML) and Bayesian Inference (BI) they did not resolve this relationship. In turn, this clade was sister to a clade including *P. melanotis*, *P. polionotus*, *P. maniculatus*, *P. keeni*, *P. leucopus*, *P. gossypinus*, *P. eremicus*, *P. californicus*, and *Osgoodomys banderanus*. Platt et al. (2015), included *Cytb* and three nuclear genes – *Adh1-12*, *Fgb-17* and *Rbp3*, and concluded that the phylogenetic position of *P. hooperi* remains uncertain due to a lack of support values and the different placement between ML and BI analyses.

An additional problem for the systematic classification of the species within *Peromyscus* is the very definition of the genus. Several revisions and classifications have recognized subgenera – *sensu lato* – (Osgood 1909; Hooper and Musser 1964; Hooper 1968) and genera – *sensu stricto* – (Carleton 1980; Carleton 1989; Musser and Carleton 2005) within *Peromyscus*. However, the current resolution of this group does not fully adhere to either of those classifications. In addition, genetic and genomic studies have demonstrated the paraphyly of *Peromyscus* (Bradley et al. 2007; Miller and Engstrom 2008; Platt et al. 2015; Sullivan et al. 2017; Castañeda-Rico et al. 2022). While clarifying the definition of *Peromyscus* is beyond the scope and objective of this manuscript, it is important to point out that whether we align to the *sensu lato* or *sensu stricto* classification of the genus, the phylogenetic placement of *P. hooperi* has not been well-resolved. However, hereafter, we recognized the genus *Peromyscus* as paraphyletic, including *Habromys*, *Megadontomys*, *Neotomodon*, *Osgoodomys*, and *Podomys* at the generic level (*sensu stricto*).

Uncertainty of the phylogenetic position of *P. hooperi* based on previous studies necessitates a reevaluation using additional sequence data. To accomplish this, we used genome-wide data, including several thousand

nuclear ultraconserved elements and whole mitochondrial genomes from a museum voucher specimen of *P. hooperi* collected by Nelson and Goldman combined with data from previous studies. These data provide new evidence about the phylogenetic placement of *P. hooperi* and its time of divergence from other peromyscines.

Materials and methods

Sample collection and laboratory methods. We used a museum specimen sample of *Peromyscus hooperi* – USNM 79619 – (ca. 2 mm² of dry skin) deposited at the Smithsonian Institution's National Museum of Natural History; and collected by E. W. Nelson and E. A. Goldman on August 14, 1896 from Carneros, Coahuila, México. We followed strict protocols to avoid contamination during sampling, as described in [McDonough et al. \(2018\)](#) and [Castañeda-Rico et al. \(2020\)](#). All pre-PCR steps were performed in a laboratory dedicated to processing ancient and historical DNA at the Center for Conservation Genomics, Smithsonian National Zoo and Conservation Biology Institute, Washington, DC. A silica column extraction protocol ([McDonough et al. 2018](#)) was used to extract DNA. We quantified DNA with a Qubit 4 fluorometer (Thermo Fisher, Waltham, MA) using a 1x dsDNA HS assay and visualized DNA with a TapeStation 4200 System (Agilent Technologies, Santa Clara, CA) using High Sensitivity D1000 reagents. A dual-indexed library was prepared using the SRSly PicoPlus NGS library prep kit (Claret Bioscience, LLC), according to the manufacturer's protocol. We performed dual indexing PCR with TruSeq-style indices ([Meyer and Kircher 2010](#)) using Kapa HiFi HotStart Uracil+ (Roche Sequencing), following the manufacturer's protocol. This library was amplified with 12 cycles of PCR. We then pooled three PCRs from the same library before cleaning to increase DNA fragment representation. We cleaned the indexed library using 1.6X solid-phased reversible immobilization (SPRI) magnetic beads ([Rohland and Reich 2012](#)), quantified concentration using a Qubit 4 fluorometer, and inspected size ranges and quality with a TapeStation 4200 System (conditions as mentioned above). Target-enrichment was performed to capture ultraconserved elements (UCE) and mitogenomes using the myBaits® UCE Tetrapods 5Kv1 kit (Daicel Arbor Biosciences) following the myBaits protocol v3, and the myBaits® Mito kit (Daicel Arbor Biosciences) for the house mouse *Mus musculus* panel, following the myBaits protocol v4. We amplified post-enrichment UCE and mitogenome libraries with 18 cycles of PCR using Kapa HiFi HotStart Ready Mix (Roche Sequencing), following the manufacturer's protocol. A 1.6X SPRI magnetic bead clean-up was performed subsequently. We again quantified and visualized the enriched libraries using a Qubit 4 fluorometer and a TapeStation 4200 System, respectively (conditions as mentioned above). Finally, captured libraries were sequenced on a partial lane of a NovaSeq 6000 SP PE 2 x 150 base pairs (bp; Illumina, Inc., San Diego, CA, US) at the Oklahoma Medical Research Foundation, Oklahoma City (combined with samples from unrelated projects).

In addition to the data generated in this study, we also reanalyzed previously published data including the following: UCEs and full mitogenomes from [Castañeda-Rico et al. \(2020, 2022\)](#), as well as *Cytb* gene sequences from [Bradley et al. \(2007\)](#), [Platt et al. \(2015\)](#), and [Sullivan et al. \(2017\)](#); Table 1 and Appendix 1).

Ultraconserved elements. We analyzed the raw data following the PHYLUCe v1.6.7 pipeline with the default parameters (Faircloth 2016 <https://github.com/faircloth-lab/phyluce>). Illuminaprocessor 2.10 ([Faircloth 2013](#)) and Trim Galore 0.6.5 (<https://github.com/FelixKrueger/TrimGalore>) were used to trim adapters, barcode regions and low-quality bases. Reads were assembled into contigs using Trinity 2.8.5 ([Grabherr et al. 2011](#)), and identified contigs matching UCE loci in the 5K UCE probe set (<https://github.com/faircloth-lab/uce-probe-sets>). A monolithic FASTA file was produced to extract sequences from each sample. We aligned FASTA sequences using MAFFT 7.4 ([Katoh and Standley 2013](#); [Nakamura et al. 2018](#)) and performed edge trimming. The resulting alignments were filtered to test them for various degrees of missing data (matrix completeness): 65 % matrix (35 % of the taxa missing for each UCE locus), 75 % matrix (25 % of taxa missing), 85 % matrix (15 % of taxa missing), 90 % matrix (10% of taxa missing), and 95 % matrix (5 % of taxa missing). Samples included in this dataset are shown in Table 1. We quantified informative sites with the PHYLUCe script *phyluce_align_get_informative_sites.py*. All of these analyses were performed on the Smithsonian Institution High Performance Computing Cluster (Smithsonian Institution, <https://doi.org/10.25572/SIHPC>).

We conducted a Maximum Likelihood (ML) analysis using RAxML 8.12 ([Stamatakis 2014](#)) with a GTRGAMMA site rate substitution model and 20 ML searches for the phylogenetic tree for each of the aforementioned data matrices (*i. e.*, 65 % to 95 % matrices). Nonparametric bootstrap replicates were generated using the -N autoMRE option which runs until convergence was reached. We reconciled the best fitting ML tree with the bootstrap replicate to obtain the final phylogenetic tree with support values using the -f b command.

We estimated the best evolutionary model of nucleotide substitution in jModelTest 2.1.1 ([Guindon and Gascuel 2003](#); [Darriba et al. 2012](#)) using the Akaike Information Criterion (AIC). The TVW+G model was selected as the best fitting model with the following parameters: base frequencies A = 0.2988, C = 0.2013, G = 0.2026, T = 0.2972; nst = 6; and gamma shape = 0.1070. A Bayesian Inference analysis (BI) using MrBayes 3.2.6 ([Huelsenbeck and Ronquist 2001](#); [Ronquist and Huelsenbeck 2003](#)) was performed on the 90 % matrix. The BI analyses comprised two independent runs with 50 million generations, sampling trees and parameters every 1,000 generations with four Markov-chains Monte Carlo (MCMC), three heated and one cold. We visualized output parameters using Tracer v1.7.1 ([Rambaut et al. 2018](#)) to check for convergence between runs and we discarded the first 25 % of the trees as burn-in.

A species tree analysis under the multispecies coalescent (MSC) model with ASTRAL-III v.5.7.8 (Zhang *et al.* 2018) was performed on the 90 % matrix. The local posterior probability – LPP – (Sayyari and Mirarab 2016) was used as branching support. We used the uce2speciestree pipeline script (Campana 2019 <https://github.com/campanam/uce2speciestree>) to generate input files for ASTRAL. This script uses RAxML to infer individual gene trees under the GTRGAMMA substitution model, and 100 bootstrap replicates.

Mitogenomes. FASTQ files were analyzed using FastQC v0.11.5 (Andrews 2010, www.bioinformatics.babraham.ac.uk/projects/fastqc). Adapter sequences and low-quality reads were removed using the default parameters (Phred:20, mean min-len:20) in Trim Galore 0.6.5 (<https://github.com/FelixKrueger/TrimGalore>). Exact duplicates were removed (-derep1,4) using Prinseq-lite v0.20.4 (Schmieder and Edwards 2011). We mapped the resulting high-quality reads to the closest available reference genome (*Peromyscus crinitus* – GenBank accession number KY707308), using the Geneious algorithm in Geneious Prime® 2021.2.2 (<https://www.geneious.com>) with default parameters (Medium-Low sensitivity, Maximum mismatches = 20 %, Maximum gaps = 10 %). A consensus sequence was generated with Geneious Prime® 2021.2.2 (<https://www.geneious.com>), using 4X as the lowest coverage to call a base, and aligned them using MAFFT 7.45 plug-in (Katoh and Standley 2013). We transferred annotations from the reference to rule out

the presence of nuclear copies of mitochondrial genes (NUMTs), and translated all protein-coding genes to check for frame shifts or stop codons.

We aligned sequences with MAFFT 7.45 plug-in (Katoh and Standley 2013) in Geneious Prime® 2021.2.2 (<https://www.geneious.com>). Samples included in this dataset are listed in Table 1. A BI analysis was conducted on a partitioned dataset using MrBayes 3.2.6 (Huelsenbeck and Ronquist 2001; Ronquist and Huelsenbeck 2003). The best model and partition scheme were estimated using PartitionFinder 2.1.1 (Lanfear *et al.* 2016). Our search was limited to the models available in MrBayes, with linked, corrected Akaike Information Criterion (AICc) and greedy parameters. The data block was defined by gene, tRNA, rRNA and D-loop selection. We conducted two independent runs with 50 million generations, sampling trees and parameters every 1,000 generations with four MCMC and parameters as mentioned above, to perform the BI analysis. Convergence between runs was checked using Tracer v1.7.1 (Rambaut *et al.* 2018), and the first 25 % of the trees was discarded as burn-in.

We performed a ML analysis using the concatenated dataset in RAxML 8.12 (Stamatakis 2014) with a GTRGAMMA site rate substitution model. Clade support was assessed by bootstrapping with the -N autoMRE option for a bootstrap convergence criterion. The -f b option was used to reconcile the best fitting ML tree with the bootstrap rep-

Table 1. Specimens examined in this study using UCE and mitogenomes with species name, accession number collection/ID study (Smithsonian Institution’s National Museum of Natural History USNM, Museum of Texas Tech University TK, and TTU associated, Museo de Zoología “Alfonso L. Herrera” Facultad de Ciencias UNAM MZFC, and University of Michigan Museum of Zoology –UMMZ), reference (the study from which the sequences were obtained or reanalyzed), GenBank BioProject, and GenBank accession numbers.

| Species | Number Scientific Collection/ID | Reference | UCE (GenBank BioProject) | Mitogenome (GenBank number) |
|----------------------------------|---------------------------------|-------------------------------------|-----------------------------|--------------------------------|
| <i>Peromyscus hooperi</i> | USNM79619/USNM79619 | This study | PRJNA880321 | OP432689 |
| <i>Peromyscus boylii</i> | | This study | | MZ433362 |
| <i>Peromyscus maniculatus</i> | | This study | | MH260579 |
| <i>Peromyscus leucopus</i> | | This study | | BK010700 |
| <i>Peromyscus megalops</i> | USNM340233/USNM340233 | Castañeda-Rico <i>et al.</i> (2022) | PRJNA838631 | ON528115 |
| <i>Peromyscus attwateri</i> | TTU143738/TK185663 | Castañeda-Rico <i>et al.</i> (2022) | PRJNA838631 | ON528112 |
| <i>Peromyscus aztecus</i> | USNM569848/USNM569848 | Castañeda-Rico <i>et al.</i> (2022) | PRJNA838631 | ON528113 |
| <i>Peromyscus polionotus</i> | USNM585473/USNM585473 | Castañeda-Rico <i>et al.</i> (2022) | PRJNA838631 | ON528117 |
| <i>Peromyscus crinitus</i> | TTU146966/TK193714 | Castañeda-Rico <i>et al.</i> (2022) | PRJNA838631 | ON528114 |
| <i>Podomys floridanus</i> | TTU97866/TK92501 | Castañeda-Rico <i>et al.</i> (2022) | PRJNA838631 | ON528118 |
| <i>Neotomodon alstoni</i> | TTU82668/TK93098 | Castañeda-Rico <i>et al.</i> (2022) | PRJNA838631 | ON528110 |
| <i>Onychomys leucogaster</i> | TTU146304/TK171574 | Castañeda-Rico <i>et al.</i> (2022) | PRJNA838631 | ON528111 |
| <i>Reithrodontomys mexicanus</i> | TTU138428/TK178510 | Castañeda-Rico <i>et al.</i> (2022) | PRJNA838631 | ON528119 |
| <i>Isthmomys pirrensis</i> | USNM565924/USNM565924 | Castañeda-Rico <i>et al.</i> (2022) | PRJNA838631 | ON528108 |
| <i>Neotoma mexicana</i> | TTU104969/TK150189 | Castañeda-Rico <i>et al.</i> (2022) | PRJNA838631 | ON528109 |
| <i>Peromyscus mekisturus</i> | UMMZ88967/UMMZ88967 | Castañeda-Rico <i>et al.</i> (2020) | PRJNA606805 | MT078818 |
| <i>Peromyscus melanophrys</i> | MZFC3907/MQ1229 | Castañeda-Rico <i>et al.</i> (2020) | PRJNA606805 | MT078816 |
| <i>Peromyscus perfulvus</i> | – /MCP119 | Castañeda-Rico <i>et al.</i> (2020) | PRJNA606805 | MT078817 |
| <i>Peromyscus pectoralis</i> | MZFC10465/FCR176 | Castañeda-Rico <i>et al.</i> (2020) | PRJNA606805 | MT078819 |
| <i>Peromyscus mexicanus</i> | MZFC11150/MRM030 | Castañeda-Rico <i>et al.</i> (2020) | PRJNA606805 | |
| <i>Habromys simulatus</i> | MZFC10104/HBR031 | Castañeda-Rico <i>et al.</i> (2020) | PRJNA606805 | |

licate to obtain the final phylogenetic tree (as mentioned above). DNA damage patterns were evaluated for the *P. hooperi* sample with mapDamage2.0 (Jónsson et al. 2013) using --rescale option.

Cytochrome b. We analyzed *Cytb* sequences extracted from the mitogenome that was generated in this study and from mitogenomes published by Sullivan et al. (2017) and Castañeda-Rico et al. (2020, 2022). We also used the *Cytb* sequences published by Bradley et al. (2007) and Platt et al. (2015) in order to compare the phylogenetic position of *P. hooperi* using genome-wide data as well as a single mitochondrial gene. The *Cytb* dataset allowed us to include more species within the genus *Peromyscus* and representatives of the genera *Habromys*, *Megadontomys*, *Neotomodon*, *Osgoodomys*, *Podomys*, *Isthmomyss*, *Onychomys*, *Reithrodontomys*, *Neotoma*, *Ochrotomys*, *Baiomys*, *Ototylomys*, *Tylomys*, *Nyctomys*, *Oryzomys* and *Sigmodon*. Samples included in this dataset are shown in Table 1 and Appendix 1.

The *Cytb* dataset was analyzed as follows: we performed alignment using MAFFT 7.45 plug-in (Katoh and Standley 2013) in Geneious Prime® 2021.2.2 (<https://www.geneious.com>). We estimated the best evolutionary model of nucleotide substitution in jModelTest 2.1.1 (Guindon and Gascuel 2003; Darriba et al. 2012) using the AIC method. The TPM3uf+I+G model was selected as the best fitting model with the following parameters: base frequencies A = 0.3896, C = 0.3336, G = 0.0500, T = 0.2267; nst = 6; proportion of invariable sites = 0.4080; and gamma shape = 0.6220. A BI analysis was run using MrBayes 3.2.6 (Huelsenbeck and Ronquist 2001; Ronquist and Huelsenbeck 2003) as mentioned above for UCE and mitogenome datasets. We used Tracer v1.7.1 (Rambaut et al. 2018) to check for convergence between runs, and the first 25 % of the trees was discarded as burn-in.

Divergence times estimation. Molecular dates of divergence were estimated in BEAST2 v2.6.6 (Bouckaert et al. 2019) using the mitogenome dataset. First, we obtained the best model and partition scheme in PartitionFinder 2.1.1 (Lanfear et al. 2016). The search was limited to the models available in BEAST, linked branch lengths, AICc model selection, and greedy schemes search. The data block was defined by codon position, tRNA, rRNA and D-loop selection, and the result was incorporated in the dating analysis. The BEAST analysis was performed under an uncorrelated lognormal relaxed molecular clock model. The calibrated Yule speciation processes model (Heled and Drummond 2012) with a randomly generated starting tree were set up as priors. We used the same three calibration points with a lognormal distribution from Castañeda-Rico et al. (2022). Calibrations were based on fossil records of 1) *Reithrodontomys* (mean = 1.8 million years ago [mya], stdev = 1.076, offset = 1.63), as used by Steppan and Schenk (2017); 2) *Onychomys* (mean = 4.9, stdev = 1.169, offset = 4.753), as used by Steppan and Schenk (2017); and 3) the most recent common ancestor of *P. attwateri* (mean = 2.7, stdev = 0.9, offset = 2.4 [Dalquest 1962; Karow et al. 1996;

Wright et al. 2020]). Two independent runs of 50 million iterations were performed, each was sampled every 1,000 iterations. We checked convergence statistics for Effective Sample Sizes (ESS) using Tracer v1.7.1 (Rambaut et al. 2018) and a 25 % of burn-in was performed on each run. We used LogCombiner v2.6.6 to combine trees and TreeAnnotator v2.6.2 to get a consensus tree with node height distribution (both packages available in BEAST). All phylogenetic and ultrametric dated trees from the UCE, mitogenome and *Cytb* datasets were visualized in FigTree 1.4.4 (<http://tree.bio.ed.ac.uk/software/figtree/>). All analyses were performed on the Smithsonian Institution High Performance Computing Cluster (Smithsonian Institution <https://doi.org/10.25572/SHPC>).

Results

Following the PHYLUCE v1.6.7 pipeline, we recovered 1,087 UCE loci (raw data are available in GenBank under BioProject PRJNA880321), and a complete mitogenome of 16,288 bp (GenBank accession number OP432689) from the *P. hooperi* sample. The average number of paired-end reads and fragment size after trimming were 13,075,112 reads and 67 bp long, respectively. The lowest-quality bases were detected at the end of the reads. We also recovered between 1,353 and 3,859 UCE loci from the reanalyzed samples. The average number of paired-end reads and fragment size after trimming for those samples ranged from 1,811,856 to 21,093,430 reads, and from 94 to 222 bp, respectively.

Ultraconserved Elements phylogenies. We recovered 9,840 contigs for *P. hooperi* after Trinity assemblies. The mean, minimum, and maximum length for contigs were 242, 201, and 3,784 bp, respectively. The incomplete matrix contained 4,406 UCE loci ($n = 18$, average = 3,136, min = 1,087, max = 3,859). A total of 1,087 UCE loci were obtained for *P. hooperi* with a mean, minimum, and maximum length of 235, 201, and 636 bp, respectively. The 65 % matrix contained 3,681 UCE loci (UL) with an average of 13.80 informative sites per locus (IS), the 75 % matrix (UL = 2,974, IS = 14.18, the 85 % matrix (UL = 1,514, IS = 14.29), the 90 % matrix (UL = 677, IS = 14.07), and the 95 % matrix (UL = 168, IS = 14.30).

The datasets representing various levels of matrix completeness yielded the same ML topology with high support values for all branches (Figure 1, phylogenetic trees obtained from the 65 %, 75 %, 85 %, and 95 % matrices are not shown). The BI tree topology, based on the 90 % matrix, showed the same topology with high posterior probability values for all branches (Figure 1). Both, ML and BI trees placed *P. hooperi* as sister to the clade containing *Podomys floridanus*, *Neotomodon alstoni*, *P. mexicanus*, *P. megalops*, *P. melanophrys*, *P. perfulvus*, *P. aztecus*, *Habromys simulatus*, *P. attwateri*, and *P. pectoralis*. The species tree supported, with high LPP values, the same phylogenetic position of *P. hooperi* (Figure 1, based on the 90 % matrix). The only difference among the species tree and the concatenated ML and BI trees, was the relationship between *P. mexicanus* and

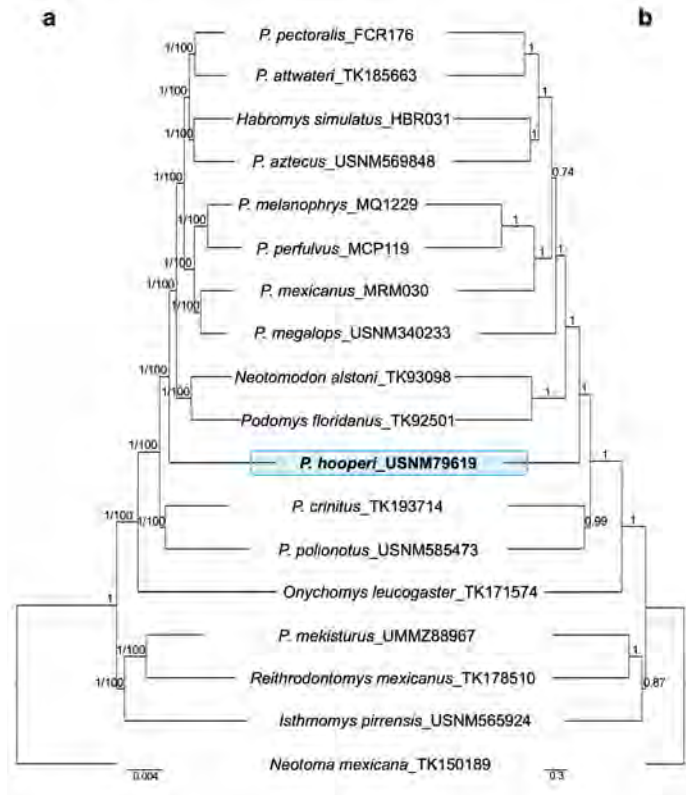


Figure 1. (a) Bayesian Inference and Maximum Likelihood phylogenies based on a 90 % matrix UCE with 677 loci. Nodal support is provided with posterior probability/ bootstrap values. (b) Species tree based on a 90 % matrix UCE with 677 loci. Nodal support is provided with local posterior probability values. The blue block highlights the phylogenetic position of *Peromyscus hooperi*.

P. megalops. These two species are sisters in the ML and BI trees but not in the species tree, where *P. megalops* is sister to the clade containing *P. mexicanus*, *P. melanophrys*, *P. perfulvus*, *P. aztecus*, *Habromys simulatus*, *P. attwateri*, and *P. pectoralis*.

Mitogenome phylogenies. The final alignment included 21 taxa and was 16,272 bp in length. BI and ML analyses, with six partitions, provided slightly different topologies (Figure 2). However, both analyses supported (pp = 1, bootstrap = 76) the placement of *P. hooperi* as sister to the clade including *Podomys floridanus*, *Neotomodon alstoni*, *P. mexicanus*, *P. megalops*, *P. melanophrys*, *P. perfulvus*, *P. boylii*, *P. aztecus*, *Habromys ixtlani*, *P. attwateri*, and *P. pectoralis*. The phylogenetic position of *P. crinitus* changed across phylogenies (Figure 2), as did the position of the clade containing *Podomys floridanus* + *Neotomodon alstoni*. However, the BI tree yielded higher support values. The DNA damage analysis showed a weak signal of damage, typical of historical DNA (Appendix 2).

Cytochrome b phylogeny. The alignment included 64 taxa, 154 sequences, and was 1,143 bp in length. The BI analysis placed *P. hooperi* sister to the clade containing *P. maniculatus*, *P. polionotus*, *P. keeni*, *P. melanotis*, *P. leucopus*, and *P. gossypinus* (Appendix 3). However, the branch support value for this phylogenetic position was low (pp = 0.53). The two samples of *P. hooperi*, one sequenced in this study (USNM 79619) and the other by [Bradley et al. \(2007;](#)

TTU 104425, GenBank accession number DQ973103) clustered together with high support (pp = 1).

Divergence time estimation of *Peromyscus hooperi*. The mitochondrial divergence dating analysis, with six data partitions, estimated a Pliocene divergence time for *P. hooperi* around 3.98 mya (95 % HPD: 3.57 to 4.47 mya; Figure 3). The divergence of *P. crinitus* was dated ca. 4.31 mya (95 % HPD: 3.80 to 4.70 mya), the split of the clade including *P. leucopus* + (*P. polionotus* + *P. maniculatus*) at ca. 4.49 mya (95 % HPD: 4.03 – 5.02 mya), and the divergence of the genus *Peromyscus* was dated ca. 5.21 mya (95 % HPD: 4.79 – 5.71 mya).

Discussion

The biological expeditions undertaken by Nelson and Goldman in México were arguably among the most important ever achieved by two naturalists for a single country ([López-Medellin and Medellin 2016](#); [Guevara 2021](#); <https://sova.si.edu/record/SIA.FARU7364>). To our knowledge, this is one of a few studies in which genome-wide data were obtained and analyzed from a specimen collected by these two naturalists (see [McDonough et al. 2022](#)). Our results not only provide new evidence about the phylogenetic position of *P. hooperi* but also joins a short list of mammal studies within the blooming field of Museomics (see [Card et al. 2021](#) for a review) that have successfully analyzed specimens collected before 1900 within a phylogeny (e. g., [Abreu-Jr et al. 2020](#); [Sacks et al. 2021](#); [Roycroft et al. 2021, 2022](#); [Castañeda-Rico et al. 2022](#); [McDonough et al. 2022](#); [Tavares et al. 2022](#)).

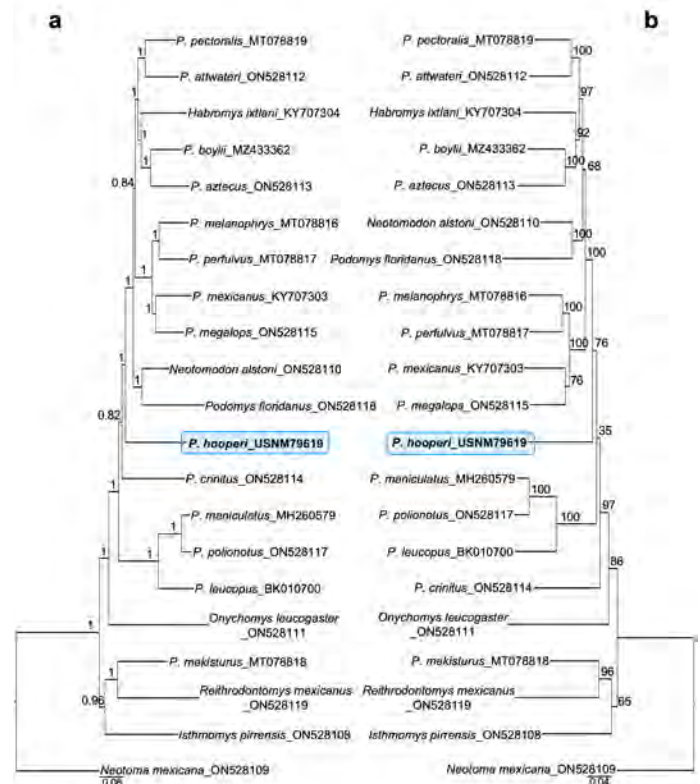


Figure 2. Mitogenome phylogenies based on Bayesian Inference (a) and Maximum Likelihood (b). Nodal support is provided with posterior probability and bootstrap values, respectively. The blue block highlights the phylogenetic position of *Peromyscus hooperi*.

Our nuclear DNA results strongly support *P. hooperi* as sister to a clade containing *Podomys floridanus*, *Neotomodon alstoni*, *Habromys simulatus*, *P. mexicanus*, *P. megalops*, *P. melanophrys*, *P. perfulvus*, *P. aztecus*, *P. attwateri*, and *P. pectoralis* (all *Peromyscus* species within the subgenus *Peromyscus*). In the mitogenome analyses, *P. boylii* (subgenus *Peromyscus*) and *H. ixtlani* joined the sister group of *P. hooperi* (Figure 1, 2). However, our results do not agree with those of [Bradley et al. \(2007\)](#), who found low support for *P. hooperi* as sister to *P. crinitus* (subgenus *Peromyscus*, *Peromyscus crinitus* species group), and both species sister to a clade including *P. melanotis*, *P. polionotus*, *P. maniculatus*, *P. keeni*, and *P. leucopus* (subgenus *Peromyscus*, *Peromyscus leucopus* and *maniculatus* species groups), *P. gossypinus*, *P. eremicus*, and *P. californicus* (subgenus *Haplomyomys*, *Peromyscus californicus* and *eremicus* species groups), and *Osgoodomys banderanus*. [Platt et al. \(2015\)](#) showed that *P. hooperi* could be related with the same species suggested by [Bradley et al. \(2007\)](#), although *P. polionotus* and *P. keeni* were not included in their study. However, the phylogenetic position of *P. hooperi* remained uncertain due to lack of strong nodal support in both of these previous studies.

Our phylogenomic analyses strongly support the placement of *P. hooperi* with the *Peromyscus mexicanus*, *megalops*, *aztecus*, *melanophrys*, and *truei* species groups (all

within the subgenus *Peromyscus*). We did include three out of the five species groups studied by [Bradley et al. \(2007\)](#). We analyzed the only member of the *Peromyscus crinitus* species group in the nuclear and mitogenome dataset, and members of the *Peromyscus maniculatus* and *leucopus* species group only in the mitogenome dataset; but we did not find that *P. hooperi* is closely related to any of those groups as previously suggested. Despite the novel data generated here, denser taxon sampling is still required to better confirm and/or determine the closest relative of *P. hooperi*. For example, phylogenetic relationships between *P. hooperi* and members of the subgenus *Haplomyomys* still require further testing. However, despite this limitation, here we have provided strong nodal support for *P. hooperi* for the first time.

The *Cytb* analysis (Appendix 3) confirmed the identity of the *P. hooperi* specimen used in this study (USNM 79619), placing it in the same clade with the only other *P. hooperi* *Cytb* sequence available ([Bradley et al. 2007](#), TTU 104425 and GenBank accession number DQ973103). In addition, the phylogenetic position of the species in this analysis is similar to [Bradley et al. \(2007\)](#) and [Platt et al. \(2015\)](#). We found that *P. hooperi* is most closely related to the *Peromyscus leucopus* and *maniculatus* species groups but with a low support (pp = 0.53); therefore, its phylogenetic posi-

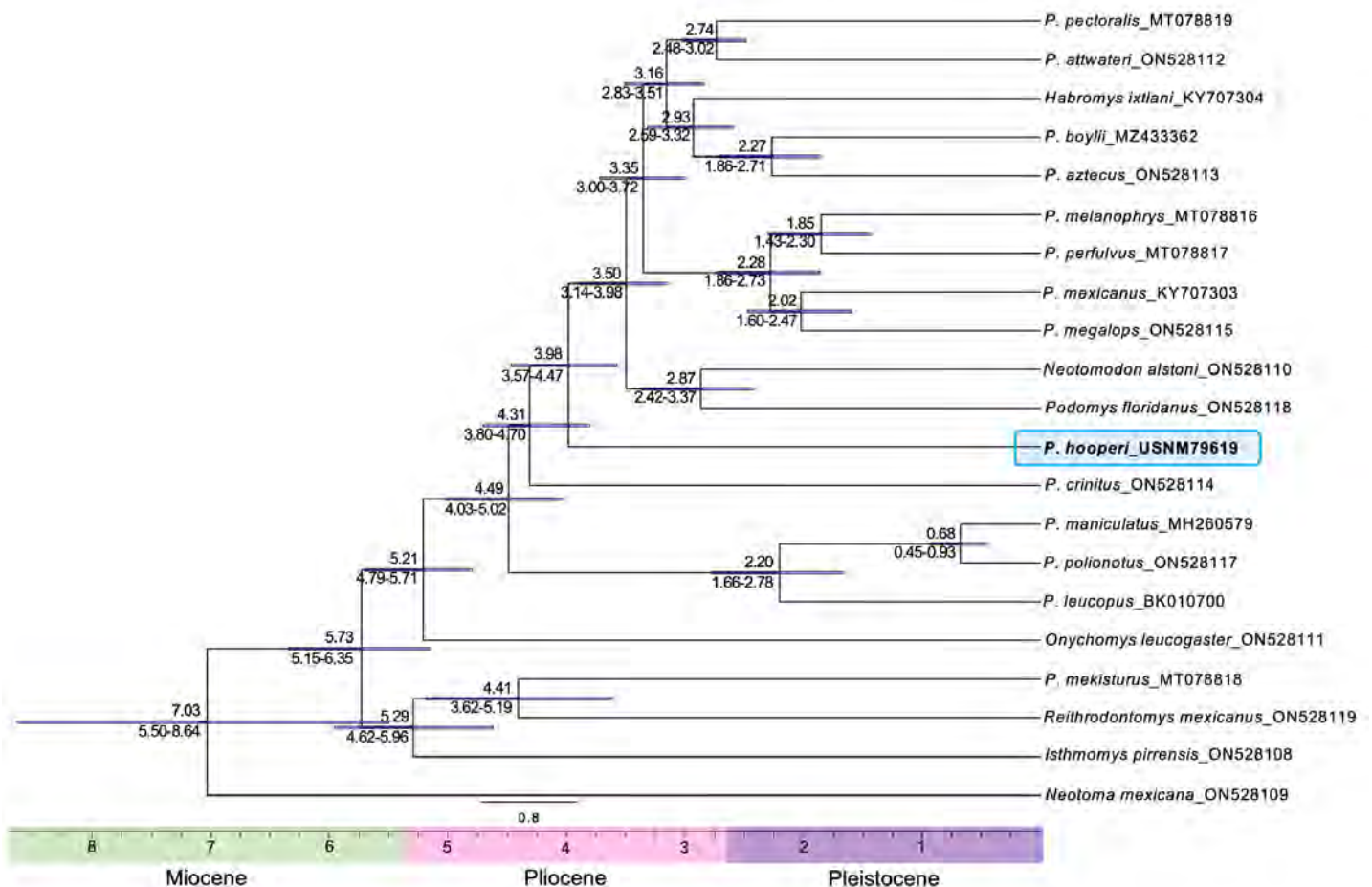


Figure 3. Dated whole mitochondrial genome phylogeny. Dates are provided in millions of years. The horizontal bars and numbers below the branches show the 95 % Highest Posterior Density. The blue block highlights the phylogenetic position of *Peromyscus hooperi*.

tion is not resolved. In conclusion, we confirmed that the phylogenetic position of the Hooper's deer mouse cannot be resolved using only *Cytb* sequences or a few genes, as [Platt et al. \(2015\)](#) documented. Our results demonstrate that genome-wide data allow a better resolution of the phylogenetic relationships of phylogenetically problematic species.

Our divergence times estimations indicated that the crown of *Peromyscus* was estimated *ca.* 5.21 mya (95 % HPD: 4.79 to 5.71 mya), and the diversification of the genus occurred *ca.* 4.49 mya (95 % HPD: 4.03 to 5.02 mya), both events during the Pliocene. We dated the split of *P. hooperi* during the Pliocene at *ca.* 3.98 mya (95 % HPD: 3.57 to 4.47 mya), following the split from *P. crinitus* at *ca.* 4.31 mya (95 % HPD: 3.80 to 4.70 mya). These dates coincide with previously dated phylogenies obtained from genome-wide data of peromyscines (e. g., [Castañeda-Rico et al. 2022](#)). They estimated the crown of the genus *Peromyscus* during the Pliocene at *ca.* 5.32 mya (95 % HPD: 4.85 to 5.98 mya), and the origin of *P. crinitus* at *ca.* 4.62 mya (95 % HPD: 4.05 to 5.28 mya), using mitogenomes. Our results also show that the *Peromyscus hooperi*, *crinitus*, *maniculatus*, and *leucopus* species groups were among the first to diverge within the genus *Peromyscus* (Figure 3), followed by the *Peromyscus megalops*, *mexicanus*, *melanophrys*, *boylii*, *aztecus*, and *truei* species groups, together with *Neotomodon*, *Podomys*, and *Habromys*. Based on our results and those of previous studies (e. g., [Hibbard 1968](#); [Riddle et al. 2000](#); [Dawson 2005](#); [Castañeda-Rico et al. 2014, 2022](#); [Platt et al. 2015](#); [Sawyer et al. 2017](#); [León-Tapia et al. 2021](#)), we suggest the Pliocene and Pleistocene as the time when speciation and diversification events took place within peromyscines, potentially associated with climatic cycles related to numerous vicariant and dispersal events.

Previous phylogenetic studies of the genus *Peromyscus* that analyzed single or few genes, provided older divergence times estimations (e. g., [Castañeda-Rico et al. 2014](#); [Platt et al. 2015](#); [Cornejo-Latorre et al. 2017](#); [Bradley et al. 2019](#)). For example, [Platt et al. \(2015\)](#), using *Cytb*, estimated the origin of *Peromyscus* and its diversification, during the Miocene, at approximately 8 mya and 5.71 mya, respectively; and the divergence of *P. hooperi* at *ca.* 5.2 mya, during the early Pliocene. However, estimates of the time to the most recent common ancestor (TMRCA) calculated from individual or few genes can be overestimated ([Duchêne et al. 2011](#)).

The evolutionary uniqueness of *P. hooperi* is supported by our results and previous studies by [Fuller et al. \(1984\)](#) and [Schmidly et al. \(1985\)](#) who found that this species does not fit well with either of the subgenera *Haplomyiomys* or *Peromyscus*. We hypothesize that *P. hooperi* will remain the sole member of the *Peromyscus hooperi* group as first proposed by [Schmidly et al. \(1985\)](#) and later supported by [Carleton \(1989\)](#) based on the morphological, karyotypic, and allozyme evidence.

The genetic and morphological uniqueness of *P. hooperi*, as well as its restricted distribution to grassland transition zones should make this a species of special concern for conservation. In addition, [Schmidly et al. \(1985\)](#) stated that *P. hooperi* is a relictual, monotypic species without close living relatives, and its survival is jeopardized/threatened by the fragile conditions of its habitat in central Coahuila as a result of overgrazing. During the last 21 years, habitat shifts from native grasslands to crops zones have increased with agricultural intensification, grain-fed cattle feedlots, and new land use policies in the Mexican states of Durango, Sinaloa, Chihuahua, Nuevo León, and particularly Coahuila where *P. hooperi* is mostly distributed ([Galván-Miyoshi et al. 2015](#); [Bonilla-Moheno and Aide 2020](#)). We recommend that future studies conduct population genetic analyses to determine the genetic diversity and structure of the different populations of *P. hooperi*. This species remains poorly known and potentially threatened by habitat loss, therefore new information is needed to determine an appropriate conservation strategy and category.

Acknowledgements

We wish to specially thank the specimen collectors, collection managers, curators and all museum staff of the Smithsonian Institution's National Museum of Natural History (NMNH) that granted the destructive sampling of the *Peromyscus hooperi* museum specimen; and the Museum of Texas Tech University (TTU), the University of Michigan Museum of Zoology (UMMZ), and the Museo de Zoología "Alfonso L. Herrera", Facultad de Ciencias, UNAM (MZFC) that granted previous sample loans. We also would like to thank the Associate Editor and two anonymous reviewers that provided comments that greatly improved the quality of this manuscript.

This manuscript is dedicated to Dr. Alfred L. Gardner (Al) for his significant contributions to the field Mammalogy through his numerous publications, research, and teachings, especially for the long-lasting impact that he has made on Mexican Mammalogy. We sincerely thank him for his invaluable help and enthusiasm to support students, researchers, and colleagues not only from Latin America but from all around the world.

Literature cited

- ABREU-JR., E. F., ET AL. 2020. Museomics of tree squirrels: a dense taxon sampling of mitogenomes reveals hidden diversity, phenotypic convergence, and the need of a taxonomic overhaul. *BMC Evolutionary Biology* 20:77.
- ANDREWS, S. 2010. FastQC: A Quality Control Tool For High Throughput Sequence Data. <http://www.bioinformatics.babraham.ac.uk/projects/fastqc>
- ÁLVAREZ-CASTAÑEDA, S. T. 2002. *Peromyscus hooperi*. *Mammalian Species* 709:1–3.
- ÁLVAREZ-CASTAÑEDA, S. T. 2016. *Peromyscus hooperi*. in IUCN 2022. The IUCN Red List of Threatened Species. Version 2022-1. www.iucnredlist.org Accessed on 22 August 2022.

- BONILLA-MOHENO, M., AND T. M. AIDE. 2020. Beyond deforestation: Land cover transition in Mexico. *Agricultural System* 178:102734.
- BRADLEY, R. D., ET AL. 2007. Toward a molecular Phylogeny for *Peromyscus*: evidence from mitochondrial cytochrome-b sequences. *Journal of Mammalogy* 88:1146–1159.
- BRADLEY, R. D., ET AL. 2019. Mitochondrial DNA sequence data indicate evidence for multiple species within *Peromyscus maniculatus*. *Special Publications Museum of Texas Tech University* 70:1–68.
- BOUCKAERT, R., ET AL. 2019. BEAST 2.5: An advanced software platform for Bayesian evolutionary analysis. *PLoS Computational Biology* 15:e1006650.
- CAMPANA, M. G. 2019. uce2speciestree. <https://github.com/campanam/uce2speciestree>. Accessed on 22 August 2022.
- CARD, D. C., ET AL. 2021. Museum Genomics. *Annual Review of Genetics* 55:633–659.
- CARLETON, M. D. 1980. Phylogenetic relationships in Neotomine–Peromyscine rodents (Muridae) and a reappraisal of the dichotomy within New World Cricetinae. *Miscellaneous Publications of the Museum of Zoology, University of Michigan* 157:1–146.
- CARLETON, M. D. 1989. Systematics and evolution. Pp. 7–141, in *Advances in the study of Peromyscus* (Rodentia) (G. L. Kirkland, Jr. and J. N. Layne, eds.). Texas Tech University Press, Lubbock, USA.
- CASTAÑEDA-RICO, S., ET AL. 2014. Evolutionary diversification and speciation in rodents of the Mexican lowlands: the *Peromyscus melanophrys* species group. *Molecular Phylogenetics and Evolution* 70:454–463.
- CASTAÑEDA-RICO, S., ET AL. 2020. Ancient DNA From Museum Specimens and Next Generation Sequencing Help Resolve the Controversial Evolutionary History of the Critically Endangered Puebla Deer Mouse. *Frontiers in Ecology and Evolution* 8:94.
- CASTAÑEDA-RICO, S., ET AL. 2022. Museomics and the holotype of a critically endangered cricetid rodent provide key evidence of an undescribed genus. *Frontiers in Ecology and Evolution* 10:930356.
- CORNEJO-LATORRE, C., ET AL. 2017. The evolutionary history of the subgenus *Haplomylomys* (Cricetidae: *Peromyscus*). *Journal of Mammalogy* 98:1627–1640.
- DALQUEST, W. W. 1962. The Good Creek formation, Pleistocene of Texas, and its fauna. *Journal of Paleontology* 36:568–582.
- DARRIBA, D., ET AL. 2012. jModelTest 2: more models, new heuristics and parallel computing. *Nature Methods* 9:772.
- DAWSON, W. 2005. Peromyscine biogeography, Mexican topography and Pleistocene climatology. Pp. 145–156, in *Contribuciones Mastozoológicas en Homenaje a Bernardo Villa* (V. Sánchez-Cordero and R. Medellín, eds.). UNAM-CONABIO, Ciudad de México, México.
- DUCHÈNE, S., ET AL. 2011. Mitogenome phylogenetics: The impact of using single regions and partitioning schemes on topology, substitution rate and divergence time estimation. *PLoS ONE*. 6:e27138.
- FAIRCLOTH, B. C. 2013. Illumiprocessor: a Trimmomatic wrapper for parallel adapter and quality trimming. doi: 10.6079/J9ILL
- FAIRCLOTH, B. C. 2016. PHYLUCE is a software package for the analysis of conserved genomic loci. *Bioinformatics* 32:786–788.
- FULLER, B., ET AL. 1984. Albumin evolution in *Peromyscus* and *Sigmodon*. *Journal of Mammalogy* 65:466–473.
- GALVÁN-MIYOSHI, Y., ET AL. 2015. Land Change Regimes and the Evolution of the Maize-Cattle Complex in Neoliberal Mexico. *Land* 4:754–777.
- GRABHERR, M. G., ET AL. 2011. Full-length transcriptome assembly from RNA-seq data without a reference genome. *Nature Biotechnology* 29:644–652.
- GUEVARA, L. The legacy of the fieldwork of E. W. Nelson and E. A. Goldman in Mexico (1892–1906) for research on poorly known mammals. 2021. *History and Philosophy of the Life Sciences* 43:31.
- GUINDON, S., AND O. GASCUEL. 2003. A simple, fast and accurate method to estimate large phylogenies by maximum-likelihood. *Systematic Biology* 52:696–704.
- HELED, J., AND A. J. DRUMMOND. 2012. Calibrated tree priors for relaxed phylogenetics and divergence time estimation. *Systematic Biology* 61:138–149.
- HIBBARD, C.W. 1968. Paleontology. Pp. 6–26, in *Biology of Peromyscus* (Rodentia) (King, J. A., ed.). Special Publication 2, American Society of Mammalogist, Oklahoma, USA.
- HOGAN, K., ET AL. 1993. Systematic and taxonomic implications of karyotypic, electrophoretic and mitochondrial DNA variation in *Peromyscus* from the Pacific Northwest. *Journal of Mammalogy* 74:819–831.
- HOOPER, E. T. 1968. Classification. Pp. 27–74, in *Biology of Peromyscus* (Rodentia) (J. A. King, ed.). Special Publication 2, The American Society of Mammalogists, Oklahoma, USA.
- HOOPER, E. T., AND G. G. MUSSER. 1964. Notes on classification of the rodent genus *Peromyscus*. *Occasional Papers of the Museum of Zoology, University of Michigan* 635:1–13.
- HUELSENBECK, J. P., AND F. RONQUIST. 2001. MRBAYES: bayesian inference of phylogeny. *Bioinformatics* 17:754–755.
- JÓNSSON, H., ET AL. 2013. mapDamage2.0: fast approximate Bayesian estimates of ancient DNA damage parameters. *Bioinformatics* 13:1682–1684.
- KAROW, P. F., ET AL. 1996. Middle Pleistocene (early Rancholabrean) vertebrates and associated marine and non-marine invertebrates from Oldsmar, Pinellas County, Florida. Pp. 97–133, in *Palaeoecology and palaeoenvironments of Late Cenozoic mammals: Tributes to the career of C. S. (Rufus) Churcher* (K. Stewart and K. Seymour, eds.). University of Toronto Press, Toronto, Canada.
- KATO, K., AND D. M. STANDLEY. 2013. MAFFT multiple sequence alignment software version 7: improvements in performance and usability. *Molecular Biology and Evolution* 30:772–780.
- LANFEAR, R., ET AL. 2016. PartitionFinder 2: new methods for selecting partitioned models of evolution for molecular and morphological phylogenetic analyses. *Molecular Biology and Evolution* 34:772–773.
- LEE, M. R., AND D. J. SCHMIDLY. 1977. A new species of *Peromyscus* (Rodentia: Muridae) from Coahuila, Mexico. *Journal of Mammalogy* 58:263–268.
- LEÓN-TAPIA, M.A., ET AL. 2021. Role of Pleistocene climatic oscillations on genetic differentiation and evolutionary history of the Transvolcanic deer mouse *Peromyscus hylocetes* (Rodentia: Cricetidae) throughout the Mexican central highlands. *Journal of Zoological Systematics and Evolutionary Research* 59:2481–2499.

- LÓPEZ-MEDELLÍN, X., AND R. MEDELLÍN. 2016. The influence of E. W. Nelson and E. A. Goldman on Mexican Mammalogy. *Special Publications Museum of Texas Tech University* 64:87–103.
- MCDONOUGH, M. M., ET AL. 2018. Performance of commonly requested destructive museum samples for mammalian genomic studies. *Journal of Mammalogy* 99:789–802.
- MCDONOUGH, M. M., ET AL. 2022. Phylogenomic systematics of the spotted skunks (Carnivora, Mephitidae, Spilogale): Additional species diversity and Pleistocene climate change as a major driver of diversification. *Molecular Phylogenetic and Evolution* 167:107266.
- MEYER, M., AND M. KIRCHER. 2010. Illumina sequencing library preparation for highly multiplexed target capture and sequencing. *Cold Spring Harbor Protocols* 2010:pdb.prot5448.
- MILLER, J. R., AND M. D. ENGSTROM. 2008. The relationships of major lineages within peromyscine rodents: a molecular phylogenetic hypothesis and systematic reappraisal. *Journal of Mammalogy* 89:1279–1295.
- MUSSER, G., AND M. D. CARLETON. 1993. Family Muridae. Pp. 501–755, *in* *Mammal Species of the World: A Taxonomic and Geographic Reference* (Wilson, D. E., and M. Reeder, eds.). Smithsonian Institution Press, Washington DC, USA.
- MUSSER, G., AND M. D. CARLETON. 2005. Superfamily Muridae. Pp. 894–1531, *in* *Mammal Species of the World: A Taxonomic and Geographic Reference* (Wilson, D. E., and M. Reeder, eds.). Johns Hopkins University Press, Baltimore, USA.
- NAKAMURA, T., ET AL. 2018. Parallelization of MAFFT for large-scale multiple sequence alignments. *Bioinformatics* 34:2490–2492.
- OSGOOD, W. H. 1909. Revision of the mice of the American genus *Peromyscus*. *North American Fauna* 28:1–285.
- PLATT, R. N. II., ET AL. 2015. What is *Peromyscus*? Evidence from nuclear and mitochondrial DNA sequences suggests the need for a new classification. *Journal of Mammalogy* 96:708–719.
- RAMBAUT, A., ET AL. 2018. Posterior summarization in Bayesian phylogenetics using Tracer 1.7. *Systematic Biology* 67:901–904.
- RIDDLE, B., ET AL. 2000. Phylogeography and Systematics of the *Peromyscus eremicus* species group and the historical biogeography of North American Warm Regional deserts. *Molecular Phylogenetics and Evolution* 17:145–160.
- ROHLAND, N., AND D. REICH. 2012. Cost-effective, high-throughput DNA sequencing libraries for multiplexed target capture. *Genome Research* 22:939–946.
- RONQUIST, F., AND J. P. HUELSENBECK. 2003. MRBAYES 3: bayesian phylogenetic inference under mixed models. *Bioinformatics* 19:1572–1574.
- ROYCROFT, E., ET AL. 2021. Museum genomics reveals the rapid decline and extinction of Australian rodents since European settlement. *Proceedings of the National Academy of Sciences* 118:e2021390118.
- ROYCROFT, E., ET AL. 2022. Sequence capture from historical museum specimens: maximizing value for population and phylogenomic studies. *Frontiers in Ecology and Evolution* 10:931644.
- SACKS, B. N., ET AL. 2021. Pleistocene origins, western ghost lineages, and the emerging phylogeographic history of the red wolf and coyote. *Molecular Ecology* 30:4292–4304.
- SCHIMIDLY, D. J., ET AL. 1985. Systematics and notes on the biology of *Peromyscus hooperi*. *Occasional Papers, Museum of Texas Tech University* 97:1–40.
- SCHMIEDER, R., AND R. EDWARDS. 2011. Quality control and pre-processing of metagenomic datasets. *Bioinformatics* 27:863–864.
- SECRETARÍA DE MEDIO AMBIENTE Y RECURSOS NATURALES. 2010. Norma Oficial Mexicana NOM-059-SEMARNAT-2010, Protección ambiental–Especies nativas de México de flora y fauna silvestres–Categorías de riesgo y especificaciones para su inclusión, exclusión o cambio–Lista de especies en riesgo. *Diario Oficial de la Federación*. México. 30 de diciembre de 2010.
- SAWYER, Y. E., ET AL. 2017. Diversification of deermice (Rodentia: genus *Peromyscus*) at their north-western range limit: genetic consequences of refugial and island isolation. *Journal of Biogeography* 44:1572–1585.
- SAYYARI, E., AND S. MIRARAB. 2016. Fast coalescent-based computation of local branch support from quartet frequencies. *Molecular Biology and Evolution* 33:1654–1668.
- STAMATAKIS, A. 2014. RAxML Version 8: a tool for phylogenetic analysis and post-analysis of large phylogenies. *Bioinformatics* 30:1312–1313.
- STEPHAN, S., AND J. J. SCHENK. 2017. Muroid rodent phylogenetics: 900-species tree reveals increasing diversification rates. *PLoS ONE* 12:e0183070.
- SULLIVAN, K. A. M., ET AL. 2017. Whole mitochondrial genomes provide increased resolution and indicate paraphyly in deer mice. *BMC Zoology* 2:11.
- TAVARES, V. C., ET AL. 2022. Historical DNA data of rare Yellow-eared bats *Vampyressa* Thomas, 1900 (Chiroptera, Phyllostomidae) clarifies phylogeny and species boundaries within the genus. *Systematics and Biodiversity* 20:1.
- WRIGHT, E. A., ET AL. 2020. Evidence from mitochondrial DNA sequences suggest a recent origin for *Peromyscus truei comanche*. *Occasional Papers Texas Tech University Museum* 367:1–19.
- ZHANG C., ET AL. 2018. ASTRAL-III: Polynomial time species tree reconstruction from partially resolved gene trees. *BMC Bioinformatics* 19:15–30.

Associated editor: Jake Esselstyn and Giovani Hernández Canchola

Submitted: September 12, 2022; Reviewed: October 25, 2022

Accepted: November 30, 2022; Published on line: January 27, 2023

Appendix 1

Specimens examined in this study using *Cytb* gene. We show the name of the species, reference (the study from which the sequences were obtained or reanalyzed), and GenBank accession number.

| Species | Study | Mitogenome (GenBank number) | <i>Cytb</i> (GenBank number) |
|----------------------------------|------------------------------|------------------------------------|------------------------------|
| <i>Onychomys leucogaster</i> | Castañeda-Rico et al. (2020) | KU168563 (To extract <i>Cytb</i>) | |
| <i>Habromys ixtlani</i> | Sullivan et al. (2017) | KY707304 (To extract <i>Cytb</i>) | |
| <i>Isthmomys pirrensis</i> | Sullivan et al. (2017) | KY707312 (To extract <i>Cytb</i>) | |
| <i>Neotoma mexicana</i> | Sullivan et al. (2017) | KY707300 (To extract <i>Cytb</i>) | |
| <i>Neotomodon alstoni</i> | Sullivan et al. (2017) | KY707310 (To extract <i>Cytb</i>) | |
| <i>Peromyscus attwateri</i> | Sullivan et al. (2017) | KY707299 (To extract <i>Cytb</i>) | |
| <i>Peromyscus aztecus</i> | Sullivan et al. (2017) | KY707306 (To extract <i>Cytb</i>) | |
| <i>Peromyscus crinitus</i> | Sullivan et al. (2017) | KY707308 (To extract <i>Cytb</i>) | |
| <i>Peromyscus megalops</i> | Sullivan et al. (2017) | KY707305 (To extract <i>Cytb</i>) | |
| <i>Peromyscus mexicanus</i> | Sullivan et al. (2017) | KY707303 (To extract <i>Cytb</i>) | |
| <i>Peromyscus pectoralis</i> | Sullivan et al. (2017) | KY707309 (To extract <i>Cytb</i>) | |
| <i>Peromyscus polionotus</i> | Sullivan et al. (2017) | KY707301 (To extract <i>Cytb</i>) | |
| <i>Podomys floridanus</i> | Sullivan et al. (2017) | KY707302 (To extract <i>Cytb</i>) | |
| <i>Reithrodontomys mexicanus</i> | Sullivan et al. (2017) | KY707307 (To extract <i>Cytb</i>) | |
| <i>Sigmodon hispidus</i> | Sullivan et al. (2017) | KY707311 (To extract <i>Cytb</i>) | |
| <i>Baiomys taylori</i> | Bradley et al. (2007) | | AF548469 |
| <i>Habromys ixtlani</i> | Bradley et al. (2007) | | DQ861395 |
| | | | DQ000482 |
| <i>Habromys ixtlani</i> | Bradley et al. (2007) | | DQ973099 |
| <i>Isthmomys pirrensis</i> | Bradley et al. (2007) | | DQ836299 |
| <i>Megadontomys cryophilus</i> | Bradley et al. (2007) | | DQ861373 |
| <i>Megadontomys thomasi</i> | Bradley et al. (2007) | | AY195795 |
| <i>Neotoma mexicana</i> | Bradley et al. (2007) | | AF294345 |
| <i>Neotomodon alstoni</i> | Bradley et al. (2007) | | AY195796 |
| | | | AY195797 |
| | | | DQ861374 |
| <i>Nyctomys sumichrasti</i> | Bradley et al. (2007) | | AY195801 |
| <i>Ochrotomys nuttalli</i> | Bradley et al. (2007) | | AY195798 |
| <i>Onychomys arenicola</i> | Bradley et al. (2007) | | AY195793 |
| <i>Oryzomys palustris</i> | Bradley et al. (2007) | | DQ185382 |
| <i>Osgoodomys banderanus</i> | Bradley et al. (2007) | | AF155383 |
| | | | DQ000473 |
| <i>Ototylomys phyllotis</i> | Bradley et al. (2007) | | AY009789 |
| <i>Peromyscus attwateri</i> | Bradley et al. (2007) | | AF155384 |
| | | | AF155385 |
| <i>Peromyscus aztecus</i> | Bradley et al. (2007) | | U89968 |
| <i>Peromyscus beatae</i> | Bradley et al. (2007) | | AF131921 |
| | | | AF131922 |
| | | | AF131914 |
| <i>Peromyscus boylii</i> | Bradley et al. (2007) | | AF155386 |
| | | | AF155392 |
| | | | AF155388 |
| <i>Peromyscus californicus</i> | Bradley et al. (2007) | | AF155393 |
| <i>Peromyscus crinitus</i> | Bradley et al. (2007) | | AY376413 |
| | | | DQ861378 |
| <i>Peromyscus crinitus</i> | Bradley et al. (2007) | | EF028168 |
| <i>Peromyscus difficilis</i> | Bradley et al. (2007) | | AY376419 AY376415 |
| | | | AY387488 |

Appendix 1

Continuation

| Species | Study | Mitogenome (GenBank number) | Cytb (GenBank number) |
|---------------------------------|------------------------------|-----------------------------|-----------------------|
| <i>Peromyscus eremicus</i> | Bradley <i>et al.</i> (2007) | | AY195799 |
| | | | AY322503 |
| <i>Peromyscus eremicus</i> | Bradley <i>et al.</i> (2007) | | DQ973100 |
| <i>Peromyscus evides</i> | Bradley <i>et al.</i> (2007) | | U89970 |
| <i>Peromyscus furvus</i> | Bradley <i>et al.</i> (2007) | | AF271032 |
| | | | AF271012 |
| | | | AF271005 |
| <i>Peromyscus gossypinus</i> | Bradley <i>et al.</i> (2007) | | DQ973101 |
| | | | DQ973102 |
| <i>Peromyscus gratus</i> | Bradley <i>et al.</i> (2007) | | AY322507 |
| | | | AY376421 |
| | | | AY376422 |
| <i>Peromyscus guatemalensis</i> | Bradley <i>et al.</i> (2007) | | EF028171 |
| | | | EF028172 |
| <i>Peromyscus gymnotis</i> | Bradley <i>et al.</i> (2007) | | EF028169 |
| | | | EF028170 |
| | | | EF028169 |
| <i>Peromyscus hooperi</i> | Bradley <i>et al.</i> (2007) | | DQ973103 |
| <i>Peromyscus hylocetes</i> | Bradley <i>et al.</i> (2007) | | U89976 |
| | | | DQ000481 |
| <i>Peromyscus keeni</i> | Bradley <i>et al.</i> (2007) | | X89787 |
| | | | AF119261 |
| <i>Peromyscus leucopus</i> | Bradley <i>et al.</i> (2007) | | AF131926 |
| | | | DQ000483 |
| <i>Peromyscus leucopus</i> | Bradley <i>et al.</i> (2007) | | DQ973104 |
| <i>Peromyscus levipes</i> | Bradley <i>et al.</i> (2007) | | AF131928 |
| | | | AY322509 |
| | | | AF155396 |
| <i>Peromyscus madrensis</i> | Bradley <i>et al.</i> (2007) | | AF155397 |
| <i>Peromyscus maniculatus</i> | Bradley <i>et al.</i> (2007) | | DQ000484 |
| | | | AY322508 |
| <i>Peromyscus maniculatus</i> | Bradley <i>et al.</i> (2007) | | DQ973111 |
| <i>Peromyscus mayensis</i> | Bradley <i>et al.</i> (2007) | | DQ836300 |
| | | | DQ836301 |
| <i>Peromyscus megalops</i> | Bradley <i>et al.</i> (2007) | | DQ000475 |
| <i>Peromyscus melanocarpus</i> | Bradley <i>et al.</i> (2007) | | EF028173 |
| <i>Peromyscus melanophrys</i> | Bradley <i>et al.</i> (2007) | | AY322510 |
| | | | AY376424 |
| <i>Peromyscus melanophrys</i> | Bradley <i>et al.</i> (2007) | | DQ973105 |
| <i>Peromyscus melanotis</i> | Bradley <i>et al.</i> (2007) | | AF155398 |
| <i>Peromyscus mexicanus</i> | Bradley <i>et al.</i> (2007) | | AY376425 |
| <i>Peromyscus mexicanus</i> | Bradley <i>et al.</i> (2007) | | EF028174 |
| <i>Peromyscus nasutus</i> | Bradley <i>et al.</i> (2007) | | AF155399 |
| | | | AY376426 |
| <i>Peromyscus nudipes</i> | Bradley <i>et al.</i> (2007) | | AY041200 |
| <i>Peromyscus oaxacensis</i> | Bradley <i>et al.</i> (2007) | | U89972 |
| <i>Peromyscus ochraventer</i> | Bradley <i>et al.</i> (2007) | | DQ973106 |

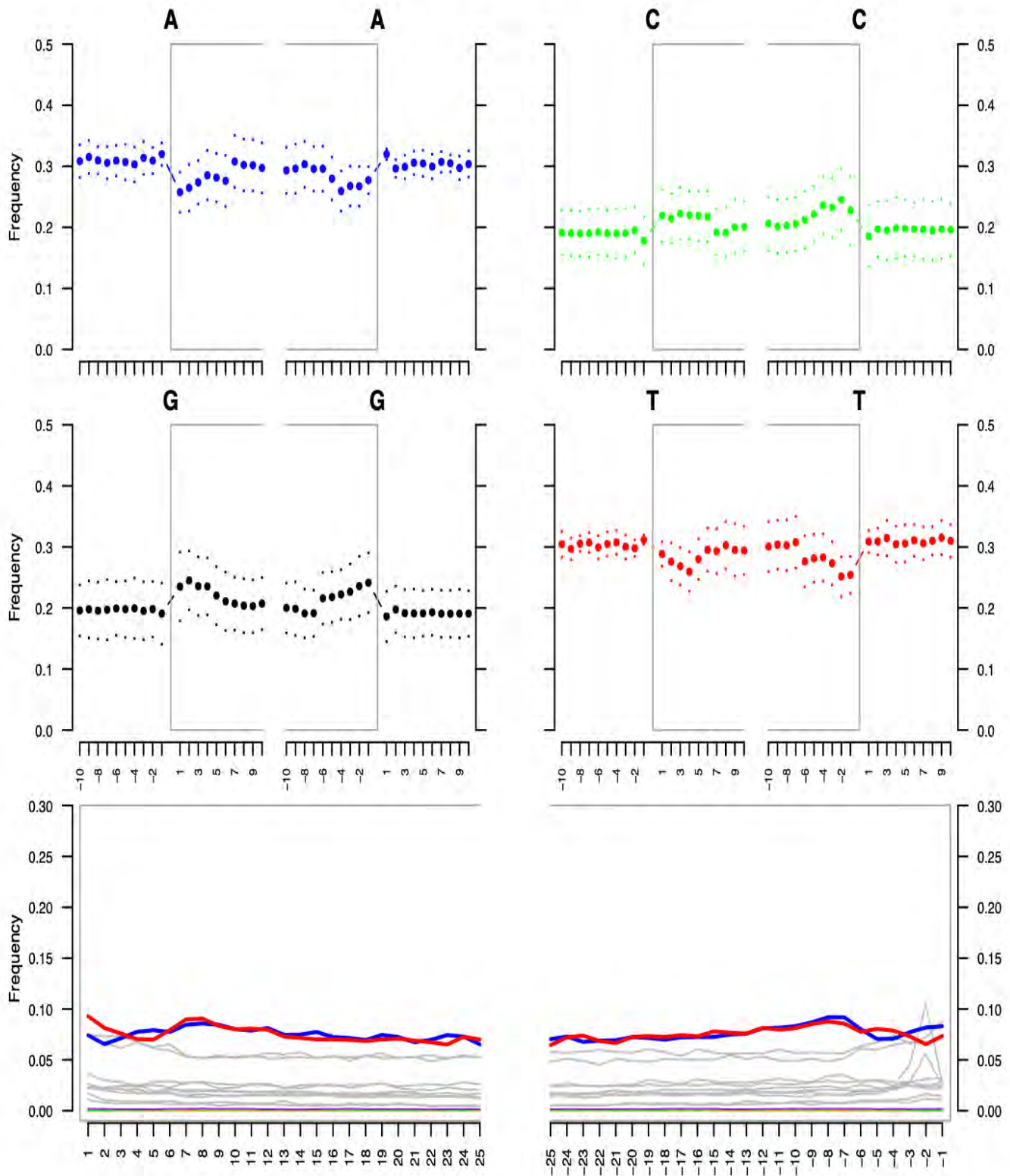
Appendix 1

Continuation

| Species | Study | Mitogenome (GenBank number) | Cytb (GenBank number) |
|------------------------------------|------------------------|-----------------------------|-----------------------|
| <i>Peromyscus pectoralis</i> | Bradley et al. (2007) | | AF155400 |
| | | | AY322511 |
| | | | AY376427 |
| <i>Peromyscus perfulvus</i> | Bradley et al. (2007) | | DQ000474 |
| <i>Peromyscus polionotus</i> | Bradley et al. (2007) | | X89792 |
| <i>Peromyscus polius</i> | Bradley et al. (2007) | | AF155403 |
| <i>Peromyscus sagax</i> | Bradley et al. (2007) | | AF155404 |
| <i>Peromyscus schmidlyi</i> | Bradley et al. (2007) | | AY322520 |
| | | | AF155405 |
| | | | AY370610 |
| <i>Peromyscus simulus</i> | Bradley et al. (2007) | | AF131927 |
| <i>Peromyscus spicilegus</i> | Bradley et al. (2007) | | AY322512 |
| | | | DQ000480 |
| | | | DQ973107 |
| <i>Peromyscus spicilegus</i> | Bradley et al. (2007) | | DQ973107 |
| <i>Peromyscus stephani</i> | Bradley et al. (2007) | | AF155411 |
| <i>Peromyscus stirtoni</i> | Bradley et al. (2007) | | DQ973108 |
| <i>Peromyscus truei</i> | Bradley et al. (2007) | | AY376433 |
| | | | AF108703 |
| | | | AY376428 |
| <i>Peromyscus winkelmanni</i> | Bradley et al. (2007) | | AF131930 |
| <i>Peromyscus zarhynchus</i> | Bradley et al. (2007) | | U89983 |
| | | | AY195800 |
| | | | DQ973109 |
| <i>Podomys floridanus</i> | Bradley et al. (2007) | | DQ973110 |
| <i>Reithrodontomys megalotis</i> | Bradley et al. (2007) | | AF176248 |
| <i>Reithrodontomys mexicanus</i> | Bradley et al. (2007) | | AY859447 |
| <i>Sigmodon hispidus</i> | Bradley et al. (2007) | | AF155420 |
| <i>Tylomys nudicaudatus</i> | Bradley et al. (2007) | | AF307839 |
| <i>Isthmomys pirrensis</i> | Platt II et al. (2015) | | FJ214681 |
| <i>Peromyscus crinitus</i> | Platt II et al. (2015) | | FJ214684 |
| <i>Peromyscus eremicus</i> | Platt II et al. (2015) | | AY322503 |
| <i>Peromyscus evides</i> | Platt II et al. (2015) | | FJ214685 |
| <i>Peromyscus levipes</i> | Platt II et al. (2015) | | DQ000477 |
| <i>Peromyscus mexicanus</i> | Platt II et al. (2015) | | JX910118 |
| <i>Peromyscus nudipes</i> | Platt II et al. (2015) | | FJ214687 |
| <i>Peromyscus ochraventer</i> | Platt II et al. (2015) | | JX910119 |
| <i>Peromyscus spicilegus</i> | Platt II et al. (2015) | | FJ214669 |
| <i>Reithrodontomys fulvescens</i> | Platt II et al. (2015) | | AF176257 |
| <i>Reithrodontomys sumichrasti</i> | Platt II et al. (2015) | | AF176256 |
| <i>Reithrodontomys mexicanus</i> | Platt II et al. (2015) | | AY859453 |

Appendix 2

Comparison of C → T terminal deamination patterns of *Peromyscus hooperi* (USNM 79619).



Appendix 3

Bayesian phylogenetic tree based on mtDNA *Cytb* sequence data. Nodal support is provided with posterior probability values. The blue block highlights the phylogenetic position of *Peromyscus hooperi*.

